

THERMAL-MECHANICAL FATIGUE BEHAVIOR OF
NICKEL-BASE SUPERALLOYS

VOL 1

by

NORMAN J. MARCHAND

B. Ing., Ecole Polytechnique de Montreal, 1980
M.Sc.A., Ecole Polytechnique de Montreal, 1982

SUBMITTED IN PARTIAL FULFILLMENT
OF THE REQUIREMENTS FOR THE
DEGREE OF

DOCTOR OF SCIENCE

at the

MASSACHUSETTS INSTITUTE OF TECHNOLOGY
January 1986

© Massachusetts Institute of Technology

Signature of Author
Department of Materials Science & Engineering
January 10, 1986

Certified by
R. M. Pelloux
Thesis Supervisor

Accepted by
Bernhardt J. Wuensch
Chairman, Departmental Graduate Committee

VOL 1
MASSACHUSETTS INSTITUTE
OF TECHNOLOGY

MAR 19 1986

LIBRARIES
Archives

THERMAL-MECHANICAL FATIGUE BEHAVIORS OF NICKEL-BASE SUPERALLOYS

by

NORMAN J. MARCHAND

Submitted to the Department of Materials Science and Engineering on January 10, 1986 in partial fulfillment of the requirements for the degree of Doctor of Science.

ABSTRACT

The thermal-mechanical fatigue (TMF) behavior of three nickel-based superalloys, which cover a wide range of ductility/strength ratio, was studied in the temperature range from 300 to 925°C. The materials investigated are Inconel X-750, Hastelloy-X and B-1900+Hf. In-phase (T_{\max} at σ_{\max} , ϵ_{\max}), out-of-phase (T_{\min} at σ_{\max} , ϵ_{\max}) and isothermal tests at T_{\min} and T_{\max} were performed under fully reversed cyclic conditions.

A microprocessor based system has been developed to control temperature and mechanical strain during the tests. The system has the ability to simultaneously control mechanical load/strain in addition to temperature. A DC electrical potential method was used to measure crack length. The electrical potential response obtained for each cycle of a given wave form and R value yields information on crack closure and crack extension per cycle.

The detailed cyclic hardening behavior of B-1900+Hf under TMF conditions was studied. The cyclic response was investigated for constant amplitude, fully reversed, strain cycling of uniaxially loaded specimens in the temperature range from 400 to 925°C. Cycling over a ductility minimum was observed to cause more cyclic hardening than isothermal fatigue experiments. In terms of mean stress and plastic strain range, out-of-phase cycling was more deleterious than in-phase cycling or isothermal cycling. On the basis of stable stress range, however, there was little difference between in-phase and out-of-phase cycling. TEM observations have shown that coarsening of γ' phase is primarily responsible for the observed behavior in TMF testing.

The thermal-mechanical fatigue crack growth (TMFCG) tests of Inconel X-750 was studied under controlled load amplitude in the temperature range from 300 to 650°C. In-phase, out-of-phase and isothermal tests at 650°C were performed on single-edge notch bars

under fully reversed cyclic conditions. A limited number of TMFCG in tension-tension ($R=0.05$) were also performed. The macroscopic crack growth rates were reported as a function of the stress intensity factor ΔK . Faster crack growth rates were measured under out-of-phase than under in-phase cycling at $R= -1$ or $R=0.05$. This behavior was rationalized by introducing the concept of an effective closure stress which was defined as the applied stress at the crossover point of the $V(\sigma)$ potential curve. This closure stress was shown to represent the effective contribution to cracking of the damage taking place during the compressive part of the cycle. Correction to the applied stress were introduced in order to take into account this damage. Correlation between TMFCG rates and ΔK_{eff} were shown to be valid provided elastic conditions prevailed in the bulk.

The TMFCG behavior of Hastelloy-X and B-1900+Hf was studied under fully reversed strain-controlled conditions in the temperature range from 400 to 925°C. The crack growth rates were first reported as a function of the strain intensity factor (ΔK_ϵ) derived from a crack compliance analysis. Out-of-phase cycling showed faster crack growth rates than isothermal or in-phase cycling at $\Delta \epsilon = 0.25\%$. Under fully plastic cycling the opposite results were observed, i.e. crack growth rates under isothermal cycling are faster than under TMF cycling. On a ΔK_ϵ basis, a strain range effect was observed in both alloys.

The results were rationalized using a corrected stress-intensity factor computed from the actual load, the closing bending moment caused by the increase of compliance with crack length, and with the effective closure stress measured with the electrical potential signal. The closure stress was shown to be controlled by the testing condition (in-phase, out-of-phase or isothermal) rather than by the strain range or by the resulting stress range. Each mode of fracture was found to be characterized by a unique crack growth rate vs ΔK_{eff} curve.

Thesis Supervisor: Dr. R. M. Pelloux

Title: Professor of Materials Engineering

Table of Contents

Abstract	2
Table of Contents	4
List of Figures	7
List of Tables	13
Acknowledgements	14
1.0 Introduction	15
2.0 Introduction to Thermal-Mechanical Fatigue	21
2.1 Definition	21
2.2 Parameters Affecting TMF	24
2.2.1 Cyclic Stress-Strain Responses	25
2.2.2 Environmental Effects	30
3.0 Review of Experimental Data	36
3.1 Introduction	36
3.2 Endurance Data	36
3.3 Fatigue Crack Propagation Data	39
3.4 Metallographic and Fractographic Data	43
3.5 Discussion	47
4.0 Experimental Procedures	53
4.1 Thermal-Mechanical Testing Requirement	53
4.2 Materials	56

4.3	Specimen Geometry.	62
4.4	Apparatus and Testing Conditions	62
5.0	Results.	70
5.1	Tensile and Creep Properties	70
5.2	Low Cycle Fatigue Properties	82
5.3	Thermal-Mechanical Fatigue Properties	
5.4	Thermal-Mechanical Fatigue Crack Growth114
	Properties114
5.4.1	Inconel X-750114
5.4.2	B-1900+Hf118
5.4.3	Hastelloy-X.124
6.0	Discussion.129
6.1	Isothermal Low Cycle Fatigue Behavior129
6.2	Cyclic Stress-Strain Responses of B-1900+Hf131
6.3	FCG of Inconel X-750142
6.4	FCG of B-1900+Hf.148
6.5	FCG of Hastelloy-X165
6.6	Correlation Parameters for In-Service Components.177
7.0	Conclusions180
8.0	Recommendations for Future Work183
9.0	References.185
Appendix 1	TMF Methods of Testing200

Appendix 2	Design of the Testing Unit	219
Appendix 3	Software for Control and Data Analysis	238
Appendix 4	Cyclic Hardening Curves and Fatigue Crack Growth Curves	358
Appendix 5	K_I -Solutions for Single Edge Notch Specimens With Fixed End Displacements	411

List of Figures

1.1	Stress-Strain-Temperature Cycles Experience at the Lower Tip of a Combuster Liner [13]	16
2.0	Proposed Terminology for High Temperature Fatigue [1].	22
2.1	Typical Stress-Strain Response Obtained at High Temperature.	26
2.2	Comparative Low-cycle Fatigue Resistance of Wrought IN-706 in Air and Vacuum.	31
3.1	Isothermal and TMF Lives of A-286 [21].	38
3.2	Comparison of TMFCG Rates in Out-of-phase and In-phase Cycling in MAR-M200 Cycled Between 315° and 927°C [27].	40
3.3	Variation of Steady State Crack Growth as a Function of the Maximum Temperature in Thermal Shock Experiment [70]	42
3.4	Temperature Dependence of Fatigue Crack Propagation in Nickel-Base Alloys [5]	51
4.1	Schematic Diagram Showing Waveforms of Temperature, Strain and Stress in Thermal and Isothermal Fatigue Tests.	54
4.2	Microstructure of Hastelloy-X. Grain Size in (a) the Transverse Direction, (b) Longitudinal Section.	58
4.3	Microstructure of X-750 Fully Heat Treated. Grain Size and MC Carbides in (a) Transverse Direction, (b) Longitudinal Section.	60
4.4	General Microstructure of B-1900+Hf Fully Heat Treated; (a) Grain Size, (b) Interdendritic spacing, fine and coarse γ' , (c) γ' size (0.9 μm)	61
4.5	Test Specimens for Monotonic Tensile and Creep Testing.	63
4.6	Test Specimen Geometries for Initial Fatigue Testing.	63
4.7	Test Specimen Geometry for TMF Testing.	64

5.1	Monotonic Tensile Response of B-1900+Hf ($\dot{\epsilon} = 0.005 \text{ min}^{-1}$)	75
5.2	Monotonic Tensile Response of Hastelloy-X ($\dot{\epsilon} = 0.005 \text{ min}^{-1}$)	76
5.3	0.2% Yield Stress Versus Representative Scatter for B-1900+Hf	77
5.4	0.2% Yield Stress Versus Representative Scatter for Hastelloy-X.	78
5.5	Specimen Rupture Life Versus Representative Rupture Life Scatter Bands for B-1900+Hf.	79
5.6	Creep Responses of Hastelloy-X at 871°C	80
5.7	Creep Responses of Hastelloy-X at 982°C	81
5.8	Strain Range Versus Number of Cycles to Failure for B-1900+Hf (T = 538°C)	90
5.9	Strain Range Versus Number of Cycles to Failure for B-1900+Hf (T = 760°C)	91
5.10	Strain Range Versus Number of Cycles to Failure for B-1900+Hf (T = 871°C)	92
5.11	Strain Range Versus Number of Cycles to Failure for B-1900+Hf (T = 982°C)	93
5.12	Strain Range Versus Number of Cycles to Failure for Hastelloy-X (T = 538 and 760°C)	94
5.13	Strain Range Versus Number of Cycles to Failure for Hastelloy-X (T = 871 and 982°C)	95
5.14	Strain Range Versus Number of Cycles to Failure as a Function of Temperature for B-1900+Hf.	96
5.15	Strain Range Versus Number of Cycles to Failure as a Function of Temperature for Hastelloy-X	97

5.16	Various Strain Components and Stress Amplitude in One Cycle (B-1900+Hf, In-phase)	102
5.17	Various Strain Components and Stress Amplitude in One Cycle (B-1900+Hf, Out-of-phase)	103
5.18	Hysteresis Loop Obtained by Plotting ϵ_{mec} and σ for B-1900+Hf (In-phase Cycling)	105
5.19	Hysteresis Loop Obtained by Plotting ϵ_{mec} and σ for B-1900+Hf (Out-of-phase Cycling)	106
5.20	Cyclic Hardening Curves of B-1900+Hf at $\Delta \epsilon_{mec} = 0.452\%$ (In-phase)	107
5.21	Cyclic Hardening Curves of B-1900+Hf at $\Delta \epsilon_{mec} = 0.4675\%$ (Out-of-phase)	108
5.22	Cyclic Hardening Curves of B-1900+Hf (In-phase)	109
5.23	Cyclic Hardening Curves of B-1900+Hf (Out-of-phase)	110
5.24	Cyclic Stress-Strain Curves of B-1900+Hf. Isothermal 538 and 871°C versus In-phase Cycling	112
5.25	Cyclic Stress-Strain Curves of B-1900+Hf. Isothermal 538 and 871°C Versus Out-of-phase Cycling.	113
5.26	Cyclic Stress-Strain Curves of B-1900+Hf. Isothermal, In-phase and Out-of-phase cycling	115
5.27	Intergranular Cracking of B-1900+Hf Cycled in In-phase Conditions. (a) Longitudinal View, (b) Transverse View, (c) Intergranular and Transgranular Cracking.	116
5.28	Transgranular Cracking of B-1900+Hf Cycled in Out-of-phase Conditions. (a) Longitudinal View, (b) Transverse View, (c) Inter-dendritic Cracking	117

5.29	Summary of the TMFCG Rates in Inconel X-750 Cycled Under Load-Controlled.	119
5.30	TMFCG Rates in B-1900+Hf Under Out-of-phase Cycling ($\Delta \epsilon_{mec} = 0.25\%$)	121
5.31	Summary of the TMFCG Rates in B-1900+Hf Cycled Under Strain-Controlled ($\Delta \epsilon_{mec} = 0.25\%$)	122
5.32	Summary of the TMFCG Rates in B-1900+Hf Cycled Under Strain-Control ($\Delta \epsilon_{mec} = 0.50\%$)	123
5.33	Influence of Frequency (Strain Rate) on the FCG Rates in B-1900+Hf Cycled Under Strain-Control ($\Delta \epsilon_{mec} = 0.25\%$)	125
5.34	Summary of the TMFCG Rates in Hastelloy-X Cycled Under Strain-Control ($\Delta \epsilon_{mec} = 0.25\%$)	127
5.35	Summary of the TMFCG Rates in Hastelloy-X Cycled Under Strain-Control ($\Delta \epsilon_{mec} = 0.50\%$)	128
6.1	Typical Dislocation Structure Obtained Under In-phase Conditions. $b = [112]$, $g = (111)$	132
6.2	Typical Dislocation Structure Obtained Under Out-of-phase Conditions. $b = [112]$, $g = (111)$	133
6.3	Dislocation Structure Observed in a Sample Cycled Under In-phase Conditions Showing Directional Coarsening of the γ' Phase. $b = [112]$, $g = (111)$	135
6.4	Potential Curves $V(T, \sigma)$, $V(T)$ and $V(\sigma)$ for TMFCG in Inconel X-750. $\Delta K \sim 25 \text{ MPa} \sqrt{\text{m}}$	143
6.5	Potential Curves $V(T, \sigma)$, $V(T)$ and $V(\sigma)$ for TMFCG in Inconel X-750. $\Delta K \sim 50 \text{ MPa} \sqrt{\text{m}}$	144
6.6	TMFCG Rates in Inconel X-750 as a Function of ΔK_{eff}	146

6.7	Out-of-phase Crack Growth Rates in B-1900+Hf as a Function of the Conventional Strain Intensity Factor in SEN and Tubular Specimens [29]	149
6.8	Effect of Frequency on the FCG Rates in B-1900+Hf as a Function of ΔK_{σ} (T_{max} , $\Delta \epsilon_{mec} = 0.25\%$)	152
6.9	FCG Rates in B-1900+Hf as a Function of ΔK_{σ} ($\Delta \epsilon_{mec} = 0.25\%$) .	153
6.10	FCG Rates in B-1900+Hf as a Function of ΔK_{σ} ($\Delta \epsilon_{mec} = 0.50\%$) .	154
6.11	Effect of Strain Range on the FCG Rates in B-1900+Hf Cycled Under Out-of-phase Conditions	156
6.12	Potential Curve $V(\sigma)$ and Stress Amplitude in B-1900+Hf Under Isothermal Cycling (T_{max})	157
6.13	Potential Curve $V(\sigma)$ and Stress Amplitude in B-1900+Hf Under In-phase Cycling	158
6.14	Potential Curve $V(\sigma)$ and Stress Amplitude in B-1900+Hf Under Out-of-phase Cycling (T_{max})	159
6.15	FCG Rates in B-1900+Hf as a Function of ΔK_{eff}	161
6.16	Variation of the Opening Stress (σ_{op}) as a Function of Crack Length in B-1900+Hf ($T = 925^{\circ}C$, $\Delta \epsilon_{mec} = 0.25\%$)	163
6.17	Out-of-phase Crack Growth Rates in Hastelloy-X as a Function of the Conventional Strain Intensity Factor in SEN and Tubular Specimens	166
6.18	FCG Rates in Hastelloy-X as a Function of ΔK_{σ} ($\Delta \epsilon_{mec} = 0.25\%$)	169
6.19	FCG Rates in Hastelloy-X as a Function of ΔK_{σ} ($\Delta \epsilon_{mec} = 0.50\%$)	170
6.20	Potential Curves $V(\sigma)$ and Stress Amplitude in Hastelloy-X Under Isothermal Testing (T_{max})	172

6.21	Potential Curves $V(\sigma)$ and Stress Amplitude in Hastelloy-X Under In-phase Cycling	173
6.22	Potential Curves $V(\sigma)$ and Stress Amplitude in Hastelloy-X Under Out-of-phase Cycling	174
6.23	Variation of the Opening Stress (σ_{op}) as a Function of Crack Length in Hastelloy-X ($T = 925^{\circ}\text{C}$, $\Delta\varepsilon_{mec} = 0.25\%$)	175
6.24	FCG RATES in Hastelloy-X as a Function of ΔK_{eff}	176

List of Tables

1.1 Potential Problems in Gas Turbine Materials. 17

2.1 Possible Types of Metal/Environmental Interactions 33

2.2 Summary of Environmental Effects on Fatigue. 34

4.1 Chemical Composition and Heat Treatment Conditions
of the Materials Tested 57

4.2 Materials and Fatigue Testing Conditions 67

5.1 Materials and Their Tensile Properties 72

5.2 Creep Test Results for B-1900+Hf 74

5.3 Short-time Creep Test Results for Hastelloy-X 74

5.4 Baseline Fatigue Test Summary at 530°C
(B-1900+Hf, $R_{\epsilon} = -1$) 84

5.5 Baseline Fatigue Test Summary at 650°C
(B-1900+Hf, $R_{\epsilon} = -1$) 84

5.6 Baseline Fatigue Test Summary at 760°C
(B-1900+Hf, $R_{\epsilon} = -1$) 85

5.7 Baseline Fatigue Test Summary at 871°C
(B-1900+Hf, $R_{\epsilon} = -1$) 86

5.8 Baseline Fatigue Test Summary at 983°C
(B-1900+Hf, $R_{\epsilon} = -1$) 88

5.9 Baseline Fatigue Test Summary of Hastelloy-X
($R_{\epsilon} = -1$) 89

5.10 Summary of the Cyclic Responses of B-1900+Hf
Under In-phase Cycling 99

5.11 Summary of the Cyclic Responses of B-1900+Hf
Under Out-of-phase Cycling. 100

Acknowledgements

The author is grateful to a number of people who assisted and encouraged him throughout this work and during the course of his stay at the Massachusetts Institute of Technology.

To the National Aeronautics and Space Administration who sponsored this work (Grant #NAG3-280). To this regard, the supervision of Drs. Marvin Hirschberg and Bob Bill is gratefully acknowledged.

To Professor R.M. Pelloux, his thesis advisor, for his invaluable technical and personal guidance.

To Professors F.A. McClintock and D.M. Parks for their review of the manuscript, but most of all, for their enlightening comments and for the many discussions on fracture mechanics and thermal-fatigue.

To Professor R.G. Ballinger for his review of the manuscript and for his help in designing the experimental set-up.

To Pete Stahl (MTS Corporation) for his assistance and guidance in repairing and improving the servo-hydraulic machine.

To Dr. Gilles L'Esperance (Ecole Polytechnique de Montreal) for his assistance in carrying-on the TEM study.

To Jeff Hill (Pratt & Whitney Aircraft) and Eric Jordan (Univ. of Conn.) for providing all the materials and specimens used in this investigation, and for the many discussions on fracture mechanics.

To Heather Ballinger who went through the pain of typing the manuscript, I am grateful.

To my close friends in the fatigue group; Ioannis, Bertrand, Jung, Glenn, Jon and Allison, for all their support and encouragement

throughout the completion of this work. Without them a considerable fraction of this thesis would not have been completed. I am eternally indebted to them.

To all my other friends; Ibrahim, Janine, John, Bob, Edmund, Arthur, Charley and Magnus, I am grateful. They have made my stay at MIT a very fruitful and pleasant one. Their friendship will always remain a very pleasant memory.

1.0 Introduction

Many fatigue problems in high temperature machinery involve thermal as well as mechanical loadings. By thermal loading it is meant that the material is subject to cyclic temperature simultaneously with cyclic stress or strain. Analysis of these conditions and consideration of the attendant fatigue damage becomes very complex and often gross simplifications are introduced.

Low cycle fatigue and thermal fatigue are recognized failure modes for structures such as gas turbine components which operate with combined temperature and strain cycling. A limited listing of materials, operating temperatures and potential life-limiting failure modes for aircraft engine components are given in Table 1.1.

The thermal fatigue cracking encountered in power plant components and gas turbine engines is due to internal constraints [1-2], arising when surfaces are heated rapidly and are prevented from expanding by the bulk section whose temperature rises more slowly. Under such circumstances, compressive plastic yielding may occur during heating and later, when the bulk material reaches the surface temperature, tensile residual stresses will be set up which, if large enough, will cause reverse plastic strains. The process may reverse on shut-down and thus a low cycle fatigue situation can arise during each start-up, shut-down operational cycle. Figure 1.1 from Moreno et al. [13] shows the kind of strain temperature cycle believed to be generated during non-uniform heating and cooling of high temperature components. The important point to note is that this fatigue cycle does not arise under isothermal conditions.

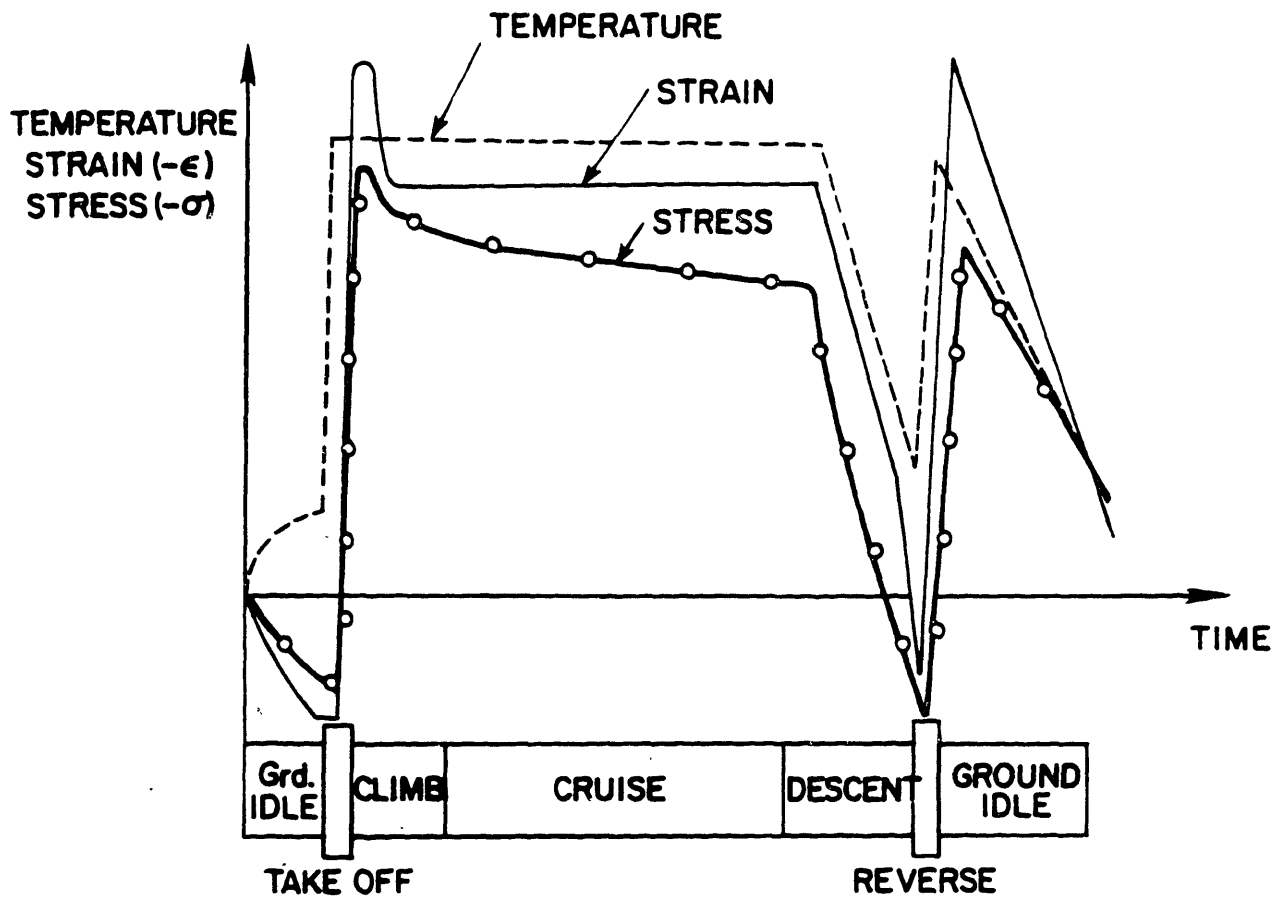


Figure 1.1 Stress-strain-temperature cycle experience at the lower tip of a combustor liner[13].

Table 1.1

POTENTIAL PROBLEMS IN GAS TURBINE MATERIALS

Component	Material Type	Temperature(°C)	Concern
compressor disk	Ni-based	< 400	burst, low cycle fatigue
compressor casing	age-hardened stainless steel or titanium alloy	< 400	high cycle fatigue
shaft	Fe-Ni-Cr	< 225	high cycle fatigue, high-strain fatigue
combustor liner	Co-based and/or Ni-based	≤1000	thermal fatigue, thermal mechanical fatigue
combustor casing	Ni-based	< 550	thermal fatigue
turbine blades	Ni-based	≤1000	thermal mechanical fatigue, high cycle fatigue
turbine disks	Ni-based	370-650	burst (over speed), low cycle fatigue, high cycle fatigue, creep fatigue

The influence of temperature on low cycle fatigue life is well documented [3-6] but the mechanisms by which temperature influences the fatigue process are not well understood. Low cycle fatigue life is generally acknowledged to be directly related to material ductility; however, as ductility increases with temperature, low cycle fatigue life normally decreases. Creep and environmental effects also are known to influence LCF behavior, but the relative contribution of these two factors is not well defined [2,4-6].

A major objective of most high-temperature fatigue research programs is to develop and verify models for thermal fatigue by comparing experimental data with analytical and/or computer-derived predictions of thermal fatigue life.

Prediction of crack propagation rates in structural components from specimen data generated in the laboratory is only possible if a parameter can be found which characterizes the severity of the stress and strain cycles near the crack tip. Such a parameter is needed to match a particular loading and crack length in a component with the correct equivalent specimen loading and crack length. In cases of cyclic loading mainly involving linear elastic deformation (small scale yielding), the stress intensity factor (ΔK) is a widely used and successful parameter. However, the stress intensity factor may not be applicable for some hot section components, since cracks may grow through regions of substantial plastic deformation.

The prediction of propagation life in engine components requires the consideration of thermal-mechanical fatigue (TMF) cycles. The problem of thermo-mechanically driven crack growth in the presence of significant inelastic strain is a challenging problem. In order for a single

parameter to be useful for predicting thermal-mechanical crack growth in components, it should satisfy the following conditions:

(1) It should predict crack growth rate from a single crack growth rate versus parameter curve. In this way, cracks of different lengths loaded in such a way as to yield the same value of the parameter, experience the same crack growth rate (similitude principle).

(2) It should correctly predict fatigue crack growth rates independent of part geometry.

(3) It should be calculable for complex real part geometries. Obviously, parameters not satisfying the above requirements would be of limited value, since component or simulated component testing would always be required to obtain crack growth rate information.

In this research program, it was proposed to assess the suitability of various parameters for correlating high temperature and thermal-mechanical crack growth rates. A parameter was sought which can correlate data for the full range of conditions from elastic stress and strain cycling to substantially plastic strain cycling. The ultimate goal of establishing such a parameter is the prediction of the propagation life of real engine components, since it is known that cracks initiate early in fatigue life.

A second goal was to combine the crack growth data generated with optical, fractographic, and TEM observations to assess a fundamental mechanistic understanding of the thermal-mechanical fatigue behavior of typical nickel-based superalloys.

To achieve these goals, the following procedure was decided upon. First, TMF was studied under linear elastic loading conditions to assess the applicability of fracture mechanics to correlate TMFCG. Then,

displacement controlled (i.e. strain controlled) TMF cycling under elastic and fully plastic conditions was studied. The TMF cyclic stress-strain behavior was combined with the crack growth data to select the parameter that best correlates the crack growth behavior.

2.0 Introduction to Thermal-Mechanical Fatigue

2.1 Definition

The subject of thermal fatigue which involves combined temperature and strain cycling, is less well understood than isothermal elevated temperature fatigue. Taira has described [7] thermal fatigue as a special case of low cycle fatigue but a more specific definition has been given by Spera [1], i.e., "thermal fatigue is the gradual deterioration and eventual cracking of a material by alternate heating and cooling during which free thermal expansion is partially or completely restrained". Spera has also proposed the following terminology by which he subdivides the general field of high temperature fatigue into thermal and isothermal categories, depending on whether temperature is cyclic or constant. As an example, thermal fatigue might result from starting and stopping of a of high temperature component, while isothermal fatigue might be the consequence of vibration during steady-state operation. The thermal fatigue category may then be subdivided into thermal-mechanical fatigue and thermal-stress fatigue, depending on whether constraints are external or internal (Figure 2.0).

As pointed out before, thermal fatigue testing can be divided into two categories, the first involving internal constraint, the second external constraint. The classic example of the former type is the use of tapered disc specimens which are alternately immersed in high and low temperature fluidized beds [8-11]. Such tests can provide a reasonable simulation of operational conditions encountered by such components as turbine blades and can readily assess the relative thermal fatigue

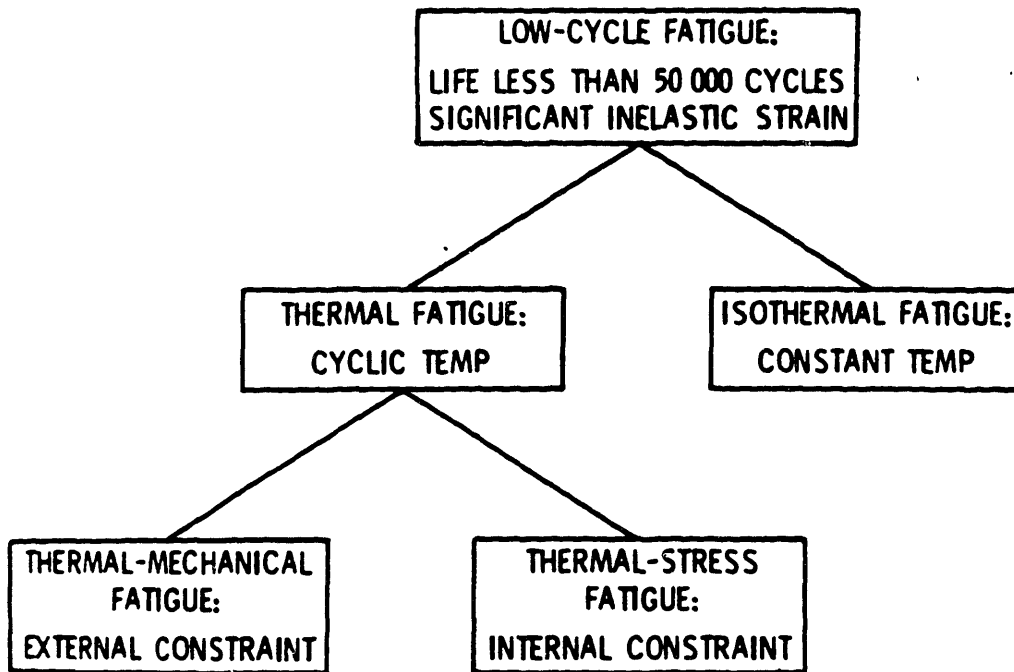


Figure 2.0 Proposed terminology for high temperature fatigue[1].

resistance of different materials. Unfortunately, stress and strain cannot be measured directly in this kind of test so that quantitative analyses are usually precluded, although use of finite element techniques has improved the situation [12-14].

External constraints are those provided by boundary forces applied to the surfaces of the body which is being heated and cooled. This type of constraint is more typical of specimen testing than it is of components in-service because designers of high-temperature equipment usually take considerable care to provide for overall thermal expansion and contraction through the use of clearances, sliding supports, bellows, etc. Thus, thermal fatigue with external constraint is primarily a laboratory testing practice in which external forces on a test specimen are used to simulate internal thermal stresses in an actual component [1].

External constraint was first used by Coffin who applied temperature cycles to hourglass type fatigue specimens held in a constraining jig [15]. The fact that most tests since then have involved isothermal strain cycling is perhaps unfortunate, since the operational fatigue situation usually involves cyclic strain resulting from and accompanying cyclic temperature. This situation has arisen partly because isothermal tests are relatively simple to perform, but also because it has often been felt that such tests carried out at the maximum service temperature should give worst-case results. However, several studies have compared fatigue resistance under thermal cycling conditions with that in isothermal tests and have shown that in many cases, the latter, rather than giving a worst-case situation,

can seriously overestimate the fatigue life under more realistic conditions [16-35].

In recent years, there has been some revision to the Coffin type approach involving cyclic temperature and external constraint, but the simple restraining jig has been replaced by servo-controlled fatigue machines in which temperature and strain cycles can be applied independently using suitable programming devices. This, in Spera's terminology, is the thermal-mechanical fatigue test [1]. In its most sophisticated form, thermal-mechanical testing involves direct strain control using high temperature extensometry with provision for automatic thermal strain compensation. Hopkins [36], Sobolev and Egorov [37], and Ellison [38] have described the state-of-the-art of this type of test.

2.2 Parameters Affecting TMF

The material properties other than ductility which are important in thermal fatigue are hot tensile strength, elastic modulus, thermal conductivity, and thermal expansion. Oxidation resistance also plays an important role in thermal fatigue. The interactions between material properties, imposed thermal cycle, and component geometry define the ability of a structure to resist thermal fatigue. However, the synergistic effects between these variables are quite complex and prediction of thermal fatigue behavior from basic properties is difficult. To clarify the situation, it is thought appropriate to review separately the mechanical response of alloys under diverse applied loading conditions and the effect of oxidation on the high temperature fatigue.

2.2.1 Cyclic Stress-Strain Responses

Largely because of the large body of information that has been accumulated, it is common to look upon the triangular wave shape test under fully reversed straining as a standard test from which one can predict other wave shape effects. This is referred to as the symmetrical hysteresis stress-strain loop with zero mean stress (Fig. 2.1a). Other wave shapes are obtained by changing various parameters (stress, temperature, strain rate, etc.); some of which are shown in Figure 2.1. The study of the material responses to changes in these parameters have allowed us to identify the main mechanical variables controlling fatigue lives and crack growth under TMF conditions.

Mean Stress

One family of shape involves strain hold period (in tension, compression or both). Figure 2.1b illustrates the tension hold. Note that the hysteresis loop will show a mean stress which is a function of the difference in the time spent in the tensile versus compressive part of the cycle. This mean stress effect can be important particularly when the plastic strain is small relative to the total strain range. In that case elastic effects dominate and a lowering of the relaxed stress with decreasing hold time is very effective in shifting the loop. On the other hand, if the plastic strain range is large relative to the total strain range, the magnitude of the relaxed stress is inconsequential, the maximum stress and relaxed stress become approximately equal and their magnitudes are controlled by plastic flow considerations.

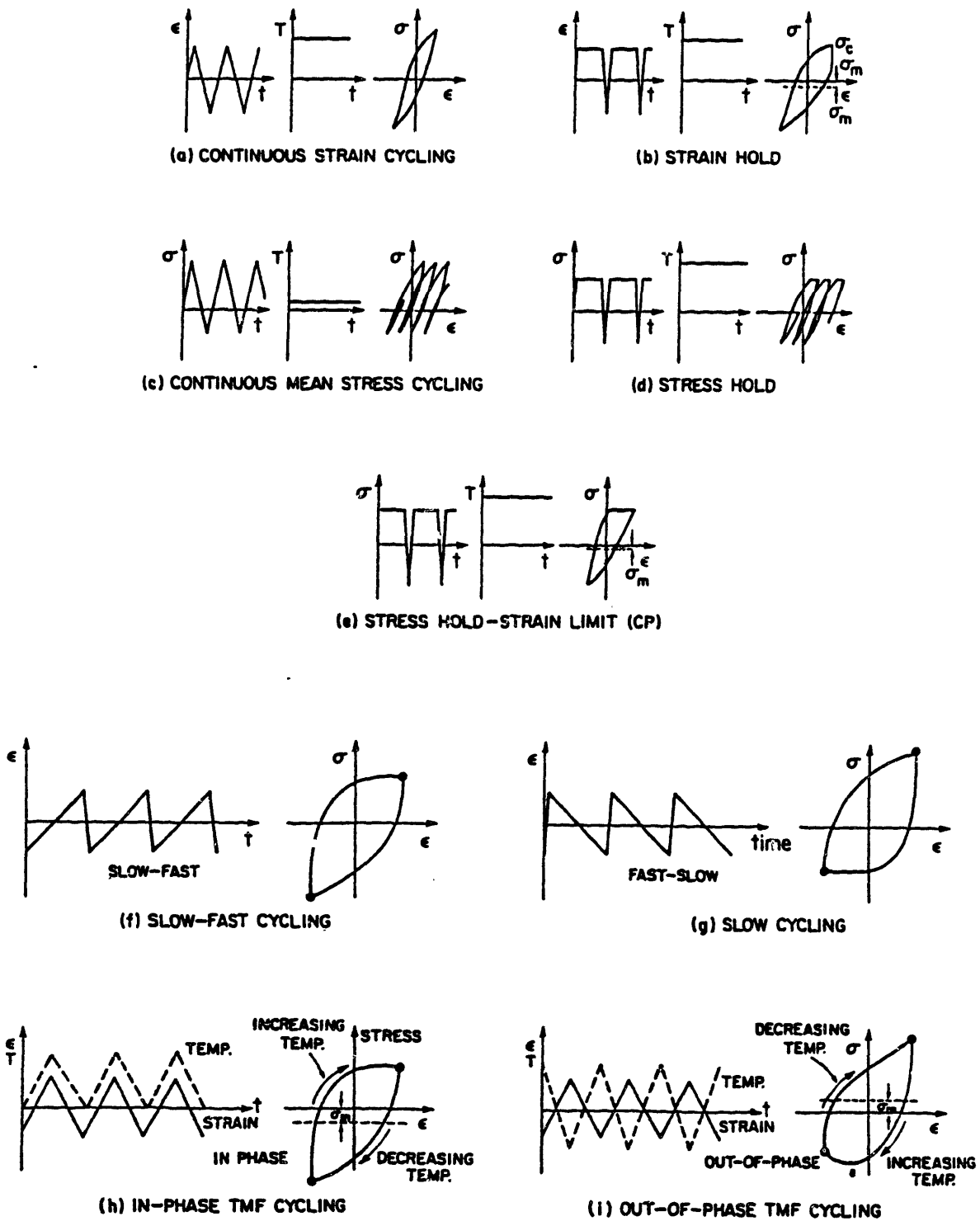


Figure 2.1 Typical stress-strain responses obtained at high temperature.

The consequences of a mean stress on fatigue life can be accounted for if one considers most of the life as spent in crack propagation, assuming that microcracks have nucleated early in the life. Here, the magnitude of the mean stress and its duration is important. Although the plastic strain range of the specimen is the same for tensile and compressive strain hold tests, the mean stress influences the local tensile plastic strain at the crack tip. A high compressive mean stress is likely to retard the amount of opening of the crack and lower the growth rate while a tensile mean stress causes a greater crack opening and enhances crack growth. Although documentation of the effect of mean stress on crack growth at high strain levels considered is lacking, there is ample evidence to support the observed effects at lower growth rates.

Ratchetting

Figure 2.1c shows a wave shape due to continuous stress cycling. Here a mean stress exists and ratchetting (incremental increase in strain) takes place, depending on the transition fatigue life. This form of ratchetting can be time independent and will occur at all temperatures, depending only on the magnitude of the mean stress and the plastic strain range. Also, time-dependent ratchetting can be expected at elevated temperature due to creep effects.

Another type of wave shape (Figure 2.1d) involves stress control. When the stress is fully reversed but hold time periods are introduced, ratchetting may lead to an increase of the strain during each cycle. The ratchetting here is the result of creep during the hold period and is

associated with the difference in the hold time period for tensile versus compressive stress.

Creep Strain

A wave shape that has received much attention is that shown in Figure 2.1e. Wave shapes in this category are identified as cp or pc, depending on whether the hold period is in tension or compression. It develops that, for the same inelastic strain and at high temperature (creep effects are sufficiently rapid to operate), the cp tests give shorter lives than the pc. Thus in Figure 2.1e, most of all the tension-going deformation is by a time-dependent mechanism, while all compression-going deformation is presumably by a time-independent process. If the microstructural features of these two distinct modes differ, as, for example; if all time-dependent deformation is by grain boundary sliding and cavities formation, and the time-independent deformation is by deformation within the grain, internal damage processes could be expected to be greater than for the equivalent deformation modes in both directions [23-24]. For example, in crack propagation, crack advance by GBS followed by plastic crack closure can be pictured as contributing to greater crack growth than crack advance by grain boundary sliding following by crack closure by the same mechanism.

Strain Rate Effects

Figures 2.1f and 2.1g show hysteresis loops of stress and plastic strains corresponding to unequal plastic strain ramp rates. One could see that unequal ramp rates generate unbalanced hysteresis loops. Where the ramp rate is slow, the corresponding stress developed just

prior to strain reversal is low; when the ramp rate is fast, the stress produced is high which is in agreement with normal stress-strain rate dependence. Thus, a slow-fast loop will be lower in tension and higher in compression, while a fast-slow is just the opposite. Correspondingly, the unequal loops will be reversed such that a slow-fast loop will have a compressive mean stress and a fast-slow loop a tensile mean stress.

Temperature

Wave shape effects are very important for thermal cycling where the effects can be accentuated by changing the temperature such that high temperature occurs during the tension-going deformation and low temperature during fast reversal. This type of temperature-strain cycling is known as in-phase cycling and is shown in Figure 2.1h. When compressive deformation occurs at high temperature and tensile deformation at low temperature, also known as out-of-phase cycling, the shape of the hysteresis loop differs from in-phase cycling. Figures 2.1g, 2.1h, and 2.1i show that rather unusual loops are produced under these conditions. In-phase cycling generates loops having a net compressive stress, while out-of-phase cycling leads to a mean tensile stress. As discussed earlier, one would conclude that out-of-phase cycling is more damaging than in-phase; this is what has been observed for nickel-base alloys [19, 27-29], tantalum alloys [20] and some low carbon steels [23-26]. However, there are numerous cases, especially with 304 and 316 SS, where the opposite effect have been observed which clearly indicate that the presence of a mean stress is not solely responsible for the shortening of fatigue life. Nevertheless, the existence of a mean stress in TMF (in-phase and out-of-phase) points

out the need for its quantitative determination under complex straining and thermal histories. This points out the importance of proper constitutive equations and models for handling these equations if problems of practical importance are to be solved.

2.2.2 Effects of Environment

During the last few years it has become a much debated question as to what extent the environment affects cyclic life at elevated temperatures. It is usually observed after testing in air that fatigue cracks are oxide-filled, and it is tempting to ascribe the well-known frequency-and time-dependence of high temperature fatigue to oxidation, since oxidation is a time-dependent process. On the other hand, creep processes also become important at high temperatures and creep is also a time-dependent process. It is a difficult problem to differentiate the effects of creep from the effects of environment because the susceptibility to environmental damage increases with temperature. This can be seen in Figure 2.2, where the fatigue lives of IN-706 are plotted versus temperature at constant frequency and strain range [39].

To clarify the situation, a number of literature surveys dealing with the effects of environment on high temperature fatigue have been written [39, 43-46]. Especially worth mentioning are the reviews by Cook and Shelton [43] and by Marshall [46], which thoroughly discuss environmental effects.

It is evident from these reviews that environment has a pronounced effect on fatigue at elevated temperatures. The most

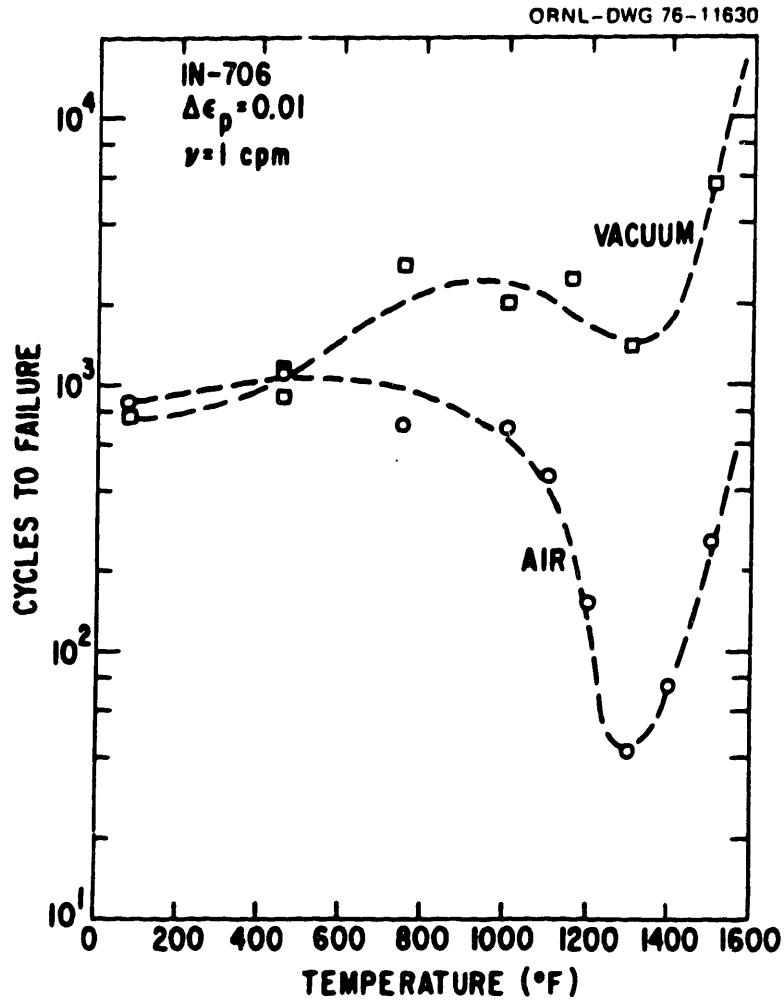


Figure 2.2 Comparative low-cycle fatigue resistance of wrought IN-706 in air and vacuum[39].

important results highlighted by these reviews may be summarized in Table 2.1 and 2.2, where the types of metal/environment interactions are listed in Table 2.1 and the principal effects on the fatigue and creep resistance listed in Table 2.2.

One can see in Table 2.2 that environmental effects have been studied mostly in terms of how an environment is changing the mechanical properties at or near the highly strained regions i.e., the surface or the crack tip of a material. Segregation of elements including O_2 and N_2 to and from grain boundaries is likely to be accentuated by plastic straining. Howes [48] concluded that the two dominant mechanisms in the formation of a thermal stress fatigue crack are local plastic strain and oxidation. After an incubation period, cracks almost invariably occur in areas of highest plastic strain [48]. Oxidation is often preferential at grain boundaries [5-6, 42-46, 48-54], forming wedges which grow in size until a crack is initiated and begins to propagate. Oxidation increases the amount of local plastic strain by reducing an alloy's strength through depletion of strengthening elements and phases. Also, plastic straining is likely to favor oxygen embrittlement at grain boundaries by a dislocation pumping mechanism [55].

Indications that the rate at which an environment affects the fatigue behavior depends on the strain amplitude have been reported by Wareing and Vaughan [3, 56], Skelton and Bucklow [57], and by Strangman et al [51, 58]. Wareing and Vaughan [3, 56] in discussing crack growth in 316 stainless steel at 625°C find a linear relation between predicted (according to Tomkins' model) and actual crack growth rate, i.e.,

Table 2.1

POSSIBLE TYPES OF METAL/ENVIRONMENTAL INTERACTIONS

Direction of mass transport	Types of metal/environment interactions
from atmosphere to metal	<ol style="list-style-type: none">1. formation of a thin adsorbed layer on the specimen2. formation of an adherent surface layer of second phase oxidation3. formation of a second phase at the surface4. formation of second phase particles at/ or grain boundary films
from metal to atmosphere	<ol style="list-style-type: none">1. evaporative loss or chemical dissolution of element from specimen to the environment

Table 2.2

SUMMARY OF ENVIRONMENT EFFECTS ON FATIGUE

Type of metal/ environment interactions	Enhancing fatigue resistance	Reducing fatigue resistance
	$N_f \uparrow$ or $\frac{da}{dN} \downarrow$	$N_f \downarrow$ or $\frac{da}{dN} \uparrow$
Adsorbed layer		-reduced surface energy of crack face ($\frac{da}{dN} \uparrow$) -reduce cohesive energy of grain boundary ($N_i \downarrow$)
Formation of an adherent surface layer (oxidation)	-disperse slip ($N_i \uparrow$) -crack blunting $\frac{da}{dN} \downarrow$ -crack closure $\frac{da}{dN} \downarrow$ -prevent crack sharpening in compression ($\frac{da}{dN}$)	-prevent slip reversal ($N_i \downarrow$) -prevent crack rewelding ($\frac{da}{dN} \uparrow$)
Formation of second phase particles or grain boundary films	-dispersing slip ($N_i \uparrow$)	-easy crack propagation path ($\frac{da}{dN} \uparrow$) -cavitation
Formation of second phase at the surface	-precipitation hardening ($N_i \uparrow$)	-loss of solid strength- ening element ($N_i \downarrow$) -cavitation
Evaporative loss or chemical dis- solution of element from specimen		-loss of solid strength- ening element ($N_i \downarrow$) -Kirkendall vacancies and voids ($\frac{da}{dN} \uparrow$)

$$\frac{da}{dN_{\text{air}}} = F_{\text{ox}} \frac{da}{dN_{\text{vacuum}}}$$

They concluded that if this is due to oxidation enhanced by plasticity, any crack growth additional oxidation contributed growth must be governed by the parameters governing plastic-controlled growth.

In another work, Skelton and Bucklow [57] show that, for the 1/2% Cr-MoV and 1% Cr-MoV steels, the oxide growth rate is accelerated by ongoing plastic straining. They also found that a fatigue crack surface displays a higher oxide growth rate than a polished and annealed surface.

Strangman et al [51, 58] have studied thermal-mechanical fatigue in nickel-base superalloys B-1900, IN-100, NX-188 and MAR-M200 with NiCoCrAlY coating. The testing was done out-of-phase and in-phase. They found an acceleration of the fatigue crack growth due to oxidation both in the substrate and in the coating for total strains above a certain limit. The previous results show that the environmental effects cannot be explained satisfactorily in terms of metal/temperature/frequency alone, and that a more global approach involving the applied strain ranges has to be considered.

3.0 Review of Experimental Data

3.1 Introduction

Two approaches have been successfully applied to practical fatigue problems: (1) The accumulation of cyclic strains (low-cycle fatigue or total endurance concept) and (2) fracture by crack growth (fracture mechanics concept). In general, these two approaches have been applied independently of each other; materials with no flaw at the initial stage of fatigue are handled by approach 1, and the materials with a flaw or flaws handled by approach 2. To combine the two approaches, the high strain fatigue (HSF) crack growth concept has been proposed. Most of the HSF crack growth data at room and elevated temperatures published between 1965 and 1982 have been reviewed by Shelton [2, 59]. However, this concept is generally overlooked and, as mentioned before, design approaches which use LEFM crack growth or total endurance data are more familiar. As a matter of fact, the thermal-mechanical fatigue problem has also been addressed separately by the two approaches.

3.2 Endurance Data

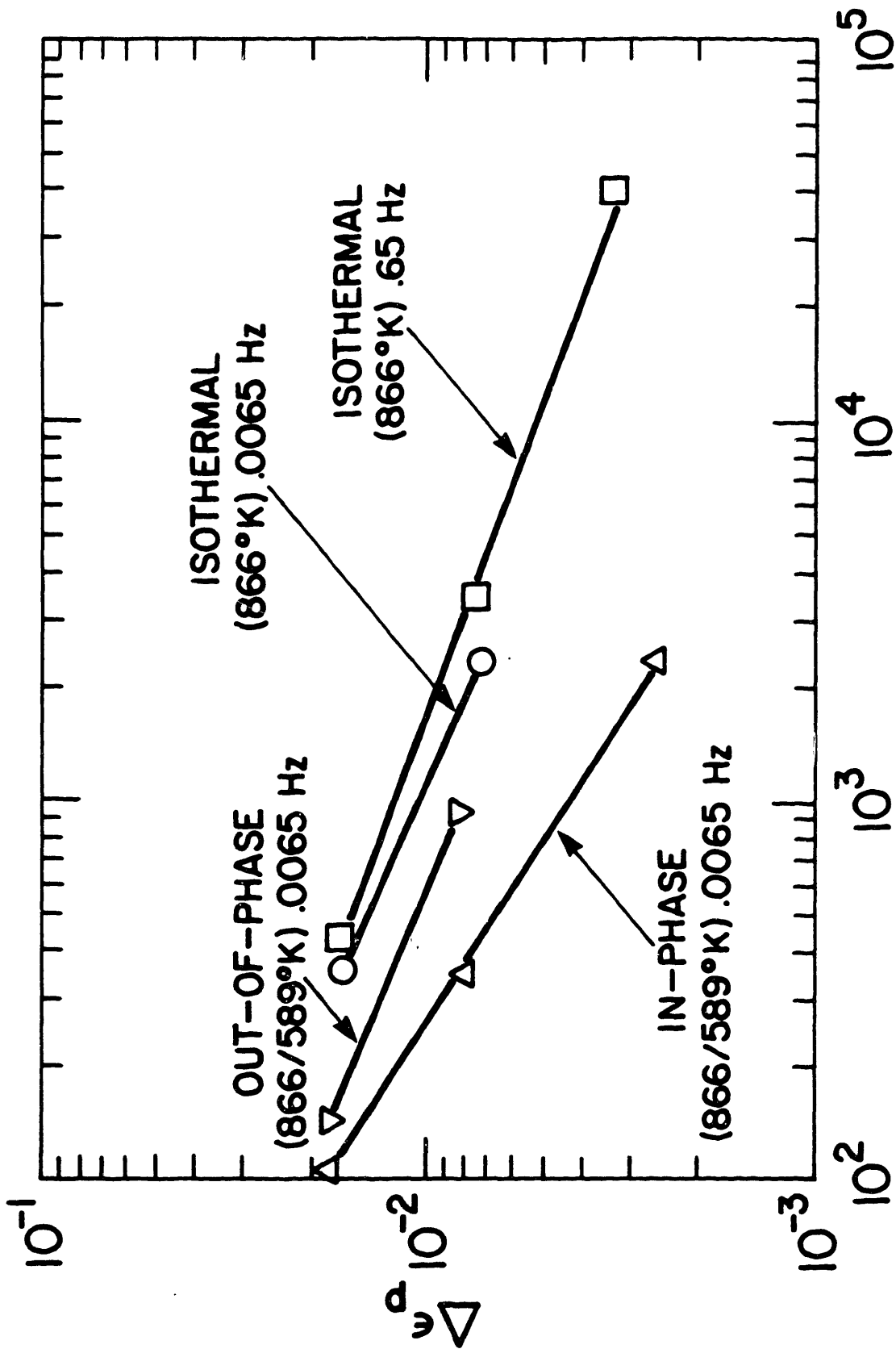
Steels

It has been pointed out by Udoguchi and Wada [17], Sheffler [20-21], Taira et al [7, 23-24], and by others [18, 25-26, 30-32, 60-62] in studies of thermal fatigue of high temperature alloys, that thermal fatigue lives are generally shorter than isothermal fatigue lives at the

mean [7], or the maximum temperature of the cycle [17-18]. Some of the results giving N_f as a function of the plastic strain range for an A-286 [21] steel are reported in Figure 3.1. These results [18, 23-26] show that in-phase cycling (i.e., maximum temperature at maximum tensile stress) is more damaging than out-of-phase (maximum temperature at compressive stress), which in turn caused fracture in fewer cycles than isothermal cycling (whether the latter was based on the mean or maximum temperature). Very similar results were found for 304 stainless steel [18, 25-26, 31]. However, when expressed in terms of total strain range ($\Delta \epsilon_{tot}$), Kuwabara and Nitta [25] found that the isothermal and out-of-phase changed rank and that this ranking was consistent with the fraction of intergranular cracks that was measured [26].

Superalloys

For the superalloy IN-738, HSF tests between 750 and 950°C in-phase or out-of-phase cycling all gave the same endurance at a given $\Delta \epsilon_{tot}$ level [48]. Other works on a coated [19] and uncoated nickel-base alloy [146] have shown that out-of-phase cycling is more damaging than in-phase and isothermal cycling, whereas the opposite behavior was observed by Bill et al. [130]. More recently, Nitta et al [66] have recently shown that the endurance of IN-738 depends on the applied strain $\Delta \epsilon_t$ being the lowest for the isothermal test (T_{max}) at low $\Delta \epsilon_t$, but the lowest for out-of-phase cycling at high $\Delta \epsilon_t$ cycled between 400 and 925°C. Their results have also shown that the thermal fatigue life of nine different superalloys was strongly dependent upon tensile and creep fracture ductilities as well as the strength of the alloys.



CYCLES TO FAILURE

Figure 3.1 Isothermal and TMF lives in A-286[21].

3.3 Fatigue Crack Growth Data

Hardly any data has been gathered on crack growth during thermal-mechanical fatigue under conditions of small plastic strains [27-29, 41, 51] and even fewer in the fully plastic strain ranges [22, 68].

Steels

During TMF cycling of 1/2 Cr-Mo-V steel in vacuum between 250 and 550°C, crack growth rates as a function of ΔK_{ϵ} were one-third those of continuous cycling at 550°C at the same plastic strain [63]. In air tests, Koizumi and Okazaki [68] found very little difference in growth rates as a function of ΔJ for 12 Cr-Mo-V-W steel thermal-mechanically cycled between 300-550°C and 350-600°C at several strain ranges. The same conclusions were derived for a 304SS cycled between 300 and 650°C. However, the validity of ΔJ for crack growth under TMF conditions need to be proven [41].

Superalloys

TMFCG tests conducted on conventionally cast Co and Ni base superalloys [27-29, 41, 51] have shown faster crack growth rate than their counterparts in isothermal conditions (at T_{max}). Typical results for a cobalt-based alloy are shown in Figure 3.2 [27] which shows that out-of-phase cycling is more deleterious than in-phase cycling. The TMF crack growth data were expressed as

$$\frac{da}{dN} = C_1 (\Delta K_{\epsilon})^m$$

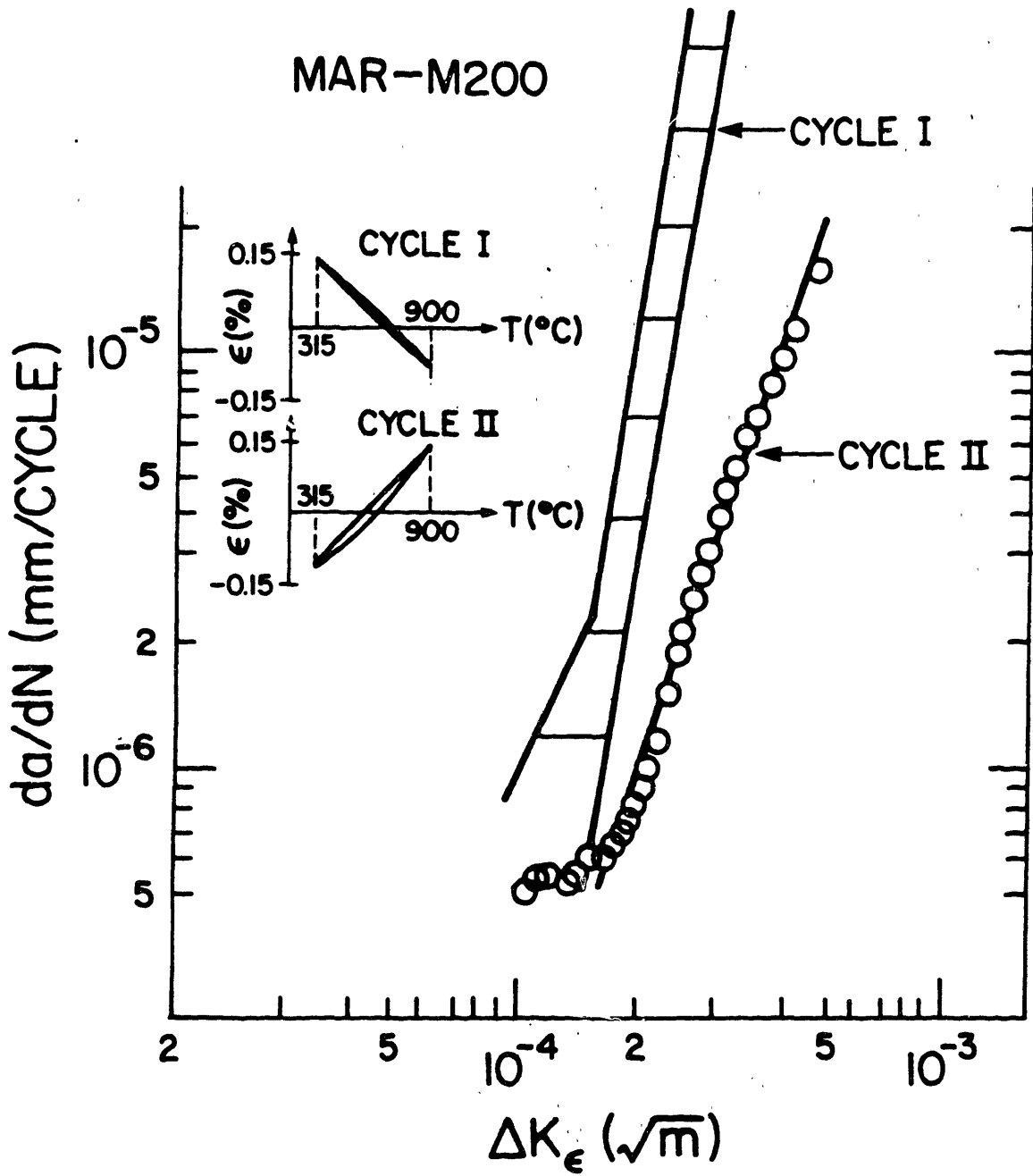


Figure 3.2 Comparison of TMFCG rates for out-of-phase and in-phase cycling in MAR-M200[27].

where ΔK_{ϵ} is the strain intensity factor. The index m was typically 3~4 for nickel-base alloy cycled from 980°C and ~6 for the cobalt-base alloy cycled from 425°C to 927°C [27].

Gemma et al [28] have also studied the TMF crack growth behavior of DS Mar-M200 and have found that crack growth rates were a minimum for a DS alloy tested parallel to the direction of grain growth. Crack growth rates prediction as a function of Θ (angle to direction of grain growth) was achieved by normalizing the ΔK_{ϵ} with the elastic modulus. Their work also indicated that under strain-controlled conditions, crack growth rates increase with increasing elastic modulus, in contrast to stress-controlled conditions for which the growth rates increase with increasing modulus [68].

In search of a correlation parameter to predict the crack propagation life of combustor liner material (Hastelloy-X), Meyers [41] has reduced the TMF data using ΔK , ΔK_{ϵ} , ΔJ , ΔCOD and Tomkin's model. All these approaches failed to correlate the TMF data within a factor of 5, which made them unattractive in predicting TMF crack growth. Furthermore, he showed that for such a parameter to exist, TMF must not involve mechanism of failure otherwise not present in isothermal testing.

Crack Growth During Thermal Stress Fatigue

Several temperature cycling experiments which consist of alternating plunging wedge-shaped disks into hot and cold fluidized beds have been carried out on various nickel-base alloys [8-12, 47, 70-71, 80, 82, 90]. For such geometries there is a fairly large (2.5-7 mm) range of uniform crack growth [12, 71]. Figure 3.3 shows that the

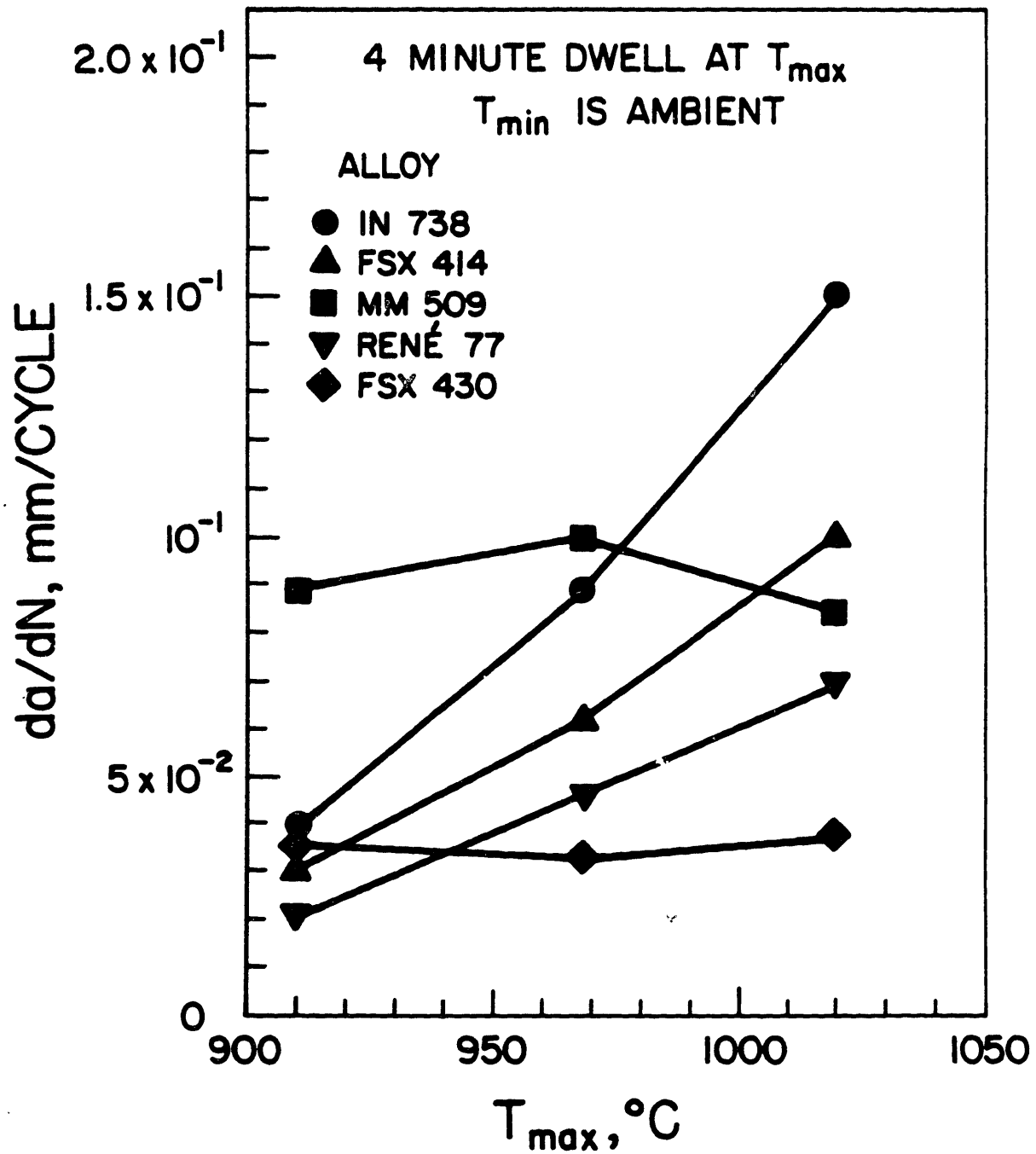


Figure 3.3 Variation of steady-state crack growth as a function of the maximum temperature in thermal shock experiment[70].

variation in uniform growth rate over the uniform range (in tapered disc experiments on several alloys) increases with increasing maximum temperature [70]. An increase in dwell time caused further crossovers in propagation rates. In these alloys, it has been shown that changes in growth rate reflects a transition in cracking mode [27, 29, 47] from trans to intergranular cracking.

3.4 Metallographic and Fractographic Data

Steels

Taira and Fujino [23-24] found from their microscopic observations on 304 SS cycled under TMF conditions that thermal cycling leaves residual grain boundary sliding which accumulates unidirectionally, in contrast to the case of isothermal fatigue. Also grain boundary cracking was often observed in the vicinity of triple points of boundaries which accommodate the strain concentration due to grain boundary sliding. Based on their finding, they concluded that the acceleration of damage is closely related to the accumulation of grain boundary cavitation in both in-phase and out-of-phase cycling. They proposed a mechanism of out-of-phase cavitation damage that involved accumulation of unreversed compressive grain boundary displacements in a low ductility material where the displacement could not be fully accommodated by intergranular deformation.

Superalloys -- cast

High temperature fatigue experiments of nickel-based superalloys have shown that crack initiation and growth behavior are very

dependent upon metallurgical variables such as carbide spacing, interdendritic spacing and grain size. It is impossible to provide a comprehensive survey here. A useful starting point is the work of Pineau et al. [42, 50, 52] and Woodford and Mowbray [71].

Thermal fatigue experiments on tapered disks of several alloys [70-71] have suggested that coarse grains at the center of the cast disks may be responsible for a deceleration in crack growth rate (see Figure 3.3), but for two alloys (IN 738 and FSX-430), larger grain size initiated cracks sooner. Initiation was intergranular, otherwise mixed, and in the transgranular mode an interdendritic path was preferred. On a $\gamma/\gamma'-\zeta$ eutectic alloy cycled under TMF conditions, Sheffler and Jackson [72] reported similar observations, i.e. preferential cracking along Ni_3Nb dendrites. In FSX-414 and FSX-430 cracking took place between $M_{23}C_6$ carbides, whereas in others (Mar-M509 and In-738) cracking of MC carbides occurred. Rene 77 failed in a transgranular manner.

Beck and Santhanan [73] demonstrated that thermal-stress fatigue resistance of a cast cobalt-base alloy can be significantly improved by changing the casting variables so as to increase the spacing of the dendritic arms in the microstructure. It is noteworthy that crack initiation periods were lengthened and propagation rates were reduced by this technique. Their work and similar work by Bizon and Spera [9] and Howes [10, 47] have shown that it is possible to deal directly with methods for improving the thermal-fatigue resistance of materials. It should be pointed out here that fluidized bed tests, as in the above, are undertaken because with these alloys, it is not yet possible to predict thermal fatigue lives from isothermal data [70].

Superalloys--directionally solidified

In a directionally solidified ingot, IN738, the greatest resistance to crack growth occurred at 45° to the columnar grain direction because there were no easy paths linking the carbides. This is in contrast with the thermal-mechanical fatigue tests performed on directionally solidified (DS) Mar-M200 which show [28] that the growth rates were a minimum for the alloy tested parallel to the direction of grain growth (i.e., crack propagation normal to the direction of grain growth). Also, the growth rate was shown to increase for the orientations in the sequence $\theta = 15^\circ, 30^\circ$ and 90° , and 45° until equivalence was reached with rates for conventionally cast B-1900. Similarly to Rene 77, DS Mar-M200 crack growth was transgranular for all orientations. At low strain intensity ranges (ΔK_E) the crack propagation path was smooth but as ΔK_E was increased the amount of interdendritic cracking increased, resulting in a much rougher fracture surface. The smooth-to-rough fracture surface transitions were rationalized in terms of the orientation dependence of crack opening displacement for a given ΔK_E . In addition, it was observed for Rene 77 that precipitate in the bulk specimen cycled in and out of solution and that a zone denuded of γ' precipitate formed by a diffusion process along the crack faces [71]. Other work on oxide-dispersion strengthened materials showed that cavitation developed at oxide particles so that cracking along grain alignment was less than the growth rate perpendicular to it [70].

It has been mentioned before that creep/TMF and simulated creep/TMF tests on DS Mar-M200 and conventionally cast B-1900 were phenomenologically indistinguishable [29]. However, the crack morphology of the simulated creep/TMF specimens differed from that

of the creep/TMF specimens. The former had a crack morphology that was typical of plane stress conditions, that is, short hairline cracks that surrounded the dominant crack. In addition the fracture surface showed changes in crack planes and growth along steep angular planes. The fracture surfaces of the latter were more typical of crack growth under plane strain conditions.

Superalloys--crack morphology

In TMF tests of nickel-based alloys, Nitta et al. [66] and Meyers [41] have found that the crack path for in-phase cycling was planar, rough and intergranular, which is similar to isothermal tests at the peak temperature. Out-of-phase cycling has shown transgranular fracture with fatigue striations and a small amount of intergranular growth. Isothermal tests at low temperature showed transgranular fracture. The degree of nonplanar growth, the extent of surface roughness and the mode of growth for the out-of-phase TMF tests fall between the features observed for the high and low temperature isothermal tests described above. This observation suggests that crack growth under TMF conditions is, in some sense, an average of that experienced in isothermal tests over the temperature range of the TMF tests [41]. This evidence offers hope that some type of superposition model may eventually predict TMF crack growth. Crack growth in in-service combustor liners tends to be nonplanar, of a moderate level of surface roughness, and chiefly transgranular, similar to the TMF tests [41]. However, as seen before, high temperature isothermal growth tends to be planar, very rough, and intergranular. This observation reinforces

the notion that isothermal tests run at the peak service temperature do not duplicate service conditions as well as TMF tests.

3.5 Discussion

The endurance and fatigue crack growth data presented and reviewed in the previous section have shown there is no general trend as to the severity of damage associated to in-phase and out-of-phase cycling. There is no hard and fast rule for relating the thermal-mechanical data to the isothermal testing data. There are many uncertainties in comparing total endurances only; for example, the number of cycles to initiation may differ, and cracking may be intergranular in isothermal tests but transgranular in the cyclic temperature tests. Obviously low endurance data will depend on initiation/propagation ratios, ductility including sensitivity to strain rate effects, T_{\max} and ΔT , σ_{\max} and σ_{mean} and microstructure.

We have seen that for all materials tested under TMF conditions, the mean stress associated with in-phase cycling is compressive whereas it is tensile for out-of-phase cycling. As also discussed earlier, the presence of a mean stress is not solely responsible for the shortening of fatigue life and the mean stress has to be taken into account with the strain ranges, that is the transition life (N_t) which is defined as the point of intersection of the elastic and plastic lines ($\epsilon_p = \epsilon_e$) on a strain cycle to failure plot. If the plastic strain range is large with respect to the elastic strain, the magnitude of the stress is likely to be controlled by plastic flow considerations and the magnitude of the mean stress (σ_m) is inconsequential. At small plastic strain (with

respect to ϵ_e), elastic effects dominate and a compressive mean stress is likely to retard the amount of opening of the crack or lower the effective stress for crack initiation and the converse is true for tensile mean stress. On the basis of the previous arguments, life predictions in terms of $\epsilon_{tot} - N_f$ should be more adequate than prediction based on ϵ_{in} vs N_f . This has been demonstrated for nickel-base alloys by Nitta et al. [66]. This fact implies that thermal fatigue life of superalloys depends not only upon the ductility but also upon the strength (elastic strain). Several reasons can be given of for the dependence of the thermal fatigue of superalloys on tensile strength [66]:

1. The transition life, which is the life from the inelastic strain dependence to the elastic strain dependence, is of the order of 10^1 for high strength superalloys. This means that life strongly depends upon strength even in the low-cycle life region ($N_f < 10^4$ cycles).

2. For high-temperature low-cycle fatigue of superalloys failure has often been shown to be governed by the product of tensile stress and inelastic strain range, i.e., the inelastic strain energy [74].

3. The failure life of superalloys depends more upon the maximum tensile stress and the depth of oxides, than on ϵ_p , because crack initiation is caused by grain boundary oxide cracking on the surface [49-50].

The dependence of thermal fatigue on strength may not be restricted to superalloys. Jaske [61] found that in order to correlate in-phase, out-of-phase, and isothermal fatigue test data for a low carbon steel, a knowledge of both cyclic stress and cyclic strain was necessary. On the basis of stabilized stress range versus cycles to failure, little

difference was observed in the behavior of specimens subjected to in-phase and out-of-phase temperature and strain cycling.

For most stainless steel, N_t is of the order of 8000 cycles in the temperature range covered by TMF tests. This explains why the mean stress has little effect on the fatigue life and why in-phase cycling is more damaging than out-of-phase cycling, as for the case of 304 and 316 SS. Grain boundary sliding is the predominant flow mechanism in 304 and 316 SS (in the temperature range 300-650°C) and it has been shown to be very important for in-phase cycling [23-24]. As the strain amplitude decreases, GBS will be less important and σ_m is likely to be of little influence until $\epsilon_e \approx \epsilon_p$. Nitta et al. [25-26, 66] and Taira et al. [23, 24] have indeed observed that the difference between the in-phase and out-of-phase life is decreasing with decreasing strain; being the same near the transition life.

The behavior of Hastelloy-X is also consistent with the above arguments. At high strain ($\epsilon_p > 0.005$) in-phase cycling leads to shorter life [30] and fast crack growth rates, whereas out-of-phase cycling gives rise to faster crack growth rate and shorter lives at low strain ($\epsilon_p < 0.0035$) [75]. It should be pointed out that the transition life is approximately equal to 800 cycles ($\epsilon_e \approx 0.0035$) at 800°C and that Hastelloy-X doesn't present a ductility minimum vs temperature as for most high strength nickel-base alloys.

We have seen that the influence of σ_m depends on the values of ϵ_p at the transition life (N_t) and that σ_m is of little influence if plastic flow dominates ($\epsilon_p/\epsilon_e > 1$). Therefore any mechanism which reduces the efficiency at which plastic flow occurs will lead to an increased importance of σ_m because it is more difficult to relax it. This is

consistent with the fact that it has been observed that when the temperature range embraces a ductility minimum in the material, out-of-phase thermal cycling gives lower endurances than isothermal and in-phase cycling [63]. This last observation also serves to explain why high strength nickel-base alloy displays faster crack growth rates and shorter life under out-of-phase TMF cycling; most of them having a ductility minimum in the temperature range covered by the tests.

The foregoing discussion has dealt with the requirement for predicting the total number of cycles to failure (N_f), and it is pertinent to question whether the predicted N_f should be taken, not as cycles to fracture but as cycles to some arbitrary load drop. In the case of thick specimens, clearly the N_f values would be different, since they would incorporate both initiation and propagation of a macroscopic crack. Thin components, however, are likely to limit crack propagation severely, so that the N_f value may be reasonably defined as cycles-to-initiation.

Considerable research effort has been directed at measuring rates of fatigue crack propagation in appropriate materials. The effect of increasing temperature upon the fatigue crack propagation rate is generally to cause an increase at a given ΔK , the extent depending on the materials. In order to obtain some insight into the factors governing the temperature dependence of fatigue crack propagation, the crack growth rates at fixed ΔK are often plotted as a function of reciprocal temperature and normalized with respect to the elastic modulus [4-5, 28, 76] (see Figure 3.4). The rate dependence at low temperatures has been shown to be much lower than at high temperatures. Conventional fracture mechanics indicates that crack growth rates are inversely proportional to elastic modulus and to fatigue flow stress. As shown by

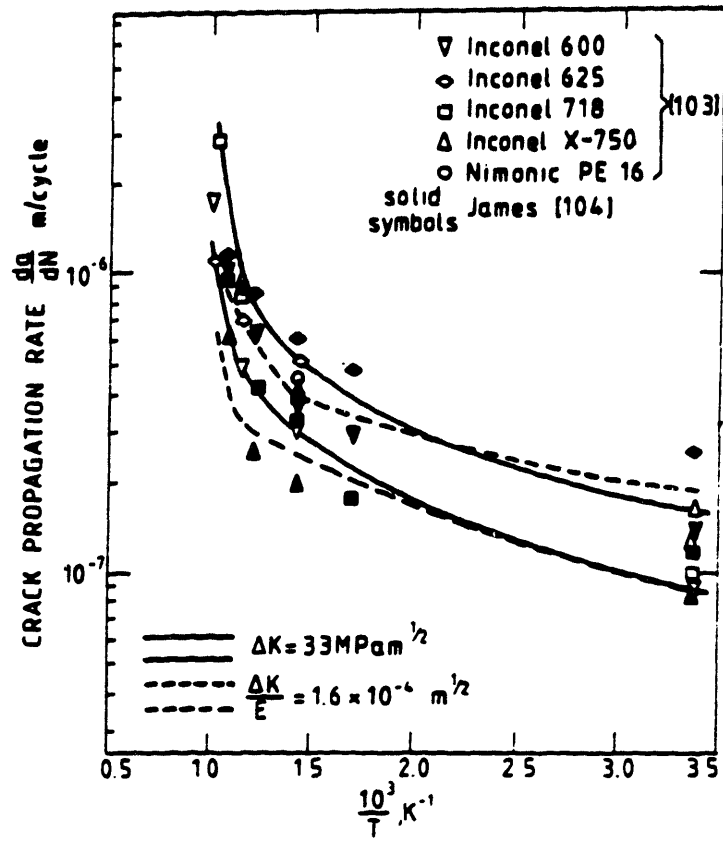


Figure 3.4 Temperature dependence of fatigue crack propagation in nickel-base alloys[5].

Lloyd [5] and Shahinian [76], the da/dN versus $1/T$ curves at fixed $\Delta K/E$, do not increase as rapidly as do similar curves at fixed ΔK . This indicates that the drop in flow stress with temperature is making a contribution at high temperatures.

Changes in the flow properties of the materials at the crack tip may be expected to induce changes in the propagation rate. A decrease in the work hardening exponent of the crack tip material caused by a decrease in strain rate or by an increase in temperature, would cause an increase in crack propagation rate. Similarly, stress relaxation reduces the effective value of σ_y . As seen before, the environment might increase the flow stress at the crack tip by oxide strengthening or reduce it by solid solution element depletion. Also, any of the possible effect of environment on the fatigue behavior might mask or enhance the effect of σ_m and ductility minimum.

Analysis of the data by Nitta et al. [26, 66], Jaske [61] and others, shows that thermal-mechanical life depends upon the tensile and fatigue ductilities as well as on the strength of the alloys. Hence, thermal fatigue life may be expected to be correctly predicted by a method which would take into account both the cyclic strength and ductility.

4.0 Experimental Procedure

4.1 Thermal-Mechanical Fatigue Testing Requirement

The testing capability and testing conditions for TMF testing of specimens are those that allow the duplication of in-service conditions. The requirements for testing facilities and test specimens for crack growth TMF testing are:

1. Strain control to simulate the thermal loading of the component since most high temperature components are under strain-controlled conditions. The mechanical strain (total strain minus thermal strain) should be controlled.
2. Strain hold time to simulate steady state conditions undergone during normal operation of nuclear reactor and gas turbine engines. During this period materials are undergoing creep and stress relaxation behavior.
3. Crack length measurement capability to obtain crack growth data in TMF conditions.
4. Controlled transient heating and cooling to simulate a component strain/temperature phase relationship (Figure 4.1).
5. Compressive load-carrying capability of the specimen to sustain compressive stresses which develop in the heating period of the cycle.

TMF crack propagation should mostly include testing of the base metal, since this type of cracking is readily studied by a fracture mechanics approach. The amount of component life spent in starting a

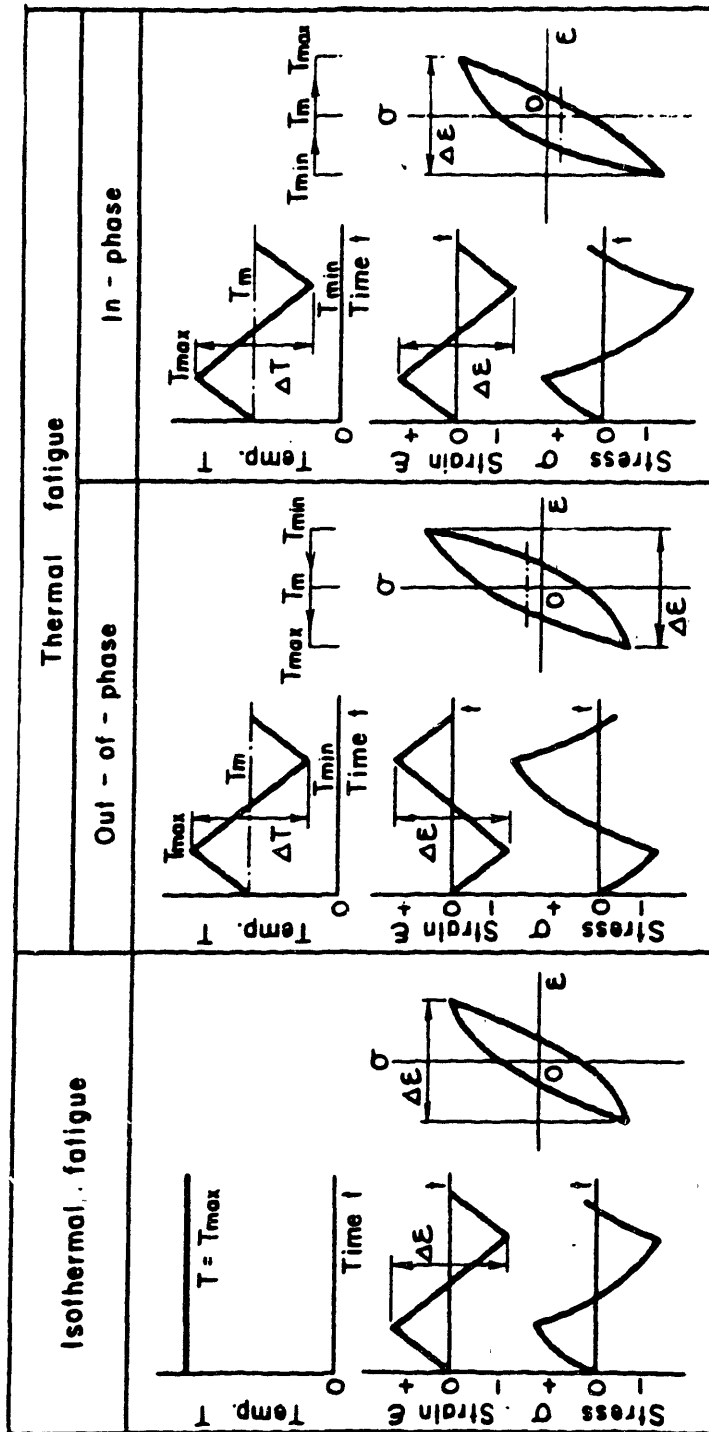


Figure 4.1 Schematic diagram showing waveforms of temperature, strain and stress in thermal and isothermal fatigue tests.

crack in the coating has to be addressed by crack initiation techniques. TMF tests should include several testing conditions in order to simulate the various strain-temperature relations at various locations in an actual component, as for example, a turbine blade.

Testing should also include both isothermal tests at the minimum and maximum temperatures of the TMF tests. The following variables should also possibly be included in the testing procedures:

1. total strain range, 0.10 to 1.0%
2. mean strain, -0.5 to 0.5%
3. crystal orientation for directionally solidified and/or single crystal materials
4. strain rate, set by the maximum transient heating and cooling rates that can be experimentally obtained.

In an extensive review, Hales [77] has described the important criteria which used to be considered when designing an experimental program to investigate fatigue at elevated temperature. He also pointed out some exhaustive reviews [78-79] which covered the various techniques available and critically examined some of them in the light of the demands placed on any testing program by modern design requirements and recent developments in understanding the physical processes in the phenomenon of high temperature fatigue. However, the present authors believe that there is still a need for a critical review of the various methods of testing to take into account the peculiarities of thermal-mechanical fatigue with a special emphasis on the recording of cyclic stress-strain behavior of various specimen geometries. The reader is referred to the Appendix I for a detailed discussion of the thermal-mechanical fatigue methods of testing.

4.2 Materials

The materials selected for this study of TMF are Hastelloy-X, Inconel X-750 and B-1900+Hf. These materials were chosen because they covered a broad range of strength and ductility. Table 4.1 gives the chemical composition and heat treatment conditions of the materials tested.

Hastelloy-X is a nickel-base solid solution strengthened superalloy. The material has a FCC gamma matrix and is strengthened by solid solution strengthening and grain boundary carbides. The solution strengthening elements are Cr and Mo. Hastelloy-X has a very high Mo content, which causes the carbides to be mainly M_6C carbides. The material also contains $M_{23}C_6$ carbides which form at temperatures up to 982°C and during cooling. The $M_{23}C_6$ carbides usually form in the grain boundaries. The material used in this study was in the form of 1 inch (25.4 mm) rod. The structure of the material was documented in the fully heat treated condition. Figure 4.2 shows the microstructure of the rod in the transverse direction. There was no major difference between the transverse and longitudinal directions. The microstructure is made up of two different grain sizes. There are large grains, $130\ \mu\text{m}$ in diameter, and small grains, $50\ \mu\text{m}$ in diameter. The average grain size is about $80\ \mu\text{m}$. The small grains are not recrystallized. This type of grain structure is common in solid solution strengthened nickel-base alloys because it is difficult to obtain a fully recrystallized grain structure and prevent the formation of embrittling phases at the same

Table 4.1

(a) Chemical Composition

Material	C	Si	Mn	P	S	Al	B	Nb	Co	Cr	Fe	Hf	Mo	W	Ta	Ti	Zr	Bi+Pb
Hastelloy-X	0.10	1.0	1.0	0.04	0.03	-	-	-	1.5	22	18.5	-	9.0	0.6	-	-	-	-
Inconel X-750	0.04	0.2	0.5	-	0.7	-	1	1.0	12.5	7	-	-	-	-	-	-	-	-
B-1900+Hf	0.09	-	-	-	6.07	0.016	0.08	9.91	7.72	0.7	1.19	5.97	0.04	4.21	0.99	0.04	0.2	0.2

(b) Heat Treatment

Material	Heat Treatment
Hastelloy-X	1177°C x 2 hrs., AC
Inconel X-750	1150°C x 4 hrs. AC, 850°C x 24 hrs. AC, 700°C x 20 hrs. AC
B-1900+Hf	1080°C x 4 hrs. AC, 900°C x 10 hrs. AC

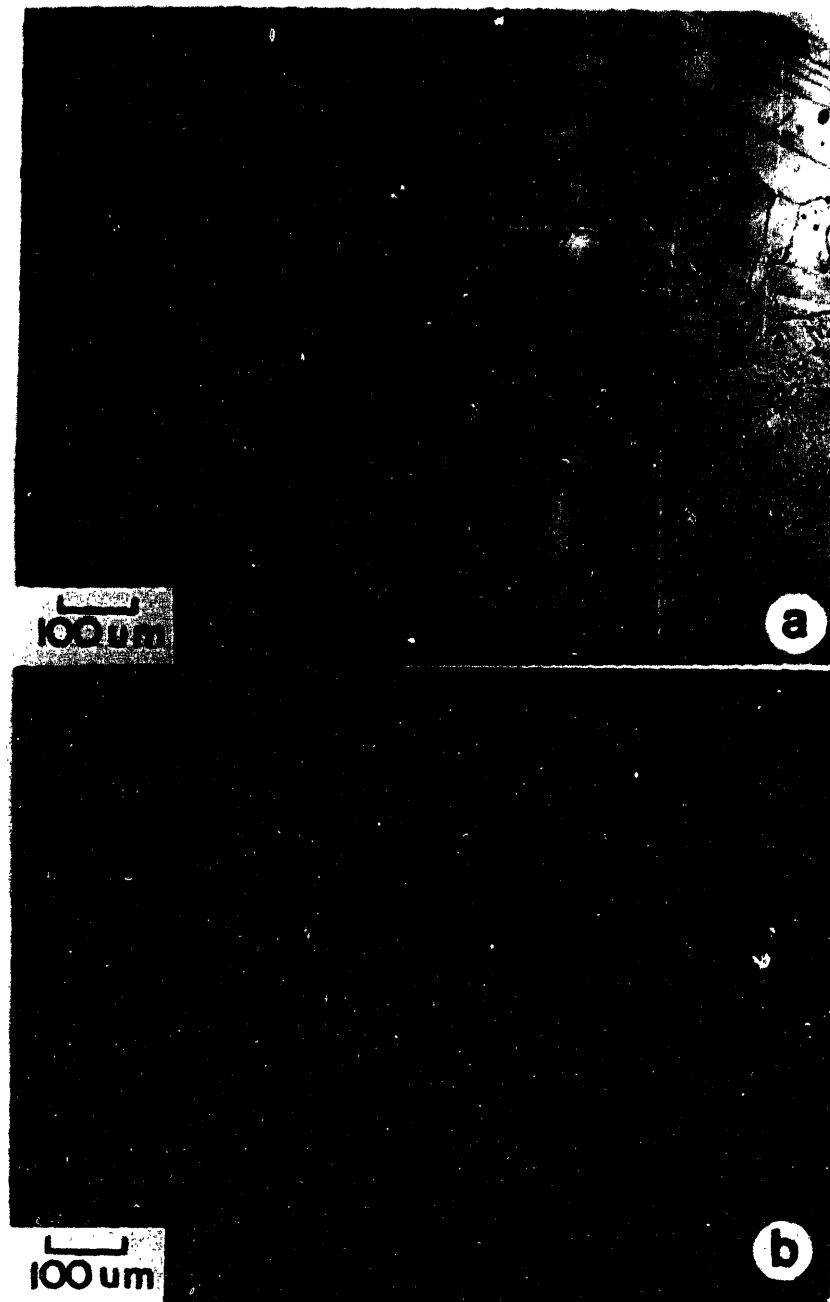


Figure 4.2 Microstructure of Hastelloy-X. Grain size in (a) the transverse direction, (b) longitudinal section.

time. In Figure 4.2, the large 6-10 μm particles are M_6C prime carbides.

Inconel X-750 is a corrosion and oxidation resistant material with good tensile and creep properties at elevated temperatures. Typical applications include land-based gas turbine parts, nuclear reactor springs, bolts, bellows and forming tools. The temperature range of interest is from 300 to 650°C. The material was supplied by International Nickel Company [122] in the form of 12.7mm thick plate in the annealed condition. It was then given a two-stage heat treatment (see Table 4.1). The grain size, as seen on micrograph 4.3, is about 130 μm and is uniform in all directions. The two-stage heat treatment produces a bimodal distribution of γ' phase: a coarse γ' phase distributed uniformly in the grains and about 0.6 μm in size, and a fine distribution of γ' about 300Å in size. The total volume fraction of γ' phase is estimated at 18%. MC carbides with little or no orientation with the matrix can be seen in micrograph 4.3. At the grain boundaries, there is a continuous network of M_{23}C_6 carbides.

The B-1900+Hf material for this program was taken from the same heat of a special quality melt of B-1900+Hf obtained from Certified Alloys Products Inc. [123] Long Beach, California. The structure of the material was documented in both the as-cast and fully heat-treated conditions. The following observations were made:

1. The grain size is about 1 to 2 mm (Figure 4.4a).
2. The fully heat treated material showed the γ' size to be about 0.9 μm (Figure 4.4c).
3. The structure has an interdendritic spacing of about 100 μm

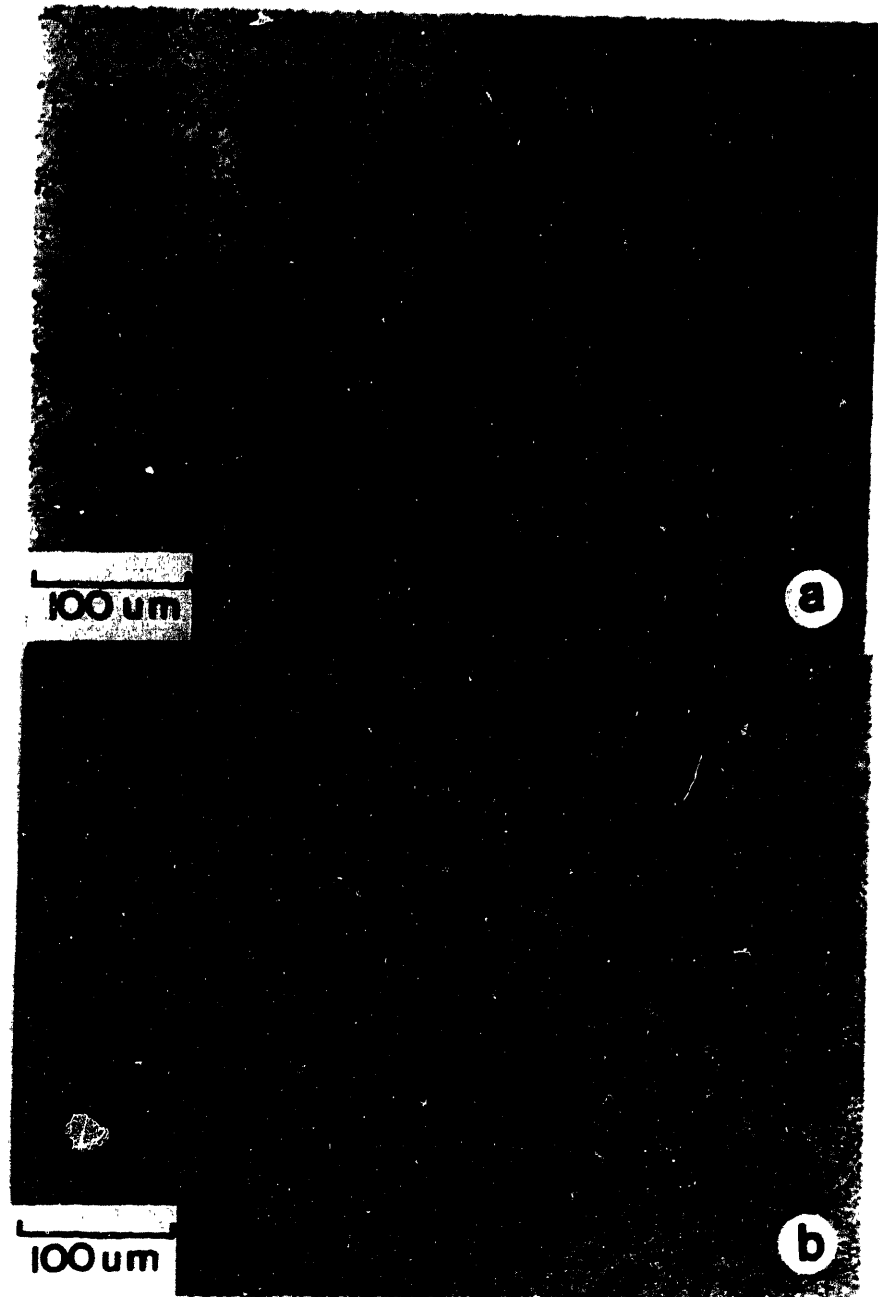


Figure 4.3 Microstructure of Inconel X-750(fully heat treated)
Grain size and carbides in (a) transverse direction,
(b) longitudinal section.

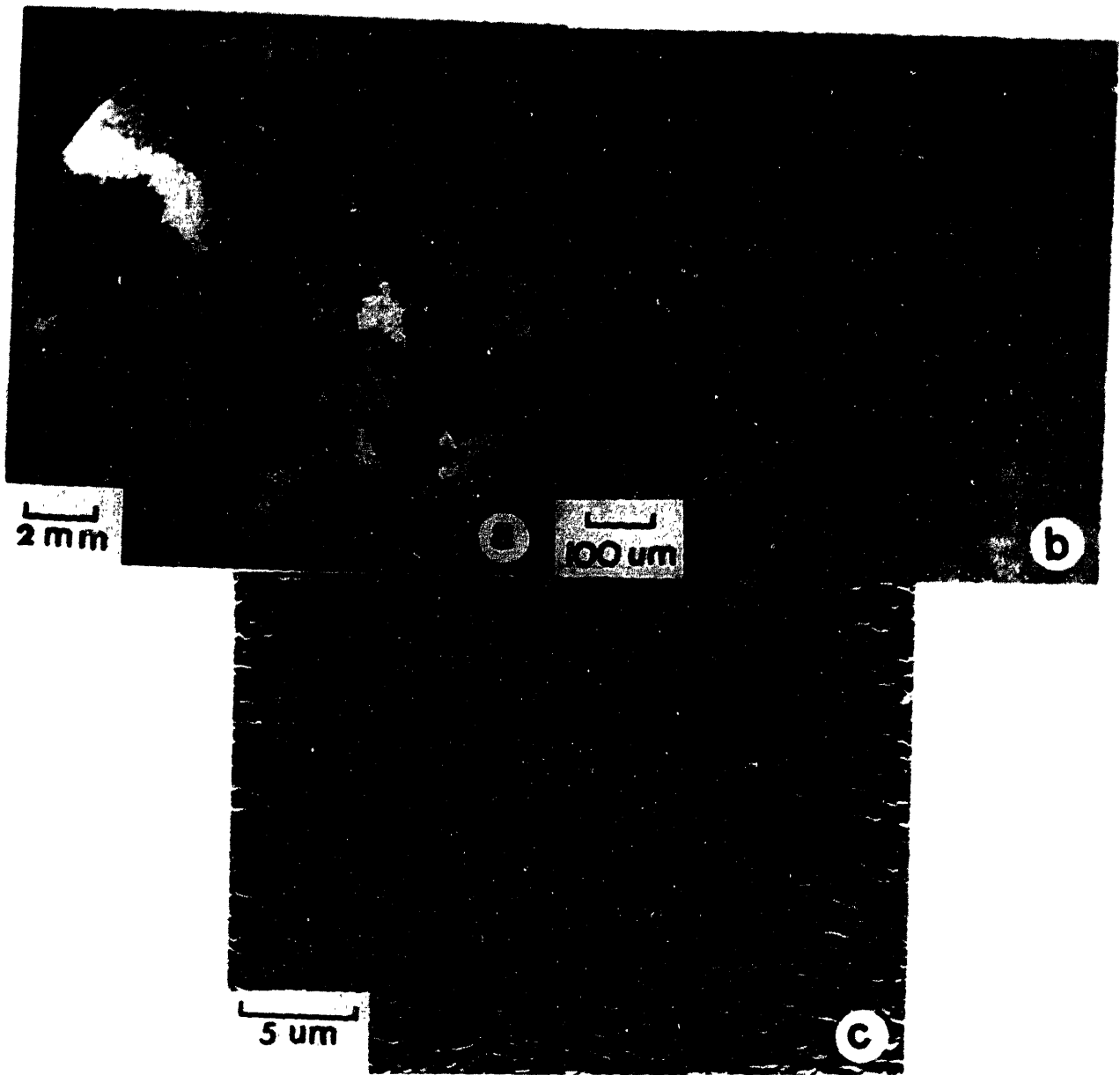


Figure 4.4 General microstructure of B-1900+Hf fully heat treated. (a) Grain size, (b) interdendritic spacing, fine and coarse γ , γ' size (0.9 μm).

with islands of γ' -eutectic surrounded by zones of fine γ' (Figure 4.4b).

4. MC carbides near the coarse γ' islands are present.

4.3 Specimen Geometry

Specimen geometries used for tensile and creep tests are shown in Figure 4.5 [123, 125]. The isothermal strain controlled fatigue specimen geometry used to provide a baseline for life prediction (initiation) is shown in Figure 4.6 [123, 125].

All the specimens used for TMF low cycle fatigue and TMFCG had a rectangular cross section of $11.7 \times 4.4 \text{ mm}^2$ (Figure 4.7). A starter notch approximately 1 mm deep cut by electro-discharge machining was used for the TMF crack growth tests. These specimens were then precracked in fatigue at 10 Hz at room temperature under a ΔK of about 20-25 MPa $\sqrt{\text{m}}$. The test section of each specimen used for cyclic properties measurements was polished with successively finer grades of silicon-carbides paper to produce a bright finish, with finishing marks parallel to the longitudinal axis of the specimen. Specimens were degreased with trichloroethylene, followed by reagent grade acetone before being heated to temperature.

4.4 Apparatus and Testing Conditions

The apparatus used in this study was a computer-controlled thermal fatigue testing system, which consisted of a closed-loop servo-controlled electro-hydraulic tension-compression fatigue machine, a

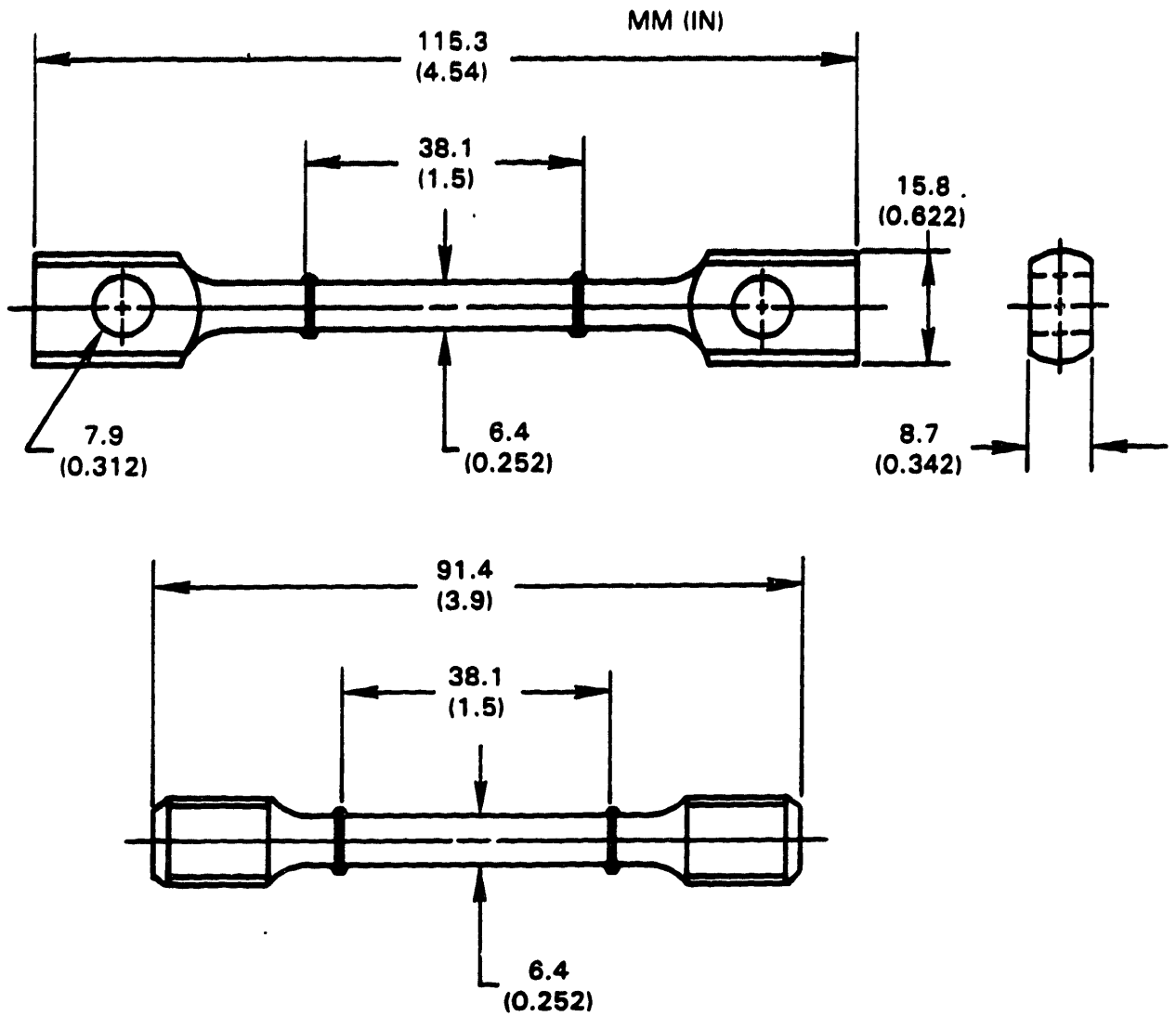


Figure 4.5 Test specimens for monotonic tensile and creep testing.

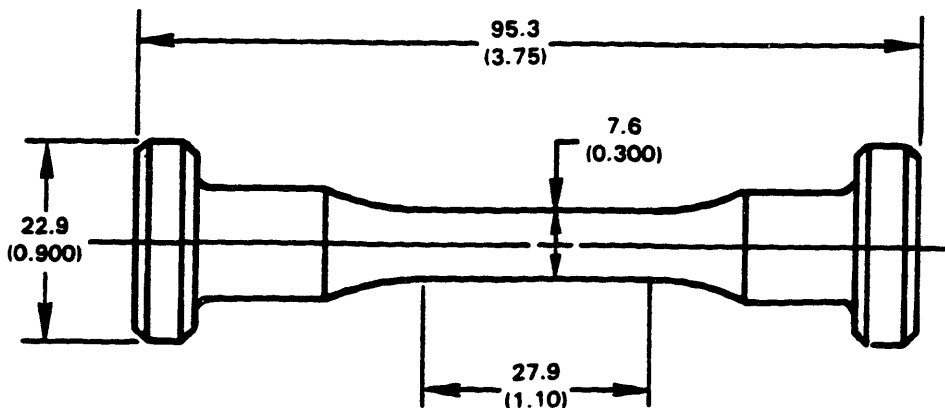
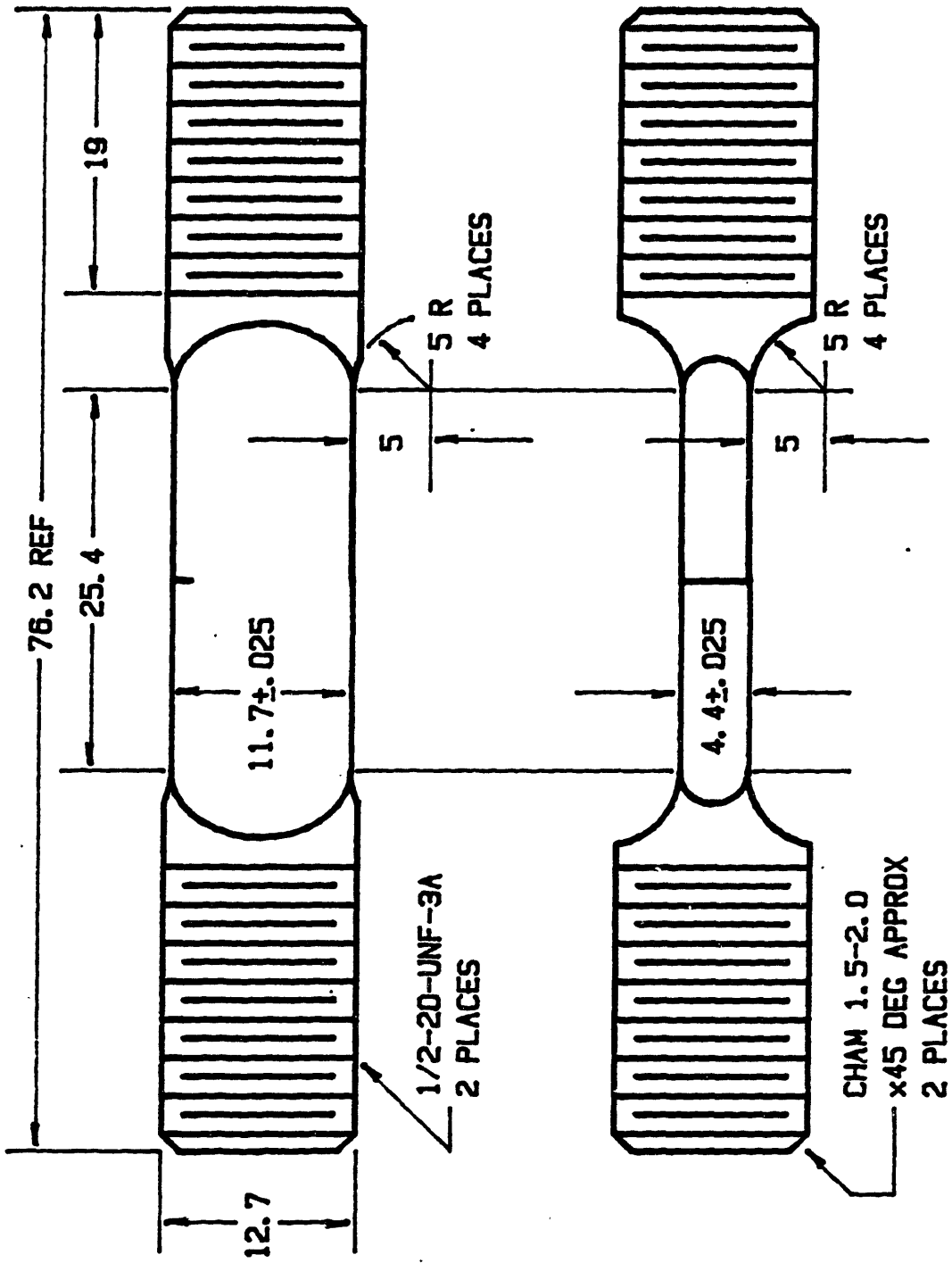


Figure 4.6 Test specimen geometry for low cycle fatigue testing.



Dimensions in mm.

Figure 4.7 Test specimen geometry for TMF testing.

high frequency oscillator for induction heating, an air compressor for cooling and a mini-computer. Appendix II describes in detail the system and its components.

The system is capable of testing specimens of different sizes and configuration (SEN, CT, hollow tube, etc.) up to loads of 25,000 lbs. The specimen alignment is assured by the use of a Wood's metal pot. Because a D.C. potential drop technique was used to monitor crack growth, the lower grip is electrically insulated from the system by means of a ceramic coating. The ends of the grips are water cooled by copper coils.

Temperature was measured with 0.2 mm diameter chromel-alumel thermocouples which were spot welded along the gauge length. By computer controlling, the temperature in the gauge length was maintained within $\pm 5^{\circ}\text{C}$ of the desired temperature for both axial and transverse directions over the entire period of the test. Temperature and strain (or stress) were computer controlled so that they were in-phase or out-of-phase for the same triangular wave shape. Therefore, specimens were in tension at low temperature and in compression at high temperature under the out-of-phase cycling, and vice versa under the in-phase fatigue. The temperature range in the TMF tests was 300 to 650°C for Inconel X-750, and 400 to 925°C for Hastelloy-X and B-1900+Hf. The tests were carried out at a frequency of 0.0056 Hz (1/3 cpm) and were run at a R-ratio ($\sigma_{\min}/\sigma_{\max}$ or $\epsilon_{\min}/\epsilon_{\max}$) of -1 or 0.05. Isothermal fatigue tests were also conducted under the same frequency at T_{\max} for comparison with the results of TMF tests. All the tests were carried out in air. Table 4.2 summarizes the experimental conditions. When possible, at least two tests at each condition were performed to

insure repeatability of the results. The software developed to run the isothermal and TMF tests, as well as the programs used to analyze the data, are described in Appendix III.

To measure the cyclic stress-strain behavior of B-1900+Hf, the strain increment technique was used. In this technique, the strain range is increased by about 10% after reaching saturation, defined as no change in stress range in 50 consecutive cycles.

There have been few attempts to measure crack length in TMF cycling using the potential drop technique [22, 49]. The method has proven to be satisfactory in isothermal conditions and it can be used for TMF testing, provided that the electrical noise is adequately filtered and the calibration curve properly corrected to take into account changes of potential with temperature. The procedures to: (1) correct the potential signals; (2) get the a/w vs N curve; and (3) analyze the potential signal to measure the closure stress, are described in detail in Appendix II.

This system, by contrast to optical measurements and compliance methods, has the capability of monitoring the crack extension during a single cycle (see Appendix II). Therefore, detailed analysis of the crack growth process can be performed and this is particularly important in trying to determine the mechanisms involved in TMFCG.

Table 4.2
Materials and Their Testing Conditions

(a) Hastelloy-X (TMFCG)

Frequency (Hz)	Temperature (°C)	Strain Range (ϵ_{tot} %)	R-ratio ($\epsilon_{min}/\epsilon_{max}$)
0.0056	400	0.25	-1
0.0056	400	0.50	-1
0.0056	925	0.25	-1
0.0056	925	0.50	-1
0.0056	400-925(In-phase)	0.25	-1
0.0056	400-925(In-phase)	0.50	-1
0.0056	925-400(Out-of-phase)	0.25	-1
0.0056	925-400(Out-of-phase)	0.50	-1

(b) Inconel X-750 (TMFCG)

Frequency (Hz)	Temperature (°C)	Stress Range (MPa)	R-ratio ($\sigma_{min}/\sigma_{max}$)
1.0	25	385	0.05
0.0056	650	385	0.05
0.0056	650	600	-1
0.0056	300-650(In-phase)	285	0.05
0.0056	300-650(In-phase)	600	-1
0.0056	650-300(Out-of-phase)	600	-1

(c) B-1900+Hf (Cyclic Properties)

Frequency (Hz)	Temperature (°C)	Strain Range (%)	N (Cycles)	R-ratio ($\epsilon_{\min}/\epsilon_{\max}$)
0.0056	400-925(In-phase)	0.2000	347	-1
0.0056	400-925 "	0.2515	337	-1
0.0056	400-925 "	0.3030	556	-1
0.0056	400-925 "	0.3580	388	-1
0.0056	400-925 "	0.3850	490	-1
0.0056	400-925 "	0.4075	383	-1
0.0056	400-925 "	0.4332	340	-1
0.0056	400-925 "	0.4525	288	-1
0.0056	400-925 "	0.4825	260	-1
0.0056	400-925 "	0.5650	54	-1
0.0056	925-400(Out-of-phase)	0.1765	475	-1
0.0056	925-400 "	0.1923	426	-1
0.0056	925-400 "	0.2153	312	-1
0.0056	925-400 "	0.2498	360	-1
0.0056	925-400 "	0.276	260	-1
0.0056	925-400 "	0.298	274	-1
0.0056	925-400 "	0.3279	274	-1
0.0056	925-400 "	0.3654	316	-1
0.0056	925-400 "	0.404	374	-1
0.0056	925-400 "	0.4370	326	-1
0.0056	925-400 "	0.4675	342	-1
0.0056	925-400 "	0.537	284	-1
0.0056	925-400 "	0.600	320	-1

(d) B-1900+Hf (TMFCG)

Frequency (Hz)	Temperature (°C)	Strain Range (%)	R-ratio ($\epsilon_{\min}/\epsilon_{\max}$)
0.10	925	0.25	-1
0.0056	925	0.25	-1
0.0056	925	0.50	-1
0.0056	400	0.50	-1
0.0056	400-925(In-phase)	0.25	-1
0.0056	400-925(In-phase)	0.50	-1
0.0056	925-400(Out-of-phase)	0.25	-1
0.0056	925-400(Out-of-phase)	0.50	-1

5.0 Results

5.1 Tensile and Creep Properties

Monotonic and creep tests were conducted to document typical engineering properties and to assess the deformation and failure mechanisms. Tensile and creep tests for B-1900+Hf and Hastelloy-X were run at Pratt & Whitney Aircraft, Hartford, Connecticut. A summary of all tensile tests and observed properties is presented in Table 5.1. Figures 5.1 to 5.4 show the monotonic tensile responses ($\dot{\epsilon} = 0.005 \text{ min}^{-1}$) and the 0.2% yield stress of B-1900+Hf and Hastelloy-X, respectively [41, 123]. Comparison of the 0.2% yield strength data (Figure 5.2 and 5.4) have shown that the results fall within the anticipated scatter. Tensile data of Inconel X-750 (Table 5.1) were shown to compare well with the published data on Inconel X-750 with similar heat treatment [124].

A summary of the test conditions and observed properties for monotonic creep tests conducted on B-1900+Hf is presented in Table 5.2. Figure 5.5 shows the observed rupture lives and the anticipated scatter for this material. Specimens tested at 871°C and 982°C have similar rupture lives for the same normalized stress, while specimens tested at 760°C show a significantly longer life for the same, or higher, normalized stress level. Examination of fracture has shown that at higher temperature (871 and 982°C) the specimens failed in an intergranular cracking mode, while the specimens tested at 760°C failed predominantly by transgranular cracking.

The short-time Hastelloy-X creep response at 871°C and 982°C are shown in Figures 5.6 and 5.7. Table 5.3 summarizes the results for various test temperatures.

Table 5.1

**Materials Tested and Their Tensile Properties
at Room and Elevated Temperature**

(a) Hastelloy-X

T (°C)	$\dot{\epsilon}$ (min ⁻¹)	Ex10 ³ (MPa)	0.2% Yield (MPa)	UTS (MPa)	Elong. (%)
21	0.008	207	367.5	787	40
505	0.008	178	294	649	43
649	0.008	161	274	572	36
760	0.008	152	259	435	38
816	0.008	145	231	----	----
871	0.008	137	175	255	50
927	0.008	127	140	----	----
982	0.008	116	91	144	48

(b) Inconel X-750

T (%)	$\dot{\epsilon}$ (min ⁻¹)	Ex10 ³ (MPa)	0.2% Yield (MPa)	UTS (MPa)	Elong. (%)
24	0.005	295	610	1000	30
300	0.005	303	616	1000	32
650	0.005	260	550	820	7

(c) B-1900+Hf

T (°C)	$\dot{\epsilon}$ (min ⁻¹)	Ex10 ³ (MPa)	0.2% Yield (MPa)	UTS (MPa)	Elong. (%)	RA (%)
RT	0.005	187.5	714	----	4.9	5.9
260	0.005	169.6	702	888	8.3	10.7
538	0.005	149.6	727	----	----	----
649	0.005	143.4	701	----	7.7	7.2
760	0.005	146.8	709	950	7.9	8.4
871	0.005	138.9	633	785	5.7	6.1
982	0.005	123.4	345	480	7.1	6.9

Table 5.2

Summary of the Creep Test Results for
B-1900+Hf

Temp. (°C)	Stress (MPa)	%Min Yield	Secondary Life (Hrs.)	CreepElong. (Min ⁻¹)	Elong. (%)
982	234	75	20.6	2.5x10 ⁻⁵	6.0
982	283	90	4.1	0.7x10 ⁻⁴	3.0
982	283	90	3.1	2.0x10 ⁻⁴	5.0
871	427	75	18.2	2.5x10 ⁻⁵	3.2
871	427	75	20.3	1.5x10 ⁻³	2.3
871	517	90	2.8	1.0x10 ⁻⁴	3.2
871	517	90	2.5	1.25x10 ⁻⁴	2.3
871	283	50	441	6.0x10 ⁻⁷	2.6
760	600	90	134.8	-----	3.1
760	670	100	30.2	7.9x10 ⁻⁶	2.9
760	670	100	49.8	7.5x10 ⁻⁶	3.78

Table 5.3

Temperature-Dependent Representation of Short-Time
Hastelloy X Creep Response

Temperature, °C	Constants for creep equation* $\epsilon_{cr} = (\sigma/A)^n (t)$	
	A	n
705	973	4.41
760	517	4.75
816	304	5.09
871	195	5.42
927	158	3.78
983	134	2.53

*Stress (σ) in MPa, creep strain (ϵ_{cr}) in percent, (t) in hours

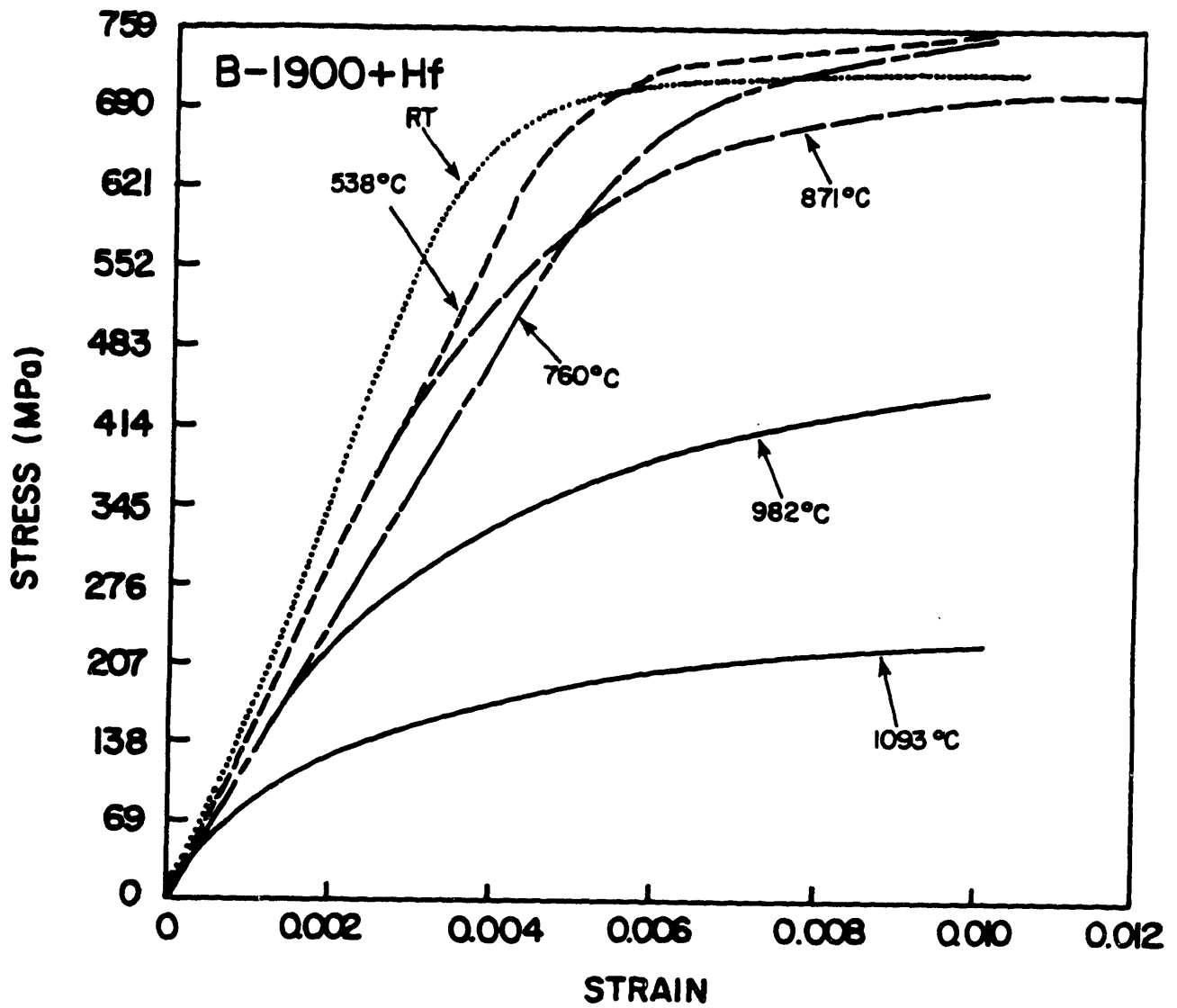


Figure 5.1 Monotonic tensile response of B-1900+Hf($\dot{\epsilon} = 0.005 \text{ min}^{-1}$)

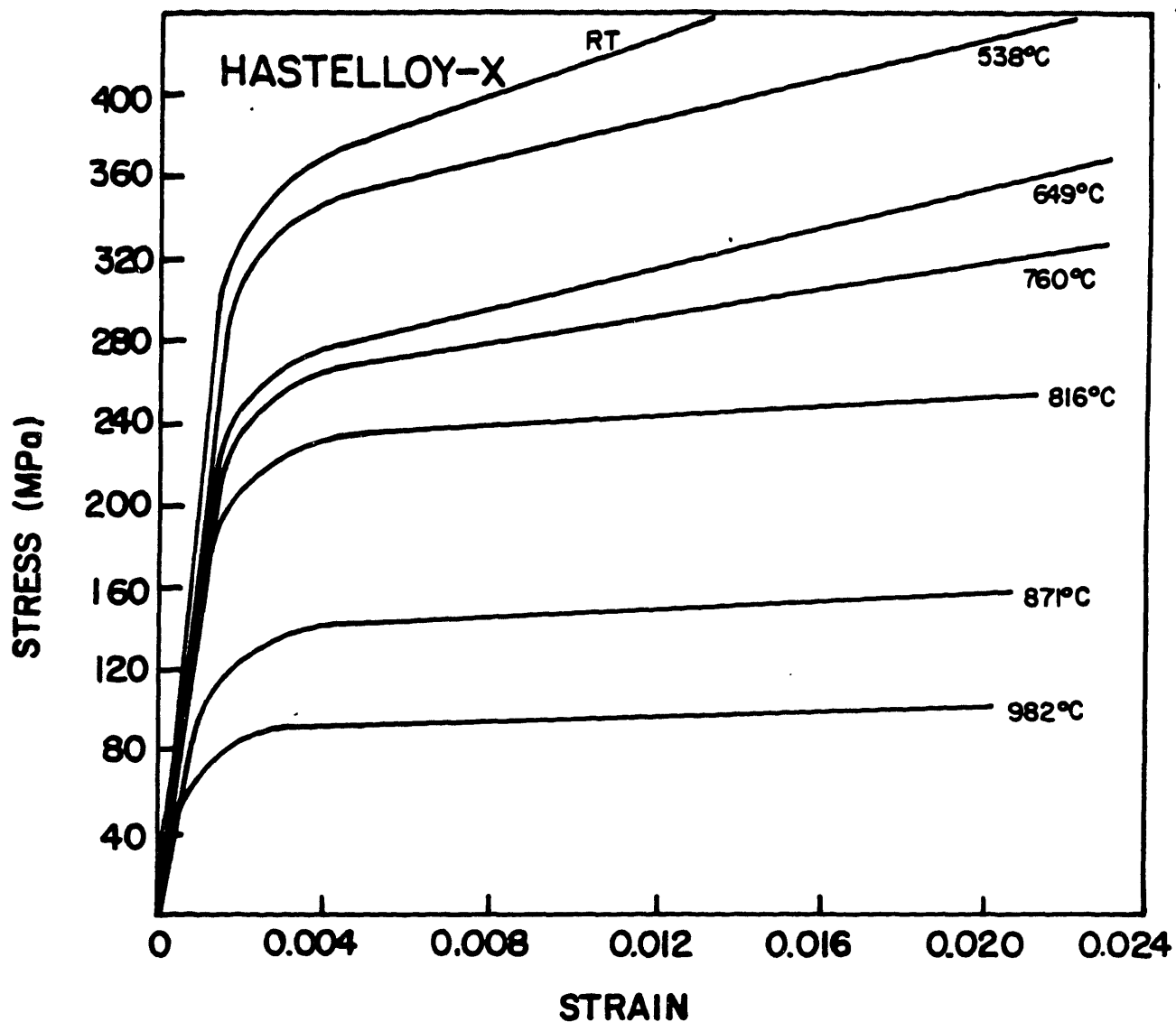


Figure 5.2 Monotonic tensile response of Hastelloy-X($\dot{\epsilon} = 0.005 \text{ min}^{-1}$)

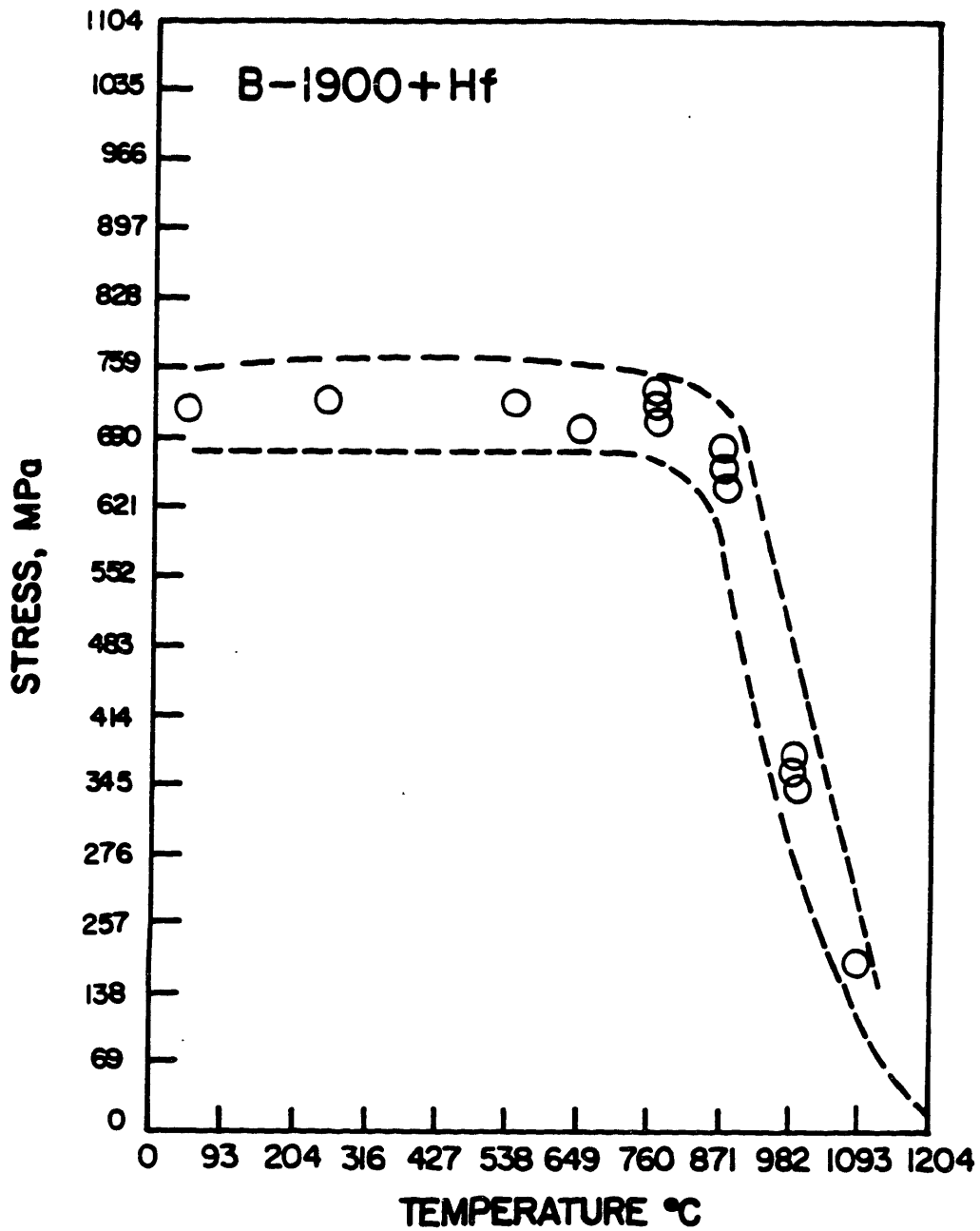


Figure 5.3 Yield stress(0.2 %) versus Representative scatter in B-1900+Hf.

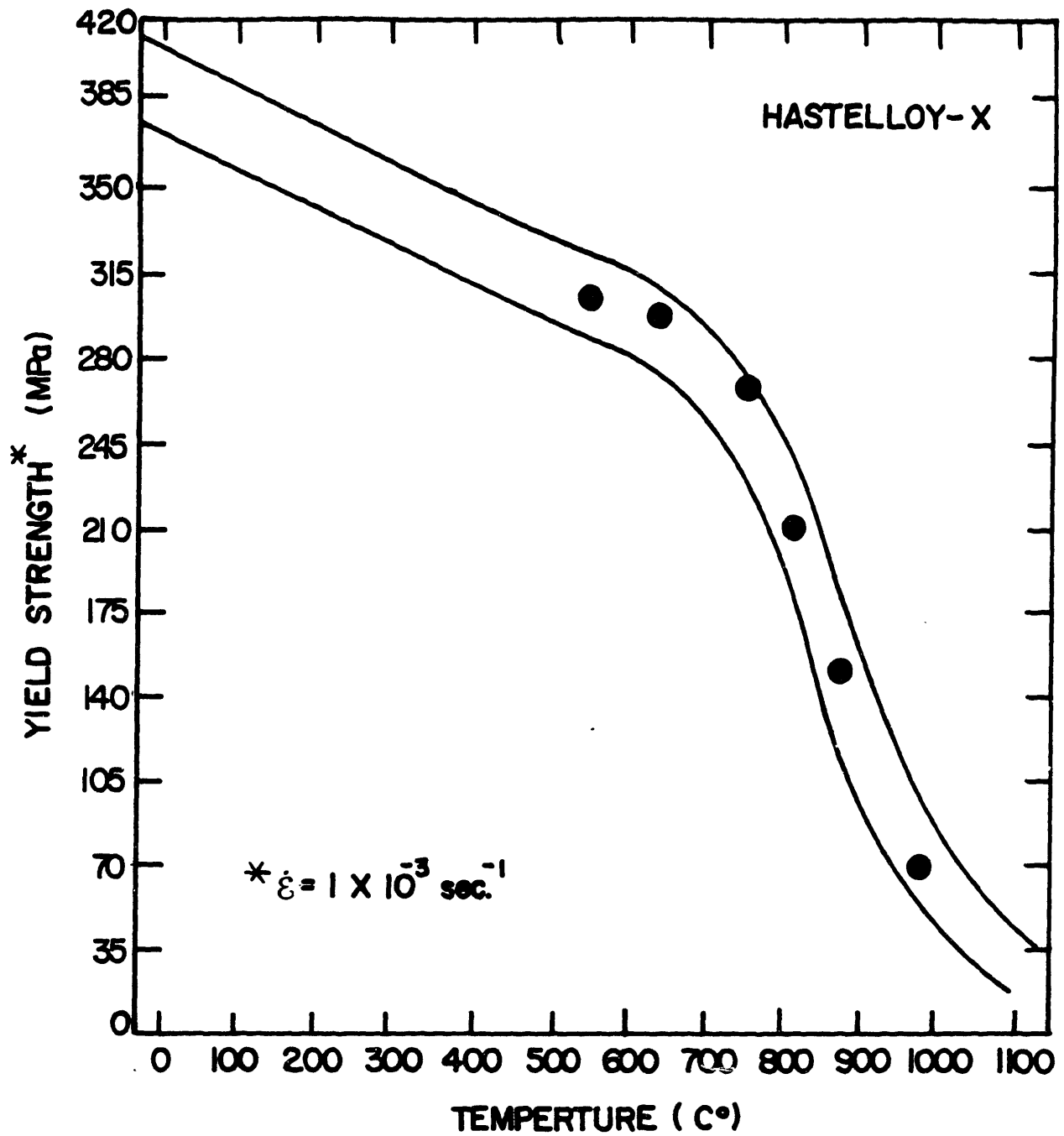


Figure 5.4 Yield stress(0.2 %) versus Representative scatter in Hastelloy-X.

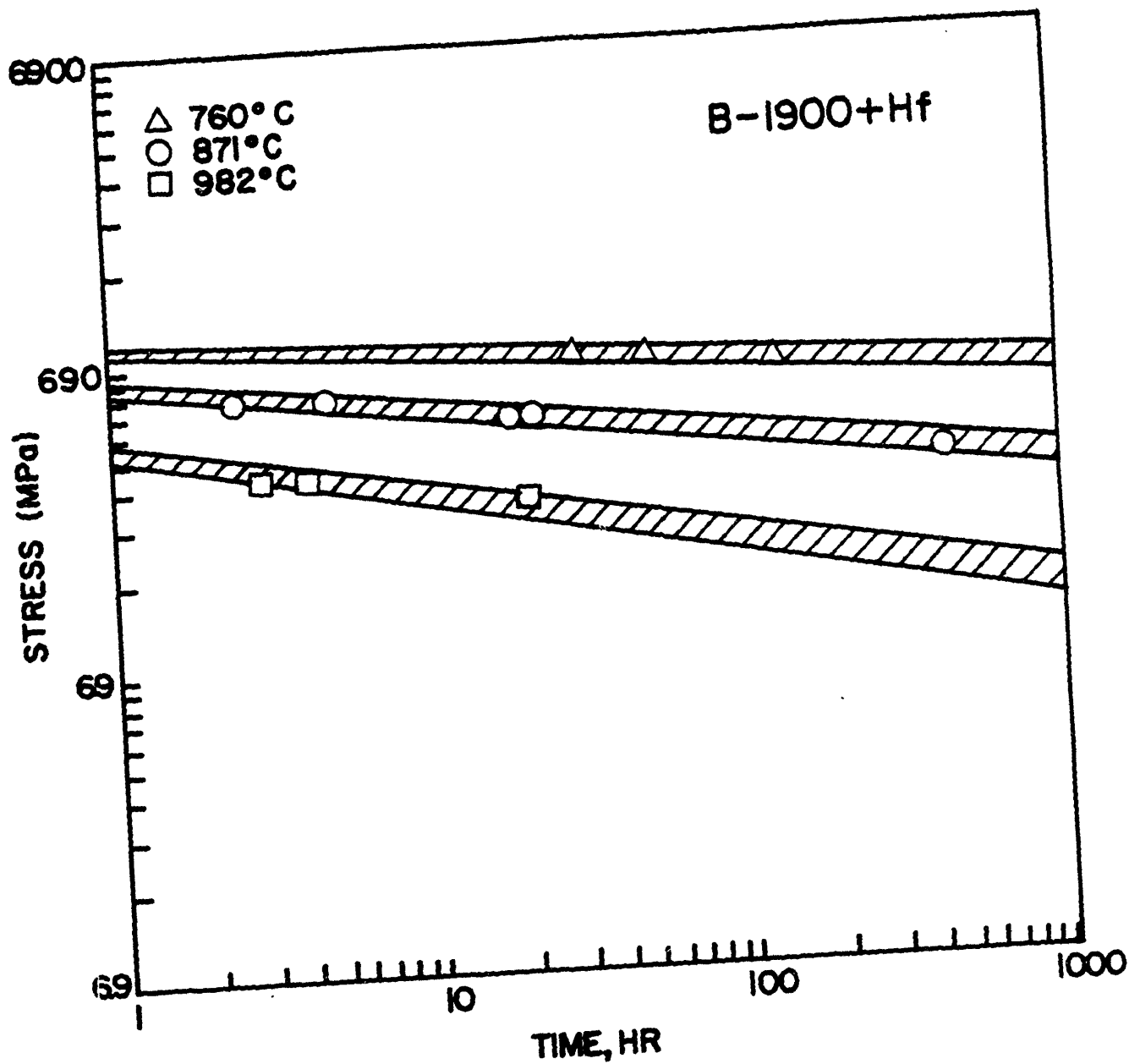


Figure 5.5 Specimen rupture life versus Representative rupture life scatter bands in B-1900+Hf.

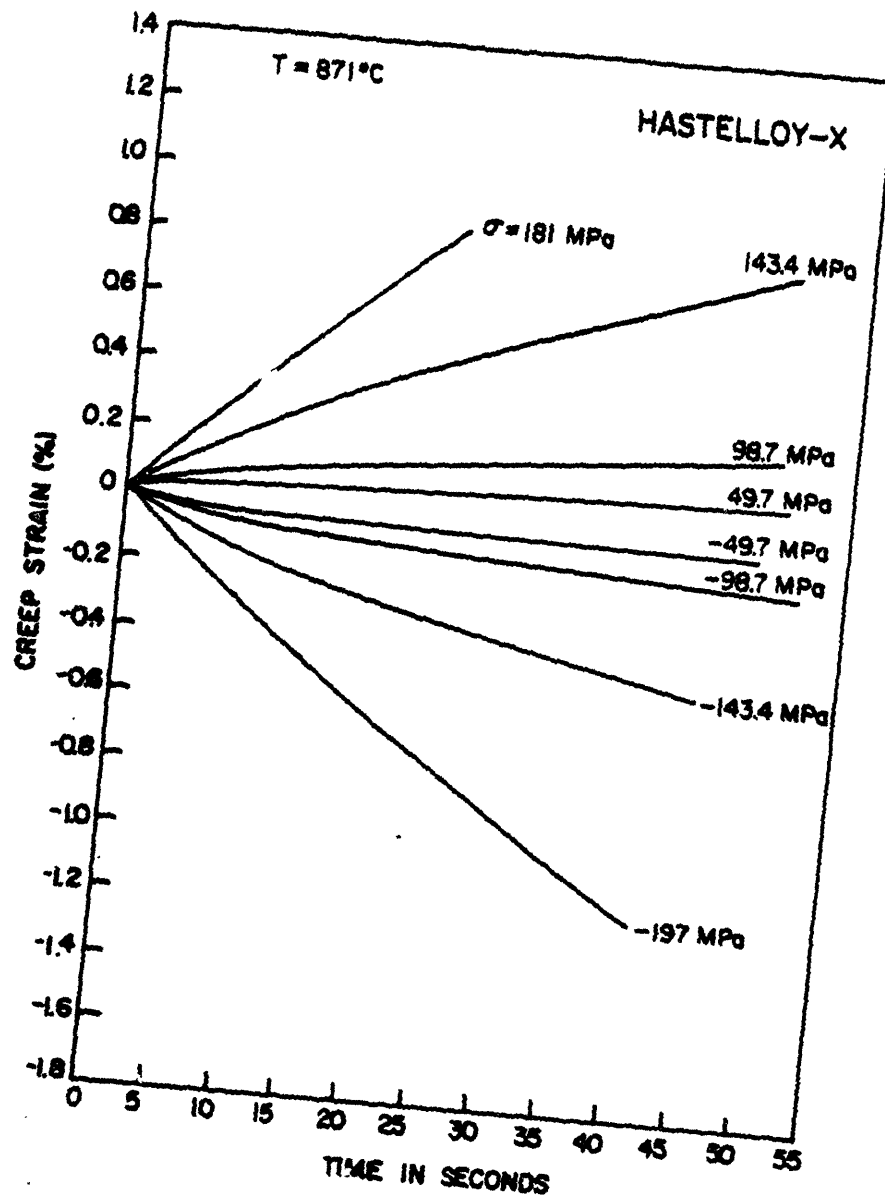


Figure 5.6 Creep responses of Hastelloy-X at 871 °C.

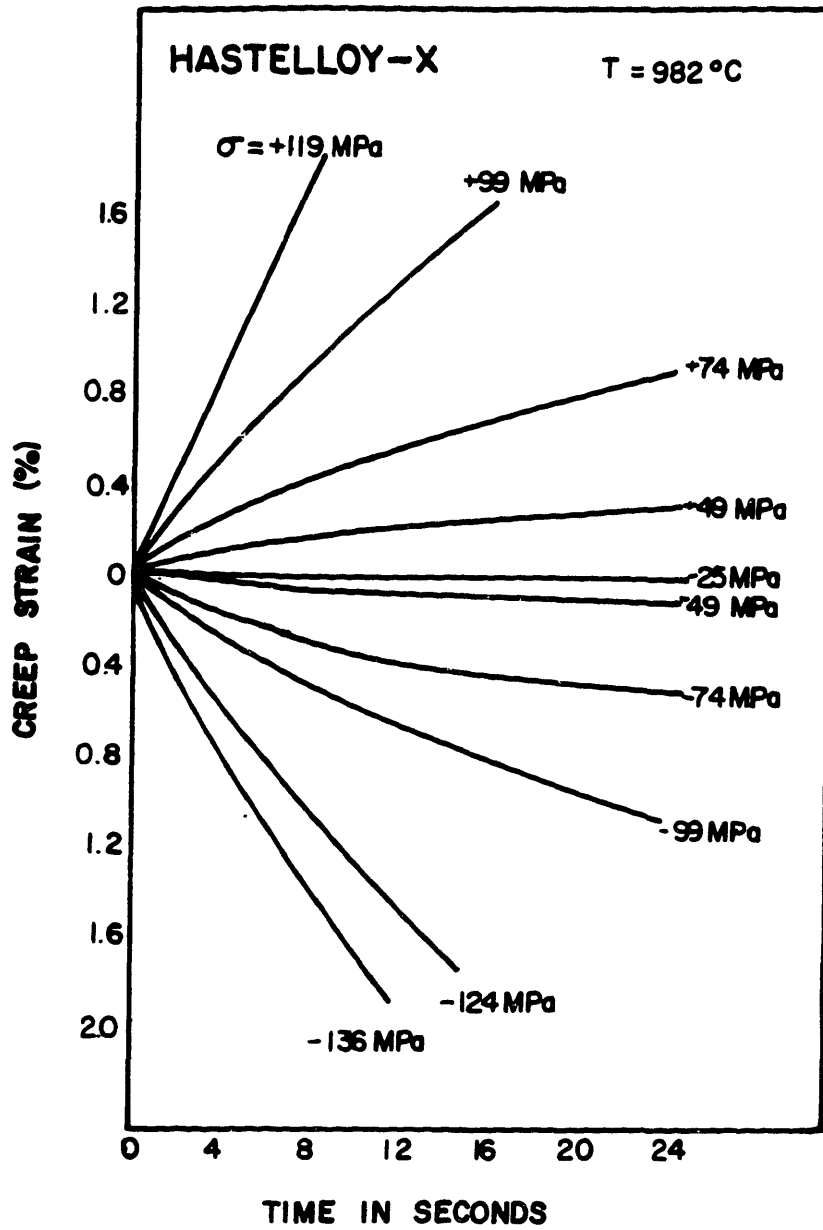


Figure 5.7 Creep responses of Hastelloy-X at 982 °C.

5.2 Low Cycle Fatigue Properties

Isothermal, strain-controlled fatigue tests were conducted to provide a baseline for life prediction model evaluation and to define crack initiation life in B-1900+Hf and Hastelloy-X [123, 125]. Major variables include strain range, strain rate (frequency) and temperature. Fully reversed ($R_e = -1$) tests were conducted at 538°C, 650°C, 760°C, 871°C, and 982°C using a symmetrical sawtooth waveform. Tables 5.4 to 5.9 summarize the testing conditions and data for B-1900+Hf and Hastelloy-X, respectively. Failure was defined as 10% tensile load drop from the steady-state values.

A review of the cyclic response histories of the tests have indicated that the high temperature tests (871 and 982°C) display a small amount of softening, while the low temperature tests (760, 650, and 538°C) tests remain constant at the smaller strain ranges, but cyclically harden at the larger strain ranges [123, 126]. In most tests, multiple cracks were observed along the gauge length of the specimens. All specimens of B-1900+Hf were found to have surface initiated fatigue cracks associated with either porosity and/or carbides [123]. Analysis of the data have also shown that the nature of the initiation site (carbide vs. porosity) was not statistically significant in determining the fatigue life. Based on these results, carbide or porosity initiation is not considered a primary variable in the analysis of the fatigue tests. Examination of the failed specimens has shown varying degrees of transgranular vs. intergranular cracking, depending upon the temperature range. In most cases, the growth mode from initiation sites was transgranular. At low temperature ($T < 871^\circ\text{C}$) the cracks

propagated transgranularly throughout the cross-section of the specimens, whereas at higher temperature ($T \geq 871^{\circ}\text{C}$), the cracks start transgranularly and surprisingly become intergranular.

Table 5.4

Summary of B-1900+Hf Fatigue Tests
(T = 538°C, R_e = -1)

Strain Range	Frequency (cpm)	Plastic Strain Range*	Stress Range (MPa)	Cyclic Life	
				First crack	10% drop
0.005	10	0.005	855	7980	13000
0.005	10	0.005	807	7536	12560
0.005	10	0.002	868	6390	7775
0.005	10	0.003	910	4665	8877
0.005	10	0.002	965	5326	9050
0.005	10	0.003	945	6840	11400
0.005	10	0.002	945	5264	8774
0.008	6.25	0.002	1331	930	1550
0.008	6.25	0.002	1420	552	920
0.008	6.25	0.0024	1441	558	930
0.010	5.00	0.0065	1585	136	227
0.010	5.00	0.0040	1537	238	397
0.010	4.99	0.0048	1606	183	305

Table 5.5

Summary of B-1900+Hf Fatigue Tests
(T = 650°C, R_e = -1)

Strain Range	Frequency (cpm)	Plastic Strain Range	Stress Range (MPa)	Cyclic Life	
				First crack	10% drop
0.008	10	0.0021	1310	418	916

Table 5.6

Summary of B-1900+Hf Fatigue Tests
(T = 760°C, R_e = -1)

Strain Range	Frequency (cpm)	Plastic Strain Range	Stress Range (MPa)	Cyclic Life	
				First crack	10% drop
0.005	10	0.004	854	3283	7539
0.005	10	0.004	890	2911	6756
0.005	10	0.005	826	3776	8864
0.008	6.25	0.0016	1230	231	723
0.008	6.24	0.0023	1148	278	910
0.008	6.00	0.0014	1210	317	958
0.005	0.9	0.0016	749	4654	1139
0.005	0.9	0.008	765	2248	5620

Table 5.7

Summary of B-1900+Hf Fatigue Tests
(T = 871°C, R_ε = -1)

Strain Range	Frequency (cpm)	Plastic Strain Range	Stress Range (MPa)	Cyclic Life	
				First crack	10% drop
0.005	10	0.00023	727	1554	3300
0.005	10	0.00023	750	808	2100
0.005	10	0.00032	773	1226	3050
0.005	10	0.00033	769	1257	3000
0.005	10	0.00022	725	1441	3500
0.005	10	0.00017	737	1032	2700
0.005	10	0.00025	726	1466	3600
0.005	10	0.00018	758	1127	2900
0.005	10	0.00028	770	912	2240
0.005	10	0.00020	753	1520	3780
0.005	10	0.00012	761	1337	3420
0.005	10	0.00021	819	1131	2488
0.005	1.0	0.00040	704	923	2656
0.005	1.0	0.00035	700	827	2110
0.005	1.0	0.00033	675	1019	2968
0.005	0.5	0.00067	645	757	2120
0.005	0.5	0.00062	630	787	2160
0.005	0.5	0.00059	625	499	1310
0.0035	14	0.00007	524	21760	67,580
0.0040	12.5	0.00009	647	3553	-----
0.0040	12.5	0.00010	629	3188	9252
0.0040	12.5	0.00006	677	3651	8100
0.0080	6.25	0.00130	998	81	383
0.0080	6.25	0.00103	1028.5	88	468
0.0080	6.25	0.00100	1012.2	93	454
0.0080	6.25	0.00129	1009.4	69	330

Table 5.7 (continued)

Strain Range	Frequency (cpm)	Plastic Strain Range	Stress Range (MPa)	Cyclic Life First crack 10% drop	
0.0080	0.625	0.00140	1019	64	325
0.0080	0.625	0.00166	923	49	272
0.0080	0.625	0.00150	984	39	208
0.0080	0.624	0.00147	962	35	189

Table 5.8

Summary of B-1900+Hf Fatigue Tests
(T = 982°C, R_e = -1)

Strain Range	Frequency (cpm)	Plastic Strain Range	Stress Range (MPa)	Cyclic Life	
				First crack	10%drop
0.005	10.	0.00117	537	406	1254
0.005	10.	0.00094	536	460	1478
0.005	10.	0.00088	525	308	-----
0.005	10.	0.00092	541	389	1207
0.005	.10	0.00143	449	337	978
0.005	.10	0.00140	502	325	911
0.005	.10	0.00142	457	382	1332
0.008	6.25	0.00275	662	67	293
0.008	6.25	0.00263	636	48	233
0.008	6.25	0.00283	649	51	241
0.008	0.625	0.00311	583	44	207

Table 5.9

Summary of Hastelloy-X Fatigue Tests
($R_{\epsilon} = -1$)

T (°C)	Strain Range	Frequency (cpm)	Plastic Strain Range	Stress Range (MPa)	Cyclic Life
538	0.005	10	0.0008	694	21,360
538	0.020	10	0.0120	1083	18,330
760	0.005	10	0.0010	622	6,100
760	0.005	10	0.0012	592	8,400
871	0.004	12.5	0.00085	403	12,600
871	0.004	12.5	0.00090	39	9,500
871	0.004	12.5	0.00080	410	12,800
871	0.005	10	0.0015	448	5,800
871	0.005	10	0.0019	397	3,800
871	0.005	10	0.0018	410	6,750
871	0.005	10	0.0017	423	4,400
871	0.005	10	0.0018	410	2,900
871	0.008	6.25	0.0050	384	1,250
871	0.008	6.25	0.0050	384	1,250
871	0.008	6.25	0.0047	423	1,120
982	0.005	10	0.00299	183	3,800
982	0.005	10	0.00280	200	3,805

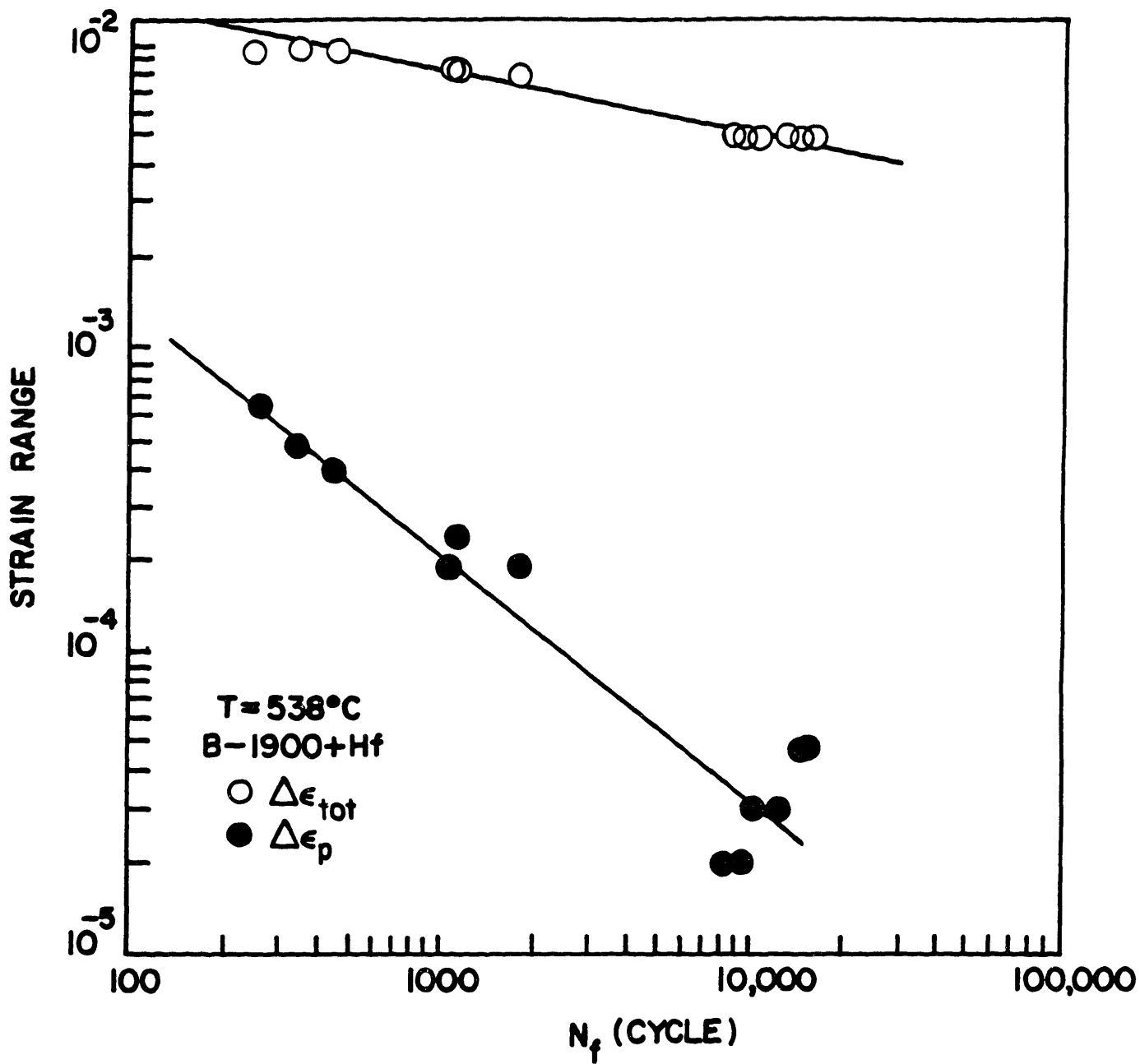


Figure 5.8 Strain range versus Number of cycles to failure in B-1900+Hf(T= 538 °C).

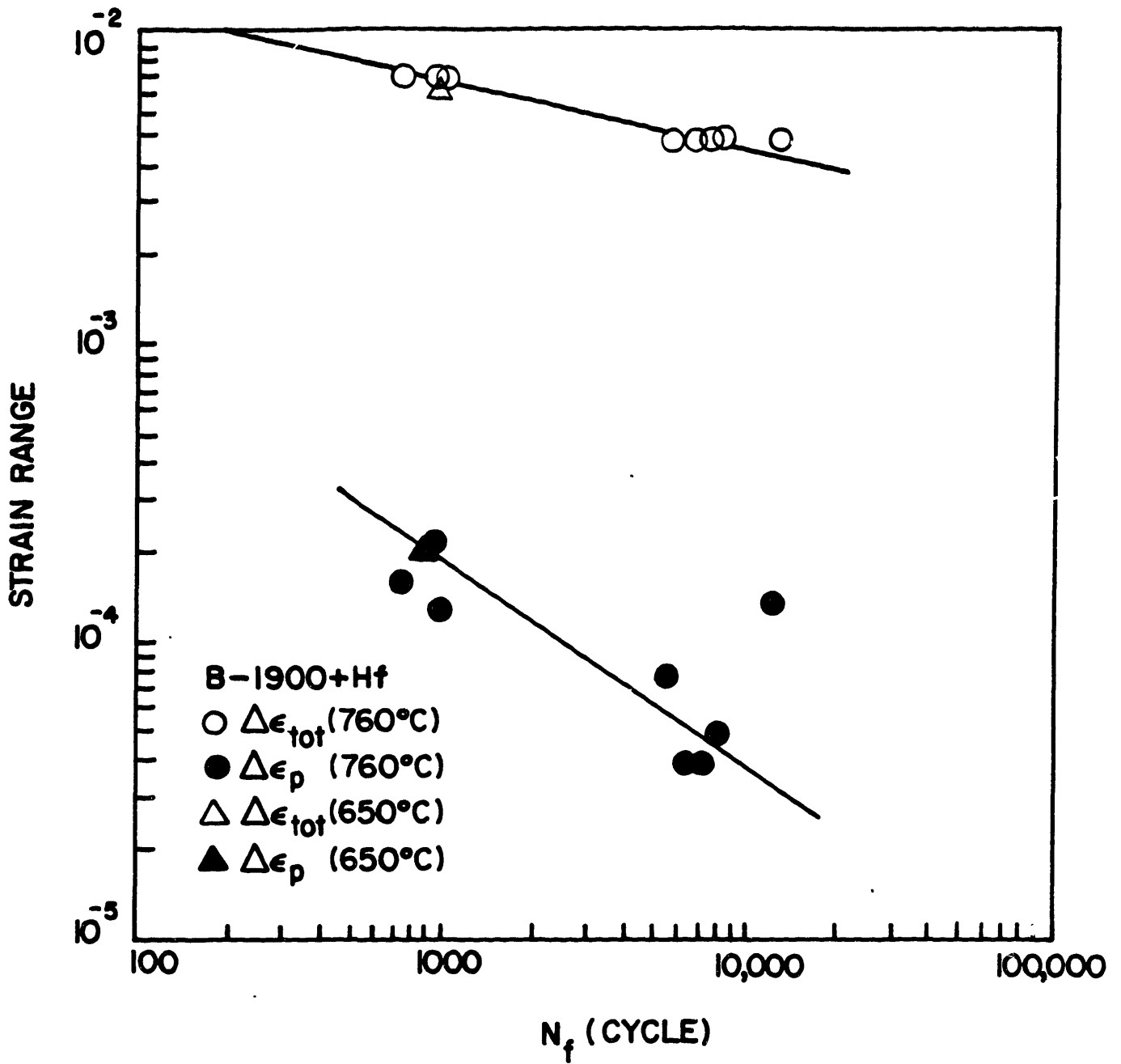


Figure 5.9 Strain range versus Number of cycles to failure in B-1900+Hf(T= 650 and 760 °C).

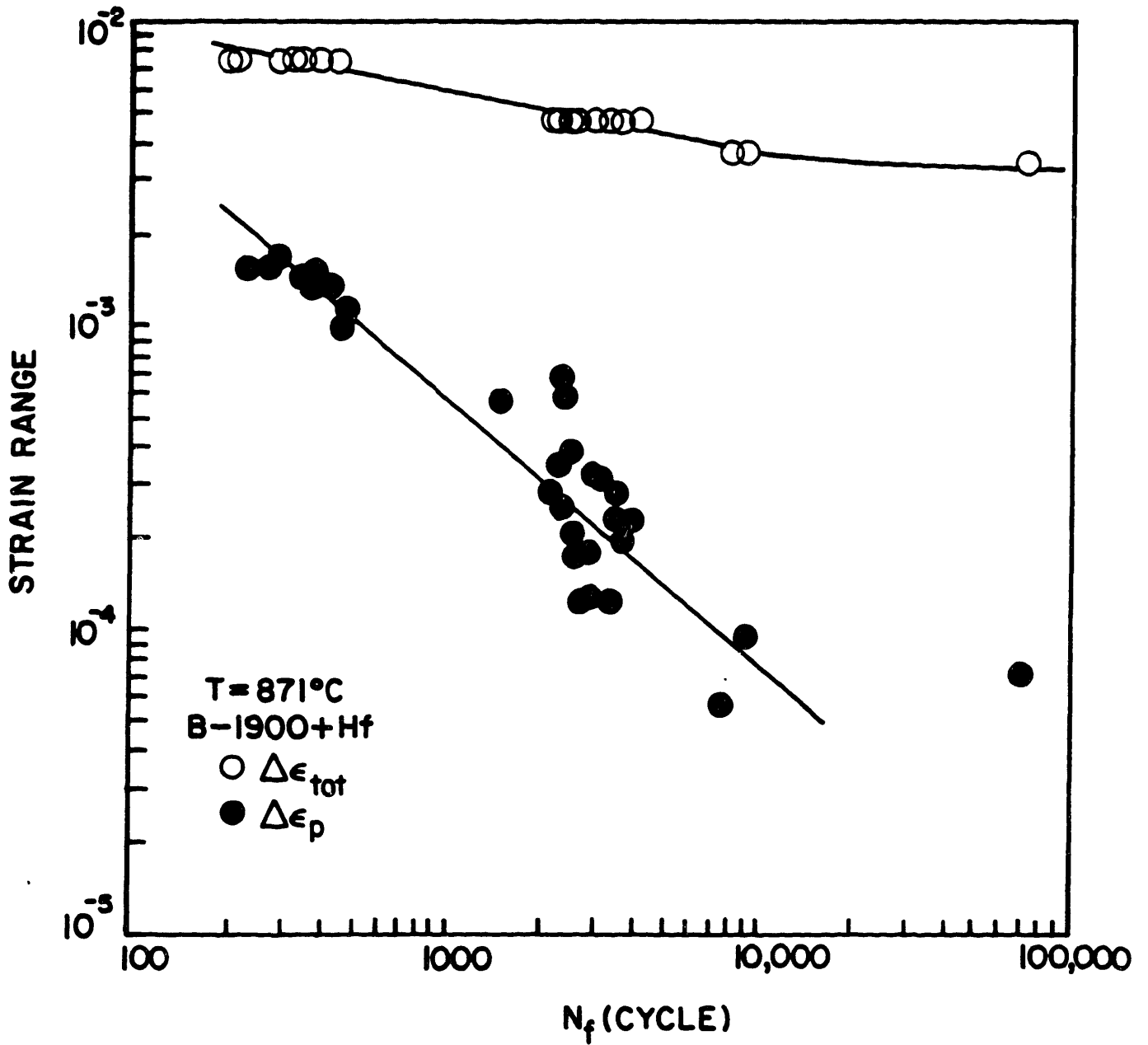


Figure 5.10 Strain range versus Number of cycles to failure in B-1900+Hf($T = 871^\circ\text{C}$).

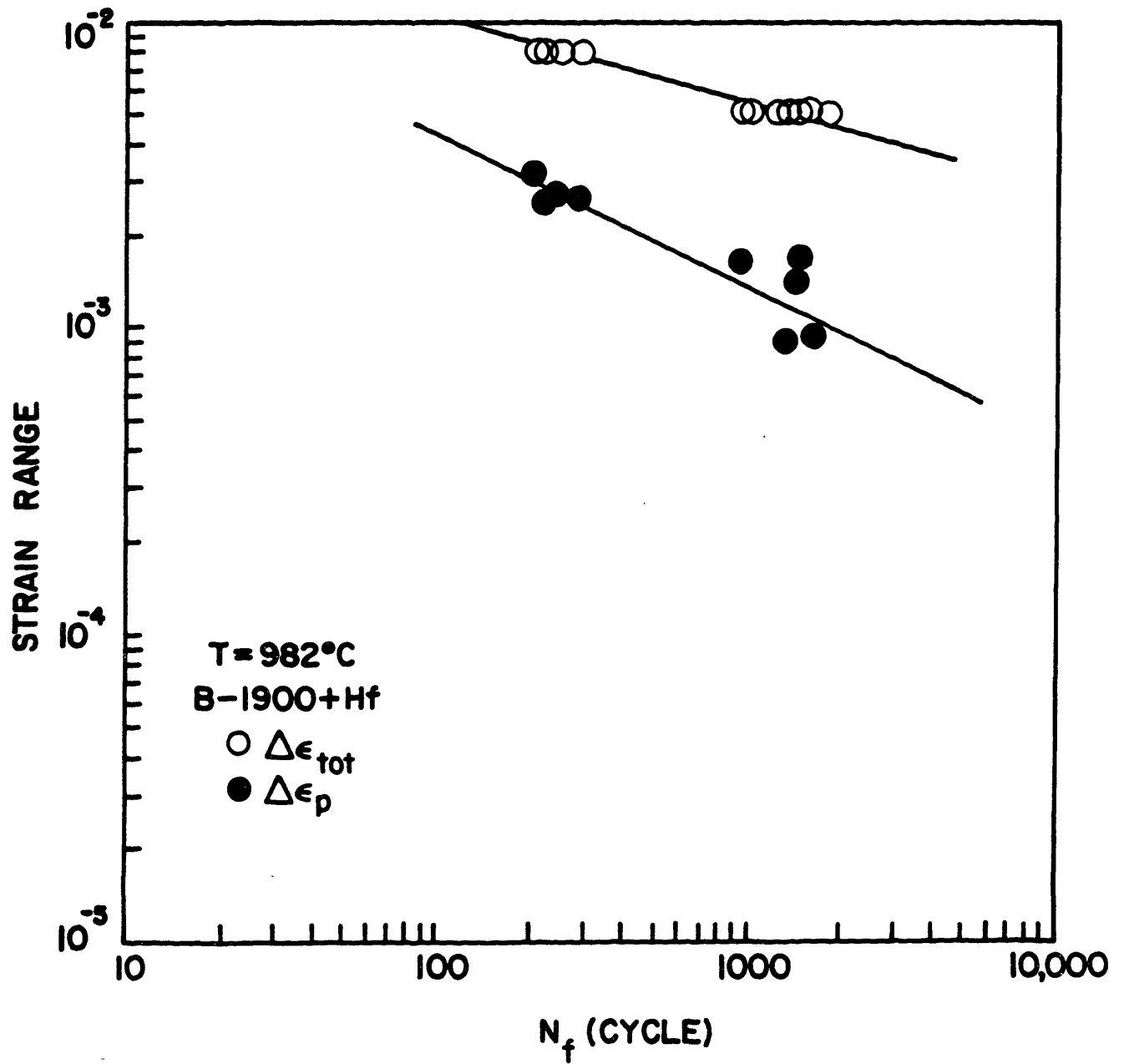


Figure 5.11 Strain range versus Number of cycles to failure in B-1900+Hf(T= 982 °C).

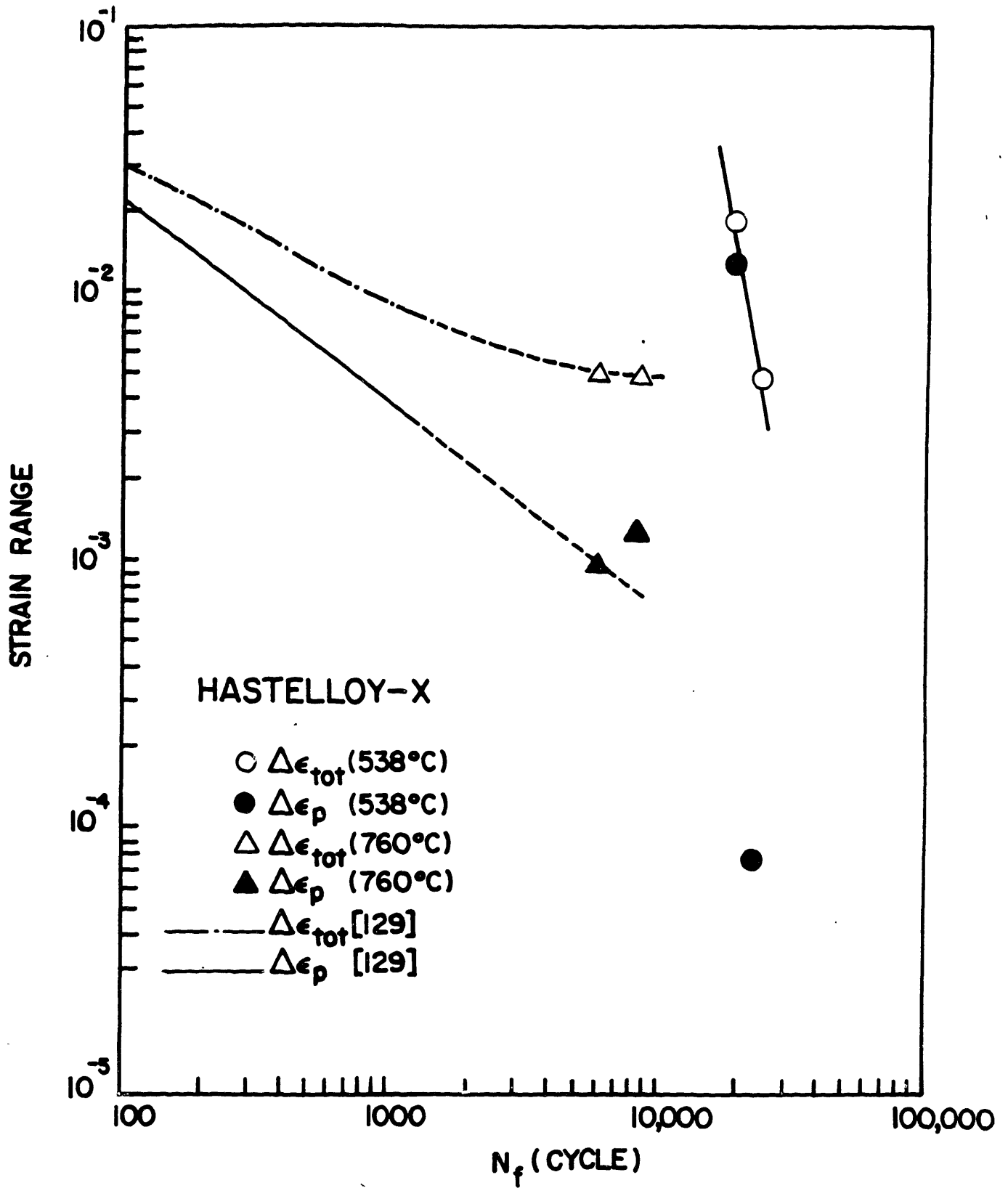


Figure 5.12 Strain range versus Number of cycles to failure in Hastelloy-X(T= 538 and 760 °C).

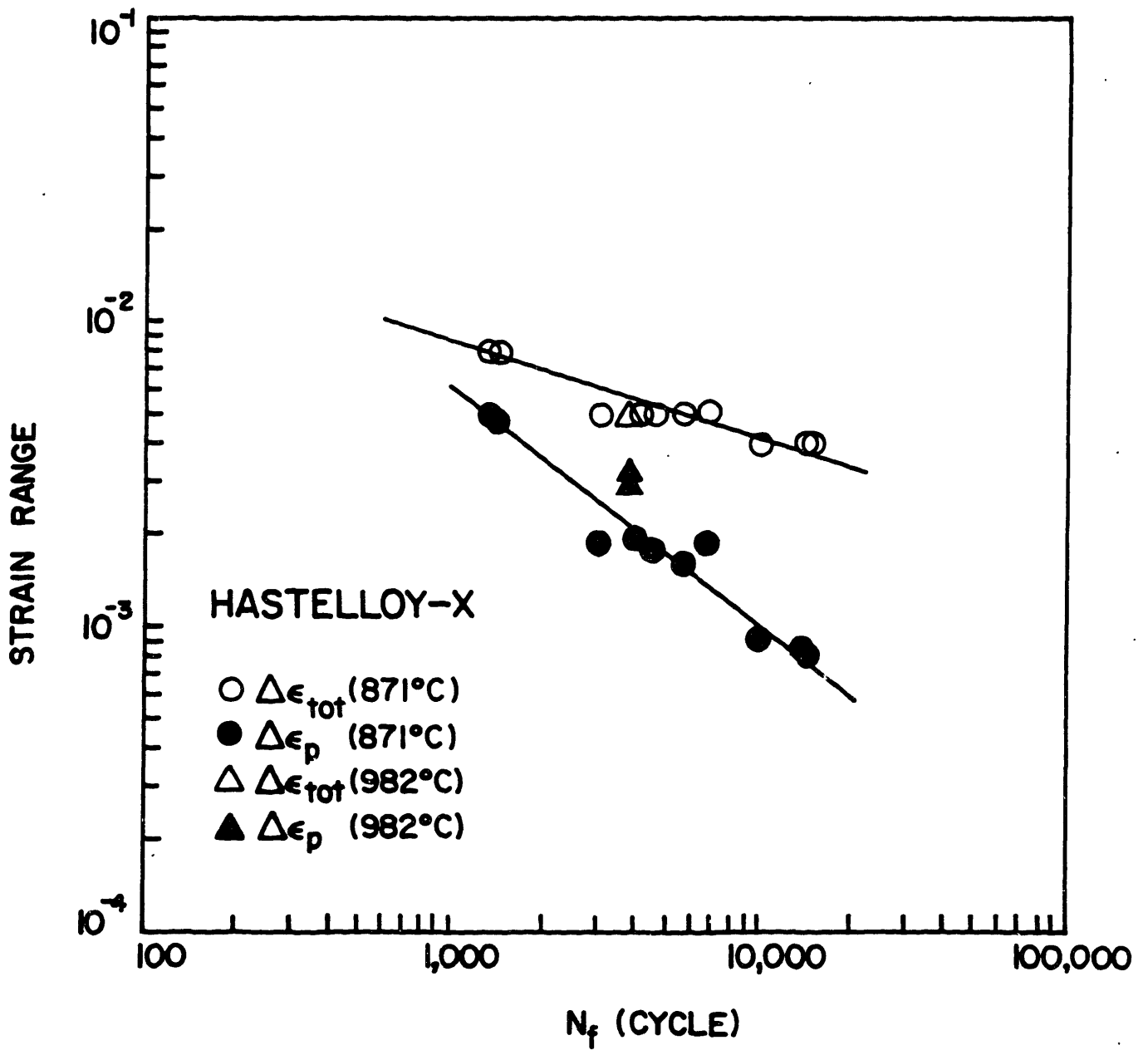


Figure 5.13 Strain range versus Number of cycles to failure in Hastelloy-X(T= 871 and 982 °C).

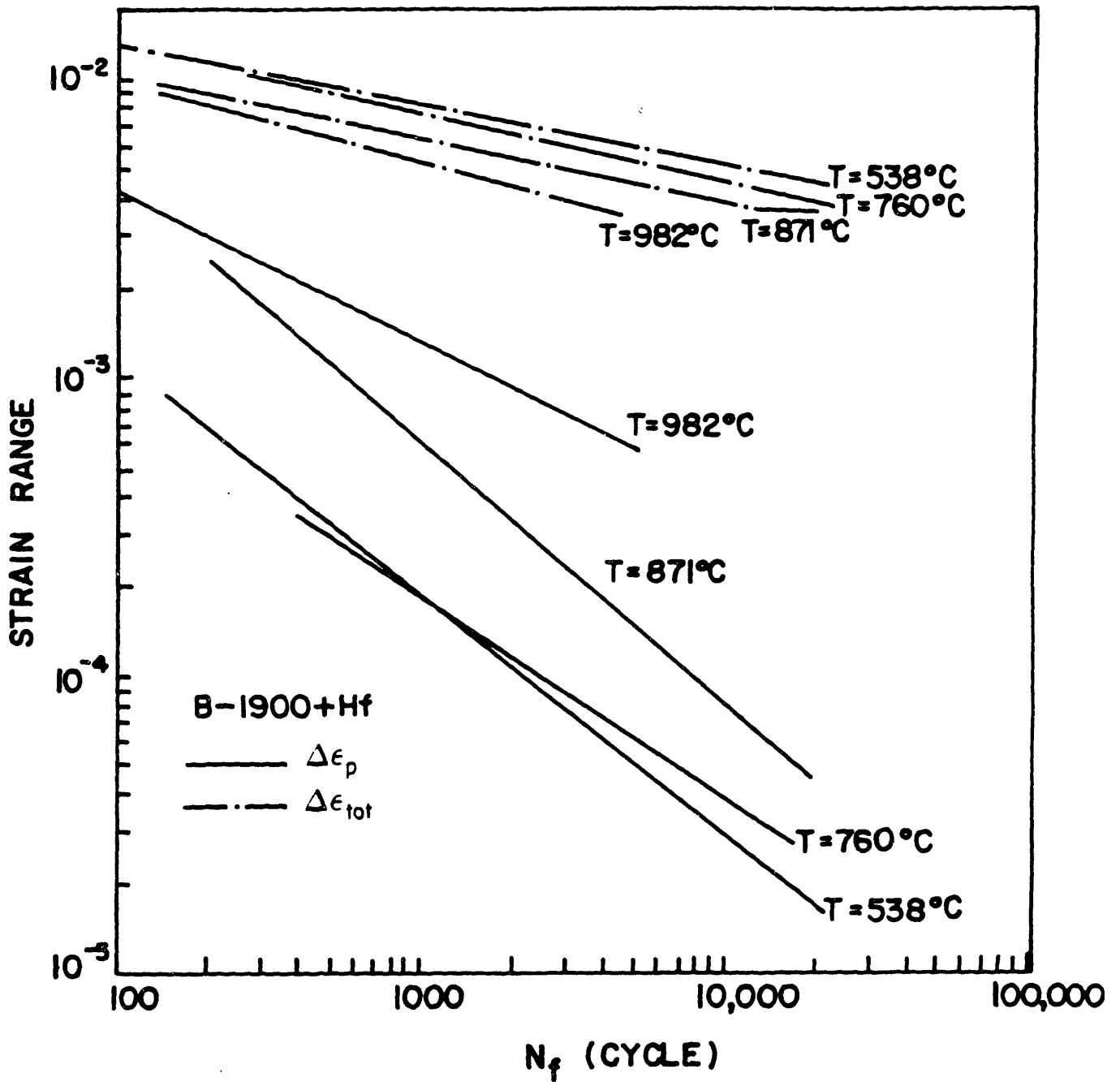


Figure 5.14 Strain range versus Number of cycles to failure as a function of temperature in B-1900+Hf.

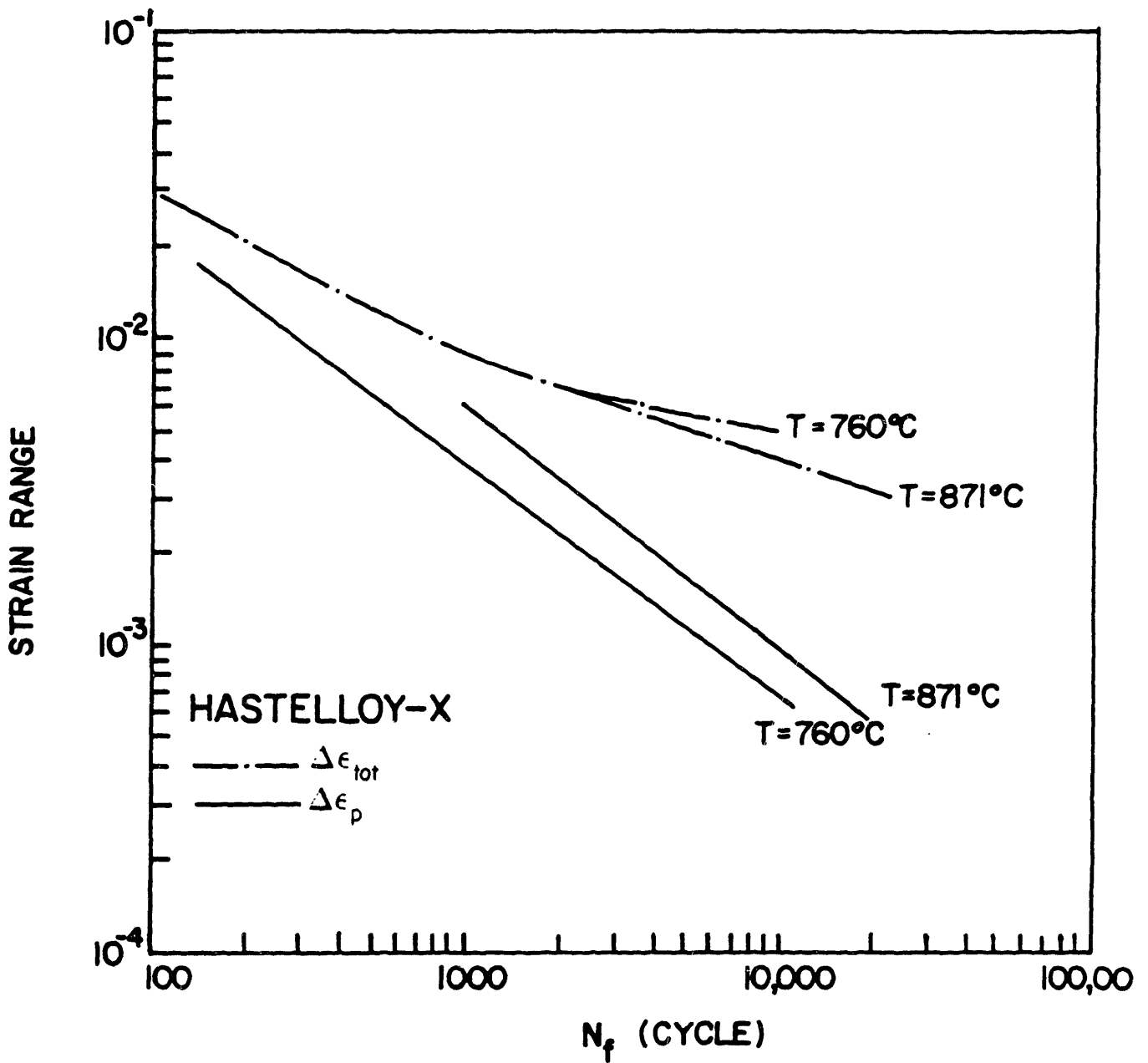


Figure 5.15 Strain range versus Number of cycles to failure as a function of temperature in Hastelloy-X.

The fatigue life in terms of total strain range ($\Delta \epsilon_p$) at various temperatures is shown in Figures 5.8 to 5.13 for both B-1900+Hf and Hastelloy-X. These figures show that the total strain range ($\Delta \epsilon_{tot}$) versus N_f correlates the data better than the inelastic strain range. This correlation is better supported by Figures 5.14 and 5.15, which show the effect of temperature on the fatigue life of B-1900+Hf and Hastelloy-X. At low temperature (538° and 760°C) there is no or little effect of the temperature, both in terms of $\Delta \epsilon_{tot}$ vs. N_f or $\Delta \epsilon_p$ vs. N_f . At higher temperature ($T > 760^\circ\text{C}$) the life (N_f) decreases with increasing temperature at constant $\Delta \epsilon_p$. Similar conclusions have also been reached by others [48-49, 66, 123, 127-128] with similar nickel-based alloys.

5.3 Thermal-Mechanical Fatigue Properties

Results of all the experiments conducted to measure the cyclic response of B-1900+Hf under TMF conditions are summarized in Tables 5.9 and 5.10, where the mechanical strain range ($\Delta \epsilon_{tot}$), the number of applied cycles at each strain range, the initial and final stress range, and final plastic strain range ($\Delta \epsilon_p$) are listed for both in-phase and out-of-phase cycling. The plastic strain ranges were taken as the width of the hysteresis loop at zero stress and, therefore, include both time-independent and time-dependent inelastic strain components. Figures 5.16 and 5.17 show the thermal strain (ϵ_{th}), the mechanical strain (ϵ_{mec}), the total strain (ϵ_{tot}), and the stress amplitude as a function of time (one cycle) for both in-phase and out-of-phase cycling. From the

Table 5.10

B-1900+Hf

In-Phase

 $T_{\max} = 925^{\circ}\text{C}$ $T_{\min} = 400^{\circ}\text{C}$

0.0056 Hz (1/3 cpm)

$\Delta \epsilon$ (%)	N	$\Delta \sigma_i$ (MPa)	$\Delta \sigma_f$ (MPa)	$\Delta \epsilon_{pf}$ (%)
.2000	347	328	356	.000
.2515	337	426	436	.000
.3030	556	527	524	.000
.3590	388	611	620	.000
.3830	490	657	664	.000
.4075	303	786	708	.012
.43215	340	745	748	.015
.45250	280	777	782	.0275
.4925	160	881	842	.0475
.5650	54	862	098	.0700

Table 5.11

B-1900+Hf
 Out-of-Phase
 $T_{\max} = 925^{\circ}\text{C}$
 $T_{\min} = 400^{\circ}\text{C}$
 0.0056 Hz (1/3 cpm)

$\Delta \epsilon$ (%)	N	$\Delta \sigma_i$ (MPa)	$\Delta \sigma_f$ (MPa)	$\Delta \epsilon_{pf}$ (%)
.1765	475	304	310	.000
.1929	426	450	369	.000
.2153	312	416	408	.000
.2498	360	460	455	.000
.2760	260	492	485	.000
.2880	274	585	558	.000
.3279	274	605	585	.012
.3654	316	650	640	.0075
.4040	374	711	684	.0145
.4370	326	754	745	.0145
.4675	222	794	787	.0325
.5370	142	885	876	.0405
.6000	60	981	950	0.0880

load-time and mechanical strain-time (Figures 5.16 - 5.17), the hysteresis loops were obtained.

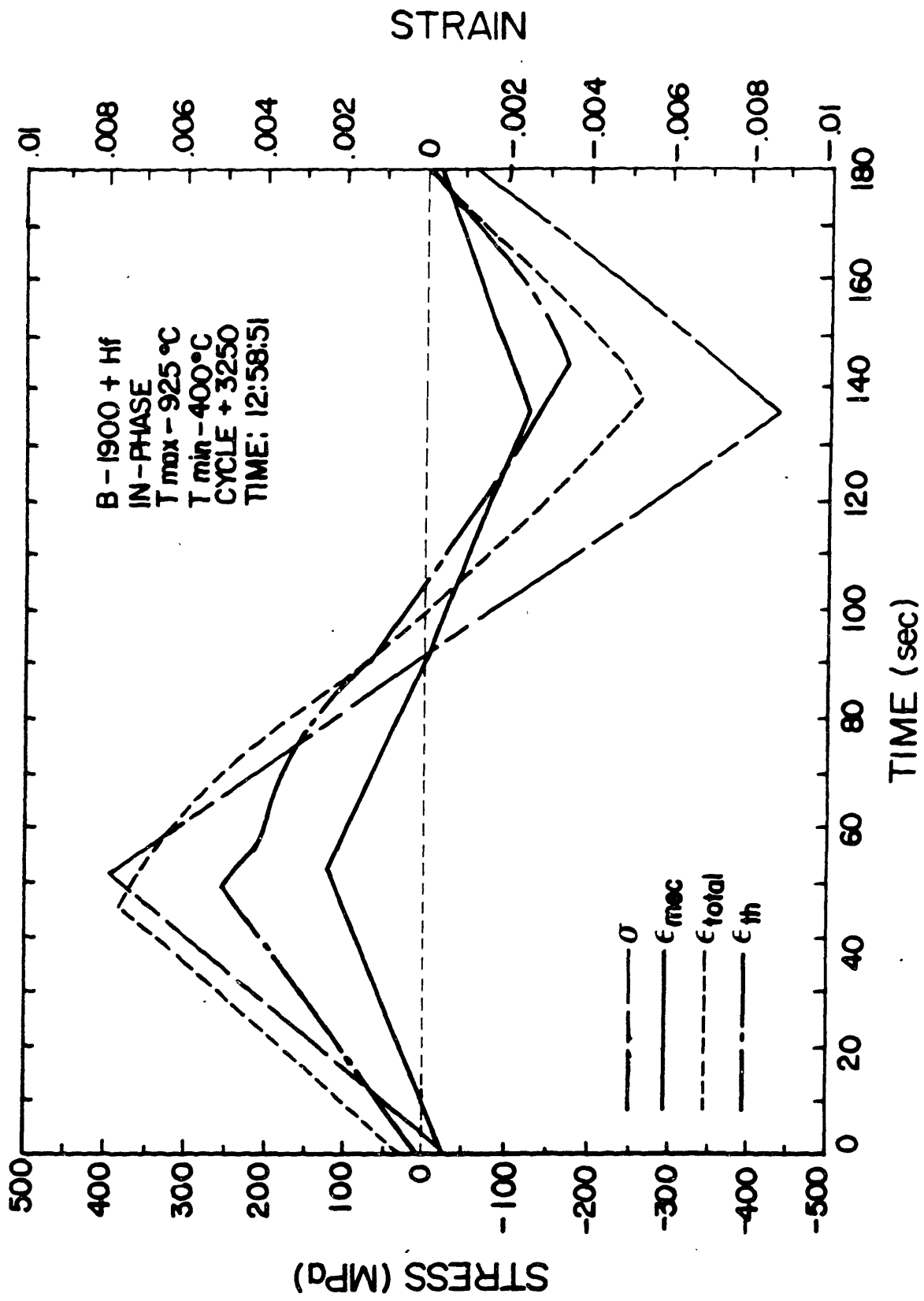


Figure 5.16 Various strain components and stress amplitude in one cycle (B-1900+Hf, in-phase).

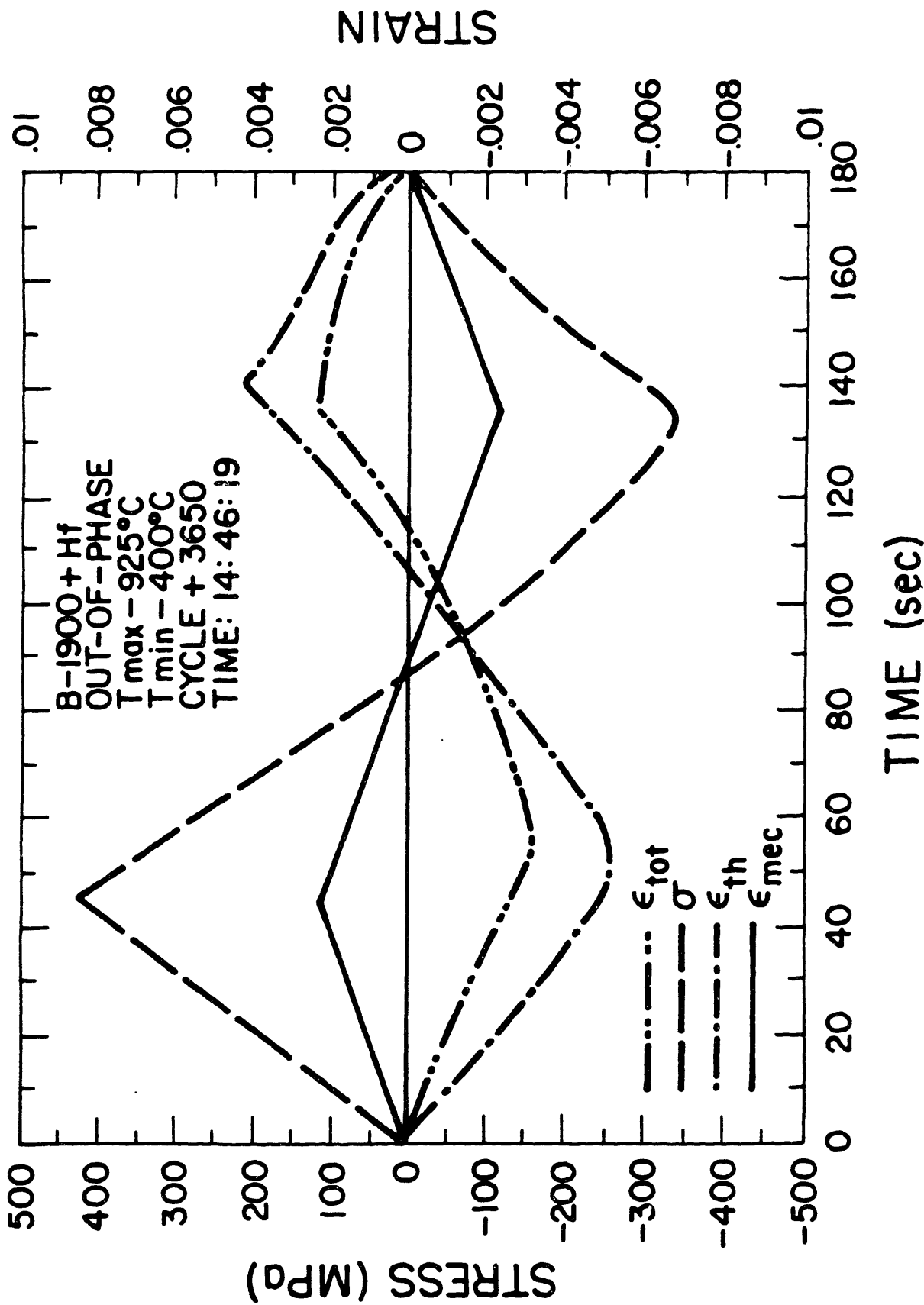


Figure 5.17 Various strain components and stress amplitude in one cycle (B-1900+Hf, out-of-phase).

Even though the mechanical strain cycling was fully reversed, the stress cycle was not symmetric about zero because the temperature was different at each extreme of the cycle. Figures 5.18 and 5.19 show examples of the loops obtained for both in-phase and out-of-phase cycling. For out-of-phase cycling, a positive (tensile) mean stress was observed and a negative mean stress was observed for the in-phase cycling. That is, for the in-phase cycle the magnitude of peak compressive stress was greater than the magnitude of peak tensile stress, or $|\sigma_{\min}| > |\sigma_{\max}|$. The opposite was true for the out-of-phase cycle where $|\sigma_{\max}| > |\sigma_{\min}|$. Figures 5.20 and 5.21 show the type of stress response for in-phase and out-of-phase cycling at fixed strain range (see Appendix IV). Figures 5.22 and 5.23 summarize the fatigue results at all strain ranges.

From Figures 5.20 to 5.23 the following conclusions can be drawn. First, one can conclude that the mean stress ($\bar{\sigma}$) does not vary much with the number of applied cycle and strain range for in-phase cycling. However, $\bar{\sigma}$ does vary with N and $\Delta \epsilon_t$ for out-of-phase cycling. It is also interesting to notice that for similar strain range, the absolute value of $\bar{\sigma}$ is higher for out-of-phase than for in-phase cycling. Another conclusion that can be drawn is that for all $\Delta \epsilon_{\text{tot}}$, in-phase cycling show σ_{\max} to harden, whereas σ_{\min} stayed almost unchanged except at high applied strain range. For out-of-phase cycling, the hardening-softening behavior depends on the applied strain range. At $\Delta \epsilon_{\text{tot}} = 0.1765\%$, σ_{\max} softened whereas σ_{\min} hardened. At $\Delta \epsilon_{\text{tot}} = 0.1923\%$, both σ_{\max} and σ_{\min} softened with the applied number of cycle. At higher $\Delta \epsilon_{\text{tot}}$, σ_{\max} hardened and σ_{\min} softened. The softening of σ_{\min} being more important than the hardening of σ_{\max} , results in a drift of $\bar{\sigma}$ to higher

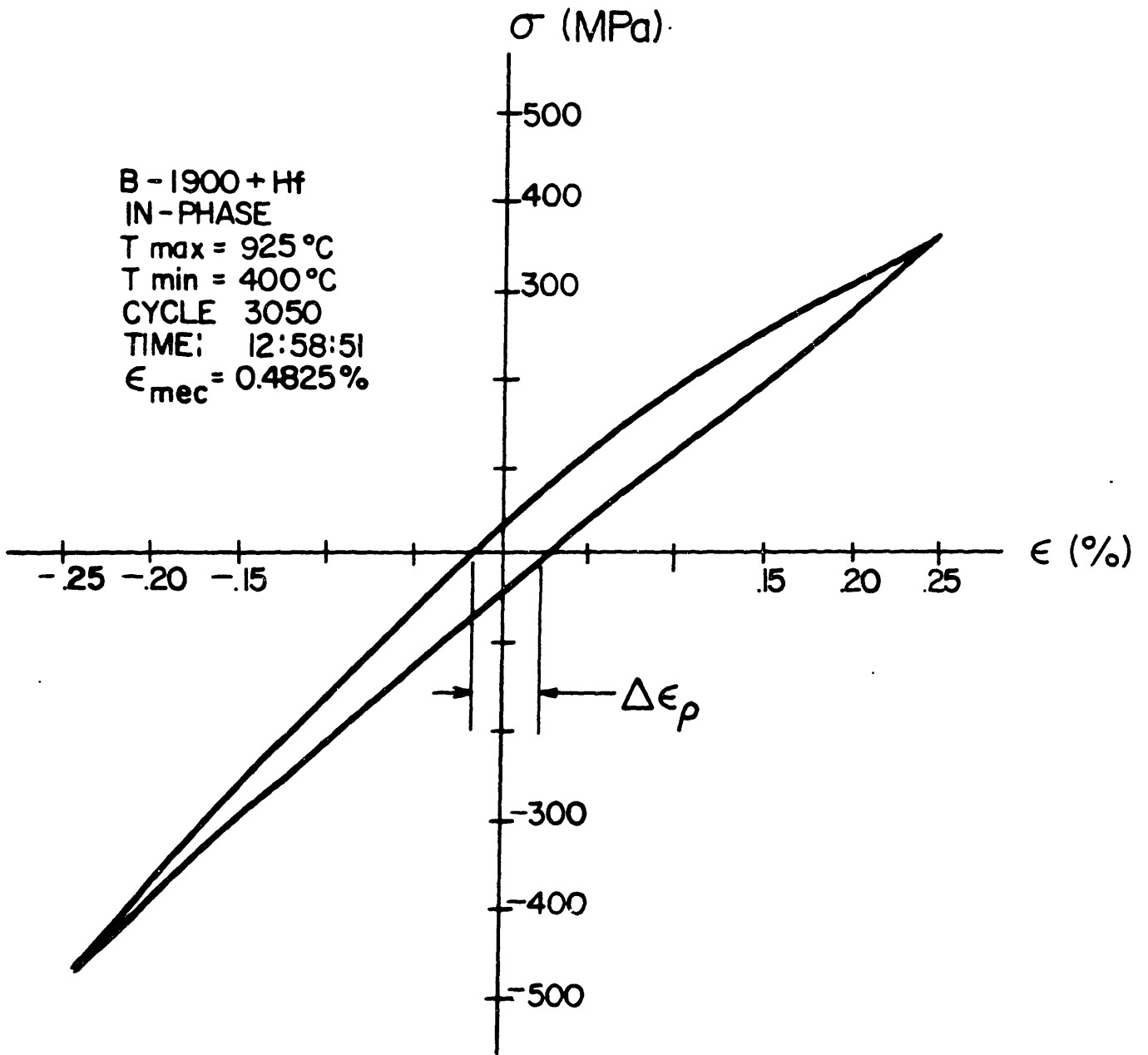


Figure 5.18 Hysteresis loop obtained in B-1900+Hf (in-phase).

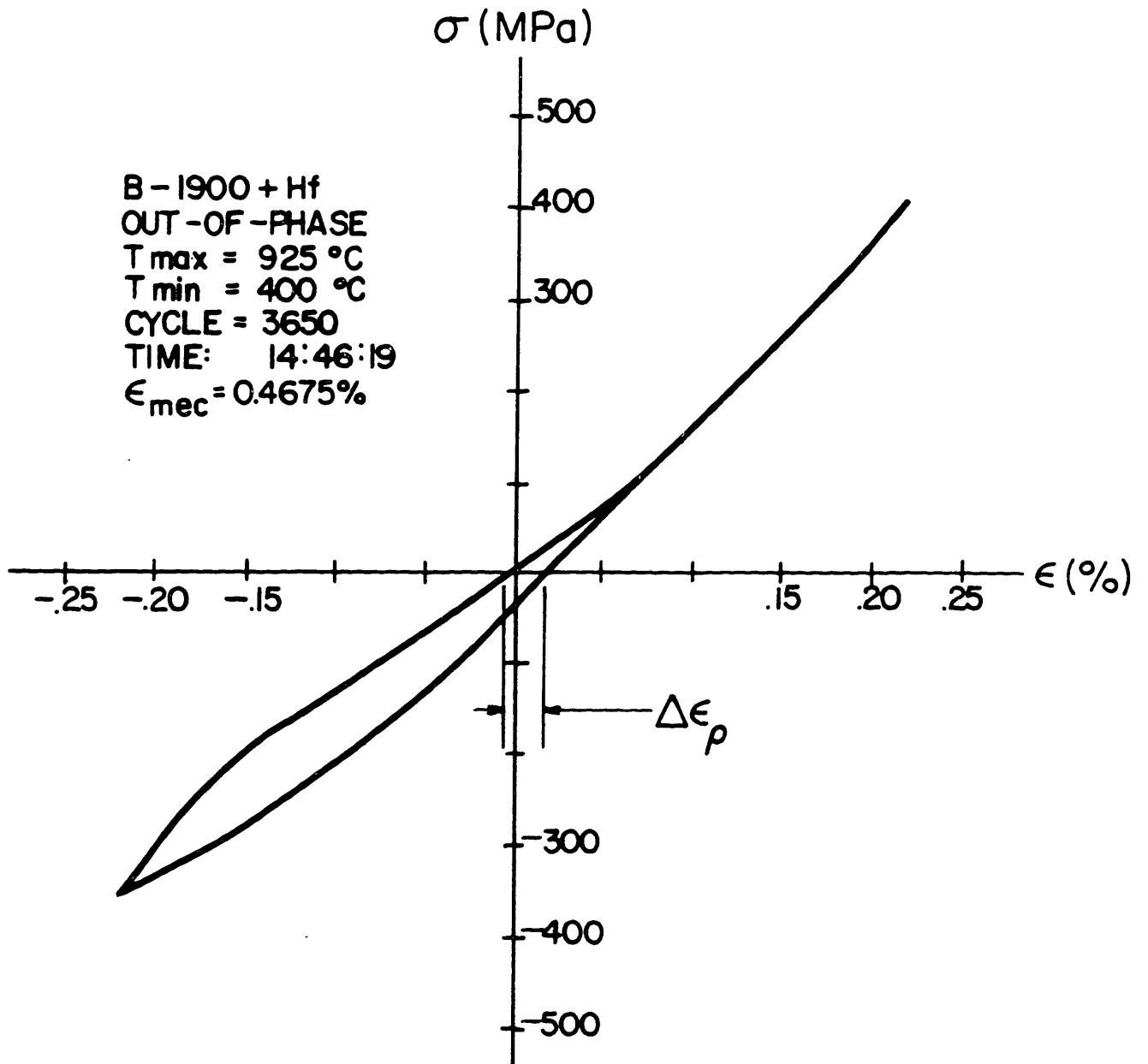


Figure 5.19 Hysteresis loop obtained in B-1900+Hf. (out-of-phase).

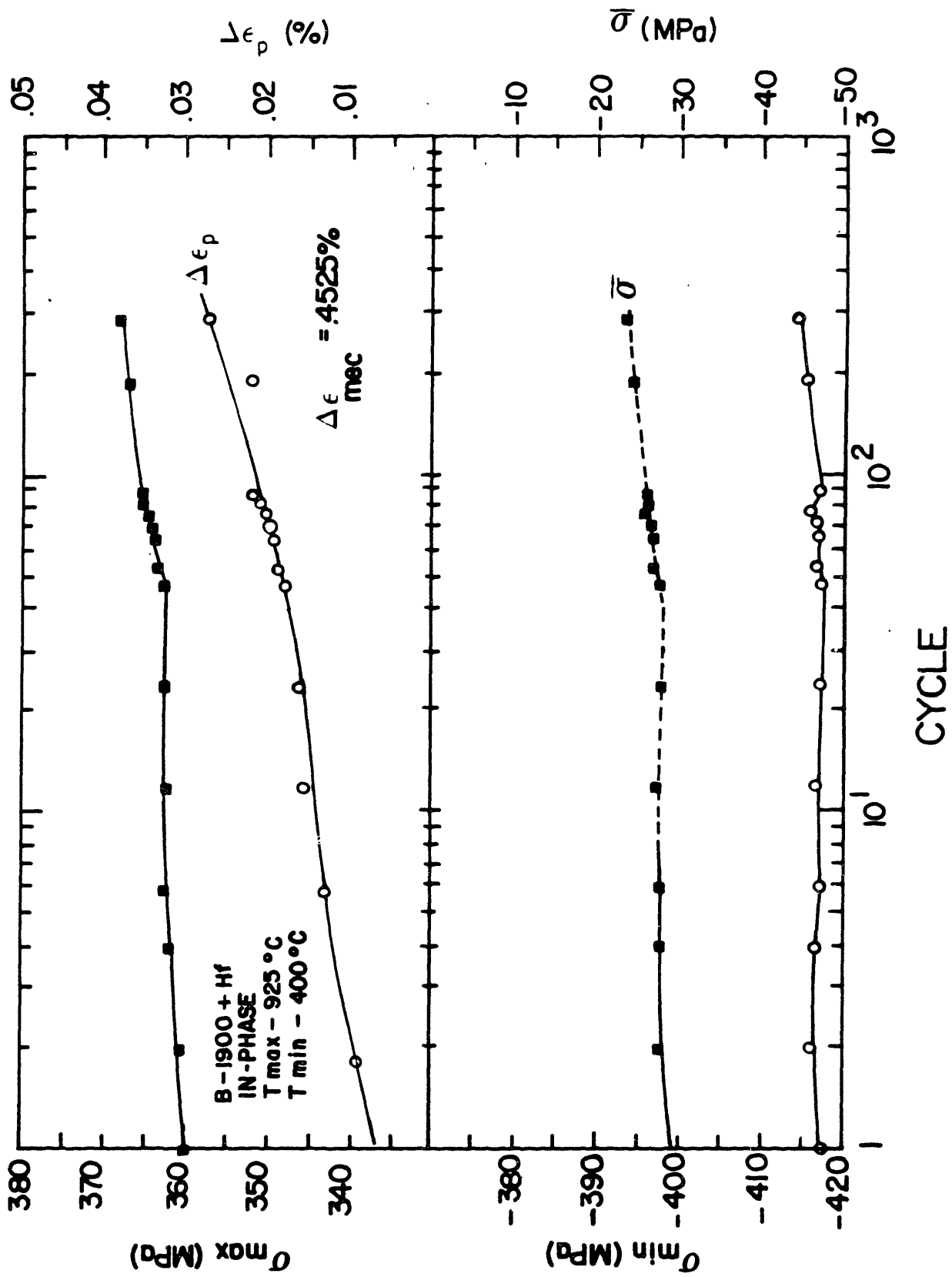


Figure 5.20 Cyclic hardening curves in B-1900+Hf (in-phase, $\Delta \epsilon_{mec} = 0.452\%$).

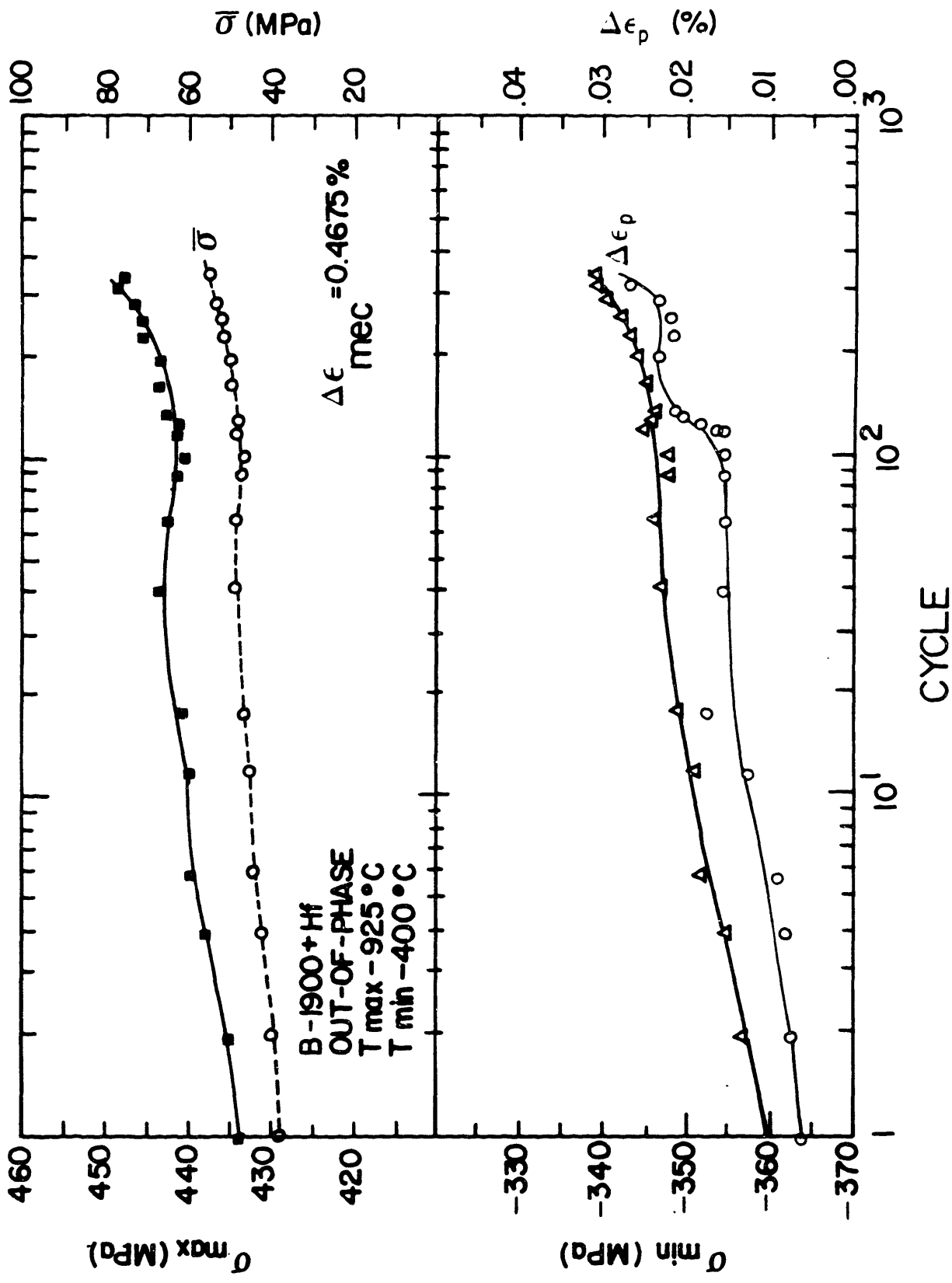


Figure 5.21 Cyclic hardening curves in B-1900+Hf (out-of-phase, $\Delta \epsilon_{\text{mec}} = 0.4675\%$).

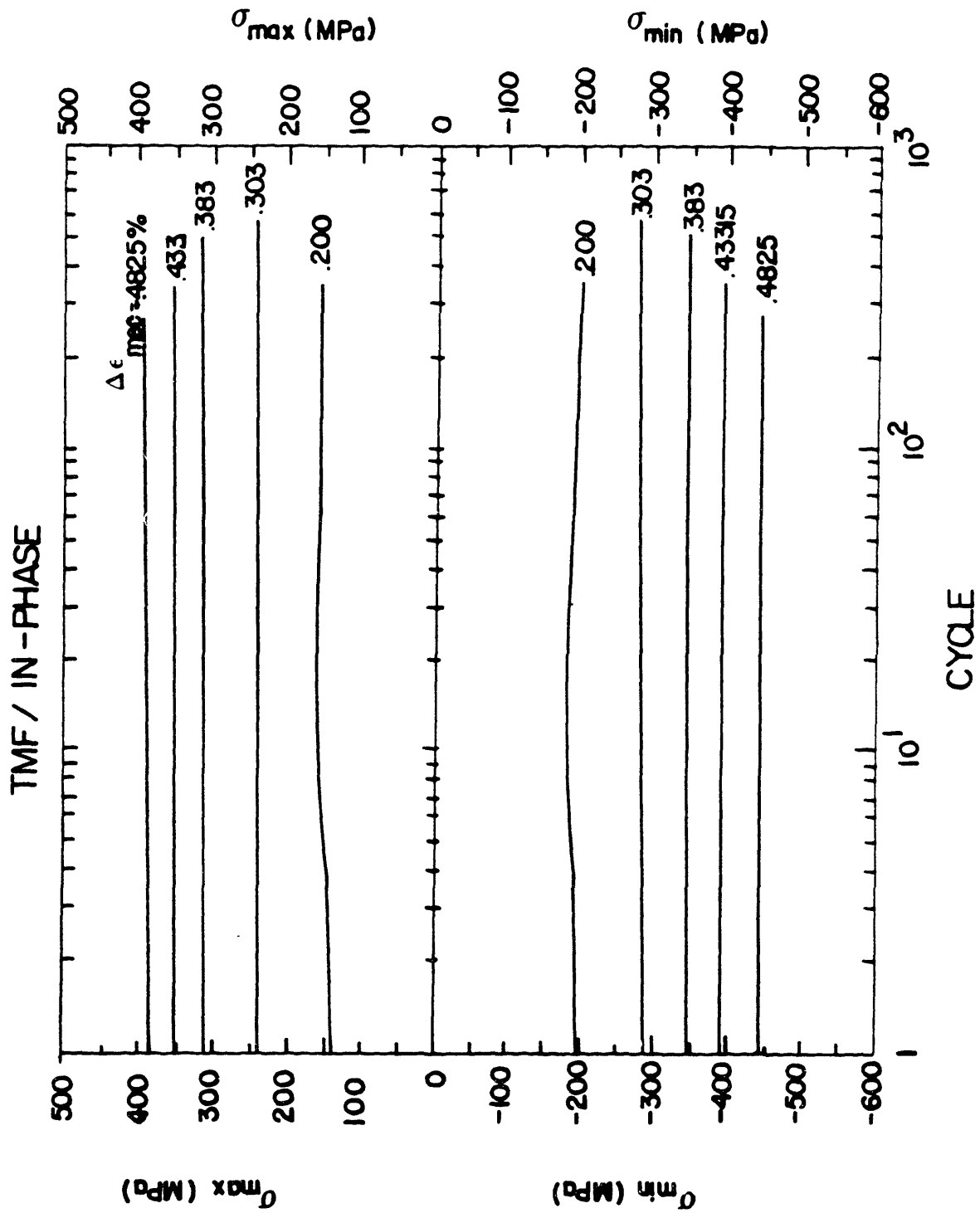
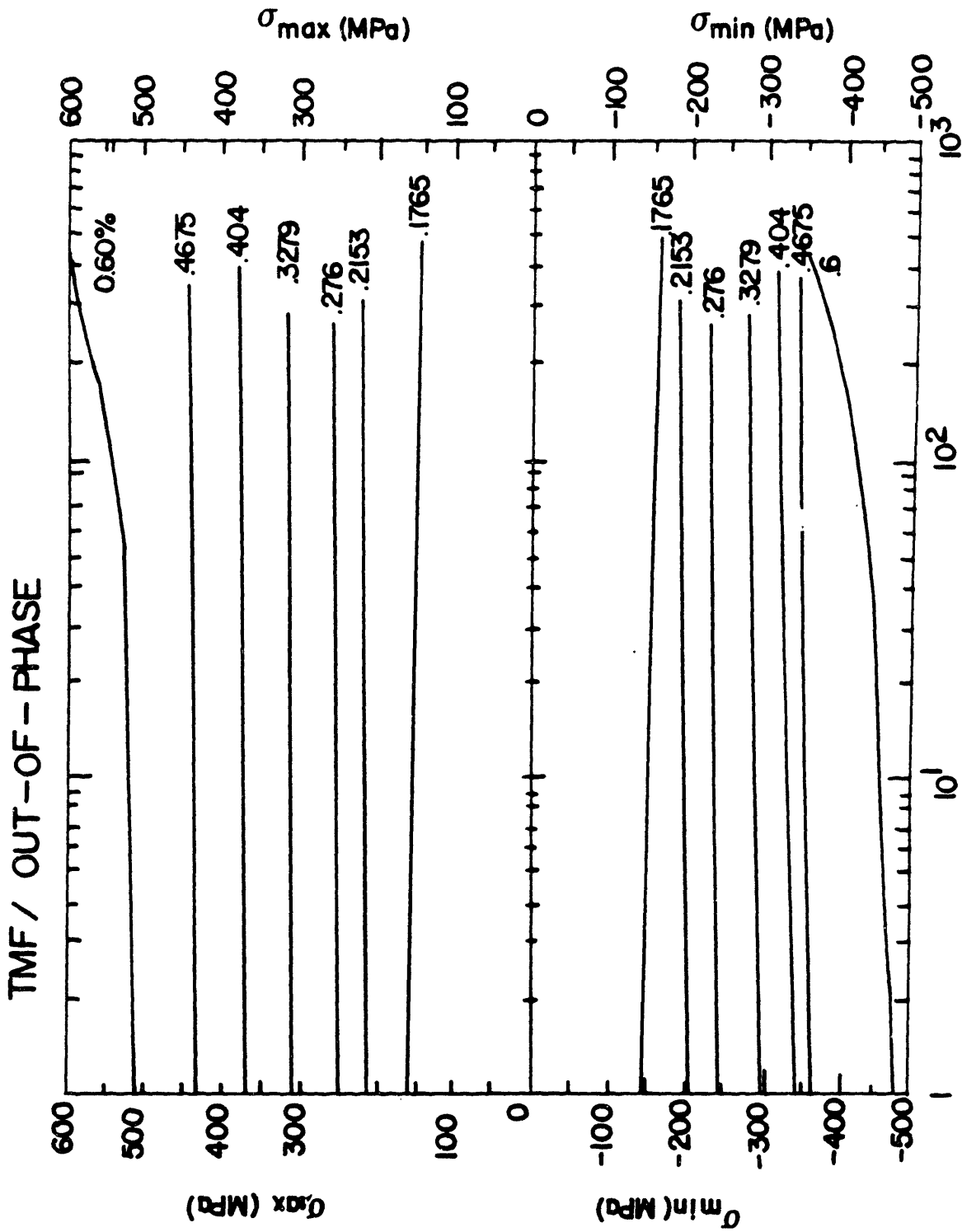


Figure 5.22 Cyclic hardening curves in B-1900+Hf(in-phase).



CYCLE

Figure 5.23 Cyclic hardening curves in B-1900+Hf(out-of-phase).

values of tensile stress. On the other hand, because σ_{\min} stayed almost unchanged and σ_{\max} hardened for in-phase cycling, the net result is a softening of the mean stress, that is $|\bar{\sigma}|$ decreases.

In this series of tests, saturation was defined such that the change in stress range ($\Delta\sigma$), in about fifty cycles, was less than or equal to two percent. The values of σ_{\max} , σ_{\min} and $\bar{\sigma}$ were plotted against the strain amplitude ($\Delta\varepsilon_{\text{tot}}/2$) to obtain the cyclic stress-strain (CSS) curves for in-phase and out-of-phase cycling. These curves are shown in Figures 5.24 and 5.25 along with the iso-thermal data obtained at 538 and 871°C [123, 126]. Interesting conclusions can be drawn from Figures 5.24 and 5.25. First, one can see that the CSS curves of in-phase, out-of-phase and isothermal testing converge at low $\Delta\varepsilon_{\text{tot}}/2$ (< 0.0012) but diverge as $\Delta\varepsilon_{\text{tot}}/2$ increases. At higher strain amplitude but lower than 0.28%, the maximum stress (σ_{\max} at 925°C) for in-phase cycling is higher than isothermal fatigue at 871°C. For $\Delta\varepsilon_{\text{tot}} > 0.28\%$, the inverse is observed, that is, a higher hardening rate for isothermal fatigue than for σ_{\max} of in-phase cycling. The hardening rate of σ_{\min} of in-phase cycling ($T = 400^\circ\text{C}$) is identical to the hardening measured for isothermal fatigue at 538°C. For out-of-phase cycling, σ_{\min} (at $T = 925^\circ\text{C}$) also show higher hardening rate than isothermal fatigue at 871°C ($\Delta\varepsilon_{\text{tot}}/2 < 0.25\%$), and a lower hardening rate for $\Delta\varepsilon_{\text{tot}}/2 > 0.25\%$ than isothermal fatigue. However, σ_{\max} (at $T = 400^\circ\text{C}$) shows a higher hardening rate than isothermal fatigue at 538°C.

The hardening behavior of in-phase and out-of-phase cycling were compared by plotting σ_{\max} of in-phase, and $|\sigma_{\min}|$ of out-of-phase on the same plot (both measured at 925°C). σ_{\min} of in-phase and σ_{\max} of out-of-phase cycling (both measured at 400°C) were also plotted.

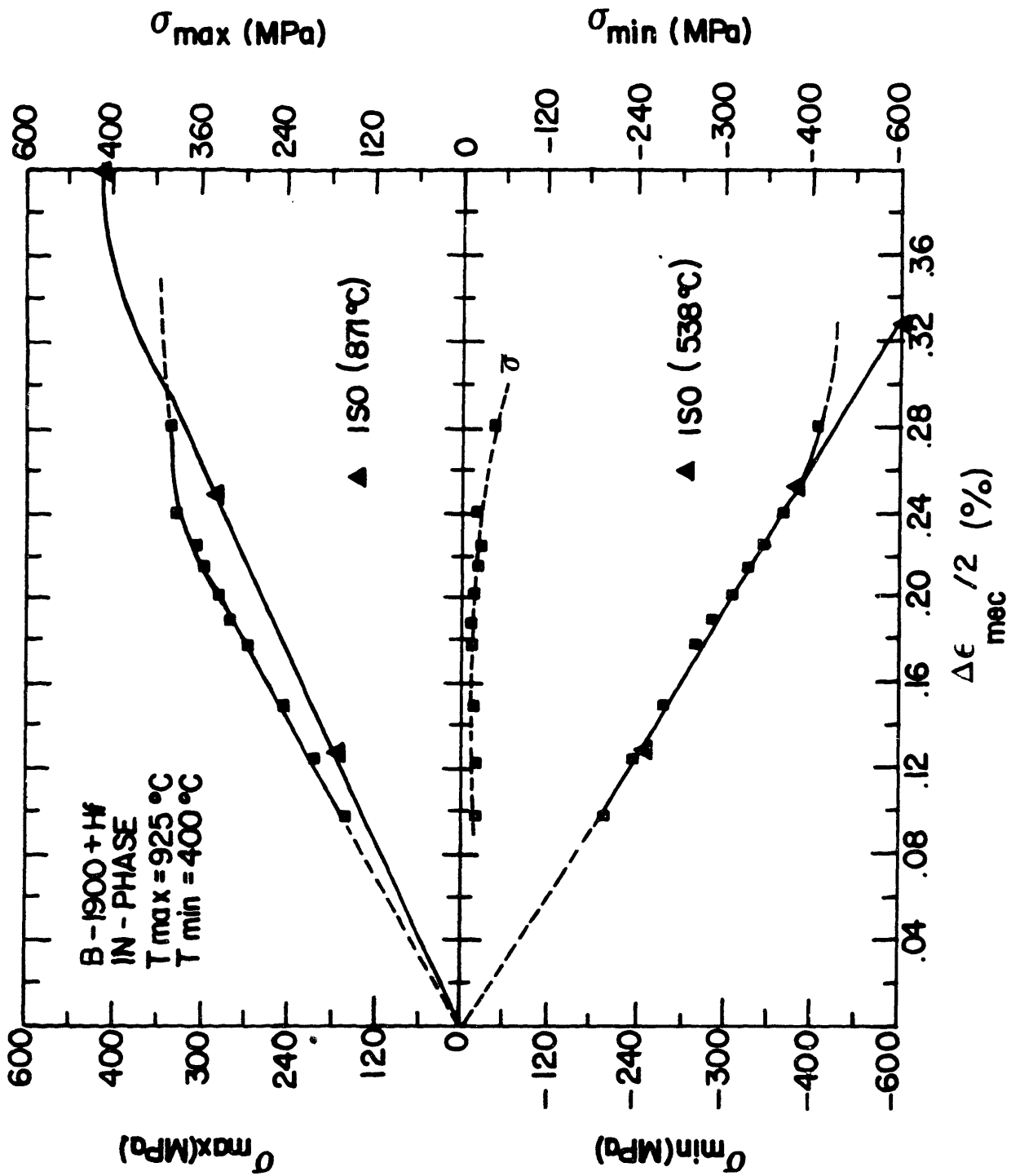


Figure 5.24 Cyclic stress-strain curves in B-1900+Hf. Isothermal (538 and 871 °C) versus in-phase cycling.

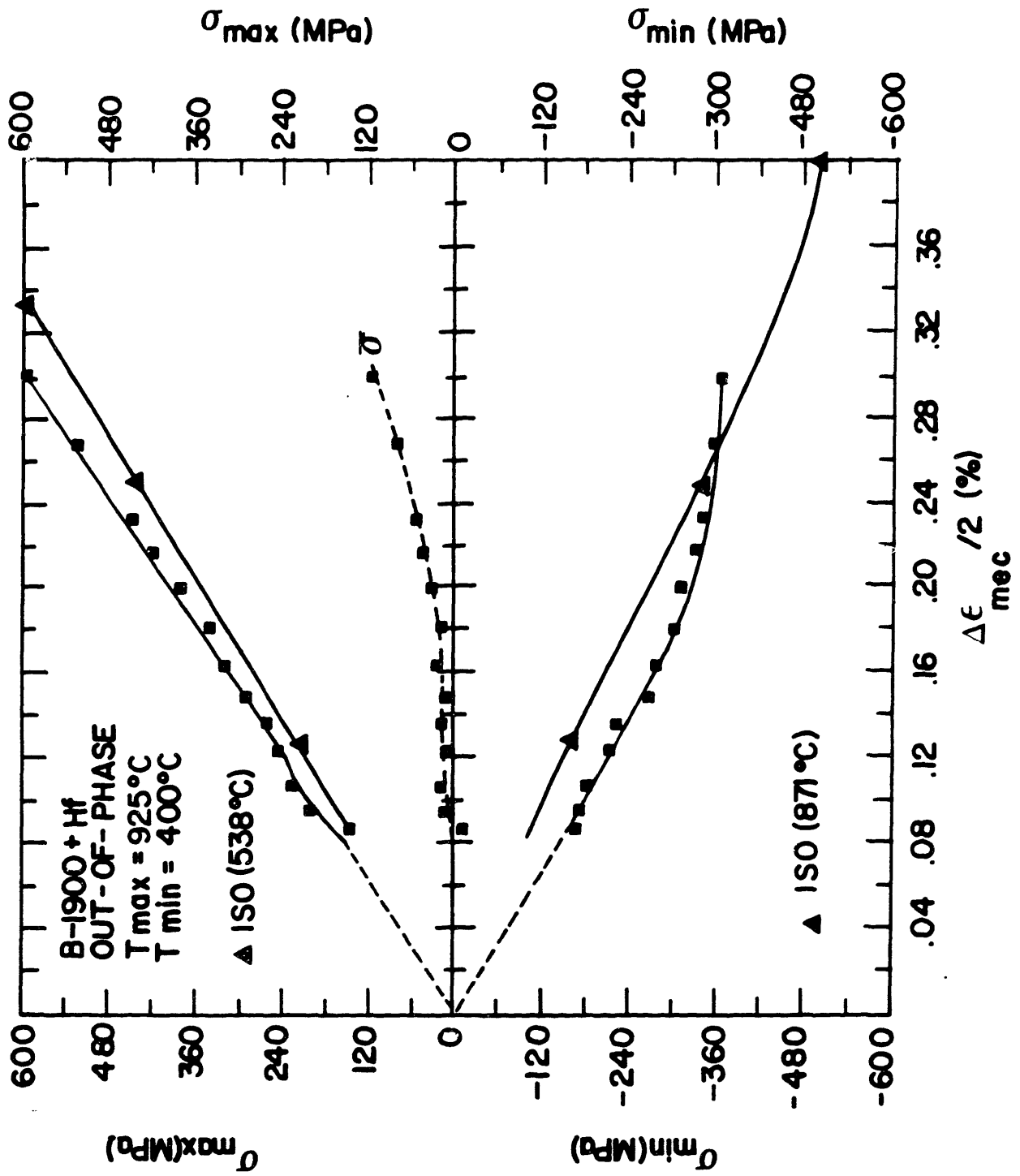


Figure 5.25 Cyclic stress-strain curves in B-1900+Hf. Isothermal (538 and 871 °C) versus out-of-phase cycling.

Figure 5.26 shows the results. One can see that the hardening at 925°C is higher for in-phase (tension) than for out-of-phase cycling (compression). However, the hardening rate at 400°C was higher for out-of-phase (tension) than for in-phase (compression) or isothermal cycling.

In order to clearly identify the process of crack growth, the long transverse and longitudinal sections perpendicular to the fracture surface were mounted for metallographic observation. For out-of-phase cycling, multiple cracks were observed along the gauge length (Figures 5.27a and 5.27b). The propagation path is transgranular and had proceeded interdendritically (Figure 5.27c). Examination of the specimen failed under in-phase cycling revealed a varying degree of transgranular and intergranular cracking (Figures 5.28a and 5.28b) with a density of surface cracks much lower than out-of-phase cycling. The fracture path, however, appears mainly intergranular (Figure 5.28c). These conclusions were supported by SEM fractographic observations.

5.4 Thermal-Mechanical Fatigue Crack Growth Properties

5.4.1 Inconel X-750

The Inconel X-750 specimens were precracked at room temperature under a cyclic stress intensity factor (ΔK_{σ}) of about 15 MPa $\sqrt{\text{m}}$. The ΔK_{σ} 's were calculated with the following expression

$$\Delta K_{\sigma} = \frac{\Delta N}{BW} (\pi a)^{1/2} \left\{ F_1(\zeta) - 6F_2(\zeta) \cdot \left(\frac{C_{12}(\zeta)}{12(L/W) + C_{22}(\zeta)} \right) \right\} \quad 5.1$$

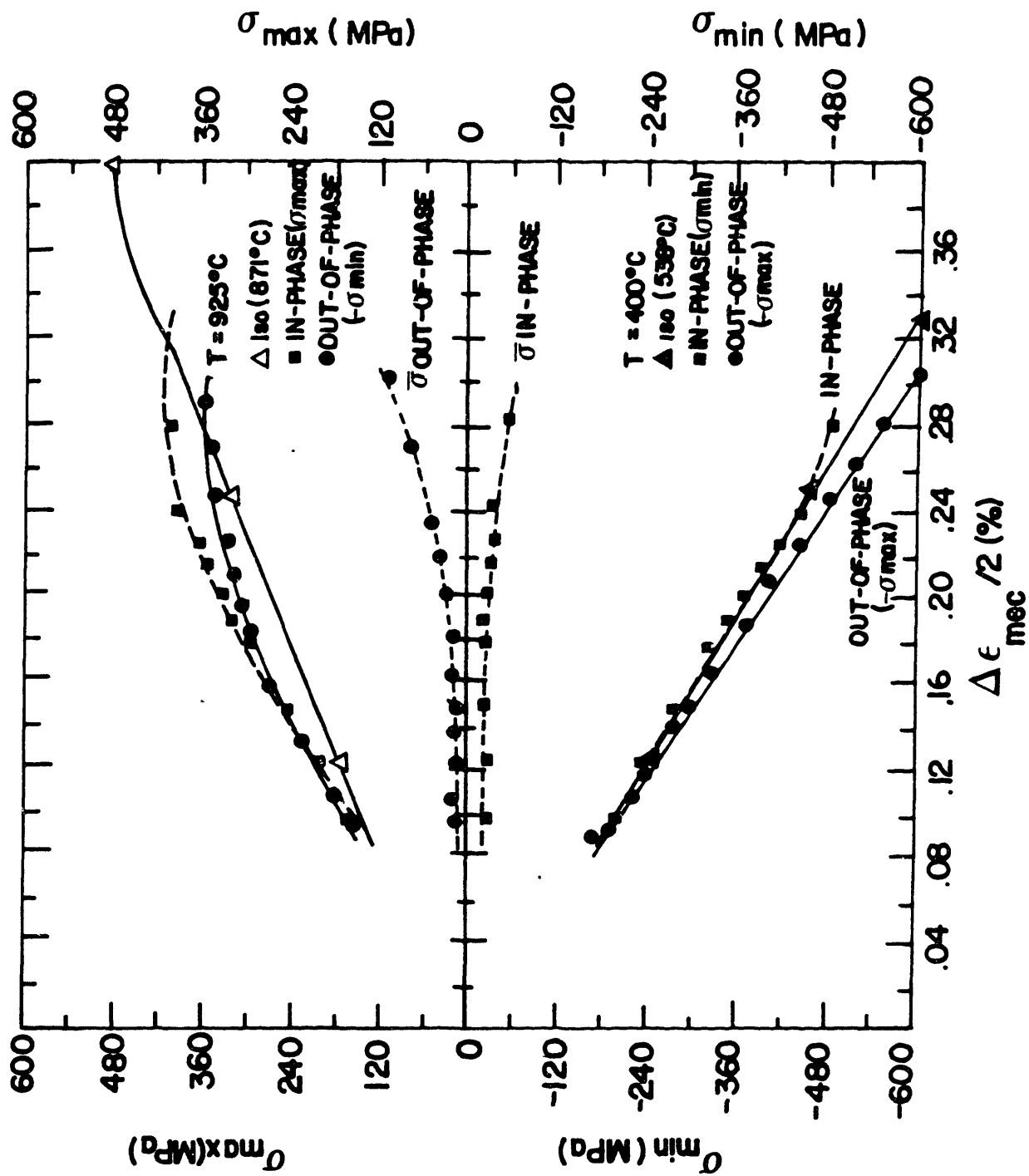


Figure 5.26 Cyclic stress-strain curves in B-1900+Hf. In-phase, out-of-phase and isothermal (538 and 871 °C).



Figure 5.27 Intergranular cracking in B-1900+Hf cycled under in-phase conditions. (a) Longitudinal section. (b) transverse section. (c) intergranular cracks.

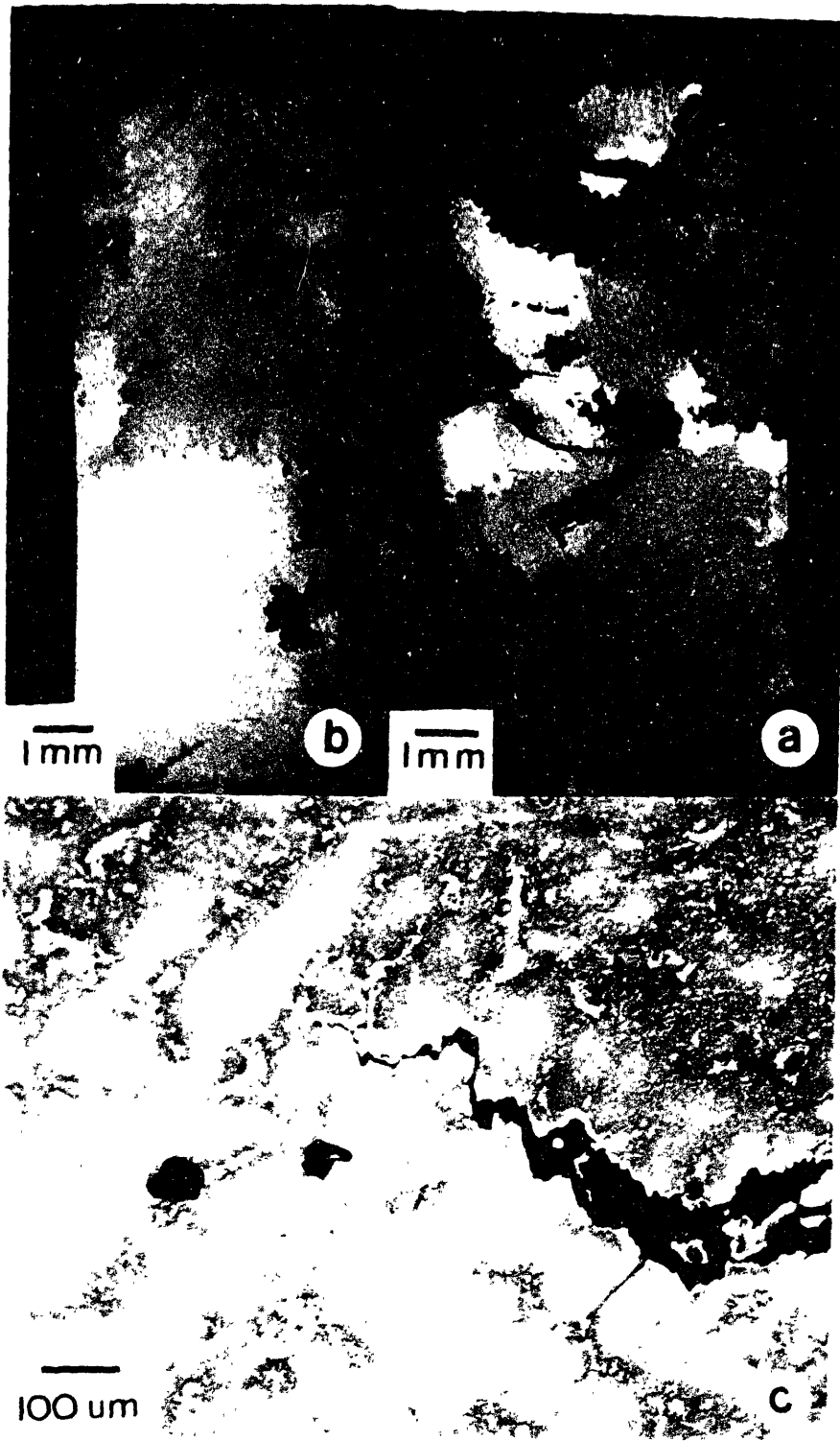


Figure 5.2: Transgranular cracking in B-1900+Hf cycled under out-of-phase conditions. (a) longitudinal section, (b) transverse section, (c) interdendritic cracking.

where $\zeta = a/w$, $F_1(\zeta)$, $F_2(\zeta)$, $C_{11}(\zeta)$, $C_{12}(\zeta)$ and $C_{22}(\zeta)$ geometry correction factors (see Appendix V). This expression was derived for an edge crack in a SEN plate with no bending. For long cracks ($a/w > 0.3$), the error between Eq. 5.1 and Harris' equation [145]

$$\Delta K_{\sigma} = \frac{\Delta N}{BW} (\pi a)^{1/2} \left\{ \frac{25}{20-13(a/w)-7(a/w)^2} \right\}^{1/2} \quad 5.2$$

is about 15% and increases steadily with increasing crack length. From the peak potential versus number of curve (see Appendix II), the crack lengths versus N_c (number of cycle) curves were obtained. The crack growth rates were computed using a seven-point incremental polynomial method. Figure 5.29 shows the crack growth data (da/dn) as a function of ΔK_{σ} ($R = 0.05$) or K_{max} ($R = -1$). This figure shows that TMF cycling is more damaging than isothermal cycling. Furthermore, it shows that fully cycling ($R = -1$) is more damaging than tension-tension cycling ($R = 0.05$) which indicates that compressive straining enhances crack growth by enhancing fracture at the crack tip during the tensile going part of the cycle. The implication of this observation will be discussed further.

Examination of the fractured specimens showed that intergranular cracking was the predominant mode of fracture for the isothermal and in-phase cycled specimens. Out-of-phase cycling shows a transgranular path of fracture.

5.4.2 B-1900+Hf

All TMFCG tests on B-1900+Hf were conducted under strain-controlled conditions. Prior to testing, the specimens were fatigue-

FATIGUE CRACK PROPAGATION

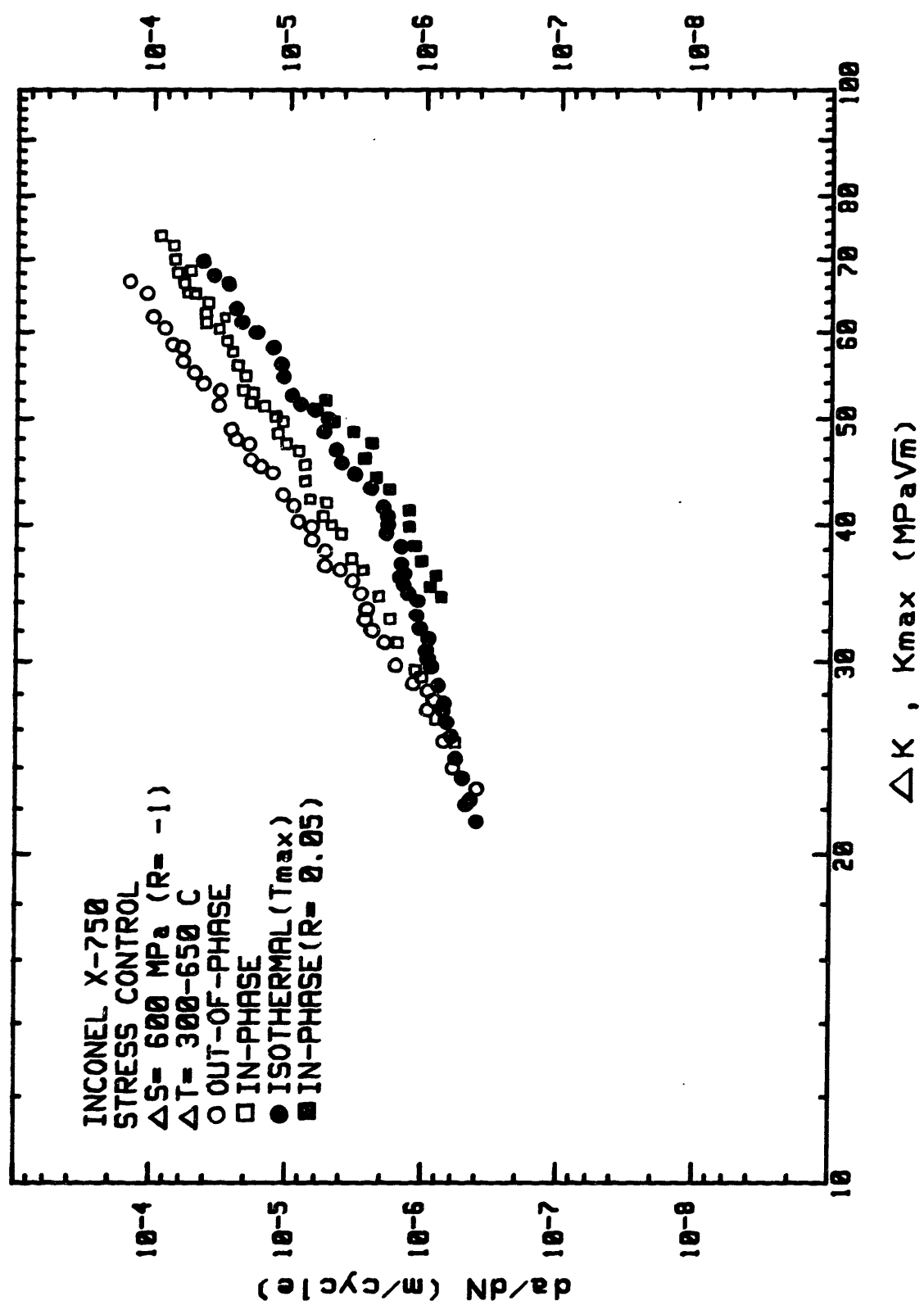


Figure 5.29 Summary of the TMFCG in Inconel X-750 cycled under load-control.

precracked in load control at 10 Hz and room temperature up to a ΔK_{σ} of about 20 MPa \sqrt{m} . Figures 5.30 to 5.32 show the crack growth rates as a function of the strain intensity factor (ΔK_{ϵ}) computed from

$$\Delta K_{\epsilon} = \Delta \epsilon \cdot (\pi a)^{1/2} \cdot \frac{F_1(\xi) \left\{ 1 - \frac{6F_2(\xi)}{F_1(\xi)} \cdot \frac{\hat{C}_{12}(\xi)}{(12\eta_b + \hat{C}_{22}(\xi))} \right\}}{\left\{ 1 + \frac{1}{\eta} \left[\hat{C}_{11}(\xi) - \frac{\hat{C}_{12}^2(\xi)}{12\eta_b + \hat{C}_{22}(\xi)} + \frac{6\hat{C}_{12}(\xi)(\eta - \eta_b)}{12\eta_b + \hat{C}_{22}(\xi)} \right] \right\}} \quad 4.2$$

also derived in Appendix V. There $\zeta = a/w$, $\eta = L/W$, $\eta_b = L_b/W$ and $C_{11}(\zeta)$, $C_{12}(\zeta)$, $C_{22}(\zeta)$, $F_1(\zeta)$ and $F_2(\zeta)$ geometry correction factors. The ΔK_{ϵ} were used for convenience because TMF is a strain-controlled process. Although ΔK_{ϵ} , as defined by Eq. 4.2, lacks physical meaning under TMF conditions, it is for the case of isothermal and elastic conditions

$$\Delta K_{\epsilon} = \Delta K / E' \quad 4.3$$

where ΔK is the stress-intensity factor derived for fixed-ends displacement loading (see Appendix V). This definition of ΔK_{ϵ} was chosen because the conventional definition lacks of mechanistic understanding and overestimates the actual ΔK_{ϵ} even under elastic conditions (see Appendix V).

Figure 5.30 shows the TMFCG rates measured during out-of-phase cycling at $\Delta \epsilon = 0.25\%$. All the data are plotted as to provide an indication of the scatter in the testing procedure. Figures 5.31 and 5.32 summarize the results for $\Delta \epsilon = 0.25\%$ and $\Delta \epsilon = 0.50\%$ at $\nu = 0.0055$ Hz (1/3 cpm). All the FCGR data measured isothermally and during TMF cycling are shown in Appendix IV.

Figure 5.31 shows that TMFCG rates are faster than their isothermal counterpart under fully elastic cycling. At higher strain ranges (Figure 5.32), the opposite behavior is observed, i.e. faster crack

FATIGUE CRACK PROPAGATION

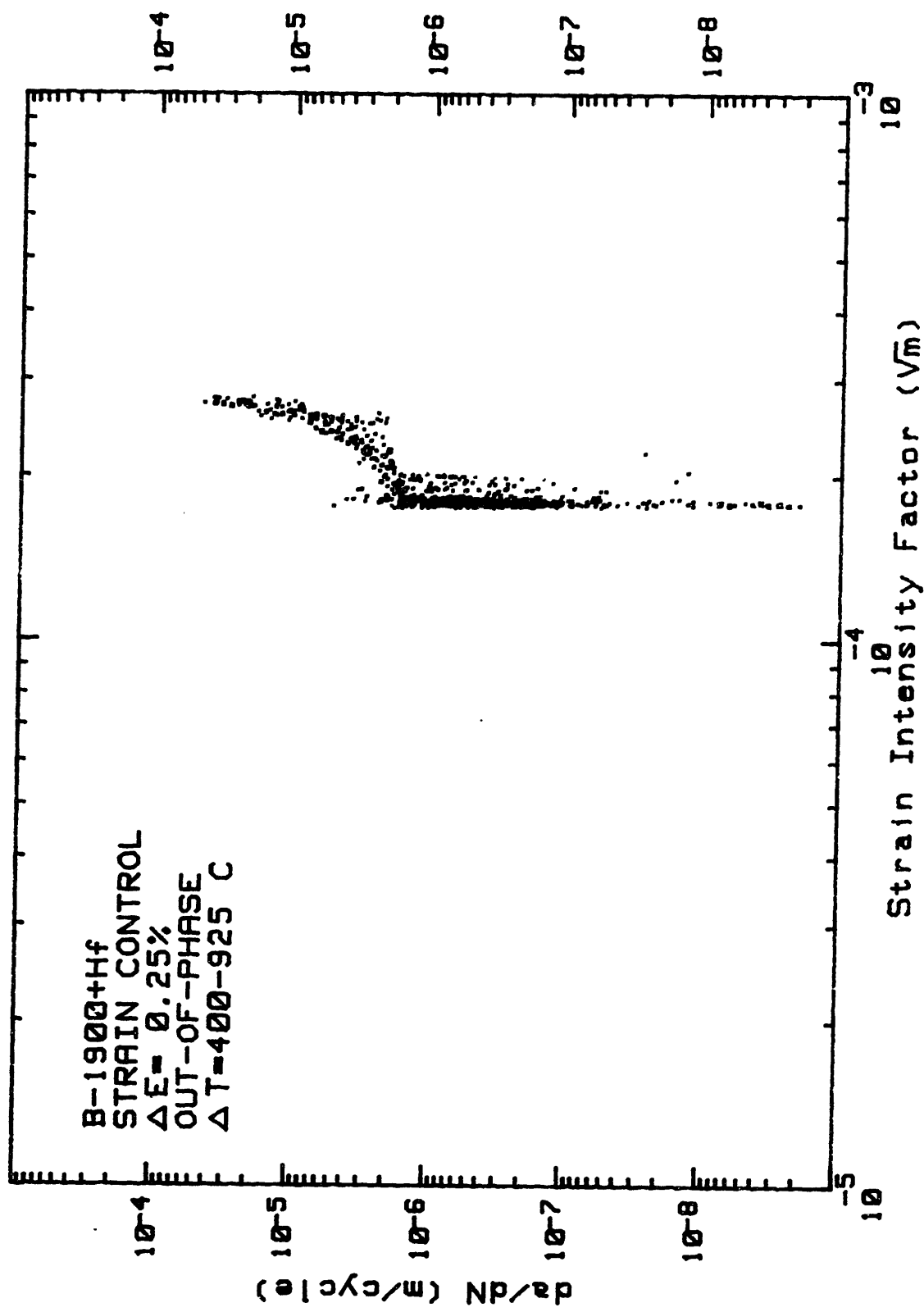


Figure 5.30 TMFCG rates in B-1900+Hf under out-of-phase cycling ($\Delta \epsilon_{mec} = 0.25\%$).

FATIGUE CRACK PROPAGATION

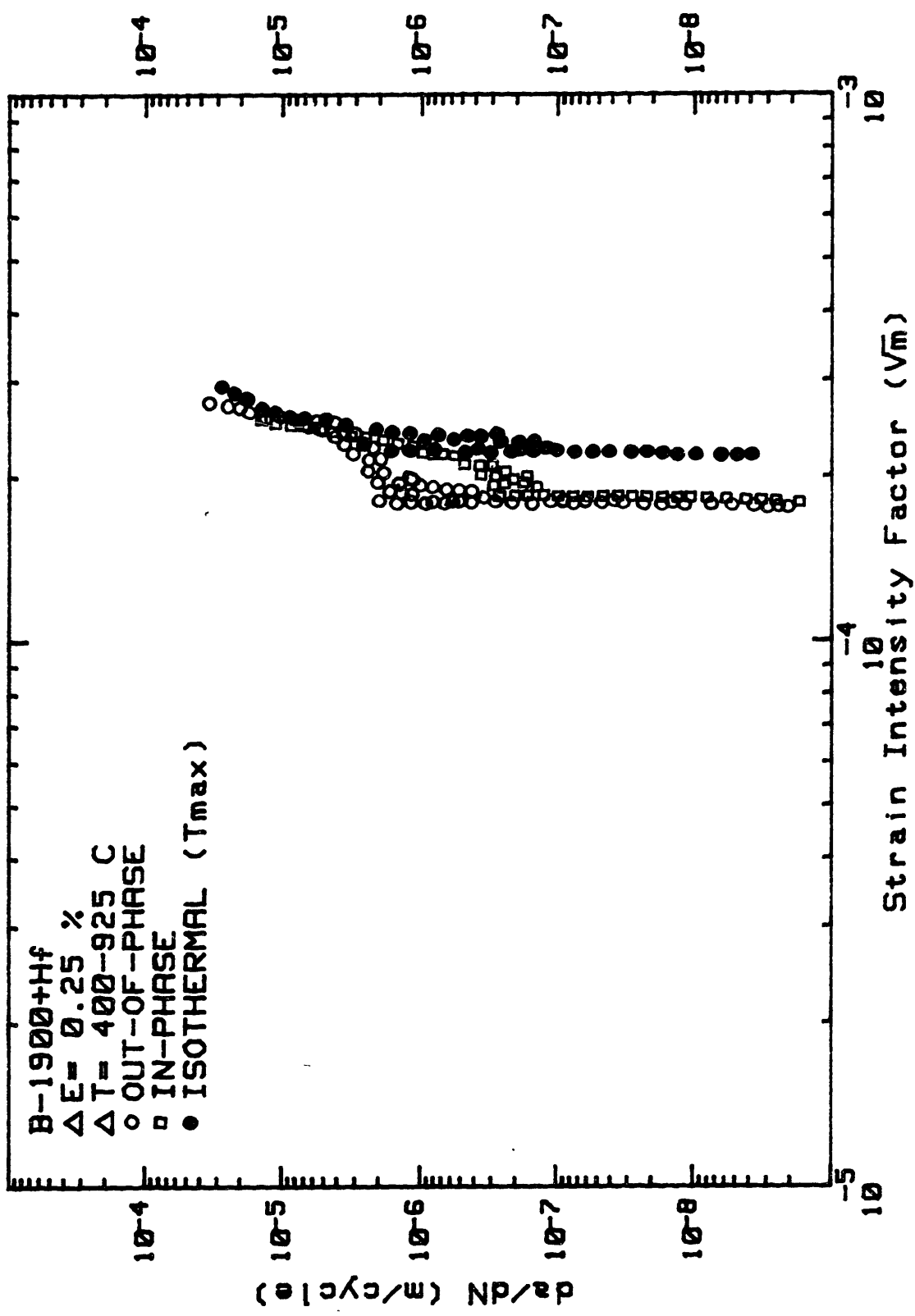


Figure 5.31 Summary of the TMFCG rates in B-1900+Hf cycled under strain-control ($\Delta \epsilon_{mec} = 0.25\%$).

FATIGUE CRACK PROPAGATION

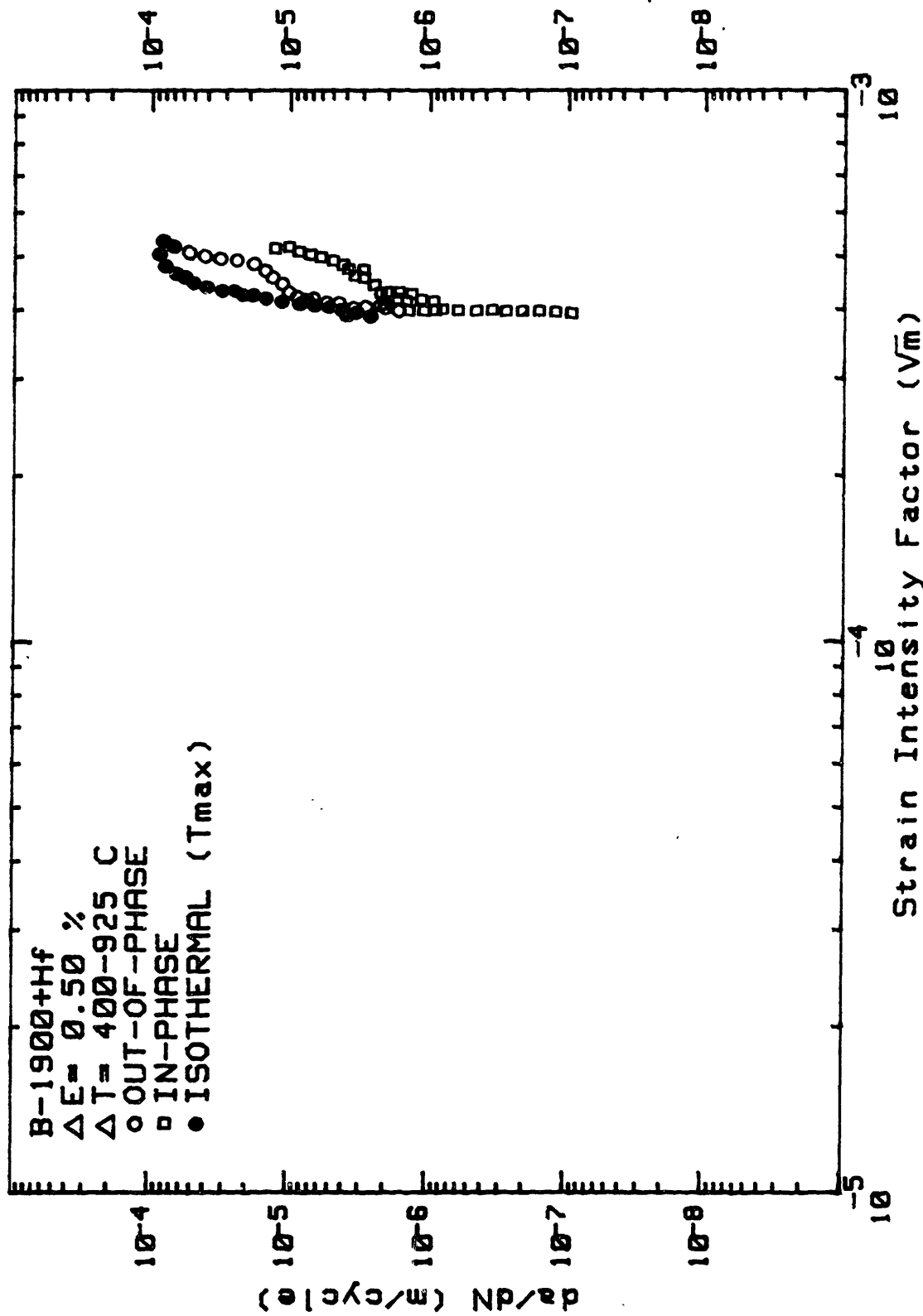


Figure 5.32 Summary of the TMFCG rates in B-1900+Hf cycled under strain-control ($\Delta \epsilon_{mec} = 0.50\%$).

growth rates are observed under isothermal conditions than under TMF conditions.

Comparison of Figures 5.31 and 5.32 shows that there is a strain range effect, i.e. the strain intensity factor does not correlate the TMF and isothermal data. In other words, if ΔK_{ϵ} is the appropriate driving force, then the growth rates data measured at low and high strain ranges would lie on a master curve.

At low strain range (Figure 5.31), a threshold, which delineates a domain of propagation and non-propagation, is observed in all cases. Under fully plastic cycling, a threshold is also observed, although less apparent. The TMF crack growth curves (Figures 5.31-5.32) show three distinct regimes characterized by their respective slopes. The isothermal tests always show two regimes: a threshold and a regime of rapid growth.

Figure 5.33 shows the effect of frequency on the crack propagation rates under displacement-controlled and isothermal conditions ($T = 925^{\circ}\text{C}$). Clearly, the crack growth rates increase with increasing frequency. As for Inconel X-750, the fracture mode is intergranular under in-phase and isothermal cycling at low frequency. For out-of-phase and isothermal cycling at high frequency (0.1 Hz), the mode of fracture is transgranular.

5.4.3 Hastelloy-X

As for B-1900+Hf, all tests were run under displacement-controlled conditions. The specimens were precracked in fatigue at room temperature prior to testing. Figure 5.34 and 5.35 summarize the

FATIGUE CRACK PROPAGATION

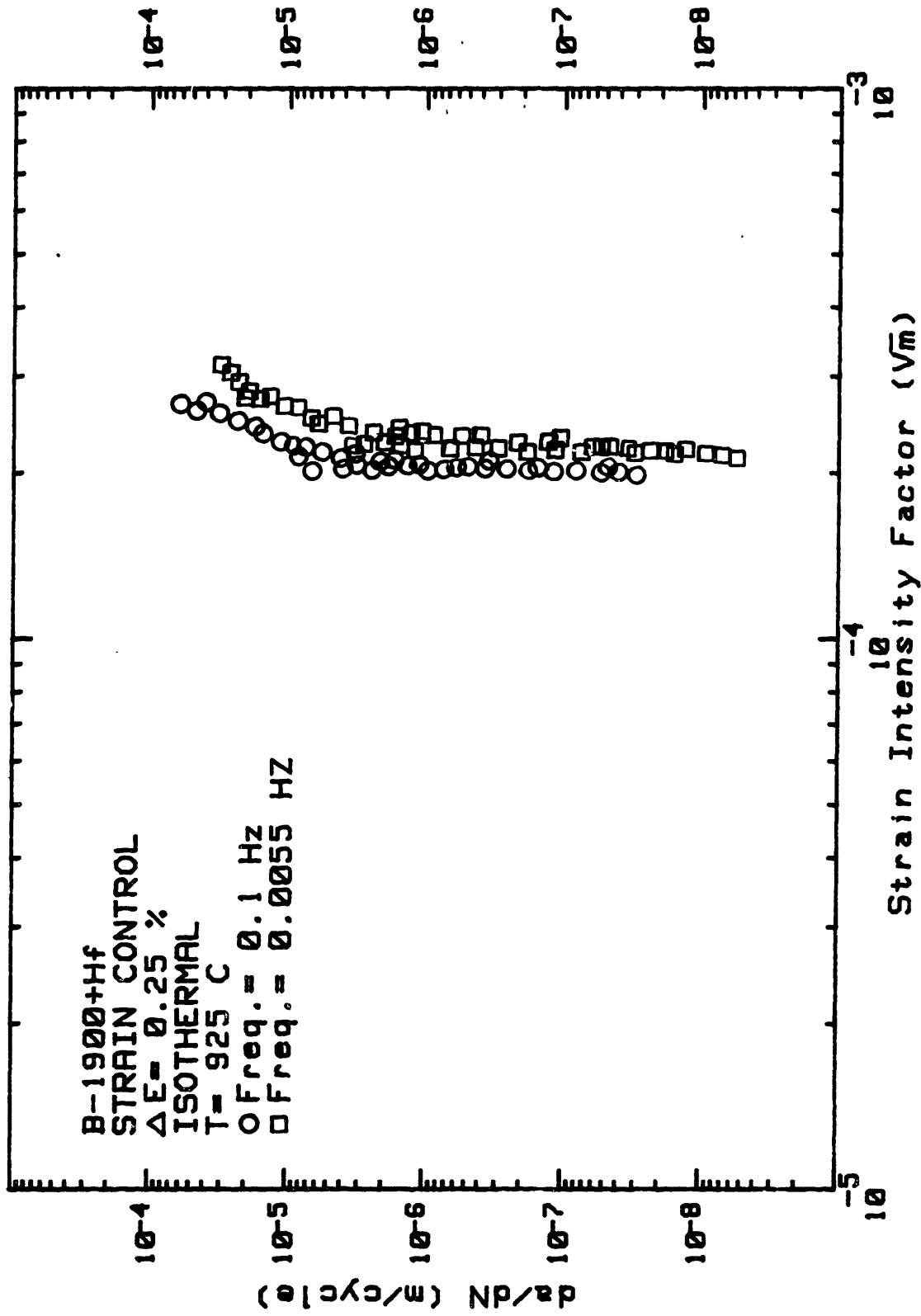


Figure 5.33 Effect of frequency on the FCG rates of B-1900+Hf cycled under strain-control.

crack growth rates as a function of the strain intensity computed with Eq. 4.2. All the FCGR curves measured isothermally and during TMF cycling are shown in Appendix IV.

Figure 5.34 shows that the crack growth rates under TMF cycling are faster than under isothermal cycling at T_{max} . Under fully plastic cycling (see Figure 5.35), the opposite behavior is observed. The crack growth data (Figures 5.34 and 5.35) show that there is a strain range effect indicating, as for the case of B-1900+Hf, that the strain intensity factor is not the universal driving force for TMF crack growth.

The fracture mode at low temperature (isothermal) is transgranular, whereas it is intergranular at high temperature. For TMF cycling, transgranular cracking is observed under out-of-phase conditions, whereas intergranular cracking is observed under in-phase cycling. These observations are consistent with what is observed for Inconel X-750 and B-1900+Hf. This indicates that there is hope to define a parameter that describes the growth rates of a crack under elastic and fully plastic conditions, for both isothermal and thermal-mechanical fatigue.

FATIGUE CRACK PROPAGATION

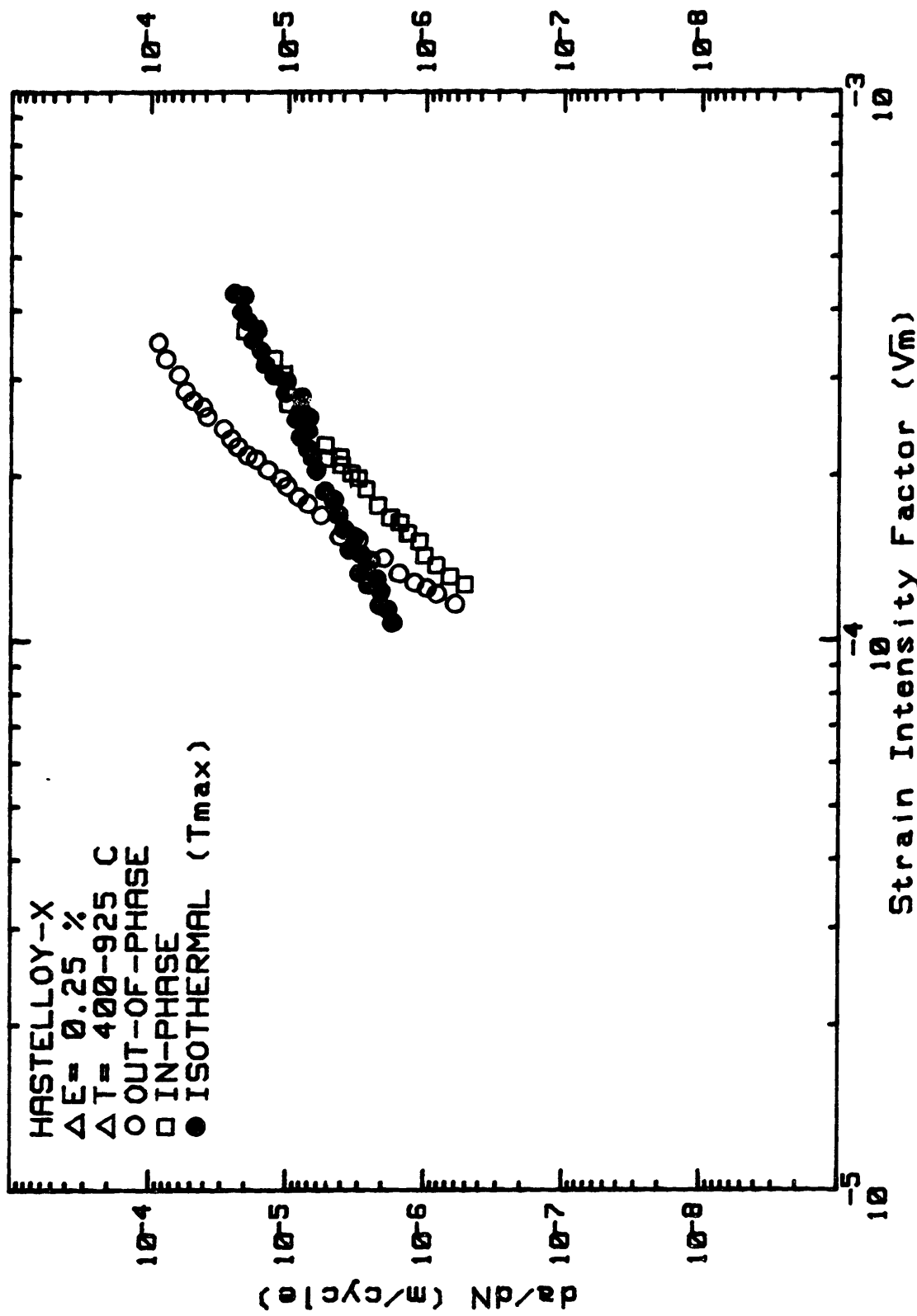


Figure 5.34 Summary of the TMFCG rates in Hastelloy-X cycled under strain-control ($\Delta \epsilon_{mec} = 0.25 \%$).

FATIGUE CRACK PROPAGATION

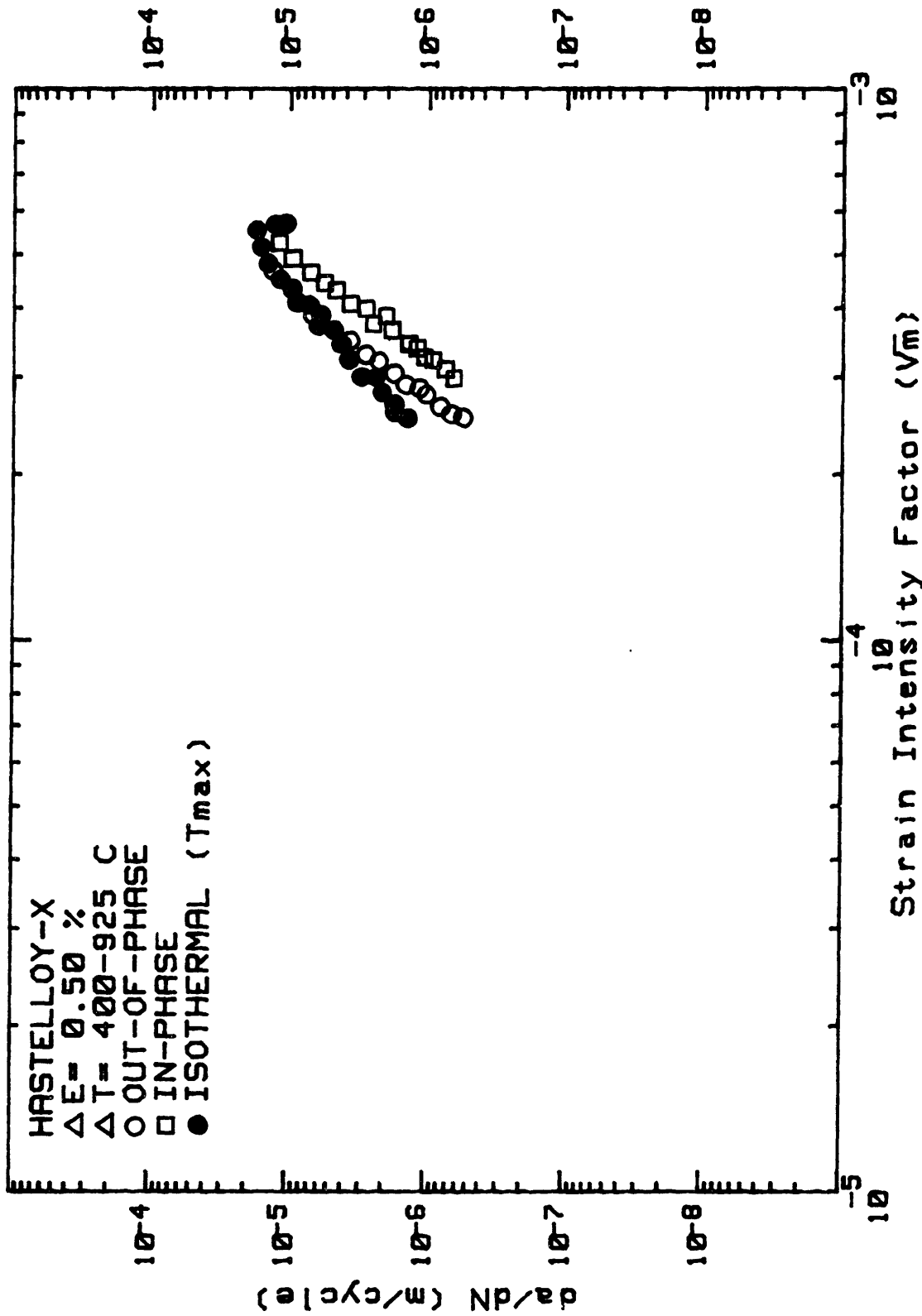


Figure 5.35 Summary of the TMFCG rates in Hastelloy-X cycled under strain-control ($\Delta \epsilon_{mec} = 0.50\%$).

6.0 Discussion

6.1 Isothermal Creep and Low Cycle Fatigue Behaviors (Life)

The creep data as shown in Figure 5.5 fall within the anticipated scatter. Extrapolation of the results to stress levels typical of those achieved during fatigue cycling (i.e., $\sigma_{\max} < 200$ MPa at $T = 925^{\circ}\text{C}$) leads to time to fracture of 10,000 hours or longer. Because the corresponding fatigue lives are in the order of 200 hours or lower, it is likely that the creep strains experienced by B-1900+Hf (or Inconel X-750) are negligible, and that most of the time-dependent damage is caused by environmental degradation rather than by creep. In other words, creep is not a significant problem for isothermal and TMF testing of B-1900+Hf and Inconel X-750 as far as the strain and temperature ranges used in this investigation are concerned. Because these strain ranges and temperature ranges are typical of those encountered in many commercial aircraft engines, the same conclusion concerning the relevance of creep damage to life predictions of these components are likely to apply.

For other materials such as Hastelloy-X, creep strains can be of significant importance because even the low stresses achieved during cycling ($\sigma_{\max} \approx 100$ MPa at 925°C) can cause creep damage as can be seen in Figures 5.6 and 5.7. In that case, changing the applied strain range not only changes the fatigue response of the material (time-dependent component), but also changes the creep response of the materials. This extra variable will add to the scatter in the results.

The results showing the isothermal life behavior of B-1900+Hf and Hastelloy-X at various temperatures (Figures 5.8-5.13) clearly indicate that low cycle fatigue, expressed in terms of strain range vs number of cycle to failure, is a stochastic process having considerable variability. It is worth noting the scatter in Figure 5.10. As mentioned before (see section 3.5), this is expected since life data depend on initiation/propagation ratios, sensitivity to strain rate, ductility, which in turn depend on the geometry of the specimen, surface finish, etc. It is obvious then, that life prediction based on life data requires the use of a stochastic parameter to take into account this variability. However, the quantitative determination of this parameter requires extensive testing. Because the models based on life data failed to recognize the fact that they are dealing with a stochastic process, the poor correlation between their predictions and the actual life is not surprising [26, 66, 128, 130]. In particular, the SRP (Strain Range Partitioning) and FS (Frequency Separation) approaches not only give poor predictions [26, 41, 66, 128, 130], but failed to predict the effect of temperature as shown in Figures 5.14 and 5.15. There are numerous new evidences that the Coffin-Manson approach (SRP, FS, etc.) is virtually identical to the growth law of small crack [149-153]. Furthermore, all these results suggest that we must pay attention to the behavior of small crack in order to solve low-cycle fatigue problems. In other words, a fracture mechanics approach is required for more adequate life predictions.

As pointed out earlier, the life data plotted in terms of total strain ranges instead of the inelastic strain ranges, provide a rationale for the effect of temperature on the fatigue life, i.e. the higher the temperature, the shorter the fatigue life. This indicates that stress-based fracture

criteria are likely to be more successful for life prediction than strain-based fracture criteria.

The fact that life data do not provide a safe way to life prediction, does not mean that these tests should not be performed. The value of these tests lies in the fact that they provide valuable information on how a material responds (hardening/softening) to some imposed cyclic conditions. From these tests, appropriate constitutive equations relating cyclic stresses and strains are derived which in turn are used in more advanced life prediction schemes like the damage-tolerant approach.

6.2 The TMF Cyclic Responses of B-1900+Hf

Typical hardening/softening behavior observed under TMF cycling are shown in Figures 5.20 and 5.21. These curves show that σ_{\max} (T = 400°C) hardened and σ_{\min} (T = 925°C) softened for out-of-phase cycling. During in-phase cycling, σ_{\max} (T = 925°C) hardened, whereas σ_{\min} (T = 400°C) remains unchanged. During isothermal fatigue, the cyclic flow stress was either unchanged or showed a small amount of softening [123] at high temperatures. Obviously, the damage occurring during TMF and isothermal fatigue are different. To rationalize the observed behaviors, transmission electron microscopy (TEM) of the failed specimens were performed with a JEOL 100CX operated at 120 KeV. The thin foils were taken parallel to the loading axis and at least two foils per specimen were made in order to get a better understanding of the average damage in the bulk specimen. Figures 6.1 and 6.2 show typical dislocations substructures obtained under in-phase and out-of-phase conditions. In all cases, coarsening of

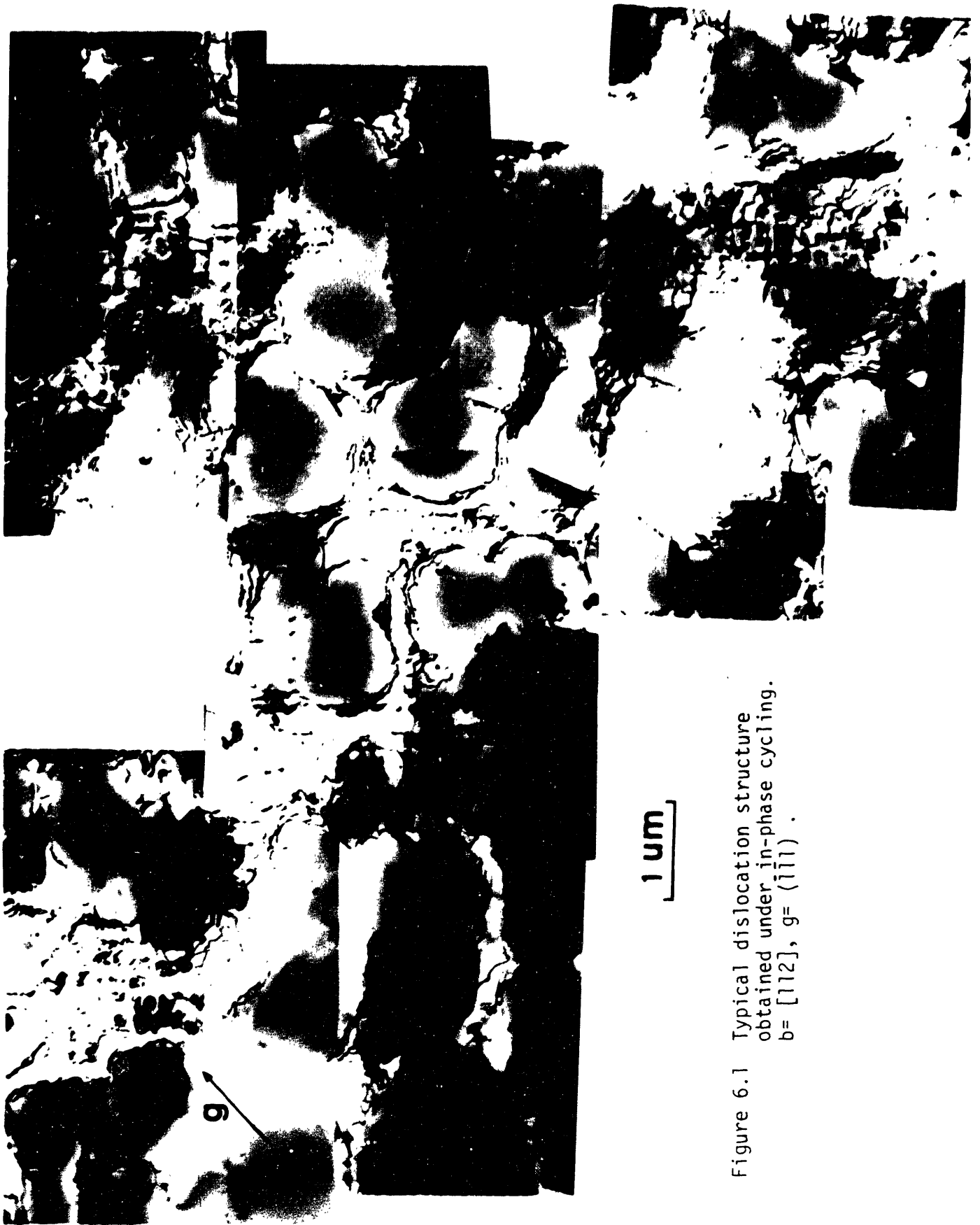


Figure 6.1 Typical dislocation structure obtained under in-phase cycling. $b = [112]$, $g = (\bar{1}\bar{1}1)$.

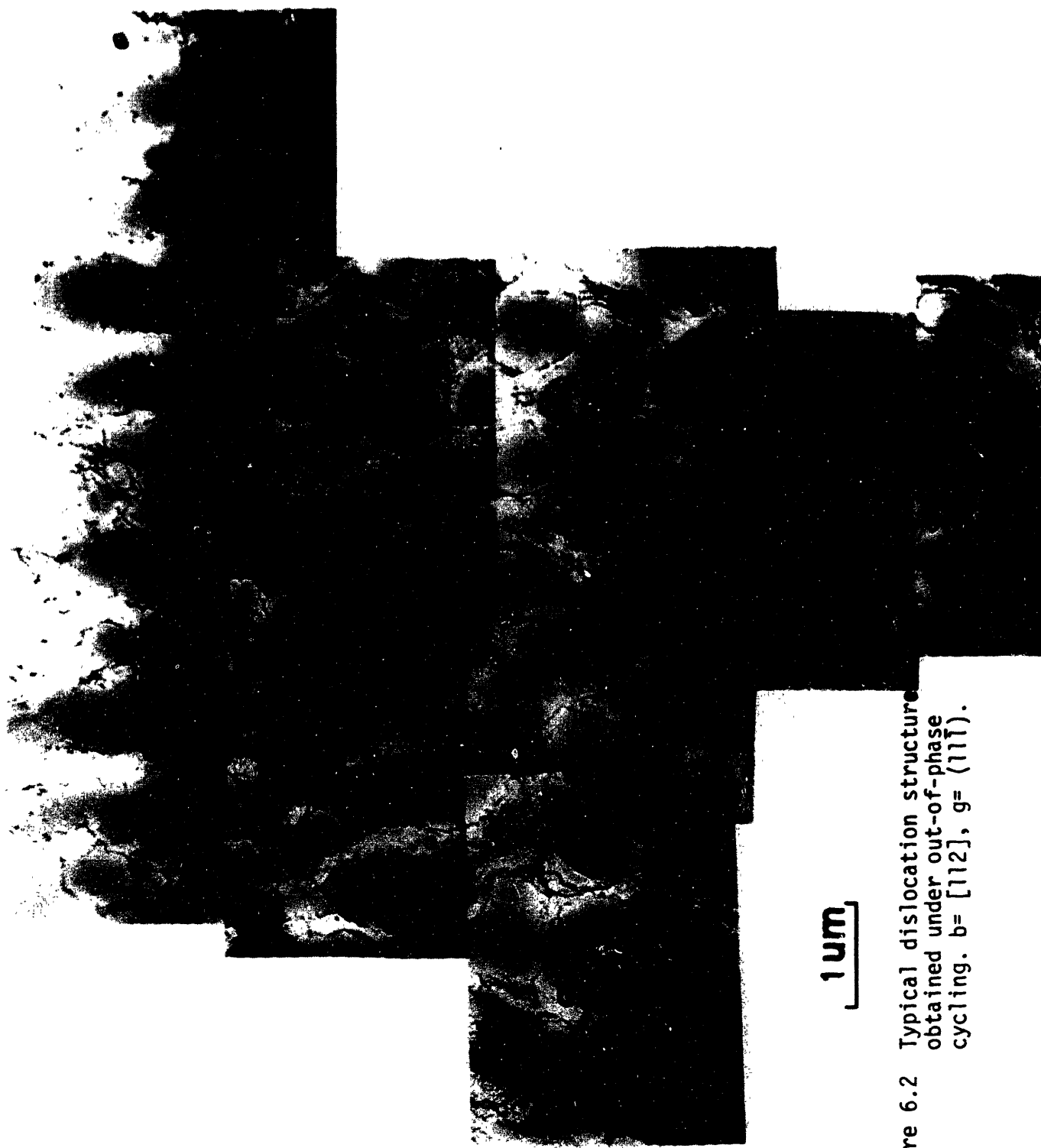


Figure 6.2 Typical dislocation structure obtained under out-of-phase cycling. $b = [112]$, $g = (11\bar{1})$.

the γ' phase has taken place, becoming more pronounced under in-phase conditions. In some grains of the specimens cycled under in-phase conditions, directional coarsening (rafting) is observed (Figure 6.3). Little or no rafting was observed under out-of-phase cycling. A tight dislocation network encapsulating the γ' can be observed in Figures 6.1 and 6.3 (in-phase cycling), whereas a loose dislocation network is observed in Figure 6.2 (out-of-phase cycling) as can be seen from the dislocation spacing. These observations show that the dislocation density is higher under in-phase than under out-of-phase cycling. The octahedral active systems were found to be $\{111\} [110]$, $\{111\} [101]$ and possibly $\{111\} [011]$ in both cases. Three Burgers vectors were identified using the invisibility criterion and assuming that the dislocations were screw in character. These Burgers vectors are $a/2[110]$, $a/2[101]$, and $a/2[011]$ indicating that at least three slip systems were operative. Comparison with specimens failed under isothermal cycling [21] shows that the dislocation density ranked in increasing order; isothermal (T_{\min} and T_{\max}), out-of-phase, and in-phase cycling.

The above results show that the two major microstructural features are: (1) changes in γ' precipitate morphology (Figures 6.1-6.3), and (2) introduction of a dislocation network about the γ' precipitates. It is well known [132-133] that coarsening of the γ' precipitates influences the mechanical behavior of nickel-base alloys. The task at hand is to separate the relative contribution of each structural feature to the cyclic behavior. In what follows, we will show that the increase in the cyclic flow stress during in-phase cycling is due to dislocation networks surrounding the γ' , and the lower flow stress under out-of-



Figure 6.3 Dislocation structure observed in a sample cycled under in-phase conditions showing directional coarsening of the γ' phase. $b = [112]$, $q = (111)$.

phase cycling and pronounced softening behavior (Figure 5.21) is a consequence of not only the dislocation networks strengthening, but also of the directional strain field around the γ' precipitates.

Cyclic Hardening/Softening Behavior

It is generally accepted that coherent particles can be sheared by dislocations and consequently, the work done in forcing the first dislocations through the particles will be important in determining the flow stress. The resistance to shear is governed by several factors:

1. The interaction of the cutting dislocation with the stress field of the precipitates.

2. If the lattice parameters of matrix and precipitate differ, then during shearing of the particles, misfit dislocations must be created at the precipitate-matrix interface. The magnitude of the Burgers vector of the interface dislocation will be the difference between the Burgers vector of the slip dislocation in the matrix and in the precipitate, i.e., $(b_m - b_p)$.

3. If the matrix and precipitate possess different atomic volumes, a hydrostatic interaction would be expected between a moving dislocation and the precipitate.

In the case of superalloys with high volume fraction of γ' (>50%), resistance to γ' - shearing is the primary strengthening mechanism. With the mean free edge-to-edge distance between the precipitates being smaller than the average precipitate size itself, dislocation shearing of the particle is favored over dislocation looping around the particles.

As previously mentioned, coarsening and rafting of γ' develop in this alloy. This feature can be attributed to the large lattice misfit (misfit $\sim -0.25\%$ [134]), which generates sufficient interfacial strain to produce misfit dislocations at elevated temperature. Significant deformation can occur only by dislocation penetration of the γ' phase and it is postulated that the misfit dislocation nets at the interface retards this process. Therefore, more hardening should be expected when rafting takes place because the dislocation networks surrounding the γ' are more intense (see Figures 6.1 & 6.3). On the other hand, it has been shown by Shah and Duhl [135] that the flow stress decreases as γ' size increases provided the cubic shape of the γ' is conserved. These two superimposed phenomena, with opposite effects with regard to the flow stress, determine the apparent flow stress. Figures 5.20 and 5.21 shows that the maximum stress (σ_{max}) of in-phase cycling (T_{max}) display continuous hardening with little appearance of stabilization. On the other hand, the σ_{min} curve of out-of-phase (T_{max}) displays continuous softening. This behavior has been previously observed on B-1900+Hf cycled in TMF [126] where continuous hardening of σ_{max} and softening of σ_{min} occurred until final fracture without evidence of saturation. This raises the question of the validity of the strain increment technique for measuring the CSS curves of low stacking-fault energy materials where continuous hardening (or softening) is observed until fracture [126, 136-137] at low applied strain. This behavior is usually rationalized in terms of planar configuration of dislocations [136, 138]. At high strain, where cross-slip takes place, saturation of the CSS curves is observed. Although B-1900+Hf is also a low stacking fault energy material, the planar configuration of dislocations alone

cannot explain the observed cyclic hardening/softening behavior (Figures 5.20-5.21).

At high temperature ($T \geq 600^\circ\text{C}$) the flow stress depends on the APB energy and thermally activated cross slip of the glide dislocations [135, 139]. The directionality of the internal stress field around the γ' is small because thermal activation is important. Therefore, the flow stress will depend on the factors controlling the internal stress. The density of misfit dislocations around the γ' particles, which depends on the γ' size and shape (rafting), affects the flow stress because it controls the internal stress on the glide dislocations. On the other hand, when coarsening takes place, the particle spacing increases, which leads to weakening because of the increased probability of avoiding shearing by Orowan-type mechanisms [140]. Under in-phase cycling, coarsening of the γ' takes place along with rafting, leading to high density of misfit dislocations without significant increase in interparticle spacing (Figure 6.3). The net result is an increase in the flow stress because the internal stress increases faster than the relaxation time required by the glide dislocation to overcome the barrier created by the misfit dislocations. During out-of-phase cycling, isotropic coarsening takes place leading to a smaller increase of misfit dislocations and a more significant increase of γ' particle spacing. The net result is a decrease in flow stress.

At low temperature the directionality of the resultant stress field around the γ' particles will also contribute to the internal stress acting on the glide dislocations [133, 135, 141]. With coarsening, the hydrostatic tensile stress field around the γ' increases and that is one of the reasons why misfit dislocations are required. It is well known that

the resistance to the movement of glide dislocations (partials), i.e., the frictional force, increases with increasing hydrostatic stress [142]. Therefore, the superposition of an external hydrostatic stress field will increase or decrease the flow stress depending on the magnitude and sign of the applied stress. If an external tensile stress field is applied, the frictional stresses increase and so does the flow stress. This corresponds to the out-of-phase cycling case where the applied stresses are tensile at low temperature (see Figure 5.21). When the applied stress field is compressive, the flow stress decreases or remains unchanged, depending on the magnitude of the net stress field [135]. During in-phase cycling, the stresses are compressive at T_{\min} and cancelled with the hydrostatic tensile stress field around the γ' . The net result is that the frictional forces on the glide dislocation are lower and the flow stress does not change much as cycling proceeds and coarsening takes place (at T_{\max}), as can be seen in Figure 5.20.

To fully understand the flow behavior with change in sign of the applied stress, we must also consider the resolved constriction stress of partial dislocations [135, 139]. The direction of the glide force per unit length, F_g/L , will reverse upon reversing the applied stress, σ [135]. While this has no physical meaning in a macroscopic sense, since it only alters the direction of glide for a particular dislocation, reversing the direction of the glide forces acting on the partial dislocation, it leads to a distinctly different physical situation. The resulting force tends to constrict the partials under an applied tensile stress and extend them under a compressive stress [135]. Since constriction of the partials is required by the cross-slip process, the flow stress appears stronger in tension than in compression where the extended partials retard cross-

slip activity. The previous argument implies that the flow behavior of B-1900+Hf is governed by octahedral slip activity. If such is the case, the flow stress can be written as

$$\sigma \propto (1/R + 1/\lambda), \quad (6.1)$$

where R is the particle size and λ the mean free distance between the two constricted nodes where the cross-slip event occurs [135]. At high temperature, λ is always smaller than R and the flow stress is governed by the dislocation network and internal stress which fixed λ [135, 143]. At low temperature, the flow stress depends on which of these two parameters (R , λ) is the smaller. If a tensile stress is applied, the partials tend to be constricted and the mean free distance between cross-slip event decreases. If a compressive stress is applied, the partials are pulled further apart (λ increases), and the flow stress is controlled by R , the particle size.

Cyclic Stress-Strain Behavior

The cyclic stress-strain curves (Figures 5.24-5.26) show that the flow stress, as a function of the strain amplitude ($\Delta \epsilon_t/2$), is higher for in-phase than out-of-phase or isothermal cycling at the maximum temperature (T_{max}). This is consistent with the fact that dislocation density increases in the order of isothermal, out-of-phase and in-phase cycling (see Figures 6.1-6.3). At low temperature (T_{min}), because cross-slip is a function of the magnitude and sign of applied stress, the flow stress is higher under out-of-phase cycling than under in-phase or isothermal cycling (see Figure 5.26).

The issue that needs to be addressed now is the cracking mode. As shown in Figures 5.27 and 5.28, fracture is transgranular and

proceeds interdendritically in out-of-phase cycling and intergranularly under in-phase cycling conditions. As expected, fracture is controlled by the favored mode of rupture in the tensile part of the cycle. Under in-phase cycling, tension occurs at high temperature where the cohesive strength of the grain boundary is low, which obviously promotes intergranular cracking. During out-of-phase cycling, the specimen is under tensile loading at low temperature and the weakest transgranular features (carbide film, secondary dendrites, inclusion stringers, etc.) control the rupture mode. The fact that the fracture mode depends on the maximum tensile stress, rather than on a critical plastic strain range, suggests that the failure criteria for B-1900+Hf is stress-based rather than strain-dependent. In other words, the testing condition (temperature and strain relationship) leading to the maximum tensile stress, will determine the number of cycles to initiation and the propagation rates.

As mentioned earlier, the major critical turbine components operate under strain-controlled conditions and, more specifically, under displacement-control. The stresses are not known a priori. Therefore, if the failure criteria in B-1900+Hf is stress-dependent, the relative crack growth rates for a given crack length can be determined from the CSS curves. Figure 5.26 shows that at low strain amplitude ($<0.25\%$) the stress range for TMF cycling is higher than for isothermal fatigue. Consequently, faster crack growth rates should be obtained for TMF cycling. Under fully plastic conditions ($\Delta\epsilon_t/2 > 0.25\%$), Figure 5.26 also shows that the isothermal stress range is higher than the stress ranges obtained under TMF cycling and faster crack growth rates are expected under isothermal cycling (T_{max}).

6.3 Fatigue Crack Growth (FCG) of Inconel X-750

The results (Figure 5.29) have shown that the crack growth rates are higher for TMF cycling than for the equivalent isothermal condition ($T = 650^{\circ}\text{C}$) which is in agreement with the results obtained on other nickel-base alloys [22, 27-29, 41, 58]. Secondly, it was observed that the crack growth rates are higher for $R = -1$ than for $R = 0.05$, which indicates that compressive stresses play an important role in the mechanics of TMFCG. Comparison between out-of-phase and in-phase cycling at $R = -1$ shows that out-of-phase cycling is more damaging than in-phase cycling at high ΔK , whereas at low ΔK , the crack growth rates are the same. The rationale of this behavior was found in the analysis of potential change within each cycle. At low ΔK , the potential curves $V(\sigma)$ which characterizes the crack geometry, i.e. crack length and crack configuration (see Appendix II), are identical for out-of-phase and in-phase cycling as can be seen in Figure 6.4. This indicates that the mechanical driving force (same stress, crack length and crack configuration) are similar and therefore identical crack growth rates are expected. As ΔK increases, the $V(\sigma)$ potential curves for both in-phase and out-of-phase cycling display different characteristic features. Figure 6.5 shows $V(\sigma)$, $V(\sigma, T)$ and $V(T)$ measured at $\Delta K \approx 50 \text{ MPa } \sqrt{\text{m}}$. The in-phase $V(\sigma)$ curve shows a smooth increase with σ_{net} ($\sigma_{\text{net}} = N/BW$) followed by a sharp increase near σ_{max} . The potential then remains quasi-stable as σ_{net} decreases and sharply falls as σ_{net} approaches zero. In the compression regime the potential smoothly decreases reaching a minimum at σ_{min} , and finally increases as the stress increases again. On the other hand, the out-of-phase $V(\sigma)$

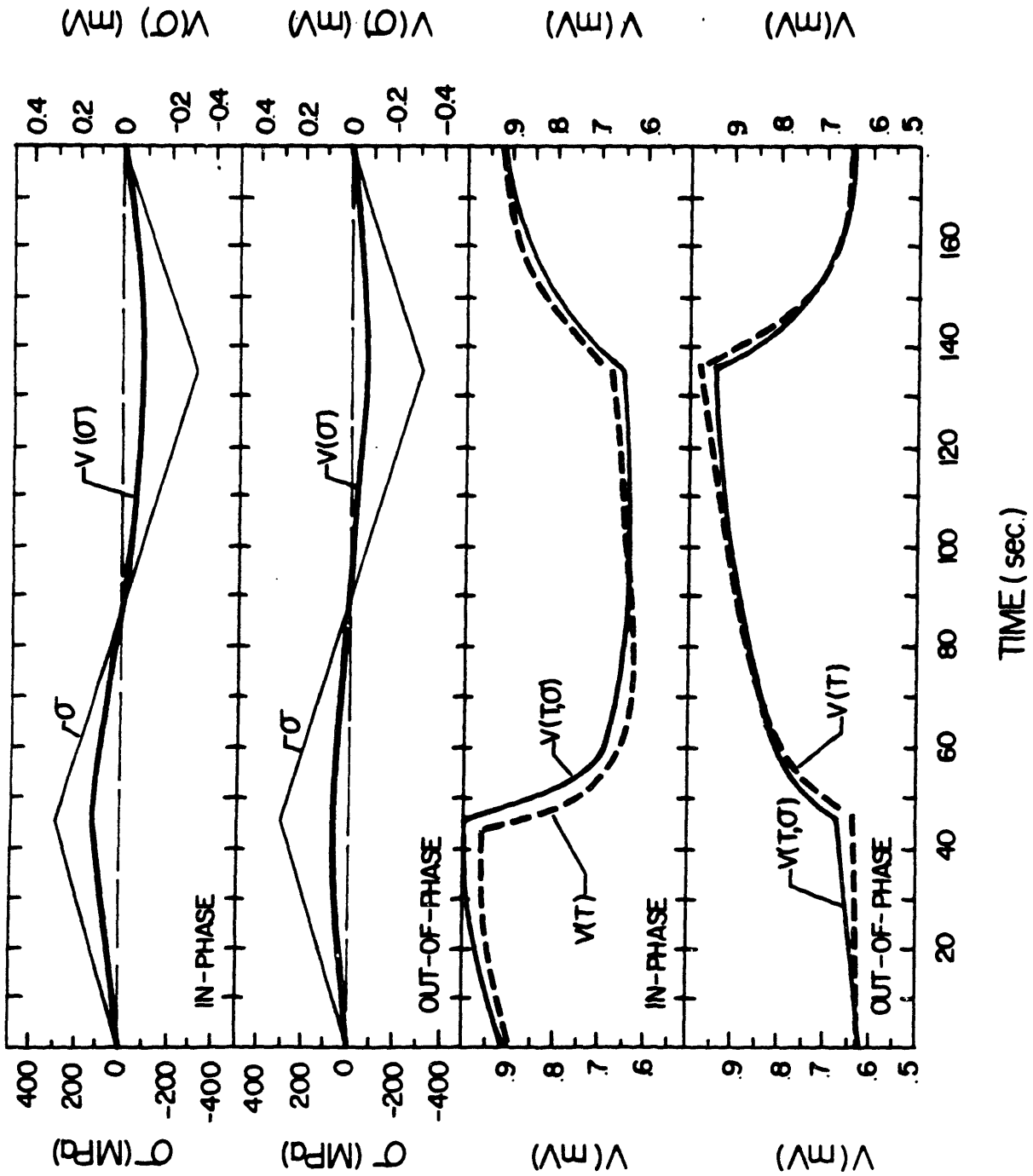


Figure 6.4 Potential curves $V(T, \sigma)$, $V(T)$, and $V(\sigma)$ for TMFCG in Inconel X-750. $\Delta K = 25 \text{ MPa}\sqrt{\text{m}}$.

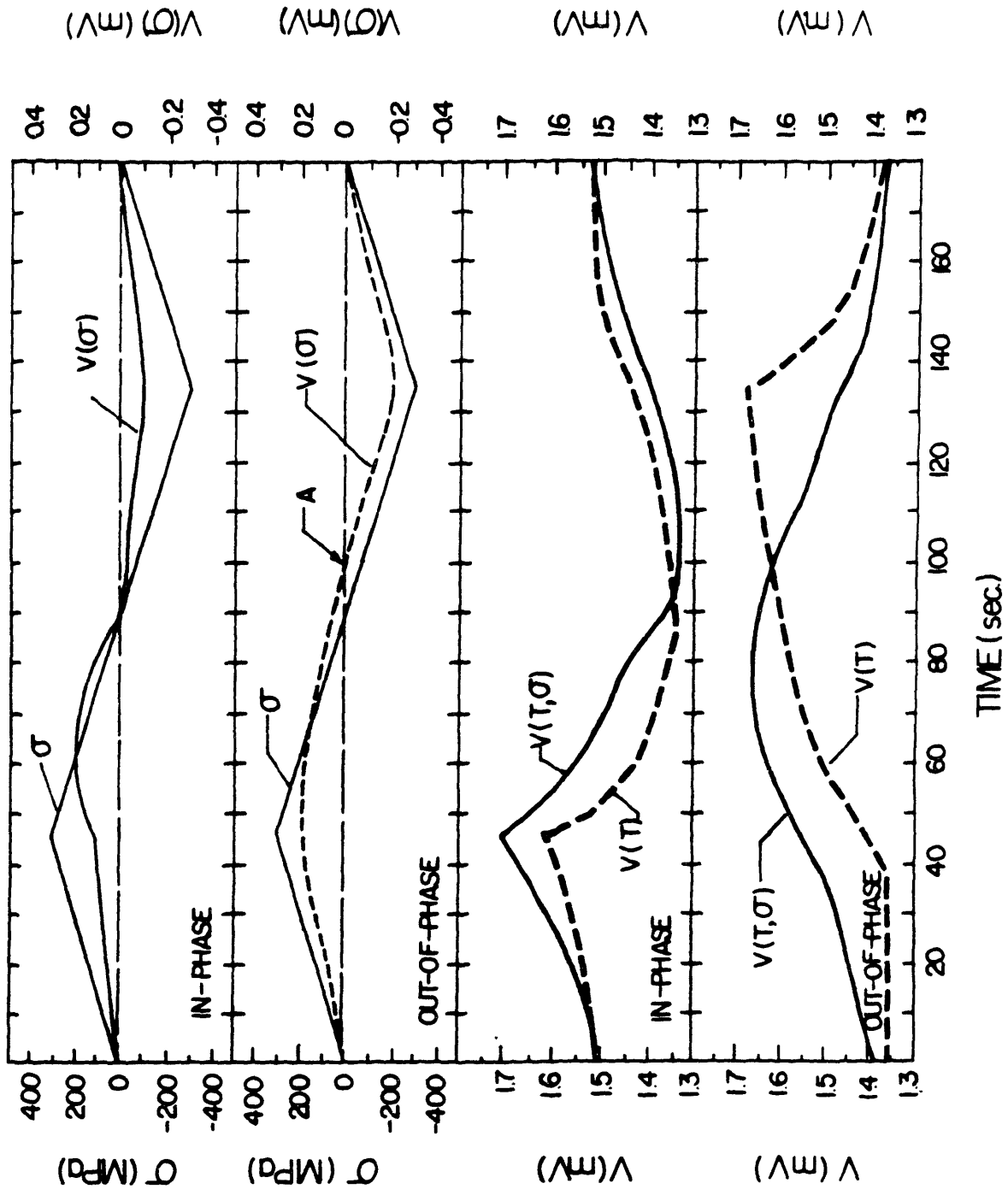


Figure 6.5 Potential curves $V(T, \sigma)$, $V(T)$, and $V(\sigma)$ for TMFCG in Inconel X-750. $\Delta K = 50 \text{ MPa}\sqrt{\text{m}}$.

potential curves show (at the same ΔK) a smooth increase with σ_{net} with a peak value at σ_{max} . The potential then decreases down to a minimum and finally increases again with σ_{net} . The most important feature of these signals is the crossover point (denoted A) for which $V(\sigma) = 0$. The crossover point represents the stress to apply to the specimen for the potential $V(\sigma, T)$ to equal $V(T)$. Because $V(T)$ is measured at zero applied stress ($\sigma_{net} = 0$) for the entire thermal cycle, the expected stress to apply is $\sigma = 0$. However, if the potential field near the crack tip is disturbed either by a non-zero residual stress-strain field or by geometrical events such as blunting, closure, etc., the $V(\sigma, T)$ potential at zero applied stress might not necessarily equal $V(T)$ and a non-zero stress is required to cancel out the contribution of this event (Δ). For out-of-phase potential, the crossover occurs at a negative stress (e.g. $\sigma = -75$ MPa at $\Delta K = 50$ MPa \sqrt{m}), whereas, it always occurs near zero stress for the in-phase potential. By first assuming that the crossover point occurs near an effective closure stress (σ_{cl}), it follows that the effective stress intensity factor (ΔK_{eff}) for crack growth will be higher for out-of-phase than for in-phase cycling (σ_{cl} is negative). If we plot the crack growth rates as a function of ΔK_{eff} ($\Delta \sigma_{eff} = \sigma_{max} - \sigma_{closure}$), we find that both in-phase and out-of-phase crack growth rates overlap as shown in Figure 6.6. This clearly shows that the stress intensity factor is a suitable parameter for correlating TMFCG data, provided the effective stress range is used.

It is important to note that the absolute amplitude of the $V(\sigma)$ signal (see Figure 6.5) in the compressive regime of the cycle, is much higher for out-of-phase than for in-phase cycling which indicates that the crack surfaces are in contact on a much larger scale than under in-

FATIGUE CRACK PROPAGATION

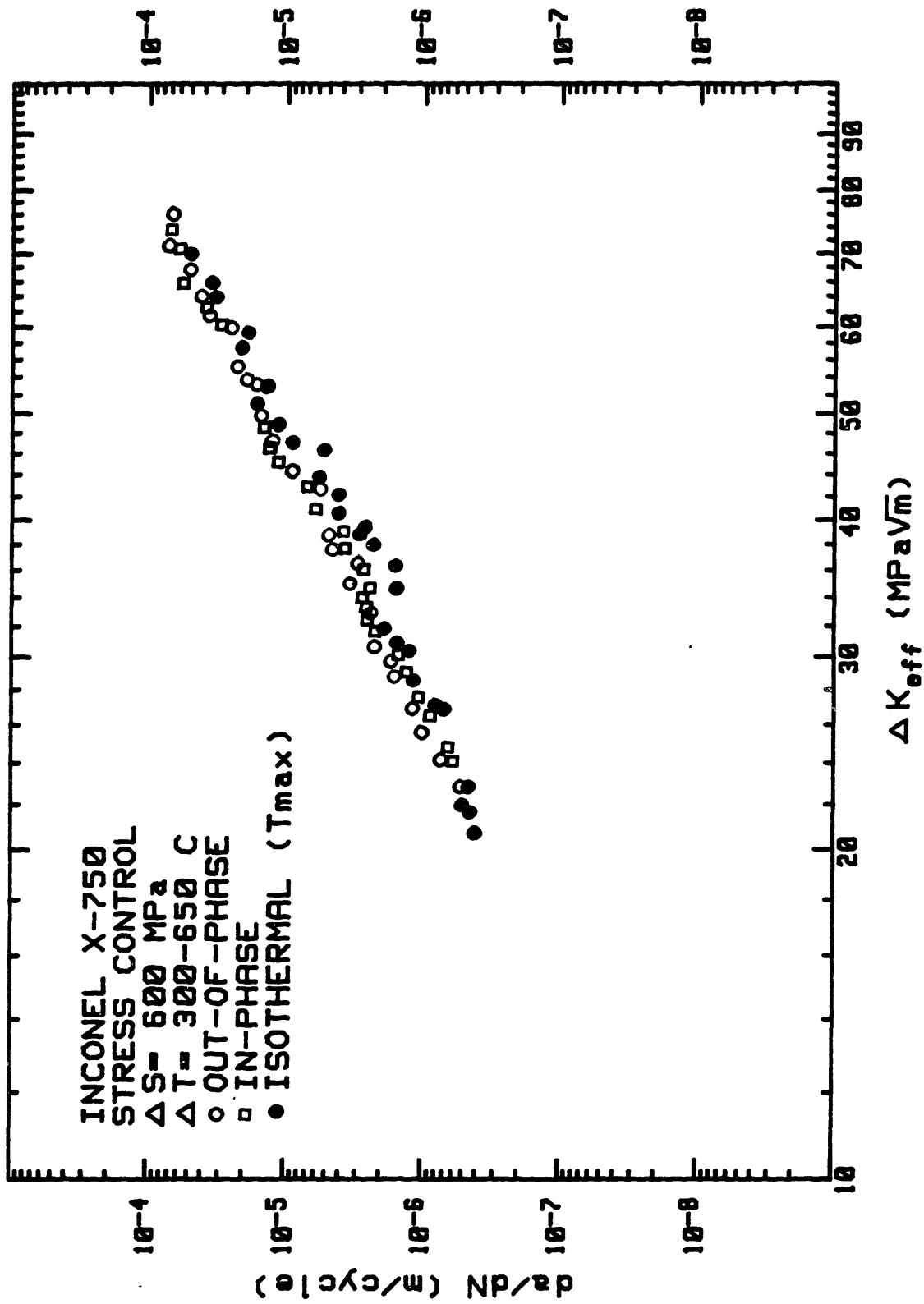


Figure 6.6 TMFCG rates in Inconel X-750 as a function of ΔK_{eff} .

phase cycling. This is in agreement with the fractographic observation which shows that out-of-phase cycling leads to transgranular crack with considerable mating, whereas, in-phase cycling leads to intergranular fracture with little evidence of mating. The higher crack growth rates at $R = -1$ than $R = 0.05$ and the fractographic observations lead to the conclusion that although there should be no cracking at the maximum temperature because of the compressive stress, some form of damage is taking place under compressive strain. Also, the surface oxide film found at high temperature will rupture at low temperature, under maximum tensile stress. This leads to a resharping of the crack tip with each cycle and results in an increase in growth rate.

The rationale for the negative closure stress in out-of-phase cycling can be found by assuming that the residual stress field at the crack tip is of tensile nature at zero applied stress and that a compressive stress has to be applied in order to cancel it and to close the crack. Assuming that the CSS behavior of Inconel X-750 is similar (in trend) to B-1900+Hf, then the validity of the previous argument is supported by Figure 5.26, which shows that for out-of-phase cycling the mean stress σ increases with increasing strain ranges. At low ΔK , the strain range near the crack tip are small [144] and the mean stress are small for all cases (see Figure 5.26). As ΔK increases, the strain range increases and so does σ . However, the increase of σ with $\Delta \epsilon_{mec}/2$ is much faster for out-of-phase than for in-phase or isothermal cycling which remain small (with respect to the stress range) for all strain amplitudes. In other words, the closure stress is becoming more and more compressive as ΔK increases, which is consistent with our measurements of σ_{cl} .

The difference in growth rates between the isothermal test (650°C) and the TMF tests can also be explained by looking at the $V(\sigma)$ potential curves at low and high ΔK . The $V(\sigma)$ curves were normalized by subtracting $(V_{\max} - V_{\min}) / 2$ from the $V(\sigma, T = \text{cst})$ signal. At low ΔK no significant differences were observed between $V(\sigma)$ potential curves of isothermal and TMF tests. At high ΔK , however, the isothermal $V(\sigma)$ potential curves show a crossover point taking place at a tensile stress. This implies that the effective driving force for cracking is reduced with respect to in-phase and out-of-phase cycling. By taking into account this σ_{cl} in the computation of ΔK , one finds that the crack growth rates in terms of ΔK_{eff} for both isothermal and TMF tests are similar as shown in Figure 6.6. The positive closure stress observed is attributed to the buildup of oxides in the wake of the crack. This is supported by fractographic observation which have shown greater oxidation for isothermal testing than for TMF cycling.

6.4 Fatigue Crack Growth (FCG) of B-1900+Hf

The applicability of fracture mechanics to correlate TMFCG data under controlled elastic displacements is confirmed by comparing our data with those of Pratt & Whitney Aircraft (P&WA) obtained on tubular specimens with an EDM slot in the center of the gage section. Because the reported data [29] are plotted in terms of the conventional ΔK_{ϵ} given by

$$\Delta K_{\epsilon} = \Delta \epsilon \cdot \sqrt{\pi a} \cdot G(a/W) \quad (6.2)$$

FATIGUE CRACK PROPAGATION

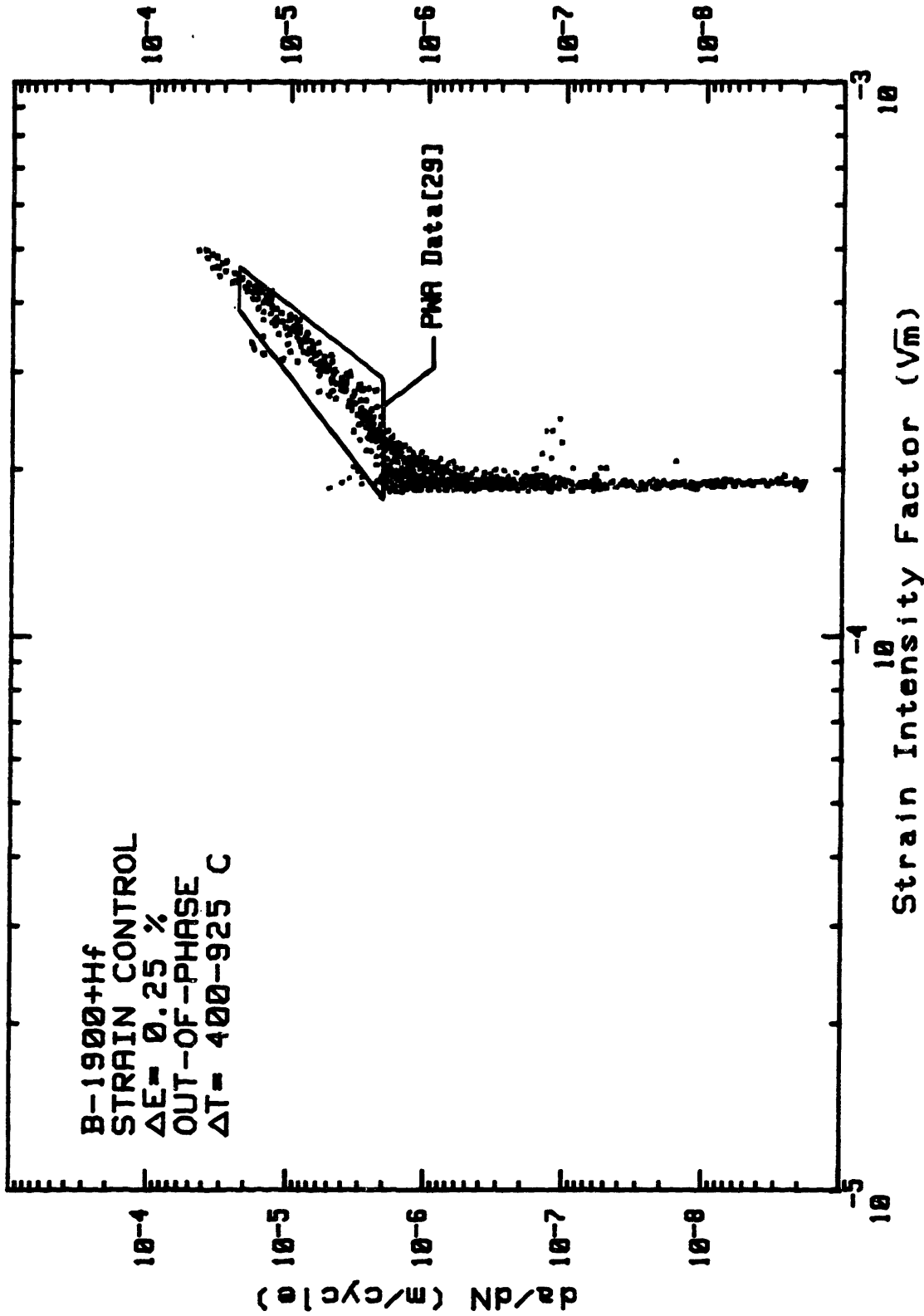


Figure 6.7 Out-of-phase crack growth rates in B-1900+Hf as a function of the conventional strain intensity factor for SEN and tubular specimens[29].

where $G(a/W)$ is the correction factor derived for stress-controlled (free rotation) stress intensity factor, the following formula was used to compute the ΔK_{ϵ} 's

$$\Delta K_{\epsilon} = \Delta \epsilon \cdot \sqrt{\pi a} \{25/20 - 13(a/W) - 7(a/W)^2\}^{1/2} \quad (6.3)$$

Figure 6.7 shows the results for $\Delta \epsilon_{mec} = 0.25\%$. As can be seen, the agreement between the two geometries is quite good which suggests that fracture mechanics is applicable provided the driving force is properly computed. Although Eq. 6.3 does not provide realistic quantitative values for the ΔK_{ϵ} 's (see Appendix V), it is used here to show that for a given material and testing conditions, equal driving forces calculated on different geometries yield identical crack growth rates. Figure 6.7 also shows that the computerized testing system has the capability of measuring crack growth rates data three orders of magnitude lower than those measured by more conventional TMF testing systems.

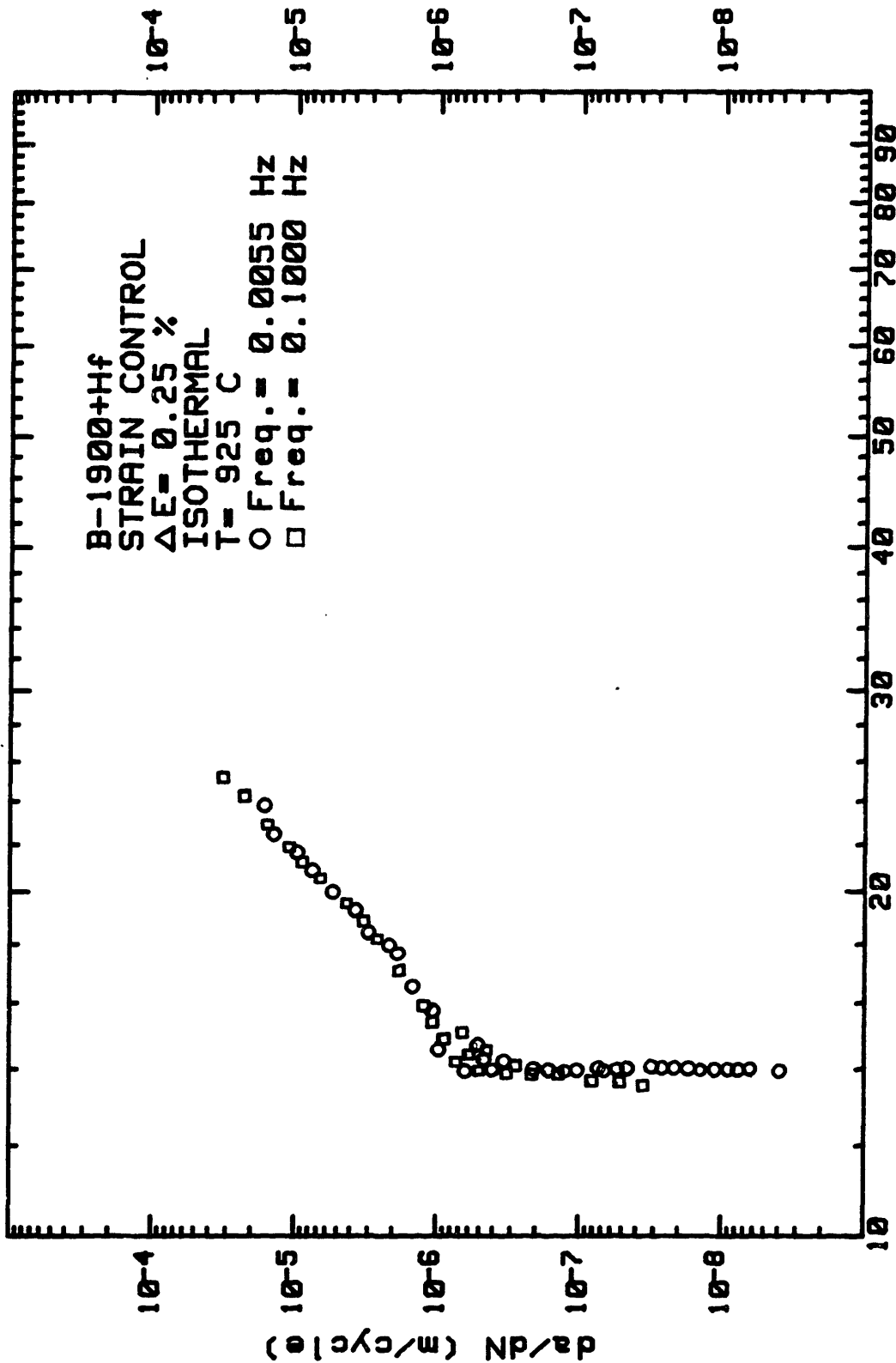
The results in Figure 5.31 show that TMF cycling is more damaging than isothermal cycling when the strain range in the bulk is fully elastic. This result is expected since for Inconel X-750 cycled under elastic stresses, the same behavior was observed (see Figure 5.29). As we know, the maximum stress (σ_{max}) achieved during cycling ranks (in increasing order) as isothermal, in-phase, and out-of-phase. Similarly, the crack growth rates also ranked in this order (see Figure 5.31). It is now logical to assume that the driving force for cracking is a stress-based parameter. In other words, even under strain-controlled cycling, the driving force for cracking is not the applied strain range as much as the maximum stress which results from the imposed cyclic straining. This point has been discussed in Section 6.2 where the modes

of cracking in B-1900+Hf indicate that the fracture criterion under TMF cycling is stress-based. Further support to this conclusion was given by the study of the effect of frequency (see Figure 5.33) which shows that as the frequency increases (at fixed strain range and temperature) the crack growth rate increases. The rationale for this behavior is that as the frequency increases, the strain rate increases and so does the stress range. If indeed the fracture criterion is stress-based rather than strain-based, an increase in stress range results in an increase in crack growth rates (in terms of the ΔK_{ϵ} 's).

Based on this idea and on the fact that the stress intensity factor was a successful parameter for Inconel X-750, all the crack growth rates data were replotted in terms of ΔK_{σ} , where ΔK_{σ} is given by Eq. 5.1. The measured loads (N_{max}) are used in the ΔK_{σ} calculations.

Figure 6.8 shows that effect of frequency disappears if the crack growth rates are plotted in term of ΔK_{σ} . This confirms the assumption that fracture in B-1900+Hf is stress-based rather than strain-based. Figures 6.9 and 6.10 show a summary of the results for $\Delta \epsilon_{mec} = 0.25\%$ and $\Delta \epsilon_{mec} = 0.50\%$. The detail results are given in Appendix IV. As expected, an increase in maximum stress by changing the testing conditions results in shifting the fatigue crack growth curves to the right, i.e., higher values of ΔK_{σ} . The shift of the FCP curves causes an increase in the apparent spread of the data between the different testing conditions. Although the spread suggests that K_{σ} is not the proper correlation parameter, comparison of Figures 6.9 and 6.10 shows that ΔK_{σ} does provide a rationale for the effect of strain range. In other words, the considerable strain range effect which exists when the crack growth data are plotted in term of ΔK_{ϵ} (see Figures 5.31 and 5.32)

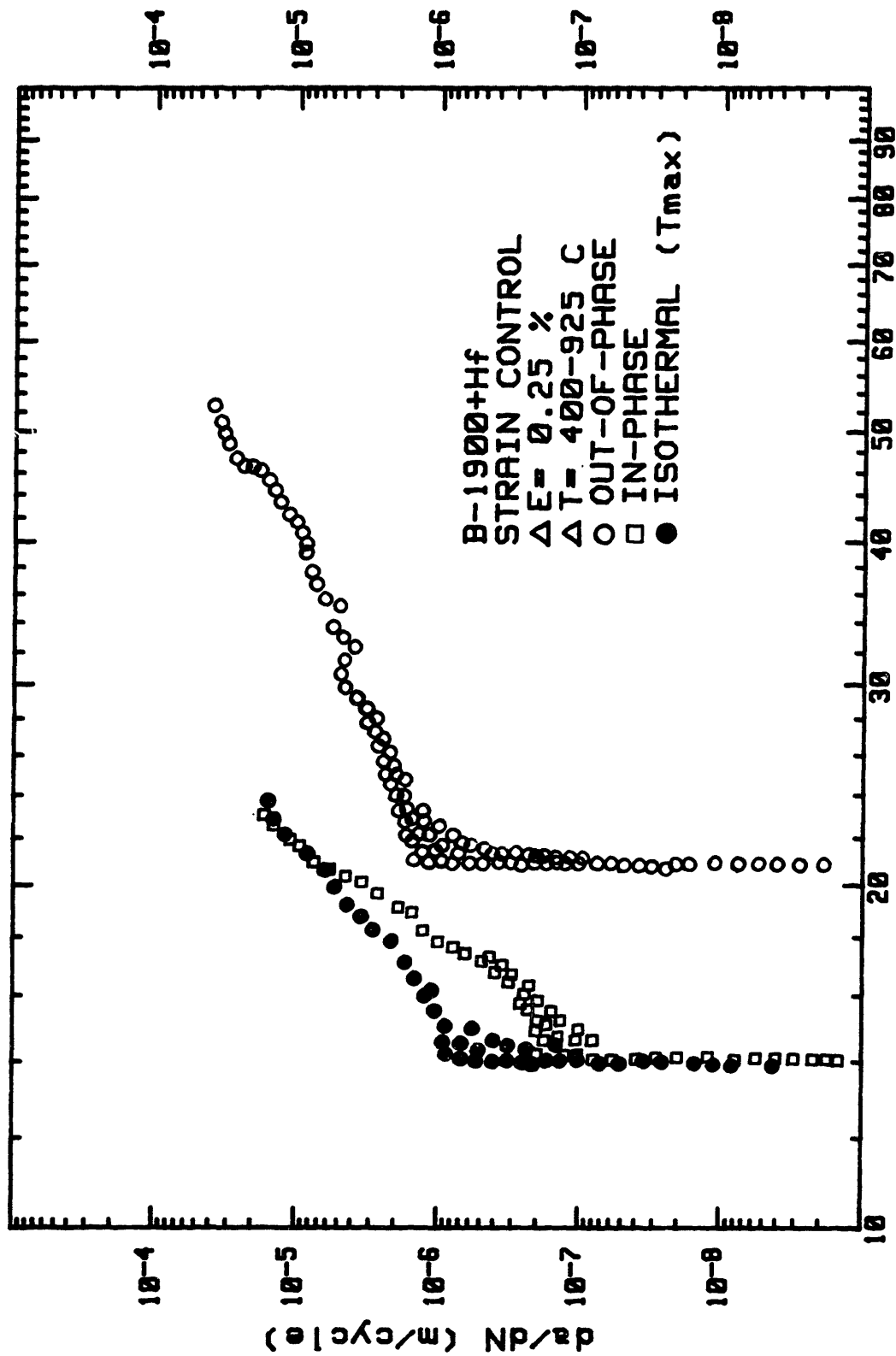
FATIGUE CRACK PROPAGATION



Stress Intensity Factor (MPa√m)

Figure 6.8 Effect of frequency on the FCG rates in B-1900+Hf as a function of ΔK_{σ} (T_{max} , $\Delta \epsilon_{mec} = 0.25\%$).

FATIGUE CRACK PROPAGATION



Stress Intensity Factor (MPa√m)

Figure 6.9 FCG rates in B-1900+Hf as a function of ΔK_{σ} ($\Delta \epsilon_{mec} = 0.25\%$)

FATIGUE CRACK PROPAGATION

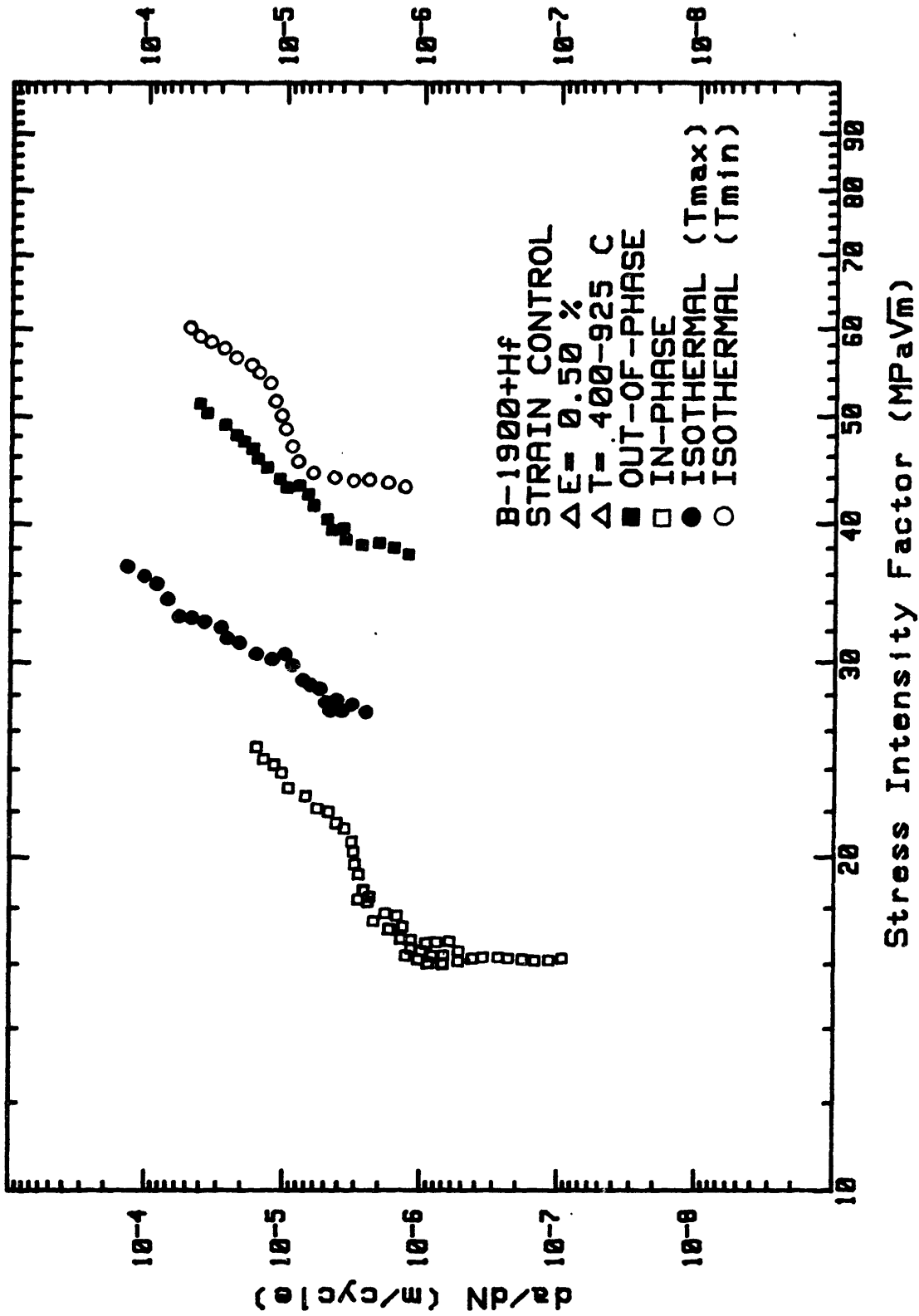
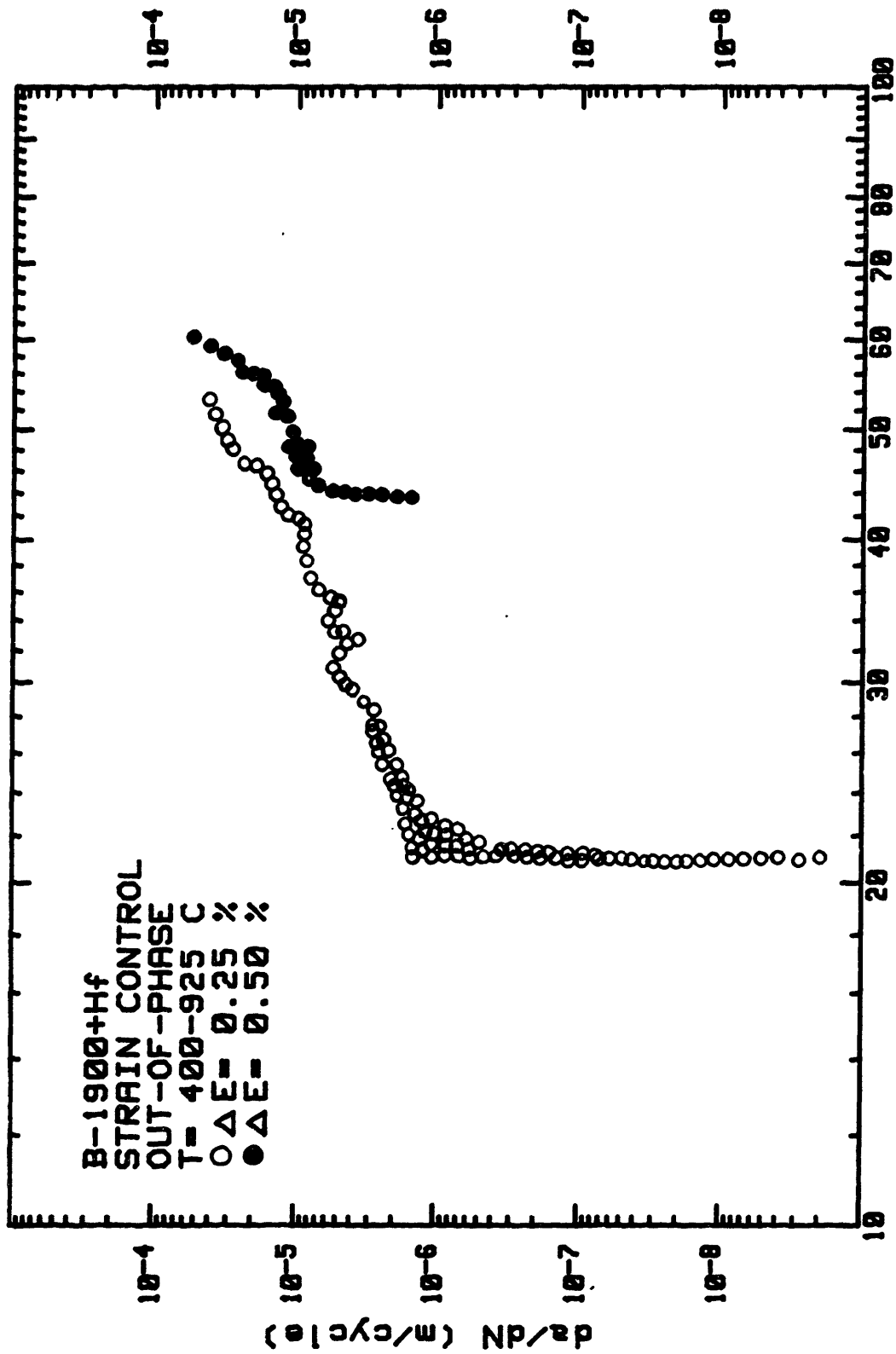


Figure 6.10 FCG rates in B-1900+Hf as a function of ΔK_{σ} ($\Delta \epsilon_{mec} = 0.50\%$)

disappears if the ΔK_{σ} is used to correlate the data. Figure 6.11 shows the correlation of the data for out-of-phase cycling at 0.25 and 0.50%. The ability of ΔK_{σ} to better rationalize the effect of strain range as compared to ΔK_{ϵ} stems from the fact that doubling the strain range does not necessarily result in doubling the stress range. Instead, an increase in $\Delta \epsilon$ results in an increase in crack growth rates which is proportional to an increase in stress range. The use of Eq. 5.1 which takes into account any non-proportional increase in stress range caused by hardening or softening at the crack tip and in the bulk material, is therefore more appropriate than the use of Eq. 5.3 which assumes a proportional increase in $\Delta \sigma$ with an increase in $\Delta \epsilon_{mec}$. As long as the plastic strain range remains small, Eq. 5.1 provides a fairly good estimate of the stress intensity factor in the material and thus a good correlation of the crack growth data with increasing strain range is expected. However, if the plastic strain range is significant (for a given $\Delta \epsilon_{mec}$), the correction for bending use in Eq. 5.1 will be incorrect because the bending (M) and normal (N) components in the specimen are coupled and cannot be determined separately (see Appendix V). This explains why the ΔK_{σ} cannot collapse the crack growth data for isothermal testing to the same extent than it does for in-phase and out-of-phase cycling because under isothermal conditions (T_{max}) and $\Delta \epsilon_{mec} = 0.50\%$, the plastic strain range is approximately 0.08% whereas it is less than 0.02% for in-phase and out-of-phase cycling.

As for Inconel X-750, the difference between in-phase, out-of-phase and isothermal crack growth data was found in the analysis of the potential drop signal. Figures 6.12, 6.13 and 6.14 show the corrected potential signal $V(\sigma)$ at two different crack lengths ($a/W \sim$

FATIGUE CRACK PROPAGATION



Stress Intensity Factor (MPa√m)

Figure 6.11 Effect of strain range on the FCG rates in B-1900+Hf cycled under out-of-phase conditions

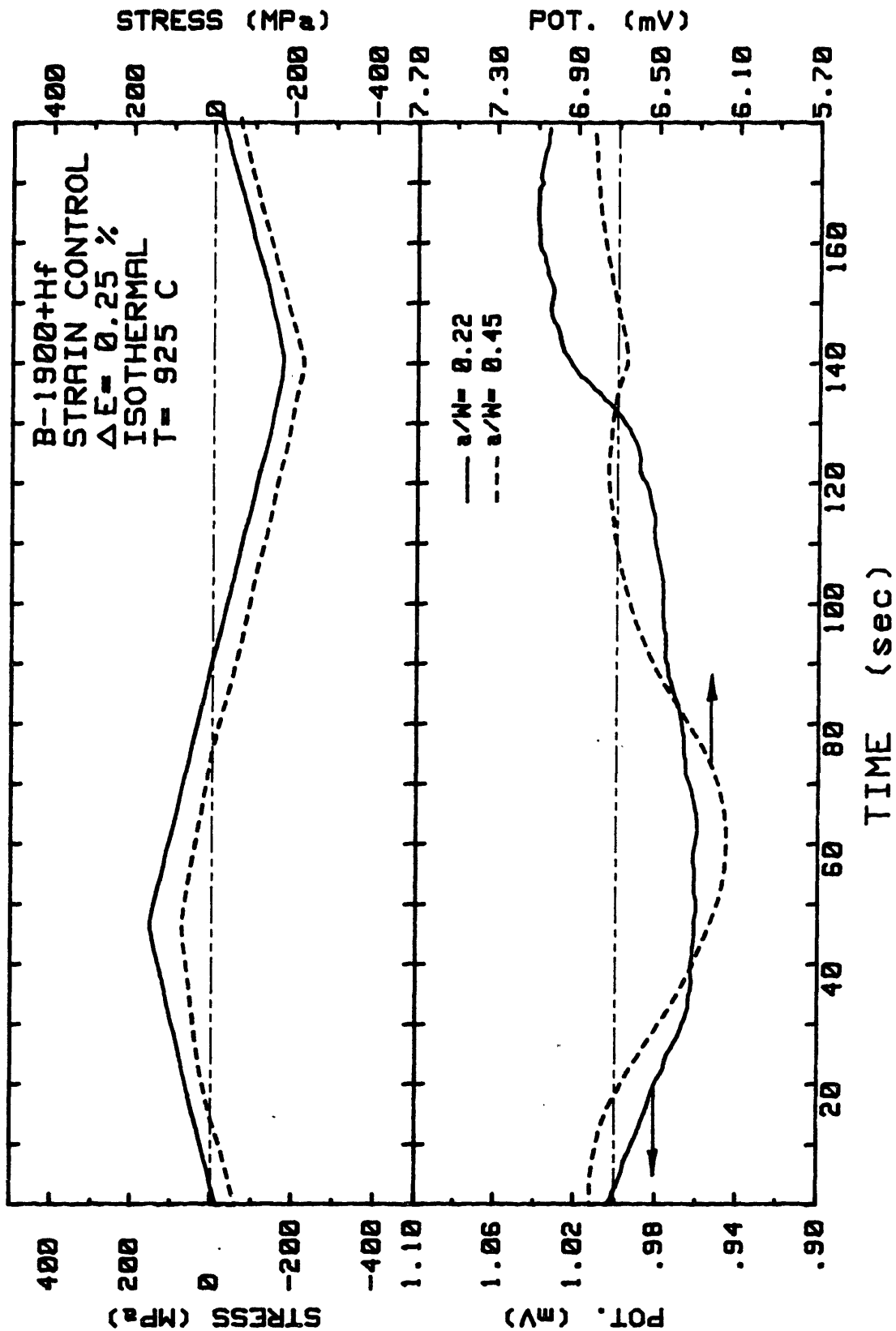


Figure 6.12 Potential curve $V(\sigma)$ and stress amplitude in B-1900+Hf under isothermal cycling (T_{max}).

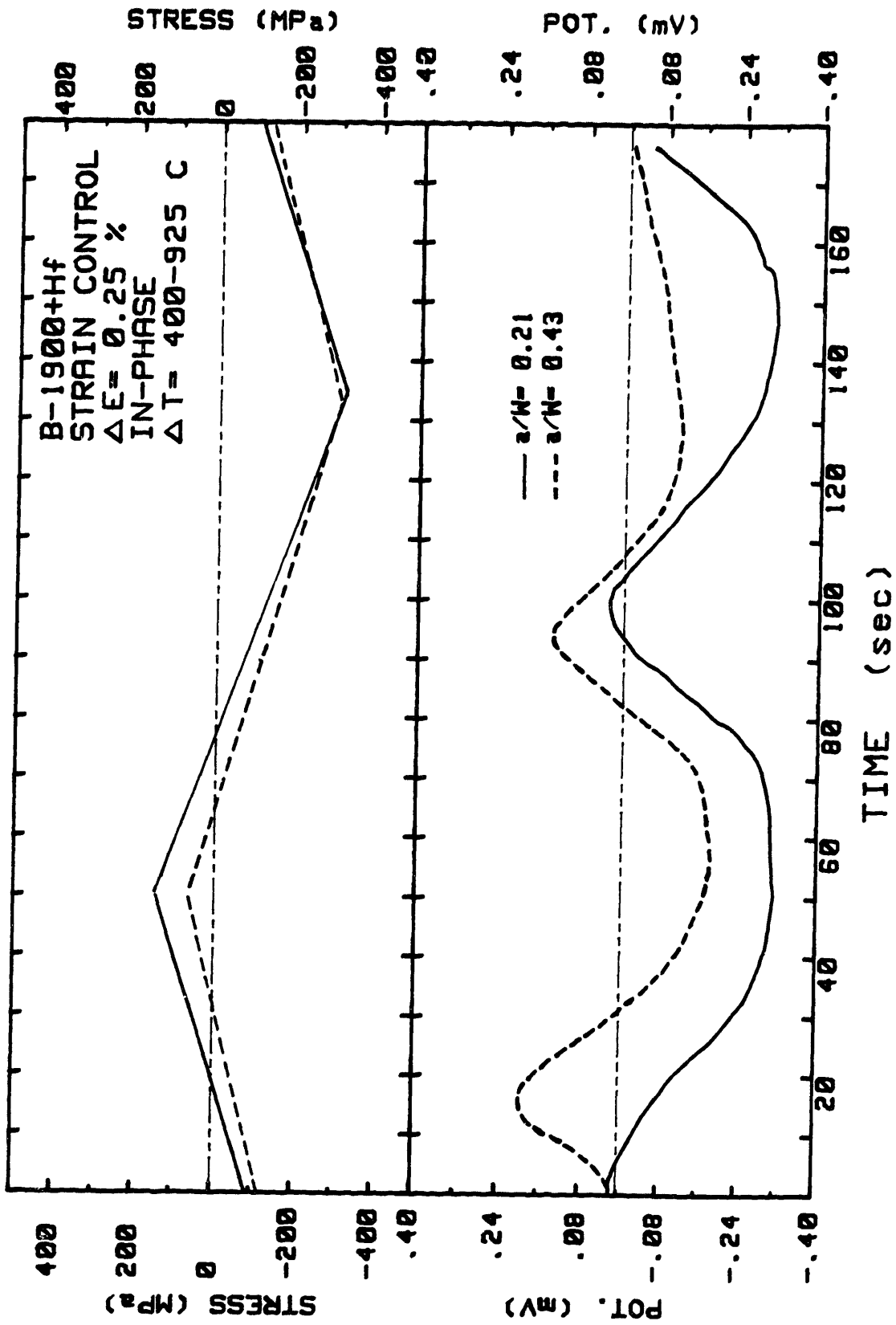


Figure 6.13 Potential curve $V(\sigma)$ and stress amplitude in B-1900+Hf under in-phase cycling.

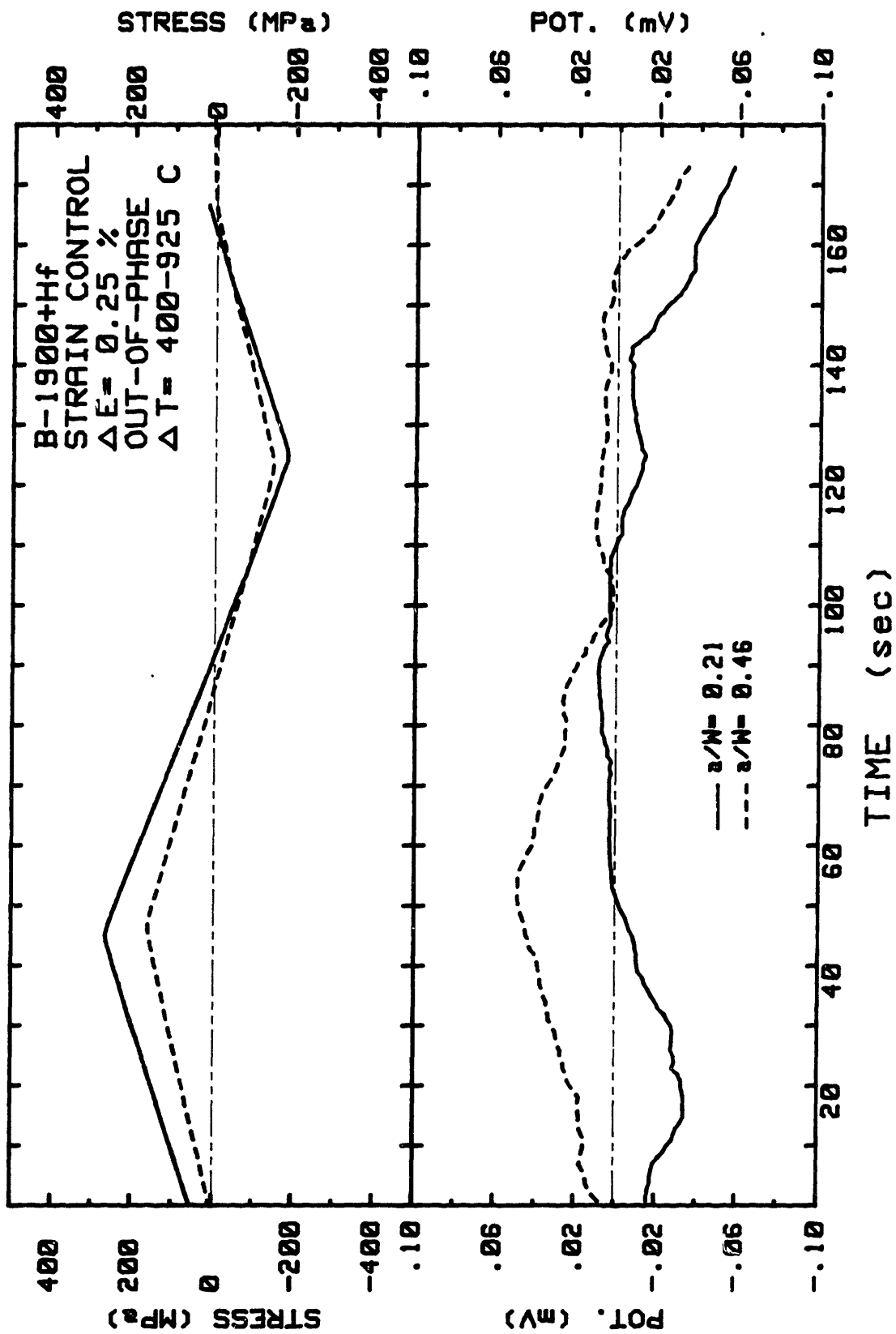


Figure 6.14 Potential curve $V(\sigma)$ and stress amplitude in B-1900+Hf under out-of-phase cycling.

0.21 and 0.45) for isothermal, in-phase, and out-of-phase testings. The following conclusions can be drawn from these figures. First, the potential signal $V(\sigma)$ are more complex than for Inconel X-750 (see Figures 6.4 and 6.5). This is expected since in these tests the stresses are not imposed but rather depend on changes in geometry (crack length) and material properties (hardening/softening) and this introduces another variable in the $V(\sigma)$ signals. Another observation is that the opening stress (σ_{op}), which is the stress at which the crack is fully open, is different from the closure stress (σ_{cl}), the stress at which the crack is completely closed. Furthermore, the difference between σ_{op} and σ_{cl} increases as the crack length increases. Finally, the magnitude of σ_{op} varies with crack length being tensile for $a/W < 0.40$ and compressive for large crack lengths ($a/W > 0.45$). The influence of crack length on σ_{op} will be discussed later.

The crack growth rates were then plotted as a function of the effective stress intensity factor (ΔK_{eff}). In the calculation of ΔK_{eff} only the opening stress (σ_{op}) were used. Figure 6.15 shows the crack growth rates as a function of ΔK_{eff} . As can be seen, the ΔK_{eff} provides a reasonable correlation for the crack growth rates and all the data fall within one of the two master curves. All the test data for which σ_{max} occurs at T_{max} (isothermal and in-phase cycling) fall in one scatterband, whereas all the low temperature data for which σ_{max} occurs at T_{min} (isothermal and out-of-phase cycling) fall in the other scatterband. In terms of mode of fracture, all the tests for which fracture is transgranular (σ_{max} at T_{min}) are grouped in one scatterband of slope 2.8, whereas all the tests which failed intergranularly (σ_{max} at T_{max}) clustered in a scatterband of slope 5.0. This clearly indicates that the

FATIGUE CRACK PROPAGATION

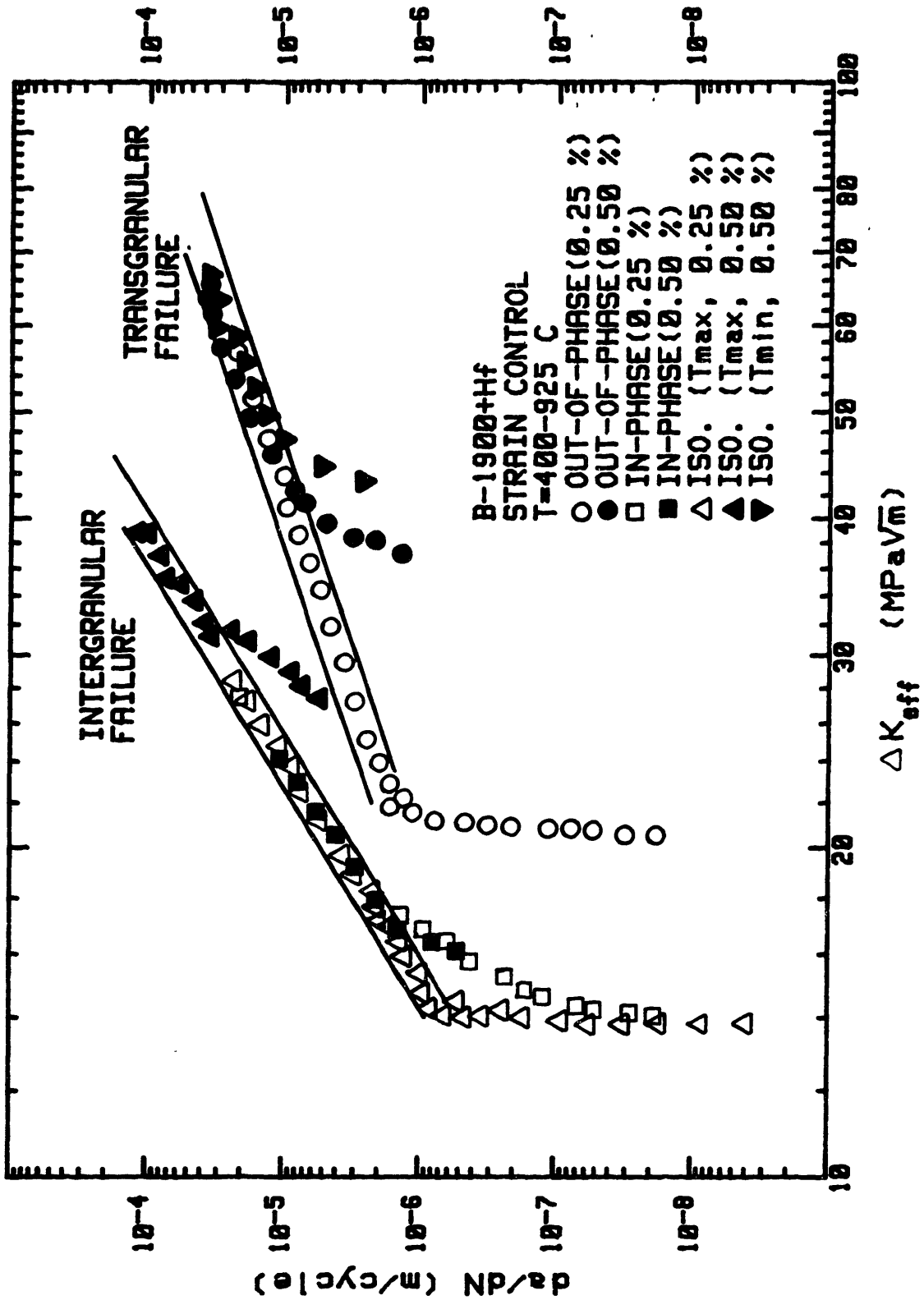


Figure 6.15 FCG rates in B-1900+Hf as a function of ΔK_{eff}

mode of fracture in B-1900+Hf is stress-based and depends only on the temperature at which σ_{max} occurs. In other words, for a given mode of fracture (fixed by the temperature at σ_{max}) there is a unique relationship between the crack growth rates and ΔK_{eff} . Furthermore, this relationship is independent of the applied strain range and cyclic history of the material.

However, the knowledge of ΔK_{eff} alone is not sufficient to allow prediction of the crack growth rates. The relationship between the strain and the temperature must be known such that the probable mode of fracture can be determined and the proper master curve (da/dN vs ΔK_{eff}) be used.

The last issue to be addressed is the variation of σ_{op} with crack length. Figure 6.16 shows the variation of σ_{op} as a function of a/W for an isothermal test ($T_{max}, \Delta \epsilon_{mec} = 0.25\%$). Also shown in this figure is the function $G(a/W)$ here defined as

$$G(a/W) = L \cdot \Delta K_{\epsilon} / \Delta \delta \quad (6.4)$$

with ΔK_{ϵ} given by Eq. 5.3, L the gauge length of the specimen, and $\Delta \delta$ the imposed displacement (see Appendix V). As can be seen in Figure 6.16, the σ_{op} is tensile when the normal component (N) dominates and ΔK_{ϵ} increases. On the other hand, when the bending component is significant, i.e. when ΔK_{ϵ} decreases with increasing crack length, the σ_{op} is compressive. It is interesting to note for this testing condition (the only one for which Eqs. 6.4 and 5.3 strictly apply), that the inflection point in the σ_{op} vs a/W results occurs at a value of a/W which yield a maximum in the $G(a/W)$ vs a/W curve. Furthermore, the fact that σ_{op} monotonically decreases between $0.35 < a/W < 0.65$ whereas K shows a monotone increase followed by a decreased, clearly

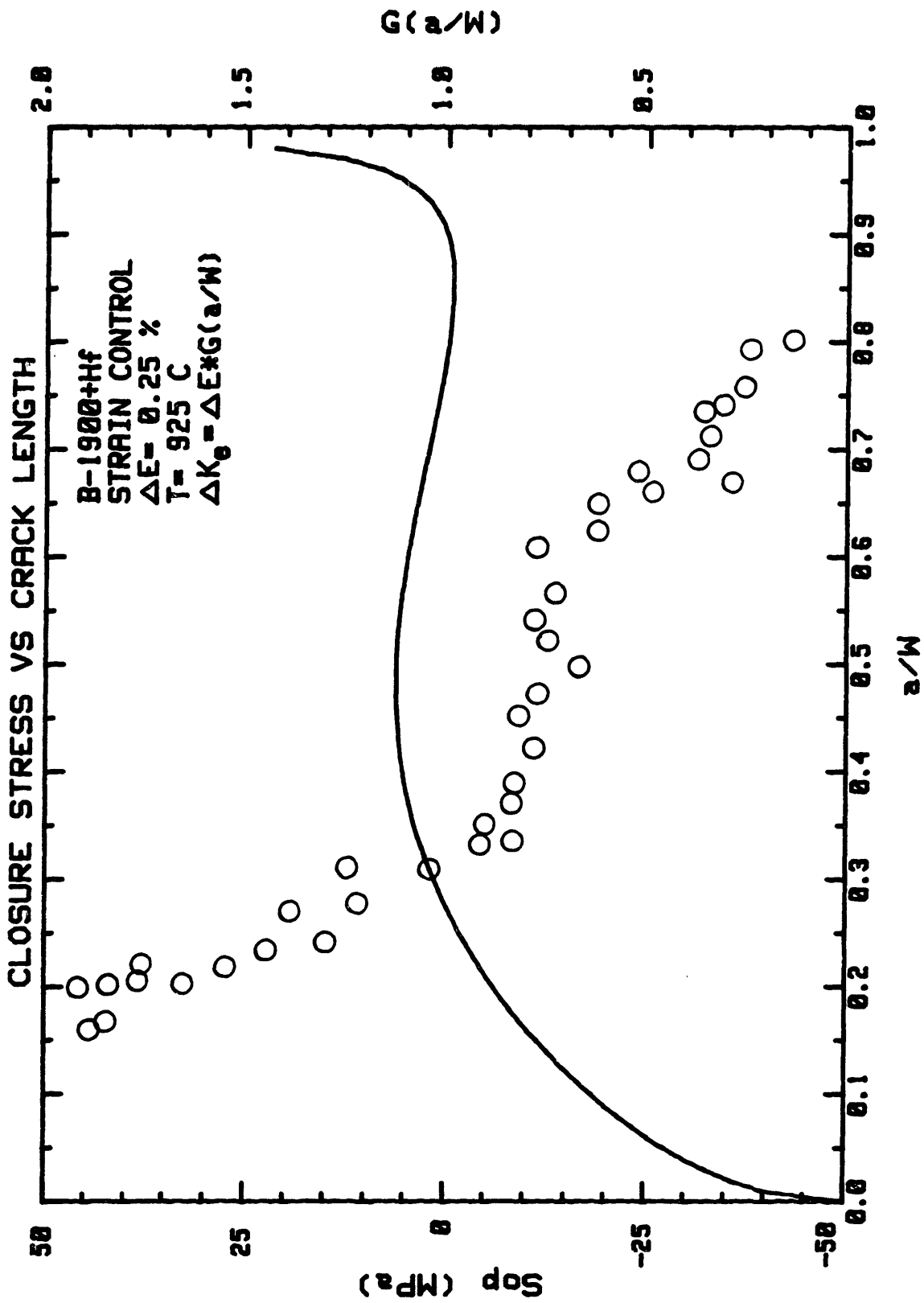


Figure 6.16 Variation of the opening stress ($\sigma_{\theta P}$) as a function of crack length in B-1900+Hf ($T = 925 \text{ C}$, $\Delta E_{mec} = 0.25 \%$).

indicates that σ_{op} is not controlled by K_{max} as sometimes observed in stress-controlled testing [147-148]. The results shown in Figure 6.16 support the argument that σ_{op} is a function of the dominant stress component (tensile or bending) in SEN specimens tested under strain controlled conditions.

An explanation for a decreasing σ_{op} with increasing crack length can be found in the work of Tanaka et al. [149-150] and Murakani et al. [151-152] which have shown (for a given crack length) that σ_{op} decreases when the plastic strain ranges increases. Furthermore, they showed that, under large cyclic plastic strains, cracks remain fully open even at the minimum stress (σ_{min}). For a center-cracked panel (CCP) specimen under remote uniform displacement (i.e., ϵ_0), Murakani [153] has obtained, using finite element analysis, an equation describing the singularity in strain distribution at the tip of a crack of length "a", i.e.,

$$\epsilon_y = C(n) \cdot \epsilon_0 \cdot (a/r)^{\alpha(n)}, \quad (6.5)$$

where $C(n)$ is a function which depends on the strain hardening exponent n , ϵ_0 the imposed remote far-field strain, and $\alpha(n)$ the singularity term which depends on the strain hardening exponent. For $n = 5$, the singularity term α is 0.52 and for $n = 13$, α is 0.64 [153]. Although not exact, Eq. 6.5 provides a rationale for the decrease in σ_{op} with increasing crack length. As "a" increases (at fixed ϵ_0), the plastic strain range ϵ_y at the crack increases and σ_{op} decreases, in agreement with the observation of Tanaka et al. [149-152]. A decrease in σ_{op} with increasing a/W has recently been reported in a CCP specimen of low carbon steel cycled under fully reversed stress conditions [149]. However, the decrease in σ_{op} with a/W is likely to be larger in SEN specimens than in CCP specimens, because the plastic strain range at the

crack tip will be larger (for a given ϵ_0). In the case of SEN specimens, ϵ_y not only depends on ϵ_0 and n as indicated by Eq. 6.5, but also will include a component which is a function of the bending moment in the specimen. In conclusion, the considerable drop of σ_{op} with increasing crack length, which leads to an increase in ΔK_{eff} , explains why the crack growth rates increase even if the material experiences a significant drop in the actual load (N_{max}) which tends to reduce ΔK_{eff} .

6.5 Fatigue Crack Growth (FCG) in Hastelloy-X

The applicability of fracture mechanics to correlate TMFCG data under displacement controlled conditions in Hastelloy-X is checked by comparing our data with those of Pratt & Whitney Aircraft (PWA) obtained on tubular specimens with an EDM slot in the center of the gage section [41]. As for B-1900+Hf, the conventional definition of the ΔK_E was used (i.e., Eq. 6.3) for purpose of comparison. Figure 6.17 shows the results for out-of-phase cycling between 400-925°C at $\Delta \epsilon_{mec} = 0.25\%$. The results of PWA (i.e., the scatterband) for out-of-phase cycling between 426-871°C and 426-927°C at a frequency of 2 min. per cycle are shown. The following comments are made concerning the data presented in Figure 6.17.

First, the 426-871°C tests data show the fastest crack growth rates of all out-of-phase tests run at a frequency of 2 min/cycle. This does not agree with the intuitive result that the higher the peak temperature in the TMF cycle, the faster should be the crack growth rate.

Secondly, the 426-871°C tests data at 2 min/cycle are in good agreement with the 400-925°C tests data at 3 min/cycle. The

FATIGUE CRACK PROPAGATION

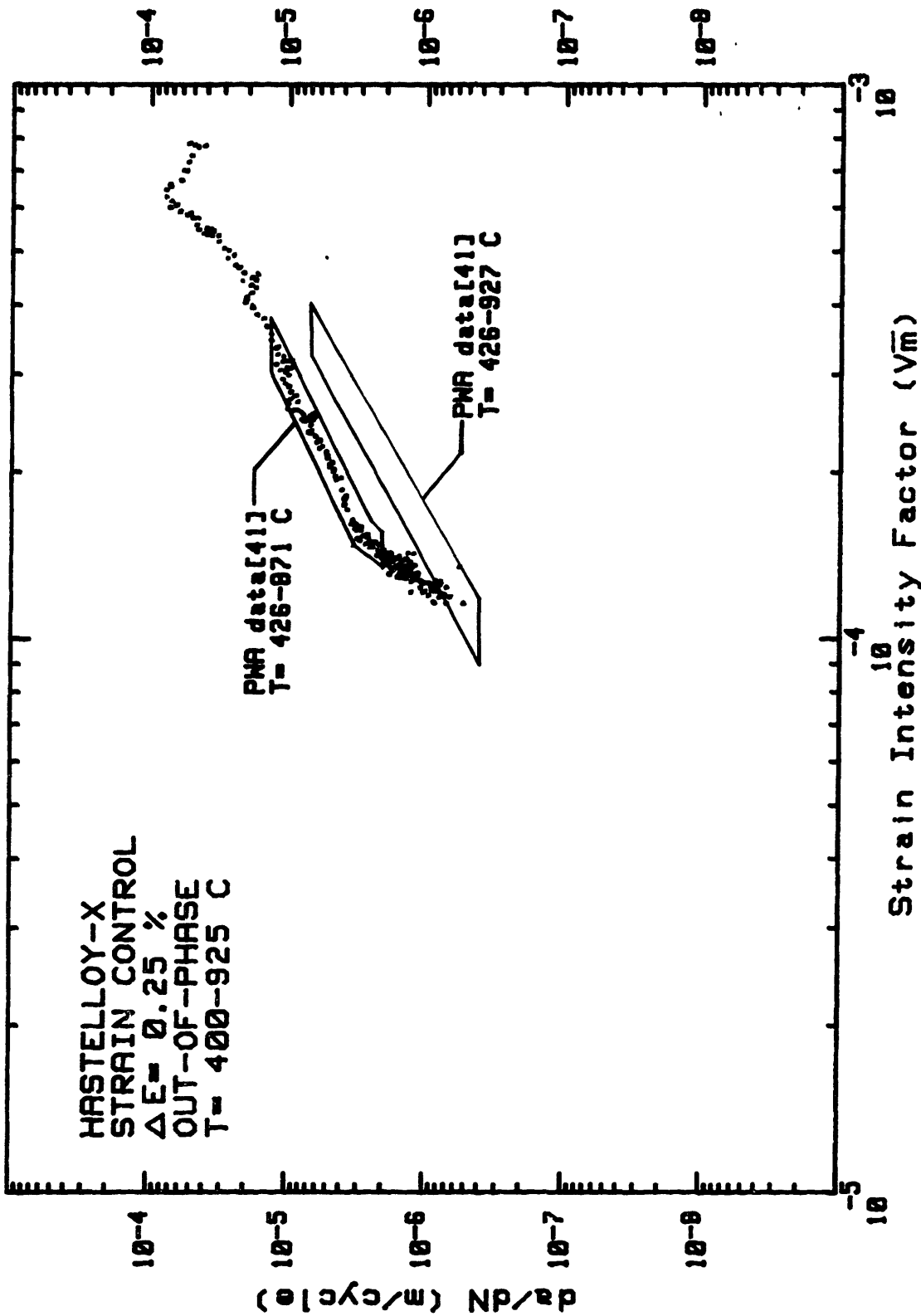


Figure 6.17 Out-of-phase crack growth rates in Hastelloy-X as a function the conventional strain intensity factor in SEN and tubular specimens[4].

explanation for these observations can be attributed to extensive ageing of the γ -matrix which takes place in the vicinity of 815-871°C [154-155]. At temperatures lower than 815°C the kinetic of $M_{23}C_6$ and Laves phase precipitation is slow because diffusion is slow. At temperatures above 875°C, the solubility of the γ -matrix is high enough and the driving force for precipitation (i.e., supersaturated concentration) is reduced. In other words, the main controlling parameter for ageing of the γ -matrix in fatigue will be the time spent in the temperature range of 815-871°C within each cycle. It is interesting to note that the time spent per cycle in the temperature range of 815-871°C is 15 sec. for the 426-871°C test, 12 sec. for the 426-927°C test, and 19 sec. for the 400-925°C test (3 min/cycle). Because the properties of the γ -matrix controls the crack growth behavior, the results shown in Figure 6.17 are not surprising. In fact, based on the previous argument, one would expect faster crack growth rates for the 400-925°C test (3 min/cycle) than for the 426-871°C test (92 min/cycle) because the time spent per cycle in the range of 815-871°C is larger. Nevertheless, the agreement between the two geometries is quite good which suggests that fracture mechanics is applicable for TMF of ductile materials like Hastelloy-X.

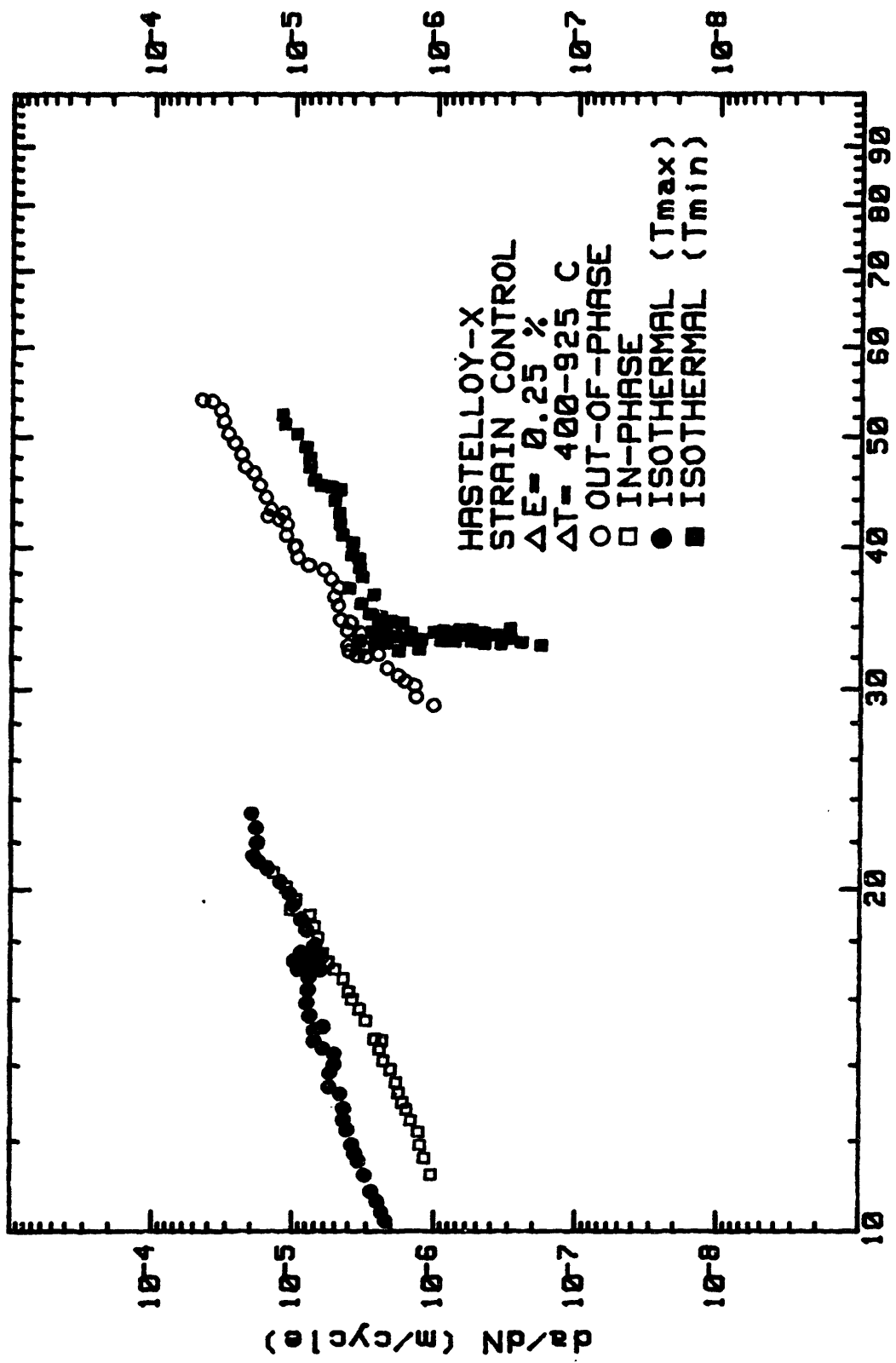
Figure 5.34 shows that the TMFCG rates under elastic cycling ($\Delta \epsilon_{mec} = 0.25\%$) are faster than those obtained under isothermal cycling at T_{max} . However, the TMFCG rates are lower than their isothermal counterpart under fully plastic cycling ($\Delta \epsilon_{mec} = 0.25\%$) which is consistent with the crack growth behavior of B-1900+Hf (see section 5.4.3). Comparison of the crack growth rates as a function of ΔK_E also shows a considerable strain range effect which clearly indicates that

ΔK_{ϵ} is not the proper driving force for TMF crack growth (see section 5.4.4).

As for Inconel X-750 and B-1900+Hf, the crack growth rates data were plotted in terms of ΔK_{σ} using Eq. 5.1. Figures 6.18 and 6.19 show the results for $\Delta \epsilon_{mec} = 0.25\%$ and $\Delta \epsilon_{mec} = 0.50\%$. As can be seen in Figures 6.18 and 6.19, the ΔK_{σ} leads to an apparent increase in scatter between the various tests data. However, a close look at the results reveals, as for B-1900+Hf, that the stress intensity factor separates the tests data which failed intergranularly, and the tests which failed transgranularly in two distinct groups. Furthermore, comparison of Figure 6.18 and 6.19 shows that ΔK_{σ} provides a very good correlation of the crack growth rates with increasing strain range. This is unexpected since for the same applied strain range, the plastic strain range in Hastelloy-X are significantly larger than for B-1900+Hf. Therefore, the ability of ΔK_{σ} to correlate the crack growth data in Hastelloy-X should be limited as compared to B-1900+Hf.

The explanation for this dichotomy can be found in the work of Murakami [153] which have shown that the strain singularity term α at the crack tip (see Eq. 6.5) is a function of the strain hardening exponent (n) and remote strain (ϵ_0). More specifically for $n = 5$, α was shown to increase with increasing ϵ_0 up to a maximum value of 0.81 (the HRR singularity is 0.83) for $\epsilon_0 \approx 0.2\%$ and to further decrease to values about 0.5 under large plastic strain ($\epsilon_0 > 2.0\%$). With ΔK_{σ} , the singularity of the strain at the crack tip is 0.5. At large plastic strain the singularity term is also close to 0.5 [153]. If, for a given mode of fracture, the response of a material to given local stress-strain distribution (at the crack tip) is unique, the observed agreement between the elastic and

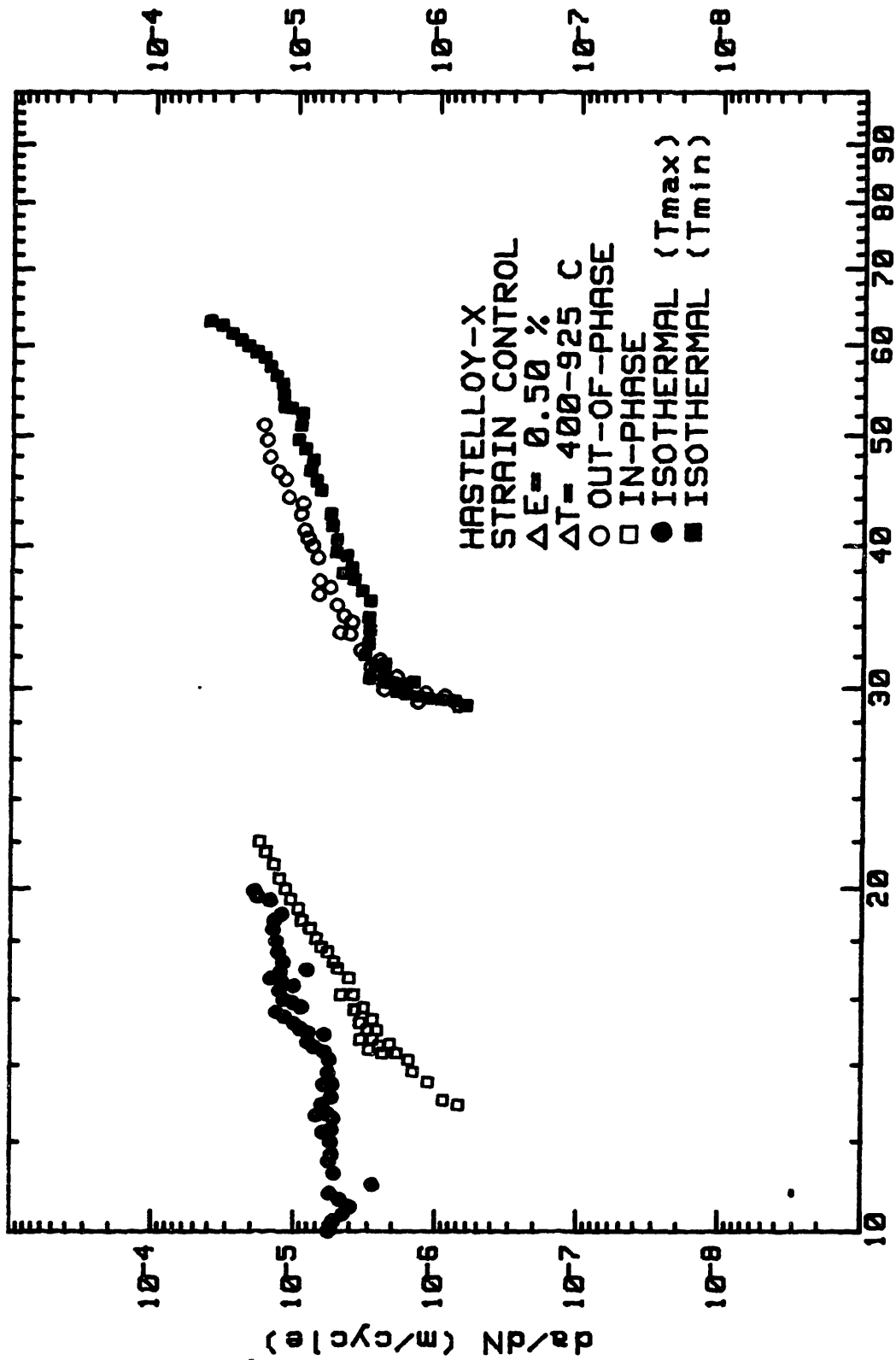
FATIGUE CRACK PROPAGATION



Stress Intensity Factor (MPa√m)

Figure 6.18 FCG rates in Hastelloy-X as a function of ΔK_{σ} ($\Delta \epsilon_{mec} = 0.25\%$)

FATIGUE CRACK PROPAGATION



Stress Intensity Factor (MPa√m)

Figure 6.19 FCG rates in Hastelloy-X as a function of ΔK_{σ} ($\Delta \epsilon_{mec} = 0.50\%$)

plastic strain cycling data is not surprising. For small plastic strains ΔK_{σ} provides a poor correlation of the data because the singularity at the crack tip is 0.83 (for $n = 5$) and the material response to this new stress-strain distribution will be different.

As for B-1900+Hf, an attempt to rationalize the effect of the various testing conditions on the crack growth rates was undertaken by using the measured values of the opening stress (σ_{op}) derived from the analysis of the potential drop signals. Figure 6.20, 6.21 and 6.22 shows the potential $V(\sigma)$ and the stress response of Hastelloy-X under isothermal, in-phase and out-of-phase cycling. A plot of σ_{op} as a function of crack length for $\Delta \epsilon_{mec} = 0.25\%$ and $T = 925^{\circ}\text{C}$ (see Figure 6.23) shows the same trend than in B-1900+Hf (see Figure 6.16). This suggests that the parameters which controlled σ_{op} are similar in both alloys. Using the value of σ_{op} , the crack growth rates as a function of ΔK_{eff} can be plotted. The result is shown in Figure 6.24. As can be seen, except for in-phase cycling, the ΔK_{eff} provides a very good correlation of the data. Furthermore, the correlation holds independently of the applied strain range and cyclic history. The implication of this result is the assumption that, for a given mode of fracture the response of the material to a particular stress-strain distribution at the crack tip is unique, is verified. On the other hand, the mode of fracture is controlled by the tensile strain rate ($\dot{\epsilon}^+$) at the crack tip. If the $\dot{\epsilon}^+$ which depends on the frequency, $\Delta \epsilon$ and a/W , is below the critical value ($\dot{\epsilon}^+_{crit}$) requires to cause intergranular fracture at temperature T , intergranular cracking occurs. The value of $\dot{\epsilon}^+_{crit}$ is a function of only the temperature for a given material and environment.

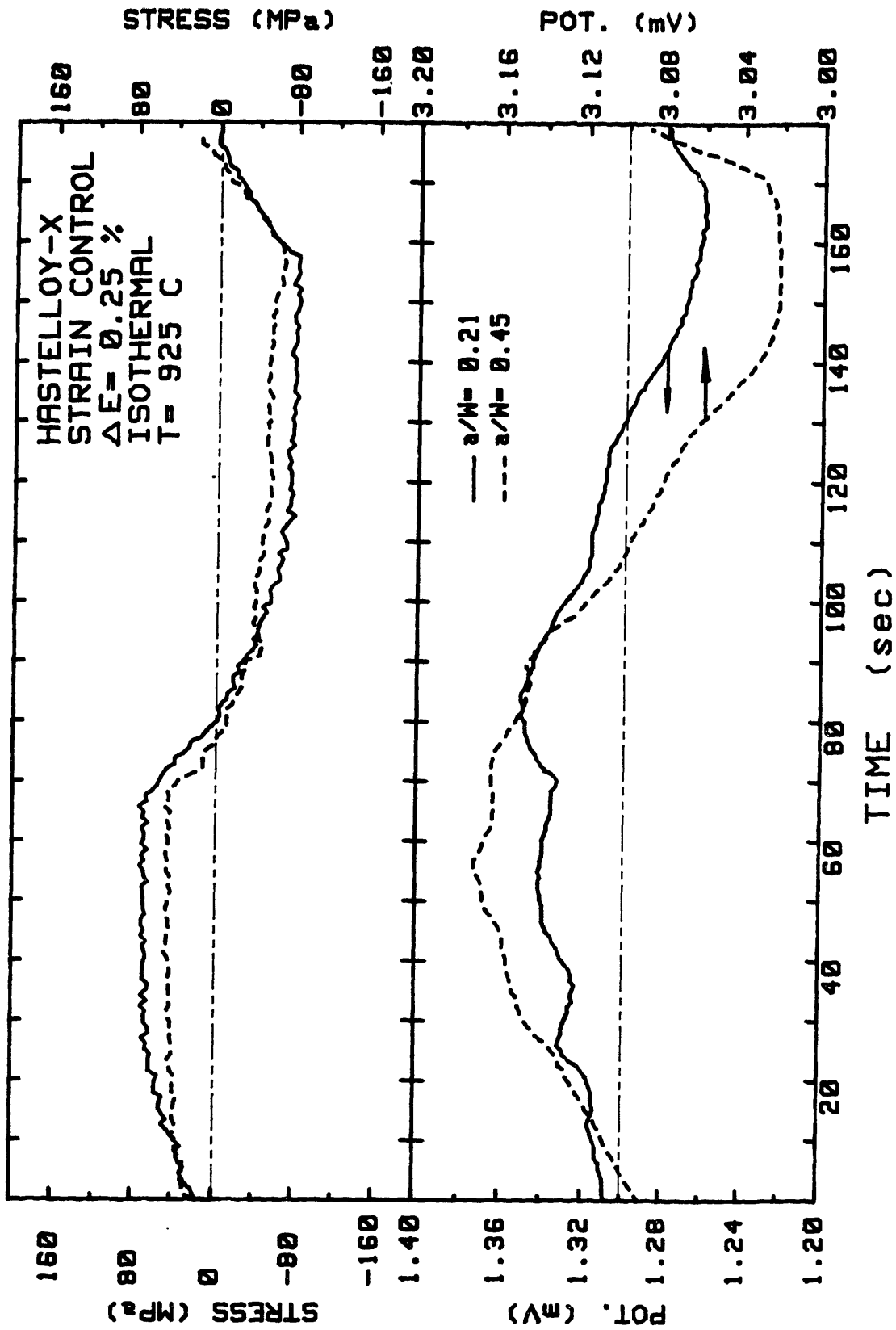


Figure 6.20 Potential curve $V(\sigma)$ and stress amplitude in Hastelloy-X under isothermal cycling (T_{max}).

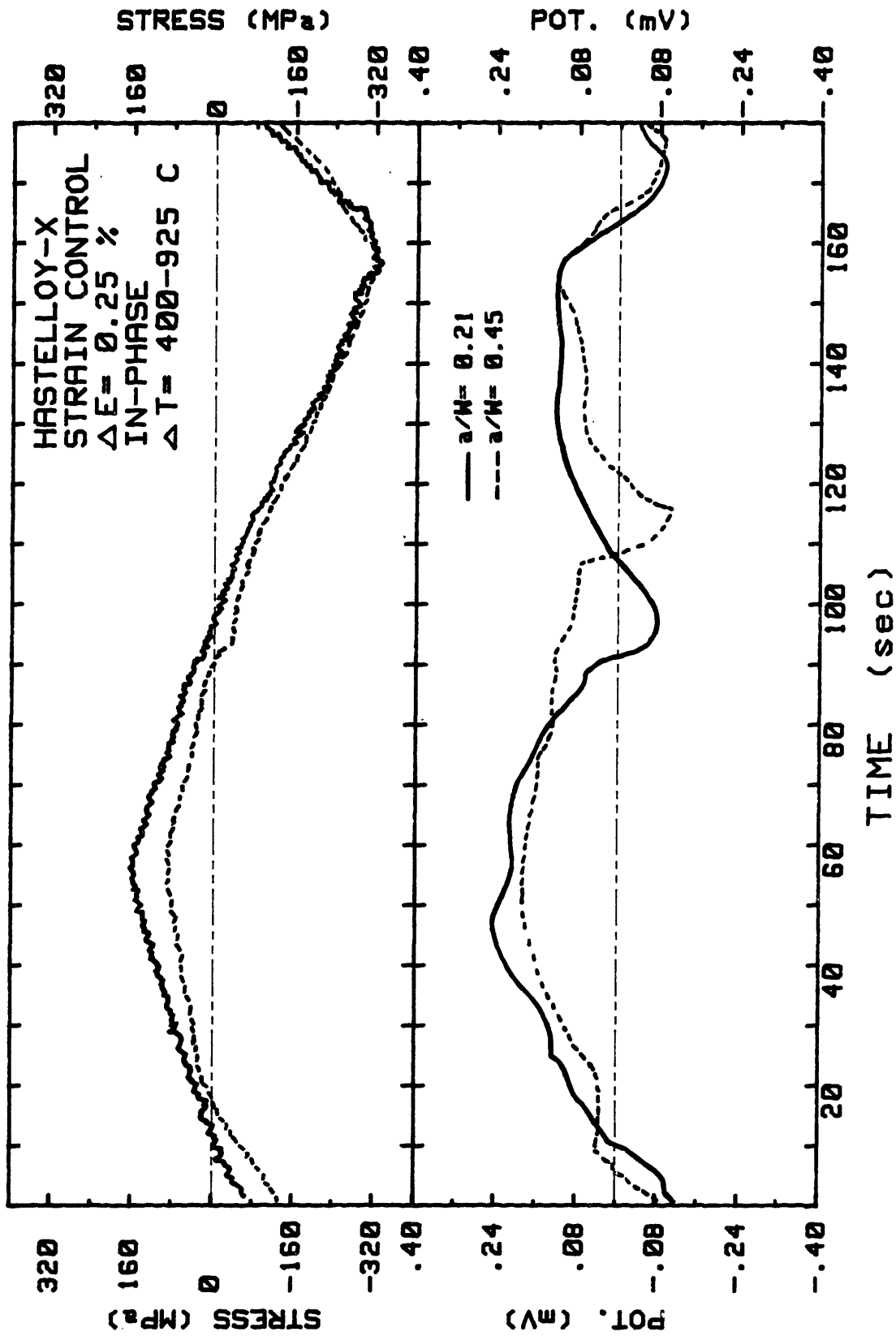


Figure 6.21 Potential curve $V(\sigma)$ and stress amplitude in Hastelloy-X under in-phase cycling.

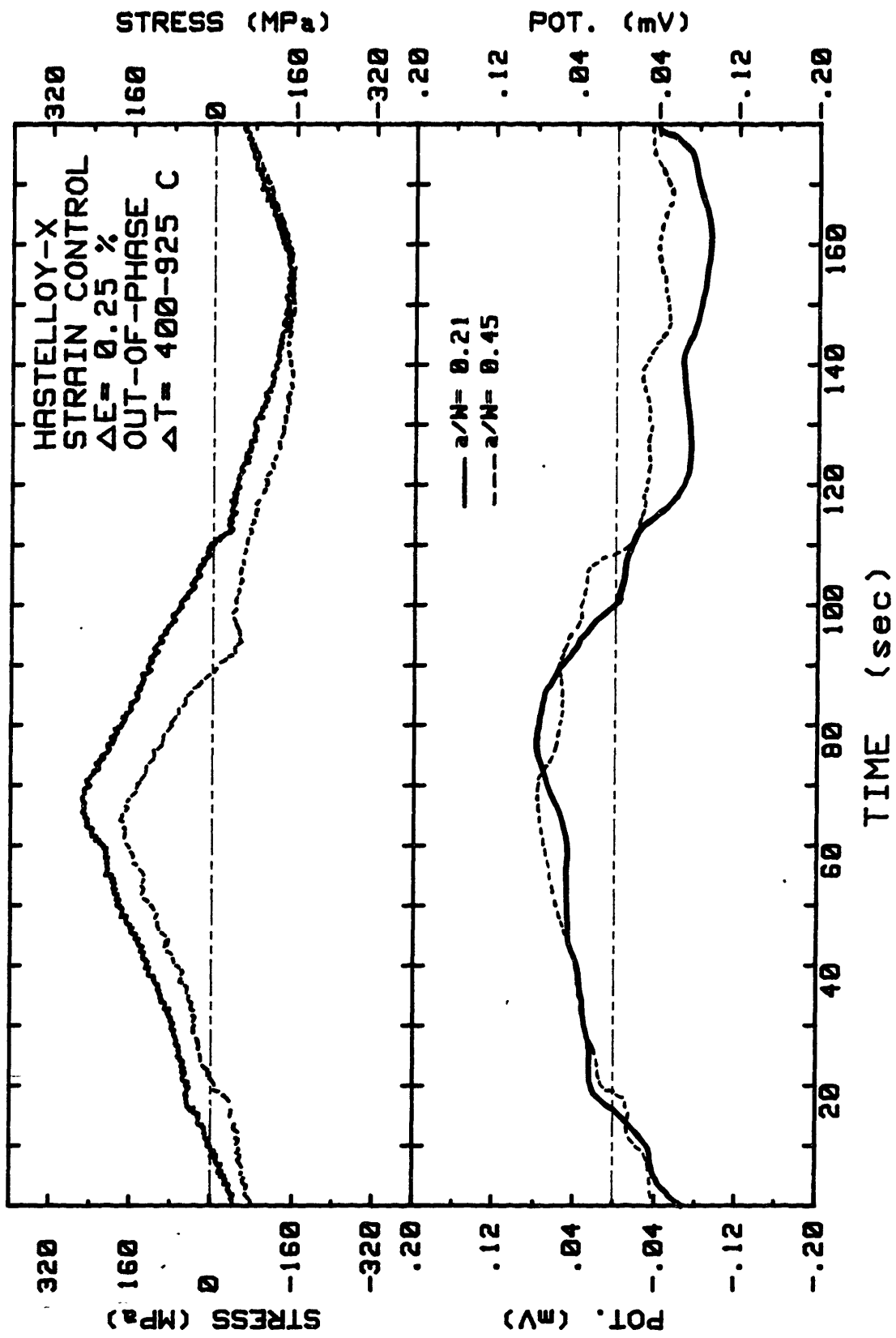


Figure 6.22 Potential curve $V(\sigma)$ and stress amplitude in Hastelloy-X under out-of-phase cycling.

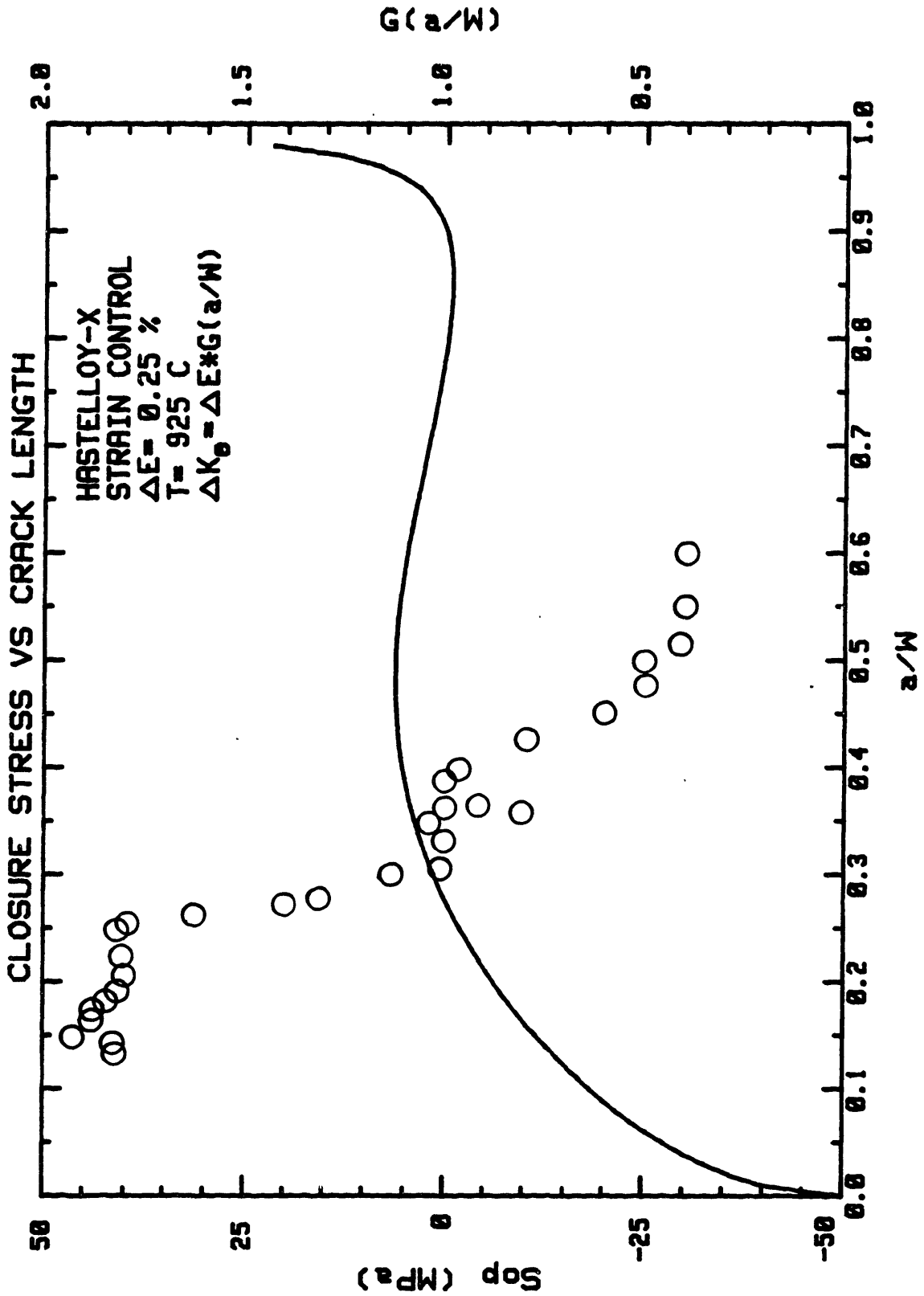


Figure 6.23 Variation of the opening stress (σ_{op}) as a function of crack length in Hastelloy-X ($T = 925 \text{ }^{\circ}\text{C}$, $\Delta E_{mec} = 0.25 \%$)

FATIGUE CRACK PROPAGATION

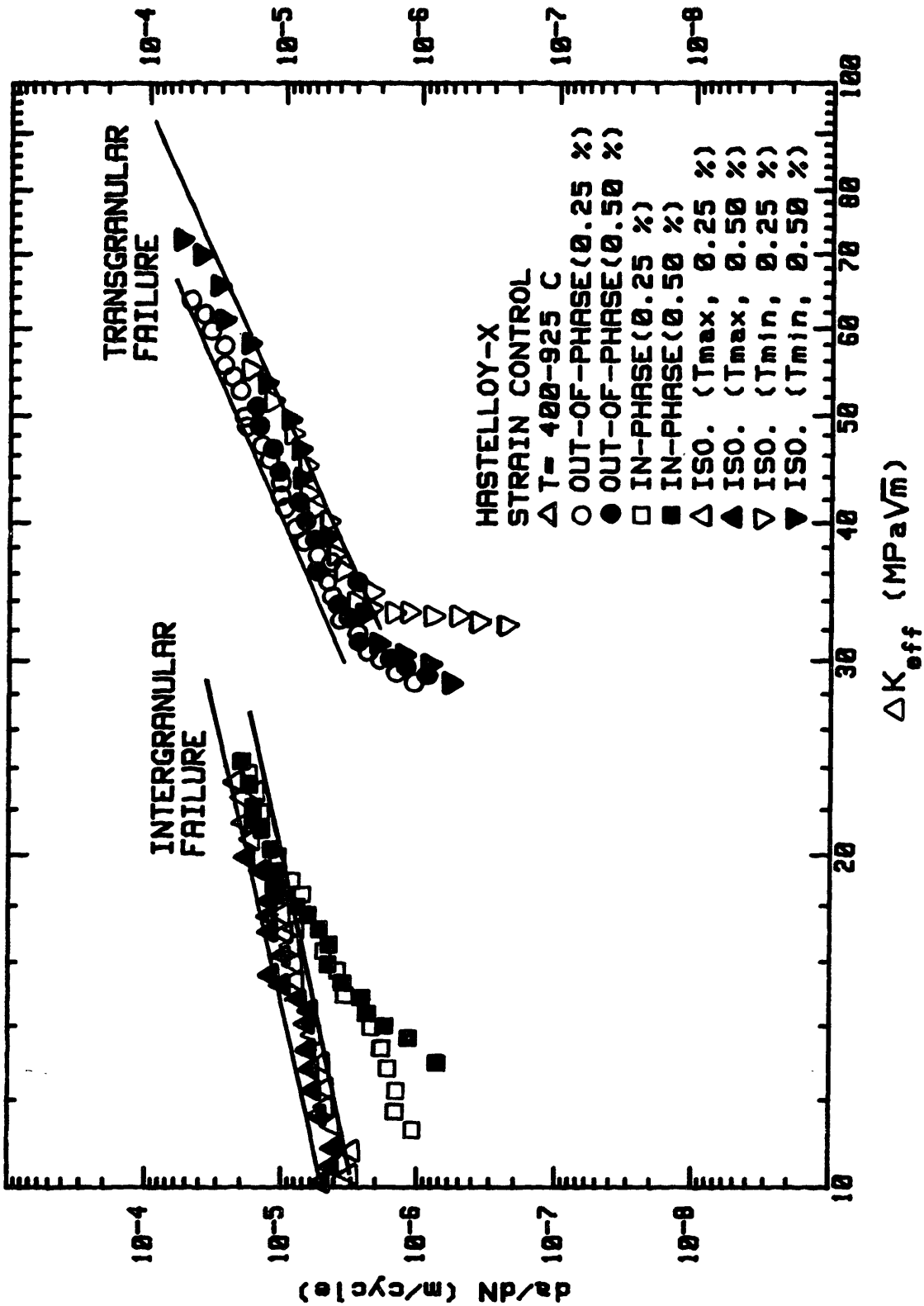


Figure 6.24 FCG rates in Hastelloy-X as a function of ΔK_{eff}

6.6 Correlation Parameters for In-Service Components

The complete description of a thermal-mechanical cycle requires a definition of the relationship between strain and temperature. The prediction of the crack propagation life of an engine component ideally requires the correct prediction of crack growth rates at all locations along the crack growth path. Cracks grow through regimes with a range of different TMF cycles. Solving an in-service component problem requires the ability to predict the crack growth rates for many different strain-temperature paths. If each different TMF cycle requires independent crack growth data, the total data base required for making life predictions would be prohibitively large. Two strategies for dealing with this problem can be used:

1. Methods of predicting TMF crack growth rates from isothermal data,
2. Develop a way of using TMF data for one type of TMF cycle (e.g., out-of-phase) to predict growth rates occurring in more complex strain-temperature (ϵ -T) cycles (see Figure 1.1).

The first approach is indeed more desirable than strategy 2 because isothermal data are more commonly available and less expensive to generate.

We have shown that ΔK_{σ} and ΔK_{eff} collapse the data to a great extent which indicates that prediction of complex ϵ -T cycles from isothermal data is possible. From isothermal testing the da/dN vs ΔK_{eff} curve is obtained, which in turn is used in prediction of crack growth rates of component (assuming that the ΔK_{eff} for the component is

known). Although the results in Figures 6.6, 6.10, 6.15 and 6.24 are promising there are still some unaccounted scatter in the results of which suggests that ΔK_{eff} might not be the universal parameter. The differences between the TMF and isothermal data might be the results of one or more of the following factors:

1. The effect of material ageing (coarsening of γ' in the case of B-1900+Hf and Inconel X-750, and carbides precipitation in Hastelloy-X),
2. Temperature change during straining might result in crack growth mechanisms that do not occur isothermally. Damage due to differential expansion of the oxide layer relative to the base metal is one possible mechanism of this type.
3. The success of the correlation parameter may depend on the path and method used for its calculation.

Although our results indicate that the best parameter for predicting TMF crack growth from isothermal data may be ΔK_{eff} , the application of ΔK_{eff} , in practice, is inconvenient because we must measure or assume the opening ratio of a crack in real components and this measurement is very difficult. Therefore, it is preferable in practice to determine the value of ΔK as a function of crack size and geometry and then estimate the crack growth rates rather than estimating ΔK_{eff} (i.e., σ_{cl}). With this respect, the prediction of complex ϵ -T cycles from TMF data is an advancement over using isothermal data at the peak temperature. This strategy involves the decomposition of complex ϵ -T cycles into more simple TMF cycles, and the use of the crack growth data (in terms of ΔK_{σ}) measured under TMF conditions to predict the growth rates of complex ϵ -T cycles. Models based on the scheme cited above might not give improved crack growth predictions

when compared to strategy 1, but they would not require the knowledge of opening ratios in complex components. The ultimate accuracy of these predictions is only limited by the extent to which complex ϵ -T crack growth is produced by unique damage mechanisms.

7.0 Conclusions

The main achievements of this work can be summarized as follows:

1. A thermal-mechanical fatigue test rig has been built around a conventional servo-hydraulic machine to simulate complex stress-strain-temperature cycles as experienced for in-service components. The system and its capabilities have been described in detail. A corrected DC potential drop technique used to accurately measure crack lengths was shown to yield better capabilities for low crack growth rate measurements ($< 10^{-6}$ m/cycles) than the conventional methods used in thermal-mechanical fatigue crack growth testing.

2. It was shown that solid specimen geometries can be used to simulate in-service thermal-mechanical fatigue crack growth conditions. The SEN geometry has some advantages over the tubular geometry in that it allows deterministic crack length measurements and the use of an accurate fracture mechanics solution.

3. Exact K-solutions for SEN specimens under fixed-end displacements controlled with no-free rotation were derived. It was shown that for this case, the use of conventional fracture mechanics K-solutions can seriously overestimate the actual K's. The conventional definition of the strain intensity factor was shown to be in error because it fails to take into account both load shedding and the closing bending moments.

4. The thermal-mechanical crack growth (TMFCG) rates in Inconel X-750 were measured under stress-controlled conditions in the temperature range from 300 to 650°C. On a stress intensity basis (ΔK_{σ})

the TMFCG rates were faster than their isothermal counterpart. Using an effective stress range ($\Delta \sigma_{\text{eff}}$) computed using measured values of the opening stress, good correlation between isothermal and TMF crack growth rates were obtained on a ΔK_{eff} -basis.

5. The cyclic stress-strain behavior for B-1900+Hf under TMF cycling differs from the isothermal behavior by showing more cyclic hardening (> 15%), both at high and low temperatures. Thus it is difficult to predict the cyclic stress-strain behavior under realistic conditions from isothermal data. The synergistic coupling between the cyclic stress-strain behavior and temperatures cannot be ignored.

6. The cyclic flow stress at elevated temperature (T_{max}) is primarily controlled by the density of misfit dislocations, which depends on the amount of isotropic and directional coarsening. At low temperature (T_{min}) the flow stress is controlled by the directionality of the stress field around the γ' , the magnitude of which depends on the sign of the applied stress.

7. Using a strain-based approach (ΔK_{ϵ}), a poor correlation between the isothermal and the TMFCG rates under elastic ($\Delta \epsilon_{\text{mec}} = 0.25\%$) and/or fully plastic ($\Delta \epsilon_{\text{mec}} = 0.50\%$) conditions were observed. A stress-based approach (ΔK_{σ}) which takes into account the hardening/softening behavior of the materials as well as the load shedding caused by extra-compliance provided by the presence of the crack was shown to rationalize the isothermal and TMF crack growth rates. Furthermore, based upon the ΔK_{eff} , the isothermal crack growth rates at T_{min} and T_{max} were shown to provide an upper and lower bounds for the TMFCG rates, respectively.

8. The cracking modes (transgranular vs. intergranular) in B-1900+Hf and Hastelloy-X are controlled by the occurrence of a critical tensile stress (σ_c) for intergranular or transgranular fracture, rather than by a critical tensile strain. Each mode of fracture is shown to be characterized by a unique crack growth rate vs. ΔK_{eff} curve.

9. The opening stress (σ_{op}) was shown to be a complex function of crack length and strain range.

10. For the materials and testing conditions used in this investigation, the crack growth rates are controlled by the mechanical driving force (ΔK_{σ} , ΔK_{eff}) only. The time-dependent components (oxidation and creep) were shown not to affect significantly the crack growth rates.

8.0 Recommendations for Future Work

The problem of thermal-mechanical fatigue in hot section engine components was extensively examined. The major areas investigated included a problem survey, experimental fracture mechanics techniques, evaluation of data correlation parameters, and prediction of crack growth under thermal-mechanical cycling. The following are the major observations and recommendations from this effort.

1. The crack propagation testing and data reduction for the various materials tested showed the necessity of the use of a physically sound data correlation parameter. The conventional strain intensity factor shows several results which make its use undesirable for TMF crack growth prediction. There was some strain range dependence on crack growth rates using both ΔK_{ϵ} and ΔK_{σ} parameters. Of the parameters extensively studied, the ΔK_{eff} was the best all-around approach for correlating high temperature and TMF data. Extensive evaluation of the ΔK_{eff} for TMF cycling is recommended.

2. The fracture mechanics analysis used a compliance approach to calculate a value for the correlation parameter. The compliance approach was originally developed for isothermal testing to obtain an experimental value of the K_{ϵ} . The compliance approach was extended for a more complicated situation, which includes spatially varying temperatures, and temperature-dependent material properties. Thus, the parameter calculated cannot be termed a "K" in the strictest sense. Further assessment of other parameters which are both theoretically justified and calculable for structural components is recommended.

3. Development of cyclic nonlinear fracture mechanics capability is recommended to better understand TMF crack growth, especially when substantial plastic strain develops.

4. There were marked differences in the specimen crack growth surface features as a function of temperature and TMF cycle. Low temperature isothermal growth was smooth and transgranular. High temperature isothermal growth was rough and intergranular. Out-of-phase TMF crack growth was moderately rough and chiefly transgranular whereas in-phase cycling was rough and intergranular. This evidence shows that not only is the temperature range and strain range important in TMF tests, but the cycle shape is also important. Crack growth in service tends to be of moderate level of surface roughness and chiefly transgranular, similar to out-of-phase TMF tests. This observation lends hope to the ultimate success of using simple TMF data to predict complex ϵ -T scheme. However, the final degree of success will be determined by the degree to which complex ϵ -T crack growth is governed by unique mechanisms not present under simple TMF conditions. Further work is recommended to further compare the damage which takes place under TMF and complex ϵ -T cycles.

9.0 References

1. D.A. Spera, "What is Thermal Fatigue?", ASTM STP 612, 1976, pp. 3-9.
2. R.P. Skelton, "The Growth of Short Cracks During High Strain Fatigue and Thermal Cycling", ASTM STP 770, 1982, pp. 337-381.
3. J. Wareing, "Mechanisms of High Temperature Fatigue and Creep-Fatigue Failure in Engineering Materials", in Fatigue at High Temperature, ed. by R.P. Skelton, Applied Sci. Pub., 1983, pp. 135-185.
4. W.J. Mills and L.A. James, "Effect of Temperature on the Fatigue Crack Propagation Behavior of Inconel X-750", *Fat. Eng. Mat. Struct.*, Vol. 3, 1980, pp. 159-175.
5. G.J. Lloyd, "High Temperature Fatigue and Creep-Fatigue Crack Propagation: Mechanics, Mechanisms and Observed Behavior in Structural Materials", in Fatigue at High Temperature, ed. by R.P. Skelton, Applied Sci. Pub., 1983, pp. 187-258.
6. L.F. Coffin, "Damage Processes in Time Dependent Fatigue--A Review", in Creep-Fatigue-Environment Interactions, ed. by R.M. Pelloux and N.S. Stoloff, AIME Pub., 1980, pp. 1-23.
7. S. Taira, "Relationship Between Thermal Fatigue and Low Cycle Fatigue at Elevated Temperature", ASTM STP 520, 1973, pp. 80-101.
8. E. Glenny, J.E. Northwood, S.W. Shaw and T.A. Taylor, "A Technique for Thermal-Shock and Thermal-Fatigue Testing Based on the Use of Fluidized Solids", J. Inst. Met., Vol. 87, 1959, pp. 194-202.
9. P. Bizon and D.A. Spera, "Thermal Stress Fatigue Behavior of 26 Superalloys", ASTM STP 612, 1976, pp. 106-122.
10. M.A. Howes, "Thermal Fatigue and Oxidation Data on TAZ-8A, Marm-200 and Udimet 700 Superalloys", NASA CR-134775, 1975.

11. K.E. Hofer and V.E. Humphreys, "Thermal Fatigue and Oxidation Data of TAZ-8A and M22 Alloys and Variations", NASA-3-17787, 1981.
12. D.F. Mowbray and J.E. McConnelee, "Nonlinear Analysis of a Tapered Disk Thermal Fatigue Specimen", ASTM STP 612, 1976, pp. 10-29.
13. V. Moreno, G.J. Meyers, A. Kaufman and G.R. Halford, "Nonlinear Structural and Life Analyses of a Combustor Liner", NASA TM-82846, 1982, 21 pgs.
14. D.A. Spera and E.C. Cox, "Description of a Computerized Method for Predicting Thermal Fatigue Life of Metals", ASTM STP 612, 1976, pp. 69-85.
15. L.F. Coffin and R.P. Wesley, "Apparatus for Study of Effects of Cyclic Thermal Stresses on Ductile Metals", Trans. ASME, 1954, pp. 123-130.
16. E.E. Baldwin, G.J. Sokol, and L.F. Coffin, "Cyclic Strain Fatigue Studies on AISI Type 347 Stainless Steel", Trans. ASTM, Vol. 57, 1957, pp. 567-576.
17. T. Udoguchi and T. Wada, "Thermal Effect on Low Cycle Fatigue Strength of Steels", Thermal Stresses and Thermal Fatigue, ed. D.J. Littler, Butterworth, London, 1971, pp. 109-123.
18. R.H. Stentz, J.T. Berling and J.B. Conway, "A Comparison of Combined Temperature and Mechanical Strain Cycling Data With Isothermal Fatigue Results", Proc. 1st Int. Conf. on Structural Mechanics in Reactor Technology, Berlin, Vol. 6, 1971, pp. 391-411.
19. U.S. Lindholm and D.L. Davidson, "Low Cycle Fatigue With Combined Thermal and Strain Cycling", ASTM STP 520, 1973, pp. 473-481.
20. K.D. Sheffler and G.S. Doble, "Thermal Fatigue Behavior of T-111 and ASTAR 811C in Ultra High Vacuum", ASTM STP 520, 1973, pp. 491-499.

21. K.D. Sheffler, "Vacuum Thermal-Mechanical Fatigue Behavior of Two Iron-Base Alloys", ASTM STP 612, 1976, pp. 214-226. (See also NASA-CR-134534.)
22. R.P. Skelton, "Environmental Crack Growth in 1/2 Cr-Mo-V Steel During Isothermal High Strain Fatigue and Temperature Cycling", Mat. Sci. Eng., Vol. 35, 1978, p. 287-298.
23. S. Taira, M. Fujino and H. Higaki, "In-Phase Thermal Fatigue Strength of Steels", J. Soc. Mat. Sci. Japan, Vol. 25, 1976, pp. 375-381.
24. N. Fujino and S. Taira, "Effect of Thermal Cycle on Low Cycle Fatigue Life of Steels and Grain Boundary Sliding Characteristics", ICM 3, Vol. 2, 1979, pp. 49-58.
25. K. Kuwabara and A. Nitta, "Effect of High Temperature Tensile Strain Holding in Thermal Fatigue Fracture", in Symposium on Creep-Fatigue Interaction, ed. R.M. Curran, ASME-MPC, New York, 1976, pp. 161-177.
26. K. Kuwabara and A. Nitta, "Thermal-Mechanical Low Cycle Fatigue Under Creep-Fatigue Interaction in Type 304 Stainless Steel", ICM 3, Vol. 2, 1979, pp. 69-78.
27. C.A. Rau, A.E. Gemma and G.R. Leverant, "Thermal-Mechanical Fatigue Crack Propagation in Nickel and Cobalt-Base Superalloys Under Various Strain-Temperature Cycles", ASTM STP 520, 1973, pp. 166-178.
28. A.E. Gemma, B.S. Langer and G.R. Leverant, "Thermal Mechanical Fatigue Crack Propagation in Anisotropic Nickel-Base Superalloy", ASTM STP 612, 1976, pp. 199-213.
29. A.E. Gemma, F.X. Ashland, and R.M. Masci, "The Effects of Stress Dwell and Varying Mean Strain on Crack Growth During Thermal Mechanical Fatigue", J. Test. Eval., Vol. 9, No. 4, 1981, pp. 209-215.
30. S. Taira, M. Fujino and R. Ohtani, "Collaborative Study of Thermal Fatigue Properties of High Temperature Alloys in Japan", Fat. Eng. Mater. Struct., Vol. 1, 1979, pp. 495-508.
31. M.J. Westwood, "Tensile Hold Time Effects on Isothermal and

- Thermal Low Cycle Fatigue of 304 Stainless Steel", ICM 3, Vol. 2, 1976, pp. 59-67.
32. V.T. Troshchenko and L.A. Zaslotskaya, "Fatigue Strength of Super-alloys Subjected to Combined Mechanical and Thermal Loading", ICM 3, Vol. 2, pp. 3-12.
 33. A.P. Gussenkov and A.G. Kasantsev, "A Kinetic Deformation Criterion for Creep Low Cycle Fatigue Under Nonisothermal Loading", ICM 3, Vol. 2, 1979, pp. 43-49.
 34. V.N. Filatov, A.S. Kruglov, S.V. Evropin and O.G. Yuren, "Non-isothermal Fatigue Testing of 12 kh18N9-Steel Within a Reactor", Zav. Labo., Vol. 47, No. 1, 1981, pp. 77-78.
 35. G.A. Tulyakov, V.A. Plekhanov and V.N. Skorobogatykh, "Installation for Low Cycle Isothermal and Nonisothermal Fatigue Tests With Complex Loading", Zav. Labo., Vol. 44, No. 9, 1978, pp. 1133-1136.
 36. S.W. Hopkins, "Low Cycle Thermal Mechanical Fatigue Testing", STM STP ;612, 1976, pp. 157-169.
 37. N.D. Sobolev and I. Egorov, "Recording Cycle Strain Diagrams Under Nonisothermal Conditions (Review)", Zav. Labo., Vol. 45, No. 5, 1979, pp. 449-452.
 38. E.G. Ellison, "Thermal-Mechanical Strain Cycling and Testing at Higher Temperatures", in Measurement of High Temperature Mechanical Properties of Materials, ed. by M.S. Loveday, M.F. Day and B.F. Dyson, HMSO Pub., 1982, pp. 204-224.
 39. L.F. Coffin, "Fatigue at Elevated Temperature", ASTM STP 520, 1973, pp. 5-34.
 40. R.L. McKnight, J.H. Laflen and G.T. Spamer, "Turbine Blade Tip Durability Analysis", NASA CR-165268, 1981, 112 pgs. *
 41. G.J. Meyers, "Fracture Mechanics Criteria for Turbine Engines and Hot Section Components", NASA CR-167896, 1982, 115 pgs.
 42. M. Clavel, C. Levailant and A. Pineau, "Influence of Micro-mechanisms of Cyclic Deformation at Elevated Temperature on

- Fatigue Behavior", in Creep-Fatigue-Environment Interactions, ed. by R.M. Pelloux and N.S. Stoloff, AIME Pub., 1980, pp. 24-45.
43. R.H. Cook and R.P. Skelton, "Environment-Dependence of the Mechanical Properties of Metals at High Temperature", *Int. Met. Rev.*, Vol. 19, Rev. 187, 1974, pp. 199-222.
 44. H.W. Grunling, K.H. Keienburg and K.K. Schweitzer, "The Interaction of High Temperature Corrosion and Mechanical Properties of Alloys" in High Temperature Alloys for Gas Turbines, ed. by Brunetand, Coutsouradis, Gibbons, Lindblom, Meadowcraft and Stickley, Reidel Pub., 1982, pp. 507-543.
 45. J.M. Davidson, K. Aning and J.K. Tien, "Hot Environment Effects on Alloy Mechanical Properties", in Symp. on Properties of High Temperature Alloys with Emphasis on Environmental Effects, Pub. by Electrochemical Soc., Princeton, NJ, 1976, pp. 175-198.
 46. P. Marshall, "The Influence of Environment in Fatigue", in Fatigue at High Temperature, ed. by R.P. Skelton, Appl. Sci. Pub., 1983, pp. 253-303.
 47. M.A.H. Howes, "Thermal Fatigue and Oxidation of Two Iron Base Alloys", ASTM STP 612, 1976, pp. 86-105.
 48. M.O. Speidel and A. Pineau, "Fatigue of High Temperature Alloys for Gas Turbines", in High Temperature Alloys for Gas Turbines, ed. by Coutsouradis, Felix, Tischmeister, Habraken, Lindblom and Speidel, Appl. Sci. Pub., 1978, pp. 469-512.
 49. S.D. Antolovich, "Aspects Metallurgiques de la Fatigue a Haute Temperature", in La Fatigue des Materiaux et Structures, ed. by C. Bathias and J.P. Bailon, Montreal University Press, 1980, pp. 465-496.
 50. A. Pineau, "High Temperature Fatigue: Creep-Fatigue Oxidation Interactions in Relation to Microstructure", in Subcritical Crack Growth Due to Fatigue, Stress Corrosion and Creep, ed. by ISPRA, Appl. Sci. Pub., in press.
 51. G.R. Leverant, T.E. Strangman and B.S. Langer, "Parameters Controlling the Thermal Fatigue Properties of Conventional Cast and Directionally Solidified Turbine Alloys", in Superalloys:

- Metallurgy and Manufacture, ed. by Kear, Muzuka, Tien and Wlodek, Claxtors Pub., 1976, pp. 285-295.
52. A. Pineau, "High Temperature Fatigue Behavior of Engineering Materials in Relation to Microstructure", in Fatigue at High Temperature, ed. by R.P. Skelton, Appl. Sci. Pub., 1983, pp. 305-364.
 53. D.H. Boone and C.P. Sullivan, "Effect of Several Metallurgical Variables on the Thermal Fatigue Behavior of Superalloys", ASTM STP 520, 1973, pp. 401-415.
 54. M. Gell and G.R. Leverant, "Mechanisms of High Temperature Fatigue", ASTM STP 520, 1973, pp. 37-67.
 55. F.E. Fujita, "Oxidation and Dislocation Mechanisms in Fatigue Crack Formation", in Fracture of Solids, ed. by D.S. Drucker and J.J. Gilman, AIME-TMS, 1963, pp. 657-670.
 56. J. Wareing and H.G. Vaughan, "The Relationship Between Striation Spacing, Macroscopic Crack Growth Rate and the Low Cycle Fatigue Life of a Type 316 Stainless Steel at 625°C", *Met. Sci.*, Vol. 11, 1977, pp. 414-424.
 57. R.P. Skelton and J.I. Bucklow, "Cyclic Oxidation and Crack Growth During High Strain Fatigue of Low Alloy Steels", *Met. Sci.*, Vol. 12, 1978, pp. 64-70.
 58. T.E. Strangman, "Thermal Fatigue of Oxidation Resistant Overlay Coatings for Superalloys", Ph.D. Dissertation, Univ. of Conn., Storrs, Conn., 1978.
 59. R.P. Skelton, "Crack Initiation and Growth in Simple Metals Components During Thermal Cycling", Fatigue at High Temperature, ed. by R.P. Skelton, Appl. Sci. Pub., 1983, pp. 1-62.
 60. H.J. Westwood and W.K. Lee, "Creep-Fatigue Crack Initiation in 1/2 Cr-Mo-V Steel", in Creep and Fracture of Engineering Materials and Structure, ed. by B. Wilshire and D.J.R. Owen, Pineridge Press, 1982, pp. 517-530.
 61. C.E. Jaske, "Thermal-Mechanical Low Cycle Fatigue of AISI 1010 Steel", ASTM STP 612, 1976, pp. 170-198.

62. A.A. Sheinker, "Exploratory Thermal-Mechanical Fatigue Results for Rene 80 in Ultrahigh Vacuum", NASA CR-159444, 1978, 16 pages.
63. S. Bhongbhobhat, "The Effect of Simultaneously Alternating Temperature and Hold Time in the Low Cycle Fatigue Behavior of Steels", in Low Cycle Fatigue Strength and Elasto-plastic Behavior of Materials, ed. by K.T. Rie and E. Harbach, DVM Pub., 1979, pp. 73-82.
64. W.R. Adams and P. Stanley, "A Programmable Machine for Simulated Thermal Fatigue Testing", J. Phys. E. Sci. Inst., Vol. 7, 1974, pp. 669-673.
65. R.A.T. Dawson, W.J. Elder, G.J. Hill and A.T. Price, "High-Strain Fatigue of Austenitic Steels", in Thermal and High Strain Fatigue, ed. by The Metals and Metallurgy Trust, London, 1967, pp. 239-269.
66. A. Nitta, K. Kuwabara and T. Kitamura, "The Characteristic of Thermal-Mechanical Fatigue Strength in Superalloys for Gas Turbines", in Proc. of the Int. Gas Turbine Congress, Tokyo, 23-28 Oct., 1983.
67. T. Koizumi and M. Okazaki, "Crack Growth and Prediction of Endurance in Thermal-Mechanical Fatigue of 12 Cr-Mo-V-W Steel", Fat. Eng. Mat. & Struct., Vol. 1, 1979, pp. 509-520.
68. K. Sadananda and P. Shahinian, "Effect of Environment on Crack Growth Behavior in Austenitic Stainless Steels Under Creep and Fatigue Conditions", Met. Trans., Vol. 11A, 1980, pp. 267-276.
69. M. Okazaki and T. Koizumi, "Crack Propagation During Low Cycle Thermal-Mechanical and Isothermal Fatigue at Elevated Temperatures", Met. Trans., Vol. 14A, 1983, pp. 1641-1648.
70. D.A. Woodford, "Thermal Fatigue Testing of Gas Turbine Materials", ICM 3, Vol. 2, 1979, pp. 33-42.
71. D.A. Woodford and D.F. Mowbray, "Effect of Material Characteristics and Test Variables on Thermal Fatigue of Cast Superalloys", Mat. Sci. & Eng., Vol. 16, 1974, pp. 5-43.

72. K.D. Scheffler and J.J. Jackson, "Stress Analysis, Thermo-Mechanical Fatigue Evaluation and Root Subcomponent Testing of Gamma/Gamma Prime-Delta Eutectic Alloy", NASA CR-135005, 1976, 52 pages.
73. C. Berk and A.T. Santhanan, "Effect of Microstructure on the Thermal Fatigue Resistance of Cast Cobalt Alloy Mar-M509", ASTM STP 612, 1976, pp. 123-140.
74. W.J. Ostergren, "A Damage Function and Associated Failure Equations for Predicting Hold Time Frequency Effects in Elevated Temperature Low-Cycle Fatigue", J. Test. Eval., Vol. 4, 1976, pp. 327-339.
75. A.E. Carden and T.B. Slade, "High Temperature Low Cycle Fatigue Experiments on Hastelloy-X", ASTM STP 459, 1969, pp. 111-129.
76. P. Shahinian, "Fatigue Crack Growth Characteristics of High Temperature Alloys", Met. Techno., Vol. 5, 1978, pp. 372-380.
77. R. Hales, "Fatigue Testing Methods at Elevated Temperature" in Fatigue High Temperature, ed. by R.P. Skelton, Appl. Sci. Pub., 1983, pp. 63-96.
78. A.E. Carden, "Thermal Fatigue Evaluation", ASTM STP 465, 1969, pp. 163-188.
79. A.E. Carden, "Fatigue at Elevated Temperature: A Review of Test Methods", ASTM STP 520, 1973, pp. 195-223.
80. T.C. Yen, "Thermal Fatigue--A Critical Review", Bull. No. 72, Welding Research Council Pub., WRCBA, 1961, 25 pages.
81. A.E. Carden, "Thermal Fatigue--An Analysis of the Conventional Experimental Method", ASTM, Vol. 63, 1963, pp. 735-758.
82. E. Glenny, "Thermal Fatigue", in High Temperature Materials in Gas Turbines, ed. by P. Sahn and M.O. Speidel, Elsevier Sci. Pub., 1974, pp. 387-395.
83. T. Slot, R.M. Stenz and J.T. Berling, "Controlled Strain Testing Procedures", ASTM STP 465, 1969, pp. 100-128.

84. E.A. Averchenkov, V.I. Egorov and N.D. Sobolev, "Method for Low Cycle Fatigue Testing of Isothermal and Nonisothermal Loading", *Zav. Lab.*, Vol. 48, No. 8, 1982, pp. 59-61.
85. N.W. Brown and K.J. Miller, "A Biaxial Fatigue Machine for Elevated Temperature Testing", *J. Test. Eval.*, Vol. 9, 1981, pp. 202-209.
86. M.W. Brown, "Low Cycle Fatigue Testing Under Multiaxial Stresses at Elevated Temperature", in Measurement of High Temperature Mechanical Properties of Materials, ed. by M.S. Loveday, M.F. Day and B.F. Dyson, HMSO, 1982, pp. 185-203.
87. J.M. Andrews and E.G. Ellison, "A Testing Rig for Cycling at High Biaxial Strains", *J. Strain Analysis*, Vol. 8, 1981, pp. 168-175.
88. C.H. Wells, "Elevated Temperature Testing Methods", ASTM STP 465, 1969, pp. 87-99.
89. L.A. James, "The Effect of Stress Ratio on the Elevated Temperature Fatigue Crack Propagation of Type 304 Stainless Steel", *Nucl. Tech.*, Vol. 14, 1972, pp. 163-170.
90. J.D. Whittenberger and P.T. Bizon, "Comparative Thermal Fatigue Resistance of Several Oxide Dispersion Strengthened Alloys", *Int. J. Fat.*, 1981, pp. 174-180.
91. C. Levailant and A. Pineau, "Assessment of High Temperature LCF Life of Austenitic Stainless Steel by Using Intergranular Damage as Correlating Parameter", ASTM STP 770, 1982, pp. 169-193.
92. P.S. Prevey and W.P. Koster, "Effect of Surface Integrity on Fatigue of Structural Alloys at Elevated Temperature", ASTM STP 520, 1973, pp. 522-536.
93. Y. Asada, R. Yuuki, D. Sumamoto, T. Sokon, K. Tokimasa, Y. Makino, M. Kitagawa and K. Shingai, "Fatigue Crack Propagation Under Elastic-Plastic Medium at Elevated Temperature", in Proc. of the 4th Int. Conf. Press. Vessel Technology, pub. by Inst. of Mech. Engrs., UK, Vol. 1, 1981, pp. 347-353.
94. G.K. Harritos, D.L. Miller and T. Nicholas, "Sustained Load Crack Growth in Inconel 718 Under Non-isothermal Conditions", *J.*

Eng. Mat. Tech., in press.

95. F. Mudry, "Etude la Rupture Ductile et de la Rupture par Clicage d'Ariers Faiblement Allies", These de Doctorat d'Etat, Universite de Technologie de Compiègne, 1982.
96. H.O. VanLeeven, "Heating Methods in Materials Testing at Elevated Temperature", ed. by Nat. Lucht., Netherlands, TMM 2087, 1961, 23 pages.
97. Numerical Methods in Thermal Problems, Proc. of the 2nd Int. Conf., ed. by G.H. Morgen and B.S. Schiefler, Pineridge Press Pub., 1982, 1383 pages.
98. ABAQUS (User's Manual - Version 4), Hibbitt, Karlsson and Sorensen, Inc., 1983.
99. P.T. Raske and W.F. Burke, "An Extensometer for Low Cycle Fatigue Tests on Anisotropic Materials at Elevated Temperature", J. Phys. E. Sci. Instrum., Vol. 12, 1979, pp. 175-176.
100. G. Sunner, "A Diametral Extensometer for Elevated Temperature High Strain Fatigue", J. Phys. E. Sci. Instrum., Vol. 1, 1968, pp. 652-654.
101. L.F. Coffin, "The Stability of Metals Under Cyclic Plastic Strain", Trans. of the ASME, J. of Basic Engr., Vol. 82, No. 3, 1960, pp. 671-682.
102. L.F. Coffin, "Instability Effects in Thermal Fatigue", ASTM STP 612, 1976, pp. 227-238.
103. K.J. Miller, Discussion of the paper by Saheb and Bui Quoc (paper C186/73) and the results by Toor (paper C168/73), in Creep and Fatigue in Elevated Temperature Applications, ed. by Inst. Mech. Engrs. and ASTM, Vol. 2, 1973, p. 23.
104. N.J. Marchand, "Fatigue Oligocyclique et Fatigue-Propagation du Cuivre et Laiton-Alpha", MS Thesis, Ecole Polytechnique de Montreal, 1983.
105. H. Teranishi and A.J. McEvily, "The Effect of Oxidation on Hold Time Fatigue Behavior of 2 1/4 Cr-Mo Steel", Met. Trans., Vol.

- 10A, 1979, pp. 1806-1808.
106. R. Hales, "The High Temperature Oxidation Behavior of Austenitic Stainless Steel", *Werkstoffe und Korrosion*, Vol. 29, 1978, pp. 393-399.
 107. J.S. Huang and R.M. Pelloux, "Low Cycle Fatigue Crack Propagation in Hastelloy-X at 25 and 760°C", *Met. Trans.*, Vol. 11A, 1982, pp. 899-904.
 108. B.A. Leich, "Microstructural Effects on the Room and Elevated Temperature Low Cycle Fatigue Behavior of Waspaloy", MS Thesis, University of Cincinnati, 1982.
 109. M.F. Day and G.F. Harrison, "Design and Calibration of Extensometers and Transducers", in Measurement of High Temperature Mechanical Properties of Materials, ed. by M.S. Loveday, M.F. Day and B.F. Dyson, HMSO, 1982, pp. 225-240.
 110. D.J. Walter and R. Hales, "An Extensometer for Creep-Fatigue Testing at Elevated Temperatures and Low Strain Ranges", *J. Strain Anal.*, Vol. 16, 1981, pp. 145-147.
 111. R. Hales and D.J. Walter, "Measurement of Strain in High Temperature Fatigue", in Measurement of High Temperature Mechanical Properties of Materials, ed. by M.S. Loveday, M.F. Day and B.F. Dyson, HMSO, 1982, pp. 241-254.
 112. C. Levaillant, B. Rezgui and A. Pineau, "Effects of Environment and Hold Times on High Temperature Low Cycle Fatigue Behavior of 316 LC Stainless Steel", *ICM3*, Vol. 2, 1979, pp. 163-172.
 113. A.J. Perry, "Review: Cavitation in Creep", *J. Mat. Sci.*, Vol. 9, 1974, pp. 1016-1039.
 114. G. Greenwood, "Creep and Cavity Growth Under Multiaxial Stresses", *Phil. Mag.*, Vol. 43, 1981, pp. 281-290.
 115. M.F. Day and G.B. Thomas, "Microstructural Assessment of Fractional Life Approach to Low Cycle Fatigue at High Temperatures", *Met. Sci.*, Vol. 13, 1979, pp. 25-33.
 116. M.S. Starkey and R.P. Skelton, "A Comparison of the Strain Inten-

- sity and Cyclic J Approaches to Crack Growth", *Fat. Eng. Mat. Struct.*, Vol. 5, 1982, pp. 329-341.
117. L.P. Wynn, "TPE 331/T76 Turboprop Propulsion Engine Durability", AFWAL-TR-82-4069, 1982, 53 pages.
 118. F. Erdogan and M. Ratwani, "Fatigue and Fracture of Cylindrical Shells Containing a Circumferential Crack", *Int. J. Fract. Mech.*, Vol. 6, 1970, pp. 379-392.
 119. R.P. Skelton, "The Effect of Microstructure and Tensile Dwell on the Growth of Short Fatigue Cracks in 316 Steel at 625°C", *Proc. of the Int. Conf. on Mechanical Behavior and Nuclear Application of Stainless Steels at Elevated Temperature*, ed. by The Metals Soc., UK, 1981, pp. 191-203.
 120. A.C. Pickard and M.A. Hicks, "Crack Length Determination Using the D.C. Electrical Potential Drop Technique--A Comparison of Calibration Methods", in *Advances in Crack Length Measurement*, ed. by C.J. Beevers, EMAS Pub., 1982, pp. 97-113.
 121. K. Krompholz, E.D. Grosser, K. Ewart and E. Moritz, "Application of the D.C. Potential Drop Technique in the High Temperature Regime", in *Advances in Crack Length Measurement*, ed. by C.J. Beevers, EMAS Pub., 1982, pp. 231-251.
 122. F. Gabrielli and R.M. Pelloux, "Effect of Environment on Fatigue and Creep Crack Growth in Inconel X-750 at Elevated Temperature", *Met. Trans.*, Vol. 13A, 1982, pp. 1083-1089.
 123. V. Moreno, "Creep-Fatigue Life Prediction for Engine Hot Section Materials (Isotropic)", NASA CR-168228, 1983, 85 pages.
 124. "Engineering Properties of Inconel X-750", Technical Bulletin T-38, Huntington Alloy Products Division of the International Nickel Company, Inc., Huntington, WV.
 125. K.P. Walker, "Research and Development Program for Nonlinear Structural Modeling with Advanced Time-Temperature Dependent Constitutive Relationships", NASA CR-165533, 1982, 187 pages.
 126. Vito Moreno and J.T. Hill, Private Communication, 1984.

127. S.D. Antolovich, S. Liu and R. Baur, "Low Cycle Fatigue Behavior of Rene 80 at Elevated Temperature", *Met. Trans.*, Vol. 12A, 1981, pp. 473-481.
128. K. Kuwabara, A. Nitta and T. Kitamura, "Thermal-Mechanical Fatigue Life Prediction in High-Temperature Component Materials for Power Plants", in Advances in Life Prediction Methods, ed. by D.A. Woodford and J.R. Whitehead, ASME MCP, 1983, pp. 131-142.
129. D.A. Jablonski, "Fatigue Behavior of Hastelloy-X at Elevated Temperature in Air, Vacuum and Oxygen Environments", Ph.D. Thesis, M.I.T., January 1978.
130. R.C. Bill, M.J. Verrille, M.A. McGaw and G.R. Halford, "Preliminary Study of Thermomechanical Fatigue of Polycrystalline MAR-M200", NASA TP-2280 AVSCOM TR 83-C-6, 1984, 16 pages.
131. V. Moreno, D.M. Nissley and L.S. Lin, "Creep-Fatigue Life Prediction for Engine Hot Section Materials", NASA CR-174844, 1984, 137 pages.
132. J.K. Tien and R.P. Gamble, "Effects of Stress Coarsening on Coherent Particle Strengthening", *Met. Trans.*, Vol. 3, 1972, pp. 2157-2162.
133. D.O. Pearson, F.O. Lemkey and B.H. Kear, "Stress Coarsening of γ' and its Influence on Creep Properties of a Single Crystal Superalloy", in Proc. of the 4th Intl. Symp. on Superalloys, ed. by J.K. Tien, ASM, Metals Park, 1980, pp. 513-520.
134. L.S. Lin and J.M. Walsh, "Lattice Misfit by Convergent-Beam Electron Diffraction--Part 1: Geometry Measurement", in Proc. of the 42nd Annual Meeting of the EMSA, 1984, pp. 520-524.
135. D.M. Shah and D.N. Duhl, "The Effect of Orientation, Temperature and Gamma Prime Size on the Yield Strength of a Single Crystal Nickel-Base Superalloy", in Superalloy 1984, ed. by M. Gell et al, AIME, Warrendale, PA, 1984, pp. 107-116.
136. J.O. Nilson, "The Influence of Nitrogen on High Temperature Low Cycle Fatigue Behavior of Austenitic Stainless Steels", *Fat. Eng. Mater. Struct.*, Vol. 7, No. 1, 1984, pp. 35-64.
137. K. Hatanaka and T. Yamada, "Effect of Grain Size on Low Cycle

- Fatigue in Low Carbon Steel", Bull. of JSME, VOL. 24, No. 196, 1981, pp. 1692-1699.
138. T. Magnin, J. Driver, J. Lepinoux and L.P. Kubin, "Aspects Microstructuraux de la Deformation Cyclique dans les Metaux et Alliages C.C. et C.F.C..1 Consolidation Cyclique", Rev. Phy. Appl., Vol. 19, 1984, pp. 467-482.
 139. G.R. Leverant, B.H. Kears and J.M. Oblack, "Creep of Precipitation-Hardened Nickel-Base Alloy Single Crystals at High Temperatures", Met. Trans., Vol. 4, 1973, pp. 355-362.
 140. R.R. Jensen and J.K. Tien, "Temperature and Strain Rate Dependence of Stress-Strain Behavior in a Nickel-Base Superalloy", Met. Trans., Vol. 16A, 1985, pp. 1049-1068.
 141. T. Miyazaki, K. Nakamura and H. Mori, "Experimental and Theoretical Investigations on Morphological Changes of γ' -Precipitates in Ni-Al Single Crystals During Uniaxial Stress-Annealing", J. Mater. Sci., Vol. 14, 1979, pp. 1827-1837.
 142. R.W.K. Honeycombe, The Plastic Deformation of Metals, 2nd Ed., Edward Arnold Pub., 1984.
 143. M. Gell and D.N. Duhl, "The Development of Single Crystal Superalloy Turbine Blades", Proc. of the N.J. Grant Symposium on Processing and Properties of Advanced High-Temperature Alloys, June 17-18, 1985, ASM Pub., in press.
 144. P. Lukas, L. Kunz, Z. Knesl, B. Weiss and R. Stickler, "Fatigue Crack Propagation Rate and the Crack Tip Plastic Strain Amplitude in Polycrystalline Copper", Mater. Sci. & Eng., Vol. 70, 1985, pp. 91-100.
 145. D.O. Harris, Trans. of ASME, J. of Basic Eng., Vol. 89, 1969, pp. 519-526.
 146. G.T. Embley and E.S. Russel, "Thermal-Mechanical Fatigue of Gas Turbine Bucket Alloys", in the Proc. of the First Parsons International Turbine Conference, Dublin, Ireland, June 1984, pp. 157-164.
 147. W. Elber, "Significance of Fatigue Crack Closure, Damage Tolerance

- in Aircraft Structures", ASTM STP 486, 1971, pp. 230-242.
148. P.C. Paris and H. Hermann, "Twenty Years of Reflection on Questions Involving Fatigue Crack Growth, Part II: Some Observations of Crack Closure", in Fatigue Threshold, EMAS Pub., Warely, U.K., 1981, pp. 11-32.
 149. T. Hoshide and K. Tanaka, "Analysis of Fatigue Crack Growth Propagation of Surface Flaws by Elastic-Plastic Fracture Mechanics", Trans. Jap. Soc. of Mech. Engrs., Vol. 48, 1982, pp. 1102-1110.
 150. K. Tanaka, "Short-Crack Fracture Mechanics in Fatigue Conditions", in Current Research on Fatigue Research on Fatigue Cracks, ed. by T. Tanaka, M. Jono, and K. Komai, JSMS Pub., Kyoto, Japan, 1985, pp. 79-100.
 151. Y. Murakami, S. Hrada, T. Endo, H. Tani-Ishi, and Y. Fukushima, "Correlations Among Growth Law of Small Cracks, Low Cycle Fatigue Law and Applicability of Miner's Rule", Eng. Frac. Mech., Vol. 18, 1983, pp. 909-924.
 152. T. Yamada, T. Moshide, S. Fujimura and M. Manabe, "Investigation of Fatigue Life Prediction Based on Analysis of Surface-Crack Growth in Low Cycle Fatigue of Smooth Specimen of Medium Carbon Steel", Trans. of the JSME, Vol. 49A, 1983, pp. 441-451.
 153. Y. Murakami, "Correlation Between Strain Singularity at Crack Tip Under Overall Plastic Deformation and the Exponent of the Coffin-Manson Law", to appear in the Proc. of the Conf. on Low Cycle Fatigue--Directions for the Future, Lake George, NY, September 30 - October 4, 1985.
 154. E.L. Wagoner, "Physical Metallurgy and Mechanical Properties of Hastelloy-X", Technical Report, Haynes-Stellite Corp., June 23, 1961.
 155. J.T. Hill, Private Communication, Pratt & Whitney Aircraft Corp., 1985.

THERMAL-MECHANICAL FATIGUE BEHAVIOR OF
NICKEL-BASE SUPERALLOYS

VOL. 2

by

NORMAN J. MARCHAND

B. Ing., Ecole Polytechnique de Montreal, 1980
M.Sc.A., Ecole Polytechnique de Montreal, 1982

SUBMITTED IN PARTIAL FULFILLMENT
OF THE REQUIREMENTS FOR THE
DEGREE OF

DOCTOR OF SCIENCE

at the

MASSACHUSETTS INSTITUTE OF TECHNOLOGY
January 1986

© Massachusetts Institute of Technology

Signature of Author

Norman Marchand

Department of Materials Science & Engineering
January 10, 1986

Certified by

R. M. Pelloux

R. M. Pelloux
Thesis Supervisor

Accepted by

Bernhardt J. Wuensch

Bernhardt J. Wuensch
Chairman, Departmental Graduate Committee

VOL. 2
MASSACHUSETTS INSTITUTE
OF TECHNOLOGY

MAR 19 1986

LIBRARIES

Archives

Appendix I

Thermal-Mechanical Fatigue Methods of Testing

1. Calibration and Recording of High Temperature Behavior

The first attempt at plotting stress-strain diagrams under thermal fatigue loading were made on the basis of Coffin's method. For instance, the diagram may be plotted by points corresponding to the half-cycles of heating and cooling. The stress is recorded by a load cell (transducers, etc.) and the strain is determined by calculation or measuring thermal or total strain at different instants of loading. Carden [78-79] explains the method of recording the parameters of thermal fatigue loading which employs the recording of the diagram of force (stress) vs mean temperature of the specimen and which makes it possible to determine the plastic strain of the specimen in any cycle. The most complicated feature in selecting the method of recording the strain parameters is the determination of the true strain at every instant of loading of the specimen. In many earlier investigations [80-82], the mean plastic strain per cycle was determined regardless of its localization caused by irregular temperature distribution and regardless of the deformation process.

In connection with the above, it is worth giving some attention to methods of direct experimental determination of strains in the critical section of the specimen at all stages of its loading.

Carden [79] suggested a method of obtaining stress-strain diagrams in thermal fatigue with the aid of two extensometers mounted

on the specimen for measuring strain in the longitudinal and transverse directions; this involves the recording of the difference in the readings of the strain gauges, and in isotropic thermal extension the component of thermal strain is automatically eliminated. This method undoubtedly permits obtaining a more accurate strain pattern in thermal fatigue; however, it has its limitations. The longitudinal extensometer measures the strain on some base, and if there is a longitudinal temperature gradient along the specimen, an error may occur in the determination of local strain. Besides, it is assumed that the Poisson ratio ν does not depend on the temperature; this is not always correct; e.g., in the case of a steel 1Kh2M, ν changes from 0.27 to 0.31 when the temperature changes within the range of 100-600°C [37].

In our opinion, the method of automatic recording of the stress-strain diagram in thermal fatigue tests using one diametral extensometer [18, 20-21, 31, 33, 61-62, 83-84] has some advantages compared with Carden's method. Similar extensometers are widely used in low cycle fatigue tests; they consist of a system of two levers connected in the central part by an elastic hinge. The ends of the levers encircle the specimen (tubular or solid) diametrically; after the other ends have been displaced and the displacement recorded by a transducer, the diametral strain of the specimen is recorded. On an installation of the Coffin type, this strain in cyclic heating and cooling of the specimen consists of a mechanical and a thermal component. To eliminate the thermal part of the strain, an electrical method of compensation is used [36, 83-84]. From the signal proportional to the total strain (transducer-induced by the extensometer), the signal proportional to the thermal strain (induced by the thermocouple welded

on at the investigated section of the specimen) is subtracted. One input of the x-y plotter receives a signal from the load-cell, the other receives the difference between the two signals proportional to the mechanical strain, and this yields the stress-strain diagram under nonisothermal conditions in coordinates of stress versus diametral strain. To obtain a diagram of the cyclic strains in terms of stress versus longitudinal strain, it is necessary to rearrange the recorded diagram and to convert the transverse strain into longitudinal strain. The total longitudinal axial strain ϵ_a can be expressed by the component of transverse strain at each instant of deformation:

$$\epsilon_a = P/A \quad (1-2\nu(T))/E(T) - 2\Delta d/d$$

where d is the diameter and Δd the change in diameter of the specimen. A is its cross-sectional area; P is the force applied to the specimen; $E(T)$ and $\nu(T)$ are the modulus of elasticity and the Poisson ratio, respectively, as functions of the temperature T .

There are similar methods of compensating for thermal strains as suggested by Slot et al. [83]; all of them involve the use of an analogue computer to obtain stress-strain diagrams in coordinates of longitudinal stress versus longitudinal strain. This is an important methodological advantage because these methods were used under conditions of independent thermal mechanical loads. However, it is generally accepted in these methods that the characteristics of elasticity E and ν remain constant at all stages of the strain cycle (i.e., their temperature dependence is not taken into account). This undoubtedly introduces an error. To calculate the change in cross-sectional area of the specimen and the elastic characteristics, a functional generator in combination with the analogue computer can be used [36].

At this point, it is important to notice that a change in the thermal loading program requires a change in the program which issues the compensating signals, whereas at moderate temperatures the previously examined method requires no correction. This problem can be ameliorated by the method described by Hopkins [36], which suggests varying the independent mechanical and thermal operating regimes. To compensate for thermal expansion and to obtain data on the magnitude of the mechanical strains, a method is used which is analogous to that described previously. The strain measuring channel receives, together with the signal from the strain meter but in opposite phase, a signal from the setting mechanisms whose program corresponds to the steady-state thermal strain of the specimen in zero-load-controlled cyclic temperature change.

Attention should be given to the arguments of Hopkins [36] and Sobolev and Egorov [37] in substantiating the method which used an analogue computer: they pointed out that it is possible that the functions expressing the temperature of thermal strain do not coincide at the heating and cooling stages. This noncoincidence can be particularly important in tests conducted with a thick-walled specimen whose deformation occurs under conditions of a nonuniform state of stress and strain and an inhomogeneous temperature field, where thermal stresses exist which were not taken into account.

The method of making torsional tests with tubular specimens has a number of methodological advantages from the point of view of recording the diagrams of nonisothermal cyclic strain, because independent programs of mechanical and thermal loading can be realized [32-33, 35]. Tulyakov et al. [35], Brown et al. [85-86], and

Andrews and Ellison [87] have described an installation with follower control system with load and temperature feedback based on this principle. The cyclic strain diagrams recorded in these tests take into account the nonuniformity of heating of the specimen which determines the change in the measuring base of the deformer because of the thermal axial strain of the specimen. We note that the use of thin-walled tubular specimens in cyclic torsion makes it possible to investigate the deformation process at very large strains where specimens in push-pull tests lose their stability.

It is difficult to reduce the hysteresis loop of thermal strain versus temperature to exactly zero. As pointed out by Hopkins [36], small changes in temperature can translate into large changes in mechanical strain if the total strain is left unchanged, whereas a small change in temperature during a cycle without changing the mechanical strain usually does not change the fatigue response of the materials. With the use of an analogue computer, accuracy is only limited by how closely it is adjusted to zero mechanical strain during the thermal cycling. Obviously, for a given thermal strain error, the test accuracy increases as the mechanical strain increases. However, to conduct these types of tests with an analogue computer is difficult and great care must be provided to insure that the proper heating and cooling compensation functions are used. With a digital computer as the programmer, this is not necessary. The computer can acquire and store the thermal strain as a function of both temperature and direction, whereas the thermal expansion compensator's output is only a function of temperature and not direction. A digital computer also allows more complex TMF testing to be conducted with no additional effort from the

operator. Such tests may include mode transfers, strains for a given time or to a given creep strain [25-26, 29, 31]. Digital computers can almost continuously read the instantaneous temperature and adjust its total strain output to compensate for any temperature error. The frequency at which the computer does this can be programmed to the maximum heating rate of the temperature equipment and the accuracy desired from the test.

These control problems never surface in isothermal tests because static temperature control is much better than dynamic temperature control, and any change in the temperature which does occur only reflects in a mean strain shift rather than a strain range shift. Fatigue life, either measured as a number of cycles to crack initiation or as a crack propagation life, is affected more by a small change in strain range than it is by the same change in mean strain [29].

2. Heating and Cooling Methods

As pointed out by Carden [79], there are several categories of heating facilities for high temperature fatigue. They are: (1) Combustion furnace heating, (2) Electric resistance heating, and (3) Electric induction heating. Because of the experimental difficulties associated with the control of temperature, combustion furnaces are seldom used in TMF experiments. However, they are sometimes used [79] in testing which tends to reproduce the environmental conditions found in the combustion stage of aircraft engines. The electrical resistance category can be subdivided into four types of methods, respectively: (a) direct resistance (self heating) [19-21, 33, 62, 78-79],

(b) electrical resistance furnace [88-89], (c) fluidized bed [8-11, 90], (d) incandescent lamps [91-94], and (e) electric blankets [95]. The electric induction heating category can be divided into the direct induction method and indirect induction heating (susceptors).

As pointed out by Van Leeuwen [96], there is a relationship between the heating method, the design of the specimen, and temperature measurement and control. Radio frequency induction requires close coil-to-specimen spacing and small grip ends, which makes difficult the mounting of additional measurement devices and obscures access to and visibility of the surface for replication, etc; also the coil has a high voltage RF potential requiring insulation and safety precaution. A temperature disturbance occurs at the thermocouple mass in the field, as well as at specimen locations unequally spaced to the coil [83]. There are also RF induction-induced ground loop problems in the instrumentation cabling.

Resistance heating induces a longitudinal temperature distribution which must be minimized by the incorporation of internal heat sinks and longer lengths of uniform cross-section. Specimen cracks normal to the current flow are accompanied by local heating at the crack tips which is not acceptable for crack propagation testing. No heating can occur after the specimen fractures as can occur with induction heating, but local melting as a result of arcing can occur during stage III final fracture. However, neither direct RF induction nor resistance heating is good for very high electrical conductivity materials, and for these materials the impedance must be matched to the output circuits in both methods. Notwithstanding these problems, both methods are still the most frequently used for TMF testing and for strain life experiments,

both methods have been proven satisfactory [19-35]. However, as mentioned before, direct resistance heating is not acceptable for crack propagation testing due to local heating at crack tips, and RF heating is used instead [27-29]. For these tests, low frequency heaters (10 KHz) are often used [28-29] because they produce lower wall thickness gradients than do the higher frequency (450 KHz) heaters and because there are fewer ground-loop problems with the 10 KHz heater than with the 450 KHz heaters. Nevertheless, it is the present author's belief that high frequency induction heating is preferable because of its fast response, making it possible to provide high heating rates and induce considerable thermal stress in specimens of small cross-section. In this case, the heating mode is close to that encountered in-service, since the heat is generated within the surface layer of the specimen. Analysis of the temperature fields in the specimens sometimes needs to be carried out with the high-frequency heaters, but numerical methods of non-stationary problems of heat conductivity using finite elements are now in our hands [12-14, 97-98]. Temperature measurement is usually accomplished by thermocouples welded onto the specimen. However, some cases of premature specimen failure due to the presence of a thermocouple have been reported [88], and optical pyrometry has been used for temperature feedback control [27-29, 36]. Few reports give calibration methods or internal analysis of the uncertainty of the readings [83].

3: Specimen Design and Measurement of Strain

Two types of machines have been used over the last 20 years for studying high temperature low cycle fatigue. One group is a natural evolution of machines used for uniaxial tensile testing, but these are generally operated in fundamentally different modes from their predecessors. The other type of machines achieves the reversed plastic strain required by deforming the material in bending. In the following, we are concerned with the specimen and appropriate extensometry used in uniaxial testing. The reader is referred to Hales [77] for a review of reverse bending testing.

An accurate measurement of strain is fundamental to mechanical fatigue testing since strain is usually the control parameter in such experiments. Also, some materials exhibit grain boundary cavitation as a result of creep-fatigue cycling and the cavities are believed to nucleate and grow as a result of deformation at slow strain rates [99]. This phenomenon has imposed extra conditions on strain measuring systems. More important, they must be stable at least over the period of the hold time and the stress relaxation behavior under nominally constant strain conditions must reflect the true behavior of the material. To perform strain-controlled tests, two methods are commonly adopted, axial and diametral strain control. These commonly employed test methods are critically assessed in the light of the need to perform tests at low (<0.5 %) strain ranges on cyclically hardening or softening behaviors.

3a. Diametral Strain Control

The majority of mechanical property tests are performed under uniaxial stress. This is true of the present state of creep-fatigue studies. Because of the difficulties experienced in attaching axial extensometers to some notch sensitive materials, many workers have used dimensional changes of the diameter to control the tests. Their measurements are usually converted to equivalent axial strain for purposes of comparison with the uniaxial data. This technique is usually used in conjunction with "hour-glass" shaped specimens. Only the strain in the narrowest portion of the specimen is considered. The diametral strain is measured by two probes which are held in contact with opposite sides of the specimen, the displacement being measured either directly or via a hinged arm, again by means of LVDTs. A full description of these techniques is given by Slot et al. [83] and by Sunner [100].

As we have seen before, diametral strain is usually converted to axial strain since this is the parameter of interest. However, this conversion is not simple since the contribution of elastic and plastic deformation changes as the system cyclically hardens and also as the axial stress relaxes during a hold period. Therefore, to control axial strain with diametral strain measurement, continuous computation of the relationship

$$\epsilon_a = \sigma / E (1/\nu_p - 1/\nu_e) - \epsilon_d / \nu_p$$

is necessary [83].

Diametral strain control with the use of "hour-glass" specimens is open to a number of serious criticisms, some of a fundamental and some of a practical nature.

Criticism of a fundamental nature

(1) The above equation for computation of axial strain requires that the volume of the material remains constant, which is not the case when creep cavitation occurs.

(2) Diametral strain measurement is inappropriate for testing weldment and other materials which have directionally variable properties [99].

(3) The method is intrinsically insensitive. For example, a typical length-to-diameter ratio is 2:1 and for a specimen 25 mm - 12 mm diameter strained to 0.2 per cent, the axial elongation is approximately 50 μm , whereas in the same test the diameter contracts by only 7-12 μm (i.e., a factor of 5 smaller than a corresponding measurement made axially).

(4) Hour-glass specimens are used because the gently changing cross-section along the gauge length does not appear to generate unacceptable stress concentration gradients and the strain at the plane of maximum cross-section is believed to be uniform. However, it is observed that cyclically strained hour-glass specimens change their shape (Figure I.1) during the progress of fatigue testing, particularly at high cyclic strains [20-21, 31, 39, 60, 79, 101-102]. These important geometrical instabilities of solid and tubular hour-glass specimens have been pointed out by Coffin [102] and Miller [103] but received surprisingly little attention. Coffin has also tried to explain these results in terms of a positional variation or gradient in the cyclic stress-strain field caused by geometry, temperature or material variations. However, his analysis relied on a simple monotonic strain distribution which assumes constant strain in every slice of the cross-section. Miller [103] and Marchand [104] have performed fully-plastic finite element

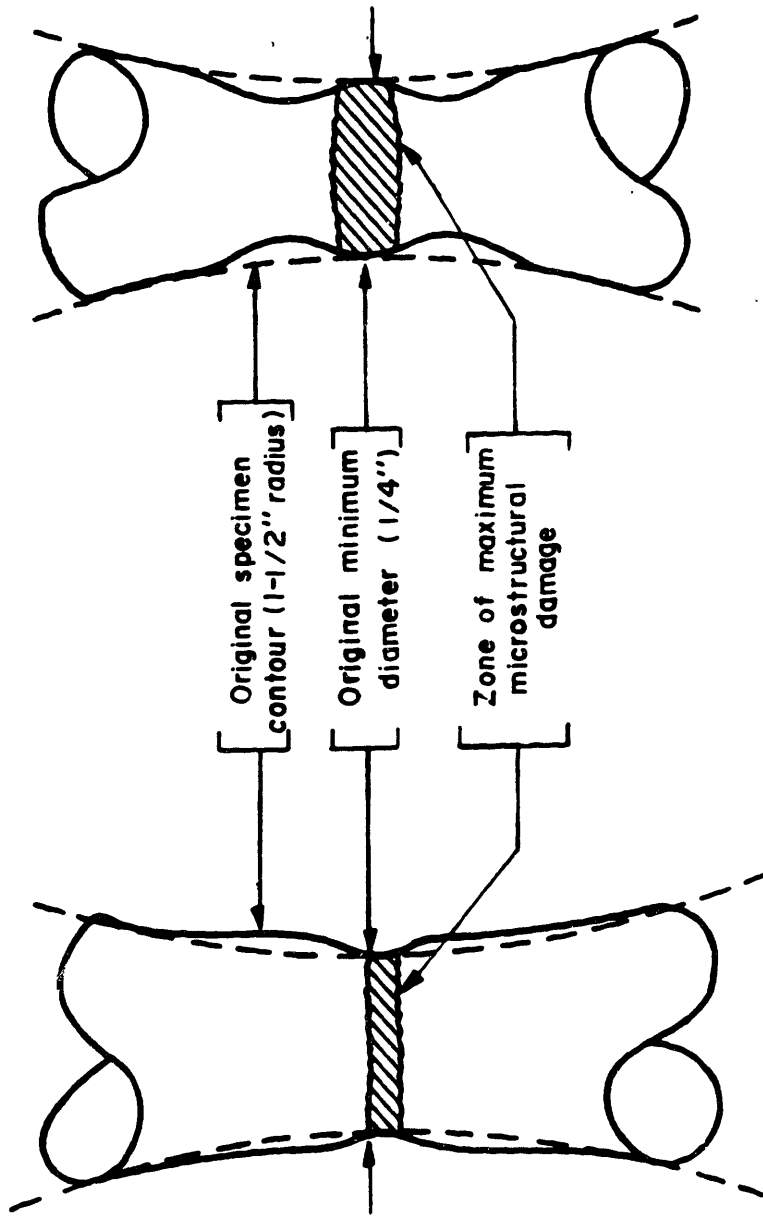


Figure I.1 Schematic illustrations of geometric changes in thermal-mechanical fatigue. (a) In-phase cycling, (b) Out-of-phase cycling [102].

analysis which show that the hour-glass profile acts as a notch, even at large radii of 40 mm (1 1/2") and clearly show the non-linearity between diametral and axial strains. Further, at high strain levels, the maximum strain will not be at the outer surface but at the core of minimum section (Figure I.2). The fact that pronounced geometric changes occurred as shown in Figure I.1 and that the final fracture takes place away from the temperature-controlled mid-point of the gauge length [21-22, 101-102], renders doubtful numerous already published results.

Criticisms of a Practical Nature

(1) Oxide growth on high temperature alloys is usually small but rapid oxide growth can initiate and produce 20-30 μm (greater than the strain being measured) of oxide in 500 hrs. [57, 105-106]. Because most oxides grow outward from the initial metal surface, lightly loaded probes of the type used in diametral extensometers are displaced by such growth. However, this displacement is interpreted as a compressive strain in the longitudinal axis of the specimen and the effect is equivalent to imposing a ratcheting strain on the system, since the servo-machine will impose a tensile mechanical strain to compensate for the diametral growth. Although examination of the specimen would show that this had occurred, it could cause the loss of a long and expensive test.

(2) Only a small volume of material is subjected to the chosen test conditions (Figure I.2). At failure, the final crack propagates through this material destroying the microstructure which had developed during the test. Consequently, metallographic examination and other measurements are difficult, thus reducing the value of the results and

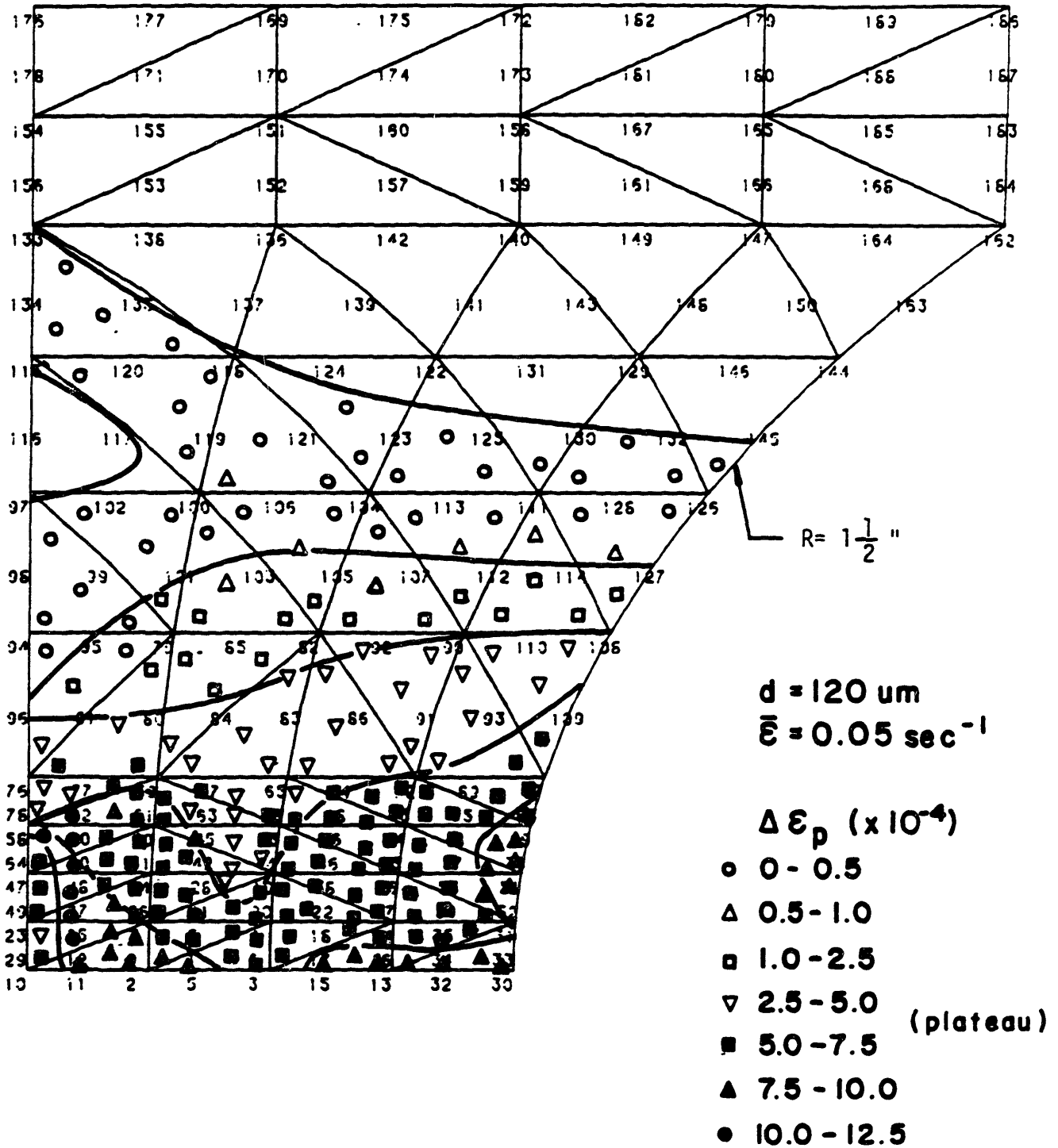


Figure I.2 Domain of iso-plastic strain in an hour-glass specimen of polycrystalline α -brass.

the testing program in developing life prediction models which may be used with confidence.

(3) The recording of crack growth data under strain-controlled conditions is nearly impossible since the crack initiates and grows in the zone where the knife-edges of the extensometer are in contact with the hour-glass specimen. There has been one attempt at measuring low cycle fatigue crack propagation rates under diametral strain-control using SEN specimens [107]. However, as in the case of hour-glass specimens, the relationship between the measured diametral strain and the axial strain was found to be non-linear under fully plastic conditions [77]. As seen before, although the measurement of diametral strain in conjunction with axial load affords in theory a method of measuring axial strain, caution is needed in interpretation of the results.

3B. Axial Strain Control

The obvious method to overcome the problems associated with the diametral strain control outlined above is to measure directly the changes of length of a defined gauge length. Axial strains are usually measured by attaching extensometer legs to knife edges machined onto the parallel section of the specimen, thereby defining the limits of the gauge length. The extensometer legs are positioned parallel to the stress axis and are extended beyond the furnace or RF coil [77, 99, 108] where these relative displacements are measured by LVDTs. This technique has proved convenient and successful on a range of materials which cyclically soften. However, certain materials, notably austenitic stainless steels [99, 109] and nickel-based alloys [111], are notch-

sensitive at elevated temperatures. The presence of the built-up notches acts as a stress-raiser, localizing strain in a small volume underneath the knife edges [77], and failure often occurs at the base of the knife edges. Changes in the profile of the knife edge can alter the propensity for fatigue crack nucleation at the base of the knife edge, but it has not proved possible to prevent this behavior. However, several authors have described some alternative methods for measuring axial strain which minimized failure at the knife edges [91-92, 99, 109-111]. All these methods rely on the high coefficient of friction of metals at high temperatures to allow side arms to be placed in contact with the specimen gauge length under low loads without slipping.

We have seen that although diametral measurements can give a measure of axial strain, there are a number of features of the method which make it less desirable than the direct measurement of axial strain. However, in order to fully appreciate the difference between the stress-strain recorded in axial and diametral strain controlled tests, it is necessary to consider the nature of both the volume changes and the closed-loop feedback system.

It is now established that during creep-fatigue testing, the creep component of the test cycle usually produces intergranular cavitation [3, 5, 42, 48-50, 91, 112]. If cavities grow purely by diffusion mechanisms, the strain developed is only in a direction which allows the applied stress to do work. It is now well-known [113-114] that under low uniaxial stresses, strain accumulates in one direction only. Therefore, the nature of the feedback system causes a difference in relaxation behavior, according to the method of strain control employed. If we consider that relaxation arises from strain conversion due to the diffuse

growth of cavities, then in the case of axial strain measurement the volume change will be detected as a change in length and stress will consequently be reduced. Reduced stress will cause the growth of cavities to decelerate and the drop in stress will be a true reflection of the creep strain accumulated. On the other hand, the diameter of the specimen, being orthogonal to the applied stress, will not change during the growth of cavities by diffusion. Because the stress is not reduced during the hold time (with no detectable change in strain), the cavities continue to grow at a rate determined by the peak stress but since no stress drop occurs, there is no method available for estimating the creep strain accumulated. However, even with the use of axial extensometers, interpretation of the stress relaxation behavior is difficult [31, 50], there are very few experimental studies devoted to the quantitative determination of the damage underlying this behavior [112, 115]. Detailed information on the microstructural process taking place is necessary in order to fully understand the relaxation behavior.

4. Fatigue Crack Growth Testing and Crack Length Measurement

The techniques and specimen geometries used for isothermal crack growth measurements at elevated temperature and under LEFM conditions are now well-established and numerous results have been obtained in the last ten years [2-4, 42, 48-50, 59, 89, 91]. Crack growth data in the high strain regime (HSF), i.e., under conditions of reversed gross plasticity in isothermal conditions, are relatively new [2, 59, 116]. Most HSF crack growth data have been obtained in push-pull testing [59] on smooth longitudinal LCF specimens. Crack propagation rates

were evaluated, either by subsequent striation measurement [2-3, 5, 59, 116] or by introducing a small starter notch and monitoring the crack growth by the potential drop technique [2, 59]. Optical measurement of crack progress has also been made on SEN specimens [107], solid center notched specimens [93, 117], and tubular center notched specimens [27-28, 41, 93]. Hardly any data have been gathered on crack growth during thermal-fatigue cycling in the plastic strain range [22, 27-29, 41, 48] and crack length measurements have been performed mostly by optical measurement [27-29, 41, 48] and by cellulose acetate replica [27] on tubular centered notched specimens. In these experiments, the surface crack lengths must be converted to a mean crack length for the tube used [41]

$$a = R \sin^{-1} (2a_p/D_o)$$

where a = mean crack length, R = mean radius of the tube, D_o = outer diameter of the tube, and $2a_p$ = total projected length measured by microscope.

Also a curvature correction factor $G(a/t)$ from Erdogan and Ratwani [118] must be used for calculating ΔK or ΔK_ϵ , the strain intensity factor. It should be noted that $G(a/t)$ was derived assuming no bulk plasticity, and the validity of this correction factor for TMF crack growth data remains to be proven. The resolution claimed [41] for optical measurements is in the range of 20-120 μm , depending on the crack tip clarity and providing the measurements are taken at maximum tensile load. The slowest growth rates reported on tubular notched specimens have been on the order of 1×10^{-6} m/cycle.

There have been few attempts to measure crack length in TMF conditions using the potential drop technique [22, 119] and 12.7 mm

diameter push-pull specimens. Using a starter notch 200 μm deep, experimenters have been able to resolve accurately a crack increment of 40 μm , and the corresponding growth rates were measured to better than 10^{-5} mm/cycle [119]. The method of potential drop has been proven satisfactory in isothermal conditions for numerous materials [120-121], and it has been shown (see Appendix II) that it can be used satisfactorily provided that the electrical noise is adequately filtered and that the calibration curve is properly corrected in order to take into account changes of potential with temperature.

Appendix II

Design of Test Unit

The apparatus which was built is a computer-controlled thermal fatigue testing system consisting primarily of a closed-loop servo-controlled electro-hydraulic tension compression fatigue machine (MTS 810 model 906.06), a high frequency oscillator for industrial heating (Lepel Model T-2.5-1-KO1-BW), an air compressor for cooling, a low frequency function generator (Exact model 504), a data acquisition and control system (HP-6942A), a programmable high resolution digital voltmeter (DVM Model 3478A), and a main frame computer (HP 9816S). Figure II.1 shows the control block diagram of this system. The system is capable of testing specimens of different size and configuration (SEN, CT, hollow tube, etc.) and to withstand a fatigue loading of 25,000 lbf (11,350 Kgf). The test specimen is mounted in a vertical plane into two end grips of high tensile steel. The specimen alignment is insured by the use of a Wood's metal pot. Because a DC potential drop technique is used to monitor crack growth, the lower grip is electrically insulated from the system by means of a ceramic coating. The ends of the end grips are water cooled by means of copper coils surrounding them.

1. The Demand-signal Generators

The demand-signal generation system provides separate demand signal for the control of specimen strain or applied stress and temperature. A programmable temperature controller is used to

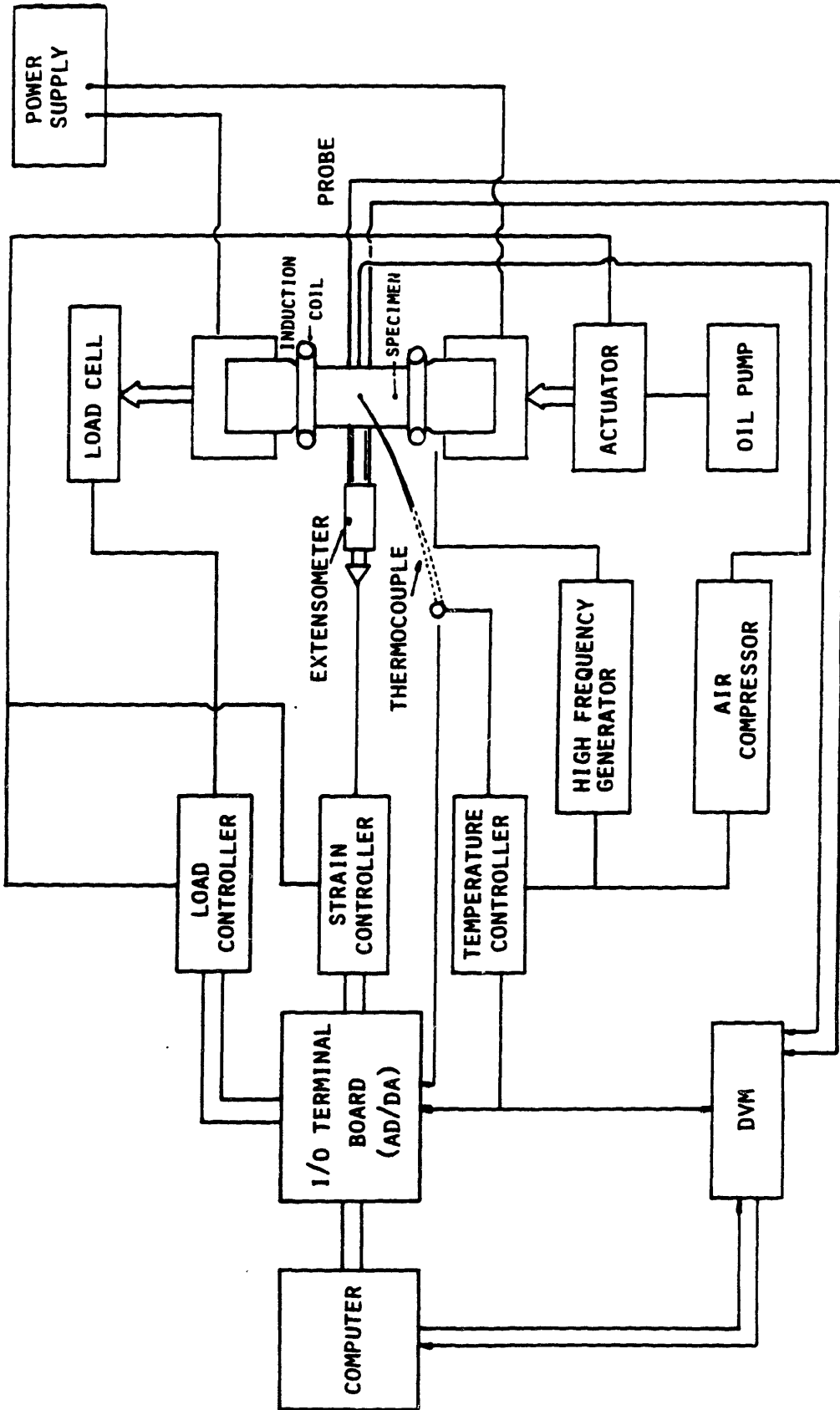


Figure II.1 Control block diagram of the testing system.

generate the driving signal to the high frequency generator, the DVM, the computer, the air valve and the frequency generator. The computer and the data acquisition and control system provide the command signals for the stress or strain controlled cycling. Proper coding and decoding of trigger signals from the temperature controller to the computer allow the system to generate any strain/stress/temperature cycling. Feedback signals from measuring points on the machine and specimen are compared continuously with the demand signals in the electronic control equipment. The difference between corresponding signals (i.e. the error) controls the power delivered to the hydraulic actuator or the heating circuit unit in such a way that the error in the test variable is reduced; careful choice of relative signal magnitudes (amplification) allows adequate control of each variable.

2. Control of Strain or Stress

Control of specimen strain is achieved by control of the displacement between two knife-edges of the strain detector attached to the specimen surface. The axial strain extensometer, machined in-house, consists of a strain gauge extensometer (SG) and a transmitter consisting of two shims which link together two sets of Invar arms, each supporting an alumina rod. The feedback signal from the SG is compared with the demand signal and the difference between the two, the error signal, is used to control the driving signal to the servovalve. The command signals (mean strain and amplitude) are sent by the Multiprogrammer (HP 6942A), which is controlled by the HP 9816S. Figure II.2 shows a block diagram of the strain controlled closed-loop

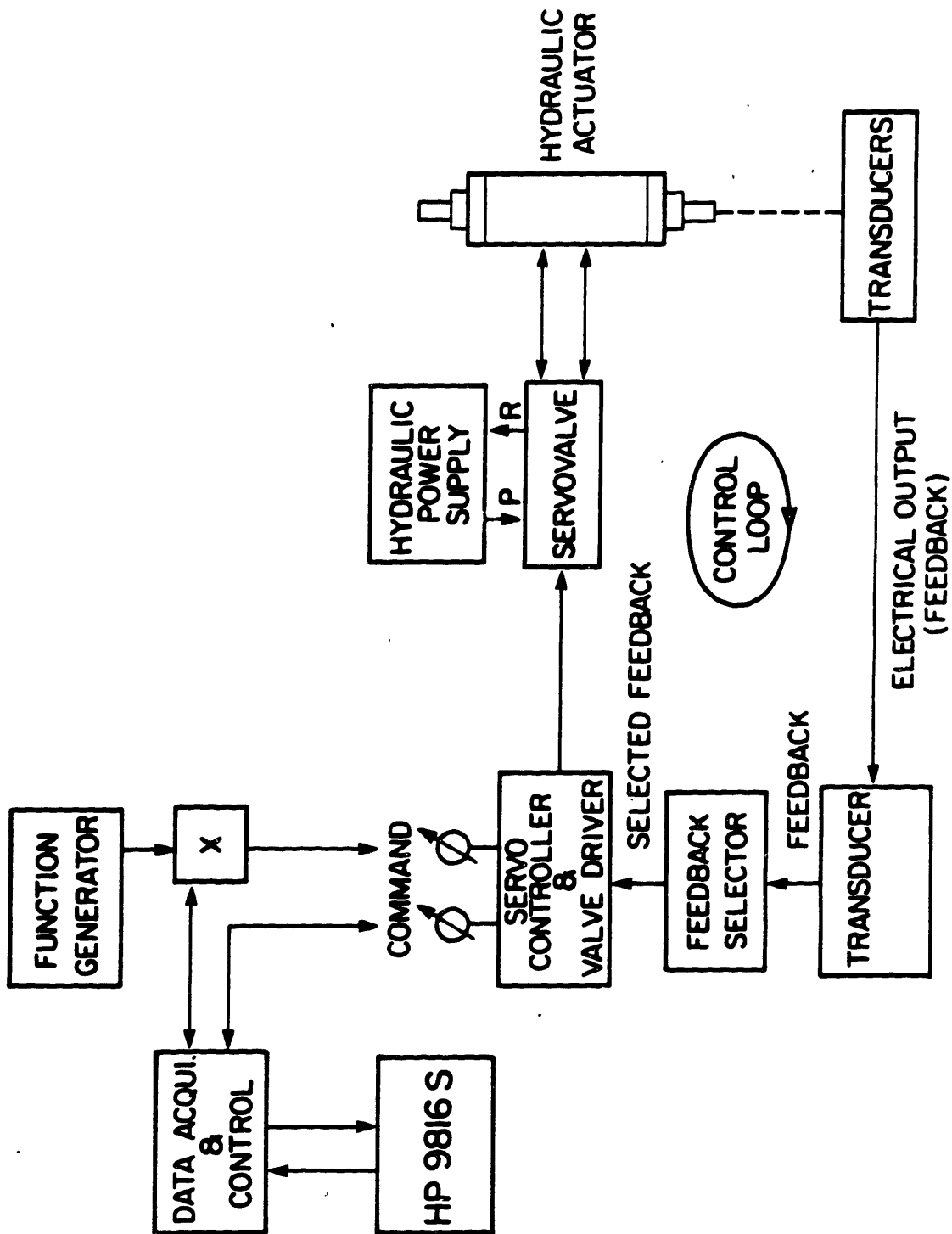


Figure II.2 Block diagram of the strain-control closed-loop unit

unit. In the system, the set point command (mean stress or strain) is fed directly to the servo-controller of the MTS unit. The amplitude signal command is also obtained by feeding the output of a D/A converter directly into the servo-controller. The procedure to continuously update the command is outlined in Section 3c.

The control of the stress applied is similar to the strain controlled except that the feedback signal is obtained from the load cell.

3. Data Acquisition and Control Unit

The command signals are sent by this data acquisition and control unit called Multiprogrammer or HP 6942A. It is composed of an internal main microprocessor, memory buffers for I/O and data storage, a real time clock and a backplane where separate plug-in cards are connected. Each plug-in I/O card is equipped with its own microprocessor.

Instructions to perform the test and values of the stress (in MPa) or strain (in %) for the mean and amplitude are typed-in on the HP 9816S at the beginning of the test. These values are then converted into their corresponding binary code and voltage and sent to the Multiprogrammer, which in turn decodes them and re-programs the appropriate I/O cards.

With the proper I/O cards, the system has the following capabilities:

1. Data acquisition
2. Measurement ranges
3. Control

4. Synthesis

3a. Acquisition

Analog measurement from up to 16 channels (can be increased to 960 channels) may be acquired, depending upon the scanner system configuration. Random access to any channel, as well as continuous scanning, are easily accomplished. Figure II.3 shows a diagram of the scanning system configuration implemented in our system. The signal may be digitized at rates up to 33 KHz by the A/D and stored on a memory card. Each memory card can store up to 64 Kbytes. The digitizing process takes place independently of all other Multiprogrammer activity, that is, data acquisition is achieved in parallel without any interruption from the control activities.

3b. Measurement Ranges

Proper switches on the A/D converters are used to select measure voltage range from $\pm 25\text{mV}$ to $\pm 10\text{V}$ full scale in the presence of 250V of common-mode voltage. The resolution can then be varied from $12 \mu\text{V}$ to 5 mV.

3c. Control and Synthesis

The twelve bits voltage D/A converters provide outputs for analog programmable instrument and stimulus of units under test (mean stress/strain and amplitude). A memory card can be used to

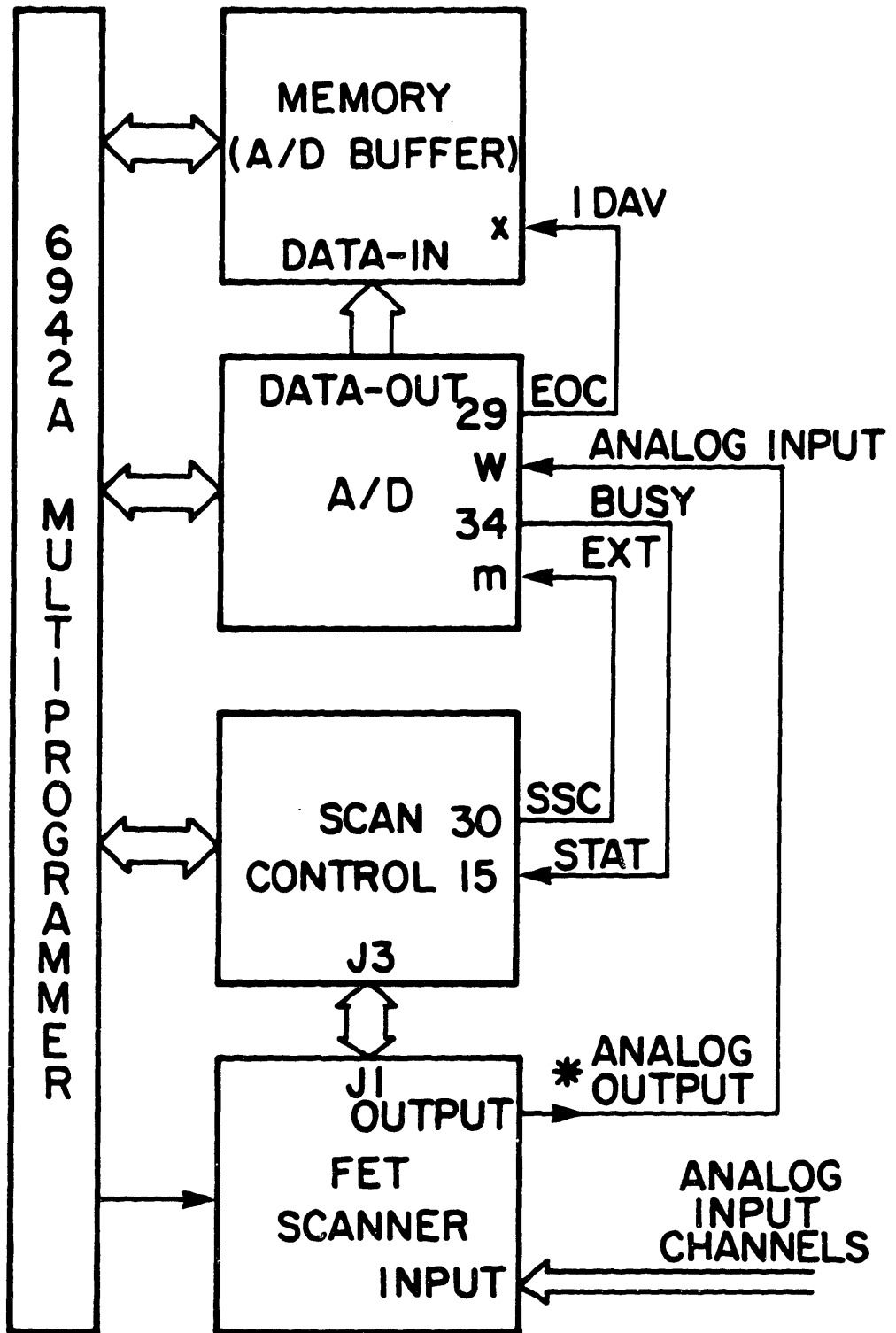


Figure II.3 Configuration for sequential scanning with buffered A/D

continuously supply preloaded data to the D/A card at rates of up to 100 KHz. Any type of waveforms may be loaded into the memory card from the computer and used as stimuli for tests. Any repeatable wave shape (sine, square, triangular, etc.) can also be preloaded into a memory card. A timer card then determined the time between each analog voltage change such that the changes are perceived in the test as continuous as possible and not as a series of step changes.

4. Control of Temperature

The specimens are heated by a radio frequency unit. For TMF tests, low frequency heaters (10 KHz) are often used [28-29] because they produce lower wall thickness gradients than the higher frequency (450 KHz) heaters and because there are fewer ground-loop problems with the 10 KHz heaters than with the 450 KHz heaters. However, it is the present author's belief that high frequency induction heating is preferable because of its fast response, making it possible to provide high heating rates capable of inducing considerable thermal stresses in specimens of small cross-section. In this case, the heating mode is close to that encountered in-service, since the heat is generated within the surface layer of the specimen. Analysis of the temperature fields in the specimens needs to be carried out with the high frequency heaters, but numerical methods of non-stationary problems of heat conductivity using finite elements are now in our hands. Temperature measurement is accomplished by thermocouples welded onto the specimen. A thermistor is used with the temperature controller to provide a stabilized cold junction.

There is a relationship between the heating method, the design of the specimen, and temperature measurement and control. Radio frequency induction requires close coil-to-specimen spacing and small grip ends which makes difficult the mounting of additional measurement devices and obscures access to and visibility of the surface for replication, etc.; also, the coil has a high voltage RF potential requiring insulation and safety precaution. A temperature disturbance occurs at the thermocouple mass in the field, as well as at specimen locations spaced to the coil. Finally, there are possible RF induction-induced group loop problems in the instrumentation cabling.

In order to minimize these potential problems, great care was taken to use properly shielded cables. The coils were machined as to maintain constant the coil-to-specimen spacing. This was achieved by using a mold having over-sized dimensions of the specimen. Before each test, the coil must be carefully positioned around the specimen as to minimize the temperature difference between the four faces of the specimen. The temperature variation along the gauge length of the specimen has been measured to be less than 10°C and accurate to $\pm 1^\circ\text{C}$.

The amplified signal from the thermocouple (Figure II.4) is compared with the demand signal which was programmed. A difference between the demand and feedback signals caused by the specimen temperature being too low, causes an increase in the power supplied to the coil. The increased power passing through the coil increases the temperature of the specimen and hence reduces the error. If the temperature is too high, the power to the coil is reduced. Compressed air is used to cool the specimen during the cool down portion of the temperature cycle. The air valve is best controlled by the

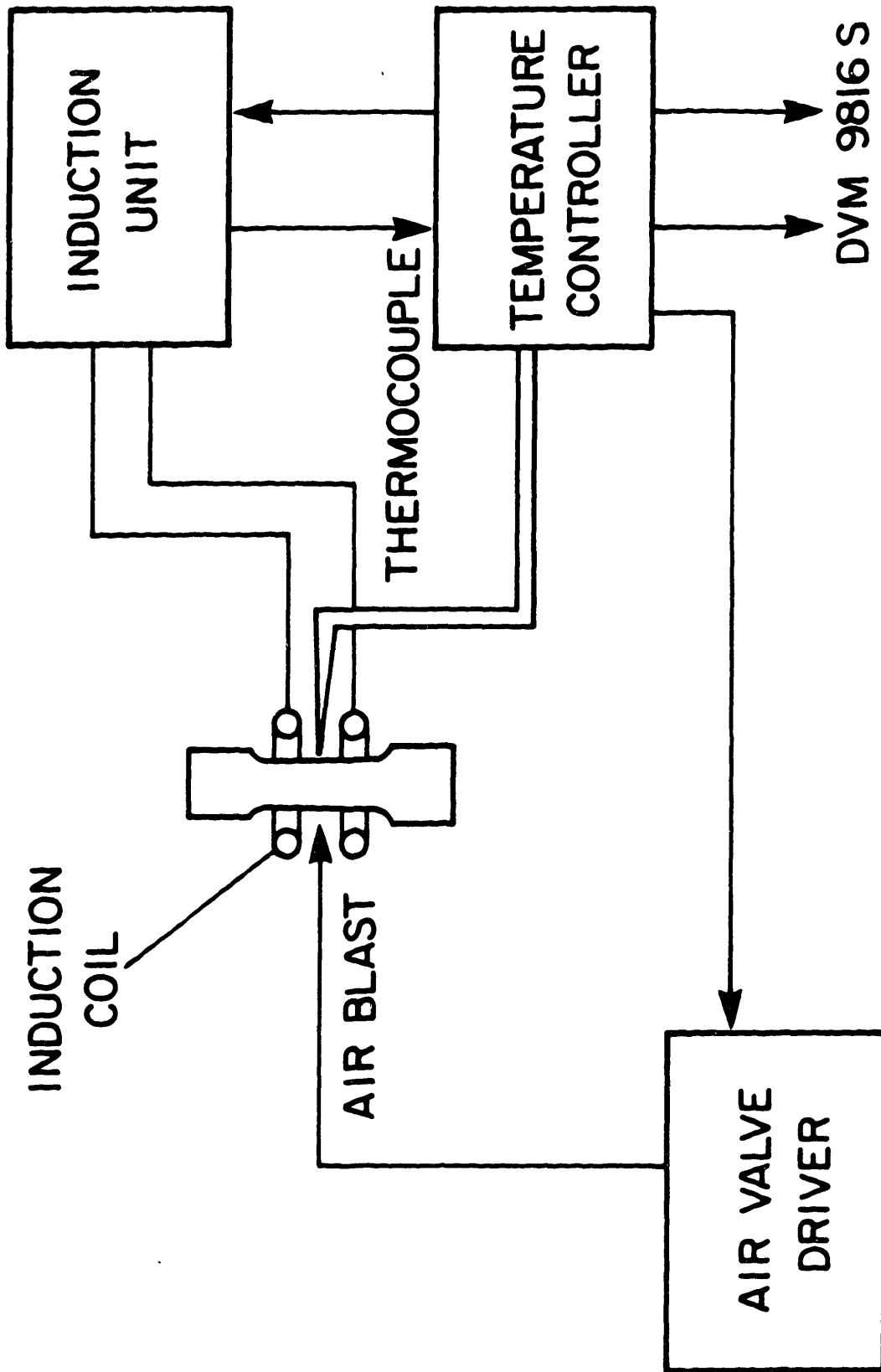


Figure 11.4 Block diagram of the temperature control unit

There is a relationship between the heating method, the design of the specimen, and temperature measurement and control. Radio frequency induction requires close coil-to-specimen spacing and small grip ends which makes difficult the mounting of additional measurement devices and obscures access to and visibility of the surface for replication, etc.; also, the coil has a high voltage RF potential requiring insulation and safety precaution. A temperature disturbance occurs at the thermocouple mass in the field, as well as at specimen locations spaced to the coil. Finally, there are possible RF induction-induced group loop problems in the instrumentation cabling.

In order to minimize these potential problems, great care was taken to use properly shielded cables. The coils were machined as to maintain constant the coil-to-specimen spacing. This was achieved by using a mold having over-sized dimensions of the specimen. Before each test, the coil must be carefully positioned around the specimen as to minimize the temperature difference between the four faces of the specimen. The temperature variation along the gauge length of the specimen has been measured to be less than 10°C and accurate to $\pm 1^\circ\text{C}$.

The amplified signal from the thermocouple (Figure II.4) is compared with the demand signal which was programmed. A difference between the demand and feedback signals caused by the specimen temperature being too low, causes an increase in the power supplied to the coil. The increased power passing through the coil increases the temperature of the specimen and hence reduces the error. If the temperature is too high, the power to the coil is reduced. Compresses air is used to cool the specimen during the cool down portion of the temperature cycle. The air valve is best controlled by the

temperature programmer, which opened or closed a solid state relay that drove the power to the air valve. With this technique, the air is always synchronized to the temperature cycle and is repeatable. The cooling rate is controlled by the heater ballasting the air blast cooling.

The limits of the system, in terms of heating and maximum temperature, were also tested. Heating rates in excess of $20^{\circ}\text{C}/\text{sec}$. have been obtained with the test rig and single edge notch specimen geometry. For faster rates, some control accuracy is sacrificed and a detailed thermal analysis has to be performed to determine the time-temperature distribution in the specimen. Using different specimen geometry and coil design, control heating rates in excess of $200^{\circ}\text{C}/\text{sec}$. were achieved with an identical heating/cooling unit. The maximum uniform temperature that can be reached is a function of the specimen geometry and specimen-to-coil distance. With the present configuration of specimen and coil design, the upper limit of the temperature cycles is 1050°C . In the development work, specimens were tested between 400 and 925°C . A six degree per second heating and cooling ramp was programmed and run. The dynamic performance of the system is shown in Figure II.5. Five thermocouples were used and the temperature of each thermocouple was always within ten degrees of the requested profile throughout the test.

5. Crack Growth Measurement

Hardly any data have been gathered on crack growth during thermal fatigue cycling in the plastic strain range and crack length measurements have been performed mostly by optical measurements

TMF TEST RIG RESPONSE (6°C/sec)

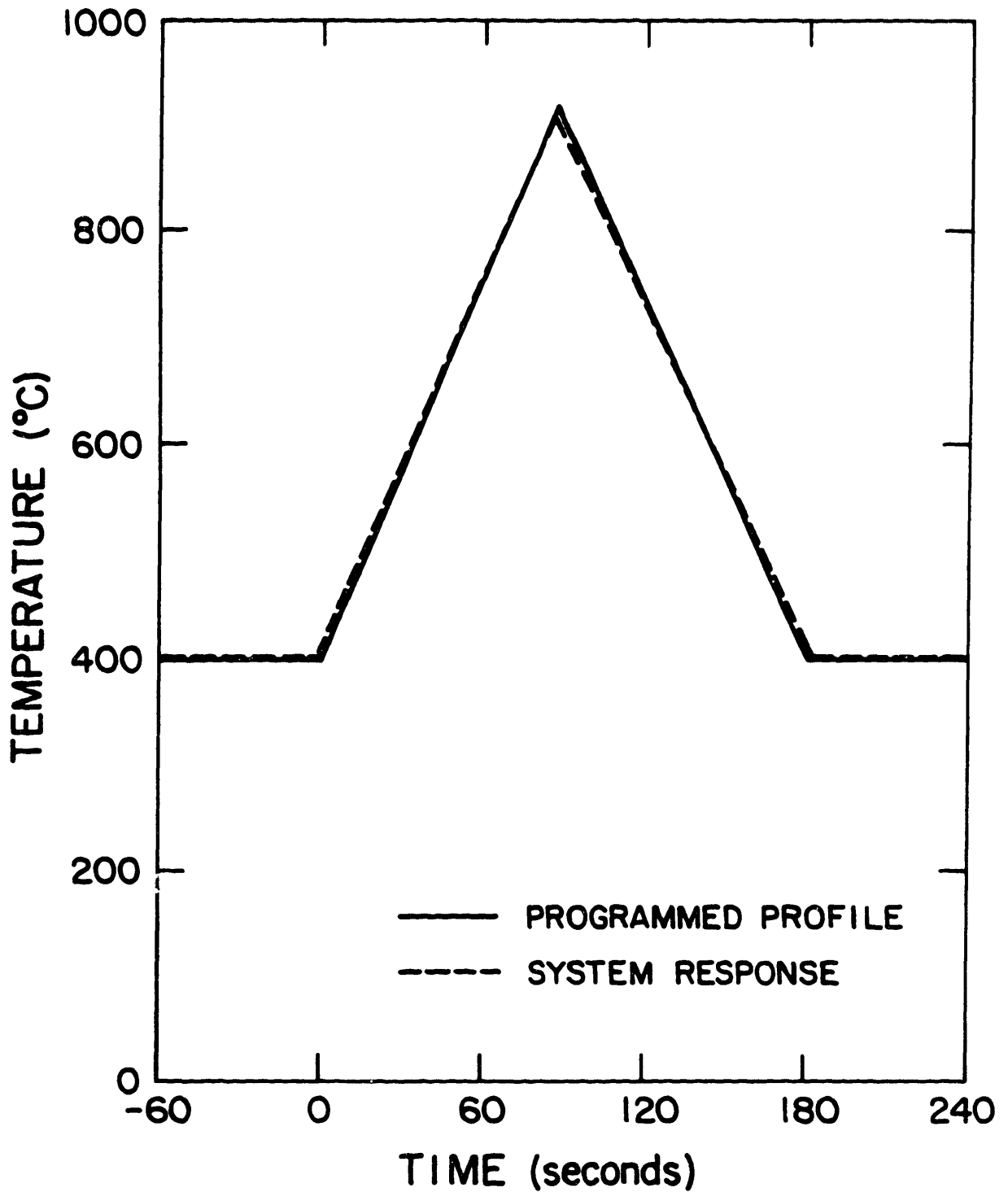


Figure II.5 Programmed profile and system response for a 6 °C/sec triangular waveform.

and by cellulose acetate replica on tubular centered notched specimens. In these experiments, the surface crack lengths must be converted to a mean crack length for the tube used (see Appendix I). The resolution claimed [41] for optical measurements is in the range of 40-120 μm , depending on the crack tip clarity and providing the measurements are taken at maximum tensile load.

There have been few attempts to measure crack length in TMF conditions using the potential drop technique [22, 119] on a 12.7 mm diameter push-pull specimen. Using a starter notch 200 μm deep, experimenters have been able to resolve accurately a crack increment of 40 μm , and the corresponding growth rates were measured to better than 10^{-8} m/cycle [119]. The method of potential drop has been used satisfactorily for isothermal conditions for numerous materials [120-121] and preliminary experiments by the authors have shown that it can be used satisfactorily provided that the electrical noises are adequately filtered and that the calibration curve is properly corrected in order to take into account changes of potential with temperature.

The electrical noises induced in the potential probes by RF heating can be eliminated by the use of a band-pass filter centered on a 430-460 KHz frequency range. Power line surges, transients, and RF induced power-line noises can be taken care of by the following technique. First, a 10 KHz band-pass filter is used to eliminate the induced-noise of the 10 KHz Master oscillator of the MTS console used to provide excitation to the servo-valves LVDT's. Second, the DVM is programmed to convert the analog signal in 10 power line cycles (PLC). In this mode, 1 PLC is used for the runup time, the A/D operation repeated ten times. The resulting ten readings are then averaged and the answer becomes a

single reading. This, with the built-in broad band filter, greatly reduces the emf noise induced by the power-line fluctuations. A schematic of the DC potential system is shown in Figure II.6. Because the potential, the temperature, the load, and the strain are recorded synchronously, it is possible to take into account the thermal variation of the potential. The procedure is the following. First, the changes in potential as a function of the temperature and strain or stress ($V(T, \sigma)$) is measured. Then a thermal cycle at zero stress is recorded ($V(T, \sigma = 0)$). The effect of the applied stress or strain is obtained by subtracting $V(T, \sigma = 0)$ from $V(T, \sigma)$ to yield $V(\sigma)$. The procedure is outlined in Figure II.7. To assess crack growth, the peak potential of each cycle ($V(T, \sigma)$) is recorded, and plots of the voltage versus applied number of cycles are obtained. Using well-known solutions [120-121] relating (V/V_0) to (a/a_0) for the single-edge notch specimen geometry, the crack lengths versus N curves are derived. Improved sensitivity can be achieved through the use of reference probes where the ratio ($V(t)/V_0$) is corrected by multiplying by (V_{ref}^0/V_{ref}), the ratio of the initial reference probe signal to the reference probe signal at time t. The resolution achieved under TMF conditions on single edge notch specimens is better than 10 μm .

A close look at the potential signals shown in Figure II.7 indicates that they can be used to generate information on the mechanisms taking place at the crack tip. By noting that $V(T, \sigma)$ and $V(T, \sigma = 0)$ are also functions of the geometry, we can write

$$V(\sigma) = V(T, \sigma, \text{geo}) - V(T, \sigma = 0, \text{geo})$$

Therefore, for a given temperature T and zero applied stress, the expected value of $V(\sigma)$ is zero is the geometry of the crack, which

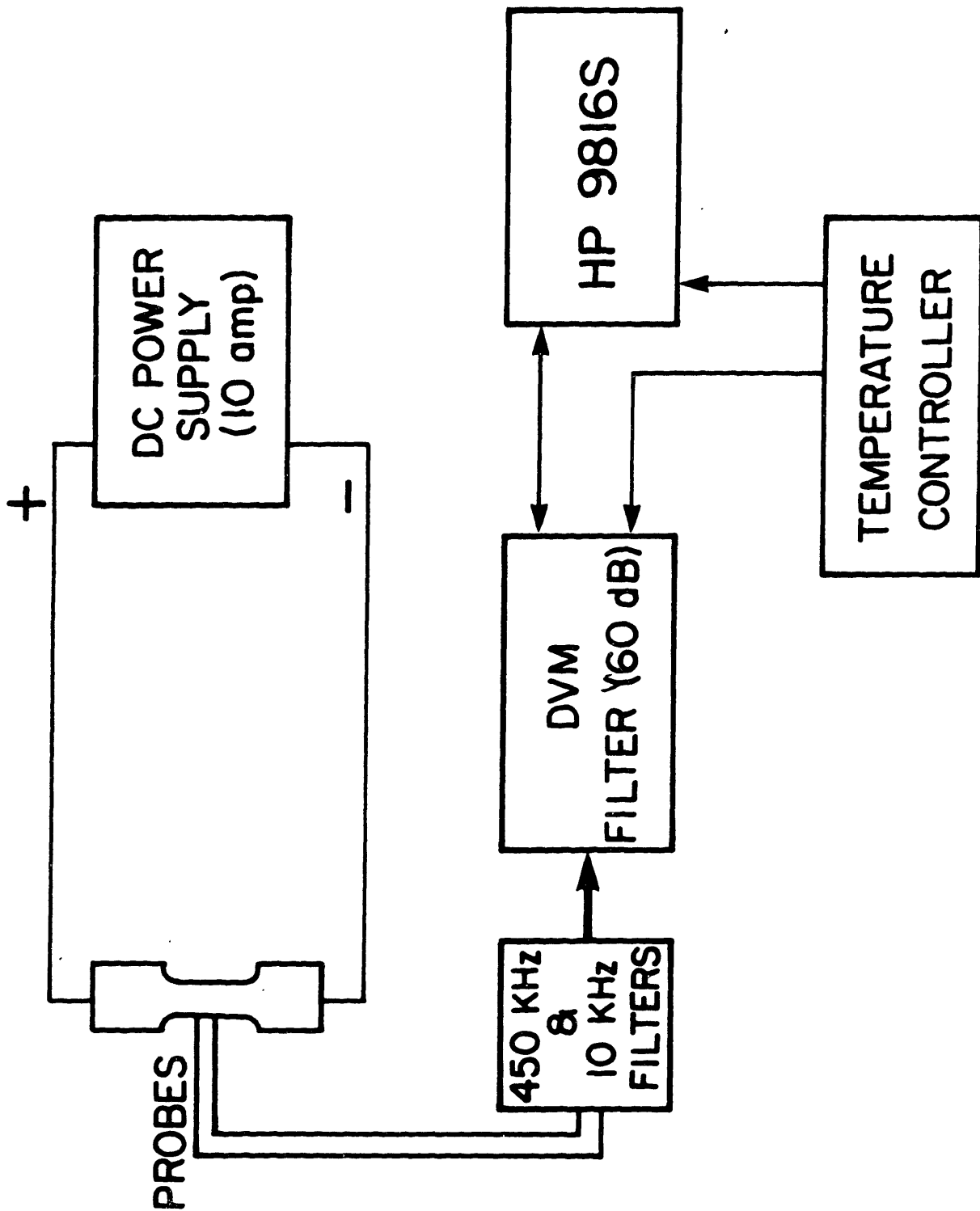


Figure II.6 Schematic of the DC potential drop system.

include crack length and configuration, in unchanged. However, if $V(\sigma)$ is not equal to zero at zero applied stress, then the geometry terms in $V(T, \sigma, \text{geo})$ and $V(T, \sigma = 0, \text{geo})$ must be different (see Equation 2). Assuming that the crack increment during the thermal cycle is negligible, then the difference associated with the geometry term is solely a function of the configuration. The applied stress required (see Figure II.7b) to give $V(\sigma) = 0$ represents the minimum necessary stress to re-establish in the specimen the same crack configuration. Because the transition point where $V(\sigma)$ equal zero corresponds to the transition between the tensile and compressive part of the cycle, it is logical to assume that this change in configuration is a change in the opening of the crack.

From Figure II.7 other information can be derived from the analysis of the $V(\sigma)$ potential curves. That is, to determine when the crack is growing within one cycle. In Figure II.7b, the $V(\sigma)$ curve for in-phase cycling shows a hump near the maximum stress, whereas at low ΔK (Figure II.7a) and for out-of-phase cycling, the $V(\sigma)$ curve is continuous without discontinuity. Such an increase in potential usually reflects a sudden increase in crack length. Therefore, it can be concluded that under this particular condition and specific loading, the crack growth was happening at the peak applied load/strain. On the other hand, for the other conditions shown in Figure II.7, it is logical to assume that the crack was growing in a continuous fashion in the tensile going part of the cycle ($0 < \sigma < \sigma_{\max}$). The crack extension during a single cycle can be estimated by comparing the values of $V(T, \sigma)$ at the beginning and at the end of the cycle. Local estimate of the crack growth rate within one cycle can be computed by dividing the

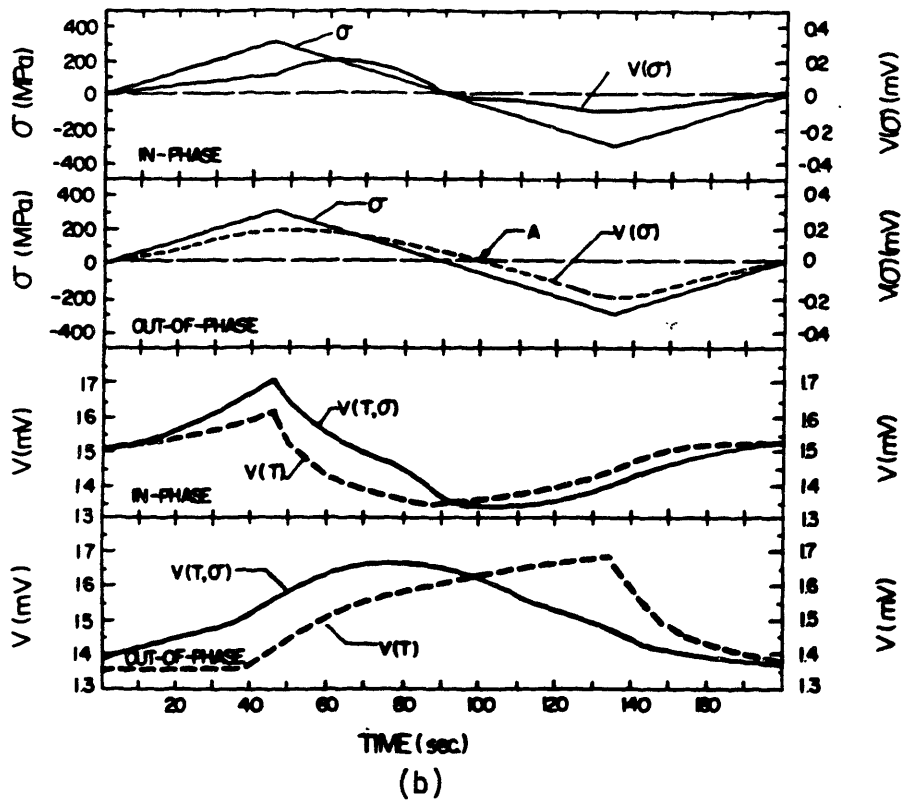
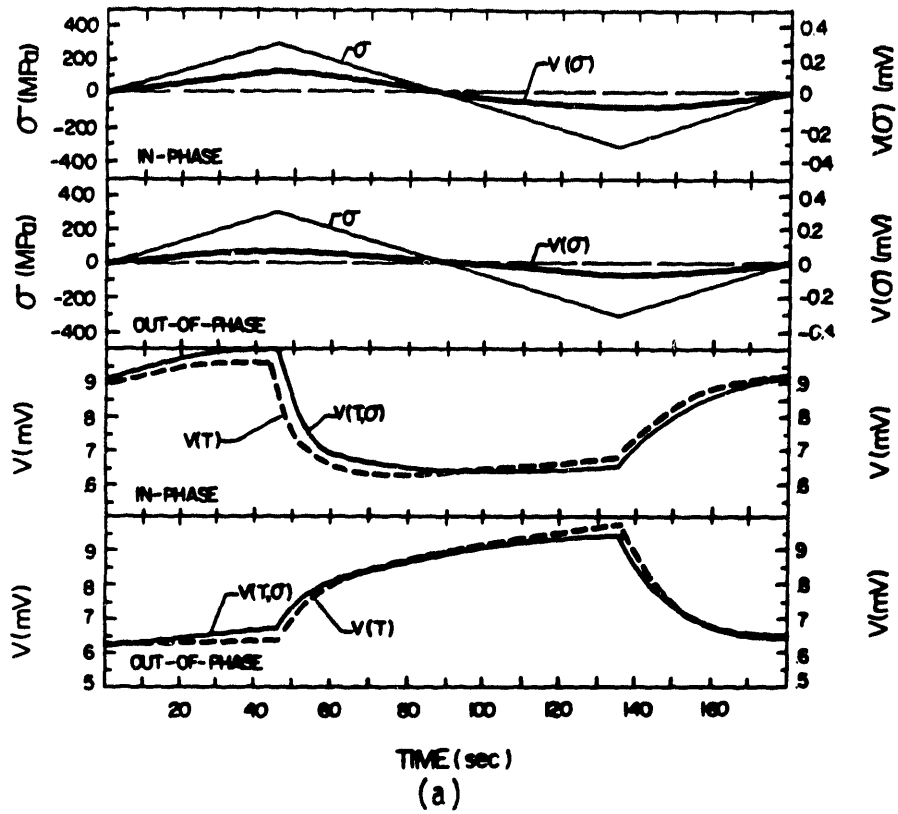


Figure II.7 Potential curves $V(T, \sigma)$, $V(T)$ and $V(\sigma)$. (a) $\Delta K = 25 \text{ MPa}\sqrt{\text{m}}$
 (b) $\Delta K = 50 \text{ MPa}\sqrt{\text{m}}$

increment in crack length by the time spent in the tension going part of the cycle (time interval for which $V(\sigma) > 0$). If a hump is seen on the $V(\sigma)$ the time interval between the hump and $V(\sigma) = 0$ must be taken.

From the above analysis of the $V(\sigma)$ curves, it can be concluded that the potential drop method has the capability of monitoring crack extension during a cycle, whereas the optical measurement and compliance methods are limited for growth measurement to no less than one cycle. Therefore, detailed analysis of the crack growth process can be achieved and this is particularly important in trying to determine the mechanisms involved with TMF crack growth.

Appendix III

Software for Control and Data Analysis

The software developed to run the isothermal and TMF tests are presented in this appendix. The programs used for data reduction and for plotting the data are also presented.

```

10! *****
20! *
30! *          PROGRAM ISO/TMF          *
40! *          *****                  *
50! *
60! *
70! *    THIS PROGRAM PERFORM THE REAL-TIME CONTROL AND DATA ACQUI- *
80! *    SITION OF ISOTHERMAL OR THERMAL-MECHANICAL FATIGUE TEST.   *
90! *
100! *    THE OPTIONS (Iso, TMF, CG, LCF) AND THE TEST PARAMETERS    *
110! *    (Load and strain scale, Mean and amplitude, and frequency) *
120! *    ARE ENTERED BY THE USER.                                    *
130! *
140! *    THE MULTI. IS PROGRAMMED ACCORDINGLY AND DISPLAYED IN REAL- *
150! *    TIME THE HYSTERISIS LOOP AND POTENTIAL.                    *
160! *
170! *
180! *****
190!
200! -----SELECT OPTIONS AND READ PARAMETERS-----
210! -----
220! LOADSUB ALL FROM "READ_PARAM"
230! CALL Read_param(Material$,Mode$,Contr_variable,Scale,Mean,Span,Gauge,Frequen
cy)
240! DELSUB Read_param
250!
260! IF Mode$="TMLCF" THEN Option_tmhcf
270! IF Mode$="TMFCG" THEN Option_tmfcg
280! IF Mode$="ISOLCF" THEN Option_isolcf
290! IF Mode$="ISOCG" THEN Option_isocg
300!
310! GOTO Finish
320!
330! -----
340! Option_tmhcf: !
350!             OPTION THERMAL-MECHANICAL LOW CYCLE FATIGUE
360! -----
370!             LOADSUB ALL FROM "TMLCF"
380!             Tmlcf(Material$,Contr_variable,Scale,Mean,Span,Gauge)
390!             GOTO Finish
400! -----
410! Option_tmfcg: !
420!             OPTION THERMAL-MECHANICAL FATIGUE CRACK GROWTH
430! -----
440!             LOADSUB ALL FROM "TMFCG"
450!             Tmfcg(Material$,Contr_variable,Scale,Mean,Span,Gauge)
460!             GOTO Finish
470! -----
480! Option_isolcf: !
490!             OPTION ISOTHERMAL LOW CYCLE FATIGUE
500! -----
510!             LOADSUB ALL FROM "ISOLCF"
520!             Isolcf(Material$,Contr_variable,Scale,Mean,Span,Gauge,Frequency)
530!             GOTO Finish
540! -----

```

```
550 Option_isocg: !
560 !           OPTION ISOTHERMAL FATIGUE CRACK GROWTH
570 !           -----
580           LOADSUB ALL FROM "ISOCG"
590           Isocg(Material$,Contr_variable,Scale,Mean,Span,Gauge,Frequency)
600           GOTO Finish
610 !           -----
620 Finish:    !
630           END
640 !           -----
```

```

10! *****
20! *
30! *          PROGRAM READ_PARAM          *
40! *          *****                    *
50! *
60! *      THIS PROGRAM IS USED BY ISO_TMF TO READ THE OPTIONS AND *
70! *      PARAMETERS REQUIRE TO RUN THE DESIRED TEST.            *
80! *
90! *      THE OPTIONS ARE:      1. ISOTHERMAL LCF (ISOLCF)      *
100! *                          2. ISOTHERMAL CG (ISOCG)       *
110! *                          3. THERMAL-MECHANICAL LCF (TMLCF) *
120! *                          4. THERMAL-MECHANICAL FCG (TMFCG) *
130! *
140! *      THE INPUTTED PARAMETERS ARE:
150! *                          1. ALLOY DESIGNATION            *
160! *                          2. LOAD AND STRAIN SCALES       *
170! *                          3. CONTROL VARIABLE (Stress or Strain) *
180! *                          4. GAUGE LENGTH                  *
190! *                          5. MEAN (Mean stress or strain) *
200! *                          6. AMPLITUDE (Stress or strain) *
210! *                          7. FREQUENCY                     *
220! *
230! *      THE PROGRAM ALSO CHECKS THE VALIDITY OF THE DATA.    *
240! *
250! *****
260! !
270! OPTION BASE 0
280! CALL Read_param(Material$,Mode$,Contr_variable,Scale,Mean,Span,Gauge,Freque
290! PRINT USING "2/,23X,K";"Program READ_PARAM terminated"
300! END
310! !
320! SUB Read_param(Material$,Mode$,Contr_variable,Scale,Mean,Span,Gauge,Freque
330! OPTION BASE 0
340! DIM Dummy$(40),Dummy1$(80)
350! Dummy$="*****"
360! Dummy1$="*****"
370! !
380! -----
390! PRINT USING 460;Dummy1$
400! PRINT USING 410
410! IMAGE 2/,20X,"ENTER TYPE OF ALLOY (10 Characters max)"
420! BEEP
430! INPUT Material$
440! -----
450! PRINT USING 460;Dummy1$
460! IMAGE 2/,80A
470! PRINT USING 480
480! IMAGE 2/,20X,"ENTER TYPE OF TESTING",/,25X,"1. ISOTHERMAL FATIGUE",/,25X,"
490! BEEP
500! INPUT Mode_type
510! IF Mode_type<>1 AND Mode_type<>2 THEN

```

```

520     PRINT USING 530
530     IMAGE 2/,20X,"INCORRECT MODE TYPE. Please re-enter"
540     BEEP 3000,1.0
550     GOTO 470
560 ELSE
570 END IF
580 !
590 -----
590 PRINT USING 460;Dummy1$
600 PRINT USING 610
610 IMAGE 2/,20X,"ENTER MODE OF TESTING",/,25X,"1. LCF (Initiation)",/,25X,"2.
    CRACK PROPAGATION (Propagation)"
620 BEEP
630 INPUT Mode_of_testing
640 IF Mode_of_testing<>1 AND Mode_of_testing<>2 THEN
650     PRINT USING 660
660     IMAGE 2/,20X,"UNDEFINED MODE OF TESTING. Please re-enter"
670     BEEP 3000,1.0
680     GOTO 600
690 ELSE
700 END IF
710 !
720 -----
720 IF Mode_type=1 THEN
730     Mode$="ISOCG"
740     IF Mode_of_testing=1 THEN Mode$="ISOLCF"
750 ELSE
760     Mode$="TMFCG"
770     IF Mode_of_testing=1 THEN Mode$="TMLCF"
780 END IF
790 PRINT USING 460;Dummy1$
800 PRINT USING 810;Dummy$,Mode$
810 IMAGE 2/,15X,40A,/,15X,"*",38X,"*",/,15X,"*",7X,6A," MODE WAS SELECTED.
    ",6X,"*"
820 IF Mode$="ISOLCF" OR Mode$="ISOCG" THEN
830     PRINT USING 840;Dummy$
840     IMAGE 15X,"*",7X,"NO DEFAULT VALUE.",14X,"*",/,15X,"*",38X,"*",/,15X
    , "*" ,38X,"*",/,15X,40A
850 ELSE
860     PRINT USING 870
870     IMAGE 15X,"*",7X,"DEFAULT VALUES ARE:",12X,"*",/,15X,"*",12X,"A. 3
    min/cycle",11X,"*"
880     PRINT USING 890;Dummy$
890     IMAGE 15X,"*",12X,"B. 3 or 4 Thermo.",8X,"*",/,15X,"*",38X,"*",/,15
    X,40A
900     END IF
910 !
920 -----
920 PRINT USING 460;Dummy1$
930 PRINT USING 940
940 IMAGE 2/,20X,"ENTER CONTROL VARIABLE?",/,25X,"1. LOAD CONTROL",/,25X,"2. S
    TRAIN CONTROL"
950 BEEP
960 INPUT Contr_variable
970 IF Contr_variable<>1 AND Contr_variable<>2 THEN
980     PRINT USING 990
990     IMAGE 2/,20X,"UNDEFINED CONTROL VARIABLE. Please re-enter"
1000    BEEP 3000,1.0

```

```

1000     BEEP 3000,1.0
1010     GOTO 930
1020     ELSE
1030     END IF
1040     !
1050     IF Contr_variable=1 THEN
1060         PRINT USING 460;Dummy1$
1070         PRINT USING 1080
1080         IMAGE 2/,20X,"ENTER LOAD SCALE? (100,50,20 or 10 %)"
1090         BEEP
1100         INPUT Load_scale
1110         Load_scale=Load_scale
1120         IF Load_scale<>100 AND Load_scale<>50 AND Load_scale<>20 AND Load_scal
e<>10 THEN
1130             PRINT USING 1140
1140             IMAGE 2/,20X,"Undefined value. Please re-enter."
1150             BEEP 3000,1.0
1160             GOTO 1070
1170         ELSE
1180         END IF
1190     !
1200     PRINT USING 460;Dummy1$
1210     PRINT USING 1220
1220     IMAGE 2/,20X, "ENTER MEAN STRESS (in MPa)?"
1230     BEEP
1240     INPUT Mean
1250     IF (Mean*11.569896)<=-(250*Load_scale) OR Mean>=(250*Load_scale) THEN
1260         PRINT USING 1270
1270         IMAGE 2/,20X,"VALUE OUT-OF-BOUND. Please re-enter."
1280         BEEP 3000,1.0
1290         GOTO 1210
1300     ELSE
1310     END IF
1320     !
1330     PRINT USING 460;Dummy1$
1340     PRINT USING 1350
1350     IMAGE 2/,20X, "ENTER STRESS AMPLITUDE (in MPa)"
1360     BEEP
1370     INPUT Span
1380     IF Span<=0 THEN
1390         PRINT USING 1400
1400         IMAGE 2/,20X,"UNDEFINED VALUE. Please re-enter"
1410         BEEP 3000,1.0
1420         GOTO 1340
1430     ELSE
1440         IF (ABS(Mean)+Span)*11.569896>=250*Load_scale THEN
1450             PRINT USING 1460
1460             IMAGE 2/,20X,"VALUE OUT-OF-BOUND, Please re-enter"
1470             BEEP 3000,1.0
1480             GOTO 1340
1490         ELSE
1500         END IF
1510     END IF
1520     !
1530     PRINT USING 460;Dummy1$
1540     PRINT USING 1550

```

```

2070     END IF
2080 ! -----
2090     PRINT USING 460;Dummy1$
2100     Emax=.05493*Strain_scale/Gauge_lenght
2110     PRINT USING 2120
2120     IMAGE 2/,20X,"ENTER MEAN STRAIN (in %)"
2130     BEEP
2140     INPUT Mean
2150     Mean=Mean/100
2160     IF Mean<=-Emax OR Mean>=Emax THEN
2170         PRINT USING 2180
2180         IMAGE 2/,20X,"VALUE OUT-OF-BOUND. Please re-enter"
2190         BEEP 3000,1.0
2200         GOTO 2110
2210     ELSE
2220     END IF
2230 ! -----
2240     PRINT USING 460;Dummy1$
2250     PRINT USING 2260
2260     IMAGE 2/,20X,"ENTER STRAIN AMPLITUDE (in %)"
2270     BEEP
2280     INPUT Span
2290     Span=Span/100
2300     IF Span<=0 THEN
2310         PRINT USING 2320
2320         IMAGE 2/,20X,"UNDEFINED VALUE. Please re-enter."
2330         BEEP 3000,1.0
2340         GOTO 2250
2350     ELSE
2360         IF (ABS(Mean)+Span)>=Emax THEN
2370             PRINT USING 2380
2380             IMAGE 2/,20X,"VALUE OUT-OF-BOUND. Please re-enter."
2390             BEEP 3000,1.0
2400             GOTO 2110
2410         ELSE
2420         END IF
2430     END IF
2440 ! -----
2450     PRINT USING 460;Dummy1$
2460     PRINT USING 2470
2470     IMAGE 2/,20X,"ENTER LOAD SCALE (100,50,20 or 10%)"
2480     BEEP
2490     INPUT Load_scale
2500     Load_scale=Load_scale
2510     IF Load_scale<>100 AND Load_scale<>50 AND Load_scale<>20 AND Load_s
cale<>10 THEN
2520         PRINT USING 2530
2530         IMAGE 2/,20X,"UNDEFINED VALUE. Please re-enter"
2540         BEEP 3000,1.0
2550         GOTO 2460
2560     ELSE
2570     END IF
2580 ! -----
2590 END IF
2600 ! -----

```

```

1550     IMAGE 2/,20X,"ENTER THE GAUGE LENGTH (in inch)"
1560     BEEP
1570     INPUT Gauge_length
1580     IF Gauge_length<.400 OR Gauge_length>.6 THEN
1590         PRINT USING 1600
1600         IMAGE 2/,20X,"GAUGE LENGHT VALUE OUT-OF-BOUND. Please re-enter."
1610         BEEP 3000,1.0
1620         GOTO 1540
1630     ELSE
1640     END IF
1650 ! -----
1660     PRINT USING 460;Dummy1$
1670     PRINT USING 1680
1680     IMAGE 2/,20X,"ENTER STRAIN SCALE (100,50,20 or 10 %)"
1690     BEEP
1700     INPUT Strain_scale
1710     Strain_scale=Strain_scale/100
1720     IF Strain_scale<>1. AND Strain_scale<>.5 AND Strain_scale<>.2 AND Stra
in_scale<>.1 THEN
1730         PRINT USING 1740
1740         IMAGE 2/,20X,"UNDEFINED VALUE. Please re-enter."
1750         BEEP 3000,1.0
1760         GOTO 1670
1770     ELSE
1780     END IF
1790 ! -----
1800     ELSE
1810 ! -----
1820     PRINT USING 460;Dummy1$
1830     PRINT USING 1840
1840     IMAGE 2/,20X,"ENTER STRAIN SCALE (100,50,20 or 10 %)"
1850     BEEP
1860     INPUT Strain_scale
1870     Strain_scale=Strain_scale/100
1880     IF Strain_scale<>1. AND Strain_scale<>.5 AND Strain_scale<>.2 AND Stra
in_scale<>.1 THEN
1890         PRINT USING 1900
1900         IMAGE 2/,20X, "Undefined value. Please re-enter"
1910         BEEP 3000,1.0
1920         GOTO 1830
1930     ELSE
1940     END IF
1950 ! -----
1960     PRINT USING 460;Dummy1$
1970     PRINT USING 1980
1980     IMAGE 2/,20X,"ENTER THE GAUGE LENGHT (in inch)"
1990     BEEP
2000     INPUT Gauge_length
2010     IF Gauge_lenght<.4 OR Gauge_lenght>.6 THEN
2020         PRINT USING 2030
2030         IMAGE 2/,20X,"GAUGE LENGHT VALUE OUT-OF-BOUND. Please re-enter."
2040         BEEP 3000,1.0
2050         GOTO 1970
2060     ELSE

```



```

2610     IF Mode_type=1 THEN
2620         PRINT USING 460;Dummy1$
2630         PRINT USING 2640
2640         IMAGE 2/,20X,"ENTER THE FREQUENCY (in Hz)"
2650         BEEP
2660         INPUT Frequency
2670         PRINT USING 2680;Frequency
2680         IMAGE 2/,25X,"INPUTTED Frequency IS ",K," Hz",/
2690         PRINT USING 2700
2700         IMAGE 30X,"1. CONTINUE",/,30X,"2. CHANGE THE FREQUENCY"
2710         BEEP
2720         INPUT Change
2730         IF Change<>1 AND Change<>2 THEN
2740             PRINT USING 2750
2750             IMAGE /,30X,"Incorrect value. Please re-enter"
2760             BEEP 3000,1.0
2770             GOTO 2690
2780         END IF
2790         IF Change=2 THEN GOTO 2630
2800         GOTO Continue
2810     END IF
2820     !
2830 Continue: !
2840     Scale=Load_scale+Strain_scale
2850     Gauge=Gauge_lenght
2860     PRINT USING 460;Dummy1$
2870     BEEP 800,2
2880     PRINT USING "/,20X,K";"** PROGRAM THE Micro_Data Track **"
2890     !
2900     SUBEND

```

```

10! *****
20! *
30! *          PROGRAM TMLCF          *
40! *          *****                *
50! *
60! *      THIS PROGRAM PERFORMS THE REAL-TIME CONTROL AND DATA      *
70! *      ACQUISITION OF THERMAL-MECHANICAL LOW CYCLE FATIGUE      *
80! *      TESTS.                                                    *
90! *
100! *      THIS PROGRAM IS CALLED BY ISO_TMF AFTER SELECTION OF THE   *
110! *      TMFLCF OPTION.                                             *
120! *
130! *      THE MICRO_DATA_TRACK MUST BE PROGRAMMED FOR 180 sec      *
140! *      PERIOD (1/3 cpm).                                          *
150! *
160! *      THE CYCLIC THERMAL STRAINS ARE FIRST MEASURED BY CYCLING   *
170! *      THE TEMPERATURE AT ZERO STRESS.                            *
180! *
190! *      THE CYCLIC DATA(Stresses, strains, and temperatures)     *
200! *      ARE RECORDED EVERY (N2/N1)=1.25 CYCLES.                   *
210! *
220! *****
230! !
240! OPTION BASE 0
250! CALL Tmlcf(Material$,Contr_variable,Scale,Mean,Span,Gauge)
260! END
270! *****
280! *****
290! !
300! SUB Tmlcf(Material$,Contr_variable,Scale,Mean,Span,Gauge)
310! DIM Load(179),Strain(179),Temp1(179),Temp2(179),Temp3(179)
320! MASS STORAGE IS "HP8290X,700,1"
330! !
340! -----DEFINE I/O CARD FUNCTION-----
350! !
360! ASSIGN @Dvm TO 720
370! ASSIGN @Multi TO 723
380! ASSIGN @Disc TO "MRZ"
390! Disc_drive=0
400! Dvm=720
410! Multi=723
420! Scanner=0
430! A_to_d=3
440! Memory1=7
450! D_to_a1=10
460! Timer=11
470! D_to_a2=12
480! Memory2=13
490! !
500! -----DEFAULT VALUES FOR THE PARAMETERS-----
510! !
520! Start=1                      !Start channel
530! Stop=5                        !Stop channel
540! Pointer=4                     !Interrupt word

```

```

550  !
560  !-----INITIALIZE THE MULTI-----
570  !-----
580  CALL Init_multi(@Multi,@Disc)
590  CALL Init_mem(@Multi,Memory1)
600  !
610  !-----INITIALIZE CONTROL PROCEDURE-----
620  !-----
630  CALL Init_control(@Multi,Memory2,Timer,D_to_a1,Contr_variable,Scale,Mean,S
pan,Gauge)
640  !
650  !-----SET INTERRUPT BRANCH FOR TRIGGER SIGNAL-----
660  !-----
670  Cycle=1                                !Set cycle counter
680  G=SPOLL(723)                            !Clear Multi SRQ
690  P=SPOLL(720)                            !Clear DVM SRQ
700  OUTPUT @Dvm;"F1R-2NSZ0"                !Set DVM ranges
710  OUTPUT @Dvm;"T2D3 TMF TEST"            !Set ext trigger and display
720  OUTPUT @Dvm;"KM01"                     !Set mask for Data Ready
730  ON INTR 7,2 GOTO Start_tmf             !Set interrupt branch
740  ENABLE INTR 7;2                        !Enable interrupt SRQ
750  BEEP
760  PRINT USING 770
770  IMAGE 2/,15X,"REMOVE CONTROL AND UTILITY PAC DISCS",2/,15X,"INSERT TWO
DISCS FOR DATA STORAGE",2/,15X,"PRESS K0(Continue) TO CONTINUE"
780  .ON KEY 0 LABEL "**CONTINUE**" GOTO 800
790 Spin: GOTO Spin
800  BEEP
810  OFF KEY
820  PRINT USING 830
830  IMAGE 20/,25X,"PROGRAM AND START THE LEPEL",2/,20X,"****WAITING FOR A
TRIGGER SIGNAL****"
840  CREATE BDAT "TEST_PARAM",1,100
850  ASSIGN @Disc TO "TEST_PARAM"
860  OUTPUT @Disc;Material$, "TMLCF",Contr_variable,Scale,Mean,Span,Gauge
870  ASSIGN @Disc TO *
880  ENTER Dvm;P
890  !
900  !-----START CYCLING AND TAKING DATA-----
910  !-----
920 Start_tmf: !
930  OUTPUT @Multi;"CY",Timer,"T"           !Start cycling
940  OUTPUT @Multi;"SC,0,0,0,0T"           !Reset Clock of Multi
950  PRINT USING 960
960  IMAGE 10/,20X,"***** TMLCF TEST IN PROGRESS *****"
970  !
980  !-----READ DATA-----
990  !-----
1000 CALL Read_data(@Multi,@Dvm,Multi,Dvm,Scanner,Memory1,Load(*),Strain(*),Temp
1(*),Temp2(*),Temp3(*))
1010 !
1020 !-----STORE DATA-----
1030 !-----
1040 CALL Store_data(@Multi,@Disc,Disc_drive,Cycle,Scale,Load(*),Strain(*),Temp
1(*),Temp2(*),Temp3(*))

```

```

1050 |
1060 | -----DISPLAY DATA-----
1070 |
1080 CALL Plot_data(Material$,Contr_variable,Scale,Span,Gauge,Cycle,Load(*),Str
ain(*)
1090 |
1100 | -----SET INTERRUPT FOR SYNCHRO. SIGNAL-----
1110 |
1120 IF Cycle<9 THEN
1130     Increment=2
1140     GOTO Synchro
1150 END IF
1160 Cycle2=INT(Cycle*1.25)
1170 Increment=Cycle2-Cycle
1180 |
1190 Synchro:
1200 Waiting=Increment-1.5
1210 Cycle=Cycle+Increment           !Update cycle counter
1220 WAIT (180*Waiting)             !Set waiting time
1230 OUTPUT @Dvm;"T2KM01"          !Ext. trigger and DVM mask
1240 ON INTR 7,2 GOTO 990           !Set interrupt branch
1250 ENABLE INTR 7;2               !Enable interrupt
1260 ENTER Dvm;P
1270 SUBEND
1280!
1290!
1300! *****
1310! *
1320! *     SUBROUTINES USED BY SUB TMFCG(Param1,Param2,...)
1330! *
1340! *****
1350!
1360!
1370 SUB Init_control(@Multi,Memory,Timer,D_to_a,Control,Scale,Mean,Span,Gauge)
1380 ALLOCATE A(4095)
1390     !__GENERATE WAVEFORM__
1400     |-----
1410     Load_scale=INT(Scale)/100
1420     Strain_scale=Scale-(Load_scale*100)
1430     IF Control=1 THEN
1440         Pmean=Mean/(Load_scale*216.078)           !Convert MPA into voltage
1450         Pmax=Span/(Load_scale*216.078)
1460     ELSE
1470         Emax=.05493*Strain_scale/Gauge
1480         Pmean=10*Mean/Emax                       !Convert Strain into voltage
1490         Pmax=10*Span/Emax
1500     END IF
1510     Coeff=800
1520     IF Pmax>5.12 THEN Coeff=400
1530     Ndata=INT(Coeff*Pmax+.5)-1
1540     Ndata2=INT(Ndata/4+.5)
1550     Ndata3=Ndata-Ndata2
1560     FOR I=0 TO Ndata2-1
1570         A(I)=Pmax*I/(Ndata2-1)
1580         A(I+Ndata3)=Pmax*(I/(Ndata2-1)-1)

```

```

1590 NEXT I
1600 FOR I=Ndata2 TO Ndata3
1610 A(I)=(Ndata-1-2*I)*Pmax/(Ndata+1-2*Ndata2)
1620 NEXT I
1630 FOR I=Ndata+1 TO 4095
1640 A(I)=0.
1650 NEXT I
1660 !
1670 !__CALCULATE THE PACE__
1680 !-----
1690 Time_int=180/Ndata
1700 Pace=INT(Time_int*500000)/1000 !Pace in msec
1710 !
1720 !__PROGRAM MULTI__AMPLITUDE
1730 !-----
1740 OUTPUT @Multi;"CC",Memory+1,"T" !Clear memory card
1750 OUTPUT @Multi;"SF",Memory,3,1,.005,12,"T" !Set format(LSB=0.005)
1760 OUTPUT @Multi;"WF",Memory+1.0,4095,"T" !Truncate memory
1770 OUTPUT @Multi;"MO",Memory,A(*),"T" !Load data into memory
1780 OUTPUT @Multi;"WF",Memory+1,Ndata,"T" !Truncate memory card
1790 OUTPUT @Multi;"WF",Memory+.1,10,"T" !Set re-circulate mode
1800 OUTPUT @Multi;"WF",Timer+.2,1,"T" !Set timer for continuous
1810 OUTPUT @Multi;"WF",Timer,Pace,"T" !output. Set Pace
1820 !
1830 !__PROGRAM MULTI-- MEAN
1840 !-----
1850 Incr=.005
1860 IF Pmean=0 THEN GOTO 1940
1870 IF Pmean<0 THEN Incr=-.005
1880 J=0
1890 OUTPUT @Multi;"QP",D_to_a,J,"T"
1900 IF ABS(J)<ABS(Pmean) THEN
1910 J=J+Incr
1920 GOTO 1890
1930 END IF
1940 DEALLOCATE A(*)
1950 SUBEND
1960!-----
1970 SUB Read_data(@Multi,@Dvm,Multi,Dvm,Scanner,Memory,Load(*),Strain(*),Temp1
(*),Temp2(*),Temp3(*))
1980 ALLOCATE Scan(4)
1990 OUTPUT @Dvm;"T1M00" !Set internal trigger and clear mask
2000 G=SPOLL(@Multi)
2010 ENTER 72310;A,B,C,D,E,F
2020 ON INTR 7,2 GOTO Interrupt
2030 ENABLE INTR 7;2
2040 OUTPUT @Multi;"CY",Scanner,"T" !Enable scanner
2050 OUTPUT @Multi;"WF",Scanner+.3,5,"T" !Set sequential mode
2060 !
2070 FOR K=0 TO 179
2080 OUTPUT @Multi;"WF",Scanner,1,"T" !Set start channel
2090 OUTPUT @Multi;"WF",Scanner+.1,5,"T" !set stop channel
2100 OUTPUT @Multi;"WF",Scanner+.2,40,"T" !Set pace(40 us)
2110 Prog_diff(@Multi,Memory,0) !Reset diff. counter
2120 Prog_write(@Multi,Memory,0) !Reset write pointer

```

```

2130     OUTPUT @Multi;"CC";Memory,"T"           !Clear Memory card
2140     Prog_mode(@Multi,Memory,56)           !Set FIFO mode
2150     Prog_refl(@Multi,Memory,4)           !Set stop pointer
2160     OUTPUT @Multi;"AC";Memory;"T"         !Armed memory card
2170     OUTPUT @Multi;"CY",Scanner,"T"       !Start pacer
2180 Wait:   GOTO Wait
2190 Interrupt: !
2200     G=SPOLL(@Multi)
2210     IF G=64 THEN
2220         ENTER 72310;A,B,C
2230         IF C<>0 THEN
2240             ENTER 72312;Address
2250             IF Address<>Memory THEN
2260                 PRINT "NOT MEMORY CARD"
2270                 PAUSE
2280             END IF
2290             OUTPUT @Multi;"WF",Scanner+.2,0,"T" !Stop scanner
2300             Prog_mode(@Multi,Memory,76) !Set FIFO lockout
2310             OUTPUT @Multi;"MR";Memory;5;"T" !MR command to get data
2320             ENTER 72305 USING "%,W";Scan(*) !Entering the data
2330             Strain(K)=Scan(0)*.005 !Convert the data into
2340             Load(K)=Scan(1)*.005 !engineering units by
2350             Temp1(K)=Scan(2)*.005 !multiplying with the
2360             Temp2(K)=Scan(3)*.005 !LSB value.
2370             Temp3(K)=Scan(4)*.005
2380             BEEP
2390             WAIT .685 !Wait set for 180
2400             ENABLE INTR 7;2
2410         ELSE
2420             BEEP 2000,.3
2430             PRINT "          *** SRQ NOT SET BY ARMED CARD ***"
2440             PAUSE
2450         END IF
2460     ELSE
2470         BEEP 2000,.3
2480         PRINT "          *** MULTI DID NOT INTERRUPT ***"
2490         PAUSE
2500     END IF
2510     NEXT K
2520     DEALLOCATE Scan(*)
2530     OUTPUT @Multi;"RC" !Read Real-time clock
2540     SUBEND
2550! -----
2560     SUB Store_data(@Multi,@Disc,Disc_drive,Cycle,Scale,Load(*),Strain(*),Temp
1(*),Temp2(*),Temp3(*))
2570     ALLOCATE X(179),Y(179)
2580     ENTER 72314;T1,T2,T3,T4 !Enter Clock values
2590     Time$=VAL$(T1*24+T2)&":"&VAL$(T3)&":"&VAL$(T4)
2600     FOR I=0 TO 179
2610         X(I)=INT((Load(I)+10)*1000)+(Strain(I)+10)/100
2620         Y(I)=DROUND(Temp1(I),3)*1000000+DROUND(Temp2(I),3)*1000+Temp3(I)
2630     NEXT I
2640     !
2650     ON ERROR GOTO Recover
2660     CREATE BDAT "COCLE"&VAL$(Cycle),1,5000

```

```

2670 ASSIGN @Disc TO "COCLE"&VAL$(Cycle)
2680 OUTPUT @Disc;Cycle,Time$,Scale,X(*),Y(*)
2690 ASSIGN @Disc TO *
2700 GOTO Out
2710 !
2720 Recover: !
2730     IF ERRN=59 OR ERRN=64 THEN
2740         IF Disc_drive=0 THEN
2750             Disc_drive=1
2760             MASS STORAGE IS ":HPB290X,700,1"
2770         ELSE
2780             Disc_drive=0
2790             MASS STORAGE IS ":HPB290X,700,0"
2800         END IF
2810     ELSE
2820         PRINT USING 2830;ERRN
2830         IMAGE 2/,25X,"ERROR NUMBER ",K,/,25X,"CHECK STORAGE UNIT",/,25X,"PROG
RAM ABORTED"
2840         PAUSE
2850     END IF
2860 Out: !
2870     DEALLOCATE X(*),Y(*)
2880     SUBEND
2890!-----
2900 SUB Init_multi(@Multi,@Disc)
2910     CLEAR 7
2920     WAIT 4.0
2930     G=SPOLL(@Multi)
2940     IF G<>64 THEN
2950         PRINT "         ***MULTI DID NOT INTERRUPT***"
2960         PAUSE
2970     END IF
2980     STATUS @Multi,3;Multi
2990     ENTER Multi*100+10;A
3000     IF A<>16384 THEN
3010         PRINT "         ***SELF TEST DID NOT SET SRQ***"
3020         PAUSE
3030     END IF
3040     ALLOCATE Ascii$[80]
3050     ON END @Disc GOTO Eof
3060 Rd_file:     ENTER @Disc;Ascii$
3070     OUTPUT @Multi;Ascii$
3080     GOTO Rd_file
3090 Eof: OFF END @Disc
3100     ASSIGN @Disc TO *
3110     DEALLOCATE Ascii$
3120     MASS STORAGE IS ":HPB290X,700,0"
3130 SUBEND
3140!-----
3150 SUB Init_mem(@Multi,Memory)
3160     Prog_mode(@Multi,Memory,254)
3170     Prog_mode(@Multi,Memory,54)
3180     Prog_ref1(@Multi,Memory,1048575)
3190     Prog_ref2(@Multi,Memory,0)
3200     Prog_read(@Multi,Memory,0)
3210     Prog_diff(@Multi,Memory,0)

```

```

3220 Prog_writa(@Multi,Memory,0)
3230 OUTPUT @Multi;"CC";Memory;"T"
3240 SUBEND
3250!-----
3260 SUB Prog_read(@Multi,Memory,Read_pointer)
3270 Read_low=Read_pointer MOD 65536
3280 Read_high=Read_pointer DIV 65536
3290 Read_low_oct=FNDec_to_octal(Read_low)
3300 Read_high_oct=FNDec_to_octal(Read_high)
3310 OUTPUT @Multi;"WF";Memory+.1;22;Memory+.2;Read_low_oct;"T"
3320 OUTPUT @Multi;"WF";Memory+.1;23;Memory+.2;Read_high_oct;"T"
3330 SUBEND
3340!-----
3350 SUB Prog_write(@Multi,Memory,Write_pointer)
3360 Write_low=Write_pointer MOD 65536
3370 Write_high=Write_pointer DIV 65536
3380 Write_low_oct=FNDec_to_octal(Write_low)
3390 Write_high_oct=FNDec_to_octal(Write_high)
3400 OUTPUT @Multi;"WF";Memory+.1;24;Memory+.2;Write_low_oct;"T"
3410 OUTPUT @Multi;"WF";Memory+.1;25;Memory+.2;Write_high_oct;"T"
3420 SUBEND
3430!-----
3440 SUB Prog_diff(@Multi,Memory,Diff_counter)
3450 Diff_low=Diff_counter MOD 65536
3460 Diff_high=Diff_counter DIV 65536
3470 Diff_low_oct=FNDec_to_octal(Diff_low)
3480 Diff_high_oct=FNDec_to_octal(Diff_high)
3490 OUTPUT @Multi;"WF";Memory+.1;20;Memory+.2;Diff_low_oct;"T"
3500 OUTPUT @Multi;"WF";Memory+.1;21;Memory+.2;Diff_high_oct;"T"
3510 SUBEND
3520!-----
3530 SUB Prog_ref1(@Multi,Memory,Ref1_reg)
3540 Ref1_low=Ref1_reg MOD 65536
3550 Ref1_high=Ref1_reg DIV 65536
3560 Ref1_low_oct=FNDec_to_octal(Ref1_low)
3570 Ref1_high_oct=FNDec_to_octal(Ref1_high)
3580 OUTPUT @Multi;"WF";Memory+.1;26;Memory+.2;Ref1_low_oct;"T"
3590 OUTPUT @Multi;"WF";Memory+.1;27;Memory+.2;Ref1_high_oct;"T"
3600 SUBEND
3610!-----
3620 SUB Prog_ref2(@Multi,Memory,Ref2_reg)
3630 Ref2_low=Ref2_reg MOD 65536
3640 Ref2_high=Ref2_reg DIV 65536
3650 Ref2_low_oct=FNDec_to_octal(Ref2_low)
3660 Ref2_high_oct=FNDec_to_octal(Ref2_high)
3670 OUTPUT @Multi;"WF";Memory+.1;30;Memory+.2;Ref2_low_oct;"T"
3680 OUTPUT @Multi;"WF";Memory+.1;31;Memory+.2;Ref2_high_oct;"T"
3690 SUBEND
3700!-----
3710 SUB Prog_mode(@Multi,Memory,Mode)
3720 OUTPUT @Multi;"WF";Memory+.3;Mode;"T"
3730 SUBEND
3740!-----
3750 SUB Read_status(@Multi,Memory,Status)

```



```

3760 STATUS @Multi,3;Multi
3770 OUTPUT @Multi;"WF";Memory+.1;1;"T RV";Memory+.2;"T"
3780 ENTER Multi*100+6;Status
3790 SUBEND
3800! -----
3810 SUB Read_read(@Multi,Memory,Read_pointer)
3820 STATUS @Multi,3;Multi
3830 OUTPUT @Multi;"WF";Memory+.1;22;"T RV";Memory+.2;"T"
3840 ENTER Multi*100+6;Read_low_oct
3850 OUTPUT @Multi;"WF";Memory+.1;23;"T RV";Memory+.2;"T"
3860 ENTER Multi*100+6;Read_high_oct
3870 Read_low=FNOctal_to_dec(Read_low_oct)
3880 Read_high=FNOctal_to_dec(Read_high_oct)
3890 Read_pointer=65536*Read_high+Read_low
3900 SUBEND
3910! -----
3920 SUB Read_write(@Multi,Memory,Write_pointer)
3930 STATUS @Multi,3;Multi
3940 OUTPUT @Multi;"WF";Memory+.1;24;"T RV";Memory+.2;"T"
3950 ENTER Multi*100+6;Write_low_oct
3960 OUTPUT @Multi;"WF";Memory+.1;25;"T RV";Memory+.2;"T"
3970 ENTER Multi*100+6;Write_high_oct
3980 Write_low=FNOctal_to_dec(Write_low_oct)
3990 Write_high=FNOctal_to_dec(Write_high_oct)
4000 Write_pointer=65536*Write_high+Write_low
4010 SUBEND
4020! -----
4030 SUB Read_diff(@Multi,Memory,Diff_counter)
4040 STATUS @Multi,3;Multi
4050 OUTPUT @Multi;"WF";Memory+.1;20;"T RV";Memory+.2;"T"
4060 ENTER Multi*100+6;Diff_low_oct
4070 OUTPUT @Multi;"WF";Memory+.1;21;"T RV";Memory+.2;"T"
4080 ENTER Multi*100+6;Diff_high_oct
4090 Diff_low=FNOctal_to_dec(Diff_low_oct)
4100 Diff_high=FNOctal_to_dec(Diff_high_oct)
4110 Diff_counter=65536*Diff_high+Diff_low
4120 SUBEND
4130! -----
4140 DEF FNDec_to_octal(Dec)
4150 Oct=Dec+2*INT(Dec/8)+20*INT(Dec/64)+200*INT(Dec/512)+2000*INT(Dec/4096)+2
0000*INT(Dec/32768)+200000*INT(Dec/262144)
4160 RETURN Oct
4170 FNEND
4180! -----
4190 DEF FNOctal_to_dec(Octal)
4200 X9=0
4210 X7=Octal
4220 X=0
4230 More: !
4240 X=X+(X7-INT(X7/10)*10)*8^X9
4250 X7=INT(X7/10)
4260 X9=X9+1
4270 IF X7<>0 THEN GOTO More
4280 RETURN X

```

```

4290 FEND
4300!
4310 SUB Plot_data(Material$,Contr_variable,Scale,Span,Gauge,Cycle,Load(*),Strain(*)
4320 ALLOCATE A(20),B(20)
4330 Load_range=INT(Scale)/100
4340 Strain_range=Scale-(Load_range*100)
4350 Conv_fac=216.078 !Factor use to convert volt into MPa for
4360 Emax=.05493*Strain_range/Gauge !a SEN geometry. Scale strain range
4370 FOR I=0 TO 20
4380 A(I)=-50+I*50/9
4390 B(I)=-40+I*2.5
4400 NEXT I
4410 DEG
4420 GINIT
4430 GRAPHICS ON
4440 BCLEAR
4450 ALPHA OFF
4460 FRAME
4470 WINDOW -66.7224080268,66.7224080268,-50,50
4480 MOVE -50,-40
4490 FOR I=0 TO 18
4500 DRAW A(I),-40
4510 IDRAW 0,1
4520 IMOVE 0,-1
4530 NEXT I
4540 C=1.
4550 D=.5
4560 FOR I=0 TO 20
4570 DRAW 50,B(I)
4580 IF 2*INT(I/2)=I THEN
4590 IDRAW -D,0
4600 IMOVE D,0
4610 ELSE
4620 IDRAW -C,0
4630 IMOVE C,0
4640 END IF
4650 NEXT I
4660 DRAW 50,40
4670 DRAW -50,40
4680 DRAW -50,10
4690 FOR I=20 TO 0 STEP -1
4700 DRAW -50,B(I)
4710 IF 2*INT(I/2)=I THEN
4720 IDRAW D,0
4730 IMOVE -D,0
4740 ELSE
4750 IDRAW C,0
4760 IMOVE -C,0
4770 END IF
4780 NEXT I
4790 MOVE -50,15
4800 FOR I=0 TO 18
4810 DRAW A(I),-15

```

```

4820    IDRAW 0,1
4830    IDRAW 0,-2
4840    IMOVE 0,1
4850    NEXT I
4860    MOVE -50,10
4870    FOR I=0 TO 18
4880        DRAW A(I),10
4890        IDRAW 0,-1
4900        IMOVE 0,1
4910    NEXT I
4920    MOVE 10,10
4930    DRAW 10,40
4940    MOVE -40,25
4950    FOR I=0 TO 20 STEP 2
4960        DRAW (-40+I),25
4970        IDRAW 0,.5
4980        IDRAW 0,-1
4990        IMOVE 0,.5
5000    NEXT I
5010    MOVE -30,15
5020    FOR I=0 TO 20 STEP 2
5030        DRAW -30,15+I
5040        IDRAW .5,0
5050        IDRAW -1,0
5060        IMOVE .5,0
5070    NEXT I
5080    CSIZE 3,.6
5090    MOVE -50,-40
5100    FOR I=2 TO 17 STEP 2
5110        MOVE A(I)-3,-43
5120        LABEL VAL$(I*10)
5130    NEXT I
5140    FOR I=1 TO 10 STEP 2
5150        MOVE 50.5,B(I)-1.5
5160        LABEL VAL$(.2*I-1.0)
5170        MOVE -55,B(I)-1.5
5180        LABEL VAL$(.2*I-1.0)
5190    NEXT I
5200    FOR I=11 TO 20 STEP 2
5210        MOVE 50.5,B(I)-1.5
5220        LABEL VAL$((I-15)*100)
5230        MOVE -58,B(I)-1.5
5240        LABEL VAL$((I-15)*100)
5250    NEXT I
5260    CSIZE 4,.6
5270    MOVE -20,-48
5280    LABEL "TIME (sec)"
5290    CSIZE 3,.6
5300    LDIR 90
5310    MOVE -56,-35
5320    LABEL "Etot (%)"
5330    MOVE 62,-35
5340    LABEL "Etot (%)"
5350    MOVE -58,-14

```

```

5360 LABEL "STRESS (MPa)"
5370 MOVE 62,-14
5380 LABEL "STRESS (MPa)"
5390 CSIZE 3.5,.6
5400 LDIR 0
5410 MOVE 15,32
5420 LABEL Material$
5430 MOVE 15,29
5440 LABEL "TMLCF"
5450 MOVE 20,26
5460 LABEL "Tmax= 926 C"
5470 MOVE 20,23
5480 LABEL "Tmin= 400 C"
5490 MOVE 15,20
5500 LABEL "CYCLE #"&VAL$(Cycle)
5510 CSIZE 3,.6
5520 MOVE -15,29
5530 DRAW -13,29
5540 DRAW -14,30
5550 DRAW -15,29
5560 MOVE -12,28
5570 IF Contr_variable=1 THEN
5580 LABEL "S= "&VAL$(2*Span)&"MPa"
5590 MOVE -15,32
5600 LABEL "STRESS CONTROL"
5610 ELSE
5620 LABEL "E= "&VAL$(2*Span)
5630 MOVE -15,32
5640 LABEL "STRAIN CONTROL"
5650 END IF
5660 MOVE -15,24
5670 LABEL "X-DIV=0.05%"
5680 MOVE -15,20
5690 LABEL "Y-DIV=100 MPa"
5700 MOVE -50,-2.5
5710 FOR I=0 TO 179
5720 B1=(((Load(I)*Load_range*Conv_fac)+500)/40)-15 !Convert volt to Mpa with
5730 A1=(I*5/9)-50 !the assumption that the
5740 DRAW A1,B1 !specimen cross section
5750 NEXT I !is (11.7*4.4)mm2.
5760 MOVE -50,-27.5
5770 FOR I=0 TO 179
5780 B1=((Strain(I)*Emax/10)+.01)*1250-40 !Plot total strain
5790 A1=(I*5/9)-50
5800 DRAW A1,B1
5810 NEXT I
5820 A1=((Strain(0)*Emax/10)+.0025)*4000-40
5830 B1=(((Load(0)*Range*Conv_fac)+500)/50)+15
5840 MOVE A1,B1
5850 FOR I=1 TO 179
5860 A1=((Strain(I)*Emax/10)+.0025)*4000-40 !Plot the hysteresis
5870 B1=(((Load(I)*Range*Conv_fac)+500)/50)+15 !loop.
5880 DRAW A1,B1
5890 NEXT I
5900 SUBEND

```

```

10! *****
20! *
30! *          PROGRAM TMFCB          *
40! *          *****                *
50! *
60! *   THIS PROGRAM PERFORMS THE REAL-TIME CONTROL AND DATA *
70! *   ACQUISITION OF THERMAL-MECHANICAL FATIGUE CRACK GROWTH *
80! *   TESTS. *
90! *
100! *   THIS PROGRAM IS CALLED BY ISO_TMF AFTER SELECTION OF THE *
110! *   TMFCB OPTION. *
120! *
130! *   THE MICRO_DATA_TRACK MUST BE PROGRAMMED FOR 180 sec *
140! *   PERIOD (1/3 cpm). *
150! *
160! *   THE CYCLIC THERMAL STRAINS ARE FIRST MEASURED BY CYCLING *
170! *   THE TEMPERATURE AT ZERO STRESS. *
180! *
190! *   THE CYCLIC DATA(Stresses, strains, temperatures, and *
200! *   potentials) ARE RECORDED EVERY 5 CYCLES. *
210! *
220! *****
230 !
240 OPTION BASE 0
250 Material$="B-1900+Hf"
260 Contr_variable=2
270 Scale=50.10
280 Mean=0.
290 Span=.00250
300 Gauge=.515
310 CALL Tmfcg(Material$,Contr_variable,Scale,Mean,Span,Gauge)
320 END
330! *****
340! *****
350 !
360 SUB Tmfcg(Material$,Contr_variable,Scale,Mean,Span,Gauge)
370 DIM Load(179),Strain(179),Temp1(179),Temp2(179),Temp3(179),Pot(179)
380 MASS STORAGE IS ":HP8290X,700,1"
390 !
400 !-----DEFINE I/O CARD FUNCTION-----
410 !-----
420 ASSIGN @Dvm TO 720
430 ASSIGN @Multi TO 723
440 ASSIGN @Disc TO "MRZ"
450 Disc_drive=0
460 Dvm=720
470 Multi=723
480 Scanner=0
490 A_to_d=3
500 Memory1=7
510 D_to_a1=10
520 Timer=11
530 D_to_a2=12
540 Memory2=13

```

```

550 |
560 |----- DEFAULT VALUES FOR THE PARAMETERS -----|
570 |-----|
580 Start=1                                !Start channel
590 Stop=5                                  !Stop channel
600 Pointer=4                              !Interrupt word
610 |
620 |----- INITIALIZE THE MULTI -----|
630 |-----|
640 CALL Init_multi(@Multi,@Disc)
650 CALL Init_mem(@Multi,Memory1)
660 |
670 |----- INITIALIZE CONTROL PROCEDURE -----|
680 |-----|
690 CALL Init_control(@Multi,Memory2,Timer,D_to_a1,Contr_variable,Scale,Mean,Span,Gauge)
700 |
710 |----- SET INTERRUPT BRANCH FOR TRIGGER SIGNAL -----|
720 |-----|
730 Cycle=1                                !Set cycle counter
740 G=SPOLL(723)                            !Clear Multi SRQ
750 P=SPOLL(720)                            !Clear DVM SRQ
760 OUTPUT @Dvm;"F1R-2N5Z0"                !Set DVM ranges
770 OUTPUT @Dvm;"T2D3 TMF TEST"            !Set ext trigger and display
780 OUTPUT @Dvm;"KM01"                     !Set mask for Data Ready
790 ON INTR 7,2 GOTO Start_tmf              !Set interrupt branch
800 ENABLE INTR 7;2                         !Enable interrupt SRQ
810 BEEP
820 PRINT USING 830
830 IMAGE 2/,15X,"REMOVE CONTROL AND UTILITY PAC DISCS",2/,15X,"INSERT TWO
DISCS FOR DATA STORAGE",2/,15X,"PRESS K0(Continue) TO CONTINUE"
840 ON KEY 0 LABEL "**CONTINUE**" GOTO 860
850 Spin: GOTO Spin
860 BEEP
870 OFF KEY
880 PRINT USING 890
890 IMAGE 2/,15X,"PROGRAM AND START THE LEPEL",2/,15X,"***WAITING FOR A T
RIGGER SIGNAL***"
900 CREATE BDAT "TEST_PARAM",1,100
910 ASSIGN @Disc TO "TEST_PARAM"
920 OUTPUT @Disc;Material$,"TMFCG",Contr_variable,Scale,Mean,Span,Gauge
930 ASSIGN @Disc TO *
940 ENTER Dvm;P
950 |
960 |----- START CYCLING AND TAKING DATA -----|
970 |-----|
980 Start_tmf: !
990 OUTPUT @Multi;"CY",Timer,"T"           !Start cycling
1000 OUTPUT @Multi;"SC,0,0,0,0T"          !Reset Clock of Multi
1010 |
1020 |----- READ DATA -----|
1030 |

```

```

1040 CALL Read_data(@Multi,@Dvm,Multi,Dvm,Scanner,Memory1,Load(*),Strain(*),Temp
p1(*),Temp2(*),Temp3(*),Pot(*))
1050 |
1060 |-----STORE DATA-----
1070 |
1080 CALL Store_data(@Multi,@Disc,Disc_drive,Cycle,Scale,Load(*),Strain(*),Temp
1(*),Temp2(*),Temp3(*),Pot(*))
1090 |
1100 |-----DISPLAY DATA-----
1110 |
1120 CALL Plot_data(Material$,Contr_variable,Scale,Span,Gauge,Cycle,Load(*),Str
ain(*),Pot(*))
1130 |
1140 |-----SET INTERRUPT FOR SYNCHRO. SIGNAL-----
1150 |
1160 IF Cycle>11 THEN GOTO Synchro
1170 IF Cycle<=5 THEN
1180     Increment=2
1190     Waiting=.5
1200 ELSE
1210     IF Cycle=7 THEN
1220         Increment=3
1230         Waiting=1.5
1240     ELSE
1250         Increment=5
1260         Waiting=3.5
1270     END IF
1280 END IF
1290 !
1300 Synchro:
1310     Cycle=Cycle+Increment           !Update cycle counter
1320     WAIT (180*Waiting)             !Set waiting time
1330     OUTPUT @Dvm;"T2KM01"          !Ext. trigger and DVM mask
1340     ON INTR 7,2 GOTO 1030         !Set interrupt branch
1350     ENABLE INTR 7;2               !Enable interrupt
1360     GRAPHICS OFF
1370     PRINT USING 1380
1380     IMAGE 10/,20X,"*****  TMFCG TEST IN PROGRESS  *****"
1390     ENTER Dvm;P
1400     SUBEND
1410 |-----
1420 |
1430 | *****
1440 | *                                     *
1450 | *          SUBROUTINES USED BY SUB TMFCG(Param1,Param2,...)          *
1460 | *                                     *
1470 | *****
1480 |
1490 |-----
1500 SUB Init_control(@Multi,Memory,Timer,D_to_a,Control,Scale,Mean,Span,Gauge)
1510 ALLOCATE A(4095)
1520     !__GENERATE WAVEFORM__
1530     !-----
1540     Load_scale=INT(Scale)/100
1550     Strain_scale=Scale-(Load_scale*100)
1560     IF Control=1 THEN

```

```

1570         Pmean=Mean/(Load_scale*216.078)      !Convert MPA into voltage
1580         Pmax=Span/(Load_scale*216.078)
1590     ELSE
1600         Emax=.05493*Strain_scale/Gauge
1610         Pmean=10*Mean/Emax                    !Convert Strain into voltage
1620         Pmax=10*Span/Emax
1630     END IF
1640     Coeff=800
1650     IF Pmax>5.12 THEN Coeff=400
1660     Ndata=INT(Coeff*Pmax+.5)-1
1670     Ndata2=INT(Ndata/4+.5)
1680     Ndata3=Ndata-Ndata2
1690     FOR I=0 TO Ndata2-1
1700         A(I)=Pmax*I/(Ndata2-1)
1710         A(I+Ndata3)=Pmax*(I/(Ndata2-1)-1)
1720     NEXT I
1730     FOR I=Ndata2 TO Ndata3
1740         A(I)=(Ndata-1-2*I)*Pmax/(Ndata+1-2*Ndata2)
1750     NEXT I
1760     FOR I=Ndata+1 TO 4095
1770         A(I)=0.
1780     NEXT I
1790     !
1800     !__CALCULATE THE PACE__
1810     !-----
1820     Time_int=180/Ndata
1830     Pace=INT(Time_int*500000)/1000           !Pace in msec
1840     !
1850     !__PROGRAM MULTI__AMPLITUDE
1860     !-----
1870     OUTPUT @Multi;"CC",Memory+1,"T"          !Clear memory card
1880     OUTPUT @Multi;"SF",Memory,3,1,.005,12,"T" !Set format(LSB=0.005)
1890     OUTPUT @Multi;"WF",Memory+1.0,4095,"T"  !Truncate memory
1900     OUTPUT @Multi;"MD",Memory,A(*),"T"      !Load data into memory
1910     OUTPUT @Multi;"WF",Memory+1,Ndata,"T"   !Truncate memory card
1920     OUTPUT @Multi;"WF",Memory+.1,10,"T"    !Set re-circulate mode
1930     OUTPUT @Multi;"WF",Timer+.2,1,"T"      !Set timer for continuous
1940     OUTPUT @Multi;"WF",Timer,Pace,"T"       !output. Set Pace
1950     !
1960     !__PROGRAM MULTI-- MEAN
1970     !-----
1980     Incr=.005
1990     IF Pmean=0 THEN GOTO 2070
2000     IF Pmean<0 THEN Incr=-.005
2010     J=0
2020     OUTPUT @Multi;"DP",D_to_a,J,"T"
2030     IF ABS(J)<ABS(Pmean) THEN
2040         J=J+Incr
2050         GOTO 2020
2060     END IF
2070     DEALLOCATE A(*)
2080     SUBEND
2090 !

```

```

2100 SUB Read_data(@Multi,@Dvm,Multi,Dvm,Scanner,Memory,Load(*),Strain(*),Temp1
(*) ,Temp2(*),Temp3(*),Pot(*))
2110 ALLOCATE Scan(4)
2120 OUTPUT @Dvm;"T1M00" !Set internal trigger and clear mask
2130 G=SPOLL(@Multi)
2140 ENTER 72310;A,B,C,D,E,F
2150 ON INTR 7,2 GOTO Interrupt
2160 ENABLE INTR 7;2
2170 OUTPUT @Multi;"CY",Scanner,"T" !Enable scanner
2180 OUTPUT @Multi;"WF",Scanner+.3,5,"T" !Set sequential mode
2190 !
2200 FOR K=0 TO 179
2210 OUTPUT @Multi;"WF",Scanner,1,"T" !Set start channel
2220 OUTPUT @Multi;"WF",Scanner+.1,5,"T" !set stop channel
2230 OUTPUT @Multi;"WF",Scanner+.2,40,"T" !Set pace(40 us)
2240 Prog_diff(@Multi,Memory,0) !Reset diff. counter
2250 Prog_write(@Multi,Memory,0) !Reset write pointer
2260 OUTPUT @Multi;"CC";Memory,"T" !Clear Memory card
2270 Prog_mode(@Multi,Memory,56) !Set FIFO mode
2280 Prog_ref1(@Multi,Memory,4) !Set stop pointer
2290 OUTPUT @Multi;"AC";Memory;"T" !Armed memory card
2300 OUTPUT @Multi;"CY",Scanner,"T" !Start pacer
2310 Wait: GOTO Wait
2320 Interrupt: !
2330 G=SPOLL(@Multi)
2340 IF G=64 THEN
2350 ENTER 72310;A,B,C
2360 IF C<>0 THEN
2370 ENTER 72312;Address
2380 IF Address<>Memory THEN
2390 PRINT "NOT MEMORY CARD"
2400 PAUSE
2410 END IF
2420 OUTPUT @Multi;"WF",Scanner+.2,0,"T" !Stop scanner
2430 Prog_mode(@Multi,Memory,76) !Set FIFO lockout
2440 OUTPUT @Multi;"MR";Memory;5;"T" !MR command to get data
2450 ENTER 72305 USING "%,W";Scan(*) !Entering the data
2460 Strain(K)=Scan(0)*.005 !Convert the data into
2470 Load(K)=Scan(1)*.005 !engineering units by
2480 Temp1(K)=Scan(2)*.005 !multiplying with the
2490 Temp2(K)=Scan(3)*.005 !LSB value.
2500 Temp3(K)=Scan(4)*.005
2510 ENTER Dvm;Pot(K) !Enter potential
2520 BEEP
2530 WAIT .685 !Wait set for 180
2540 ENABLE INTR 7;2
2550 ELSE
2560 BEEP 2000,.3
2570 PRINT " *** SRQ NOT SET BY ARMED CARD ***"
2580 PAUSE
2590 END IF
2600 ELSE
2610 BEEP 2000,.3
2620 PRINT " *** MULTI DID NOT INTERRUPT ***"
2630 PAUSE

```

```

2640     END IF
2650     NEXT K
2660     DEALLOCATE Scan(*)
2670     OUTPUT @Multi;"RC"                                !Read Real-time clock
2680     SUBEND
2690!-----
2700     SUB Store_data(@Multi,@Disc,Disc_drive,Cycle,Scale,Load(*),Strain(*),Temp
1(*),Temp2(*),Temp3(*),Pot(*))
2710     ALLOCATE X(179),Y(179)
2720     ENTER 72314;T1,T2,T3,T4                            !Enter Clock values
2730     Time$=VAL$(T1*24+T2)&":"&VAL$(T3)&":"&VAL$(T4)
2740     FOR I=0 TO 179
2750         X(I)=INT((Load(I)+10)*1000)+(Strain(I)+10)/100
2760         Y(I)=DROUND(Temp1(I),3)*1000000+DROUND(Temp2(I),3)*1000+Temp3(I)
2770     NEXT I
2780     !
2790     ON ERROR GOTO Recover
2800     CREATE BDAT "CYCLE"&VAL$(Cycle),1,5000
2810     ASSIGN @Disc TO "CYCLE"&VAL$(Cycle)
2820     OUTPUT @Disc;Cycle,Time$,Scale,X(*),Y(*),Pot(*)
2830     ASSIGN @Disc TO *
2840     GOTO Out
2850     !
2860 Recover: !
2870     IF ERRN=59 OR ERRN=64 THEN
2880         IF Disc_drive=0 THEN
2890             Disc_drive=1
2900             MASS STORAGE IS ":HP8290X,700,1"
2910         ELSE
2920             Disc_drive=0
2930             MASS STORAGE IS ":HP8290X,700,0"
2940         END IF
2950     ELSE
2960         PRINT USING 2970;ERRN
2970         IMAGE 2/,25X,"ERROR NUMBER ",K,/,25X,"CHECK STORAGE UNIT",/,25X,"PROG
RAM ABORTED"
2980         PAUSE
2990     END IF
3000 Out: !
3010     DEALLOCATE X(*),Y(*)
3020     SUBEND
3030!-----
3040 SUB Init_multi(@Multi,@Disc)
3050     CLEAR 7
3060     WAIT 4.0
3070     G=SPOLL(@Multi)
3080     IF G<>64 THEN
3090         PRINT "          ***MULTI DID NOT INTERRUPT***"
3100         PAUSE
3110     END IF
3120     STATUS @Multi,3;Multi
3130     ENTER Multi*100+10;A
3140     IF A<>16384 THEN
3150         PRINT "          ***SELF TEST DID NOT SET SRQ***"

```

```

3160     PAUSE
3170     END IF
3180     ALLOCATE Ascii$(80)
3190     ON END @Disc GOTO Eof
3200 Rd_file:     ENTER @Disc;Ascii$
3210     OUTPUT @Multi;Ascii$
3220     GOTO Rd_file
3230 Eof: OFF END @Disc
3240     ASSIGN @Disc TO *
3250     DEALLOCATE Ascii$
3260     MASS STORAGE IS ":HP8290X,700,0"
3270 SUBEND
3280!-----
3290 SUB Init_mem(@Multi,Memory)
3300     Prog_mode(@Multi,Memory,254)
3310     Prog_mode(@Multi,Memory,54)
3320     Prog_ref1(@Multi,Memory,1048575)
3330     Prog_ref2(@Multi,Memory,0)
3340     Prog_read(@Multi,Memory,0)
3350     Prog_diff(@Multi,Memory,0)
3360     Prog_write(@Multi,Memory,0)
3370     OUTPUT @Multi;"CC";Memory;"T"
3380 SUBEND
3390!-----
3400 SUB Prog_read(@Multi,Memory,Read_pointer)
3410     Read_low=Read_pointer MOD 65536
3420     Read_high=Read_pointer DIV 65536
3430     Read_low_oct=FNDec_to_octal(Read_low)
3440     Read_high_oct=FNDec_to_octal(Read_high)
3450     OUTPUT @Multi;"WF";Memory+.1;22;Memory+.2;Read_low_oct;"T"
3460     OUTPUT @Multi;"WF";Memory+.1;23;Memory+.2;Read_high_oct;"T"
3470 SUBEND
3480!-----
3490 SUB Prog_write(@Multi,Memory,Write_pointer)
3500     Write_low=Write_pointer MOD 65536
3510     Write_high=Write_pointer DIV 65536
3520     Write_low_oct=FNDec_to_octal(Write_low)
3530     Write_high_oct=FNDec_to_octal(Write_high)
3540     OUTPUT @Multi;"WF";Memory+.1;24;Memory+.2;Write_low_oct;"T"
3550     OUTPUT @Multi;"WF";Memory+.1;25;Memory+.2;Write_high_oct;"T"
3560 SUBEND
3570!-----
3580 SUB Prog_diff(@Multi,Memory,Diff_counter)
3590     Diff_low=Diff_counter MOD 65536
3600     Diff_high=Diff_counter DIV 65536
3610     Diff_low_oct=FNDec_to_octal(Diff_low)
3620     Diff_high_oct=FNDec_to_octal(Diff_high)
3630     OUTPUT @Multi;"WF";Memory+.1;20;Memory+.2;Diff_low_oct;"T"
3640     OUTPUT @Multi;"WF";Memory+.1;21;Memory+.2;Diff_high_oct;"T"
3650 SUBEND
3660!-----
3670 SUB Prog_ref1(@Multi,Memory,Ref1_reg)
3680     Ref1_low=Ref1_reg MOD 65536
3690     Ref1_high=Ref1_reg DIV 65536

```

```

3700 Ref1_low_oct=FNDec_to_octal(Ref1_low)
3710 Ref1_high_oct=FNDec_to_octal(Ref1_high)
3720 OUTPUT @Multi;"WF";Memory+.1;26;Memory+.2;Ref1_low_oct;"T"
3730 OUTPUT @Multi;"WF";Memory+.1;27;Memory+.2;Ref1_high_oct;"T"
3740 SUBEND
3750! -----
3760 SUB Prog_ref2(@Multi,Memory,Ref2_reg)
3770 Ref2_low=Ref2_reg MOD 65536
3780 Ref2_high=Ref2_reg DIV 65536
3790 Ref2_low_oct=FNDec_to_octal(Ref2_low)
3800 Ref2_high_oct=FNDec_to_octal(Ref2_high)
3810 OUTPUT @Multi;"WF";Memory+.1;30;Memory+.2;Ref2_low_oct;"T"
3820 OUTPUT @Multi;"WF";Memory+.1;31;Memory+.2;Ref2_high_oct;"T"
3830 SUBEND
3840! -----
3850 SUB Prog_mode(@Multi,Memory,Mode)
3860 OUTPUT @Multi;"WF";Memory+.3;Mode;"T"
3870 SUBEND
3880! -----
3890 SUB Read_status(@Multi,Memory,Status)
3900 STATUS @Multi,3;Multi
3910 OUTPUT @Multi;"WF";Memory+.1;1;"T RV";Memory+.2;"T"
3920 ENTER Multi*100+6;Status
3930 SUBEND
3940! -----
3950 SUB Read_read(@Multi,Memory,Read_pointer)
3960 STATUS @Multi,3;Multi
3970 OUTPUT @Multi;"WF";Memory+.1;22;"T RV";Memory+.2;"T"
3980 ENTER Multi*100+6;Read_low_oct
3990 OUTPUT @Multi;"WF";Memory+.1;23;"T RV";Memory+.2;"T"
4000 ENTER Multi*100+6;Read_high_oct
4010 Read_low=FNOctal_to_dec(Read_low_oct)
4020 Read_high=FNOctal_to_dec(Read_high_oct)
4030 Read_pointer=65536*Read_high+Read_low
4040 SUBEND
4050! -----
4060 SUB Read_write(@Multi,Memory,Write_pointer)
4070 STATUS @Multi,3;Multi
4080 OUTPUT @Multi;"WF";Memory+.1;24;"T RV";Memory+.2;"T"
4090 ENTER Multi*100+6;Write_low_oct
4100 OUTPUT @Multi;"WF";Memory+.1;25;"T RV";Memory+.2;"T"
4110 ENTER Multi*100+6;Write_high_oct
4120 Write_low=FNOctal_to_dec(Write_low_oct)
4130 Write_high=FNOctal_to_dec(Write_high_oct)
4140 Write_pointer=65536*Write_high+Write_low
4150 SUBEND
4160! -----
4170 SUB Read_diff(@Multi,Memory,Diff_counter)
4180 STATUS @Multi,3;Multi
4190 OUTPUT @Multi;"WF";Memory+.1;20;"T RV";Memory+.2;"T"
4200 ENTER Multi*100+6;Diff_low_oct
4210 OUTPUT @Multi;"WF";Memory+.1;21;"T RV";Memory+.2;"T"

```

```

4220 ENTER Multi*100+6;Diff_high_oct
4230 Diff_low=FNOctal_to_dec(Diff_low_oct)
4240 Diff_high=FNOctal_to_dec(Diff_high_oct)
4250 Diff_counter=65536*Diff_high+Diff_low
4260 SUBEND
4270! -----
4280 DEF FNDec_to_octal(Dec)
4290 Oct=Dec+2*INT(Dec/8)+20*INT(Dec/64)+200*INT(Dec/512)+2000*INT(Dec/4096)+2
0000*INT(Dec/32768)+200000*INT(Dec/262144)
4300 RETURN Oct
4310 FNEND
4320! -----
4330 DEF FNOctal_to_dec(Octal)
4340 X9=0
4350 X7=Octal
4360 X=0
4370 More: !
4380 X=X+(X7-INT(X7/10)*10)*8^X9
4390 X7=INT(X7/10)
4400 X9=X9+1
4410 IF X7<>0 THEN GOTO More
4420 RETURN X
4430 FNEND
4440! -----
4450 SUB Plot_data(Material$,Contr_variable,Scale,Span,Gauge,Cycle,Load(*),Stra
in(*),Pot(*)).
4460 ALLOCATE A(20),B(20)
4470 Load_range=INT(Scale)/100.
4480 Strain_range=Scale-(Load_range*100)
4490 Conv_fac=216.078 !Factor use to convert volt into MPa for
4500 Emax=.05493*Strain_range/Gauge !a SEN geometry. Scale strain range
4510 FOR I=0 TO 20
4520 A(I)=-50+I*50/9
4530 B(I)=-40+I*2.5
4540 NEXT I
4550 DEG
4560 GINIT
4570 GRAPHICS ON
4580 GCLEAR
4590 ALPHA OFF
4600 FRAME
4610 WINDOW -66.7224080268,66.7224080268,-50,50
4620 MOVE -50,-40
4630 FOR I=0 TO 18
4640 DRAW A(I),-40
4650 IDRAW 0,1
4660 IMOVE 0,-1
4670 NEXT I
4680 C=.5
4690 D=1
4700 FOR I=0 TO 20
4710 DRAW 50,B(I)
4720 IF I>=10 THEN
4730 C=1

```

```

4740     D=.5
4750     ELSE
4760     END IF
4770     IF 2*INT(I/2)=I THEN
4780         IDRAW -D,0
4790         IMOVE D,0
4800     ELSE
4810         IDRAW -C,0
4820         IMOVE C,0
4830     END IF
4840     NEXT I
4850     DRAW 50,40
4860     DRAW -50,40
4870     DRAW -50,10
4880     FOR I=20 TO 0 STEP -1
4890         DRAW -50,B(I)
4900         IF I<=10 THEN
4910             C=.5
4920             D=1.0
4930         ELSE
4940         END IF
4950         IF 2*INT(I/2)=I THEN
4960             IDRAW D,0
4970             IMOVE -D,0
4980         ELSE
4990             IDRAW C,0
5000             IMOVE -C,0
5010         END IF
5020     NEXT I
5030     MOVE -50,15
5040     FOR I=0 TO 18
5050         DRAW A(I),-15
5060         IDRAW 0,1
5070         IDRAW 0,-2
5080         IMOVE 0,1
5090     NEXT I
5100     MOVE -50,10
5110     FOR I=0 TO 18
5120         DRAW A(I),10
5130         IDRAW 0,-1
5140         IMOVE 0,1
5150     NEXT I
5160     MOVE 10,10
5170     DRAW 10,40
5180     MOVE -40,25
5190     FOR I=0 TO 20 STEP 2
5200         DRAW (-40+I),25
5210         IDRAW 0,.5
5220         IDRAW 0,-1
5230         IMOVE 0,.5
5240     NEXT I
5250     MOVE -30,15
5260     FOR I=0 TO 20 STEP 2
5270         DRAW -30,15+I

```

```
5280 IDRAW .5,0
5290 IDRAW -1,0
5300 IMOVE .5,0
5310 NEXT I
5320 CSIZE 3,.6
5330 MOVE -50,-40
5340 FOR I=2 TO 17 STEP 2
5350 MOVE A(I)-3,-43
5360 LABEL VAL$(I*10)
5370 NEXT I
5380 FOR I=0 TO 10 STEP 2
5390 MOVE 50.5,B(I)-1.5
5400 LABEL VAL$(.5+I*.50)
5410 MOVE -55,B(I)-1.5
5420 LABEL VAL$(.5+I*.50)
5430 NEXT I
5440 FOR I=11 TO 20 STEP 2
5450 MOVE 50.5,B(I)-1.5
5460 LABEL VAL$((I-15)*100)
5470 MOVE -58,B(I)-1.5
5480 LABEL VAL$((I-15)*100)
5490 NEXT I
5500 CSIZE 4,.6
5510 MOVE -20,-48
5520 LABEL "TIME (sec)"
5530 CSIZE 3,.6
5540 LDIR 90
5550 MOVE -56,-38
5560 LABEL "POT. (mV)"
5570 MOVE 58,-38
5580 LABEL "POT. (mV)"
5590 MOVE -58,-14
5600 LABEL "STRESS (MPa)"
5610 MOVE 62,-14
5620 LABEL "STRESS (MPa)"
5630 CSIZE 3.5,.6
5640 LDIR 0
5650 MOVE 15,32
5660 LABEL Material$
5670 MOVE 15,29
5680 LABEL "TMFCG"
5690 MOVE 20,26
5700 LABEL "Tmax= 926 C"
5710 MOVE 20,23
5720 LABEL "Tmin= 400 C"
5730 MOVE 15,20
5740 LABEL "CYCLE #"&VAL$(Cycle)
5750 CSIZE 3,.6
5760 MOVE -15,29
5770 DRAW -13,29
5780 DRAW -14,30
5790 DRAW -15,29
5800 MOVE -12,28
5810 IF Contr_variable=1 THEN
```

```

5820 LABEL "S= "&VAL$(2*Span)&"MPa"
5830 MOVE -15,32
5840 LABEL "STRESS CONTROL"
5850 ELSE
5860 LABEL "E= "&VAL$(2*Span)
5870 MOVE -15,32
5880 LABEL "STRAIN CONTROL"
5890 END IF
5900 MOVE -15,24
5910 LABEL "X-DIV=0.05%"
5920 MOVE -15,20
5930 LABEL "Y-DIV=100 MPa"
5940 MOVE -50,-2.5
5950 FOR I=0 TO 179 !Convert volt to Mpa with
5960 B1=(((Load(I)*Load_range*Conv_fac)+500)/40)-15 !the assumption that the
5970 A1=(I*5/9)-50 !specimen cross section
5980 DRAW A1,B1 !is (11.7*4.4)mm2.
5990 NEXT I
6000 MOVE -50,-27.5
6010 FOR I=0 TO 179 !Plot potential
6020 B1=(Pot(I)*1000-.5)*5-40
6030 A1=(I*5/9)-50
6040 DRAW A1,B1
6050 NEXT I
6060 A1=((Strain(0)*Emax/10)+.0025)*4000-40
6070 B1=(((Load(0)*Range*Conv_fac)+500)/50)+15
6080 MOVE A1,B1
6090 FOR I=1 TO 179
6100 A1=((Strain(I)*Emax/10)+.0025)*4000-40 !Plot the hysteresis
6110 B1=(((Load(I)*Range*Conv_fac)+500)/50)+15 !loop.
6120 DRAW A1,B1
6130 NEXT I
6140 SUBEND

```



```

10! *****
20! *
30! *          PROGRAM ISOCCG          *
40! *          *****                *
50! *
60! *      THIS PROGRAM PERFORMS THE REAL-TIME CONTROL AND DATA *
70! *      ACQUISITION OF ISOTHERMAL LOW CYCLE FATIGUE CRACK *
80! *      GROWTH TESTS. *
90! *
100! *      THIS PROGRAM IS CALLED BY ISO_TMF AFTER SELECTION OF THE *
110! *      ISOCCG OPTION. *
120! *
130! *      THE CYCLIC DATA(Stresses, strains and potentials) ARE *
140! *      RECORDED EVERY 5 CYCLES. *
150! *
160! *****
170! !
180! OPTION BASE 0
190! CALL Isocg(Material$,Contr_variable,Scale,Mean,Span,Gauge,Frequency)
200! END
210! *****
220! *****
230! !
240! SUB Isocg(Material$,Contr_variable,Scale,Mean,Span,Gauge,Frequency)
250! MASS STORAGE IS ":HP8290X,700,1"
260! !
270! -----DEFINE I/O CARD FUNCTION-----
280! !
290! ASSIGN @Multi TO 723
300! ASSIGN @Dvm TO 720
310! ASSIGN @Disc TO "MRZ"
320! Disc_drive=0
330! Multi=723
340! Scanner=0
350! A_to_d=3
360! Memory1=7
370! D_to_a1=10
380! Timer=11
390! D_to_a2=12
400! Memory2=13
410! !
420! -----DEFAULT VALUES FOR THE PARAMETERS-----
430! !
440! Start=1                                !Start channel
450! Stop=2                                  !Stop channel
460! Cycle_per_block=1
470! Data_per_cycle=200
480! Gauge_factor=.05493
490! !
500! -----INITIALIZE THE MULTI-----
510! !
520! CALL Init_multi(@Multi,@Disc)
530! CALL Init_mem(@Multi,Memory1)
540! !

```

```

550 |-----INITIALIZE CONTROL PROCEDURE-----
560 |-----
570 CALL Init_control(@Multi,Memory2,Timer,D_to_a1,Contr_variable,Scale,Mean,Span,Gauge,Gauge_factor,Frequency,Ndata,Pace,Paces)
580 OUTPUT @Dvm;"F1R-2N4T1Z0D3 ISOCS"
590 |-----
600 |-----INITIALIZE READING PROCEDURE-----
610 |-----
620 CALL Init_read(Cycle_per_block,Data_per_cycle,Frequency,Pace1,Pace2,Ref_count)
630 ALLOCATE Scan(Ref_count),Pot((Ref_count+1)/2-1)
640 |-----
650 BEEP
660 Cycle=1 !Set cycle counter
670 Next_cycle=3 !Set Next_cycle counter
680 G=SPOLL(723) !Clear Multi SRQ
690 PRINT USING 700
700 IMAGE 2/,15X,"REMOVE CONTROL AND UTILITY PAC DISCS",2/,15X,"INSERT TWO DISCS FOR DATA STORAGE",2/,15X,"PRESS K0(Continue) TO CONTINUE"
710 ON KEY 0 LABEL "**CONTINUE**" GOTO 730
720 Spin: GOTO Spin
730 OFF KEY
740 CREATE BDAT "TEST_PARAM",1,100
750 ASSIGN @Disc TO "TEST_PARAM"
760 OUTPUT @Disc;Material$,"ISOCS",Contr_variable,Scale,Mean,Span,Gauge,Frequency
770 ASSIGN @Disc TO *
780 CALL Plot_frame(Material$,Contr_variable,Mean,Span,Frequency)
790 DELSUB Plot_frame
800 PRINT USING 810
810 IMAGE 20/,25X,"MULTIPROGRAMMER IS READY",2/,20X,"****WAITING FOR THE START COMMAND****"
820 ON KEY 0 LABEL " START CYCLING" GOTO Start_iso
830 Wait: GOTO Wait
840 |-----
850 |-----START CYCLING AND TAKING DATA-----
860 |-----
870 Start_iso:
880 OFF KEY
890 |-----
900 |-----READ DATA-----
910 |-----
920 OUTPUT @Multi;"WF",Timer+.2,0,"T"
930 IF Frequency>.185 THEN OUTPUT @Multi;"WF",Timer,Paces,"T"
940 OUTPUT @Multi;"WF",Timer+.2,1,"T"
950 CALL Read_data(@Multi,@Dvm,Frequency,Timer,Pace,Paces,Scanner,Memory1,Pace1,Pace2,Ref_count,Scan(*),Pot(*))
960 |-----STORE DATA-----
970 |-----
980 CALL Store_data(@Disc,Disc_drive,Cycle,Ref_count,Scan(*),Pot(*))
990 |-----
1000 |-----DISPLAY DATA-----
1010 |-----
1020 CALL Plot_data(Contr_variable,Scale,Span,Gauge,Gauge_factor,Cycle,Ref_count,Scan(*),Pot(*),Exponent,Min,Vo)

```

```

1030 !
1040 ! ----- SET WAITING FOR SYNCHRO. SIGNAL -----
1050 ! -----
1060 Synchro: !
1070 OUTPUT @Multi;"WF",Timer+.2,0,"T" !Stop cycling
1080 ON INTR 7 GOTO Complete
1090 ENABLE INTR 7;2
1100 OUTPUT @Multi;"RV",Memory2+1,Memory2+1.1,Memory2+1.2,Memory2+1.3,"T"
1110 ENTER 72306;A1,B1,C1,D1 !Read read and ref.pointers
1120 OUTPUT @Multi;"WF",Memory2+1.1,C1-A1,"T" !Set diff. counter
1130 OUTPUT @Multi;"WF",Memory2+.1,2,"T" !Set FIFO mode
1140 OUTPUT @Multi;"WF",Memory2+1.0,1,"T" !Set ref. word
1150 OUTPUT @Multi;"WF",Memory2+1.3,A1,"T" !set read pointer
1160 OUTPUT @Multi;"AC",Memory2+1,"T" !Arm card
1170 OUTPUT @Multi;"WF",Timer+.2,1,"T" !Set continuous mode
1180 OUTPUT @Multi;"CY",Timer,"T" !Resume cycling
1190 Spin2: GOTO Spin2
1200 Complete: !
1210 OUTPUT @Multi;"WF",Timer+.2,0,"T" !Set one-shot mode
1220 OUTPUT @Multi;"DC",Memory2+1,"T" !Disarm card
1230 OUTPUT @Multi;"RC" !Read real-time clock(T2)
1240 ENTER 72314;A1,B1,C1,D1 !Enter real-time clock(T1)
1250 ENTER 72314;A2,B2,C2,D2 !Enter real-time clock(T2)
1260 T1=60*(A1*60*24+B1*60+C1)+D1
1270 T2=60*(A2*60*24+B2*60+C2)+D2
1280 Time_delay=T2-T1 !Compute elapsed time
1290 Wait_time=(Next_cycle-Cycle-1)/Frequency !Wait between read data
1300 IF Wait_time<Time_delay THEN
1310 Cycle=INT(Cycle+1.5+Time_delay*Frequency)
1320 Next_cycle=Cycle+5
1330 IF Cycle<7 THEN Next_cycle=Cycle+2
1340 OUTPUT @Multi;"CC",Memory2+1,"T" !Clear card
1350 OUTPUT @Multi;"WF",Memory2+.1,10,"T" !Set re-circulate mode
1360 OUTPUT @Multi;"WF",Memory2+1.0,Ndata,"T" !Set ref. word
1370 OUTPUT @Multi;"WF",Memory2+1.2,Ndata+1,"T" !Set write pointer
1380 OUTPUT @Multi;"WF",Memory2+1.3,0,"T" !Set read pointer
1390 OUTPUT @Multi;"WF",Timer+.2,1,"T" !Set continuous mode
1400 GOTO 910
1410 ELSE
1420 Cycle=Next_cycle
1430 Next_cycle=Cycle+5
1440 IF Cycle<7 THEN Next_cycle=Cycle+2
1450 Waitime=Wait_time-INT(Time_delay*Frequency+.5)/Frequency
1460 OUTPUT @Multi;"CC",Memory2+1,"T" !Clear card
1470 OUTPUT @Multi;"WF",Memory2+.1,10,"T" !Set re-circulate mode
1480 OUTPUT @Multi;"WF",Memory2+1.0,Ndata,"T" !Set ref. word
1490 OUTPUT @Multi;"WF",Memory2+1.2,Ndata+1,"T" !Set write pointer
1500 OUTPUT @Multi;"WF",Memory2+1.3,0,"T" !Set read pointer
1510 OUTPUT @Multi;"WF",Timer+.2,1,"T" !Set continuous mode
1520 OUTPUT @Multi;"CY",Timer,"T" !Resume cycling
1530 WAIT Waitime !Wait next read data
1540 GOTO 910
1550 END IF
1560 SUBEND

```

```

1570! -----
1580!
1590! *****
1600! *
1610! *      SUBROUTINES USED BY SUB ISOGB(Param1,Param2,...)      *
1620! *
1630! *****
1640!
1650! -----
1660 SUB Init_control(@Multi,Memory,Timer,D_to_a,Control,Scale,Mean,Span,Gauge,
Gauge_factor,Frequency,Ndata,Pace,Paces)
1670   !__GENERATE WAVEFORM__
1680   !-----
1690   Load_scale=INT(Scale)/100
1700   Strain_scale=Scale-(Load_scale*100)
1710   IF Control=1 THEN
1720       Pmean=Mean/(Load_scale*216.078)           !Convert MPA into voltage
1730       Pmax=Span/(Load_scale*216.078)
1740   ELSE
1750       Emax=Gauge_factor*Strain_scale/Gauge
1760       Pmean=10*Mean/Emax                       !Convert Strain into voltage
1770       Pmax=10*Span/Emax
1780   END IF
1790   Coeff=800
1800   IF Pmax>5.12 THEN Coeff=400
1810   Ndata=INT(Coeff*Pmax+.5)-1
1820   ALLOCATE A(Ndata)
1830   Ndata2=INT(Ndata/4+.5)
1840   Ndata3=Ndata-Ndata2
1850   FOR I=0 TO Ndata2-1
1860       A(I)=Pmax*I/(Ndata2-1)
1870       A(I+Ndata3)=Pmax*(I/(Ndata2-1)-1)
1880   NEXT I
1890   FOR I=Ndata2 TO Ndata3
1900       A(I)=(Ndata-1-2*I)*Pmax/(Ndata+1-2*Ndata2)
1910   NEXT I
1920   !
1930   !__CALCULATE THE PACE__
1940   !-----
1950   Time_int=1/(Ndata*Frequency)
1960   Pace=INT(Time_int*500000)/1000                !Pace in msec
1970   Paces=Pace
1980   IF Frequency>.185 THEN Paces=INT(500000/(Ndata*.185))/1000
1990   !
2000   !__PROGRAM MULTI__AMPLITUDE
2010   !-----
2020   OUTPUT @Multi;"CC",Memory+1,"T"              !Clear memory card
2030   OUTPUT @Multi;"SF",Memory,3,1,.005,12,"T"  !Set format(LSB=0.005)
2040   OUTPUT @Multi;"WF",Memory+1.0,Ndata,"T"    !Truncate memory
2050   OUTPUT @Multi;"MO",Memory,A(*),"T"        !Load data into memory
2060   OUTPUT @Multi;"WF",Memory+.1,10,"T"       !Set re-circulate mode
2070   OUTPUT @Multi;"WF",Timer+.2,1,"T"         !Set timer for continuous
2080   OUTPUT @Multi;"WF",Timer,Pace,"T"         !output. Set Pace
2090   !

```

```

2100 !__PROGRAM MULTI-- MEAN
2110 ! -----
2120 Incr=.005
2130 IF Pmean=0 THEN GOTO 2210
2140 IF Pmean<0 THEN Incr=-.005
2150 J=0
2160 OUTPUT @Multi;"OP",D_to_a,J,"T"
2170 IF ABS(J)<ABS(Pmean) THEN
2180     J=J+Incr
2190     GOTO 2160
2200 END IF
2210 DEALLOCATE A(*)
2220 SUBEND
2230!
2240 SUB Read_data(@Multi,@Dvm,Frequency,Timer,Pace,Paces,Scanner,Memory,Pace1,
Pace2,Ref_count,Scan(*),Pot(*))
2250     G=SPOLL(@Multi)
2260     ENTER 72310;A,B,C,D,E,F
2270     ON INTR 7 GOTO Interrupt           !Set interrupt branch
2280     ENABLE INTR 7;2                   !Enable Interrupt
2290     OUTPUT @Multi;"CY",Scanner,"T"    !Enable scanner
2300     OUTPUT @Multi;"WF",Scanner+.3,5,"T" !Set sequential mode
2310     !
2320     OUTPUT @Multi;"WF",Scanner,1,"T"   !Set start channel
2330     OUTPUT @Multi;"WF",Scanner+.1,2,"T" !set stop channel
2340     OUTPUT @Multi;"WF",Scanner+.2,Pace1,"T" !Set pace(in usec)
2350     Prog_diff(@Multi,Memory,0)        !Reset diff. counter
2360     Prog_write(@Multi,Memory,0)       !Reset write pointer
2370     OUTPUT @Multi;"CC";Memory,"T"     !Clear Memory card
2380     Prog_mode(@Multi,Memory,56)       !Set FIFO mode
2390     Prog_ref1(@Multi,Memory,Ref_count) !Set stop pointer
2400     OUTPUT @Multi;"AC";Memory,"T"     !Armed memory card
2410     OUTPUT @Multi;"SC",0,0,0,0T"     !Reset clock
2420     OUTPUT @Multi;"CY",Timer,"T"     !Start cycling
2430     OUTPUT @Multi;"CY",Scanner,"T"   !Start pacer
2440     FOR I=0 TO (Ref_count+1)/2-1
2450         ENTER @Dvm;Pot(I)             !Read potential
2460         WAIT Pace2
2470     NEXT I
2480 Spin:     GOTO Spin
2490 Interrupt: !
2500     OUTPUT @Multi;"WF",Timer+.2,0,"T" !Check pace
2510     OUTPUT @Multi;"RC"                 !Read real-time clock(T1)
2520     IF Frequency>.185 THEN OUTPUT @Multi;"WF",Timer,Pace,"T"
2530     OUTPUT @Multi;"WF",Timer+.2,1,"T" !Set continuous mode
2540     OUTPUT @Multi;"CY",Timer,"T"     !Continue cycling
2550     G=SPOLL(@Multi)
2560     IF G=64 THEN
2570         ENTER 72310;A,B,C
2580         IF C<>0 THEN
2590             ENTER 72312;Address
2600             IF Address<>Memory THEN
2610                 PRINT "NOT MEMORY CARD"
2620                 PAUSE
2630             END IF

```

```

2640         OUTPUT @Multi;"WF",Scanner+.2,0,"T"           !Stop scanner
2650         Prog_mode(@Multi,Memory,76)                   !Set FIFO lockout
2660         OUTPUT @Multi;"MR";Memory;Ref_count+1;"T"!MR command to get data
2670         ENTER 72305 USING "%,W";Scan(*)                !Entering the data
2680     ELSE
2690         BEEP 2000,.3
2700         PRINT "          *** SRQ NOT SET BY ARMED CARD ***"
2710         PAUSE
2720     END IF
2730     ELSE
2740         BEEP 2000,.3
2750         PRINT "          *** MULTI DID NOT INTERRUPT ***"
2760         PAUSE
2770     END IF
2780 SUBEND
2790!
2800 SUB Store_data(@Disc,Disc_drive,Cycle,Ref_count,Scan(*),Pot(*))
2810 ALLOCATE X(199)
2820 FOR I=0 TO Ref_count STEP 2
2830     X(I/2)=INT((Scan(I)+10)*1000)+(Scan(I+1)+10)/100
2840 NEXT I
2850 ON ERROR GOTO Recover
2860 CREATE BDAT "CYCLE"&VAL$(Cycle),1,4000
2870 ASSIGN @Disc TO "CYCLE"&VAL$(Cycle)
2880 OUTPUT @Disc;Cycle,X(*),Pot(*)
2890 ASSIGN @Disc TO *
2900 GOTO Out
2910 !
2920 Recover: !
2930     IF ERRN=59 OR ERRN=64 THEN
2940         IF Disc_drive=0 THEN
2950             Disc_drive=1
2960             MASS STORAGE IS ":HP8290X,700,1"
2970         ELSE
2980             Disc_drive=0
2990             MASS STORAGE IS ":HP8290X,700,0"
3000         END IF
3010     ELSE
3020         BEEP 2000,1
3030         PRINT USING 3040;ERRN
3040         IMAGE 2/,25X,"ERROR NUMBER ",K,/,25X,"CHECK STORAGE UNIT",/,25X,"PROG
RAM ABORTED"
3050         PAUSE
3060     END IF
3070     GOTO 2860
3080 Out: !
3090     DEALLOCATE X(*)
3100 SUBEND
3110!
3120 SUB Init_multi(@Multi,@Disc)
3130     CLEAR 7
3140     WAIT 4.0
3150     @=SPOLL(@Multi)

```

```

3160 IF B<>64 THEN
3170 PRINT "      ***MULTI DID NOT INTERRUPT***"
3180 PAUSE
3190 END IF
3200 STATUS @Multi,3;Multi
3210 ENTER Multi*100+10;A
3220 IF A<>16384 THEN
3230 PRINT "      ***SELF TEST DID NOT SET SRQ***"
3240 PAUSE
3250 END IF
3260 ALLOCATE Ascii$[80]
3270 ON END @Disc GOTO Eof
3280 Rd_file: ENTER @Disc;Ascii$
3290 OUTPUT @Multi;Ascii$
3300 GOTO Rd_file
3310 Eof: OFF END @Disc
3320 ASSIGN @Disc TO *
3330 DEALLOCATE Ascii$
3340 MASS STORAGE IS ":HP8290X,700,0"
3350 SUBEND

```

```

3360!-----

```

```

3370 SUB Init_mem(@Multi,Memory)
3380 Prog_mode(@Multi,Memory,254)
3390 Prog_mode(@Multi,Memory,54)
3400 Prog_ref1(@Multi,Memory,1048575)
3410 Prog_ref2(@Multi,Memory,0)
3420 Prog_read(@Multi,Memory,0)
3430 Prog_diff(@Multi,Memory,0)
3440 Prog_write(@Multi,Memory,0)
3450 OUTPUT @Multi;"CC";Memory;"T"
3460 SUBEND

```

```

3470!-----

```

```

3480 SUB Prog_read(@Multi,Memory,Read_pointer)
3490 Read_low=Read_pointer MOD 65536
3500 Read_high=Read_pointer DIV 65536
3510 Read_low_oct=FNDec_to_octal(Read_low)
3520 Read_high_oct=FNDec_to_octal(Read_high)
3530 OUTPUT @Multi;"WF";Memory+.1;22;Memory+.2;Read_low_oct;"T"
3540 OUTPUT @Multi;"WF";Memory+.1;23;Memory+.2;Read_high_oct;"T"
3550 SUBEND

```

```

3560!-----

```

```

3570 SUB Prog_write(@Multi,Memory,Write_pointer)
3580 Write_low=Write_pointer MOD 65536
3590 Write_high=Write_pointer DIV 65536
3600 Write_low_oct=FNDec_to_octal(Write_low)
3610 Write_high_oct=FNDec_to_octal(Write_high)
3620 OUTPUT @Multi;"WF";Memory+.1;24;Memory+.2;Write_low_oct;"T"
3630 OUTPUT @Multi;"WF";Memory+.1;25;Memory+.2;Write_high_oct;"T"
3640 SUBEND

```

```

3650!-----

```

```

3660 SUB Prog_diff(@Multi,Memory,Diff_counter)
3670 Diff_low=Diff_counter MOD 65536
3680 Diff_high=Diff_counter DIV 65536
3690 Diff_low_oct=FNDec_to_octal(Diff_low)

```

```

3700 Diff_high_oct=FNDec_to_octal(Diff_high)
3710 OUTPUT @Multi;"WF";Memory+.1;20;Memory+.2;Diff_low_oct;"T"
3720 OUTPUT @Multi;"WF";Memory+.1;21;Memory+.2;Diff_high_oct;"T"
3730 SUBEND
3740! -----
3750 SUB Prog_ref1(@Multi,Memory,Ref1_reg)
3760 Ref1_low=Ref1_reg MOD 65536
3770 Ref1_high=Ref1_reg DIV 65536
3780 Ref1_low_oct=FNDec_to_octal(Ref1_low)
3790 Ref1_high_oct=FNDec_to_octal(Ref1_high)
3800 OUTPUT @Multi;"WF";Memory+.1,26;Memory+.2;Ref1_low_oct;"T"
3810 OUTPUT @Multi;"WF";Memory+.1,27;Memory+.2;Ref1_high_oct;"T"
3820 SUBEND
3830! -----
3840 SUB Prog_ref2(@Multi,Memory,Ref2_reg)
3850 Ref2_low=Ref2_reg MOD 65536
3860 Ref2_high=Ref2_reg DIV 65536
3870 Ref2_low_oct=FNDec_to_octal(Ref2_low)
3880 Ref2_high_oct=FNDec_to_octal(Ref2_high)
3890 OUTPUT @Multi;"WF";Memory+.1;30;Memory+.2;Ref2_low_oct;"T"
3900 OUTPUT @Multi;"WF";Memory+.1;31;Memory+.2;Ref2_high_oct;"T"
3910 SUBEND
3920! -----
3930 SUB Prog_mode(@Multi,Memory,Mode)
3940 OUTPUT @Multi;"WF";Memory+.3;Mode;"T"
3950 SUBEND
3960! -----
3970 SUB Read_status(@Multi,Memory,Status)
3980 STATUS @Multi,3;Multi
3990 OUTPUT @Multi;"WF";Memory+.1;1;"T RV";Memory+.2;"T"
4000 ENTER Multi*100+6;Status
4010 SUBEND
4020! -----
4030 SUB Read_read(@Multi,Memory,Read_pointer)
4040 STATUS @Multi,3;Multi
4050 OUTPUT @Multi;"WF";Memory+.1;22;"T RV";Memory+.2;"T"
4060 ENTER Multi*100+6;Read_low_oct
4070 OUTPUT @Multi;"WF";Memory+.1;23;"T RV";Memory+.2;"T"
4080 ENTER Multi*100+6;Read_high_oct
4090 Read_low=FNOctal_to_dec(Read_low_oct)
4100 Read_high=FNOctal_to_dec(Read_high_oct)
4110 Read_pointer=65536*Read_high+Read_low
4120 SUBEND
4130! -----
4140 SUB Read_write(@Multi,Memory,Write_pointer)
4150 STATUS @Multi,3;Multi
4160 OUTPUT @Multi;"WF";Memory+.1;24;"T RV";Memory+.2;"T"
4170 ENTER Multi*100+6;Write_low_oct
4180 OUTPUT @Multi;"WF";Memory+.1;25;"T RV";Memory+.2;"T"
4190 ENTER Multi*100+6;Write_high_oct
4200 Write_low=FNOctal_to_dec(Write_low_oct)
4210 Write_high=FNOctal_to_dec(Write_high_oct)
4220 Write_pointer=65536*Write_high+Write_low

```



```

4230 SUBEND
4240! -----
4250 SUB Read_diff(@Multi,Memory,Diff_counter)
4260   STATUS @Multi,3;Multi
4270   OUTPUT @Multi;"WF";Memory+.1;20;"T RV";Memory+.2;"T"
4280   ENTER Multi*100+6;Diff_low_oct
4290   OUTPUT @Multi;"WF";Memory+.1;21;"T RV";Memory+.2;"T"
4300   ENTER Multi*100+6;Diff_high_oct
4310   Diff_low=FNOctal_to_dec(Diff_low_oct)
4320   Diff_high=FNOctal_to_dec(Diff_high_oct)
4330   Diff_counter=65536*Diff_high+Diff_low
4340 SUBEND
4350! -----
4360 DEF FNDec_to_octal(Dec)
4370   Oct=Dec+2*INT(Dec/8)+20*INT(Dec/64)+200*INT(Dec/512)+2000*INT(Dec/4096)+2
0000*INT(Dec/32768)+200000*INT(Dec/262144)
4380   RETURN Oct
4390 FNEND
4400! -----
4410 DEF FNOctal_to_dec(Octal)
4420   X9=0
4430   X7=Octal
4440   X=0
4450 More:   !
4460   X=X+(X7-INT(X7/10)*10)*8^X9
4470   X7=INT(X7/10)
4480   X9=X9+1
4490   IF X7<>0 THEN GOTO More
4500   RETURN X
4510 FNEND
4520! -----
4530 SUB Plot_frame(Material$,Contr_variable,Mean,Span,Frequency)
4540 ALLOCATE A(20),B(20)
4550 FOR I=0 TO 4
4560   A(I)=25*I-50
4570 NEXT I
4580 FOR I=0 TO 20
4590   B(I)=3*I-40
4600 NEXT I
4610 DEG
4620 BINIT
4630 GCLEAR
4640 ALPHA ON
4650 GRAPHICS OFF
4660 FRAME
4670 WINDOW -66.7224080268,66.7224080268,-50,50
4680 MOVE -50,-40
4690 FOR I=0 TO 3
4700   FOR J=1 TO 9
4710     DRAW 25*LBT(J*10^I)-50,-40
4720     IF J=1 THEN
4730       IDRAW 0,1
4740       IMOVE 0,-1

```

```

4750     ELSE
4760         IDRAW 0,.5
4770         IMOVE 0,-.5
4780     END IF
4790 NEXT J
4800 NEXT I
4810 C=.5
4820 D=1.0
4830 FOR I=0 TO 20
4840     DRAW 50,B(I)
4850     IF 2*INT(I/2)=I THEN
4860         IDRAW -D,0
4870         IMOVE D,0
4880     ELSE
4890         IDRAW -C,0
4900         IMOVE C,0
4910     END IF
4920 NEXT I
4930 FOR I=3 TO 0 STEP -1
4940     FOR J=9 TO 1 STEP -1
4950         DRAW 25*LGT(J*10^I)-50,20
4960         IF J=1 THEN
4970             IDRAW 0,-1
4980             IMOVE 0,1
4990         ELSE
5000             IDRAW 0,-.5
5010             IMOVE 0,.5
5020         END IF
5030     NEXT J
5040 NEXT I
5050 FOR I=20 TO 0 STEP -1
5060     DRAW -50,B(I)
5070     IF 2*INT(I/2)=I THEN
5080         IDRAW D,0
5090         IMOVE -D,0
5100     ELSE
5110         IDRAW C,0
5120         IMOVE -C,0
5130     END IF
5140 NEXT I
5150 MOVE -50,-10
5160 FOR I=0 TO 3
5170     FOR J=1 TO 9
5180         DRAW 25*LGT(J*10^I)-50,-10
5190         IF J=1 THEN
5200             IDRAW 0,1
5210             IDRAW 0,-2
5220             IMOVE 0,1
5230         ELSE
5240             IDRAW 0,.5
5250             IDRAW 0,-1
5260             IMOVE 0,.5
5270         END IF
5280     NEXT J

```

```

5290 NEXT I
5300 MOVE 50,20
5310 DRAW 50,40
5320 DRAW -50,40
5330 DRAW -50,20
5340 CSIZE 3,.6
5350 MOVE -50,-44
5360 LABEL VAL$(1)
5370 FOR I=1 TO 4
5380     MOVE A(I)-3,-44
5390     LABEL VAL$(10^I)
5400 NEXT I
5410 FOR I=0 TO 8 STEP 2
5420     MOVE -56,3*I-41
5430     LABEL USING "D.D";I/2
5440     MOVE 51,3*I-41
5450     LABEL USING "D.D";I/2
5460 NEXT I
5470 CSIZE 4,.6
5480 MOVE -5,-48
5490 LABEL "CYCLE"
5500 CSIZE 3,.6
5510 LDIR 90
5520 MOVE -58,-32
5530 IDRAW 0,3
5540 IDRAW -1.5,-1.5
5550 IDRAW 1.5,-1.5
5560 MOVE -57,-28
5570 LABEL "V/Vo"
5580 MOVE -58,-3
5590 IDRAW 0,3
5600 IDRAW -1.5,-1.5
5610 IDRAW 1.5,-1.5
5620 MOVE -57,1
5630 IF Contr_variable=1 THEN
5640     LABEL "E/2(X 10 )"
5650     IMOVE -3.5,14.6
5660     LABEL "-"
5670 ELSE
5680     LABEL "S/2 (MPa)"
5690 END IF
5700 LDIR -90
5710 MOVE 59,16
5720 IDRAW 0,-3
5730 IDRAW 1.5,1.5
5740 IDRAW -1.5,1.5
5750 MOVE 59,12
5760 IF Contr_variable=1 THEN
5770     LABEL "E/2(X 10 )"
5780     IMOVE 3.5,-14.6
5790     LABEL "-"
5800 ELSE
5810     LABEL "S/2 (MPa)"

```

```

5820 END IF
5830 MOVE 59,-20
5840 IDRAW 0,-3
5850 IDRAW 1.5,1.5
5860 IDRAW -1.5,1.5
5870 MOVE 59,-24
5880 LABEL "V/Vo"
5890 LDIR 0
5900 CSIZE 3.5,.6
5910 MOVE -45,34
5920 LABEL Material$
5930 MOVE -45,30
5940 LABEL "ISQCG"
5950 MOVE -45,26
5960 LABEL "Frequency= "&VAL$(Frequency)&" Hz"
5970 IF Contr_variable=1 THEN
5980     MOVE 15,34
5990     LABEL "STRESS CONTROL"
6000     MOVE 15,31
6010     IDRAW 3,0
6020     IDRAW -1.5,1.5
6030     IDRAW -1.5,-1.5
6040     MOVE 19,30
6050     LABEL "S = "&VAL$(Span*2)&" (MPa)"
6060 ELSE
6070     MOVE 15,34
6080     LABEL "STRAIN CONTROL"
6090     MOVE 15,31
6100     IDRAW 3,0
6110     IDRAW -1.5,1.5
6120     IDRAW -1.5,-1.5
6130     MOVE 19,30
6140     LABEL "E = "&VAL$(Span*2)
6150 END IF
6160 MOVE 19,26
6170 LABEL "R = "&VAL$(DROUND((Mean-Span)/(Mean+Span),2))
6180 SUBEND
6190!
6200 SUB Init_read(Cycle_per_block,Data_per_cycle,Frequency,Pace1,Pace2,Ref_count)
6210 Ref_count=(Cycle_per_block*Data_per_cycle*2)-1
6220 IF Frequency>=.185 THEN
6230     Pace1=INT(1.E+6/(Data_per_cycle*2*.185)-30)           !Pace in usec
6240     Pace2=0.
6250 ELSE
6260     Pace1=INT(1.E+6/(Data_per_cycle*2*Frequency)-30)       !Pace in usec
6270     Pace2=DROUND((1/Frequency-1/37)/200,3)
6280 END IF
6290 SUBEND
6300!
6310 SUB Plot_data(Contr_variable,Scale,Span,Gauge,Gauge_factor,Cycle,Ref_count
,Scan(*),Pot(*),Exponent,Min,Vo)
6320 ALPHA OFF
6330 GRAPHICS ON
6340 CSIZE 3,.6
6350 Indice=1

```

```

6360 Max=0
6370 Maxim=0
6380 IF Contr_variable=1 THEN Indice=0
6390 FOR I=74 TO 124 STEP 2
6400 J=I+Indice
6410 IF Scan(J)*.005>Max THEN Maximum=Scan(J)*.005
6420 IF Scan(J+200)*.005<Min THEN Minimum=Scan(J+200)*.005
6430 IF Pot(I/2)>Maxim THEN Maxim=Pot(I/2)
6440 IF Pot(I/2+1)>Maxim THEN Maxim=Pot(I/2+1)
6450 NEXT I
6460 Range=Maximum-Minimum
6470 Vmax=Maxim
6480 Load_scale=INT(Scale)/100
6490 Strain_scale=Scale-(Load_scale*100)
6500 IF Cycle>1 THEN GOTO Data
6510 CALL Scale_frame(Contr_variable,Scale,Gauge,Gauge_factor,Range,Min,Expon
ent)
6520 Vo=Vmax
6530 Data: !
6540 X=25*LGT(Cycle)-50
6550 IF Contr_variable=1 THEN
6560 Strain_ampli=Range*Strain_scale*Gauge_factor/(Gauge*20)
6570 Y1=4*(Strain_ampli*(10^Exponent)-Min)
6580 ELSE
6590 Stress_ampli=Range*Load_scale*216.078/2
6600 Y1=.2*(Stress_ampli-Min)
6610 END IF
6620 MOVE X-.7,3*Y1-11.3
6630 LABEL "x"
6640 MOVE X-.7,6*(Vmax/Vo)-41.3
6650 LABEL "x"
6660 SUBEND
6670! -----
6680 SUB Scale_frame(Contr_variable,Scale,Gauge,Gauge_factor,Range,Min,Exponen
t)
6690 Load_scale=INT(Scale)/100
6700 Strain_scale=Scale-(Load_scale*100)
6710 IF Contr_variable=1 THEN
6720 Strain_ampli=Range*Strain_scale*Gauge_factor/(Gauge*20)
6730 FOR Multiplier=0 TO 5
6740 IF Strain_ampli*10^Multiplier>1 AND Strain_ampli*10^Multiplier<10 TH
EN Exponent=Multiplier
6750 NEXT Multiplier
6760 A=Strain_ampli*10^Exponent
6770 IF A<2.5 THEN
6780 Min=0.
6790 ELSE
6800 IF A<5.0 THEN
6810 Min=2.5
6820 ELSE
6830 IF A<7.5 THEN
6840 Min=5.0
6850 ELSE
6860 Min=7.5

```

```

6870         END IF
6880         END IF
6890     END IF
6900 ELSE
6910     Stress_ampli=Range*Load_scale*216.078/2
6920     Norme=INT(Stress_ampli/100)*100
6930     A=Stress_ampli-Norme
6940     IF A<25 THEN
6950         Min=Norme
6960         IF A<12.5 THEN Min=Norme-25
6970     ELSE
6980         IF A<50 THEN
6990             Min=Norme+25
7000             IF A<37.5 THEN Min=Norme
7010         ELSE
7020             IF A<75 THEN
7030                 Min=Norme+50
7040                 IF A<62.5 THEN Min=Norme+25
7050             ELSE
7060                 Min=Norme+75
7070                 IF A<77.5 THEN Min=Norme+50
7080             END IF
7090         END IF
7100     END IF
7110 END IF
7120 A$="3D"
7130 Facto=5
7140 IF Contr_variable=1 THEN
7150     A$="D.D"
7160     Facto=.50
7170 END IF
7180 FOR I=2 TO 10 STEP 2
7190     MOVE -56,3*I-11.5
7200     LABEL USING A$;(Facto*I+Min)
7210     MOVE 51,3*I-11.5
7220     LABEL USING A$;(Facto*I+Min)
7230 NEXT I
7240 CSIZE 3,.6
7250 LDIR 90
7260 IF Contr_variable=1 THEN
7270     MOVE -57,1
7280     IMOVE -1,16.6
7290     LABEL USING "D";Exponent
7300     LDIR -90
7310     MOVE 59,12
7320     IMOVE .5,-16.6
7330     LABEL USING "D";Exponent
7340 END IF
7350 LDIR 0
7360 SUBEND

```

```

10! *****
11!
12!
13!
14!
15!
16!
17!
18!
19!
20!
21!
22!
23!
24!
25!
26!
27!
28!
29!
30!
31!
32!
33!
34!
35!
36!
37!
38!
39!
40!
41!
42!
43!
44!
45!
46!
47!
48!
49!
50!
51!
52!
53!
54!

```

PROGRAM ISOLCF

THIS PROGRAM PERFORMS THE REAL-TIME CONTROL AND DATA ACQUISITION OF ISOTHERMAL LOW CYCLE FATIGUE TESTS.

THIS PROGRAM IS CALLED BY ISO_TMF AFTER SELECTION OF THE ISOLCF OPTION.

THE CYCLIC DATA(Stresses, and strains) ARE RECORDED (N2/N1)=1.25 CYCLES.

```

!
OPTION BASE 0
CALL Isolcf(Material$,Contr_variable,Scale,Mean,Span,Gauge,Frequency)
END
*****
*****
!
SUB Isolcf(Material$,Contr_variable,Scale,Mean,Span,Gauge,Frequency)
MASS STORAGE IS ":HP8290X,700,1"
!
-----DEFINE I/O CARD FUNCTION-----
!
ASSIGN @Multi TO 723
ASSIGN @Disc TO "MRZ"
Disc_drive=0
Multi=723
Scanner=0
A_to_d=3
Memory1=7
D_to_a1=10
Timer=11
D_to_a2=12
Memory2=13
Ndata=0
Pace=0
!
-----DEFAULT VALUES FOR THE PARAMETERS-----
!
Start=1 !Start channel
Stop=2 !Stop channel
Pointer=1 !Interrupt word
Cycle_per_block=12
Data_per_cycle=200
Gauge_factor=.05493
!
-----INITIALIZE THE MULTI-----
!
CALL Init_multi(@Multi,@Disc)
CALL Init_mem(@Multi,Memory1)

```

```

550 |
560 |-----INITIALIZE CONTROL PROCEDURE-----
570 |-----
580 CALL Init_control(@Multi,Memory2,Timer,D_to_a1,Contr_variable,Scale,Mean,Span,Gauge,Gauge_factor,Frequency,Ndata)
590 |
600 |-----INITIALIZE READING PROCEDURE-----
610 |-----
620 CALL Init_read(Frequency,Pace,Cycle_per_block,Data_per_cycle,Ref_count)
630 ALLOCATE Scan(Ref_count)
640 |
650 |-----SET INTERRUPT BRANCH FOR THE START SIGNAL-----
660 |-----
670 BEEP
680 Cycle=1 !Set cycle counter
690 Next_cycle=2 !Set Next_cycle counter
700 PRINT USING 710
710 IMAGE 2/,15X,"REMOVE CONTROL AND UTILITY PAC DISCS",2/,15X,"INSERT TWO DISCS FOR DATA STORAGE",2/,15X,"PRESS K0(Continue) TO CONTINUE"
720 ON KEY 0 LABEL "**CONTINUE**" GOTO 740
730 Spin: GOTO Spin
740 OFF KEY
750 CREATE BDAT "TEST_PARAM",1,100
760 ASSIGN @Disc TO "TEST_PARAM"
770 OUTPUT @Disc;Material$, "ISOLCF",Contr_variable,Scale,Mean,Span,Gauge,Frequency
780 ASSIGN @Disc TO *
790 CALL Plot_frame(Material$,Contr_variable,Mean,Span,Frequency)
800 DELSUB Plot_frame
810 PRINT USING 820
820 IMAGE 20/,25X,"MULTIPROGRAMMER IS READY",2/,20X,"****WAITING FOR THE START COMMAND****"
830 ON KEY 0 LABEL " START CYCLING" GOTO Start_iso
840 Wait: GOTO Wait
850 |
860 |-----START CYCLING AND TAKING DATA-----
870 |-----
880 Start_iso: !
890 OFF KEY
900 OUTPUT @Multi;"SC,0,0,0,0T" !Reset Clock of Multi
910 OUTPUT @Multi;"CY",Timer,"T" !Start cycling
920 |
930 |-----READ DATA-----
940 |-----
950 CALL Read_data(@Multi,Multi,Scanner,Memory1,Pace,Ref_count,Scan(*))
960 |-----STORE DATA-----
970 |-----
980 CALL Store_data(@Disc,Disc_drive,Cycle,Next_cycle,Ref_count,Scan(*))
990 |
1000 |-----DISPLAY DATA-----
1010 |-----
1020 CALL Plot_data(Contr_variable,Scale,Span,Gauge,Gauge_factor,Cycle,Next_cycle,Ref_count,Scan(*),Exponent,Exp,Min,Mini)

```



```

1030 !
1040 !-----SET WAITING FOR SYNCHRO. SIGNAL-----
1050 !
1060 Synchro:
1070 OUTPUT @Multi;"WF",Timer+.2,0,"T"           !Stop cycling
1080 ON INTR 7 GOTO Complete
1090 ENABLE INTR 7;2
1100 OUTPUT @Multi;"RV",Memory2+1,Memory2+1.1,Memory2+1.2,Memory2+1.3,"T"
1110 ENTER 72306;A1,B1,C1,D1                       !Read card pointers
1120 OUTPUT @Multi;"WF",Memory2+1.1,C1-A1,"T"     !Set differential counter
1130 OUTPUT @Multi;"WF",Memory2+.1,2,"T"         !Set FIFO output mode
1140 OUTPUT @Multi;"WF",Memory2+1.0,1,"T"        !Set reference word
1150 OUTPUT @Multi;"WF",Memory2+1.3,A1,"T"       !Set read pointer
1160 OUTPUT @Multi;"AC",Memory2+1,"T"           !Arm card for interrupt
1170 OUTPUT @Multi;"WF",Timer+.2,1,"T"         !Reset timer(continuous)
1180 OUTPUT @Multi;"CY",Timer,"T"              !Complete the cycle
1190 Spin2: GOTO Spin2
1200 Complete: !
1210 OUTPUT @Multi;"WF",Timer+.2,0,"T"           !Stop Timer
1220 OUTPUT @Multi;"DC",Memory2+1,"T"           !Disarm card
1230 OUTPUT @Multi;"RC"                          !Set real-time clock(T2)
1240 ENTER 72314;A1,B1,C1,D1                     !Read real-time clock(T1)
1250 ENTER 72314;A2,B2,C2,D2                     !Read real-time clock(T2)
1260 T1=60*(A1*60*24+B1*60+C1)+D1
1270 T2=60*(A2*60*24+B2*60+C2)+D2
1280 Time_delay=T2-T1
1290 Wait_time=(Next_cycle-Cycle-1)/Frequency     !Wait between cycles
1300 IF Wait_time<Time_delay THEN
1310     Cycle=INT(Cycle+1.5+Time_delay*Frequency)
1320     Next_cycle=INT(Cycle*1.25)
1330     OUTPUT @Multi;"CC",Memory2+1,"T"         !Clear card
1340     OUTPUT @Multi;"WF",Memory2+.1,10,"T"     !Set re-circulate mode
1350     OUTPUT @Multi;"WF",Memory2+1.0,Ndata,"T" !Set ref. word
1360     OUTPUT @Multi;"WF",Memory2+1.2,Ndata+1,"T"!Set write pointer
1370     OUTPUT @Multi;"WF",Memory2+1.3,0,"T"     !Set read pointer
1380     OUTPUT @Multi;"WF",Timer+.2,1,"T"       !Set continuous mode
1390     OUTPUT @Multi;"CY",Timer,"T"            !Resume cycling
1400     GOTO 940
1410 ELSE
1420     Cycle=Next_cycle
1430     Waitime=Wait_time-((T2-T1)*Frequency)     !Compute wait
1440     OUTPUT @Multi;"CC",Memory2+1,"T"         !Clear card
1450     OUTPUT @Multi;"WF",Memory2+.1,10,"T"     !Set re-circulate mode
1460     OUTPUT @Multi;"WF",Memory2+1.0,Ndata,"T" !Set ref. word
1470     OUTPUT @Multi;"WF",Memory2+1.2,Ndata+1,"T"!Set write word
1480     OUTPUT @Multi;"WF",Memory2+1.3,0,"T"     !Set read pointer
1490     OUTPUT @Multi;"WF",Timer+.2,1,"T"       !Set continuous mode
1500     OUTPUT @Multi;"CY",Timer,"T"            !Resume cycling
1510     WAIT Waitime                             !Wait for next reading
1520     GOTO 940
1530 END IF
1540 SUBEND
1550!-----
1560!

```

```

1570! *****
1580! *
1590! *      SUBROUTINES USED BY SUB ISOLCF(Param1,Param2,...)
1600! *
1610! *****
1620!
1630!
1640 SUB Init_control(@Multi,Memory,Timer,D_to_a,Control,Scale,Mean,Span,Gauge,
Gauge_factor,Frequency,Ndata)
1650 !__GENERATE WAVEFORM__
1660 !-----
1670 Load_scale=INT(Scale)/100
1680 Strain_scale=Scale-(Load_scale*100)
1690 IF Control=1 THEN
1700     Pmean=Mean/(Load_scale*216.078)      !Convert MPA into voltage
1710     Pmax=Span/(Load_scale*216.078)
1720 ELSE
1730     Emax=Gauge_factor*Strain_scale/Gauge
1740     Pmean=10*Mean/Emax                  !Convert Strain into voltage
1750     Pmax=10*Span/Emax
1760 END IF
1770 Coeff=800
1780 IF Pmax>5.12 THEN Coeff=400
1790 Ndata=INT(Coeff*Pmax+.5)-1
1800 ALLOCATE A(Ndata)
1810 Ndata2=INT(Ndata/4+.5)
1820 Ndata3=Ndata-Ndata2
1830 FOR I=0 TO Ndata2-1
1840     A(I)=Pmax*I/(Ndata2-1)
1850     A(I+Ndata3)=Pmax*(I/(Ndata2-1)-1)
1860 NEXT I
1870 FOR I=Ndata2 TO Ndata3
1880     A(I)=(Ndata-1-2*I)*Pmax/(Ndata+1-2*Ndata2)
1890 NEXT I
1900 !
1910 !__CALCULATE THE PACE__
1920 !-----
1930 Time_int=1/(Ndata*Frequency)
1940 Pace=INT(Time_int*500000)/1000      !Pace in msec
1950 !__PROGRAM MULTI__AMPLITUDE
1960 !-----
1970 OUTPUT @Multi;"CC",Memory+1,"T"      !Clear memory card
1980 OUTPUT @Multi;"SF",Memory,3,1,.005,12,"T" !Set format(LSB=0:005)
1990 OUTPUT @Multi;"MO",Memory,A(*),"T"    !Load data into memory
2000 OUTPUT @Multi;"WF",Memory+1.0,Ndata,"T" !Truncate memory
2010 OUTPUT @Multi;"WF",Memory+.1,10,"T"   !Set re-circulate mode
2020 OUTPUT @Multi;"WF",Timer+.2,1,"T"     • !Set timer for continuous
2030 OUTPUT @Multi;"WF",Timer,Pace,"T"     !output. Set Pace
2040 !
2050 !__PROGRAM MULTI-- MEAN
2060 !-----
2070 Incr=.005
2080 IF Pmean=0 THEN GOTO 2160
2090 IF Pmean<0 THEN Incr=-.005

```

```

2100 J=0
2110 OUTPUT @Multi;"OP",D_to_a,J,"T"
2120 IF ABS(J)<ABS(Pmean) THEN
2130     J=J+Incr
2140     GOTO 2110
2150 END IF
2160 DEALLOCATE A(*)
2170 SUBEND
2180!
-----
2190 SUB Read_data(@Multi,Multi,Scanner,Memory,Pace,Ref_count,Scan(*)
2200     G=SPOLL(@Multi)
2210     ENTER 72310;A,B,C,D,E,F
2220     ON INTR 7,2 GOTO Interrupt
2230     ENABLE INTR 7;2
2240     OUTPUT @Multi;"CY",Scanner,"T"           !Enable scanner
2250     OUTPUT @Multi;"WF",Scanner+.3,5,"T"      !Set sequential mode
2260     !
2270     OUTPUT @Multi;"WF",Scanner,1,"T"         !Set start channel
2280     OUTPUT @Multi;"WF",Scanner+.1,2,"T"      !set stop channel
2290     OUTPUT @Multi;"WF",Scanner+.2,Pace,"T"   !Set pace(in usec)
2300     Prog_diff(@Multi,Memory,0)              !Reset diff. counter
2310     Prog_write(@Multi,Memory,0)            !Reset write pointer
2320     OUTPUT @Multi;"CC";Memory,"T"          !Clear Memory card
2330     Prog_mode(@Multi,Memory,56)            !Set FIFO mode
2340     Prog_ref1(@Multi,Memory,Ref_count)      !Set stop pointer
2350     OUTPUT @Multi;"AC";Memory;"T"          !Armed memory card
2360     OUTPUT @Multi;"CY",Scanner,"T"         !Start pacer
2370 Wait:   GOTO Wait
2380 Interrupt:   !
2390     OUTPUT @Multi;"RC"                     !Read real-time clock(T1)
2400     G=SPOLL(@Multi)
2410     IF G=64 THEN
2420         ENTER 72310;A,B,C
2430         IF C<>0 THEN
2440             ENTER 72312;Address
2450             IF Address<>Memory THEN
2460                 PRINT "NOT MEMORY CARD"
2470                 PAUSE
2480             END IF
2490             OUTPUT @Multi;"WF",Scanner+.2,0,"T" !Stop scanner
2500             Prog_mode(@Multi,Memory,76)       !Set FIFO lockout
2510             OUTPUT @Multi;"MR";Memory;Ref_count+1;"T"!MR command to get data
2520             ENTER 72305 USING "%,W";Scan(*)   !Entering the data
2530         ELSE
2540             BEEP 2000,.3
2550             PRINT "          *** SRQ NOT SET BY ARMED CARD ***"
2560             PAUSE
2570         END IF
2580     ELSE
2590         BEEP 2000,.3
2600         PRINT "          *** MULTI DID NOT INTERRUPT ***"
2610         PAUSE
2620     END IF

```

```

2630 SUBEND
2640! -----
2650 SUB Store_data(@Disc,Disc_drive,Cycle,Next_cycle,Ref_count,Scan(*))
2660 ALLOCATE X(199)
2670 Start=0
2680 Stop=399
2690 Init_cycle=Cycle
2700 Transfer: !
2710 Next_cycle=INT(Init_cycle*1.25)
2720 IF Next_cycle=Init_cycle THEN Next_cycle=Init_cycle+1
2730 FOR I=0 TO 399 STEP 2
2740 J=I+Start
2750 X(I/2)=INT((Scan(J)+10)*1000)+(Scan(J+1)+10)/100
2760 NEXT I
2770 ON ERROR GOTO Recover
2780 CREATE BDAT "CYCLE"&VAL$(Init_cycle),1,4000
2790 ASSIGN @Disc TO "CYCLE"&VAL$(Init_cycle)
2800 OUTPUT @Disc;Init_cycle,X(*)
2810 ASSIGN @Disc TO *
2820 Enough: !
2830 Init_cycle=Init_cycle+1
2840 Start=Stop+1
2850 Stop=Stop+400
2860 IF Stop>Ref_count THEN GOTO Out
2870 IF Init_cycle<Next_cycle THEN GOTO Enough
2880 GOTO Transfer
2890 !
2900 Recover: !
2910 IF ERRN=59 OR ERRN=64 THEN
2920 IF Disc_drive=0 THEN
2930 Disc_drive=1
2940 MASS STORAGE IS ":HP8290X,700,1"
2950 ELSE
2960 Disc_drive=0
2970 MASS STORAGE IS ":HP8290X,700,0"
2980 END IF
2990 ELSE
3000 BEEP 2000,1
3010 PRINT USING 3020;ERRN
3020 IMAGE 2/,25X,"ERROR NUMBER ",K,/,25X,"CHECK STORAGE UNIT",/,25X,"PROG
RAM ABORTED"
3030 PAUSE
3040 END IF
3050 GOTO 2780
3060 Out: !
3070 DEALLOCATE X(*)
3080 SUBEND
3090! -----
3100 SUB Init_multi(@Multi,@Disc)
3110 CLEAR 7
3120 WAIT 4.0
3130 G=SPOLL(@Multi)
3140 IF G<>64 THEN
3150 PRINT " ***MULTI DID NOT INTERRUPT***"

```

```

3160     PAUSE
3170   END IF
3180   STATUS @Multi,3;Multi
3190   ENTER Multi*100+10;A
3200   IF A<>16384 THEN
3210     PRINT "      ***SELF TEST DID NOT SET SRQ***"
3220     PAUSE
3230   END IF
3240   ALLOCATE Ascii#[80]
3250   ON END @Disc GOTO Eof
3260 Rd_file:   ENTER @Disc;Ascii$
3270   OUTPUT @Multi;Ascii$
3280   GOTO Rd_file
3290 Eof: OFF END @Disc
3300   ASSIGN @Disc TO *
3310   DEALLOCATE Ascii$
3320   MASS STORAGE IS ":HP8290X,700,0"
3330 SUBEND
3340!-----
3350 SUB Init_mem(@Multi,Memory)
3360   Prog_mode(@Multi,Memory,254)
3370   Prog_mode(@Multi,Memory,54)
3380   Prog_ref1(@Multi,Memory,1048575)
3390   Prog_ref2(@Multi,Memory,0)
3400   Prog_read(@Multi,Memory,0)
3410   Prog_diff(@Multi,Memory,0)
3420   Prog_write(@Multi,Memory,0)
3430   OUTPUT @Multi;"CC";Memory;"T"
3440 SUBEND
3450!-----
3460 SUB Prog_read(@Multi,Memory,Read_pointer)
3470   Read_low=Read_pointer MOD 65536
3480   Read_high=Read_pointer DIV 65536
3490   Read_low_oct=FNDec_to_octal(Read_low)
3500   Read_high_oct=FNDec_to_octal(Read_high)
3510   OUTPUT @Multi;"WF";Memory+.1;22;Memory+.2;Read_low_oct;"T"
3520   OUTPUT @Multi;"WF";Memory+.1;23;Memory+.2;Read_high_oct;"T"
3530 SUBEND
3540!-----
3550 SUB Prog_write(@Multi,Memory,Write_pointer)
3560   Write_low=Write_pointer MOD 65536
3570   Write_high=Write_pointer DIV 65536
3580   Write_low_oct=FNDec_to_octal(Write_low)
3590   Write_high_oct=FNDec_to_octal(Write_high)
3600   OUTPUT @Multi;"WF";Memory+.1;24;Memory+.2;Write_low_oct;"T"
3610   OUTPUT @Multi;"WF";Memory+.1;25;Memory+.2;Write_high_oct;"T"
3620 SUBEND
3630!-----
3640 SUB Prog_diff(@Multi,Memory,Diff_counter)
3650   Diff_low=Diff_counter MOD 65536
3660   Diff_high=Diff_counter DIV 65536
3670   Diff_low_oct=FNDec_to_octal(Diff_low)
3680   Diff_high_oct=FNDec_to_octal(Diff_high)
3690   OUTPUT @Multi;"WF";Memory+.1;20;Memory+.2;Diff_low_oct;"T"

```

```

3700  OUTPUT @Multi;"WF";Memory+.1;21;Memory+.2;Diff_high_oct;"T"
3710  SUBEND
3720! -----
3730  SUB Prog_ref1(@Multi,Memory,Ref1_reg)
3740  Ref1_low=Ref1_reg MOD 65536
3750  Ref1_high=Ref1_reg DIV 65536
3760  Ref1_low_oct=FNDec_to_octal(Ref1_low)
3770  Ref1_high_oct=FNDec_to_octal(Ref1_high)
3780  OUTPUT @Multi;"WF";Memory+.1;26;Memory+.2;Ref1_low_oct;"T"
3790  OUTPUT @Multi;"WF";Memory+.1;27;Memory+.2;Ref1_high_oct;"T"
3800  SUBEND
3810! -----
3820  SUB Prog_ref2(@Multi,Memory,Ref2_reg)
3830  Ref2_low=Ref2_reg MOD 65536
3840  Ref2_high=Ref2_reg DIV 65536
3850  Ref2_low_oct=FNDec_to_octal(Ref2_low)
3860  Ref2_high_oct=FNDec_to_octal(Ref2_high)
3870  OUTPUT @Multi;"WF";Memory+.1;30;Memory+.2;Ref2_low_oct;"T"
3880  OUTPUT @Multi;"WF";Memory+.1;31;Memory+.2;Ref2_high_oct;"T"
3890  SUBEND
3900! -----
3910  SUB Prog_mode(@Multi,Memory,Mode)
3920  OUTPUT @Multi;"WF";Memory+.3;Mode;"T"
3930  SUBEND
3940! -----
3950  SUB Read_status(@Multi,Memory,Status)
3960  STATUS @Multi,3;Multi
3970  OUTPUT @Multi;"WF";Memory+.1;1;"T RV";Memory+.2;"T"
3980  ENTER Multi*100+6;Status
3990  SUBEND
4000! -----
4010  SUB Read_read(@Multi,Memory,Read_pointer)
4020  STATUS @Multi,3;Multi
4030  OUTPUT @Multi;"WF";Memory+.1;22;"T RV";Memory+.2;"T"
4040  ENTER Multi*100+6;Read_low_oct
4050  OUTPUT @Multi;"WF";Memory+.1;23;"T RV";Memory+.2;"T"
4060  ENTER Multi*100+6;Read_high_oct
4070  Read_low=FNOctal_to_dec(Read_low_oct)
4080  Read_high=FNOctal_to_dec(Read_high_oct)
4090  Read_pointer=65536*Read_high+Read_low
4100  SUBEND
4110! -----
4120  SUB Read_write(@Multi,Memory,Write_pointer)
4130  STATUS @Multi,3;Multi
4140  OUTPUT @Multi;"WF";Memory+.1;24;"T RV";Memory+.2;"T"
4150  ENTER Multi*100+6;Write_low_oct
4160  OUTPUT @Multi;"WF";Memory+.1;25;"T RV";Memory+.2;"T"
4170  ENTER Multi*100+6;Write_high_oct
4180  Write_low=FNOctal_to_dec(Write_low_oct)
4190  Write_high=FNOctal_to_dec(Write_high_oct)
4200  Write_pointer=65536*Write_high+Write_low
4210  SUBEND
4220! -----
4230  SUB Read_diff(@Multi,Memory,Diff_counter)
4240  STATUS @Multi,3;Multi

```

```

4250 OUTPUT @Multi;"WF";Memory+.1;20;"T RV";Memory+.2;"T"
4260 ENTER Multi*100+6;Diff_low_oct
4270 OUTPUT @Multi;"WF";Memory+.1;21;"T RV";Memory+.2;"T"
4280 ENTER Multi*100+6;Diff_high_oct
4290 Diff_low=FNOctal_to_dec(Diff_low_oct)
4300 Diff_high=FNOctal_to_dec(Diff_high_oct)
4310 Diff_counter=65536*Diff_high+Diff_low
4320 SUBEND
4330! -----
4340 DEF FNDec_to_octal(Dec)
4350 Oct=Dec+2*INT(Dec/8)+20*INT(Dec/64)+200*INT(Dec/512)+2000*INT(Dec/4096)+2
0000*INT(Dec/32768)+200000*INT(Dec/262144)
4360 RETURN Oct
4370 FNEND
4380! -----
4390 DEF FNOctal_to_dec(Octal)
4400 X9=0
4410 X7=Octal
4420 X=0
4430 More: !
4440 X=X+(X7-INT(X7/10)*10)*8^X9
4450 X7=INT(X7/10)
4460 X9=X9+1
4470 IF X7<>0 THEN GOTO More
4480 RETURN X
4490 FNEND
4500! -----
4510 SUB Plot_frame(Material$,Contr_variable,Mean,Span,Frequency)
4520 ALLOCATE A(20),B(20)
4530 FOR I=0 TO 4
4540 A(I)=25*I-50
4550 NEXT I
4560 FOR I=0 TO 20
4570 B(I)=3*I-40
4580 NEXT I
4590 DEG
4600 GINIT
4610 GCLEAR
4620 ALPHA ON
4630 GRAPHICS OFF
4640 FRAME
4650 WINDOW -66.7224080268,66.7224080268,-50,50
4660 MOVE -50,-40
4670 FOR I=0 TO 3
4680 FOR J=1 TO 9
4690 DRAW 25*LG(T(J*10^I))-50,-40
4700 IF J=1 THEN
4710 IDRAW 0,1
4720 IMOVE 0,-1
4730 ELSE
4740 IDRAW 0,.5
4750 IMOVE 0,-.5
4760 END IF
4770 NEXT J

```

```

4780 NEXT I
4790 C=.5
4800 D=1.0
4810 FOR I=0 TO 20
4820   DRAW 50,B(I)
4830   IF 2*INT(I/2)=I THEN
4840     IDRAW -D,0
4850     IMOVE D,0
4860   ELSE
4870     IDRAW -C,0
4880     IMOVE C,0
4890   END IF
4900 NEXT I
4910 FOR I=3 TO 0 STEP -1
4920   FOR J=9 TO 1 STEP -1
4930     DRAW 25*LGT(J*10^I)-50,20
4940     IF J=1 THEN
4950       IDRAW 0,-1
4960       IMOVE 0,1
4970     ELSE
4980       IDRAW 0,-.5
4990       IMOVE 0,.5
5000     END IF
5010   NEXT J
5020 NEXT I
5030 FOR I=20 TO 0 STEP -1
5040   DRAW -50,B(I)
5050   IF 2*INT(I/2)=I THEN
5060     IDRAW D,0
5070     IMOVE -D,0
5080   ELSE
5090     IDRAW C,0
5100     IMOVE -C,0
5110   END IF
5120 NEXT I
5130 MOVE -50,-10
5140 FOR I=0 TO 3
5150   FOR J=1 TO 9
5160     DRAW 25*LGT(J*10^I)-50,-10
5170     IF J=1 THEN
5180       IDRAW 0,1
5190       IDRAW 0,-2
5200       IMOVE 0,1
5210     ELSE
5220       IDRAW 0,.5
5230       IDRAW 0,-1
5240       IMOVE 0,.5
5250     END IF
5260   NEXT J
5270 NEXT I
5280 MOVE 50,20
5290 DRAW 50,40
5300 DRAW -50,40
5310 DRAW -50,20
5320 CSIZE 3,.6

```



```
5330 MOVE -50,-44
5340 LABEL VAL$(1)
5350 FOR I=1 TO 4
5360     MOVE A(I)-3,-44
5370     LABEL VAL$(10^I)
5380 NEXT I
5390 CSIZE 4,.6
5400 MOVE -5,-48
5410 LABEL "CYCLE"
5420 CSIZE 3,.6
5430 LDIR 90
5440 MOVE -58,-36
5450 IDRAW 0,3
5460 IDRAW -1.5,-1.5
5470 IDRAW 1.5,-1.5
5480 MOVE -57,-32
5490 LABEL "Ep(X 10  )"
5500 IMOVE -3.5,13
5510 LABEL "--"
5520 MOVE -58,-3
5530 IDRAW 0,3
5540 IDRAW -1.5,-1.5
5550 IDRAW 1.5,-1.5
5560 MOVE -57,1
5570 IF Contr_variable=1 THEN
5580     LABEL "E/2(X 10  )"
5590     IMOVE -3.5,14.6
5600     LABEL "--"
5610 ELSE
5620     LABEL "S/2 (MPa)"
5630 END IF
5640 LDIR -90
5650 MOVE 59,16
5660 IDRAW 0,-3
5670 IDRAW 1.5,1.5
5680 IDRAW -1.5,1.5
5690 MOVE 59,12
5700 IF Contr_variable=1 THEN
5710     LABEL "E/2(X 10  )"
5720     IMOVE 3.5,-14.6
5730     LABEL "--"
5740 ELSE
5750     LABEL "S/2 (MPa)"
5760 END IF
5770 MOVE 59,-16
5780 IDRAW 0,-3
5790 IDRAW 1.5,1.5
5800 IDRAW -1.5,1.5
5810 MOVE 59,-20
5820 LABEL "Ep(X 10  )"
5830 IMOVE 3.5,-13
5840 LABEL "--"
5850 LDIR 0
5860 CSIZE 3.5,.6
```

```

5870 MOVE -45,34
5880 LABEL Material$
5890 MOVE -45,30
5900 LABEL "ISOLCF"
5910 MOVE -45,26
5920 LABEL "Frequency= "&VAL$(Frequency)&" Hz"
5930 IF Contr_variable=1 THEN
5940     MOVE 15,34
5950     LABEL "STRESS CONTROL"
5960     MOVE 15,31
5970     IDRAW 3,0
5980     IDRAW -1.5,1.5
5990     IDRAW -1.5,-1.5
6000     MOVE 19,30
6010     LABEL "S = "&VAL$(Span*2)&" (MPa)"
6020 ELSE
6030     MOVE 15,34
6040     LABEL "STRAIN CONTROL"
6050     MOVE 15,31
6060     IDRAW 3,0
6070     IDRAW -1.5,1.5
6080     IDRAW -1.5,-1.5
6090     MOVE 19,30
6100     LABEL "E = "&VAL$(Span*2)
6110 END IF
6120 MOVE 19,26
6130 LABEL "R = "&VAL$(DROUND((Mean-Span)/(Mean+Span),2))
6140 SUBEND
6150!-----
6160 SUB Init_read(Frequency,Pace,Cycle_per_block,Data_per_cycle,Ref_count)
6170 Ref_count=(Cycle_per_block*Data_per_cycle*2)-1
6180 Pace=INT(1.E+6/(Data_per_cycle*2*Frequency))-30      !Pace in usec
6190 SUBEND
6200!-----
6210 SUB Plot_data(Contr_variable,Scale,Span,Gauge,Gauge_factor,Cycle,Next_cycle,Ref_count,Scan(*),Exponent,Expo,Min,Mini)
6220 ALPHA OFF
6230 GRAPHICS ON
6240 CSIZE 3,.6
6250 Start=0
6260 Stop=399
6270 Indice=1
6280 Transfer:
6290     Next_cycle=INT(Cycle*1.25)
6300     IF Next_cycle=Cycle THEN Next_cycle=Cycle+1
6310     IF Contr_variable=1 THEN Indice=0
6320     FOR I=Start+74 TO Start+124 STEP 2
6330         J=I+Indice
6340         IF Scan(J)*.005>Max THEN Maximum=Scan(J)*.005
6350         IF Scan(J+200)*.005<Min THEN Minimum=Scan(J+200)*.005
6360         IF ABS(Scan(J+50))*0.005<.10 THEN Maxim=Scan(J+50)*.005
6370         IF ABS(Scan(J+250))*0.005<.10 THEN Minim=Scan(J+250)*.005
6380     NEXT I

```

```

6390     Range=Maximum-Minimum
6400     Ep_range=Scan(Maxim+1)-Scan(Minim+1)
6410     Load_scale=INT(Scale)/100
6420     Strain_scale=Scale-(Load_scale*100)
6430     IF Cycle>1 THEN GOTO Data
6440     CALL Scale_frame(Contr_variable,Scale,Gauge,Gauge_factor,Range,Ep_range,
Min,Mini,Exponent,Expo)
6450 Data: !
6460     X=25*LGT(Cycle)-50
6470     IF Contr_variable=1 THEN
6480         Strain_ampli=Range*Strain_scale*Gauge_factor/(Gauge*20)
6490         Y1=4*(Strain_ampli*(10^Exponent)-Min)
6500     ELSE
6510         Stress_ampli=Range*Load_scale*216.078/2
6520         Y1=.2*(Stress_ampli-Min)
6530     END IF
6540     MOVE X-.7,3*Y1-11.3
6550     LABEL "x"
6560     Ep=Ep_range*Strain_scale*Gauge_factor/(Gauge*10)
6570     MOVE X-.7,12*(Ep*(10^Expo)-Mini)-41.3
6580     LABEL "x"
6590 Enough: !
6600     Cycle=Cycle+1
6610     Start=Stop+1
6620     Stop=Stop+400
6630     IF Stop>Ref_count THEN GOTO Out
6640     IF Cycle<Next_cycle THEN GOTO Enough
6650     GOTO Transfer
6660 Out: !
6670     Cycle=Cycle-1
6680     SUBEND
6690!
-----
6700     SUB Scale_frame(Contr_variable,Scale,Gauge,Gauge_factor,Range,Ep_range,Min,Mini,Exponent,Expo)
6710     Load_scale=INT(Scale)/100
6720     Strain_scale=Scale-(Load_scale*100)
6730     IF Contr_variable=1 THEN
6740         Strain_ampli=Range*Strain_scale*Gauge_factor/(Gauge*20)
6750         FOR Multiplier=0 TO 5
6760             IF Strain_ampli*10^Multiplier>1 AND Strain_ampli*10^Multiplier<10 TH
EN Exponent=Multiplier
6770             NEXT Multiplier
6780             A=Strain_ampli*10^Exponent
6790             IF A<2.5 THEN
6800                 Min=0.
6810             ELSE
6820                 IF A<5.0 THEN
6830                     Min=2.5
6840                 ELSE
6850                     IF A<7.5 THEN
6860                         Min=5.0
6870                     ELSE
6880                         Min=7.5
6890                     END IF

```

```

6900         END IF
6910     END IF
6920 ELSE
6930     Stress_ampli=Range*Load_scale*216.078/2
6940     Norme=INT(Stress_ampli/100)*100
6950     A=Stress_ampli-Norme
6960     IF A<25 THEN
6970         Min=Norme
6980         IF A<12.5 THEN Min=Norme-25
6990     ELSE
7000         IF A<50 THEN
7010             Min=Norme+25
7020             IF A<37.5 THEN Min=Norme
7030         ELSE
7040             IF A<75 THEN
7050                 Min=Norme+50
7060                 IF A<62.5 THEN Min=Norme+25
7070             ELSE
7080                 Min=Norme+75
7090                 IF A<77.5 THEN Min=Norme+50
7100             END IF
7110         END IF
7120     END IF
7130 END IF
7140 Ep=Ep_range*Strain_scale*Gauge_factor/(Gauge*10)
7150 FOR Multiplier=0 TO 5
7160     IF Ep*10^Multiplier>1 AND Ep*10^Multiplier<10 THEN Expo=Multiplier
7170 NEXT Multiplier
7180 A=Ep*10^Expo
7190 IF A<2.5 THEN
7200     Mini=0.
7210 ELSE
7220     IF A<5.0 THEN
7230         Mini=2.5
7240     ELSE
7250         IF A<7.5 THEN
7260             Mini=5.0
7270         ELSE
7280             Mini=7.5
7290         END IF
7300     END IF
7310 END IF
7320 CSIZE 3,.5
7330 FOR I=0 TO 8 STEP 2.
7340     MOVE -56,3*I-41
7350     LABEL USING "D.D";(.25*I+Mini)
7360     MOVE 51,3*I-41
7370     LABEL USING "D.D";(.25*I+Mini)
7380 NEXT I
7390 A$="3D"
7400 Facto=5
7410 IF Contr_variable=1 THEN
7420     A$="D.D"
7430     Facto=.50

```

```
7440 END IF
7450 FOR I=2 TO 10 STEP 2
7460     MOVE -56,3*I-11.5
7470     LABEL USING A$;(Facto*I+Min)
7480     MOVE 51,3*I-11.5
7490     LABEL USING A$;(Facto*I+Min)
7500 NEXT I
7510 CSIZE 3,.6
7520 LDIR 90
7530 MOVE -57,-32
7540 IMOVE -.5,16
7550 LABEL USING "D";Expo
7560 IF Contr_variable=1 THEN
7570     MOVE -57,1
7580     IMOVE -1,16.6
7590     LABEL USING "D";Exponent
7600     LDIR -90
7610     MOVE 59,12
7620     IMOVE .5,-16.6
7630     LABEL USING "D";Exponent
7640 END IF
7650 LDIR -90
7660 MOVE 59,-20
7670 IMOVE .5,-14
7680 LABEL USING "D";Expo
7690 LDIR 0
7700 SUBEND
```

```

10! *****
20! *
30! *          PROGRAM THERMAL_STRAINS          *
40! *          *****                          *
50! *
60! *          THIS PROGRAM PERFORMS THE REAL-TIME CONTROL AND DATA          *
70! *          ACQUISITION OF THERMAL STRAINS TESTS MEASUREMENTS.          *
80! *
90! *          THE MICRO_DATA_TRACK MUST BE PROGRAMMED FOR 180 sec          *
100! *          PERIOD (1/3 cpm).
110! *
120! *          THE CYCLIC THERMAL STRAINS ARE MEASURED BY CYCLING THE          *
130! *          TEMPERATURE AT ZERO STRESS.
140! *
150! *****
160 !
170 OPTION BASE 0
180 CALL Read_param(Material$,Mode,Scale,Mean,Span,Gauge)
190 DELSUB Read_param
200 CALL Thermal_strain(Material$,Mode,Scale,Mean,Span,Gauge)
210 END
220! *****
230! *****
240 !
250 SUB Thermal_strain(Material$,Mode,Scale,Mean,Span,Gauge)
260 ALLOCATE Load(4095),Strain(4095),Temp1(4095),Temp2(4095),Temp3(4095)
270 MASS STORAGE IS ":HPB290X,700,1"
280 !
290 !-----DEFINE I/O CARD FUNCTION-----
300 !
310 ASSIGN @Dvm TO 720
320 ASSIGN @Multi TO 723
330 ASSIGN @Disc TO "MRZ"
340 Disc_drive=0
350 Dvm=720
360 Multi=723
370 Scanner=0
380 A_to_d=3
390 Memory1=7
400 D_to_a1=10
410 Timer=11
420 D_to_a2=12
430 Memory2=13
440 !
450 !-----DEFAULT VALUES FOR THE PARAMETERS-----
460 !
470 Start=1                                !Start channel
480 Stop=5                                  !Stop channel
490 Pointer=20479                            !Interrupt word(4906*5)
500 IF Mode=1 THEN
510     ALLOCATE Pot(1)
520 ELSE
530     ALLOCATE Pot(809)
540 END IF

```

```

550      !
560      !-----INITIALIZE THE MULTI-----!
570      !
580      CALL Init_multi(@Multi,@Disc)
590      CALL Init_mem(@Multi,Memory1)
600      !
610      !-----SET INTERRUPT BRANCH FOR TRIGGER SIGNAL-----!
620      !
630      Cycle=1                      !Set cycle counter
640      G=SPOLL(723)                  !Clear Multi SRQ
650      P=SPOLL(720)                  !Clear DVM SRQ
660      BEEP
670      PRINT USING 680
680      IMAGE 20/,15X,"REMOVE CONTROL AND UTILITY PAC DISCS.",2/,15X,"INSERT ONE F
LOPPY(in right disc) FOR "
690      PRINT USING 700
700      IMAGE 1/,15X,"DATA STORAGE.  PRESS K0 TO CONTINUE."
710      ON KEY 0 LABEL "**CONTINUE**" GOTO 730
720 Spin: GOTO Spin
730      BEEP
740      OFF KEY
750      CREATE BDAT "Thermal",1,100
760      ASSIGN @Disc TO "Thermal"
770      OUTPUT @Disc;Material$, "THERMAL_STRAIN",Mode,Scale,Mean,Span,Gauge
780      ASSIGN @Disc TO *
790      PRINT USING 800
800      IMAGE 20/,25X,"PROGRAM AND START THE LEPEL",2/,20X,"****WAITING FOR A TRIG
GER SIGNAL****"
810      PRINT USING 820
820      IMAGE 5/,15X,"*****  THERMAL STRAINS MEASUREMENT IN PROGRESS  *****"
830      OUTPUT @Dvm;"F1R-2N5Z0"          !Set DVM range
840      OUTPUT @Dvm;"T2D3 TMF TEST"      !Set ext trigger and display
850      OUTPUT @Dvm;"KM01"              !Set mask for Data Ready
860      ON INTR 7,2 GOTO Start_tmf      !Set interrupt branch
870      ENABLE INTR 7;2                 !Enable interrupt SRQ
880      ENTER Dvm;P
890      !
900      !-----START CYCLING AND TAKING DATA-----!
910      !
920 Start_tmf:      !
930      BEEP
940      OUTPUT @Multi;"SC,0,0,0,0T"      !Reset Clock of Multi
950      !
960      !-----READ DATA-----!
970      !
980      CALL Read_data(@Multi,@Dvm,Multi,Dvm,Scanner,Memory1,Mode,Load(*),Strain(*
),Pot(*),Temp1(*),Temp2(*),Temp3(*))
990      !
1000     !-----STORE DATA-----!
1010     !
1020     CALL Store_data(@Multi,@Disc,Disc_drive,Mode,Cycle,Scale,Load(*),Strain(*
),Pot(*),Temp1(*),Temp2(*),Temp3(*))
1030     !
1040     !-----DISPLAY DATA-----!

```

```

1050 ! -----
1060 CALL Plot_data(Material$,Scale,Span,Gauge,Cycle,Load(*),Strain(*),Temp1(*)
,Temp2(*),Temp3(*))
1070 !
1080 !-----SET INTERRUPT FOR SYNCHRO. SIGNAL-----
1090 !
1100 IF Cycle<9 THEN
1110     Increment=2
1120     GOTO Synchro
1130 END IF
1140 Cycle2=INT(Cycle*1.25)
1150 Increment=Cycle2-Cycle
1160 !
1170 Synchro: !
1180 Waiting=Increment-1.5
1190 Cycle=Cycle+Increment !Update cycle counter
1200 WAIT (180*Waiting) !Set waiting time
1210 CALL Init_mem(@Multi,Memory1) !Reset memory card
1220 OUTPUT @Dvm;"T2KM01" !Ext. trigger and DVM mask
1230 ON INTR 7,2 GOTO 970 !Set interrupt branch
1240 ENABLE INTR 7;2 !Enable interrupt
1250 ENTER Dvm;P
1260 SUBEND
1270! -----
1280!
1290! *****
1300! * *
1310! * SUBROUTINES USED BY SUB TMFC6(Param1,Param2,...) *
1320! * *
1330! *****
1340!
1350! -----
1360!
1370 SUB Read_data(@Multi,@Dvm,Multi,Dvm,Scanner,Memory,Mode,Load(*),Strain(*)
,Pot(*),Temp1(*),Temp2(*),Temp3(*))
1380 ALLOCATE INTEGER Scan(20479)
1390 OUTPUT @Dvm;"T1M00"
1400 G=SPOLL(@Multi)
1410 ENTER 72310;A,B,C
1420 ON INTR 7,2 GOTO Interrupt
1430 ENABLE INTR 7;2
1440 OUTPUT @Multi;"CY",Scanner,"T" !Enable scanner
1450 OUTPUT @Multi;"WF",Scanner+.3,5,"T" !Set sequential mode
1460 !
1470 OUTPUT @Multi;"WF",Scanner,1,"T" !Set start channel
1480 OUTPUT @Multi;"WF",Scanner+.1,5,"T" !set stop channel
1490 OUTPUT @Multi;"WF",Scanner+.2,8759,"T" !Set pace(40 us)
1500 Prog_diff(@Multi,Memory,0) !Reset diff. counter
1510 Prog_write(@Multi,Memory,0) !Reset write pointer
1520 OUTPUT @Multi;"CC";Memory,"T" !Clear Memory card
1530 Prog_mode(@Multi,Memory,56) !Set FIFO mode
1540 Prog_ref1(@Multi,Memory,20479) !Set stop pointer
1550 OUTPUT @Multi;"AC";Memory;"T" !Armed memory card
1560 OUTPUT @Multi;"CY",Scanner,"T" !Start pacer

```



```

1570     IF Mode=1 THEN GOTO Wait
1580     FOR I=0 TO 809                                !If require read
1590         ENTER @Dvm;Pot(I)                        !potential change
1600     NEXT I                                        !with temperature
1610 Wait:  GOTO Wait
1620 Interrupt:  !
1630     BEEP
1640     G=SPOLL(@Multi)
1650     IF G=64 THEN
1660         ENTER 72310;A,B,C
1670         IF C<>0 THEN
1680             ENTER 72312;Address
1690             IF Address<>Memory THEN
1700                 PRINT "NOT MEMORY CARD"
1710                 PAUSE
1720             END IF
1730             OUTPUT @Multi;"WF",Scanner+.2,0,"T"    !Stop scanner
1740             Prog_mode(@Multi,Memory,76)           !Set FIFO lockout
1750             OUTPUT @Multi;"MR";Memory;20480;"T"   !MR command to get data
1760             ENTER 72305 USING "%,W";Scan(*)       !Entering the data
1770             FOR K=0 TO 20479 STEP 5
1780                 J=INT(K/5)
1790                 Strain(J)=Scan(K)*.005
1800                 Load(J)=Scan(K+1)*.005
1810                 Temp1(J)=Scan(K+2)*.005
1820                 Temp2(J)=Scan(K+3)*.005
1830                 Temp3(J)=Scan(K+4)*.005
1840             NEXT K
1850             ENABLE INTR 7;2
1860         ELSE
1870             BEEP 2000,.3
1880             PRINT "          *** SRQ NOT SET BY ARMED CARD   ***"
1890             PAUSE
1900         END IF
1910     ELSE
1920         BEEP 2000,.3
1930         PRINT "          *** MULTI DID NOT INTERRUPT   ***"
1940         PAUSE
1950     END IF
1960     DEALLOCATE Scan(*)
1970     OUTPUT @Multi;"RC"                            !Read Real-time clock
1980     SUBEND
1990! -----
2000     SUB Store_data(@Multi,@Disc,Disc_drive,Mode,Cycle,Scale,Load(*),Strain(*)
,Pot(*),Temp1(*),Temp2(*),Temp3(*))
2010     !
2020     FOR I=0 TO 4095
2030         Temp1(I)=(Temp1(I))+Temp2(I)+Temp3(I))/3
2040         Temp2(I)=(Load(I)+10)*1000+(Strain(I)+10)/100
2050     NEXT I
2060     ON ERROR GOTO Recover
2070     MASS STORAGE IS ":HP8290X,700,0"
2080     CREATE BDAT "CYCLE"&VAL$(Cycle),15,5000
2090     ASSIGN @Disc TO "CYCLE"&VAL$(Cycle)

```

```

2100 IF Mode=1 THEN
2110   OUTPUT @Disc;Cycle,Scale,Temp1(*),Temp2(*)
2120 ELSE
2130   OUTPUT @Disc;Cycle,Scale,Temp1(*),Temp2(*),Pot(*)
2140 END IF
2150 ASSIGN @Disc TO *
2160 GOTO Out
2170 Recover:      IF ERRN=64 THEN MASS STORAGE IS ":HPB290X,700,1"
2180               GOTO 2080
2190 !
2200 Out: !
2210   SUBEND
2220!
-----
2230 SUB Init_multi(@Multi,@Disc)
2240   CLEAR 7
2250   WAIT 4.0
2260   G=SPOLL(@Multi)
2270   IF G<>64 THEN
2280     PRINT "      ***MULTI DID NOT INTERRUPT***"
2290     PAUSE
2300   END IF
2310   STATUS @Multi,3;Multi
2320   ENTER Multi*100+10;A
2330   IF A<>16384 THEN
2340     PRINT "      ***SELF TEST DID NOT SET SRQ***"
2350     PAUSE
2360   END IF
2370   ALLOCATE Ascii$[80]
2380   ON END @Disc GOTO Eof
2390 Rd_file:   ENTER @Disc;Ascii$
2400   OUTPUT @Multi;Ascii$
2410   GOTO Rd_file
2420 Eof: OFF END @Disc
2430   ASSIGN @Disc TO *
2440   DEALLOCATE Ascii$
2450   MASS STORAGE IS ":HPB290X,700,0"
2460 SUBEND
2470!
-----
2480 SUB Init_mem(@Multi,Memory)
2490   Prog_mode(@Multi,Memory,254)
2500   Prog_mode(@Multi,Memory,54)
2510   Prog_ref1(@Multi,Memory,1048575)
2520   Prog_ref2(@Multi,Memory,0)
2530   Prog_read(@Multi,Memory,0)
2540   Prog_diff(@Multi,Memory,0)
2550   Prog_write(@Multi,Memory,0)
2560   OUTPUT @Multi;"CC";Memory;"T"
2570 SUBEND
2580!
-----
2590 SUB Prog_read(@Multi,Memory,Read_pointer)
2600   Read_low=Read_pointer MOD 65536
2610   Read_high=Read_pointer DIV 65536
2620   Read_low_oct=FNDec_to_octal(Read_low)
2630   Read_high_oct=FNDec_to_octal(Read_high)

```

```

2640 OUTPUT @Multi;"WF";Memory+.1;22;Memory+.2;Read_low_oct;"T"
2650 OUTPUT @Multi;"WF";Memory+.1;23;Memory+.2;Read_high_oct;"T"
2660 SUBEND
2670!-----
2680 SUB Prog_write(@Multi,Memory,Write_pointer)
2690 Write_low=Write_pointer MOD 65536
2700 Write_high=Write_pointer DIV 65536
2710 Write_low_oct=FNDec_to_octal(Write_low)
2720 Write_high_oct=FNDec_to_octal(Write_high)
2730 OUTPUT @Multi;"WF";Memory+.1;24;Memory+.2;Write_low_oct;"T"
2740 OUTPUT @Multi;"WF";Memory+.1;25;Memory+.2;Write_high_oct;"T"
2750 SUBEND
2760!-----
2770 SUB Prog_diff(@Multi,Memory,Diff_counter)
2780 Diff_low=Diff_counter MOD 65536
2790 Diff_high=Diff_counter DIV 65536
2800 Diff_low_oct=FNDec_to_octal(Diff_low)
2810 Diff_high_oct=FNDec_to_octal(Diff_high)
2820 OUTPUT @Multi;"WF";Memory+.1;20;Memory+.2;Diff_low_oct;"T"
2830 OUTPUT @Multi;"WF";Memory+.1;21;Memory+.2;Diff_high_oct;"T"
2840 SUBEND
2850!-----
2860 SUB Prog_ref1(@Multi,Memory,Ref1_reg)
2870 Ref1_low=Ref1_reg MOD 65536
2880 Ref1_high=Ref1_reg DIV 65536
2890 Ref1_low_oct=FNDec_to_octal(Ref1_low)
2900 Ref1_high_oct=FNDec_to_octal(Ref1_high)
2910 OUTPUT @Multi;"WF";Memory+.1;26;Memory+.2;Ref1_low_oct;"T"
2920 OUTPUT @Multi;"WF";Memory+.1;27;Memory+.2;Ref1_high_oct;"T"
2930 SUBEND
2940!-----
2950 SUB Prog_ref2(@Multi,Memory,Ref2_reg)
2960 Ref2_low=Ref2_reg MOD 65536
2970 Ref2_high=Ref2_reg DIV 65536
2980 Ref2_low_oct=FNDec_to_octal(Ref2_low)
2990 Ref2_high_oct=FNDec_to_octal(Ref2_high)
3000 OUTPUT @Multi;"WF";Memory+.1;30;Memory+.2;Ref2_low_oct;"T"
3010 OUTPUT @Multi;"WF";Memory+.1;31;Memory+.2;Ref2_high_oct;"T"
3020 SUBEND
3030!-----
3040 SUB Prog_mode(@Multi,Memory,Mode)
3050 OUTPUT @Multi;"WF";Memory+.3;Mode;"T"
3060 SUBEND
3070!-----
3080 SUB Read_status(@Multi,Memory,Status)
3090 STATUS @Multi,3;Multi
3100 OUTPUT @Multi;"WF";Memory+.1;1;"T RV";Memory+.2;"T"
3110 ENTER Multi*100+6;Status
3120 SUBEND
3130!-----
3140 SUB Read_read(@Multi,Memory,Read_pointer)
3150 STATUS @Multi,3;Multi
3160 OUTPUT @Multi;"WF";Memory+.1;22;"T RV";Memory+.2;"T"
3170 ENTER Multi*100+6;Read_low_oct

```

```

3180  OUTPUT @Multi;"WF";Memory+.1;23;"T RV";Memory+.2;"T"
3190  ENTER Multi*100+6;Read_high_oct
3200  Read_low=FNOctal_to_dec(Read_low_oct)
3210  Read_high=FNOctal_to_dec(Read_high_oct)
3220  Read_pointer=65536*Read_high+Read_low
3230  SUBEND
3240! -----
3250  SUB Read_write(@Multi,Memory,Write_pointer)
3260  STATUS @Multi,3;Multi
3270  OUTPUT @Multi;"WF";Memory+.1;24;"T RV";Memory+.2;"T"
3280  ENTER Multi*100+6;Write_low_oct
3290  OUTPUT @Multi;"WF";Memory+.1;25;"T RV";Memory+.2;"T"
3300  ENTER Multi*100+6;Write_high_oct
3310  Write_low=FNOctal_to_dec(Write_low_oct)
3320  Write_high=FNOctal_to_dec(Write_high_oct)
3330  Write_pointer=65536*Write_high+Write_low
3340  SUBEND
3350! -----
3360  SUB Read_diff(@Multi,Memory,Diff_counter)
3370  STATUS @Multi,3;Multi
3380  OUTPUT @Multi;"WF";Memory+.1;20;"T RV";Memory+.2;"T"
3390  ENTER Multi*100+6;Diff_low_oct
3400  OUTPUT @Multi;"WF";Memory+.1;21;"T RV";Memory+.2;"T"
3410  ENTER Multi*100+6;Diff_high_oct
3420  Diff_low=FNOctal_to_dec(Diff_low_oct)
3430  Diff_high=FNOctal_to_dec(Diff_high_oct)
3440  Diff_counter=65536*Diff_high+Diff_low
3450  SUBEND
3460! -----
3470  DEF FNDec_to_octal(Dec)
3480  Oct=Dec+2*INT(Dec/8)+20*INT(Dec/64)+200*INT(Dec/512)+2000*INT(Dec/4096)+2
0000*INT(Dec/32768)+200000*INT(Dec/262144)
3490  RETURN Oct
3500  FNEND
3510! -----
3520  DEF FNOctal_to_dec(Octal)
3530  X9=0
3540  X7=Octal
3550  X=0
3560  More:  !
3570  X=X+(X7-INT(X7/10)*10)*8^X9
3580  X7=INT(X7/10)
3590  X9=X9+1
3600  IF X7<>0 THEN GOTO More
3610  RETURN X
3620  FNEND
3630! -----
3640  SUB Plot_data(Material$,Scale,Span,Gauge,Cycle,Load(*),Strain(*),Temp1(*),
Temp2(*),Temp3(*))
3650  ALLOCATE A(20),B(20)
3660  Load_range=INT(Scale)/100
3670  Strain_range=Scale-(Load_range*100)
3680  Conv_fac=216.078
3690  Emax=.05555*Strain_range/Gauge.

```

```
3700 FOR I=0 TO 20
3710   A(I)=-50+I*50/9
3720   B(I)=-40+I*2.5
3730 NEXT I
3740 DEG
3750 GINIT
3760 GRAPHICS ON
3770 GCLEAR
3780 ALPHA OFF
3790 FRAME
3800 WINDOW -66.7224080268,66.7224080268,-50,50
3810 MOVE -50,-40
3820 FOR I=0 TO 18
3830   DRAW A(I),-40
3840   IDRAW 0,1
3850   IMOVE 0,-1
3860 NEXT I
3870 C=1.
3880 D=.5
3890 FOR I=0 TO 20
3900   DRAW 50,B(I)
3910   IF 2*INT(I/2)=I THEN
3920     IDRAW -D,0
3930     IMOVE D,0
3940   ELSE
3950     IDRAW -C,0
3960     IMOVE C,0
3970   END IF
3980 NEXT I
3990 DRAW 50,40
4000 DRAW -50,40
4010 DRAW -50,10
4020 FOR I=20 TO 0 STEP -1
4030   DRAW -50,B(I)
4040   IF 2*INT(I/2)=I THEN
4050     IDRAW D,0
4060     IMOVE -D,0
4070   ELSE
4080     IDRAW C,0
4090     IMOVE -C,0
4100   END IF
4110 NEXT I
4120 MOVE -50,-15
4130 FOR I=0 TO 18
4140   DRAW A(I),-15
4150   IDRAW 0,1
4160   IDRAW 0,-2
4170   IMOVE 0,1
4180 NEXT I
4190 MOVE -50,10
4200 FOR I=0 TO 18
4210   DRAW A(I),10
4220   IDRAW 0,-1
4230   IMOVE 0,1
```

```

4240 NEXT I
4250 MOVE 10,10
4260 DRAW 10,40
4270 MOVE -40,25
4280 FOR I=0 TO 20 STEP 2
4290     DRAW (-40+I),25
4300     IDRAW 0,.5
4310     IDRAW 0,-1
4320     IMOVE 0,.5
4330 NEXT I
4340 MOVE -30,15
4350 FOR I=0 TO 20 STEP 2
4360     DRAW -30,15+I
4370     IDRAW .5,0
4380     IDRAW -1,0
4390     IMOVE .5,0
4400 NEXT I
4410 CSIZE 3,.6
4420 MOVE -50,-40
4430 FOR I=2 TO 17 STEP 2
4440     MOVE A(I)-3,-43
4450     LABEL VAL$(I*10)
4460 NEXT I
4470 FOR I=1 TO 10 STEP 2
4480     MOVE 50.5,B(I)-1.5
4490     LABEL USING "S.D";.2*I-1.0
4500     MOVE -55,B(I)-1.5
4510     LABEL USING "S.D";.2*I-1.0
4520 NEXT I
4530 FOR I=11 TO 20 STEP 2
4540     MOVE -58,B(I)-1.5
4550     LABEL VAL$((I-15)*100)
4560 NEXT I
4570 FOR I=11 TO 20 STEP 2
4580     MOVE 51.5,B(I)-1.5
4590     LABEL VAL$(70*(I-10)+300)
4600 NEXT I
4610 CSIZE 4,.6
4620 MOVE -20,-48
4630 LABEL "TIME (sec)"
4640 CSIZE 3,.6
4650 LDIR 90
4660 MOVE -56,-35
4670 LABEL "Etot (%)"
4680 LDIR -90
4690 MOVE 58,-20
4700 LABEL "Etot (%)"
4710 LDIR 90
4720 MOVE -58,-14
4730 LABEL "STRESS (MPa)"
4740 LDIR -90
4750 MOVE 58,10
4760 LABEL "TEMPERATURE (C)"
4770 CSIZE 3.5,.6

```

```

4780 LDIR 0
4790 MOVE 15,32
4800 LABEL Material$
4810 MOVE 15,29
4820 LABEL "Thermal Strain"
4830 MOVE 20,26
4840 LABEL "Analysis"
4850 MOVE 15,23
4860 LABEL "Tmax= 926 C"
4870 MOVE 15,20
4880 LABEL "Tmin= 400 C"
4890 MOVE 15,17
4900 LABEL "CYCLE #"&VAL$(Cycle)
4910 CSIZE 3,.6
4920 MOVE -15,29
4930 DRAW -13,29
4940 DRAW -14,30
4950 DRAW -15,29
4960 MOVE -12,28
4970 LABEL "S= "&VAL$(2*Span)&"MPa"
4980 MOVE -15,32
4990 LABEL "STRESS CONTROL"
5000 MOVE -15,24
5010 LABEL "X-DIV=0.05%"
5020 MOVE -15,20
5030 LABEL "Y-DIV=100 MPa"
5040 MOVE -50,-2.5
5050 FOR I=0 TO 4095
5060 B1=(((Load(I)*Load_range*Conv_fac)+500)/40)-15
5070 A1=(I*100/4095)-50
5080 DRAW A1,B1
5090 NEXT I
5100 MOVE -50,-2.5
5110 FOR I=0 TO 4095
5120 B1=2.5*(Temp1(I)*1000-300)/70-15
5130 A1=(I*100/4095)-50
5140 DRAW A1,B1
5150 NEXT I
5160 MOVE -50,-27.5
5170 FOR I=0 TO 4095
5180 B1=((1.5*Strain(I)*Emax/10)+.01)*1250-40 !Plot thermal strain
5190 A1=(I*100/4095)-50
5200 DRAW A1,B1
5210 NEXT I
5220 A1=((1.5*Strain(0)*Emax/10)+.0025)*4000-40
5230 B1=(((Load(0)*Range*Conv_fac)+500)/50)+15
5240 MOVE A1,B1
5250 FOR I=1 TO 4095 STEP 5
5260 A1=((1.5*Strain(I)*Emax/10)+.0025)*4000-40 !Plot hysteresis loop
5270 B1=(((Load(I)*Range*Conv_fac)+500)/50)+15
5280 DRAW A1,B1
5290 NEXT I
5300 SUBEND
5310!
-----

```

```

5320 SUB Read_param(Material$,Mode,Scale,Mean,Span,Gauge)
5330 OPTION BASE 0
5340 ALLOCATE Dummy${40},Dummy1${80}
5350 Dummy$="*****"
5360 Dummy1$="*****"
5370 !
5380 PRINT USING 5440;Dummy1$
5390 PRINT USING 5400
5400 IMAGE 2/,20X,"ENTER TYPE OF ALLOY (10 Characters max)"
5410 BEEP
5420 INPUT Material$
5430 !
5440 IMAGE 2/,80A
5450 PRINT USING 5440;Dummy1$
5460 PRINT USING 5470
5470 IMAGE 2/,20X,"ENTER MODE OF TESTING",/,25X,"1. LCF (Initiation)",/,25X,"2.
CRACK PROPAGATION (Propagation)"
5480 BEEP
5490 INPUT Mode_of_testing
5500 IF Mode_of_testing<>1 AND Mode_of_testing<>2 THEN
5510 PRINT USING 5520
5520 IMAGE 2/,20X,"UNDEFINED MODE OF TESTING. Please re-enter"
5530 BEEP 3000,1.0
5540 GOTO 5460
5550 ELSE
5560 END IF
5570 !
5580 PRINT USING 5440;Dummy1$
5590 PRINT USING 5600
5600 IMAGE 2/,20X,"ENTER CONTROL VARIABLE?",/,25X,"1. LOAD CONTROL",/,25X,"2. S
TRAIN CONTROL"
5610 BEEP
5620 INPUT Contr_variable
5630 IF Contr_variable<>1 AND Contr_variable<>2 THEN
5640 PRINT USING 5650
5650 IMAGE 2/,20X,"UNDEFINED CONTROL VARIABLE. Please re-enter"
5660 BEEP 3000,1.0
5670 GOTO 5590
5680 ELSE
5690 END IF
5700 !
5710 IF Contr_variable=1 THEN
5720 PRINT USING 5440;Dummy1$
5730 PRINT USING 5740
5740 IMAGE 2/,20X,"ENTER LOAD SCALE? (100,50,20 or 10 %)"
5750 BEEP
5760 INPUT Load_scale
5770 Load_scale=Load_scale
5780 IF Load_scale<>100 AND Load_scale<>50 AND Load_scale<>20 AND Load_scal
e<>10 THEN
5790 PRINT USING 5800
5800 IMAGE 2/,20X,"Undefined value. Please re-enter."
5810 BEEP 3000,1.0
5820 GOTO 5730
5830 ELSE

```



```

5840     END IF
5850 ! -----
5860     PRINT USING 5440;Dummy1$
5870     PRINT USING 5880
5880     IMAGE 2/,20X, "ENTER MEAN STRESS (in MPa)?"
5890     BEEP
5900     INPUT Mean
5910     IF (Mean*11.569896)<=-(250*Load_scale) OR Mean>=(250*Load_scale) THEN
5920         PRINT USING 5930
5930         IMAGE 2/,20X, "VALUE OUT-OF-BOUND. Please re-enter."
5940         BEEP 3000,1.0
5950         GOTO 5870
5960     ELSE
5970     END IF
5980 ! -----
5990     PRINT USING 5440;Dummy1$
6000     PRINT USING 6010
6010     IMAGE 2/,20X, "ENTER STRESS AMPLITUDE (in MPa)"
6020     BEEP
6030     INPUT Span
6040     IF Span<=0 THEN
6050         PRINT USING 6060
6060         IMAGE 2/,20X, "UNDEFINED VALUE. Please re-enter"
6070         BEEP 3000,1.0
6080         GOTO 6000
6090     ELSE
6100         IF (ABS(Mean)+Span)*11.569896>=250*Load_scale THEN
6110             PRINT USING 6120
6120             IMAGE 2/,20X, "VALUE OUT-OF-BOUND, Please re-enter"
6130             BEEP 3000,1.0
6140             GOTO 6000
6150         ELSE
6160         END IF
6170     END IF
6180 ! -----
6190     PRINT USING 5440;Dummy1$
6200     PRINT USING 6210
6210     IMAGE 2/,20X, "ENTER THE GAUGE LENGTH (in inch)"
6220     BEEP
6230     INPUT Gauge_length
6240     IF Gauge_length<.400 OR Gauge_length>.6 THEN
6250         PRINT USING 6260
6260         IMAGE 2/,20X, "GAUGE LENGHT VALUE OUT-OF-BOUND. Please re-enter."
6270         BEEP 3000,1.0
6280         GOTO 6200
6290     ELSE
6300     END IF
6310 ! -----
6320     PRINT USING 5440;Dummy1$
6330     PRINT USING 6340
6340     IMAGE 2/,20X, "ENTER STRAIN SCALE (100,50,20 or 10 %)"
6350     BEEP
6360     INPUT Strain_scale
6370     Strain_scale=Strain_scale/100

```

```

6380     IF Strain_scale<>1. AND Strain_scale<>.5 AND Strain_scale<>.2 AND Stra
in_scale<>.1 THEN
6390         PRINT USING 6400
6400         IMAGE 2/,20X,"UNDEFINED VALUE. Please re-enter."
6410         BEEP 3000,1.0
6420         GOTO 6330
6430     ELSE
6440     END IF
6450 !-----
6460     ELSE
6470 !-----
6480         PRINT USING 5440;Dummy1$
6490         PRINT USING 6500
6500         IMAGE 2/,20X,"ENTER STRAIN SCALE (100,50,20 or 10 %)"
6510         BEEP
6520         INPUT Strain_scale
6530         Strain_scale=Strain_scale/100
6540         IF Strain_scale<>1. AND Strain_scale<>.5 AND Strain_scale<>.2 AND Stra
in_scale<>.1 THEN
6550             PRINT USING 6560
6560             IMAGE 2/,20X, "Undefined value. Please re-enter"
6570             BEEP 3000,1.0
6580             GOTO 6490
6590         ELSE
6600         END IF
6610 !-----
6620         PRINT USING 5440;Dummy1$
6630         PRINT USING 6640
6640         IMAGE 2/,20X,"ENTER THE GAUGE LENGHT (in inch)"
6650         BEEP
6660         INPUT Gauge_lenght
6670         IF Gauge_lenght<.4 OR Gauge_lenght>.6 THEN
6680             PRINT USING 6690
6690             IMAGE 2/,20X,"GAUGE LENGHT VALUE OUT-OF-BOUND. Please re-enter."
6700             BEEP 3000,1.0
6710             GOTO 6630
6720         ELSE
6730         END IF
6740 !-----
6750         PRINT USING 5440;Dummy1$
6760         Emax=.05493*Strain_scale/Gauge_lenght
6770         PRINT USING 6780
6780         IMAGE 2/,20X,"ENTER MEAN STRAIN (in %)"
6790         BEEP
6800         INPUT Mean
6810         Mean=Mean/100
6820         IF Mean<=-Emax OR Mean>=Emax THEN
6830             PRINT USING 6840
6840             IMAGE 2/,20X,"VALUE OUT-OF-BOUND. Please re-enter"
6850             BEEP 3000,1.0
6860             GOTO 6770
6870         ELSE
6880         END IF
6890 !-----
6900         PRINT USING 5440;Dummy1$

```

```

6910     PRINT USING 6920
6920     IMAGE 2/,20X,"ENTER STRAIN AMPLITUDE (in %)"
6930     BEEP
6940     INPUT Span
6950     Span=Span/100
6960     IF Span<=0 THEN
6970         PRINT USING 6980
6980         IMAGE 2/,20X,"UNDEFINED VALUE. Please re-enter."
6990         BEEP 3000,1.0
7000         GOTO 6910
7010     ELSE
7020         IF (ABS(Mean)+Span)>=Emax THEN
7030             PRINT USING 7040
7040             IMAGE 2/,20X,"VALUE OUT-OF-BOUND. Please re-enter."
7050             BEEP 3000,1.0
7060             GOTO 6770
7070         ELSE
7080             END IF
7090     END IF
7100     ! -----
7110     PRINT USING 5440;Dummy1$
7120     PRINT USING 7130
7130     IMAGE 2/,20X,"ENTER LOAD SCALE (100,50,20 or 10%)"
7140     BEEP
7150     INPUT Load_scale
7160     Load_scale=Load_scale
7170     IF Load_scale<>100 AND Load_scale<>50 AND Load_scale<>20 AND Load_s
cale<>10 THEN
7180         PRINT USING 7190
7190         IMAGE 2/,20X,"UNDEFINED VALUE. Please re-enter"
7200         BEEP 3000,1.0
7210         GOTO 7120
7220     ELSE
7230         END IF
7240     END IF
7250     Continue: !
7260     Scale=Load_scale+Strain_scale
7270     Gauge=Gauge_lenght
7280     Mode=Mode_of_testing
7290     PRINT USING 5440;Dummy1$
7300     BEEP 800,2
7310     PRINT USING "/,20X,K";"** PROGRAM THE Micro_Data Track **"
7320     !
7330     SUBEND

```

```

10! *****
20! *
30! *          PROGRAM FCP          *
40! *          *****            *
50! *
60! *    THIS PROGRAM PERFORMS THE REAL-TIME CONTROL AND DATA *
70! *    ACQUISITION OF FATIGUE CRACK GROWTH TESTS.           *
80! *
90! *    THE CYCLIC DATA(Stresses and potentials) ARE         *
100! *    RECORDED EVERY 5 CYCLES.                               *
110! *
120! *****
130! !
140! OPTION BASE 0
150! CALL Read_param(Material$,Scale,Mean,Span,Frequency)
160! !DELSUB Read_param
170! CALL Fcp(Material$,Scale,Mean,Span,Frequency)
180! END
190! *****
200! *****
210! !
220! SUB Fcp(Material$,Scale,Mean,Span,Frequency)
230! MASS STORAGE IS ":HP8290X,700,1"
240! !
250! !-----DEFINE I/O CARD FUNCTION-----!
260! !
270! ASSIGN @Multi TO 723
280! ASSIGN @Dvm TO 720
290! ASSIGN @Disc TO "MRZ"
300! Disc_drive=0
310! Multi=723
320! Scanner=0
330! A_to_d=3
340! Memory1=7
350! D_to_a1=10
360! Timer=11
370! D_to_a2=12
380! Memory2=13
390! !
400! !-----DEFAULT VALUES FOR THE PARAMETERS-----!
410! !-----!
420! Start=2                                !Start channel
430! Stop=2                                  !Stop channel
440! Cycle_per_block=1
450! Data_per_cycle=200
460! IF Frequency>=20. THEN
470!     Increment=249
480! ELSE
490!     IF Frequency>=10 THEN
500!         Increment=149
510!     ELSE
520!         IF Frequency>=1 THEN
530!             Increment=49
540!         ELSE

```

```

550         Increment=4
560         IF Increment>=.1 THEN Increment=9
570     END IF
580 END IF
590 END IF
600 !
610 !-----INITIALIZE THE MULTI-----!
620 !
630 CALL Init_multi(@Multi,@Disc)
640 CALL Init_mem(@Multi,Memory1)
650 !
660 !
670 !-----INITIALIZE READING PROCEDURE-----!
680 !-----!
690 CALL Init_read(Cycle_per_block,Data_per_cycle,Frequency,Pace1,Pace2,Ref_co
unt)
700 ALLOCATE Scan(Ref_count),Pot(Ref_count)
710 !-----!
720 BEEP
730 Cycle=1 !Set cycle counter
740 Next_cycle=Cycle+Increment !Set Next_cycle counter
750 G=SPOLL(723) !Clear Multi SRQ
760 PRINT USING 770
770 IMAGE 20/,15X,"REMOVE CONTROL AND UTILITY PAC DISCS",2/,15X,"INSERT TWU DI
SCS FOR DATA STORAGE",2/,15X,"PRESS K0(Continue) TO CONTINUE"
780 ON KEY 0 LABEL "**CONTINUE**" GOTO 800
790 Spin: GOTO Spin
800 OFF KEY
810 CREATE BDAT "TEST_PARAM",1,100
820 ASSIGN @Disc TO "TEST_PARAM"
830 OUTPUT @Disc;Material$, "FCP",Scale,Mean,Span,Frequency
840 ASSIGN @Disc TO *
850 CALL Plot_frame(Material$,Scale,Mean,Span,Frequency,Max)
860 !DELSUB Plot_frame
870 PRINT USING 880
880 IMAGE 20/,25X,"MULTIPROGRAMMER IS READY",2/,20X,"***WAITING FOR THE S
TART COMMAND***"
890 ON KEY 0 LABEL " START CYCLING" GOTO Start_fcp
900 Wait: GOTO Wait
910 !
920 !-----START CYCLING AND TAKING DATA-----!
930 !-----!
940 Start_fcp:!
950 OFF KEY
960 Vmax1=0
970 !-----* CONTROL PROCEDURE-----!
980 !-----!
990 OUTPUT @Dvm;"F1R-2N4T1Z0D3 *FCP*"
1000 CALL Init_control(@Multi,Memory2,Timer,D_to_ai,Scale,Mean,Span,Frequency,N
data,Pace,Paces)
1010 !
1020 !-----READ DATA-----!
1030 !-----!
1040 OUTPUT @Multi;"WF",Timer+.2,0,"T"

```

```

1050 IF Frequency>.185 THEN OUTPUT @Multi;"WF",Timer,Paces,"T"
1060 OUTPUT @Multi;"WF",Timer+.2,1,"T"
1070 CALL Read_data(@Multi,@Dvm,Frequency,Timer,Pace,Paces,Scanner,Memory1,Pace
1,Pace2,Ref_count,Scan(*),Pot(*))
1080 !-----DISPLAY DATA-----
1090 !-----
1100 CALL Plot_data(Frequency,Max,Cycle,Pot(*),Vo,Vmax)
1110 Vmax2=Vmax
1120 !
1130 !-----STORE DATA-----
1140 !-----
1150 CALL Store_data(@Disc,Disc_drive,Cycle,Scan(*),Pot(*),Vmax1,Vmax2)
1160 !
1170 !-----SET WAITING FOR SYNCHRO. SIGNAL-----
1180 !-----
1190 Synchro:
1200 OUTPUT @Multi;"WF",Timer+.2,0,"T" !Stop cycling
1210 OUTPUT @Multi;"RC" !Read real-time clock(T2)
1220 ENTER 72314;A1,B1,C1,D1 !Enter real-time clock(T1)
1230 ENTER 72314;A2,B2,C2,D2 !Enter real-time clock(T2)
1240 T1=60*(A1*60*24+B1*60+C1)+D1
1250 T2=60*(A2*60*24+B2*60+C2)+D2
1260 Time_delay=T2-T1 !Compute elapsed time
1270 Wait_time=Increment/Frequency !Wait between read data
1280 IF Wait_time<Time_delay THEN
1290 Cycle=INT(Cycle+1.5+Time_delay*Frequency)
1300 Next_cycle=Cycle+Increment
1310 OUTPUT @Multi;"WF",Timer+.2,1,"T" !Set continuous mode
1320 Vmax1=Vmax2
1330 GOTO 1030
1340 ELSE
1350 Cycle=Next_cycle
1360 Next_cycle=Cycle+Increment+INT(Time_delay*Frequency+.5)
1370 Waitime=Wait_time
1380 Vmax1=Vmax2
1390 OUTPUT @Multi;"WF",Timer+.2,1,"T" !Set continuous mode
1400 OUTPUT @Multi;"CY",Timer,"T" !Resume cycling
1410 WAIT Waitime !Wait next read data
1420 GOTO 1030
1430 END IF
1440 SUBEND
1450!-----

```

```

1460!
1470! *****
1480! *
1490! *          SUBROUTINES USED BY SUB FCP(Param1,Param2,...)          *
1500! *
1510! *****
1520!
1530!
-----
1540 SUB Init_control(@Multi,Memory,Timer,D_to_a,Scale,Mean,Span,Frequency,Ndat
a,Pace,Paces)
1550  !__GENERATE WAVEFORM__
1560  ! -----
1570  Load_scale=INT(Scale)/100
1580  Pmean=Mean/(Load_scale*216.078)      !Convert MPA into voltage
1590  Pmax=Span/(Load_scale*216.078)      !Convert MPa into voltage
1600  Coeff=800
1610  IF Pmax>5.12 THEN Coeff=400
1620  Ndata=INT(Coeff*Pmax+.5)-1
1630  ALLOCATE A(Ndata)
1640  Ndata2=INT(Ndata/4+.5)
1650  Ndata3=Ndata-Ndata2
1660  FOR I=0 TO Ndata2-1
1670    A(I)=Pmax*I/(Ndata2-1)
1680    A(I+Ndata3)=Pmax*(I/(Ndata2-1)-1)
1690  NEXT I
1700  FOR I=Ndata2 TO Ndata3
1710    A(I)=(Ndata-1-2*I)*Pmax/(Ndata+1-2*Ndata2)
1720  NEXT I
1730  !
1740  !__CALCULATE THE PACE__
1750  ! -----
1760  Time_int=1/(Ndata*Frequency)
1770  Pace=INT(Time_int*500000)/1000      !Pace in msec
1780  Paces=Pace
1790  IF Frequency>.185 THEN Paces=INT(500000/(Ndata*.185))/1000
1800  !
1810  !__PROGRAM MULTI__AMPLITUDE
1820  ! -----
1830  OUTPUT @Multi;"CC",Memory+1,"T"      !Clear memory card
1840  OUTPUT @Multi;"SF",Memory,3,1,.005,12,"T" !Set format(LSB=0.005)
1850  OUTPUT @Multi;"WF",Memory+1.0,Ndata,"T" !Truncate memory
1860  OUTPUT @Multi;"MD",Memory,A(*),"T"      !Load data into memory
1870  OUTPUT @Multi;"WF",Memory+.1,10,"T"      !Set re-circulate mode
1880  OUTPUT @Multi;"WF",Timer+.2,1,"T"      !Set timer for continuous
1890  OUTPUT @Multi;"WF",Timer,Pace,"T"      !output. Set Pace
1900  !
1910  !__PROGRAM MULTI-- MEAN
1920  ! -----
1930  Incr=.005
1940  IF Pmean=0 THEN GOTO 2020
1950  IF Pmean<0 THEN Incr=-.005
1960  J=0
1970  OUTPUT @Multi;"OP",D_to_a,J,"T"
1980  IF ABS(J)<ABS(Pmean) THEN

```

```

1990      J=J+Incr
2000      GOTO 1970
2010      END IF
2020      DEALLOCATE A(*)
2030      SUBEND
2040!
-----
2050      SUB Read_data(@Multi,@Dvm,Frequency,Timer,Pace,Paces,Scanner,Memory,Pace1,
Pace2,Ref_count,Scan(*),Pot(*))
2060      G=SPOLL(@Multi)
2070      ENTER 72310;A,B,C,D,E,F
2080      ON INTR 7 GOTO Interrupt          !Set interrupt branch
2090      ENABLE INTR 7;2                  !Enable Interrupt
2100      OUTPUT @Multi;"CY",Scanner,"T"  !Enable scanner
2110      OUTPUT @Multi;"WF",Scanner+.3,S,"T" !Set sequential mode
2120      !
2130      OUTPUT @Multi;"WF",Scanner,2,"T" !Set start channel
2140      OUTPUT @Multi;"WF",Scanner+.1,2,"T" !set stop channel
2150      OUTPUT @Multi;"WF",Scanner+.2,Pace1,"T" !Set pace(in usec)
2160      Prog_diff(@Multi,Memory,0)      !Reset diff. counter
2170      Prog_write(@Multi,Memory,0)     !Reset write pointer
2180      OUTPUT @Multi;"CC";Memory,"T"   !Clear Memory card
2190      Prog_mode(@Multi,Memory,56)     !Set FIFO mode
2200      Prog_ref1(@Multi,Memory,Ref_count) !Set stop pointer
2210      OUTPUT @Multi;"AC";Memory;"T"   !Armed memory card
2220      OUTPUT @Multi;"SC,0,0,0,0T"     !Reset clock
2230      OUTPUT @Multi;"CY",Timer,"T"    !Start cycling
2240      OUTPUT @Multi;"CY",Scanner,"T"   !Start pacer
2250      FOR I=0 TO Ref_count
2260          ENTER @Dvm;Pot(I)           !Read potential
2270          WAIT Pace2
2280      NEXT I
2290      Spin: GOTO Spin
2300      Interrupt: !
2310          OUTPUT @Multi;"WF",Timer+.2,0,"T" !Check pace
2320          OUTPUT @Multi;"RC"           !Read real-time clock(T1)
2330          IF Frequency>.185 THEN OUTPUT @Multi;"WF",Timer,Pace,"T"
2340          OUTPUT @Multi;"WF",Timer+.2,1,"T" !Set continuous mode
2350          OUTPUT @Multi;"CY",Timer,"T" !Continue cycling
2360          G=SPOLL(@Multi)
2370          IF G=64 THEN
2380              ENTER 72310;A,B,C
2390              IF C<>0 THEN
2400                  ENTER 72312;Address
2410                  IF Address<>Memory THEN
2420                      PRINT "NOT MEMORY CARD"
2430                      PAUSE
2440                  END IF
2450                  OUTPUT @Multi;"WF",Scanner+.2,0,"T" !Stop scanner
2460                  Prog_mode(@Multi,Memory,76) !Set FIFO lockout
2470                  OUTPUT @Multi;"MR";Memory;Ref_count+1;"T"!MR command to get data
2480                  ENTER 72305 USING "%,W";Scan(*) !Entering the data
2490              ELSE
2500                  BEEP 2000,.3
2510                  PRINT "          *** SRQ NOT SET BY ARMED CARD ***"

```



```

2520         PAUSE
2530         END IF
2540         ELSE
2550             BEEP 2000,.3
2560             PRINT "             *** MULTI DID NOT INTERRUPT ***"
2570             PAUSE
2580         END IF
2590     SUBEND
2600!-----
2610 SUB Store_data(@Disc,Disc_drive,Cycle,Scan(*),Pot(*),Vmax1,Vmax2)
2620 ON ERROR GOTO Recover
2630 IF ABS(Vmax2-Vmax1)*1000<.005 THEN GOTO Out
2640 CREATE BDAT "CYCLE"&VAL$(Cycle),1,4000
2650 ASSIGN @Disc TO "CYCLE"&VAL$(Cycle)
2660 OUTPUT @Disc;Cycle,Scan(*),Pot(*)
2670 ASSIGN @Disc TO *
2680 GOTO Out
2690 !
2700 Recover: !
2710     IF ERRN=59 OR ERRN=64 THEN
2720         IF Disc_drive=0 THEN
2730             Disc_drive=1
2740             MASS STORAGE IS ":HPB290X,700,1"
2750         ELSE
2760             Disc_drive=0
2770             MASS STORAGE IS ":HPB290X,700,0"
2780         END IF
2790     ELSE
2800         BEEP 2000,1
2810         PRINT USING 2820;ERRN
2820         IMAGE 2/,25X,"ERROR NUMBER ",K,/,25X,"CHECK STORAGE UNIT",/,25X,"PROG
RAM ABORTED"
2830         PAUSE
2840         END IF
2850         GOTO 2640
2860 Out: !
2870     SUBEND
2880!-----
2890 SUB Init_multi(@Multi,@Disc)
2900     CLEAR 7
2910     WAIT 4.0
2920     G=SPOLL(@Multi)
2930     IF G<>64 THEN
2940         PRINT "             ***MULTI DID NOT INTERRUPT***"
2950         PAUSE
2960     END IF
2970     STATUS @Multi,3;Multi
2980     ENTER Multi*100+10;A
2990     IF A<>16384 THEN
3000         PRINT "             ***SELF TEST DID NOT SET SRQ***"
3010         PAUSE
3020     END IF
3030     ALLOCATE Ascii$(80)
3040     ON END @Disc GOTO Eof

```

```

3050 Rd_file:   ENTER @Disc;Ascii$
3060   OUTPUT @Multi;Ascii$
3070   GOTO Rd_file
3080 Eof: OFF END @Disc
3090   ASSIGN @Disc TO *
3100   DEALLOCATE Ascii$
3110   MASS STORAGE IS ":HPB290X,700,0"
3120 SUBEND
3130! -----
3140 SUB Init_mem(@Multi,Memory)
3150   Prog_mode(@Multi,Memory,254)
3160   Prog_mode(@Multi,Memory,54)
3170   Prog_ref1(@Multi,Memory,1048575)
3180   Prog_ref2(@Multi,Memory,0)
3190   Prog_read(@Multi,Memory,0)
3200   Prog_diff(@Multi,Memory,0)
3210   Prog_write(@Multi,Memory,0)
3220   OUTPUT @Multi;"CC";Memory;"T"
3230 SUBEND
3240! -----
3250 SUB Prog_read(@Multi,Memory,Read_pointer)
3260   Read_low=Read_pointer MOD 65536
3270   Read_high=Read_pointer DIV 65536
3280   Read_low_oct=FNDec_to_octal(Read_low)
3290   Read_high_oct=FNDec_to_octal(Read_high)
3300   OUTPUT @Multi;"WF";Memory+.1;22;Memory+.2;Read_low_oct;"T"
3310   OUTPUT @Multi;"WF";Memory+.1;23;Memory+.2;Read_high_oct;"T"
3320 SUBEND
3330! -----
3340 SUB Prog_write(@Multi,Memory,Write_pointer)
3350   Write_low=Write_pointer MOD 65536
3360   Write_high=Write_pointer DIV 65536
3370   Write_low_oct=FNDec_to_octal(Write_low)
3380   Write_high_oct=FNDec_to_octal(Write_high)
3390   OUTPUT @Multi;"WF";Memory+.1;24;Memory+.2;Write_low_oct;"T"
3400   OUTPUT @Multi;"WF";Memory+.1;25;Memory+.2;Write_high_oct;"T"
3410 SUBEND
3420! -----
3430 SUB Prog_diff(@Multi,Memory,Diff_counter)
3440   Diff_low=Diff_counter MOD 65536
3450   Diff_high=Diff_counter DIV 65536
3460   Diff_low_oct=FNDec_to_octal(Diff_low)
3470   Diff_high_oct=FNDec_to_octal(Diff_high)
3480   OUTPUT @Multi;"WF";Memory+.1;20;Memory+.2;Diff_low_oct;"T"
3490   OUTPUT @Multi;"WF";Memory+.1;21;Memory+.2;Diff_high_oct;"T"
3500 SUBEND
3510! -----
3520 SUB Prog_ref1(@Multi,Memory,Ref1_reg)
3530   Ref1_low=Ref1_reg MOD 65536
3540   Ref1_high=Ref1_reg DIV 65536
3550   Ref1_low_oct=FNDec_to_octal(Ref1_low)
3560   Ref1_high_oct=FNDec_to_octal(Ref1_high)
3570   OUTPUT @Multi;"WF";Memory+.1,26;Memory+.2;Ref1_low_oct;"T"
3580   OUTPUT @Multi;"WF";Memory+.1,27;Memory+.2;Ref1_high_oct;"T"
3590 SUBEND

```

```

3600!
-----
3610 SUB Prog_ref2(@Multi,Memory,Ref2_reg)
3620   Ref2_low=Ref2_reg MOD 65536
3630   Ref2_high=Ref2_reg DIV 65536
3640   Ref2_low_oct=FNDec_to_octal(Ref2_low)
3650   Ref2_high_oct=FNDec_to_octal(Ref2_high)
3660   OUTPUT @Multi;"WF";Memory+.1;30;Memory+.2;Ref2_low_oct;"T"
3670   OUTPUT @Multi;"WF";Memory+.1;31;Memory+.2;Ref2_high_oct;"T"
3680 SUBEND
3690!
-----
3700 SUB Prog_mode(@Multi,Memory,Mode)
3710   OUTPUT @Multi;"WF";Memory+.3;Mode;"T"
3720 SUBEND
3730!
-----
3740 SUB Read_status(@Multi,Memory,Status)
3750   STATUS @Multi,3;Multi
3760   OUTPUT @Multi;"WF";Memory+.1;1;"T RV";Memory+.2;"T"
3770   ENTER Multi*100+6;Status
3780 SUBEND
3790!
-----
3800 SUB Read_read(@Multi,Memory,Read_pointer)
3810   STATUS @Multi,3;Multi
3820   OUTPUT @Multi;"WF";Memory+.1;22;"T RV";Memory+.2;"T"
3830   ENTER Multi*100+6;Read_low_oct
3840   OUTPUT @Multi;"WF";Memory+.1;23;"T RV";Memory+.2;"T"
3850   ENTER Multi*100+6;Read_high_oct
3860   Read_low=FNOctal_to_dec(Read_low_oct)
3870   Read_high=FNOctal_to_dec(Read_high_oct)
3880   Read_pointer=65536*Read_high+Read_low
3890 SUBEND
3900!
-----
3910 SUB Read_write(@Multi,Memory,Write_pointer)
3920   STATUS @Multi,3;Multi
3930   OUTPUT @Multi;"WF";Memory+.1;24;"T RV";Memory+.2;"T"
3940   ENTER Multi*100+6;Write_low_oct
3950   OUTPUT @Multi;"WF";Memory+.1;25;"T RV";Memory+.2;"T"
3960   ENTER Multi*100+6;Write_high_oct
3970   Write_low=FNOctal_to_dec(Write_low_oct)
3980   Write_high=FNOctal_to_dec(Write_high_oct)
3990   Write_pointer=65536*Write_high+Write_low
4000 SUBEND
4010!
-----
4020 SUB Read_diff(@Multi,Memory,Diff_counter)
4030   STATUS @Multi,3;Multi
4040   OUTPUT @Multi;"WF";Memory+.1;20;"T RV";Memory+.2;"T"
4050   ENTER Multi*100+6;Diff_low_oct
4060   OUTPUT @Multi;"WF";Memory+.1;21;"T RV";Memory+.2;"T"
4070   ENTER Multi*100+6;Diff_high_oct
4080   Diff_low=FNOctal_to_dec(Diff_low_oct)
4090   Diff_high=FNOctal_to_dec(Diff_high_oct)
4100   Diff_counter=65536*Diff_high+Diff_low
4110 SUBEND
4120!
-----

```

```

4120!
4130 DEF FNDec_to_octal(Dec)
4140   Oct=Dec+2*INT(Dec/8)+20*INT(Dec/64)+200*INT(Dec/512)+2000*INT(Dec/4096)+2
0000*INT(Dec/32768)+200000*INT(Dec/262144)
4150   RETURN Oct
4160 FNEND
4170!
4180 DEF FNOctal_to_dec(Octal)
4190   X9=0
4200   X7=Octal
4210   X=0
4220 More:   !
4230   X=X+(X7-INT(X7/10)*10)*8^X9
4240   X7=INT(X7/10)
4250   X9=X9+1
4260   IF X7<>0 THEN GOTO More
4270   RETURN X
4280 FNEND
4290!
4300 SUB Plot_frame(Material$,Scale,Mean,Span,Frequency,Max)
4310 ALLOCATE A(20),B(20)
4320 IF Frequency>=10 THEN
4330   Max=7
4340 ELSE
4350   IF Frequency>=1 THEN
4360     Max=6
4370   ELSE
4380     IF Frequency>=.1 THEN
4390       Max=5
4400     ELSE
4410       Max=4
4420     END IF
4430   END IF
4440 END IF
4450 FOR I=0 TO Max
4460   A(I)=(100/Max)*I-50
4470 NEXT I
4480 FOR I=0 TO 20
4490   B(I)=3*I-40
4500 NEXT I
4510 DEG
4520 BINIT
4530 BCLEAR
4540 ALPHA ON
4550 GRAPHICS OFF
4560 FRAME
4570 WINDOW -66.7224080268,66.7224080268,-50,50
4580 LDIR 0
4590 C=.75
4600 D=1.5
4610 MOVE -50,-40
4620 FOR I=0 TO Max-1
4630   FOR J=2 TO 10 STEP 2
4640     DRAW (100/Max)*LGT(J*10^I)-50,-40
4650     IF J=10 THEN

```

```

4660         IDRAW 0,D
4670         IMOVE 0,-D
4680     ELSE
4690         IDRAW 0,C
4700         IMOVE 0,-C
4710     END IF
4720     NEXT J
4730     NEXT I
4740     FOR I=0 TO 20
4750         DRAW 50,B(I)
4760         IF 2*INT(I/2)=I THEN
4770             IDRAW -D,0
4780             IMOVE D,0
4790         ELSE
4800             IDRAW -C,0
4810             IMOVE C,0
4820         END IF
4830     NEXT I
4840     FOR I=Max-1 TO 0 STEP -1
4850         FOR J=10 TO 2 STEP -2
4860             DRAW (100/Max)*LBT(J*10^I)-50,20
4870             IF J=10 THEN
4880                 IDRAW 0,-D
4890                 IMOVE 0,D
4900             ELSE
4910                 IDRAW 0,-C
4920                 IMOVE 0,C
4930             END IF
4940         NEXT J
4950     NEXT I
4960     FOR I=20 TO 0 STEP -1
4970         DRAW -50,B(I)
4980         IF 2*INT(I/2)=I THEN
4990             IDRAW D,0
5000             IMOVE -D,0
5010         ELSE
5020             IDRAW C,0
5030             IMOVE -C,0
5040         END IF
5050     NEXT I
5060     MOVE 50,20
5070     DRAW 50,40
5080     DRAW -50,40
5090     DRAW -50,20
5100     CSIZE 3,.6
5110     MOVE -50,-43
5120     LABEL USING "D";1
5130     FOR I=1 TO Max
5140         MOVE A(I)+1,-43
5150         LABEL USING "D";I
5160         IMOVE -3,1
5170         LABEL USING "DD";10
5180     NEXT I
5190     FOR I=0 TO 18 STEP 2

```

```

5200     MOVE -56,3*I-41
5210     LABEL USING "D.D";I/4
5220     MOVE 51,3*I-41
5230     LABEL USING "D.D";I/4
5240     NEXT I
5250     CSIZE 4,.6
5260     MOVE -5,-49
5270     LABEL "CYCLE"
5280     CSIZE 3,.6
5290     LDIR 90
5300     MOVE -58,-13
5310     IDRAW 0,3
5320     IDRAW -1.5,-1.5
5330     IDRAW 1.5,-1.5
5340     MOVE -57,-9
5350     LABEL "V/Vo"
5360     LDIR -90
5370     MOVE 59,-4
5380     IDRAW 0,-3
5390     IDRAW 1.5,1.5
5400     IDRAW -1.5,1.5
5410     MOVE 59,-8
5420     LABEL "V/Vo"
5430     LDIR 0
5440     CSIZE 3.5,.6
5450     MOVE -45,34
5460     LABEL Material$
5470     MOVE -45,30
5480     LABEL "FCP"
5490     MOVE -45,26
5500     LABEL "Frequency= "&VAL$(Frequency)&" Hz"
5510     MOVE 15,34
5520     LABEL "STRESS CONTROL"
5530     MOVE 15,31
5540     IDRAW 3,0
5550     IDRAW -1.5,1.5
5560     IDRAW -1.5,-1.5
5570     MOVE 19,30
5580     LABEL "S = "&VAL$(Span*2)&" (MPa)"
5590     MOVE 19,26
5600     LABEL "R = "&VAL$(DROUND((Mean-Span)/(Mean+Span),2))
5610     SUBEND
5620! -----
5630     SUB Init_read(Cycle_per_block,Data_per_cycle,Frequency,Pace1,Pace2,Ref_cou
nt)
5640     Ref_count=(Cycle_per_block*Data_per_cycle)-1
5650     IF Frequency>=.185 THEN
5660         Pace1=INT(1.E+6/(Data_per_cycle*.185)-30)           !Pace in usec
5670         Pace2=0.
5680     ELSE
5690         Pace1=INT(1.E+6/(Data_per_cycle*Frequency)-30)       !Pace in usec
5700         Pace2=DROUND((1/Frequency-1/37)/200,3)
5710     END IF
5720     SUBEND

```

```

5730! -----
5740 SUB Plot_data(Frequency,Max,Cycle,Pot(*),Vo,Vmax)
5750 ALPHA OFF
5760 GRAPHICS ON
5770 CSIZE 3,.6
5780 Maximum=0
5790 FOR J=37 TO 62
5800     IF Pot(J)>Maximum THEN Maximum=Pot(J)
5810 NEXT J
5820     Vmax=Maximum
5830 Vmax=.55
5840     IF Cycle>1 THEN GOTO Data
5850     Vo=Vmax
5860     MOVE -50,0
5870 Data: !
5880     X=(100/Max)*LGT(Cycle)-50
5890     DRAW X,12*(Vmax/Vo)-40
5900     SUBEND
5910! -----
5920 SUB Read_param(Material$,Scale,Mean,Span,Frequency)
5930 ALLOCATE Dummy$(40),Dummy1$(80)
5940 Dummy$="*****"
5950 Dummy1$="*****"
*****
5960 IMAGE 2/,80A
5970 !
5980 PRINT USING 5960;Dummy1$
5990 IMAGE 2/,80A
6000 PRINT USING 6010
6010 IMAGE 2/,20X,"ENTER TYPE OF ALLOY (10 Characters max)"
6020 BEEP
6030 INPUT Material$
6040     PRINT USING 5960;Dummy1$
6050     PRINT USING 6060
6060     IMAGE 2/,20X,"ENTER LOAD SCALE? (100,50,20 or 10 %)"
6070     BEEP
6080     INPUT Load_scale
6090     Load_scale=Load_scale
6100     IF Load_scale<>100 AND Load_scale<>50 AND Load_scale<>20 AND Load_scal
e<>10 THEN
6110         PRINT USING 6120
6120         IMAGE 2/,20X,"Undefined value. Please re-enter."
6130         BEEP 3000,1.0
6140         GOTO 6050
6150     ELSE
6160     END IF
6170     PRINT USING 5960;Dummy1$
6180     PRINT USING 6190
6190     IMAGE 2/,20X, "ENTER MEAN STRESS (in MPa)?"
6200     BEEP
6210     INPUT Mean
6220     IF (Mean*11.569896)<=-(250*Load_scale) OR Mean>=(250*Load_scale) THEN
6230         PRINT USING 6240
6240         IMAGE 2/,20X,"VALUE OUT-OF-BOUND. Please re-enter."

```

```

6250      BEEP 3000,1.0
6260      GOTO 6180
6270      ELSE
6280      END IF
6290      PRINT USING 5960;Dummy1$
6300      PRINT USING 6310
6310      IMAGE 2/,20X, "ENTER STRESS AMPLITUDE (in MPa)"
6320      BEEP
6330      INPUT Span
6340      IF Span<=0 THEN
6350          PRINT USING 6360
6360          IMAGE 2/,20X, "UNDEFINED VALUE. Please re-enter"
6370          BEEP 3000,1.0
6380          GOTO 6300
6390      ELSE
6400          IF (ABS(Mean)+Span)*11.569896>=250*Load_scale THEN
6410              PRINT USING 6420
6420              IMAGE 2/,20X, "VALUE OUT-OF-BOUND, Please re-enter"
6430              BEEP 3000,1.0
6440              GOTO 6300
6450          ELSE
6460          END IF
6470      END IF
6480      PRINT USING 5960;Dummy1$
6490      PRINT USING 6500
6500      IMAGE 2/,20X, "ENTER THE FREQUENCY (in Hz)"
6510      BEEP
6520      INPUT Frequency
6530      PRINT USING 6540;Frequency
6540      IMAGE 2/,25X, "INPUTTED Frequency IS ",K, " Hz",/
6550      PRINT USING 6560
6560      IMAGE 30X, "1. CONTINUE",/,30X, "2. CHANGE THE FREQUENCY"
6570      BEEP
6580      INPUT Change
6590      IF Change<>1 AND Change<>2 THEN
6600          PRINT USING 6610
6610          IMAGE /,30X, "Incorrect value. Please re-enter"
6620          BEEP 3000,1.0
6630          GOTO 6550
6640      END IF
6650      IF Change=2 THEN GOTO 6490
6660      GOTO Continue
6670      !
6680      Continue: !
6690      Scale=Load_scale
6700      PRINT USING 5960;Dummy1$
6710      BEEP 800,2
6720      PRINT USING "/,20X,K,/,30X,K"; "*** PROGRAM THE Micro_Data Track **", "IF REQ
UIRED"
6730      !
6740      SUBEND

```



```

10      !           PROGRAM DATA_ANALYSIS
20      !
30      ! This program analyses the data obtained from isothermal
40      ! and thermal-mechanical fatigue tests. It analyses the
50      ! potential signal and the corresponding hysteresis loop.
60      ! The (potential vs cycles) curve is first obtained. Then
70      ! the fatigue crack growth rates are derived and plotted.
80      ! The cyclic stress and strain hardening curves are also
90      ! obtained and stored in memory.
100     !
110     DUMP DEVICE IS 701,EXPANDED
120     OPTION BASE 0
130     COM Load(359),Strain(359),Pot(359),Temp(359),X(359),Y(359)
140     COM /Param/ Crack(999),Cycles(999),Range,INTEGER Cycle,W,Z,Nmax
150     COM /Time/ A$[10]
160     ALLOCATE Stress_max(999),Stress_min(999)
170     INTEGER Option
180     Material$="HASTELLOY-X"
190     Tmax$="401"
200     Tmin$="399"
210     Range$="0.50"
220     Counter=-1
230     Cycle=-3
240     W=0
250     MASS STORAGE IS ":HPB290X,700,0"
260     PRINTER IS 1
270     PRINT " "
280     PRINT " "
290     PRINT "      Enter one of the following options:"
300     PRINT "                1. manual entering"
310     PRINT "                2. automatic entering"
320     INPUT Option
330     PRINT " "
340     PRINT " "
350     PRINT "      Enter the final cycle number"
360     INPUT Nmax
370     PRINT " "
380     PRINT " "
390     PRINT "      DO YOU WANT A GRAPHICS DISPLAY OF THE"
400     PRINT "      CYCLIC DATA? Y/N "
410     INPUT B$
420     IF Cycle>=Nmax THEN GOTO 770
430     IF Option=1 THEN
440         PRINT " "
450         PRINT " "
460         PRINT "      Enter Cycle number?"
470         INPUT Cycle
480     ELSE
490         Cycle=Cycle+4
500     END IF
510     IF B$="N" OR B$="n" THEN
520         CALL Read_data
530         CALL Pot_time(Stress_max(*),Stress_min(*),Counter)
540     ELSE

```

```

550     CALL Read_data
560     CALL Plot(Material$,Range$,Tmax$,Tmin$)
570     CALL Pot_time(Stress_max(*),Stress_min(*),Counter)
580     WAIT 2.0
590     ALPHA ON
600     GRAPHICS OFF
610     PRINT " "
620     PRINT " "
630     PRINT "     DO YOU WANT A PRINTED COPY OF THE"
640     PRINT "     PREVIOUS DISPLAY?  Y/N"
650     INPUT B1$
660     IF B1$="Y" OR B1$="y" THEN
670         ALPHA OFF
680         GRAPHICS ON
690         DUMP GRAPHICS #701
700         PRINTER IS 701
710         PRINT CHR$(12)
720         PRINTER IS 1
730     ELSE
740     END IF
750 END IF
760 GOTO 420
770 PRINTER IS 1
780 CALL Volt_time(Material$,Range$,Tmax$,Tmin$,Stress_max(*),Stress_min(*),Counter)
790 CALL Fcgr(Material$,Range$,Tmax$,Tmin$,Stress_max(*),Stress_min(*),Counter)
800 CALL Store_dadn(Stress_max(*),Stress_min(*),Counter)
810 !
820 GRAPHICS OFF
830 PRINT " "
840 PRINT " "
850 PRINT "     PLEASE ENTER TYPE OF FCGR CURVE"
860 PRINT "         1. da/dN = f(K-stress)"
870 PRINT "         2. da/dN = f(K-strain)"
880 PRINT "         3. da/dN = f(J)"
890 PRINT "         4. da/dN = f(COD)"
900 INPUT A1
910 IF A1=1 OR A1=2 THEN
920     IF A1=1 THEN
930         LOADSUB ALL FROM "STRESS_INT"
940         CALL Stress_int
950         DELSUB Stress_int
960     ELSE
970         LOADSUB ALL FROM "STRAIN_INT"
980         CALL Strain_int
990         DELSUB Strain_int
1000    END IF
1010 ELSE
1020     IF A1=3 THEN
1030         LOADSUB ALL FROM "J_INTEGRAL"
1040         CALL J_integral
1050         DELSUB J_integral
1060     ELSE
1070         LOADSUB ALL FROM "DEL_COD"

```

```

1080          CALL Cod
1090          DELSUB Cod
1100          END IF
1110 END IF
1120 PRINT " "
1130 PRINT " "
1140 PRINT "      DO YOU WANT TO CONTINUE?"
1150 PRINT "          Y/N"
1160 INPUT B$
1170 IF B$="Y" THEN
1180     GOTO 820
1190 ELSE
1200     FOR I=0 TO 10
1210         PRINT " "
1220     NEXT I
1230     PRINT "          ****PROGRAM TERMINATED****"
1240 END IF
1250 END
1260! -----
1270 SUB Read_data
1280 OPTION BASE 0
1290 COM Load(359),Strain(359),Pot(359),Temp(359),X(359),Y(359)
1300 COM /Time/ A$[10]
1310 COM /Param/ Crack(999),Cycles(999),Range,INTEGER Cycle,W,Z,Nmax
1320 INTEGER Dummy
1330 IF Cycle>1 THEN GOTO 1420
1340 PRINT " "
1350 PRINT " "
1360 PRINT "      INSERT the floppies containing the data. Make sure"
1370 PRINT "      that floppy#1 is in the left drive, floppy #2 is in"
1380 PRINT "      the right drive, floppy#3 is in the left drive,"
1390 PRINT "      floppy#4 in the right drive, etc."
1400 ON KEY 0 LABEL "CONTINUE" GOTO Proceed
1410 Idle:      GOTO Idle
1420 Proceed:  !
1430     ON ERROR GOTO Recover
1440     !
1450     ASSIGN @Disc TO "CYCLE"&VAL$(Cycle)
1460     ENTER @Disc;Z,Dummy,Range,A$,X(*),Y(*)
1470     ASSIGN @Disc TO *
1480     FOR I=0 TO 359
1490         Load(I)=((INT(X(I))/1000)-10)
1500         Strain(I)=((X(I)-INT(X(I)))*100)-10
1510         Temp(I)=INT(Y(I))/1000
1520         Pot(I)=Y(I)-INT(Y(I))
1530     NEXT I
1540     BEEP
1550     GOTO End
1560 Recover: !
1570     IF ERRN=56 OR ERRN=64 THEN
1580         IF W=0 THEN
1590             W=1
1600             MASS STORAGE IS ":HP8290X,700,1"
1610             GOTO 1440

```

```

1620     ELSE
1630         W=0
1640         MASS STORAGE IS ":HP8290X,700,0"
1650         PRINT "    INSERT floppy#3 into left drive and"
1660         PRINT "    floppy#4 into right drive."
1670         ON KEY 0 LABEL "CONTINUE" GOTO 1440
1680     END IF
1690 ELSE
1700     PRINT " "
1710     PRINT " "
1720     PRINT "    ERROR NUMBER =";ERRN
1730     PRINT "    PLEASE CHECK STORAGE UNITS."
1740     PRINT "    PROGRAM TERMINATED."
1750     PAUSE
1760 END IF
1770 End:    !
1780 SUBEND
1790! -----
1800 SUB Plot(Material$,Range$,Tmax$,Tmin$)
1810 OPTION BASE 0
1820 COM Load(359),Strain(359),Pot(359),Temp(359),X(359),Y(359)
1830 COM /Time/ A$[10]
1840 COM /Param/ Crack(999),Cycles(999),Range,INTEGER Cycle,W,Z,Nmax
1850 DIM A(20),B(20)
1860 DEG
1870 GINIT
1880 GRAPHICS ON
1890 GCLEAR
1900 ALPHA OFF
1910 FRAME
1920 WINDOW -66.7224080268,66.7224080268,-50,50
1930 FOR I=0 TO 20
1940     A(I)=-50+I*50/9
1950     B(I)=-40+I*2.5
1960 NEXT I
1970 MOVE -50,-40
1980 FOR I=0 TO 18
1990     DRAW A(I),-40
2000     IDRAW 0,1
2010     IDRAW 0,-1
2020 NEXT I
2030 C=.5
2040 D=1
2050 FOR I=0 TO 20
2060     DRAW 50,B(I)
2070     IF I>=10 THEN
2080         C=1
2090         D=.5
2100     ELSE
2110     END IF
2120     IF 2*INT(I/2)=I THEN
2130         IDRAW -D,0
2140         IDRAW D,0
2150     ELSE

```

```

2160     IDRAW -C,0
2170     IDRAW C,0
2180     END IF
2190     NEXT I
2200     DRAW 50,40
2210     DRAW -50,40
2220     DRAW -50,10
2230     FOR I=20 TO 0 STEP -1
2240         DRAW -50,B(I)
2250         IF I<=10 THEN
2260             C=.5
2270             D=1.0
2280         ELSE
2290             END IF
2300         IF 2*INT(I/2)=I THEN
2310             IDRAW D,0
2320             IDRAW -D,0
2330         ELSE
2340             IDRAW C,0
2350             IDRAW -C,0
2360         END IF
2370     NEXT I
2380     MOVE -50,15
2390     FOR I=0 TO 18
2400         DRAW A(I),-15
2410         IDRAW 0,1
2420         IDRAW 0,-2
2430         IDRAW 0,1
2440     NEXT I
2450     MOVE -50,10
2460     FOR I=0 TO 18
2470         DRAW A(I),10
2480         IDRAW 0,-1
2490         IDRAW 0,1
2500     NEXT I
2510     MOVE 10,10
2520     DRAW 10,40
2530     MOVE -40,25
2540     FOR I=0 TO 20 STEP 2
2550         DRAW (-40+I),25
2560         IDRAW 0,.5
2570         IDRAW 0,-1
2580         IDRAW 0,.5
2590     NEXT I
2600     MOVE -30,15
2610     FOR I=0 TO 20 STEP 2
2620         DRAW -30,15+I
2630         IDRAW .5,0
2640         IDRAW -1,0
2650         IDRAW .5,0
2660     NEXT I
2670     CSIZE 3,.6
2680     MOVE -50,-40
2690     FOR I=2 TO 17 STEP 2

```

```

2700     MOVE A(I)-3,-43
2710     LABEL USING "K";(I*20)
2720     NEXT I
2730     Mini=Pot(0)
2740     Maxi=Pot(0)
2750     FOR I=1 TO 359
2760     IF Pot(I)>Maxi THEN Maxi=Pot(I)
2770     IF Pot(I)<Mini THEN Mini=Pot(I)
2780     NEXT I
2790     Min_scale=.8
2800     Factor=1.0
2810     IF Mini*1000>Min_scale THEN
2820         Min_scale=Min_scale+.5
2830         GOTO 2810
2840     END IF
2850     Min_scale=Min_scale-.5
2860     IF Maxi*1000>Min_scale+1.0 THEN Factor=Factor*2.0
2870     FOR I=0 TO 10 STEP 2
2880         MOVE -55,B(I)-1.5
2890         LABEL USING "K";Factor*.1*I+Min_scale
2900     NEXT I
2910     FOR I=1 TO 10 STEP 2
2920         MOVE 52,B(I)-1.5
2930         LABEL USING "S.D";I/10-.5
2940     NEXT I
2950     FOR I=11 TO 20 STEP 2
2960         MOVE 50.5,B(I)-1.5
2970         LABEL VAL$((I-15)*100)
2980         MOVE -58,B(I)-1.5
2990         LABEL VAL$((I-15)*100)
3000     NEXT I
3010     CSIZE 4,.6
3020     MOVE -20,-48
3030     LABEL "TIME (sec)"
3040     CSIZE 3,.6
3050     LDIR 90
3060     MOVE -56,-38
3070     LABEL "POT. (mV)"
3080     MOVE -58,-14
3090     LABEL "STRESS (MPa)"
3100     LDIR -90
3110     MOVE 62,8
3120     LABEL "STRESS (MPa)"
3130     MOVE 60,-18
3140     LABEL "STRAIN (%)"
3150     CSIZE 3.5,.6
3160     LDIR 0
3170     MOVE 15,32
3180     LABEL Material$
3190     MOVE 15,29
3200     LABEL "TEMPERATURE"
3210     MOVE 20,26
3220     LABEL "Tmax= "&Tmax$&" C"
3230     MOVE 20,23

```

```

3240 LABEL "Tmin= "&Tmin$&" C"
3250 MOVE 15,20
3260 LABEL "CYCLES #"&VAL$(Cycle)&" & #"&VAL$(Cycle+1)
3270 MOVE 15,17
3280 LABEL "TIME: "&A$
3290 CSIZE 3,.6
3300 MOVE -15,29
3310 DRAW -13,29
3320 DRAW -14,30
3330 DRAW -15,29
3340 MOVE -12,28
3350 IF Z=1 THEN
3360 LABEL "S= 800 MPa"
3370 MOVE -15,32
3380 LABEL "STRESS CONTROL"
3390 ELSE
3400 LABEL "E= "&Range$&"%"
3410 MOVE -15,32
3420 LABEL "STRAIN CONTROL"
3430 END IF
3440 MOVE -15,24
3450 LABEL "X-DIV=0.05%"
3460 MOVE -15,20
3470 LABEL "Y-DIV=100 MPa"
3480 MOVE -50,-2.5
3490 FOR I=0 TO 358
3500 IF ABS(Load(I)-Load(I+1))>.5 THEN GOTO 3540
3510 B1=(((Load(I)*Range*216.078)+500)/40)-15
3520 A1=(I*5/18)-50
3530 DRAW A1,B1
3540 NEXT I
3550 FOR I=1 TO 358
3560 IF ABS(Strain(I)-Strain(I-1))>.08 THEN GOTO 3640
3570 IF Strain(I)=Strain(I-1) THEN GOTO 3640
3580 IF ABS(Load(I)-Load(I+1))>.5 THEN GOTO 3640
3590 B1=(((.15*Strain(I)*.005555/.515)+.0025)*5000-40
3600 A1=(I*5/18)-50
3610 MOVE A1,B1
3620 IMOVE -.667,-.8
3630 LABEL "."
3640 NEXT I
3650 MOVE -50,-27.5
3660 FOR I=0 TO 359
3670 A1=(I*5/18)-50
3680 B1=(Pot(I)*1000-Min_scale)*25/Factor-40
3690 DRAW A1,B1
3700 NEXT I
3710 A1=((.15*Strain(0)*.005555/.515)+.0025)*4000-40
3720 B1=(((Load(0)*Range*216.078)+500)/50)+15
3730 MOVE A1,B1
3740 FOR I=1 TO 359
3750 PRINT I,Load(I),Strain(I)
3760 IF ABS(Strain(I)-Strain(I-1))>.08 THEN GOTO 3820
3770 IF Strain(I)=Strain(I-1) THEN GOTO 3820

```

```

3780     A1=((.15*Strain(I)*.005555/.515)+.0025)*4000-40
3790     B1=(((Load(I)*Range*216.078)+500)/50)+15
3800     MOVE A1,B1
3810     LABEL ". "
3820     NEXT I
3830     SUBEND
3840!
-----
3850 SUB Pot_time(Stress_max(*),Stress_min(*),K)
3860 OPTION BASE 0
3870 COM Load(359),Strain(359),Pot(359),Temp(359),X(359),Y(359)
3880 COM /Time/ A#[10]
3890 COM /Param/ Crack(999),Cycles(999),Range,INTEGER Cycle,W,Z,Nmax
3900 INTEGER I,J,L
3910 L=0
3920 K=K+1
3930 Max=Pot(L)
3940 FOR I=1 TO 179
3950     J=I+L
3960     IF Pot(J)>Max THEN Max=Pot(J)
3970 NEXT I
3980 Max_stress=Load(L+30)
3990 Min_stress=Load(179+L-29)
4000 FOR I=30 TO 70
4010     J=I+L
4020     IF Load(J)>Max_stress AND Load(J)<Max_stress+.25 THEN Max_stress=Load(J)
4030     IF Load(179+L-I)<Min_stress AND Load(179+L-I)>Min_stress-.25 THEN Min_str
ess=Load(179+L-I)
4040 NEXT I
4050 Cycles(K)=INT(Cycle+(L/180))
4060 Crack(K)=Max
4070 Stress_max(K)=Max_stress
4080 Stress_min(K)=Min_stress
4090 PRINTER IS 1
4100 PRINT USING 4110;K,Cycles(K),Crack(K),Stress_max(K),Stress_min(K)
4110 IMAGE 5X,K,5X,K,5X,K,5X,K,5X,K
4120 L=L+180
4130 IF L>180 THEN GOTO 4150
4140 GOTO 3920
4150 PRINT " "
4160 PRINTER IS 1
4170 SUBEND
4180!
-----
4190 SUB Fcgr(Material$,Tmax$,Range$,Tmin$,Stress_max(*),Stress_min(*),Counter)
4200 OPTION BASE 0
4210 COM Load(359),Strain(359),Pot(359),Temp(359),X(359),Y(359)
4220 COM /Time/ A#[10]
4230 COM /Param/ Crack(999),Cycles(999),Range,INTEGER Cycle,W,Z,Nmax
4240 DIM A(20),B(20)
4250 !
4260 PRINT " "
4270 PRINT " "
4280 PRINT "     DO YOU WANT THE EXPERIMENTAL CALIBRATION?"
4290 PRINT "           Y/N"
4300 INPUT B$
4310 IF B$="Y" THEN

```



```

4320 PRINT " "
4330 PRINT " "
4340 PRINT " PLEASE ENTER THE INITIAL AND FINAL"
4350 PRINT " CRACK LENGHT (in mm)"
4360 INPUT Crack_init, Crack_final
4370 PRINT " "
4380 PRINT " "
4390 PRINT " PLEASE ENTER THE INITIAL AND FINAL"
4400 PRINT " VOLTAGE (in milivolt)"
4410 INPUT Volt_init, Volt_final
4420 Cal_slope=(Crack_init-Crack_final)/(Volt_init-Volt_final)
4430 Cal_coeff=Crack_init-Cal_slope*Volt_init
4440 FOR I=0 TO Counter
4450 Crack(I)=Cal_slope*Crack(I)*1000+Cal_coeff
4460 NEXT I
4470 ELSE
4480 PRINT " "
4490 PRINT " "
4500 PRINT " PLEASE ENTER THE INITIAL CRACK LENGHT"
4510 PRINT " (in mm)"
4520 INPUT Crack_init
4530 PRINT " "
4540 PRINT " "
4550 PRINT " PLEASE ENTER THE INITIAL VOLTAGE"
4560 PRINT " (in milivolt)"
4570 INPUT Volt_init
4580 PRINT " "
4590 PRINT " "
4600 PRINT " PLEASE ENTER PROBES Y-SPACING"
4610 PRINT " (in mm)"
4620 INPUT Y_spacing
4630 RAD
4640 P1=PI*Y_spacing/23.4
4650 P2=(EXP(P1)+EXP(-P1))/2
4660 P3=COS(PI*Crack_init/23.4)
4670 P4=P2/P3
4680 P5=LOG(P4+SQR(P4^2-1))
4690 P6=P5/Volt_init
4700 P1=23.4/P1
4710 P2=P2*2
4720 FOR I=0 TO Counter
4730 P3=Crack(I)*1000
4740 Crack(I)=P1*Arc(P2/(EXP(P3*P6)+EXP(-P3*P6)))
4750 NEXT I
4760 END IF
4770 DEG
4780 GINIT
4790 GRAPHICS ON
4800 SCLEAR
4810 ALPHA OFF
4820 WINDOW -66.7224080268,66.7224080268,-50,50
4830 FOR I=0 TO 20
4840 B(I)=-40+I*4.0
4850 NEXT I

```

```

4860 MOVE -50,-40
4870 FOR J=0 TO 3
4880     FOR I=2 TO 10 STEP 2
4890         A1=25*LGT(I*10^J)-50
4900         DRAW A1,-40
4910         IF I<10 THEN
4920             IDRAW 0,.7
4930             IDRAW 0,-.7
4940         ELSE
4950             IDRAW 0,1.4
4960             IDRAW 0,-1.4
4970         END IF
4980     NEXT I
4990 NEXT J
5000 C=.7
5010 D=1.4
5020 FOR I=0 TO 20
5030     DRAW 50,B(I)
5040     IF 2*INT(I/2)=I THEN
5050         IDRAW -D,0
5060         IDRAW D,0
5070     ELSE
5080         IDRAW -C,0
5090         IDRAW C,0
5100     END IF
5110 NEXT I
5120 FOR J=3 TO 0 STEP -1
5130     FOR I=10 TO 2 STEP -2
5140         A1=25*LGT(I*10^J)-50
5150         DRAW A1,40
5160         IF I<10 THEN
5170             IDRAW 0,-C
5180             IDRAW 0,C
5190         ELSE
5200             IDRAW 0,-D
5210             IDRAW 0,D
5220         END IF
5230     NEXT I
5240 NEXT J
5250 DRAW -50,40
5260 FOR I=20 TO 0 STEP -1
5270     DRAW -50,B(I)
5280     IF 2*INT(I/2)=I THEN
5290         IDRAW D,0
5300         IDRAW -D,0
5310     ELSE
5320         IDRAW C,0
5330         IDRAW -C,0
5340     END IF
5350 NEXT I
5360 CSIZE 3,.6
5370 MOVE -51,-45
5380 LABEL "1"
5390 FOR I=1 TO 4

```

```

5400     MOVE LGT(10^I)*25-53,-45
5410     LABEL VAL$(10)
5420     IMOVE 4,5
5430     LABEL VAL$(I)
5440     NEXT I
5450     FOR I=2 TO 18 STEP 2
5460         MOVE 50.5,B(I)-1.5
5470         LABEL VAL$(I*.05)
5480         MOVE -55,B(I)-1.5
5490         LABEL VAL$(I*.05)
5500     NEXT I
5510     CSIZE 4,.6
5520     MOVE -58,0
5530     LABEL "A"
5540     LDIR 90
5550     MOVE -55,-.5
5560     LABEL "I"
5570     LDIR 0
5580     MOVE -58,-4
5590     LABEL "W"
5600     MOVE 56,-0
5610     LABEL "A"
5620     LDIR 90
5630     MOVE 59,-.5
5640     LABEL "I"
5650     LDIR 0
5660     MOVE 56,-4
5670     LABEL "W"
5680     MOVE -5,-49
5690     LABEL "CYCLE"
5700     MOVE 15,32
5710     LABEL Material$
5720     MOVE 15,29
5730     LABEL "TEMPERATURE"
5740     MOVE 20,26
5750     LABEL "Tmax= "&Tmax$&" C"
5760     MOVE 20,23
5770     LABEL "Tmin= "&Tmin$&" C"
5780     MOVE -40,29
5790     DRAW -38,29
5800     DRAW -39,30
5810     DRAW -40,29
5820     MOVE -37,28
5830     IF Z=1 THEN
5840         LABEL "S= 800 MPa"
5850         MOVE -40,32
5860         LABEL "STRESS CONTROL"
5870     ELSE
5880         LABEL "E= "&Range$&"%"
5890         MOVE -40,32
5900         LABEL "STRAIN CONTROL"
5910     END IF
5920     !
5930     FOR I=0 TO Counter

```

```

5940     A1=LGT(Cycles(I))*25-50
5950     B1=(Crack(I)/11.7)*80-40
5960     MOVE A1-1,B1-1.667
5970     LABEL ". "
5980     NEXT I
5990     SUBEND
6000!-----
6010     SUB Store_dadn(Stress_max(*),Stress_min(*),Counter)
6020     OPTION BASE 0
6030     COM Load(359),Strain(359),Pot(359),Temp(359),X(359),Y(359)
6040     COM /Time/ A$(10)
6050     COM /Param/ Crack(999),Cycles(999),Range,INTEGER Cycle,W,Z,Nmax
6060     ALLOCATE Z$(19),Z1$(19),Z2$(19),Z3$(19),Z4$(19),Dummy1(399),Dummy2(399)
6070     GRAPHICS OFF
6080     ALPHA ON
6090     PRINT " "
6100     PRINT " "
6110     PRINT "          DO YOU WANT TO SAVE THE A VS N DATA?"
6120     PRINT "                                (Y/N)"
6130     INPUT B$
6140     IF B$((">Y" AND B$((">N" THEN GOTO 6090
6150     IF B$="Y" THEN
6160         PRINT " "
6170         PRINT " "
6180         PRINT "          INSERT THE FLOPPY DISC INTO DRIVE#0.  MAKE"
6190         PRINT "          SURE THAT IT HAS BEEN INITIALIZED "
6200         ON KEY 0 LABEL "CONTINUE" GOTO Proceed
6210     Idle:          GOTO Idle
6220     Proceed:      !
6230         PRINT " "
6240         PRINT " "
6250         PRINT "          ENTER FILE NAME?"
6260         INPUT Z$
6270         PRINT " "
6280         PRINT " "
6290         PRINT "          ENTER MATERIAL?"
6300         INPUT Z1$
6310         PRINT " "
6320         PRINT " "
6330         PRINT "          ENTER TESTING CONDITION?"
6340         PRINT "          (In-phase, out-of-phase, isothermal)"
6350         INPUT Z2$
6360         PRINT " "
6370         PRINT " "
6380         PRINT "          ENTER TEMPERATURE RANGE (in C)"
6390         INPUT Z3$
6400         PRINT " "
6410         PRINT " "
6420         PRINT "          ENTER STRAIN RANGE (in %)"
6430         INPUT Z4$
6440         FOR I=0 TO Counter
6450             Dummy1(I)=Cycles(I)+(Crack(I)/100)
6460             Dummy2(I)=((Stress_max(I)+10)*1000)+((Stress_min(I)+10)/100)
6470         NEXT I

```

```

6480 MASS STORAGE IS ":HPB290X,700,0"
6490 CREATE BDAT Z$,1,8400
6500 ASSIGN @Disc TO Z$
6510 OUTPUT @Disc;Z1$,Z2$,Z3$,Z4$,Counter,Dummy1(*),Dummy2(*)
6520 ASSIGN @Disc TO *
6530 GOTO End_sub
6540 ELSE
6550 GOTO End_sub
6560 END IF
6570 End_sub: !
6580 DEALLOCATE Z$,Z1$,Z2$,Z3$,Z4$,Dummy1(*),Dummy2(*)
6590 SUBEND
6600!-----
6610 SUB Volt_time(Material$,Range$,Tmax$,Tmin$,Stress_max(*),Stress_min(*),Counter)
6620 OPTION BASE 0
6630 COM Load(359),Strain(359),Pot(359),Temp(359),X(359),Y(359)
6640 COM /Time/ A$[10]
6650 COM /Param/ Crack(999),Cycles(999),Range,INTEGER Cycle,W,Z,Nmax
6660 DIM A(20),B(20)
6670 DEG
6680 GINIT
6690 GRAPHICS ON
6700 GCLEAR
6710 ALPHA OFF
6720 WINDOW -66.7224080268,66.7224080268,-50,50
6730 FOR I=0 TO 20
6740 B(I)=-40+I*4.0
6750 NEXT I
6760 MOVE -50,-40
6770 FOR J=0 TO 3
6780 FOR I=2 TO 10 STEP 2
6790 A1=25*LGT(I*10^J)-50
6800 DRAW A1,-40
6810 IF I<10 THEN
6820 IDRAW 0,.7
6830 IDRAW 0,-.7
6840 ELSE
6850 IDRAW 0,1.4
6860 IDRAW 0,-1.4
6870 END IF
6880 NEXT I
6890 NEXT J
6900 C=.7
6910 D=1.4
6920 FOR I=0 TO 20
6930 DRAW 50,B(I)
6940 IF 2*INT(I/2)=I THEN
6950 IDRAW -D,0
6960 IDRAW D,0
6970 ELSE
6980 IDRAW -C,0
6990 IDRAW C,0
7000 END IF

```

```

7010 NEXT I
7020 FOR J=3 TO 0 STEP -1
7030   FOR I=10 TO 2 STEP -2
7040     A1=25*LBT(I*10^J)-50
7050     DRAW A1,40
7060     IF I<10 THEN
7070       IDRAW 0,-C
7080       IDRAW 0,C
7090     ELSE
7100       IDRAW 0,-D
7110       IDRAW 0,D
7120     END IF
7130   NEXT I
7140 NEXT J
7150 DRAW -50,40
7160 FOR I=20 TO 0 STEP -1
7170   DRAW -50,B(I)
7180   IF 2*INT(I/2)=I THEN
7190     IDRAW D,0
7200     IDRAW -D,0
7210   ELSE
7220     IDRAW C,0
7230     IDRAW -C,0
7240   END IF
7250 NEXT I
7260 CSIZE 3,.6
7270 MOVE -51,-45
7280 LABEL "1"
7290 FOR I=1 TO 4
7300   MOVE LBT(10^I)*25-53,-45
7310   LABEL "10"
7320   IMOVE 4,5
7330   LABEL VAL$(I)
7340 NEXT I
7350 FOR I=2 TO 18 STEP 2
7360   MOVE 50.5,B(I)-1.5
7370   LABEL VAL$(I*.25)
7380   MOVE -56,B(I)-1.5
7390   LABEL VAL$(I*.25)
7400 NEXT I
7410 CSIZE 4,.6
7420 MOVE -58,-20
7430 LDIR 90
7440 LABEL "VOLTAGE (in mV)"
7450 MOVE 58,20
7460 LDIR -90
7470 LABEL "VOLTAGE (in mV)"
7480 LDIR 0
7490 MOVE -5,-49
7500 LABEL "CYCLE"
7510 MOVE 15,32
7520 LABEL Material$
7530 MOVE 15,29
7540 LABEL "TEMPERATURE"

```

```

7550 MOVE 20,26
7560 LABEL "Tmax= "&Tmax$&" C"
7570 MOVE 20,23
7580 LABEL "Tmin= "&Tmin$&" C"
7590 MOVE -40,29
7600 DRAW -38,29
7610 DRAW -39,30
7620 DRAW -40,29
7630 MOVE -37,28
7640 IF Z=1 THEN
7650     LABEL "S= 800 MPa"
7660     MOVE -40,32
7670     LABEL "STRESS CONTROL"
7680 ELSE
7690     LABEL "E= "&Range$&"%"
7700     MOVE -40,32
7710     LABEL "STRAIN CONTROL"
7720 END IF
7730 !
7740 FOR I=0 TO Counter
7750     A1=LBT(Cycles(I))*25-51
7760     B1=Crack(I)*16000-41.667
7770     MOVE A1,B1
7780     LABEL "."
7790 NEXT I
7800 WAIT 3.0
7810 SUBEND
7820!-----

```

```

10      !                      PROGRAM STRAIN_INT
20      OPTION BASE 0
30      COM /Param/ Crack(999),Cycles(999),Range,INTEGER Cycle,W,Z,Nmax
40      Z=2
50      CALL Strain_int
60      END
70      !
80      SUB Strain_int
90      OPTION BASE 0
100     COM /Param/ Crack(999),Cycles(999),Range,INTEGER Cycle,W,Z,Nmax
110     ALLOCATE Delk(999),Dadn(999)
120     ALLOCATE Bb(3),A(10),N(10),Z1$(19),Z2$(19),Z3$(19),Z4$(19)
130     ALLOCATE C11(99),C12(99),C22(99)
140     !
150     Select:                      !*****
160     PRINT " "
170     PRINT " "
180     PRINT "      ENTER FILE NAME?"
190     INPUT Z$
200     !
210     Read_data:                  !*****
220     !-----
230     CALL Read_const(C11(*),C12(*),C22(*))
240     MASS STORAGE IS ":HP8290X,700,1"
250     ASSIGN @Disc TO Z$
260     ENTER @Disc;Z1$,Z2$,Z3$,Z4$,Nmaxx,Crack(*)
270     ASSIGN @Disc TO *
280     MASS STORAGE IS ":HP8290X,700,0"
290     Nmax=Nmaxx
300     FOR I=0 TO Nmax
310         Cycles(I)=INT(Crack(I))
320         Crack(I)=(Crack(I)-Cycles(I))*100
330     NEXT I
340     !-----
350     Plot_frame:                  !*****
360     DEG
370     GINIT
380     !PLOTTER IS 705,"HPGL"
390     GRAPHICS ON
400     BCLEAR
410     LDIR 0
420     WINDOW -66.7224080268,66.7224080268,-50,50
430     CSIZE 3,.6
440     MOVE -50,-40
450     FOR I=-5 TO -4
460         FOR J=1 TO 10
470             A1=50*(LBT(J*10^I)+5)-50
480             DRAW A1,-40
490             IF J=10 THEN
500                 IDRAW 0,1.8
510                 IDRAW 0,-1.8
520             ELSE
530                 IDRAW 0,.8
540                 IDRAW 0,-.8

```



```

550     END IF
560     NEXT J
570     NEXT I
580     FOR J=-9 TO -4
590         FOR I=1 TO 9
600             A1=(LGT(I*10^J)+9)*80/6-40
610             DRAW 50,A1
620             IF I>1 THEN
630                 IDRAW -.8,0
640                 IDRAW .8,0
650             ELSE
660                 IDRAW -1.8,0
670                 IDRAW 1.8,0
680             END IF
690         NEXT I
700     NEXT J
710     FOR I=-4 TO -5 STEP -1
720         FOR J=10 TO 1 STEP -1
730             A1=50*(LGT(J*10^I)+5)-50
740             DRAW A1,40
750             IF J=10 THEN
760                 IDRAW 0,-1.8
770                 IDRAW 0,1.8
780             ELSE
790                 IDRAW 0,-.8
800                 IDRAW 0,.8
810             END IF
820         NEXT J
830     NEXT I
840     FOR J=-4 TO -9 STEP -1
850         FOR I=9 TO 1 STEP -1
860             A1=(LGT(I*10^J)+9)*80/6-40
870             DRAW -50,A1
880             IF I>1 THEN
890                 IDRAW .8,0
900                 IDRAW -.8,0
910             ELSE
920                 IDRAW 1.8,0
930                 IDRAW -1.8,0
940             END IF
950         NEXT I
960     NEXT J
970     DRAW -50,-40
980     FOR I=-5 TO -3
990         A1=(LGT(10^I)+5)*50-50
1000        MOVE A1,-40
1010        IMOVE -1.5,-3.0
1020        LABEL VAL$(I)
1030        IMOVE -1.6,.4
1040        LABEL "10"
1050    NEXT I
1060    MOVE 50,-40
1070    FOR I=-8 TO -4
1080        A1=(LGT(10^I)+9)*80/6-40

```

```

1090     MOVE 50,A1
1100     IMOVE 1.5,-1.5
1110     LABEL "10"
1120     IMOVE 2.8,3.5
1130     LABEL VAL$(I)
1140     NEXT I
1150     MOVE -50,40
1160     FOR I=-4 TO -8 STEP -1
1170         A1=(LGT(10^I)+9)*80/6-40
1180         MOVE -50,A1
1190         IMOVE -7.0,-1.5
1200         LABEL "10"
1210         IMOVE 2.8,3.5
1220         LABEL VAL$(I)
1230     NEXT I
1240     CSIZE 3.5,.6
1250     MOVE -25,-48
1260     LABEL "Strain Intensity Factor (Vm)"
1270     MOVE -25,-48
1280     IMOVE 51,3.1
1290     IDRAW 1.6,0
1300     LDIR 90
1310     MOVE -58,-15
1320     LABEL "da/dN (m/cycle)"
1330     LDIR 0
1340     MOVE -24,42
1350     LABEL "FATIGUE CRACK PROPAGATION"
1360     MOVE -45,30
1370     LABEL Z1$
1380     MOVE -45,27
1390     LABEL "STRAIN CONTROL"
1400     MOVE -45,25
1410     IDRAW 2,0
1420     IDRAW -1,1.5
1430     IDRAW -1,-1.5
1440     MOVE -42,24
1450     LABEL "E= "&Z4$&"%"
1460     MOVE -45,21
1470     LABEL Z2$
1480     MOVE -45,18
1490     LABEL "T="&Z3$&" C"
1500     MOVE--45,15
1510     LABEL "Frequency= 0.1 Hz"
1520     MOVE -45,13
1530     IDRAW 2,0
1540     IDRAW -1,1.5
1550     IDRAW -1,-1.5
1560     MOVE -42,12
1570     LABEL "K from Eq. 32"
1580     MOVE -45,9
1590     LABEL "L /W= 2.5"
1600     MOVE -43,8
1610     LABEL "b"
1620     MOVE -50,-40

```

```

1630 !
1640 Plot_data: !*****
1650 Lw=2.17
1660 Lb=2.50
1670 K=-1
1680 Deltae=VAL(Z4$)/100
1690 Npts=Nmax-6
1700 FOR I=0 TO Npts
1710   L=0
1720   K=K+1
1730   K1=K+6
1740   FOR J=K TO K1
1750     L=L+1
1760     A(L)=Crack(J)
1770     N(L)=Cycles(J)
1780   NEXT J
1790   C1=.5*(N(1)+N(7))
1800   C2=.5*(N(7)-N(1))
1810   Sx=0
1820   Sx2=0
1830   Sx3=0
1840   Sx4=0
1850   Sy=0
1860   Syx=0
1870   Syx2=0
1880   FOR J=1 TO 7
1890     Xx=(N(J)-C1)/C2
1900     Yy=A(J)
1910     Sx=Sx+Xx
1920     Sx2=Sx2+Xx^2
1930     Sx3=Sx3+Xx^3
1940     Sx4=Sx4+Xx^4
1950     Sy=Sy+Yy
1960     Syx=Syx+Xx*Yy
1970     Syx2=Syx2+Yy*Xx^2
1980   NEXT J
1990   Den=7.0*(Sx2*Sx4-Sx3^2)-Sx*(Sx*Sx4-Sx2*Sx3)+Sx2*(Sx*Sx3-Sx2^2)
2000   T2=Sy*(Sx2*Sx4-Sx3^2)-Syx*(Sx*Sx4-Sx2*Sx3)+Syx2*(Sx*Sx3-Sx2^2)
2010   Bb(1)=T2/Den
2020   T3=7.0*(Syx*Sx4-Syx2*Sx3)-Sx*(Sy*Sx4-Syx2*Sx2)+Sx2*(Sy*Sx3-Syx*Sx2)
2030   Bb(2)=T3/Den
2040   T4=7.0*(Sx2*Syx2-Sx3*Syx)-Sx*(Sx*Syx2-Sx3*Sy)+Sx2*(Sx*Syx-Sx2*Sy)
2050   Bb(3)=T4/Den
2060   Yb=Sy/7.0
2070   Rss=0
2080   Tss=0
2090   FOR J=1 TO 7
2100     Xx=(N(J)-C1)/C2
2110     Yhat=Bb(1)+Bb(2)*Xx+Bb(3)*Xx^2
2120     Rss=Rss+(A(J)-Yhat)^2
2130     Tss=Tss+(A(J)-Yb)^2
2140   NEXT J
2150   R2=1.0-Rss/Tss
2160   Dadn(I)=Bb(2)/C2+2.0*Bb(3)*(N(4)-C1)/C2^2

```

```

2170   Xx=(N(4)-C1)/C2
2180   Ar=Bb(1)+Bb(2)*Xx+Bb(3)*Xx^2
2190   !-----
2200   T=Ar/11.7
2210   K11=INT((T+.005)*100)-1
2220   F11=FNF11(T)
2230   F22=FNF22(T)
2240   Factor1=1-(6*(F22/F11)*C12(K11)/(C22(K11)+12*Lb))
2250   A11=C12(K11)^2/(12*Lb+C22(K11))
2260   A22=6*C12(K11)*(Lw-Lb)/(12*Lb+C22(K11))
2270   Factor2=(1+(C11(K11)-A11+A22)/Lw)
2280   Ft=SQR(PI*Ar/1000)*F11*Factor1/Factor2
2290   !Ft=SQR(25/(20-13*T-7*T^2))      !Harris' formula
2300   Delk(I)=Deltae*Ft
2310   IF T>=.55 THEN Delk(I)=100
2320   NEXT I
2330   BEEP 3000,1
2340   ALPHA OFF
2350   !
2360   FOR I=0 TO Npts
2370     A1=(LGT(Delk(I))+5)*50-50
2380     A2=(LGT(ABS(Dadn(I))/1000)+9)*80/6-40
2390     MOVE A1,A2
2400     IMOVE -1.3344481605,-1
2410     LABEL ". ."
2420   NEXT I
2430   PENUP
2440   MOVE -50,-40
2450   PAUSE
2460   SUBEND
2470!-----
2480   DEF FNF11(I)
2490   RAD
2500   IF I=0 THEN
2510     F11=2/SQR(PI)
2520     GOTO 2570
2530   END IF
2540   A=SQR(2*TAN(PI*I/2)/(PI*I))
2550   B=(.752+2.02*I+.37*(1-SIN(PI*I/2))^3)/COS(PI*I/2)
2560   F11=A*B
2570   RETURN F11
2580   FNF11
2590!-----
2600   DEF FNF22(I)
2610   RAD
2620   IF I=0 THEN
2630     F22=2/SQR(PI)
2640     GOTO 2690
2650   END IF
2660   A=SQR(2*TAN(PI*I/2)/(PI*I))
2670   B=(.923+.199*(1-SIN(PI*I/2))^4)/COS(PI*I/2)
2680   F22=A*B
2690   RETURN F22
2700   FNF22

```

2710! -----
2720 SUB Read_const(C11(*),C12(*),C22(*))
2730 DATA .39655E-03,.1594E-02,.36060E-02,.64504E-02,.10149E-01,.14728E-0
1,.20217E-01,.26652E-01,.34072E-01,.42522E-01
2740 DATA .52051E-01,.62715E-01,.74576E-01,.87699E-01,.10216,.11804,.1354
2,.15441,.17510,.19761
2750 DATA .22207,.24861,.27738,.30854,.34225,.37872,.41813,.46073,.50674,
.55643
2760 DATA .61009,.66802,.73057,.79811,.87105,.94981,1.0349,1.1268,1.2262,
1.3335
2770 DATA 1.4497,1.5753,1.7114,1.8586,2.0182,2.1912,2.3789,2.5827,2.8040,
3.0447
2780 DATA 3.3065,3.5917,3.9026,4.2418,4.6124,5.0177,5.4615,5.9481,6.4823,
7.0697
2790 DATA 7.7166,8.4301,9.2186,10.091,11.060,12.136,13.336,14.676,16.176,
17.861
2800 DATA 19.759,21.905,24.337,27.106,30.271,33.905,38.097,42.958,48.629,
55.284
2810 DATA 63.151,72.522,83.782,97.441,114.19,135.00,161.19,194.73,238.50,
296.92
2820 DATA 377.05,490.68,658.66,920.72,1359.9,2174.0,3930.5,8822.6,31809.,
31809.
2830! -----
2840 READ C11(*)
2850! -----
2860 DATA .23631E-02,.9402E-02,.21068E-01,.37333E-01,.58192E-01,.83658E-0
1,.11377,.14857,.18815,.23259
2870 DATA .28201,.33655,.39637,.46164,.53256,.60936,.69228,.78161,.87763,
.98069
2880 DATA 1.0911,1.2093,1.3358,1.4708,1.6151,1.7690,1.9332,2.1083,2.2950,
2.4940
2890 DATA 2.7062,2.9324,3.1735,3.4305,3.7047,3.9970,4.3090,4.6419,4.9973,
5.3769
2900 DATA 5.7826,6.2163,6.6802,7.1768,7.7085,8.2785,8.8898,9.5459,10.251,
11.008
2910 DATA 11.824,12.702,13.650,14.672,15.777,16.974,18.269,19.676,21.204,
22.867
2920 DATA 24.680,26.659,28.826,31.200,33.808,36.680,39.849,43.356,47.246,
51.573
2930 DATA 56.403,61.811,67.889,74.744,82.510,91.347,101.45,113.07,126.50,
142.13
2940 DATA 160.45,182.09,207.87,238.89,276.62,323.09,381.14,454.87,550.30,
676.68
2950 DATA 848.67,1090.7,1445.7,1995.3,2909.4,4591.0,8192.0,18147.,64577.,
64577.
2960! -----

```
2970 READ C12(*)
2980!-----
2990 DATA .14082E-01,.55459E-01,.12310,.21611,.33375,.47539,.64052,.82877
,1.0399,1.2736
3000 DATA 1.5299,1.8089,2.1105,2.4352,2.7830,3.1545,3.5500,3.9703,4.4159,
4.8876
3010 DATA 5.3863,5.9128,6.4683,7.0540,7.6710,8.3207,9.0047,9.7247,10.482,
11.280
3020 DATA 12.118,13.001,13.931,14.909,15.939,17.025,18.168,19.374,20.646,
21.988
3030 DATA 23.405,24.901,26.484,28.158,29.930,31.807,33.798,35.911,38.155,
40.541
3040 DATA 43.081,45.787,48.673,51.756,55.052,58.582,62.366,66.430,70.801,
75.509
3050 DATA 80.590,86.083,92.034,98.493,105.52,113.18,121.55,130.73,140.81,
151.93
3060 DATA 164.22,177.85,193.03,210.01,229.06,250.55,274.91,302.67,334.49,
371.20
3070 DATA 413.86,463.83,522.87,593.31,678.29,782.09,910.72,1072.8,1280.9,
1554.3
3080 DATA 1923.4,2438.8,3189.1,4341.7,6244.1,9717.6,17100.,37358.,131140,
131140
3090!-----
3100 READ C22(*)
3110!-----
3120 SUBEND
```

```

10      !                PROGRAM  STRESS_INT
20      OPTION BASE 0
30      COM /Param/ Crack(999),Cycles(999),Range,INTEGER Cycle,W,Z,Nmax
40      Z=2
50      CALL Stress_int
60      END
70      !
80      SUB Stress_int
90      OPTION BASE 0
100     COM /Param/ Crack(999),Cycles(999),Range,INTEGER Cycle,W,Z,Nmax
110     ALLOCATE Delk(1300),Dadn(1300)
120     ALLOCATE Bb(3),A(10),N(10),Z1$(19),Z2$(19),Z3$(19),Z4$(19)
130     ALLOCATE C11(99),C12(99),C22(99)
140     ALLOCATE Dummy1(199),Dummy2(199)
150     ALLOCATE Stress_max(199),Stress_min(199)
160     !
170     Select:                !*****
180     PRINT " "
190     PRINT " "
200     PRINT "      ENTER FILE NAME?"
210     INPUT Z$
220     PRINT " "
230     PRINT " "
240     PRINT "      ENTER MODULUS(in MPa)?"
250     INPUT Modulus
260     PRINT " "
270     PRINT " "
280     PRINT "      ENTER POISSON RATIO?"
290     INPUT Poisson
300     !
310     Read_data:            !*****
320     !-----
330     CALL Read_const(C11(*),C12(*),C22(*))
340     MASS STORAGE IS ":HPB290X,700,1"
350     ASSIGN @Disc TO Z$
360     ENTER @Disc;Z1$,Z2$,Z3$,Z4$,Counter,Dummy1(*),Dummy2(*)
370     ASSIGN @Disc TO *
380     MASS STORAGE IS ":HPB290X,700,0"
390     FOR I=0 TO Counter
400         Cycles(I)=INT(Dummy1(I))
410         Crack(I)=(Dummy1(I)-Cycles(I))*100
420         Stress_max(I)=INT(Dummy2(I))/1000-10
430         Stress_min(I)=(Dummy2(I)-INT(Dummy2(I)))*100-10
440     NEXT I
450     DEALLOCATE Dummy1(*),Dummy2(*)
460     CALL Stress_cycle(Counter,Stress_max(*),Stress_min(*),Cycles(*),Crack(*),Z
1$,Z2$,Z3$,Z4$)
470     !-----
480     Plot_frame:          !*****
490     DEG
500     GINIT
510     !PLOTTER IS 705,"HPGL"
520     GRAPHICS ON
530     GCLEAR

```

```

540 LDIR 0
550 WINDOW -66.7224080268,66.7224080268,-50,50
560 CSIZE 3,.6
570 MOVE -50,-40
580 FOR I=10 TO 100 STEP 2
590     A1=100*(LGT(I/10))-50
600     DRAW A1,-40
610     IF INT(I/10)<(I/10) THEN
620         IDRAW 0,.8
630         IDRAW 0,-.8
640     ELSE
650         IDRAW 0,1.8
660         IDRAW 0,-1.8
670     END IF
680 NEXT I
690 FOR J=-9 TO -4
700     FOR I=1 TO 9
710         A1=(LGT(I*10^J)+9)*80/6-40
720         DRAW 50,A1
730         IF I>1 THEN
740             IDRAW -.8,0
750             IDRAW .8,0
760         ELSE
770             IDRAW -1.8,0
780             IDRAW 1.8,0
790         END IF
800     NEXT I
810 NEXT J
820 FOR I=100 TO 10 STEP -2
830     A1=100*(LGT(I/10))-50
840     DRAW A1,40
850     IF INT(I/10)<(I/10) THEN
860         IDRAW 0,-.8
870         IDRAW 0,.8
880     ELSE
890         IDRAW 0,-1.8
900         IDRAW 0,1.8
910     END IF
920 NEXT I
930 FOR J=-4 TO -9 STEP -1
940     FOR I=9 TO 1 STEP -1
950         A1=(LGT(I*10^J)+9)*80/6-40
960         DRAW -50,A1
970         IF I>1 THEN
980             IDRAW .8,0
990             IDRAW -.8,0
1000        ELSE
1010            IDRAW 1.8,0
1020            IDRAW -1.8,0
1030        END IF
1040    NEXT I
1050 NEXT J
1060 DRAW -50,-40
1070 FOR I=1 TO 9

```



```

1080     A1=LGT(I)*100-50
1090     MOVE A1,-40
1100     IMOVE -1.5,-3.0
1110     LABEL VAL$(I*10)
1120     NEXT I
1130     MOVE 50,-40
1140     FOR I=-8 TO -4
1150         A1=(LGT(10^I)+9)*80/6-40
1160         MOVE 50,A1
1170         IMOVE 1.5,-1.5
1180         LABEL "10"
1190         IMOVE 2.8,3.5
1200         LABEL VAL$(I)
1210     NEXT I
1220     MOVE -50,40
1230     FOR I=-4 TO -8 STEP -1
1240         A1=(LGT(10^I)+9)*80/6-40
1250         MOVE -50,A1
1260         IMOVE -7.0,-1.5
1270         LABEL "10"
1280         IMOVE 2.8,3.5
1290         LABEL VAL$(I)
1300     NEXT I
1310     CSIZE 3.5,.6
1320     MOVE -28,-48
1330     LABEL "Stress Intensity Factor (MPaVm)"
1340     MOVE -28,-48
1350     IMOVE 57,3.1
1360     IDRAW 1.6,0
1370     LDIR 90
1380     MOVE -58,-15
1390     LABEL "da/dN (a/cycle)"
1400     LDIR 0
1410     MOVE -24,42
1420     LABEL "FATIGUE CRACK PROPAGATION"
1430     MOVE -45,30
1440     LABEL Z1$
1450     MOVE -45,27
1460     LABEL "STRAIN CONTROL"
1470     MOVE -45,25
1480     IDRAW 2,0
1490     IDRAW -1,1.5
1500     IDRAW -1,-1.5
1510     MOVE -42,24
1520     LABEL "E= "&Z4$&"%"
1530     MOVE -45,21
1540     LABEL Z2$
1550     MOVE -45,18
1560     LABEL "T="&Z3$&" C"
1570     MOVE -50,-40
1580     PENUP
1590     !PAUSE
1600     !

```

```

1610 Plot_data:                !*****
1620 Lw=2.17
1630 Lb=2.5
1640 K=-1
1650 Npts=Counter-6
1660 FOR I=0 TO Npts
1670   !Deltap=(Stress_max(I+3)-Stress_min(I+3))*21.6078*5!K using stress range
1680   Deltap=Modulus*VAL(Z4$)/(100*(1-Poisson)) !K using Modulus
1690   L=L+1
1700   K=K+1
1710   K1=K+6
1720   FOR J=K TO K1
1730     L=L+1
1740     A(L)=Crack(J)
1750     N(L)=Cycles(J)
1760   NEXT J
1770   C1=.5*(N(1)+N(7))
1780   C2=.5*(N(7)-N(1))
1790   Sx=0
1800   Sx2=0
1810   Sx3=0
1820   Sx4=0
1830   Sy=0
1840   Syx=0
1850   Syx2=0
1860   FOR J=1 TO 7
1870     Xx=(N(J)-C1)/C2
1880     Yy=A(J)
1890     Sx=Sx+Xx
1900     Sx2=Sx2+Xx^2
1910     Sx3=Sx3+Xx^3
1920     Sx4=Sx4+Xx^4
1930     Sy=Sy+Yy
1940     Syx=Syx+Xx*Yy
1950     Syx2=Syx2+Yy*Xx^2
1960   NEXT J
1970   Den=7.0*(Sx2*Sx4-Sx3^2)-Sx*(Sx*Sx4-Sx2*Sx3)+Sx2*(Sx*Sx3-Sx2^2)
1980   T2=Sy*(Sx2*Sx4-Sx3^2)-Syx*(Sx*Sx4-Sx2*Sx3)+Syx2*(Sx*Sx3-Sx2^2)
1990   Bb(1)=T2/Den
2000   T3=7.0*(Syx*Sx4-Syx2*Sx3)-Sx*(Sy*Sx4-Syx2*Sx2)+Sx2*(Sy*Sx3-Syx*Sx2)
2010   Bb(2)=T3/Den
2020   T4=7.0*(Sx2*Syx2-Sx3*Syx)-Sx*(Sx*Syx2-Sx3*Sy)+Sx2*(Sx*Syx-Sx2*Sy)
2030   Bb(3)=T4/Den
2040   Yb=Sy/7.0
2050   Rss=0
2060   Tss=0
2070   FOR J=1 TO 7
2080     Xx=(N(J)-C1)/C2
2090     Yhat=Bb(1)+Bb(2)*Xx+Bb(3)*Xx^2
2100     Rss=Rss+(A(J)-Yhat)^2
2110     Tss=Tss+(A(J)-Yb)^2
2120   NEXT J
2130   R2=1.0-Rss/Tss
2140   Dadn(I)=Bb(2)/C2+2.0*Bb(3)*(N(4)-C1)/C2^2
2150   Xx=(N(4)-C1)/C2

```

```

2160 Ar=Bb(1)+Bb(2)*Xx+Bb(3)*Xx^2
2170 ! -----
2180 T=Ar/11.7
2190 K11=INT((T+.005)*100)-1
2200 F11=FNF11(T)
2210 F22=FNF22(T)
2220 Factor1=1-(6*(F22/F11)*C12(K11)/(C22(K11)+12*Lb))
2230 A11=C12(K11)^2/(12*Lb+C22(K11))
2240 A22=6*C12(K11)*(Lw-Lb)/(12*Lb+C22(K11))
2250 Factor2=(1+(C11(K11)-A11+A22)/Lw)
2260 Ft=SQR(PI*Ar/1000)*F11*Factor1/Factor2 !K using modulus
2270 ! Ft=SQR(PI*Ar/1000)*F11*Factor1 !K using stress range
2280 Delk(I)=Deltap*Ft
2290 PRINT Delk(I),Dadn(I)
2300 IF T>=.60 THEN Delk(I)=100000
2310 NEXT I
2320 BEEP 3000,1
2330 ALPHA OFF
2340 !
2350 FOR I=0 TO Npts
2360 A1=LBT(Delk(I)/10)*100-50
2370 A2=(LBT(ABS(Dadn(I))/1000)+9)*80/6-40
2380 MOVE A1,A2
2390 IMOVE -1.3344481605,-1
2400 LABEL ". ."
2410 NEXT I
2420 PENUP
2430 MOVE -50,-40
2440 PAUSE
2450 SUBEND
2460 ! -----
2470 DEF FNF11(I)
2480 RAD
2490 IF I=0 THEN
2500 F11=2/SQR(PI)
2510 GOTO 2560
2520 END IF
2530 A=SQR(2*TAN(PI*I/2)/(PI*I))
2540 B=(.752+2.02*I+.37*(1-SIN(PI*I/2))^3)/COS(PI*I/2)
2550 F11=A*B
2560 RETURN F11
2570 FNEND
2580 ! -----
2590 DEF FNF22(I)
2600 RAD
2610 IF I=0 THEN
2620 F22=2/SQR(PI)
2630 GOTO 2680
2640 END IF
2650 A=SQR(2*TAN(PI*I/2)/(PI*I))
2660 B=(.923+.199*(1-SIN(PI*I/2))^4)/COS(PI*I/2)
2670 F22=A*B
2680 RETURN F22
2690 FNEND

```

```

2700!
-----
2710 SUB Read_const(C11(*),C12(*),C22(*))
2720 DATA .39655E-03,.1594E-02,.36060E-02,.64504E-02,.10149E-01,.14728E-01,.202
17E-01,.26652E-01,.34072E-01,.42522E-01
2730 DATA .52051E-01,.62715E-01,.74576E-01,.87699E-01,.10216,.11804,.13542,.154
41,.17510,.19761
2740 DATA .22207,.24861,.27738,.30854,.34225,.37872,.41813,.46073,.50674,.55643
2750 DATA .61009,.66802,.73057,.79811,.87105,.94981,1.0349,1.1268,1.2262,1.3335
2760 DATA 1.4497,1.5753,1.7114,1.8586,2.0182,2.1912,2.3789,2.5827,2.8040,3.0447
2770 DATA 3.3065,3.5917,3.9026,4.2418,4.6124,5.0177,5.4615,5.9481,6.4823,7.0697
2780 DATA 7.7166,8.4301,9.2186,10.091,11.060,12.136,13.336,14.676,16.176,17.861
2790 DATA 19.759,21.905,24.337,27.106,30.271,33.905,38.097,42.958,48.629,55.284
2800 DATA 63.151,72.522,83.782,97.441,114.19,135.00,161.19,194.73,238.50,296.92
2810 DATA 377.05,490.68,658.66,920.72,1359.9,2174.0,3930.5,8822.6,31809.,31809.
2820 READ C11(*)
2830!-----
2840 DATA .23631E-02,.9402E-02,.21068E-01,.37333E-01,.58192E-01,.83658E-01,.113
77,.14857,.18815,.23259
2850 DATA .28201,.33655,.39637,.46164,.53256,.60936,.69228,.78161,.87763,.98069
2860 DATA 1.0911,1.2093,1.3358,1.4708,1.6151,1.7690,1.9332,2.1083,2.2950,2.4940
2870 DATA 2.7062,2.9324,3.1735,3.4305,3.7047,3.9970,4.3090,4.6419,4.9973,5.3769
2880 DATA 5.7826,6.2163,6.6802,7.1768,7.7085,8.2785,8.8898,9.5459,10.251,11.008
2890 DATA 11.824,12.702,13.650,14.672,15.777,16.974,18.269,19.676,21.204,22.867
2900 DATA 24.680,26.659,28.826,31.200,33.808,36.680,39.849,43.356,47.246,51.573
2910 DATA 56.403,61.811,67.889,74.744,82.510,91.347,101.45,113.07,126.50,142.13
2920 DATA 160.45,182.09,207.87,238.89,276.62,323.09,381.14,454.87,550.30,676.68
2930 DATA 848.67,1090.7,1445.7,1995.3,2909.4,4591.0,8192.0,18147.,64577.,64577.
2940 READ C12(*)
2950!-----
2960 DATA .14082E-01,.55459E-01,.12310,.21611,.33375,.47539,.64052,.82877,1.039
9,1.2736
2970 DATA 1.5299,1.8089,2.1105,2.4352,2.7830,3.1545,3.5500,3.9703,4.4159,4.8876
2980 DATA 5.3863,5.9128,6.4683,7.0540,7.6710,8.3207,9.0047,9.7247,10.482,11.280
2990 DATA 12.118,13.001,13.931,14.909,15.939,17.025,18.168,19.374,20.646,21.988
3000 DATA 23.405,24.901,26.484,28.158,29.930,31.807,33.798,35.911,38.155,40.541
3010 DATA 43.081,45.787,48.673,51.756,55.052,58.582,62.366,66.430,70.801,75.509
3020 DATA 80.590,86.083,92.034,98.493,105.52,113.18,121.55,130.73,140.81,151.93
3030 DATA 164.22,177.85,193.03,210.01,229.06,250.55,274.91,302.67,334.49,371.20
3040 DATA 413.86,463.83,522.87,593.31,678.29,782.09,910.72,1072.8,1280.9,1554.3
3050 DATA 1923.4,2438.8,3189.1,4341.7,6244.1,9717.6,17100.,37358.,131140,131140
3060 READ C22(*)
3070 SUBEND
3080!-----

```

```

3090 SUB Stress_cycle(Counter,Stress_max(*),Stress_min(*),Cycles(*),Crack(*),Z1
$,Z2$,Z3$,Z4$)
3100 ALLOCATE A(20),B(20)
3110 FOR I=0 TO 20
3120   A(I)=25*I-50
3130   B(I)=3*I-40
3140 NEXT I
3150 DEG
3160 GINIT
3170 GCLEAR
3180 ALPHA OFF
3190 GRAPHICS ON
3200 FRAME
3210 WINDOW -66.722,66.722,-50,50
3220 MOVE -50,-40
3230 FOR I=0 TO 3
3240   FOR J=1 TO 9
3250     DRAW 25*LGT(J*10^I)-50,-40
3260     IF J=1 THEN
3270       IDRAW 0,1
3280       IDRAW 0,-1
3290     ELSE
3300       IDRAW 0,.5
3310       IDRAW 0,-.5
3320     END IF
3330   NEXT J
3340 NEXT I
3350 C=.5
3360 D=1.0
3370 FOR I=0 TO 20
3380   DRAW 50,B(I)
3390   IF 2*INT(I/2)=I THEN
3400     IDRAW -D,0
3410     IDRAW D,0
3420   ELSE
3430     IDRAW -C,0
3440     IDRAW C,0
3450   END IF
3460 NEXT I
3470 FOR I=3 TO 0 STEP -1
3480   FOR J=9 TO 1 STEP -1
3490     DRAW 25*LGT(J*10^I)-50,20
3500     IF J=1 THEN
3510       IDRAW 0,-1
3520       IDRAW 0,1
3530     ELSE
3540       IDRAW 0,-.5
3550       IDRAW 0,.5
3560     END IF
3570   NEXT J
3580 NEXT I
3590 FOR I=20 TO 0 STEP -1
3600   DRAW -50,B(I)
3610   IF 2*INT(I/2)=I THEN
3620     IDRAW D,0

```

```

3630     IDRAW -D,0
3640     ELSE
3650     IDRAW C,0
3660     IDRAW -C,0
3670     END IF
3680     NEXT I
3690     MOVE -50,-10
3700     FOR I=0 TO 3
3710     FOR J=1 TO 9
3720     DRAW 25*LGT(J*10^I)-50,-10
3730     IF J=1 THEN
3740     IDRAW 0,1
3750     IDRAW 0,-2
3760     IDRAW 0,1
3770     ELSE
3780     IDRAW 0,.5
3790     IDRAW 0,-1
3800     IDRAW 0,.5
3810     END IF
3820     NEXT J
3830     NEXT I
3840     MOVE 50,20
3850     DRAW 50,40
3860     DRAW -50,40
3870     DRAW -50,20
3880     CSIZE 3,.6
3890     MOVE -50,-44
3900     LABEL VAL$(1)
3910     FOR I=1 TO 4
3920     MOVE A(I)-3,-44
3930     LABEL VAL$(10^I)
3940     NEXT I
3950     FOR I=0 TO 8 STEP 2
3960     MOVE -56,B(I)-1
3970     LABEL USING "Z.D";I/10
3980     MOVE 51,B(I)-1
3990     LABEL USING "Z.D";I/10
4000     NEXT I
4010     FOR I=10 TO 20 STEP 2
4020     MOVE -56,B(I)-1
4030     LABEL USING "DDD";500*(I-10)/10
4040     MOVE 51,B(I)-1
4050     IF I=10 THEN LABEL USING "D";500*(I-10)/10
4060     IF I=12 THEN LABEL USING "DDD";500*(I-10)/10
4070     IF I>12 THEN LABEL USING "DDD";500*(I-10)/10
4080     NEXT I
4090     CSIZE 4,.6
4100     MOVE -5,-48
4110     LABEL "CYCLE"
4120     CSIZE 3,.6
4130     LDIR 90
4140     MOVE -58,-27
4150     LABEL "a/W"
4160     MOVE -58,-3

```

```

4170 LABEL "Smax (MPa)"
4180 LDIR -90
4190 MOVE 59,13
4200 LABEL "Smin (MPa)"
4210 MOVE 59,-22
4220 LABEL "a/W"
4230 LDIR 0
4240 CSIZE 3.5,.6
4250 MOVE -45,34
4260 LABEL Z1$
4270 MOVE -45,31
4280 LABEL "STRAIN CONTROL"
4290 MOVE -45,28
4300 LABEL Z2$
4310 MOVE -45,26
4320 IDRAW 3,0
4330 IDRAW -1.5,1.5
4340 IDRAW -1.5,-1.5
4350 MOVE -41,25
4360 LABEL "T= "&Z3$&" C"
4370 MOVE -45,23
4380 IDRAW 3,0
4390 IDRAW -1.5,1.5
4400 IDRAW -1.5,-1.5
4410 MOVE -41,22
4420 LABEL "E= "&Z4$&" %"
4430!
-----
4440 FOR I=0 TO Counter
4450   X=25*LGT(Cycles(I))-50
4460   Y=30*(Crack(I)/11.7)-40
4470   MOVE X,Y
4480   IMOVE -1,-2
4490   LABEL "."
4500 NEXT I
4510!
-----
4520 MOVE -50,0
4530 Previous1=Stress_max(0)*21.6078*5
4540 Previous2=Stress_max(0)*21.6078*5
4550 FOR I=0 TO Counter
4560   X=25*LGT(Cycles(I))-50
4570   Load=Stress_max(I)*21.6078*5
4580   IF Load>Previous1+75 OR Load<Previous1-75 THEN Alpha1
4590   IF Load>Previous2+75 OR Load<Previous2-75 THEN Alpha1
4600   GOTO 4640
4610 Alpha1:!
4620   Load=Previous1
4630   Stress_max(I)=Load/(21.6078*5)
4640   !
-----
4650   Y=30*Load/500-10
4660   MOVE X-1,Y-2
4670   LABEL "+"
4680   Previous2=Previous1
4690   Previous1=Load
4700 NEXT I

```

```

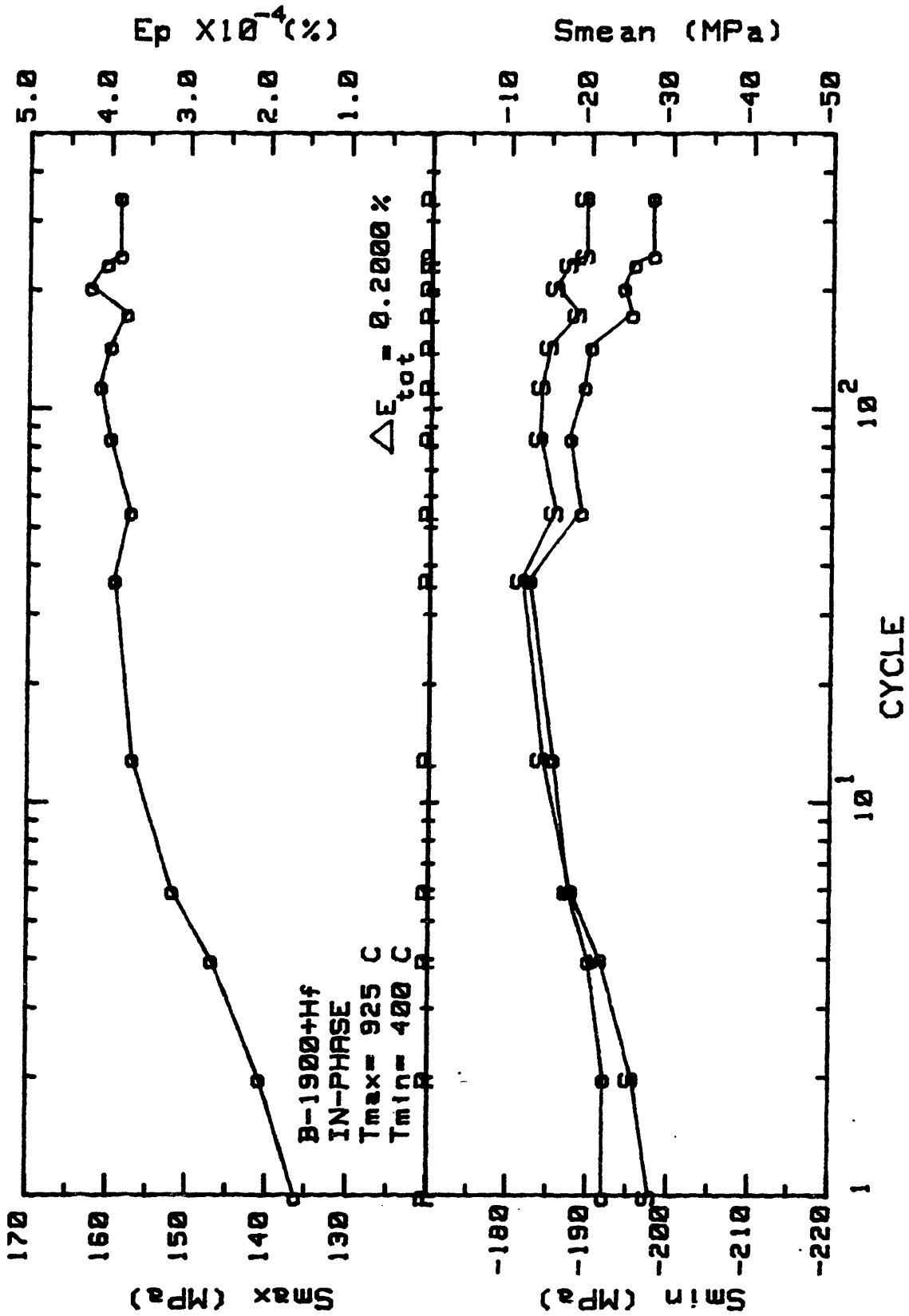
4710! -----
4720 MOVE -50,0
4730 Previous1=-Stress_min(0)*21.6078*5
4740 Previous2=-Stress_min(0)*21.6078*5
4750 FOR I=0 TO Counter
4760   X=25*LGT(Cycles(I))-50
4770   Load=-Stress_min(I)*21.6078*5
4780   IF Load>Previous1+50 OR Load<Previous1-50 THEN Alpha
4790   IF Load>Previous2+50 OR Load<Previous2-50 THEN Alpha
4800   GOTO 4840
4810 Alpha: !
4820     Load=Previous1
4830     Stress_min(I)=-Load/(21.6078*5)
4840     ! -----
4850     Y=30*Load/500-10
4860     MOVE X-1,Y-1
4870     LABEL "-"
4880     Previous2=Previous1
4890     Previous1=Load
4900 NEXT I
4910 PAUSE
4920 SUBEND

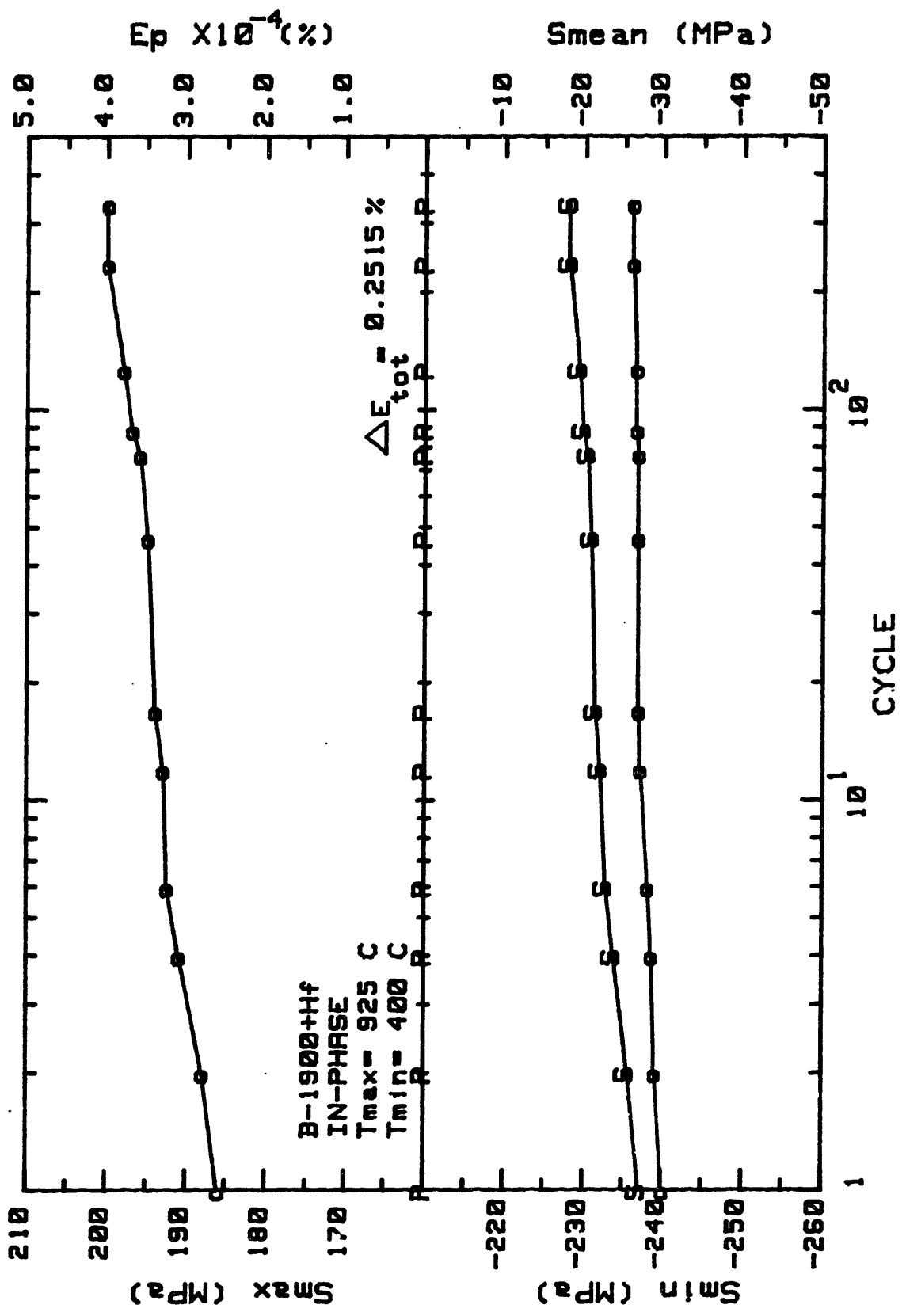
```

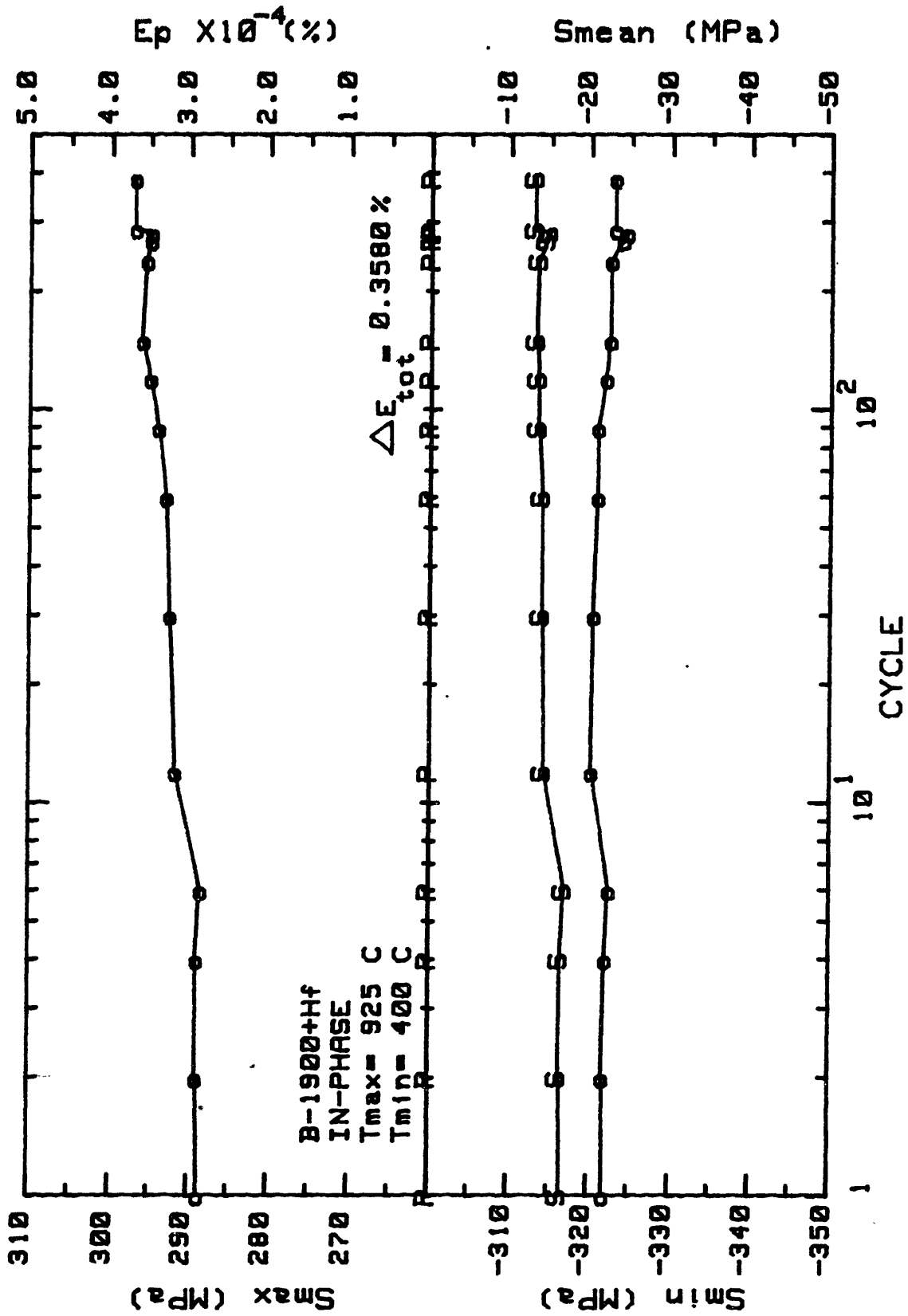

Appendix IV

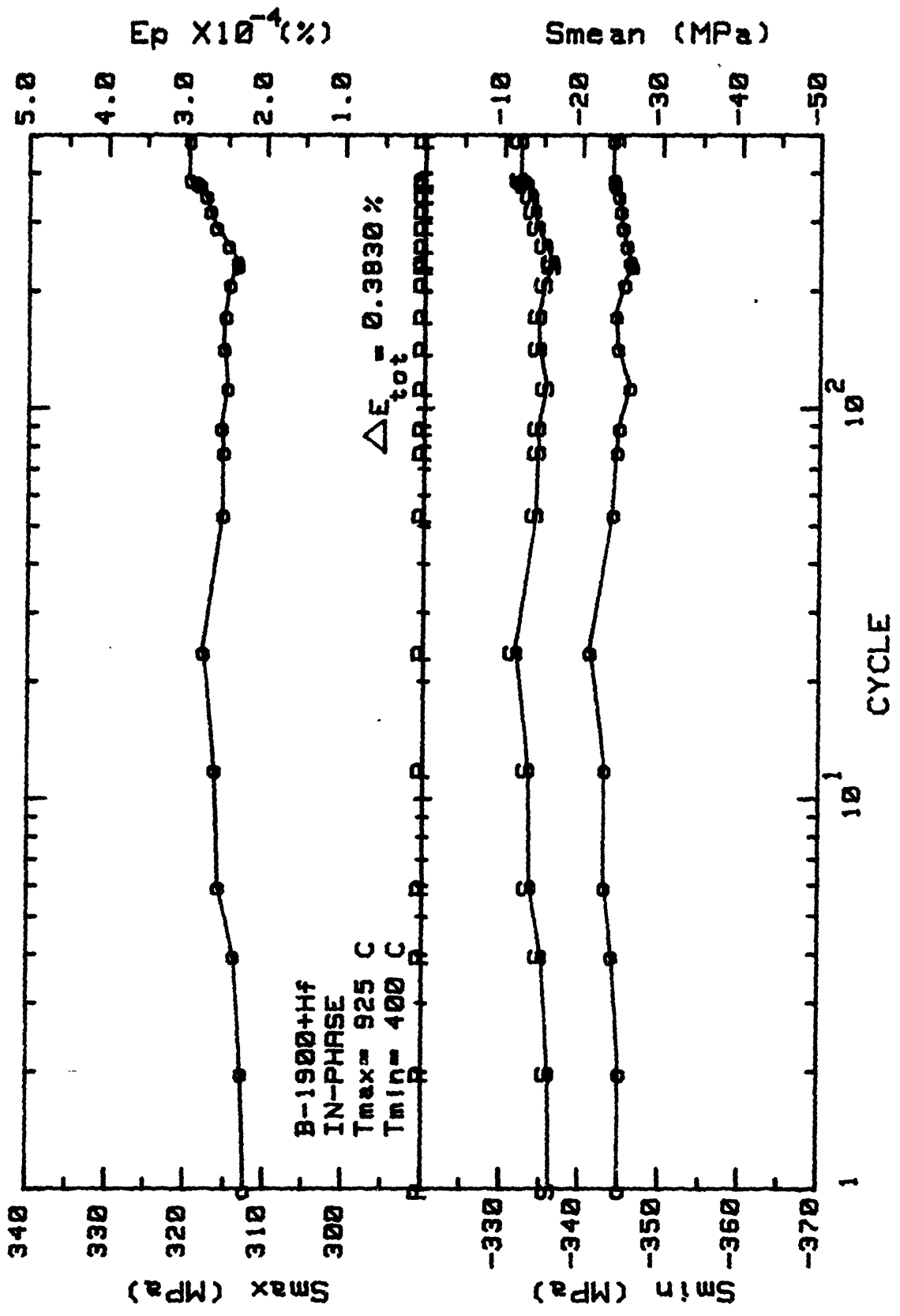
In this appendix the cyclic stress-strain curves obtained under TMF conditions for B-1900+Hf are presented. The crack growth rates as a function of the strain intensity factor (ΔK_{ϵ}) are also presented for $\Delta \epsilon = 0.25\%$ and 0.50% .

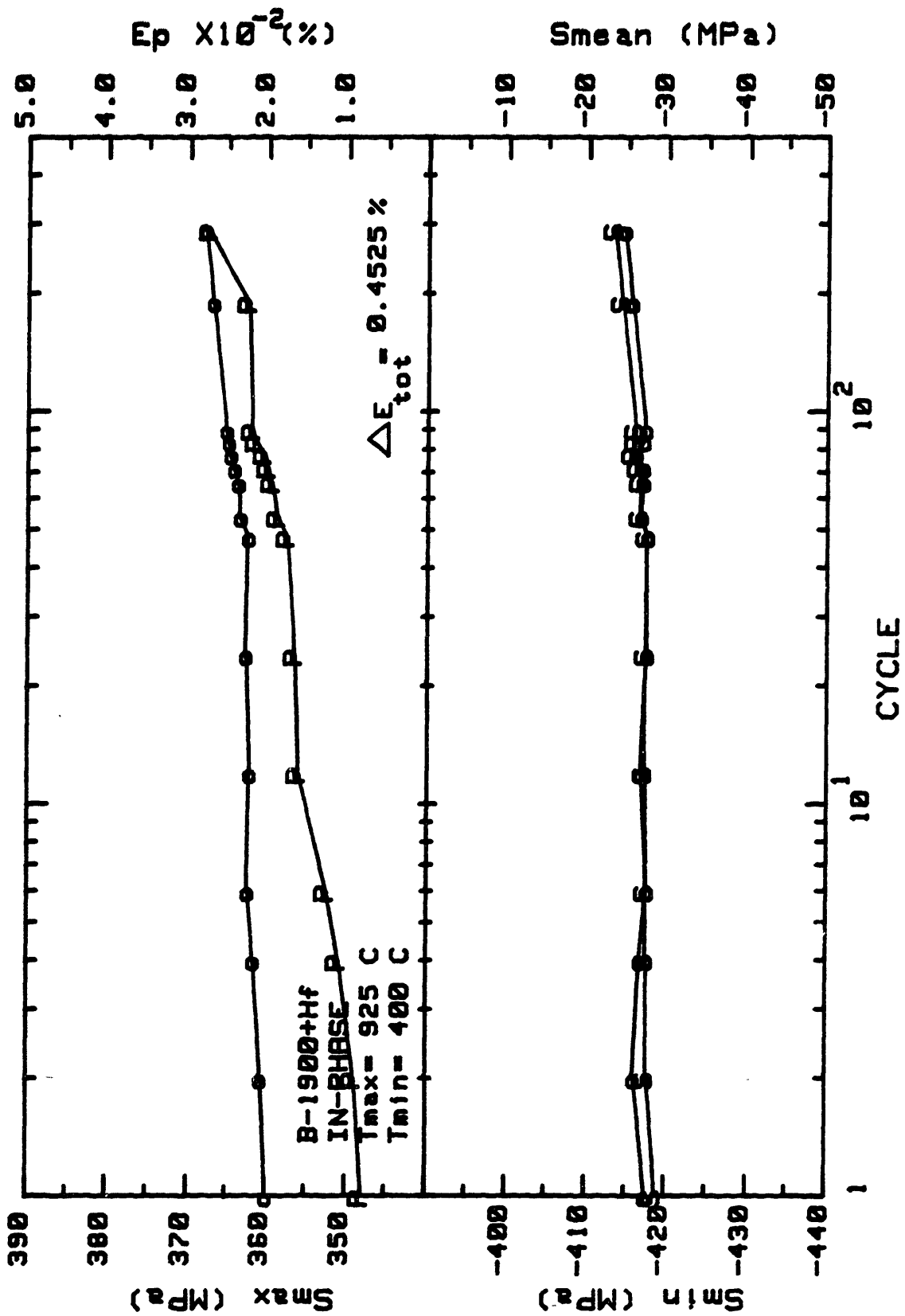
Each cyclic hardening/softening curves show the maximum stress, minimum stress, plastic strain range and mean stress as a function of the applied number of cycles. All data points on the FCG curves are shown as an indication of the scatter and resolution of the testing procedure.

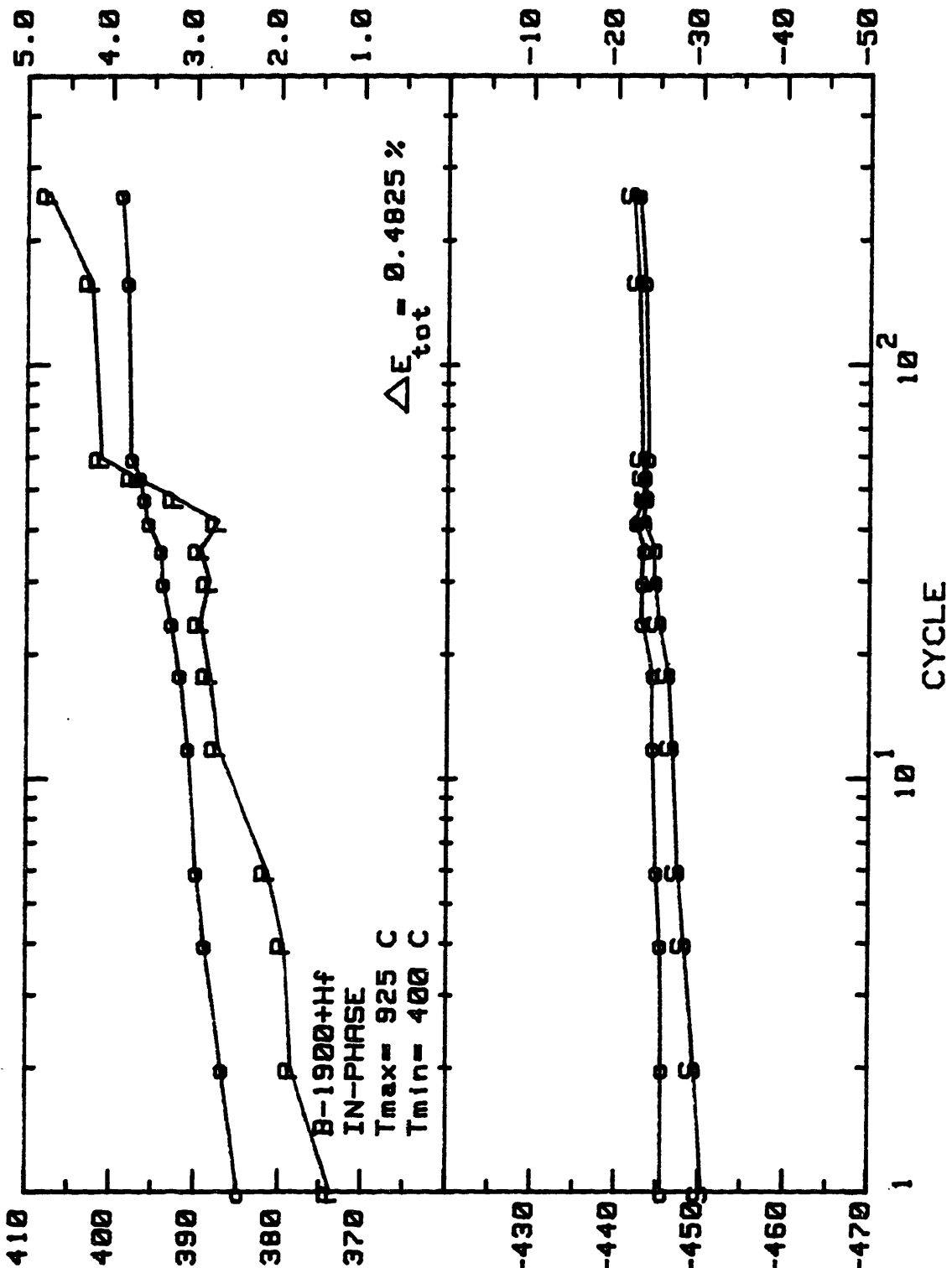
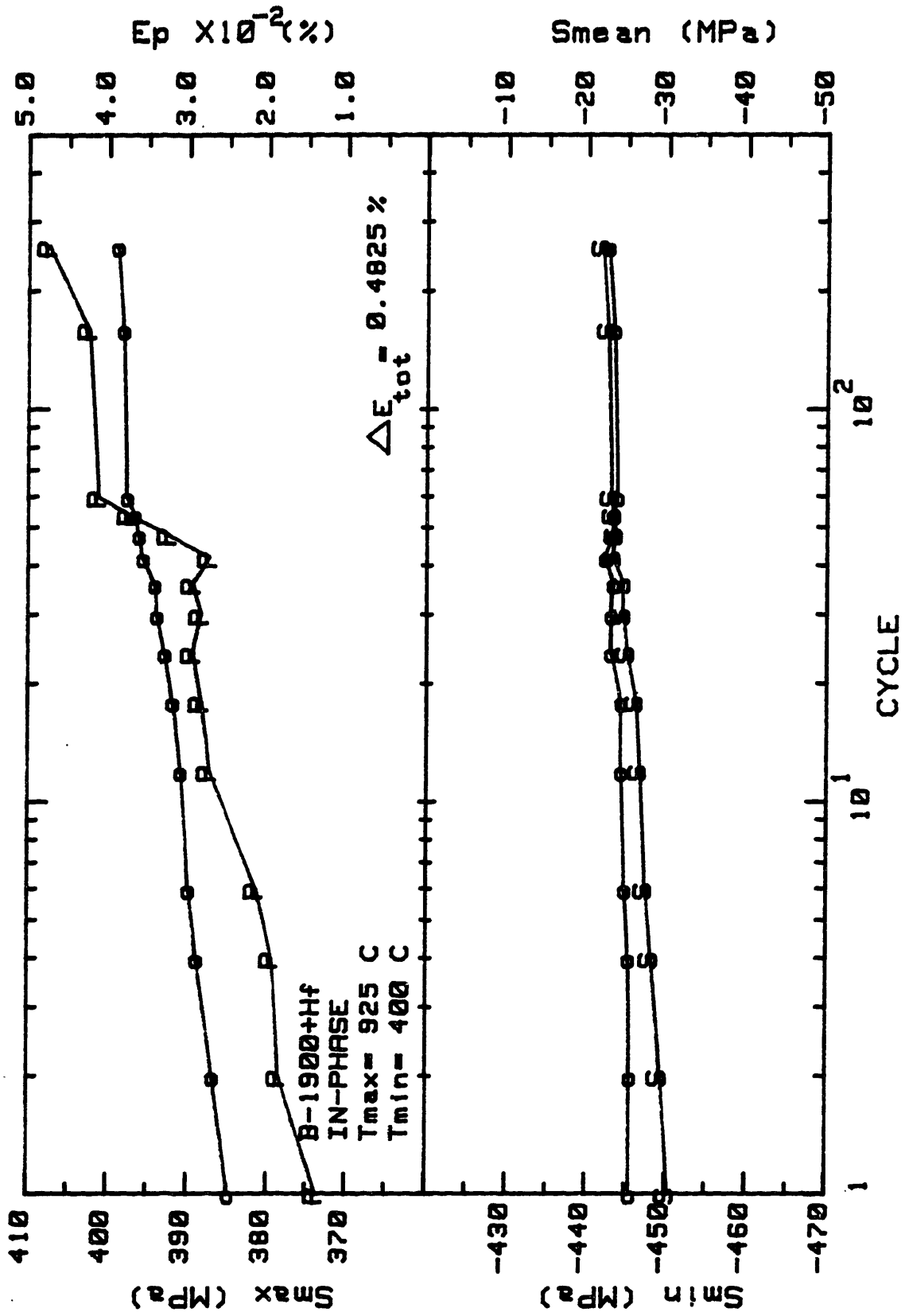


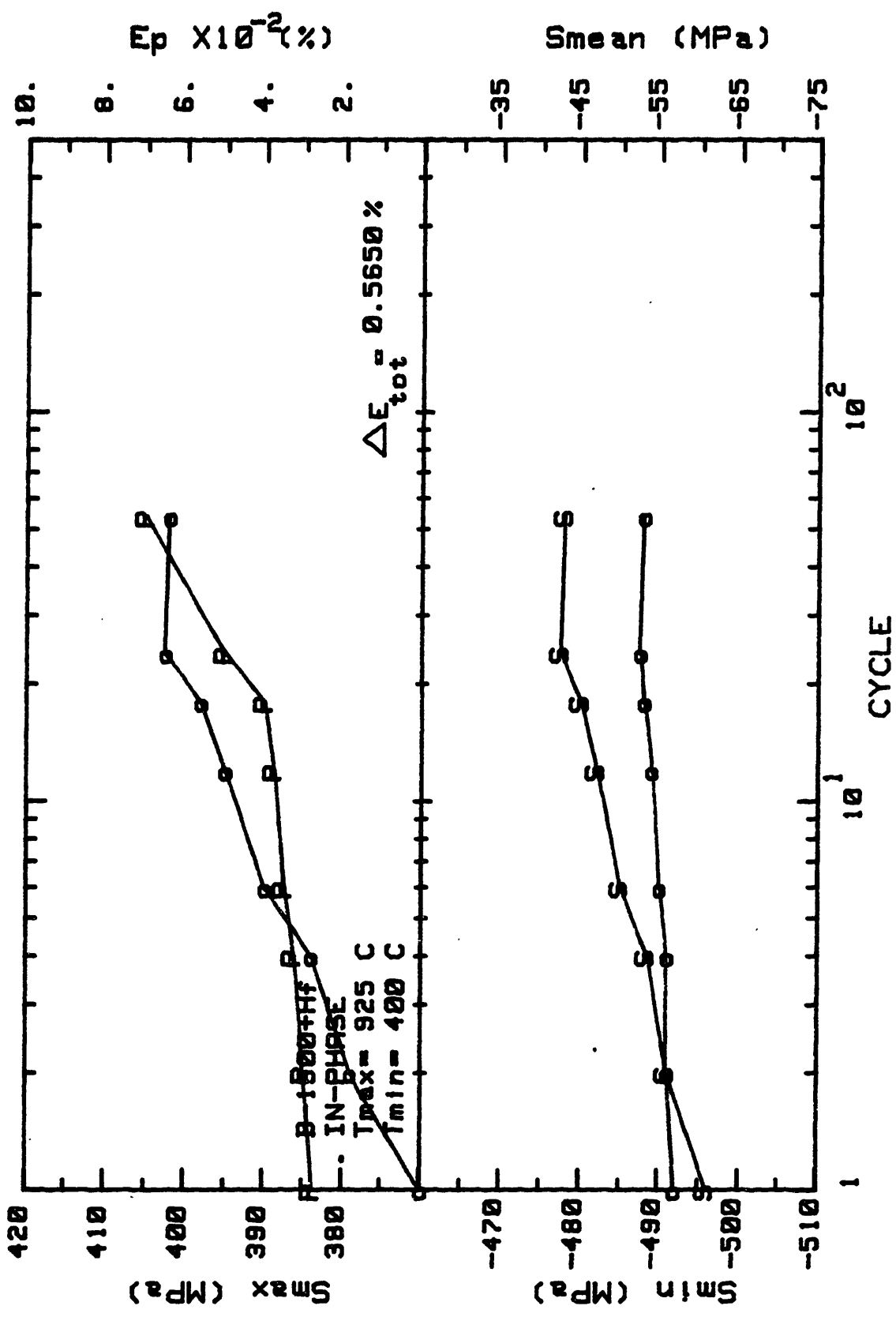


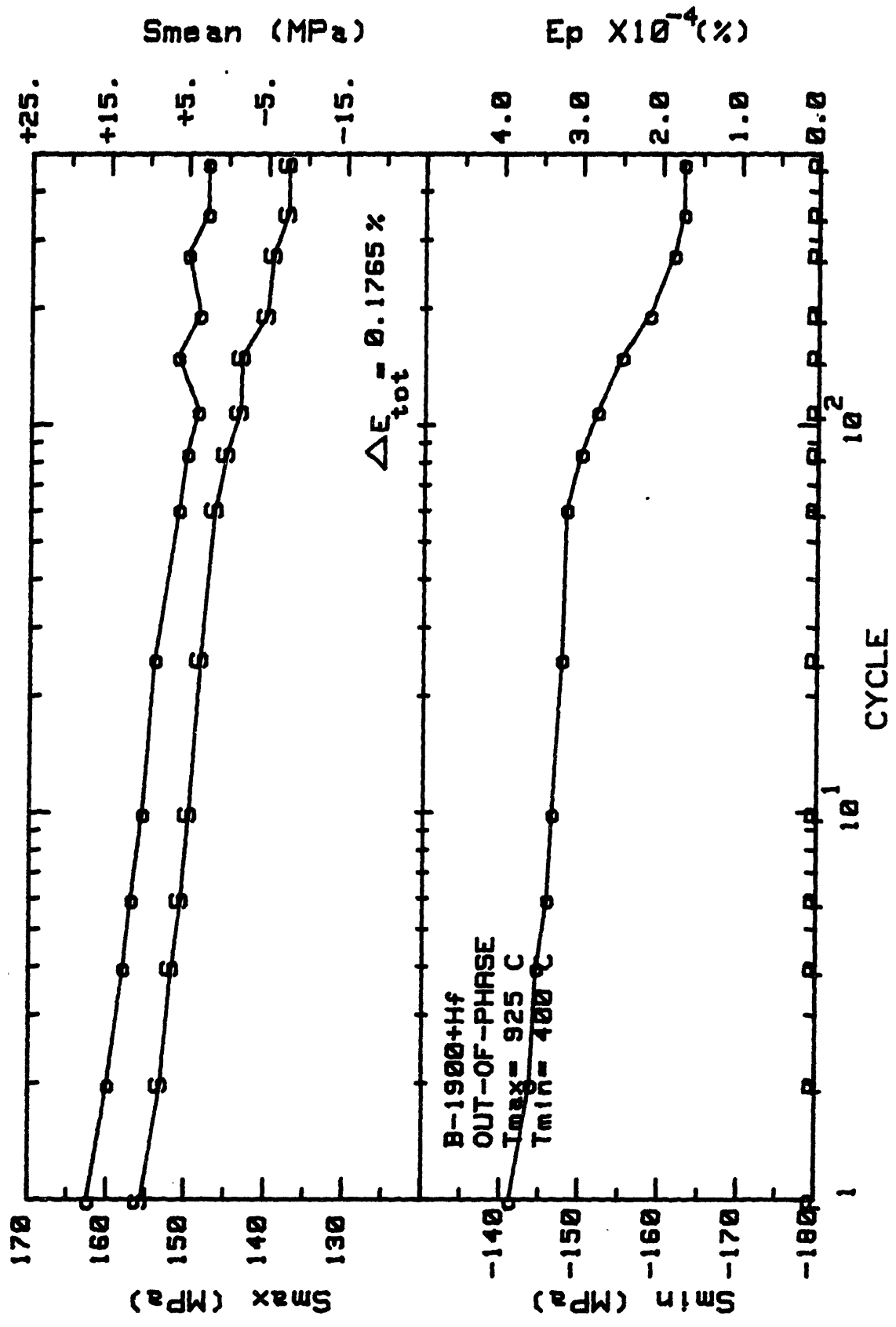


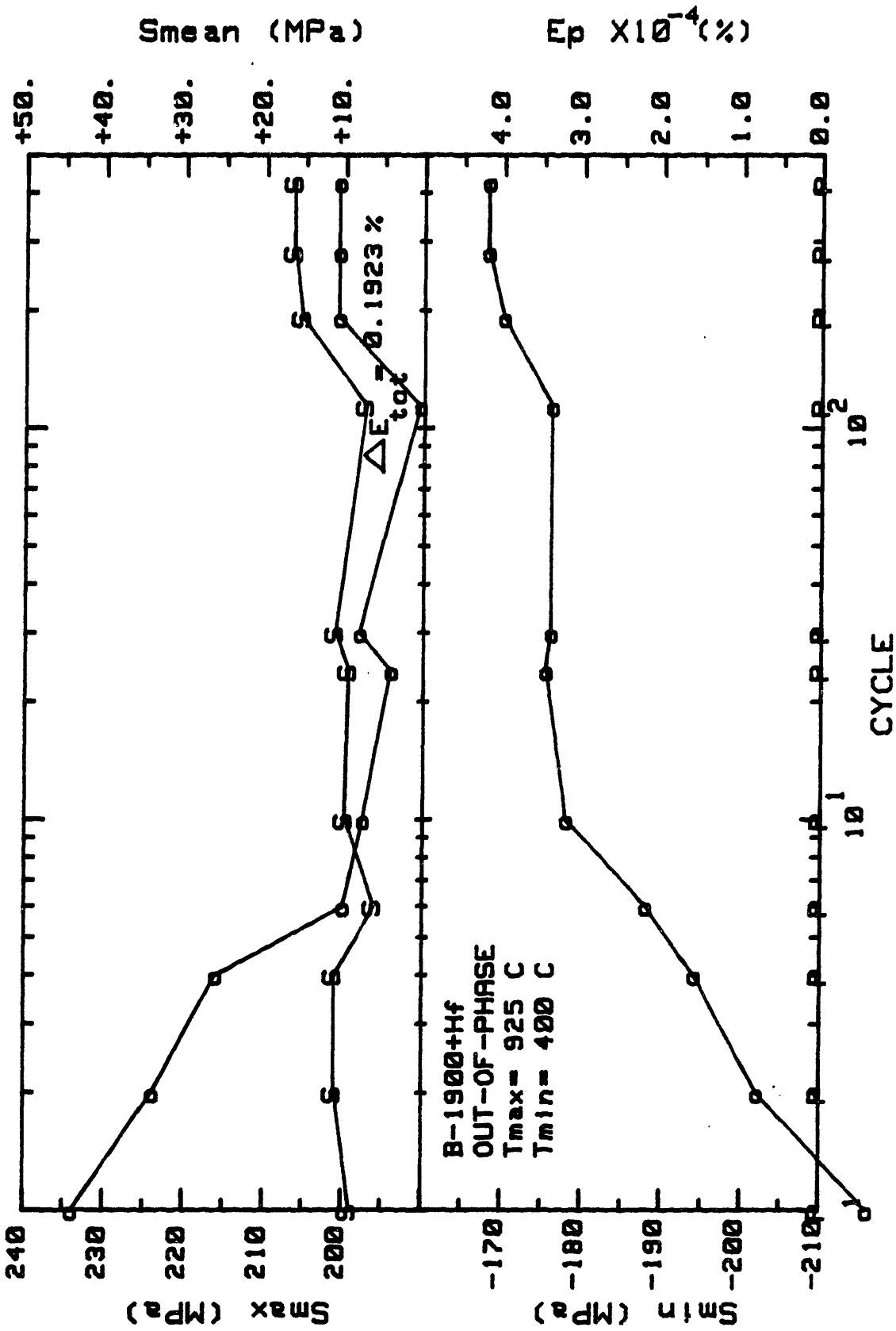


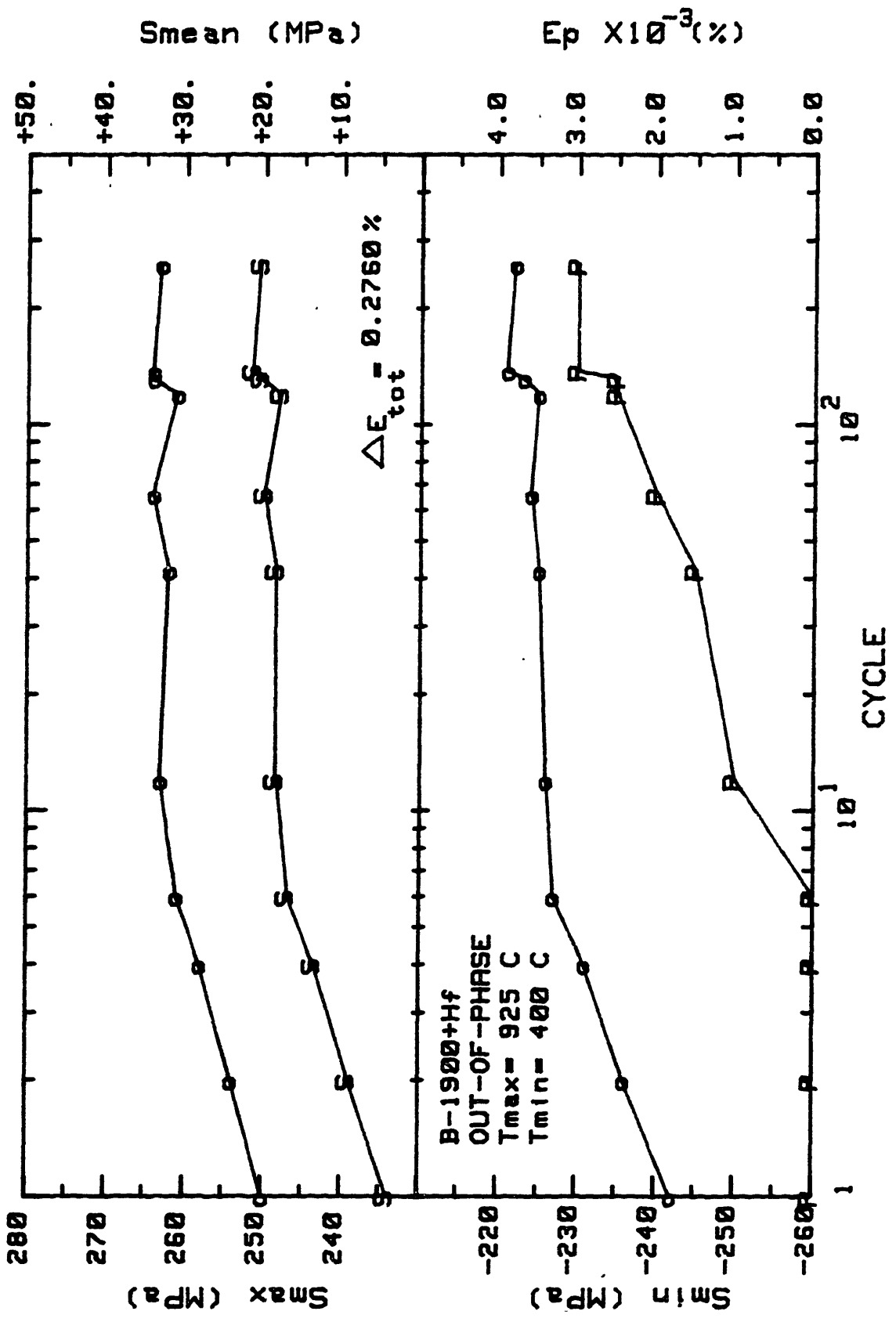


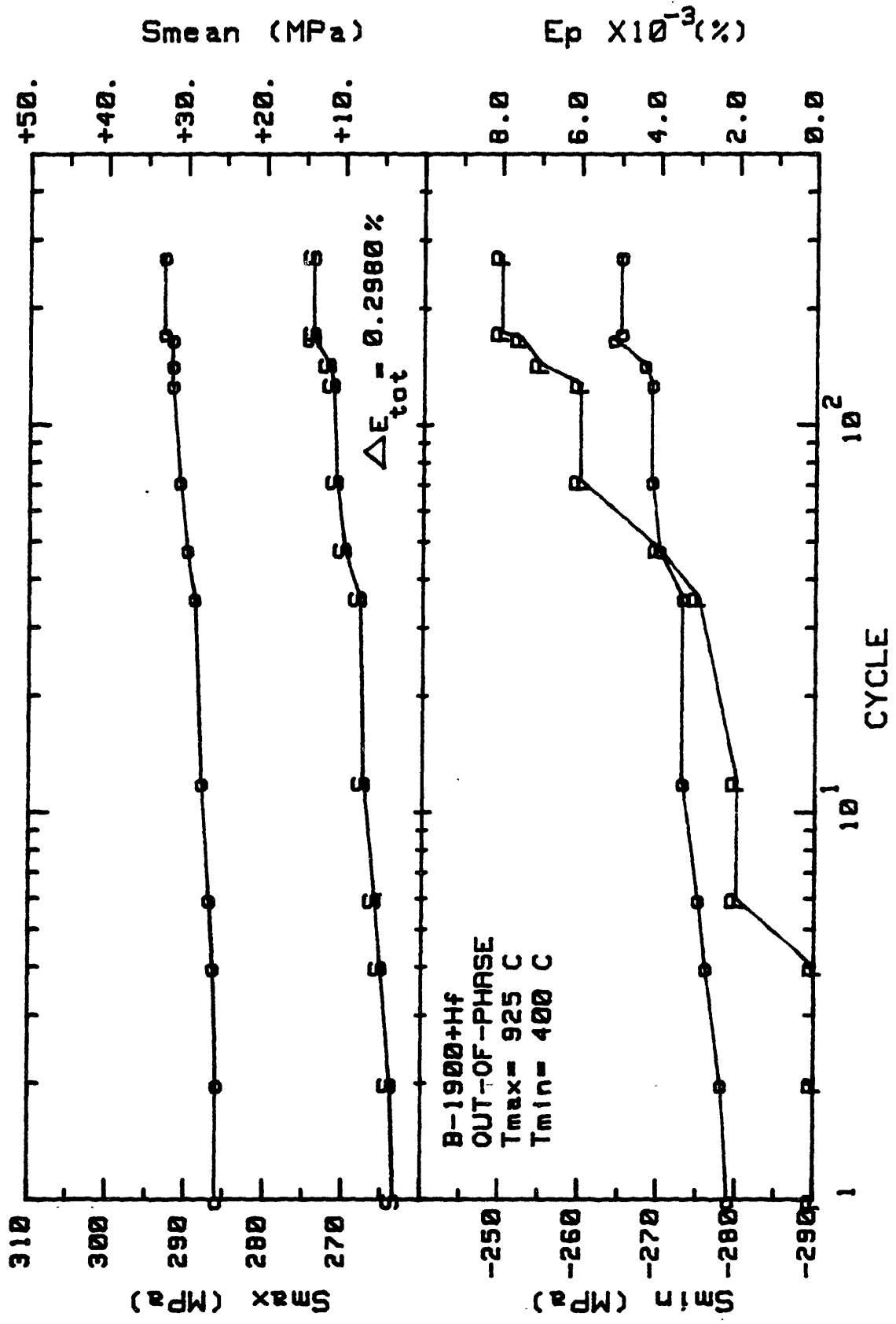


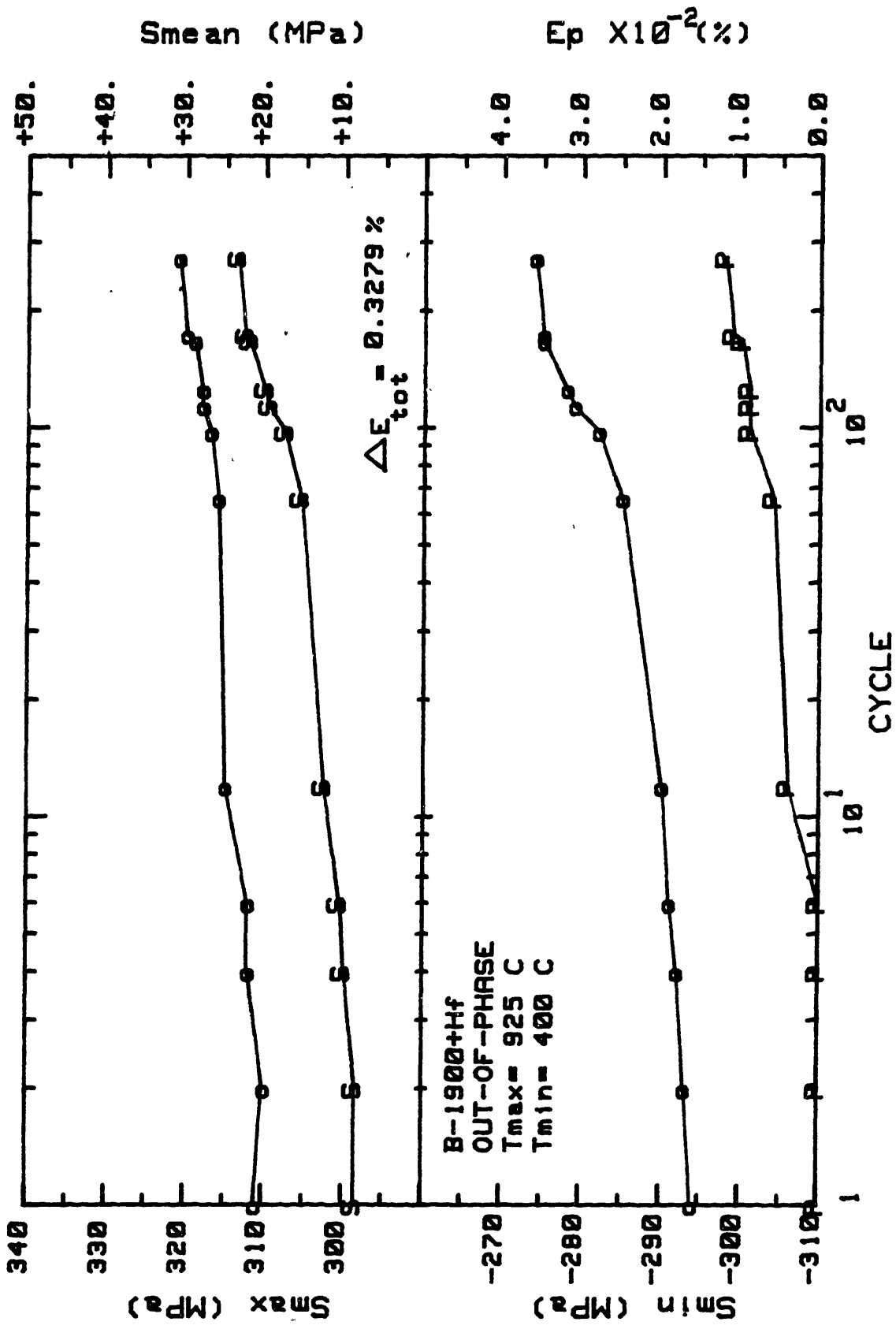


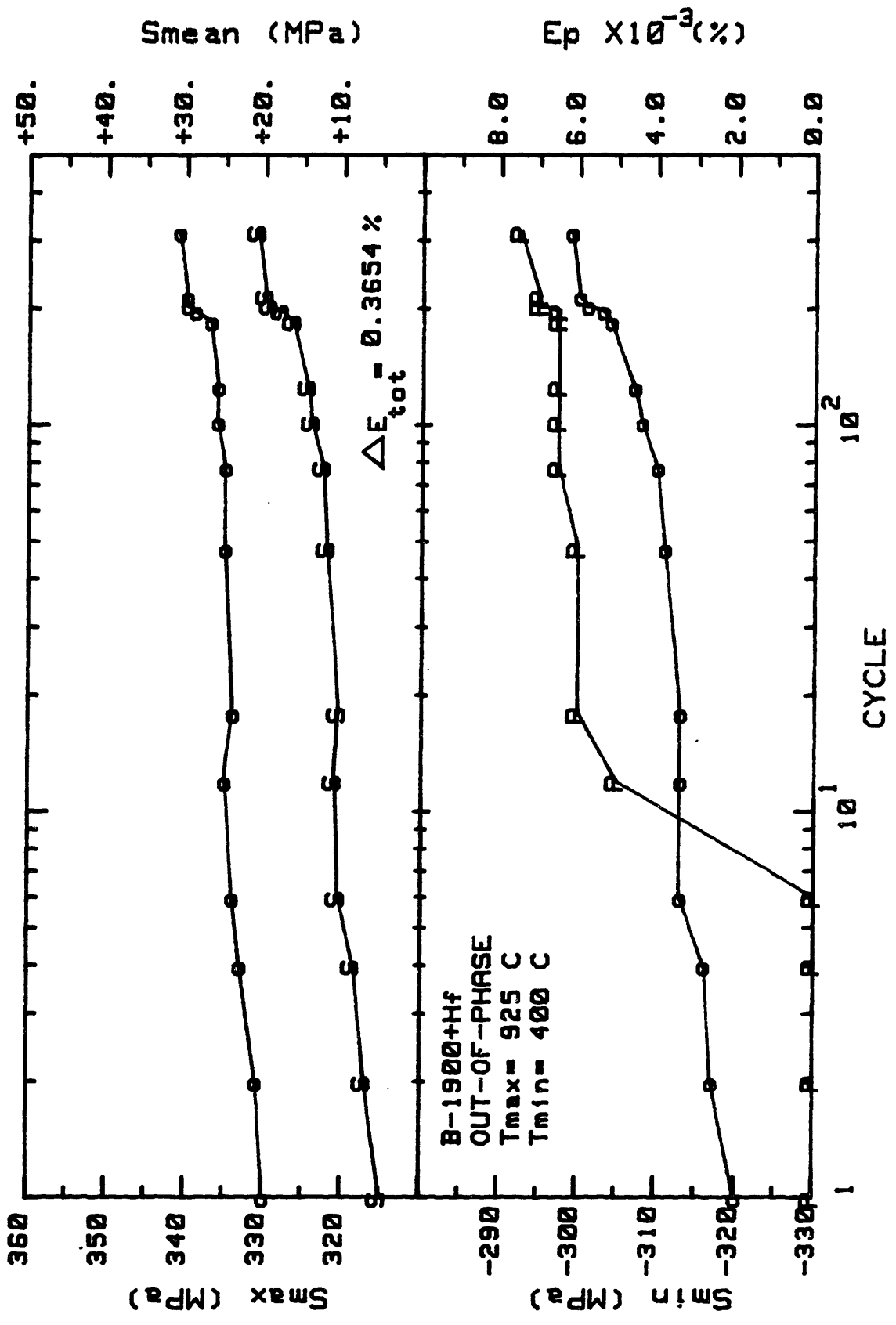


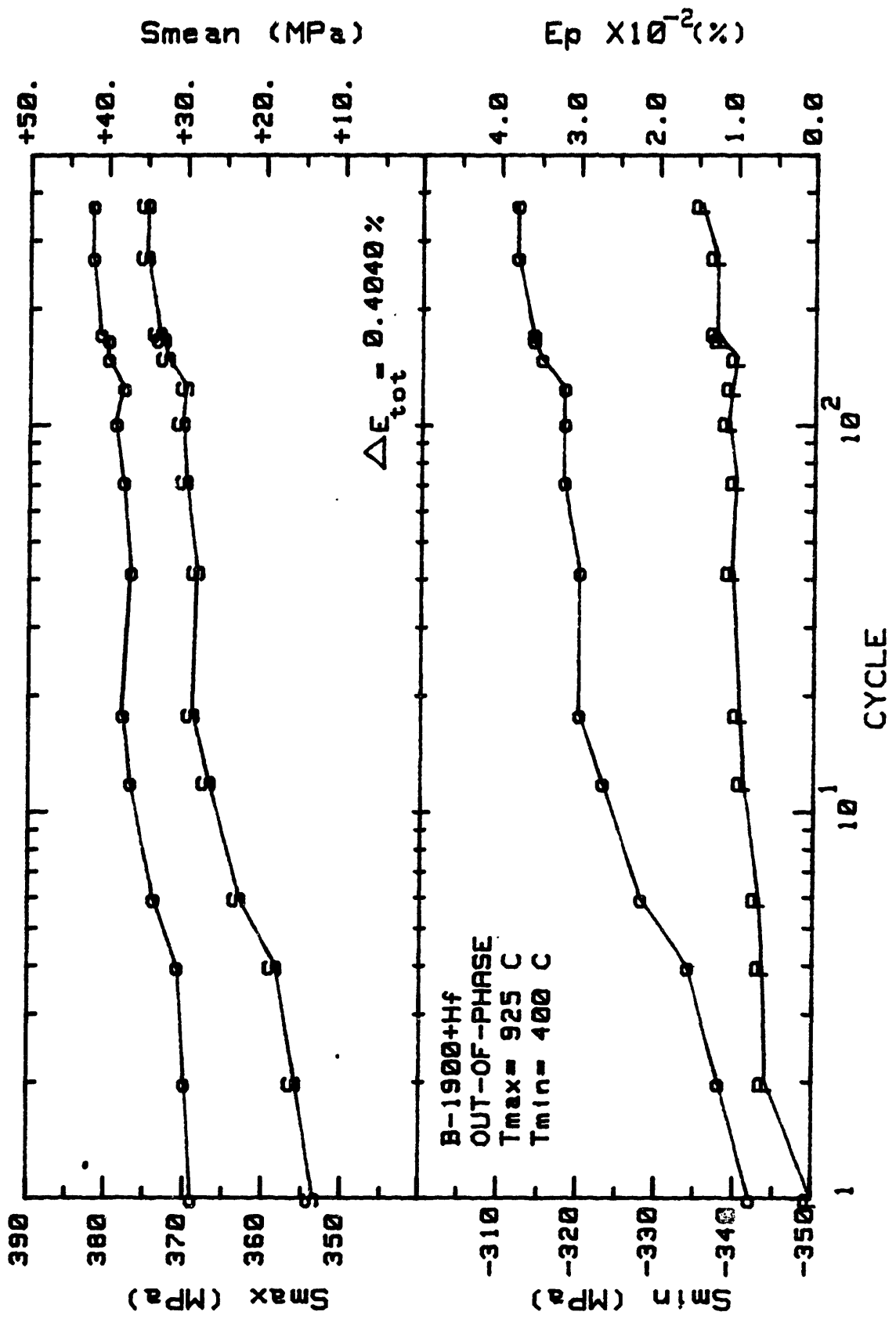


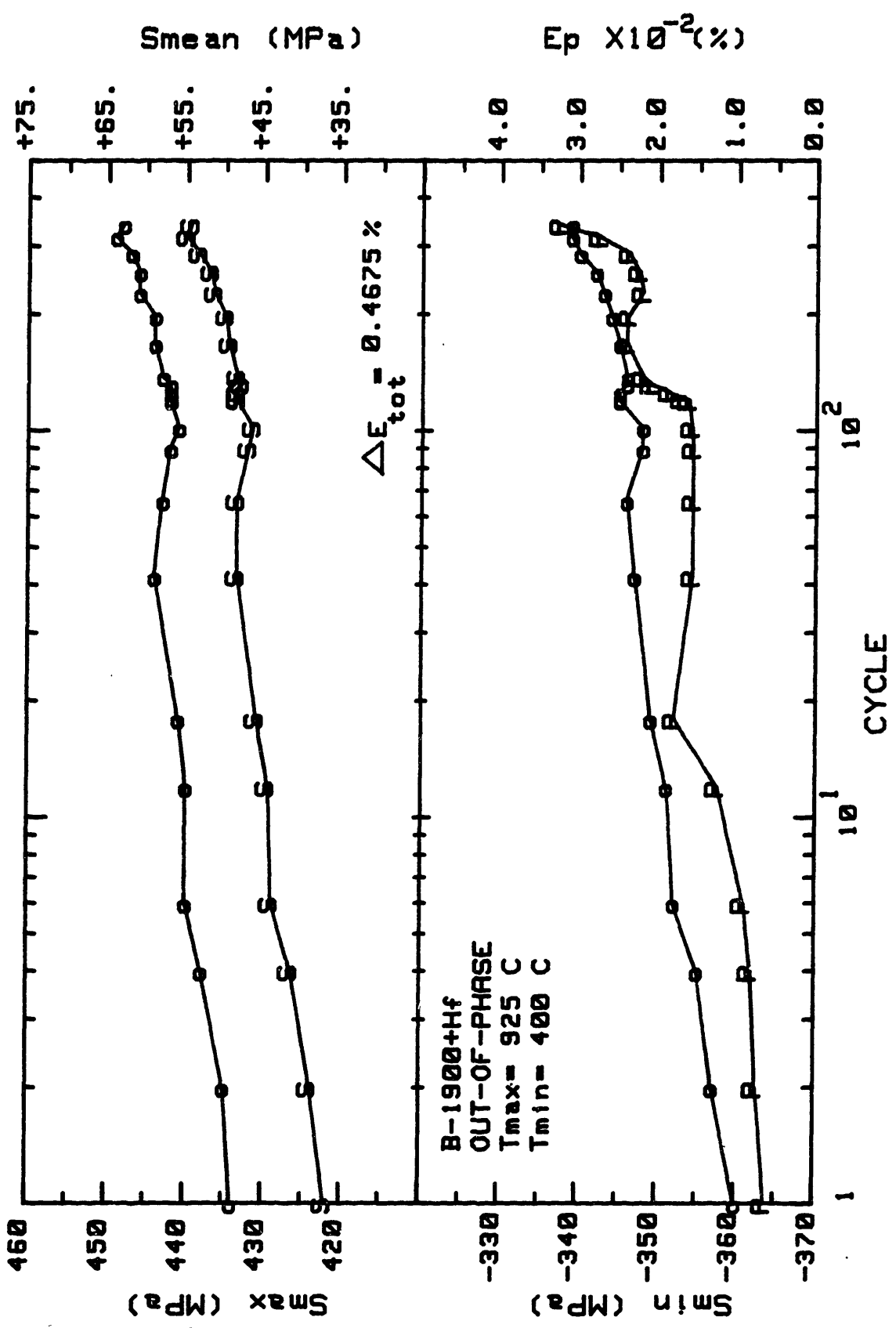


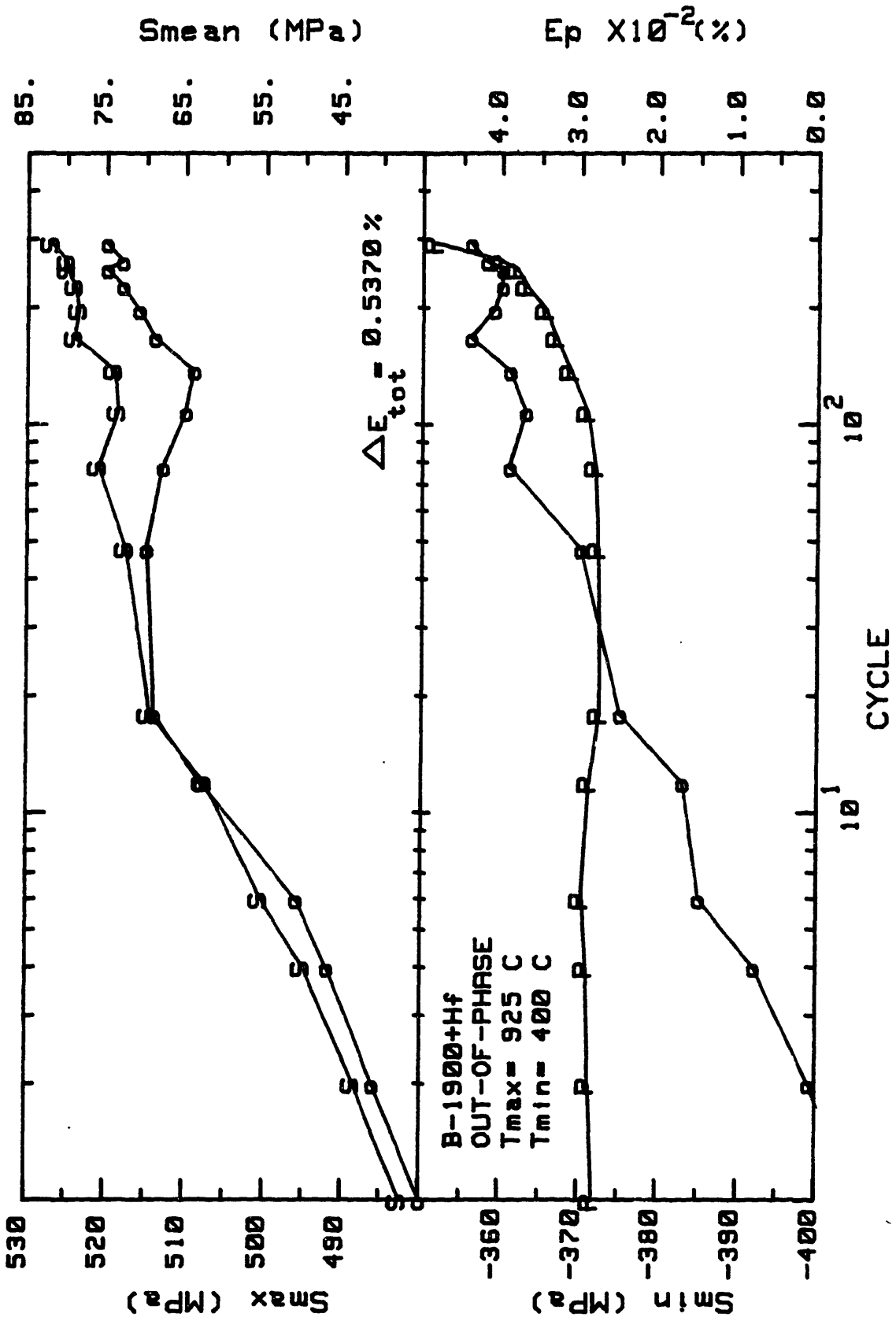


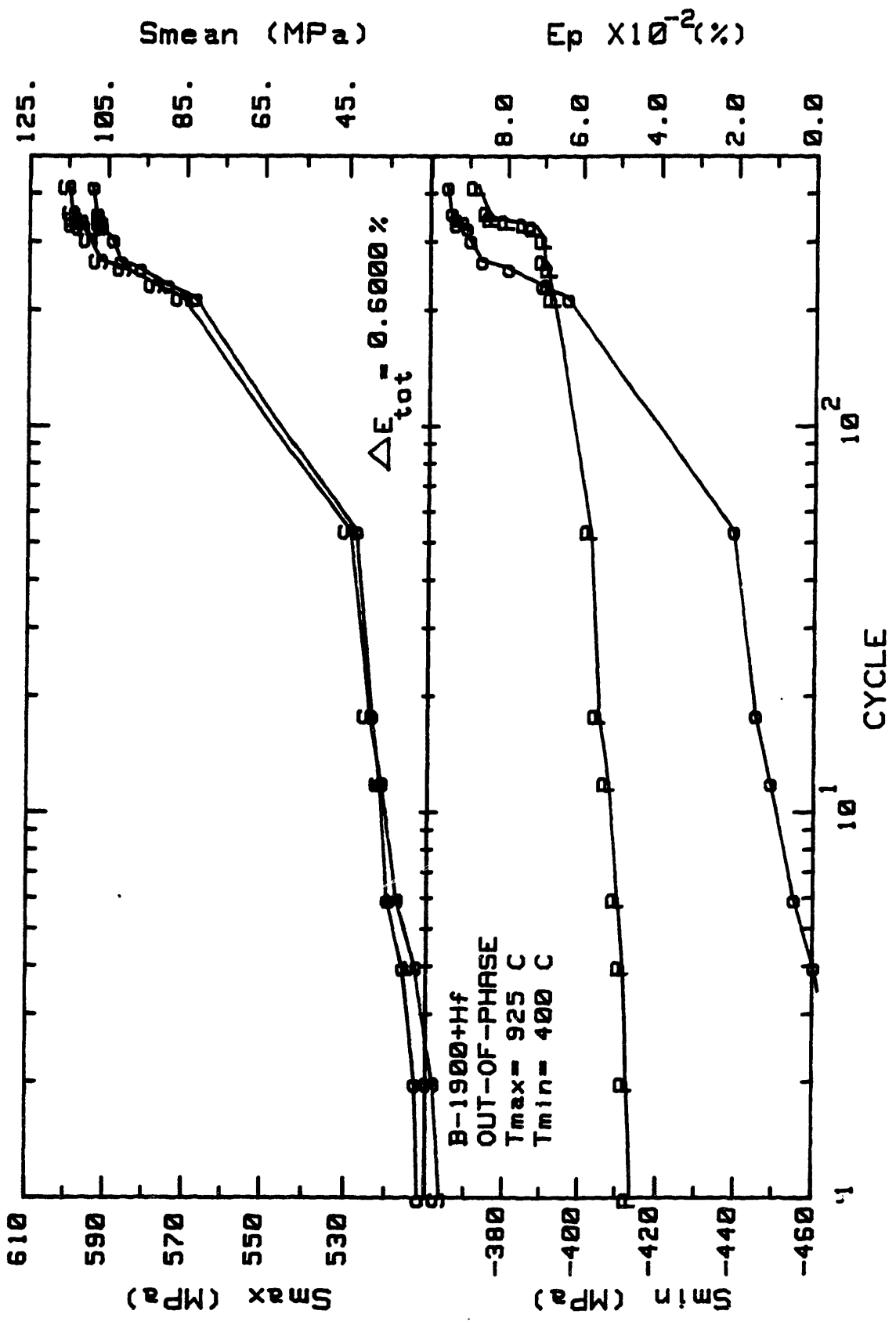


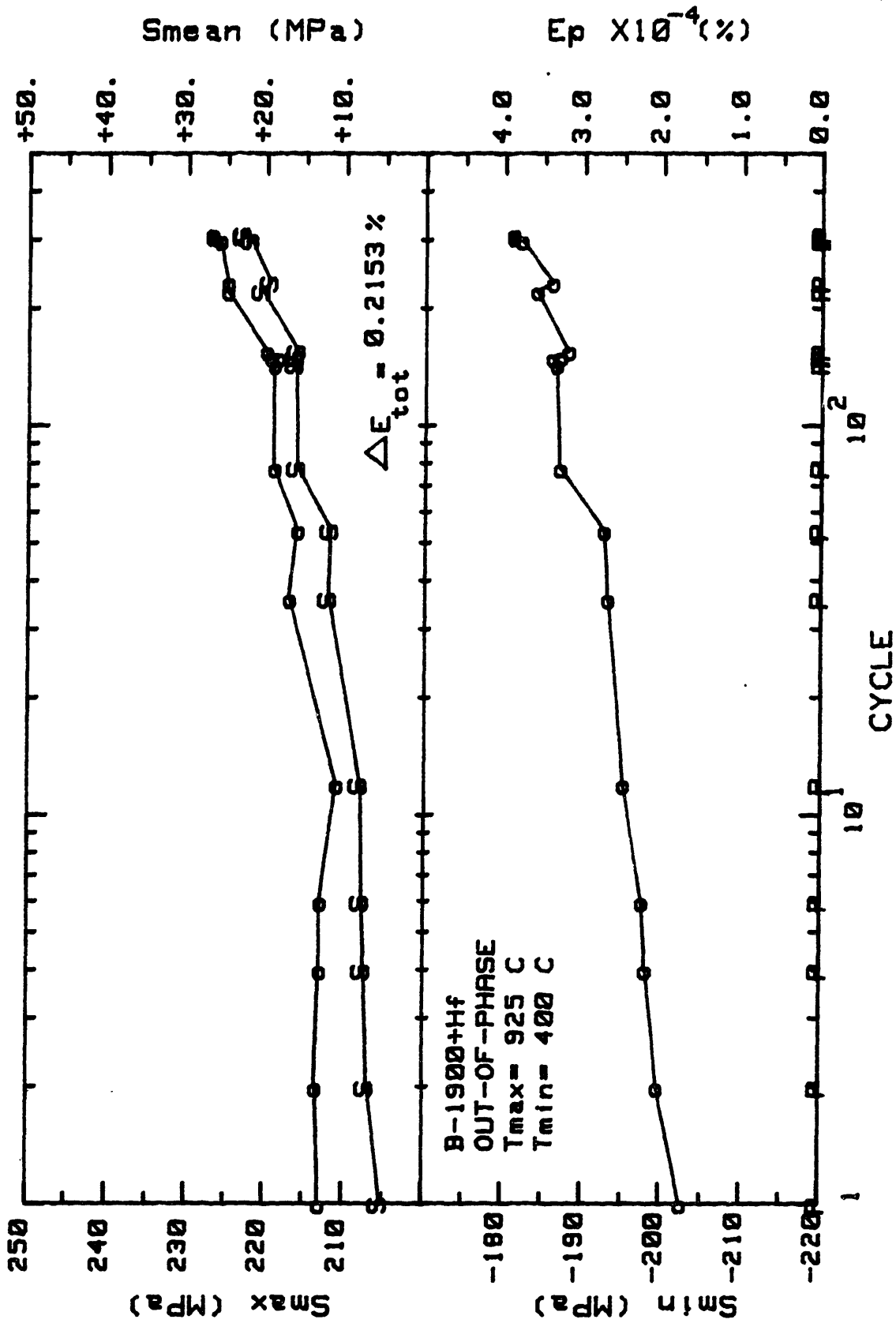


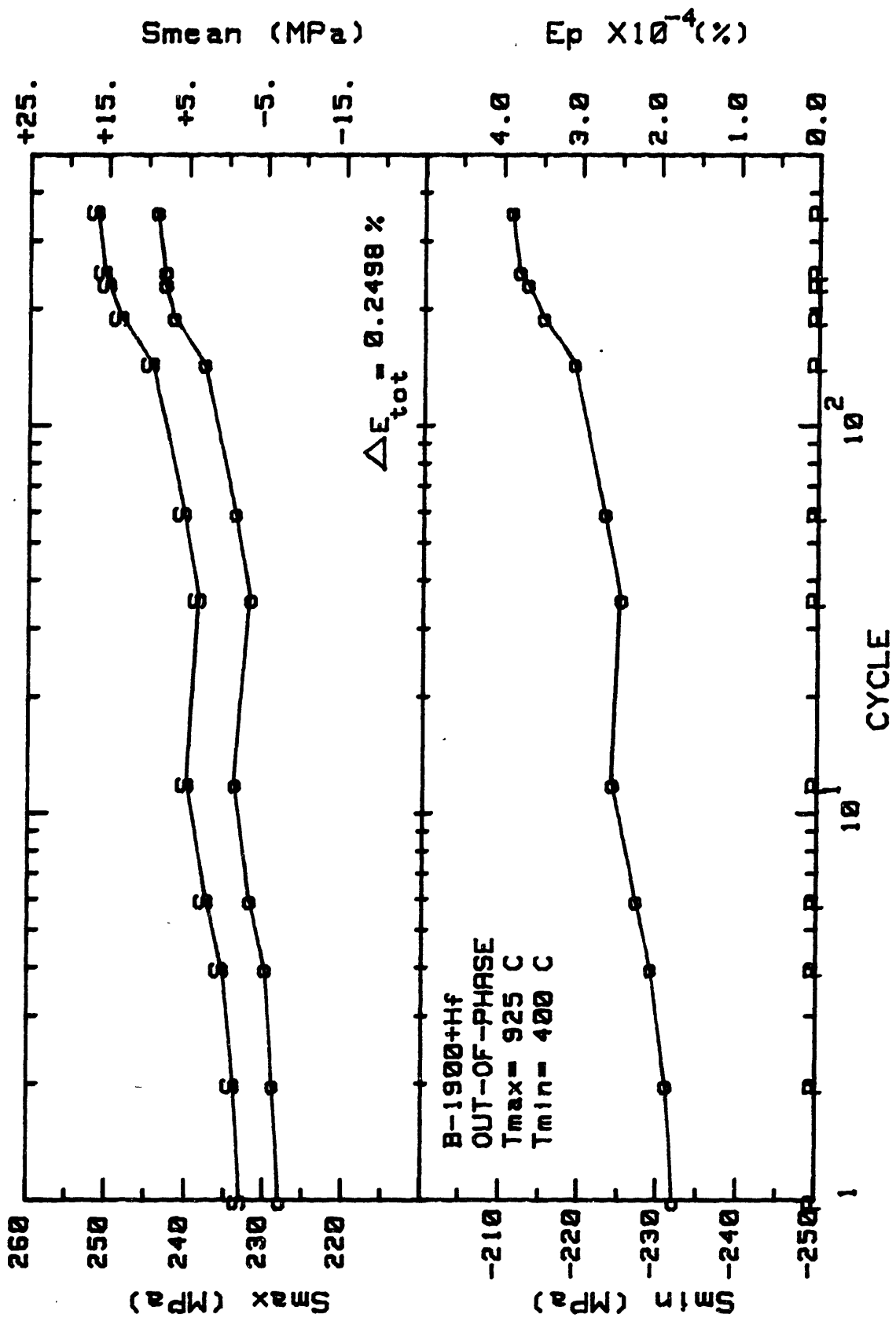






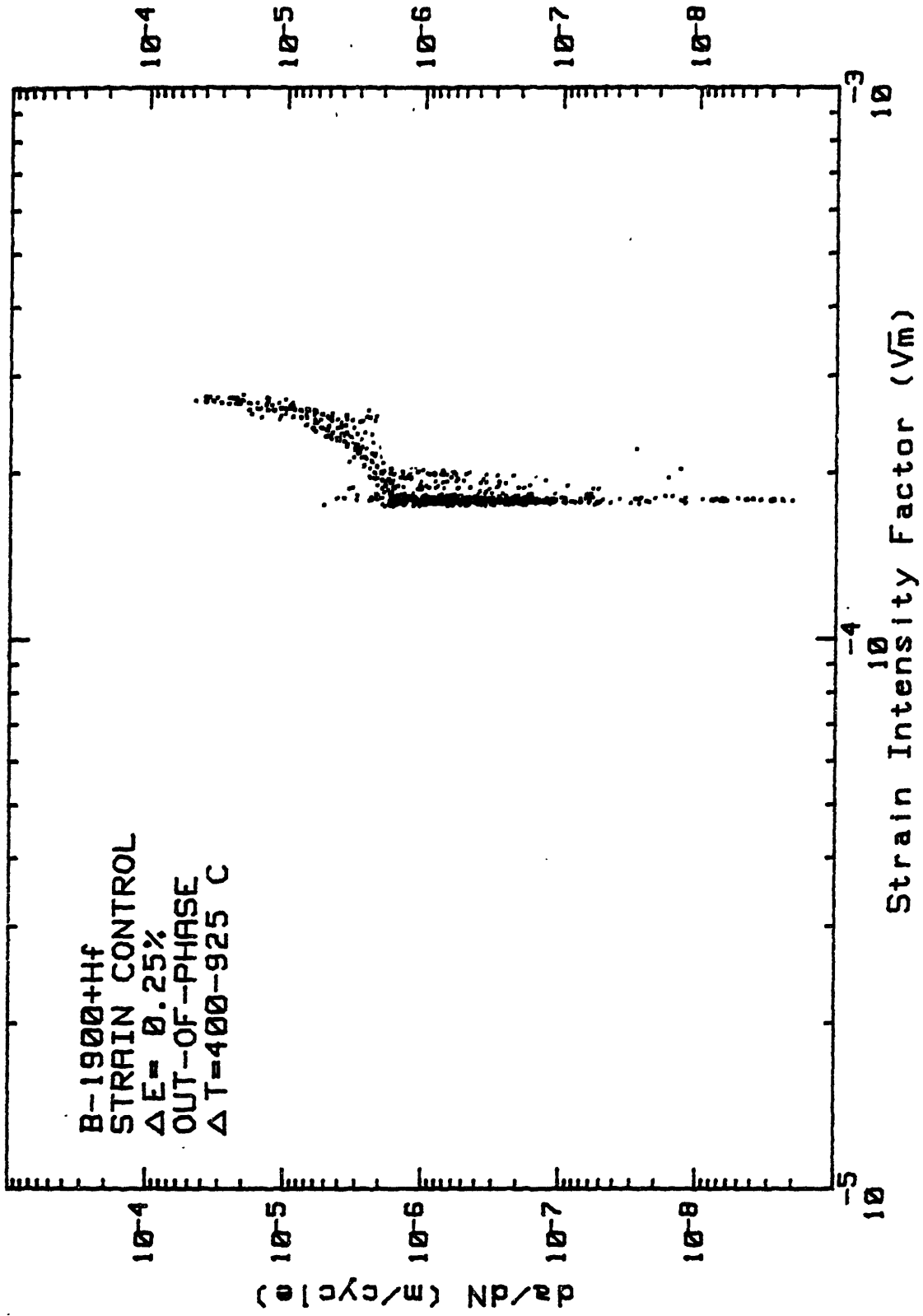






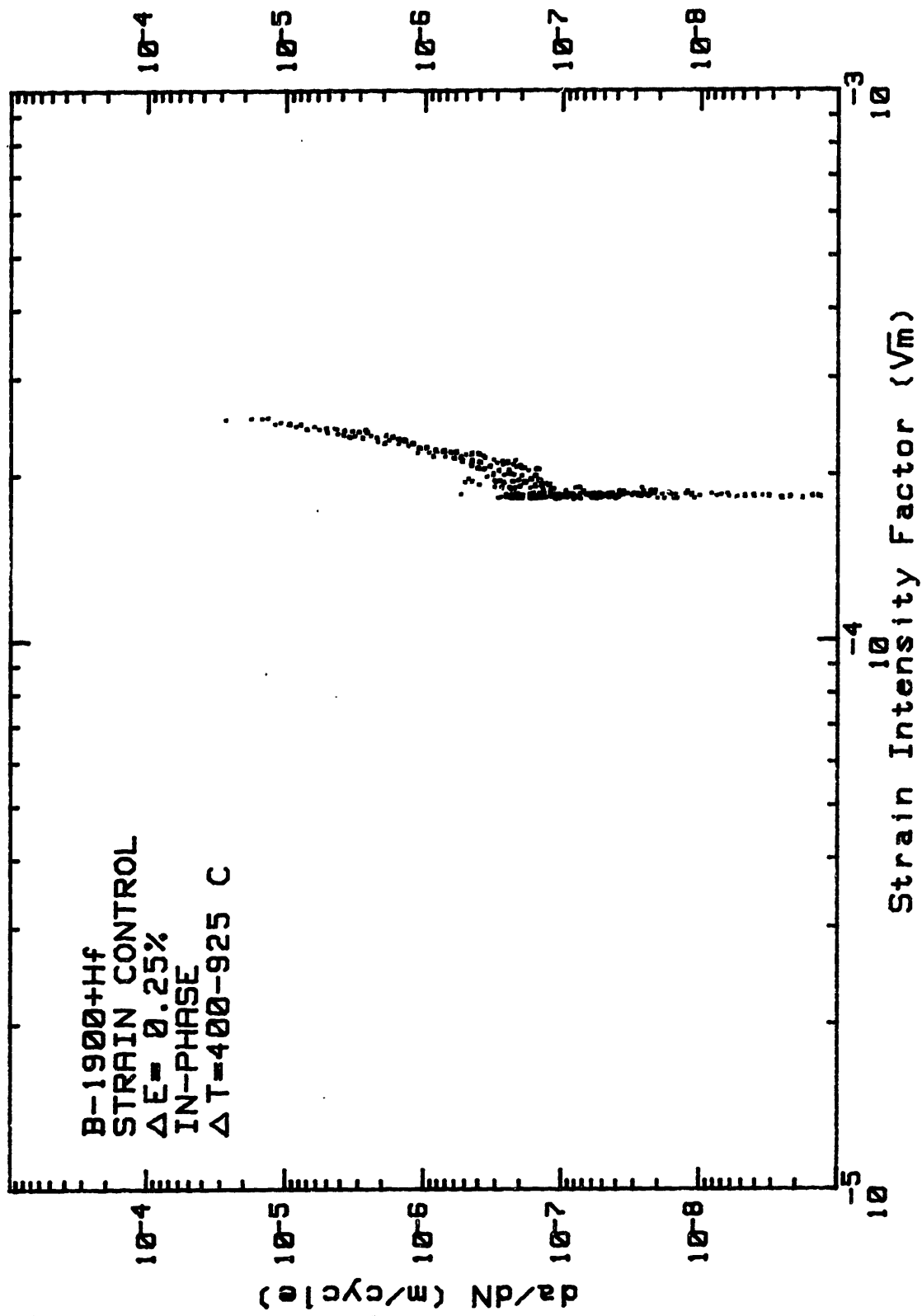
FATIGUE CRACK PROPAGATION

B-1900+Hf
STRAIN CONTROL
 $\Delta E = 0.25\%$
OUT-OF-PHASE
 $\Delta T = 400-925 \text{ C}$



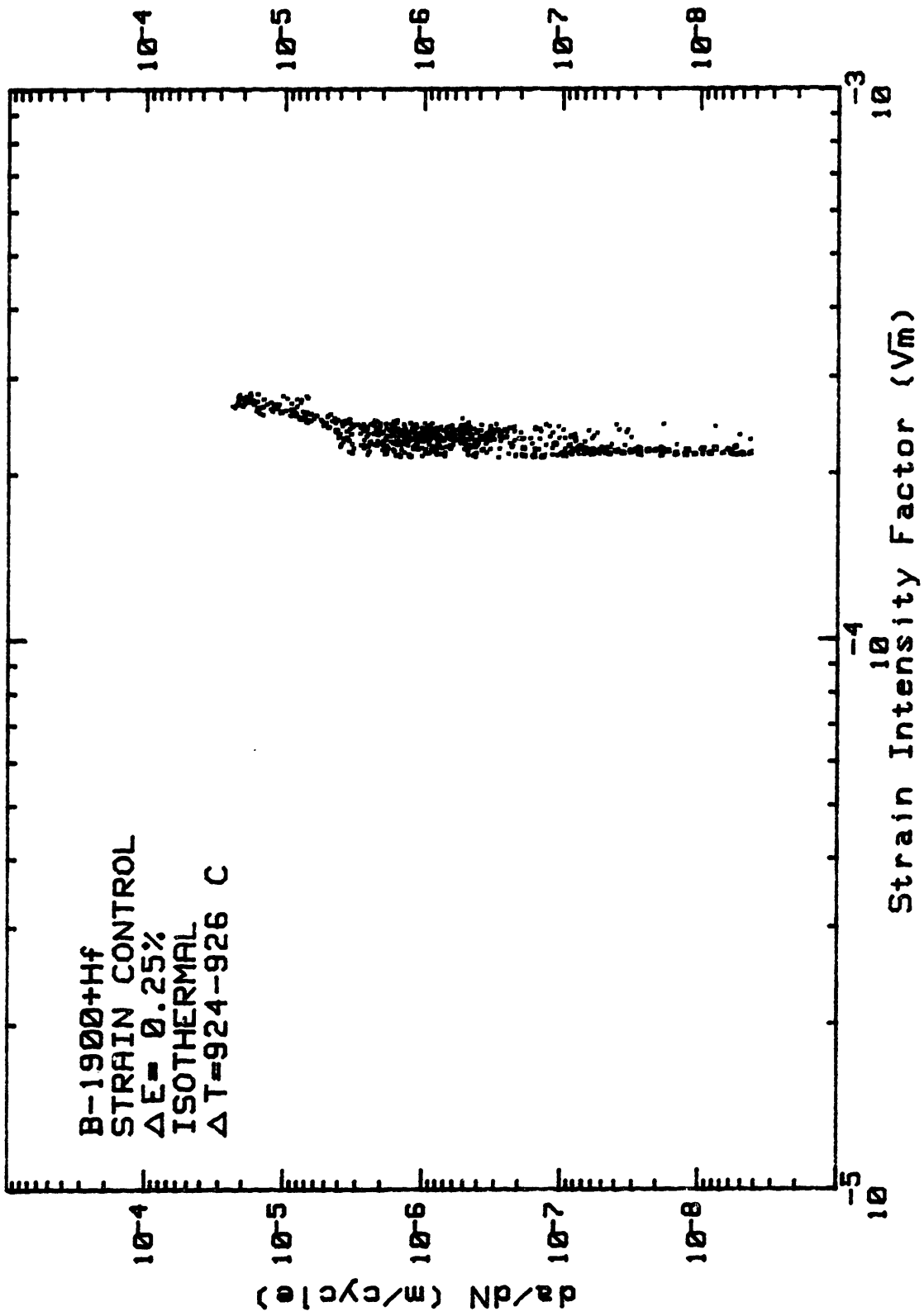
FATIGUE CRACK PROPAGATION

B-1900+Hf
STRAIN CONTROL
 $\Delta E = 0.25\%$
IN-PHASE
 $\Delta T = 400-925$ C



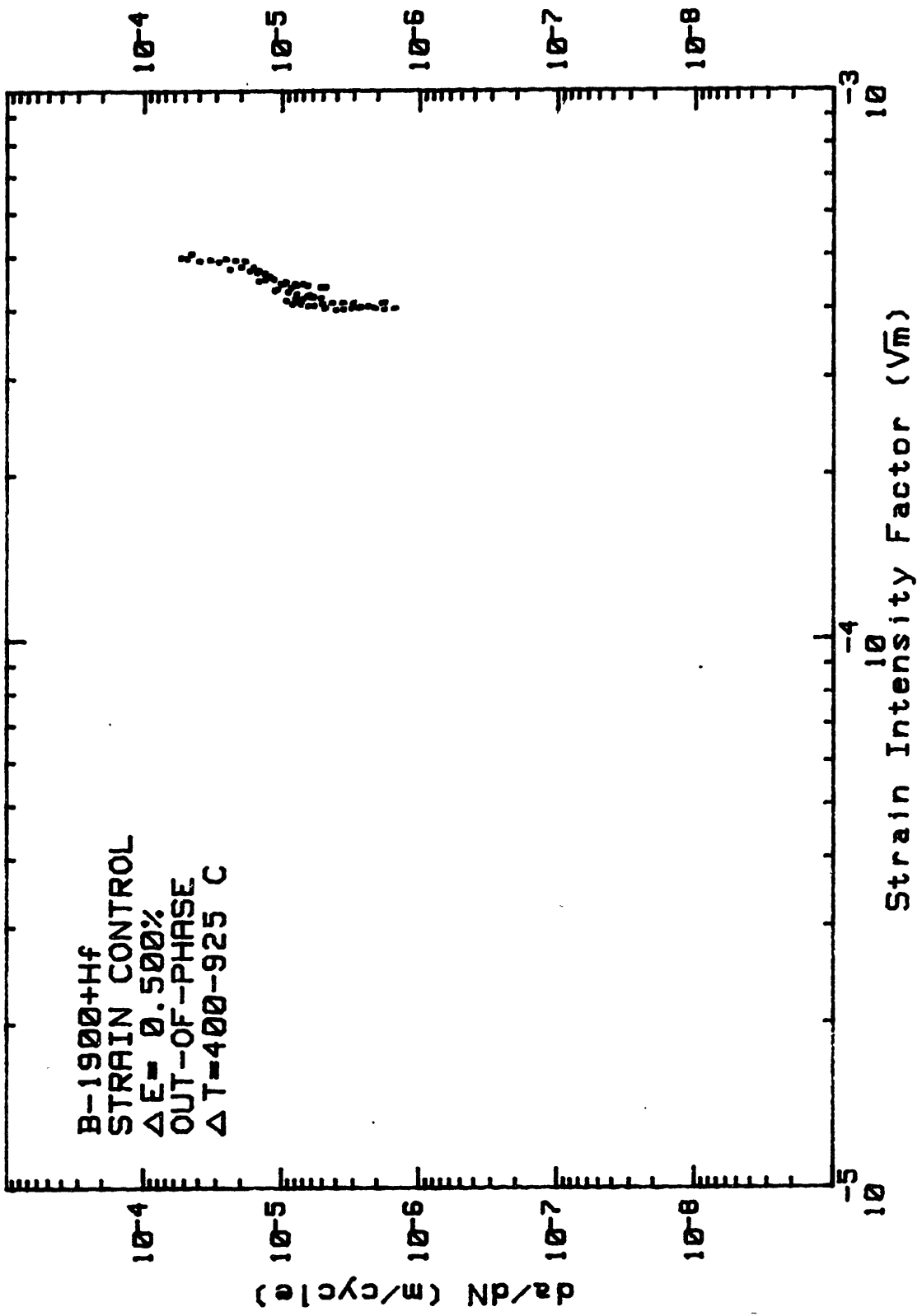
FATIGUE CRACK PROPAGATION

B-1900+Hf
STRAIN CONTROL
 $\Delta E = 0.25\%$
ISOTHERMAL
 $\Delta T = 924 - 926 \text{ C}$



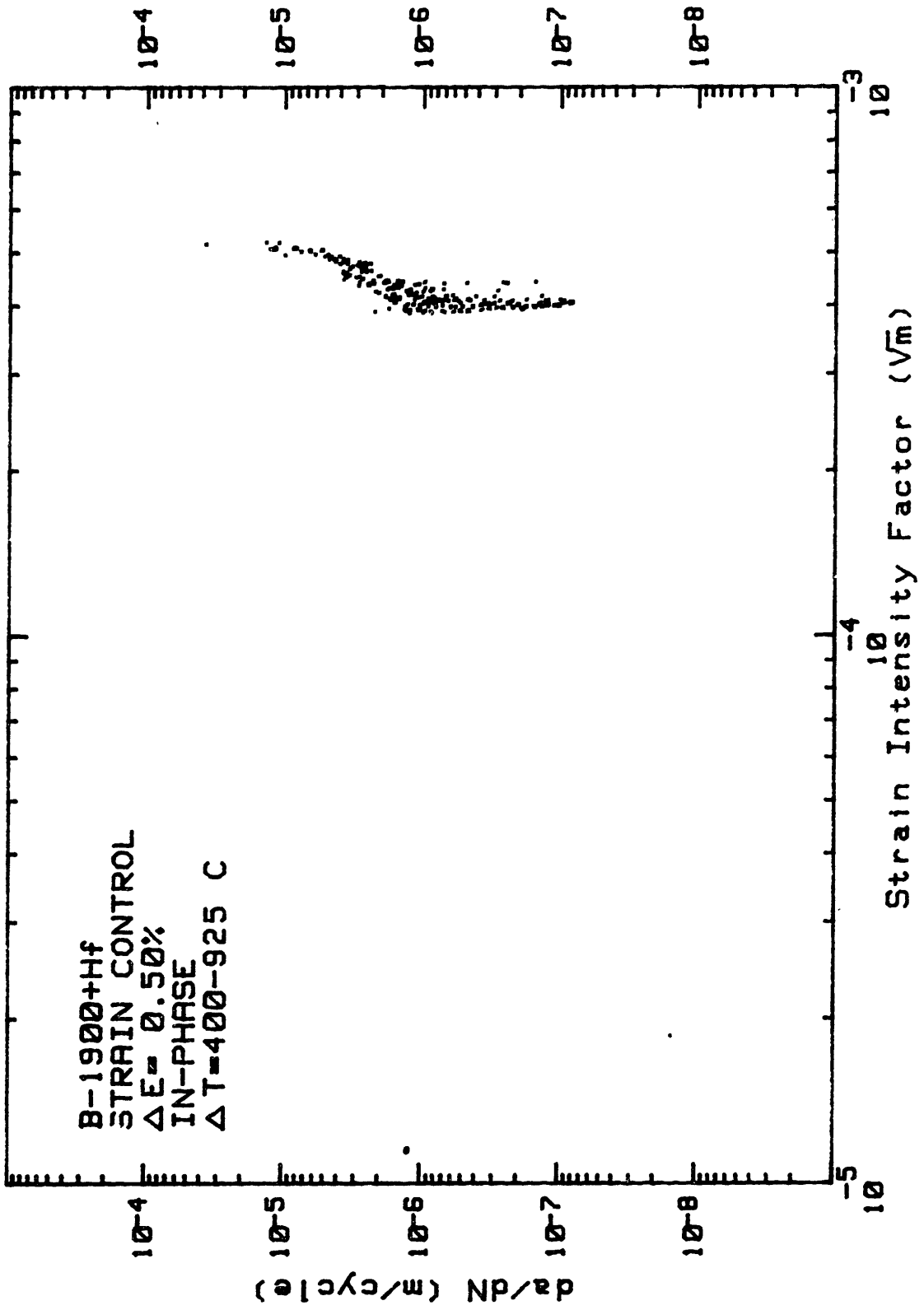
FATIGUE CRACK PROPAGATION

B-1900+Hf
STRAIN CONTROL
 $\Delta E = 0.500\%$
OUT-OF-PHASE
 $\Delta T = 400-925 \text{ C}$



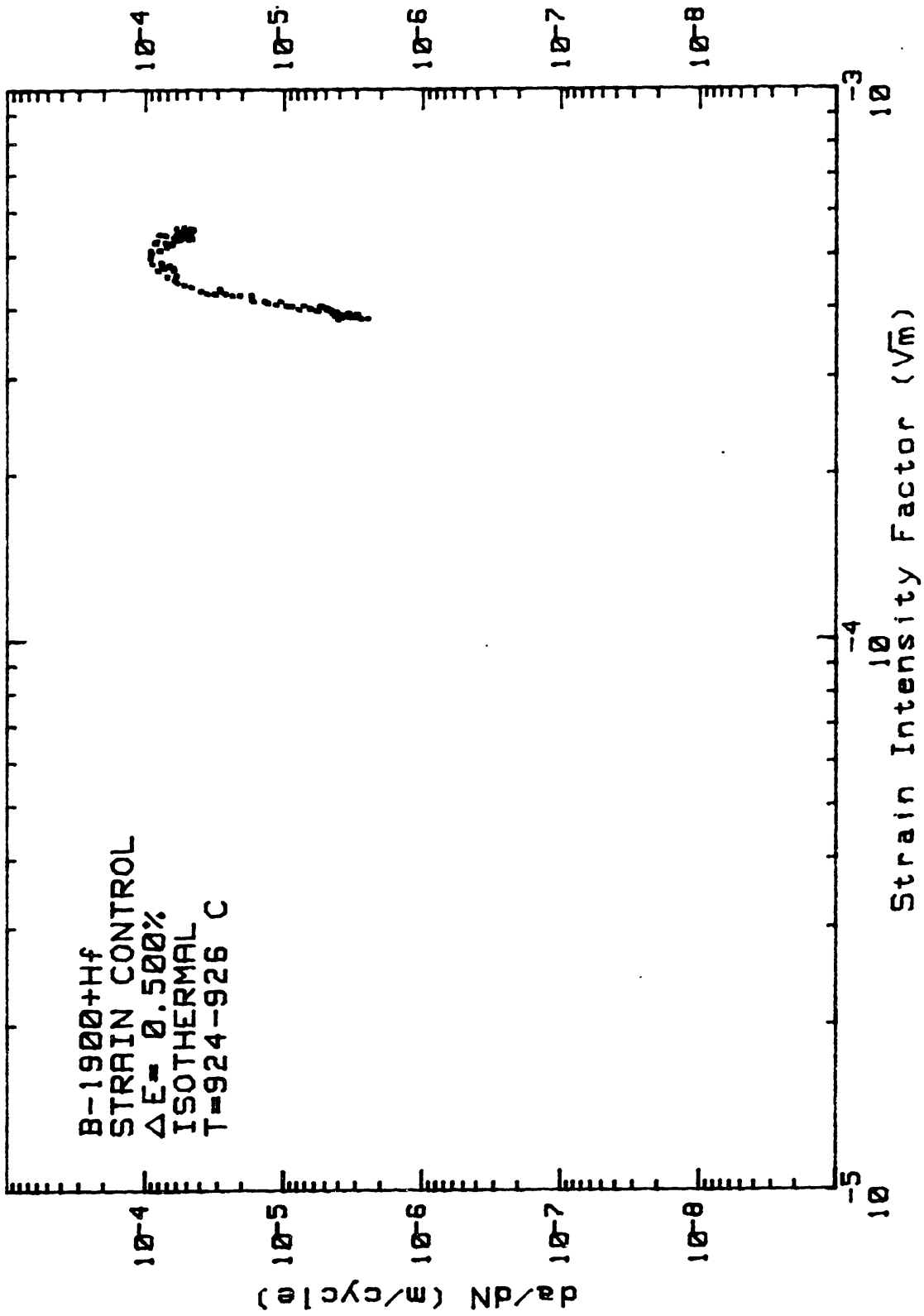
FATIGUE CRACK PROPAGATION

B-1900+Hf
STRAIN CONTROL
 $\Delta E = 0.50\%$
IN-PHASE
 $\Delta T = 400-925 \text{ C}$



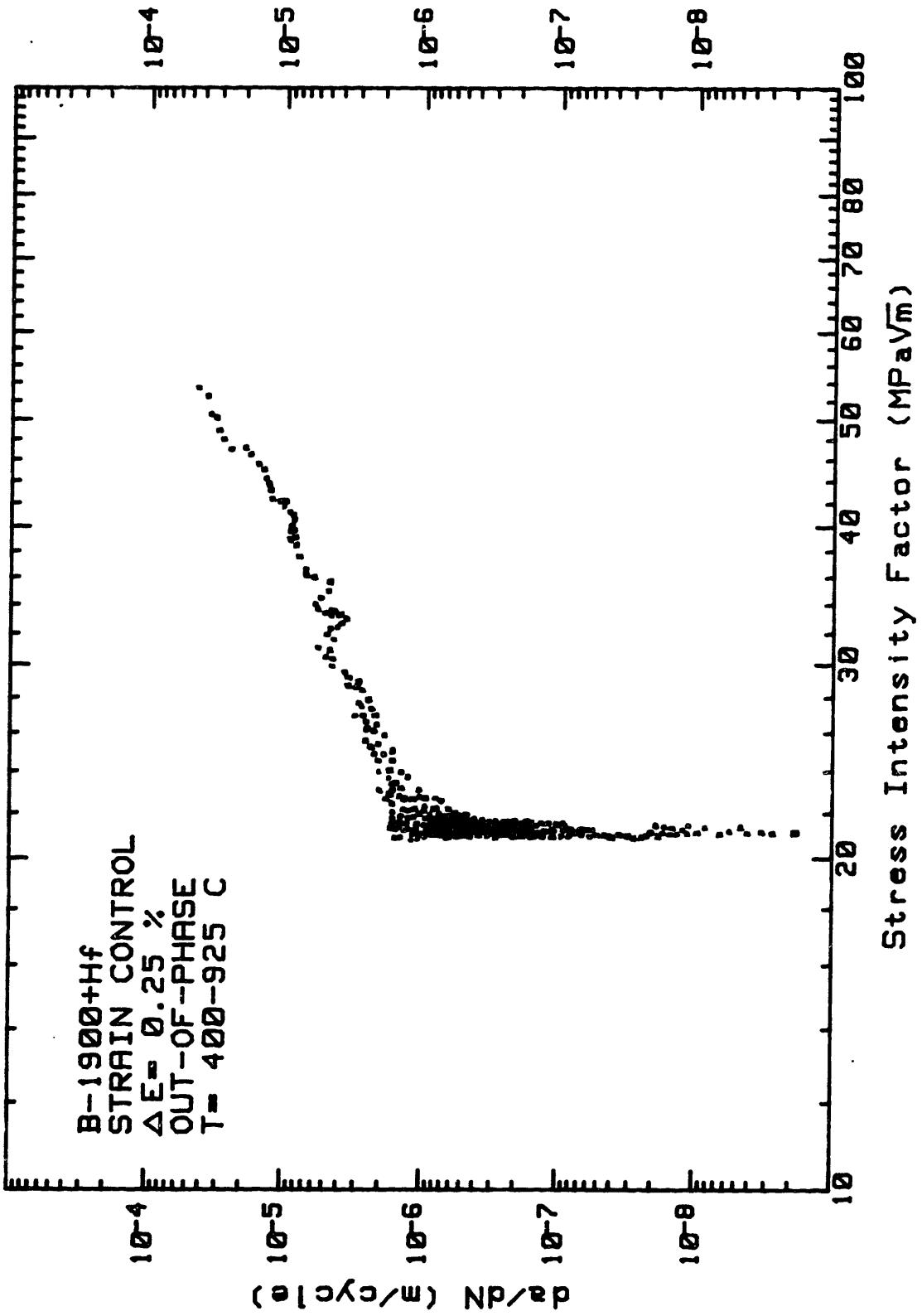
FATIGUE CRACK PROPAGATION

B-1900+Hf
STRAIN CONTROL
 $\Delta E = 0.500\%$
ISOTHERMAL
T=924-926 C



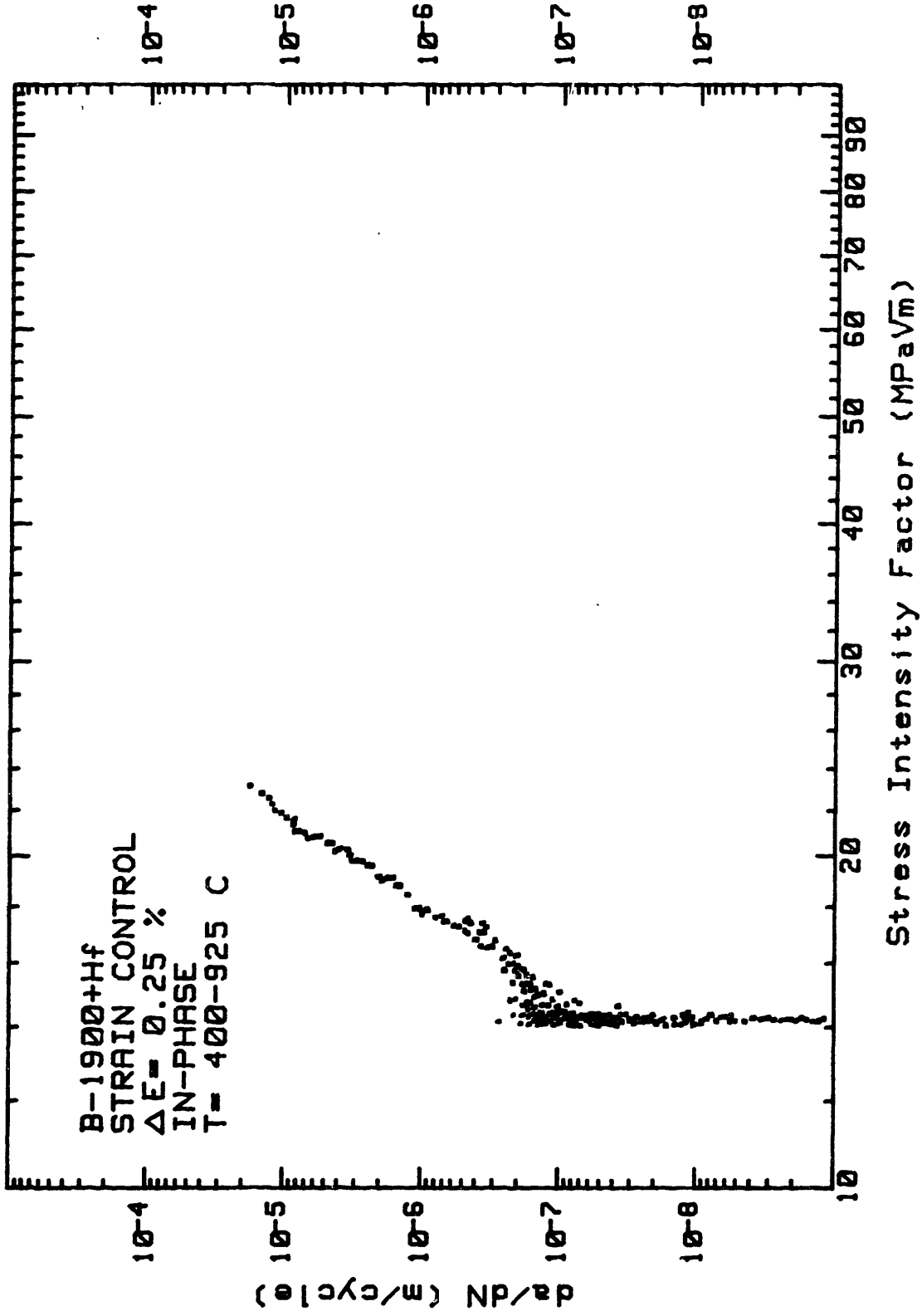
FATIGUE CRACK PROPAGATION

B-1900+Hf
STRAIN CONTROL
 $\Delta E = 0.25\%$
OUT-OF-PHASE
T = 400-925 C



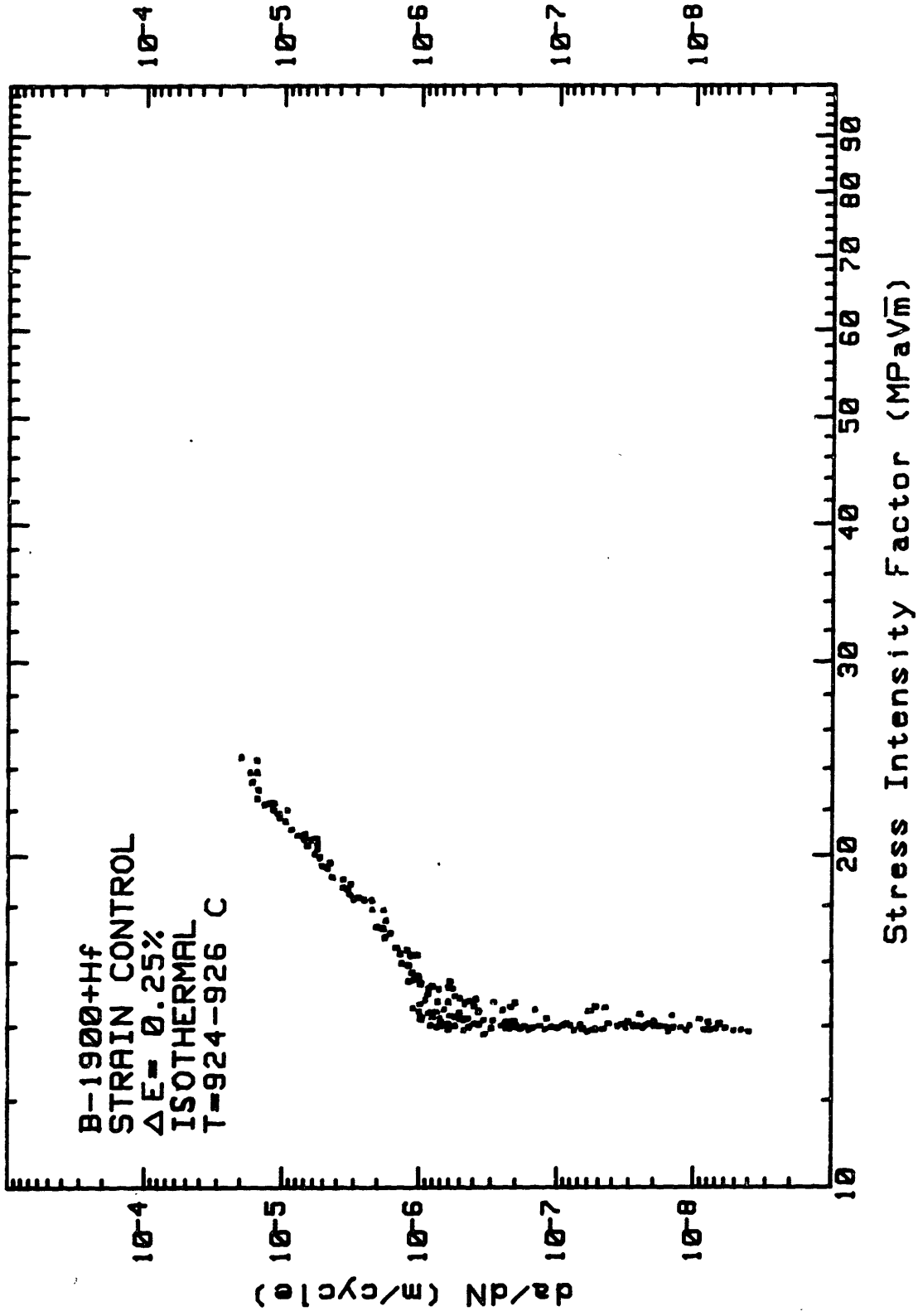
FATIGUE CRACK PROPAGATION

B-1900+Hf
STRAIN CONTROL
 $\Delta E = 0.25\%$
IN-PHASE
T = 400-925 C



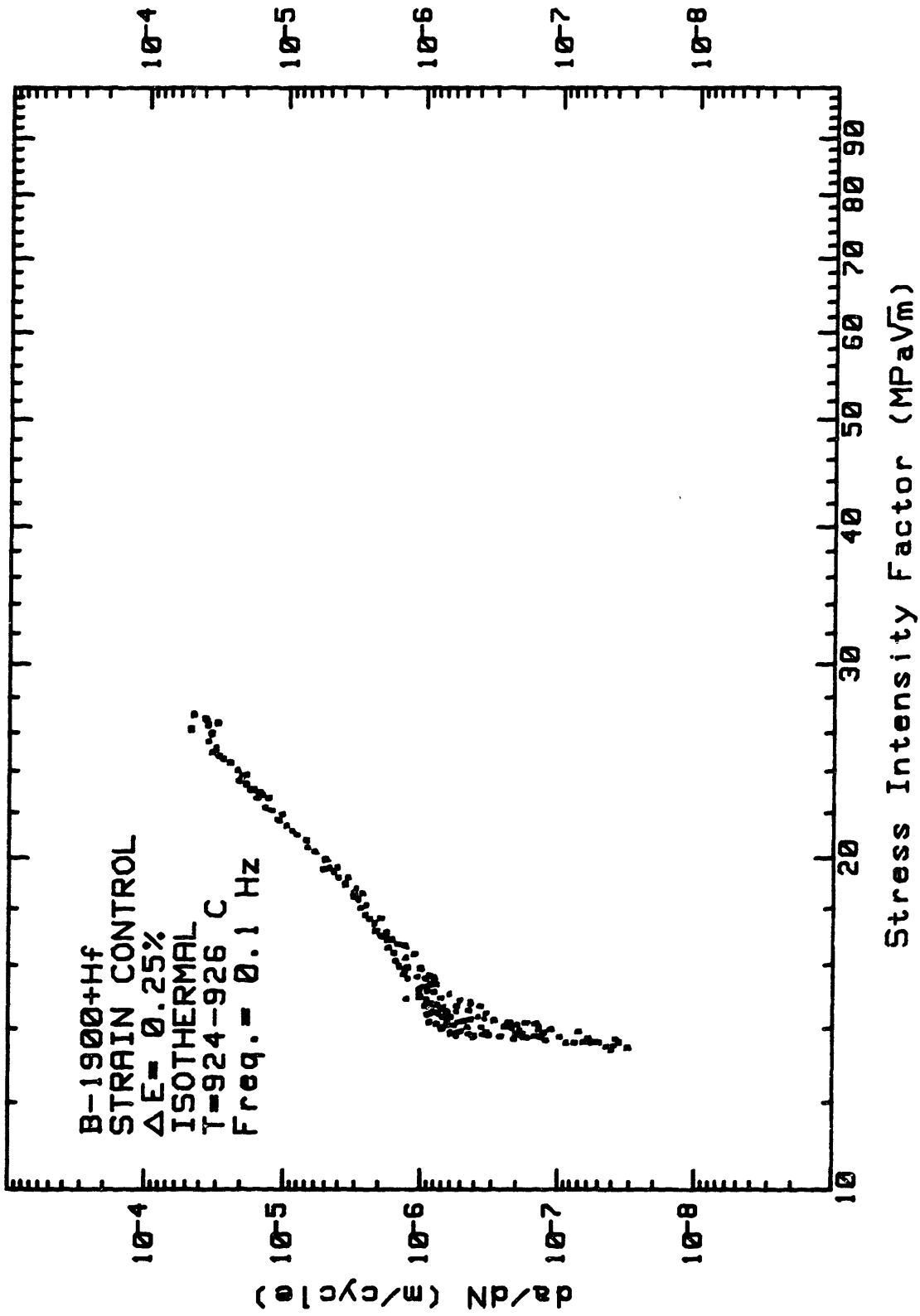
FATIGUE CRACK PROPAGATION

B-1900+Hf
STRAIN CONTROL
 $\Delta E = 0.25\%$
ISOTHERMAL
T=924-926 C



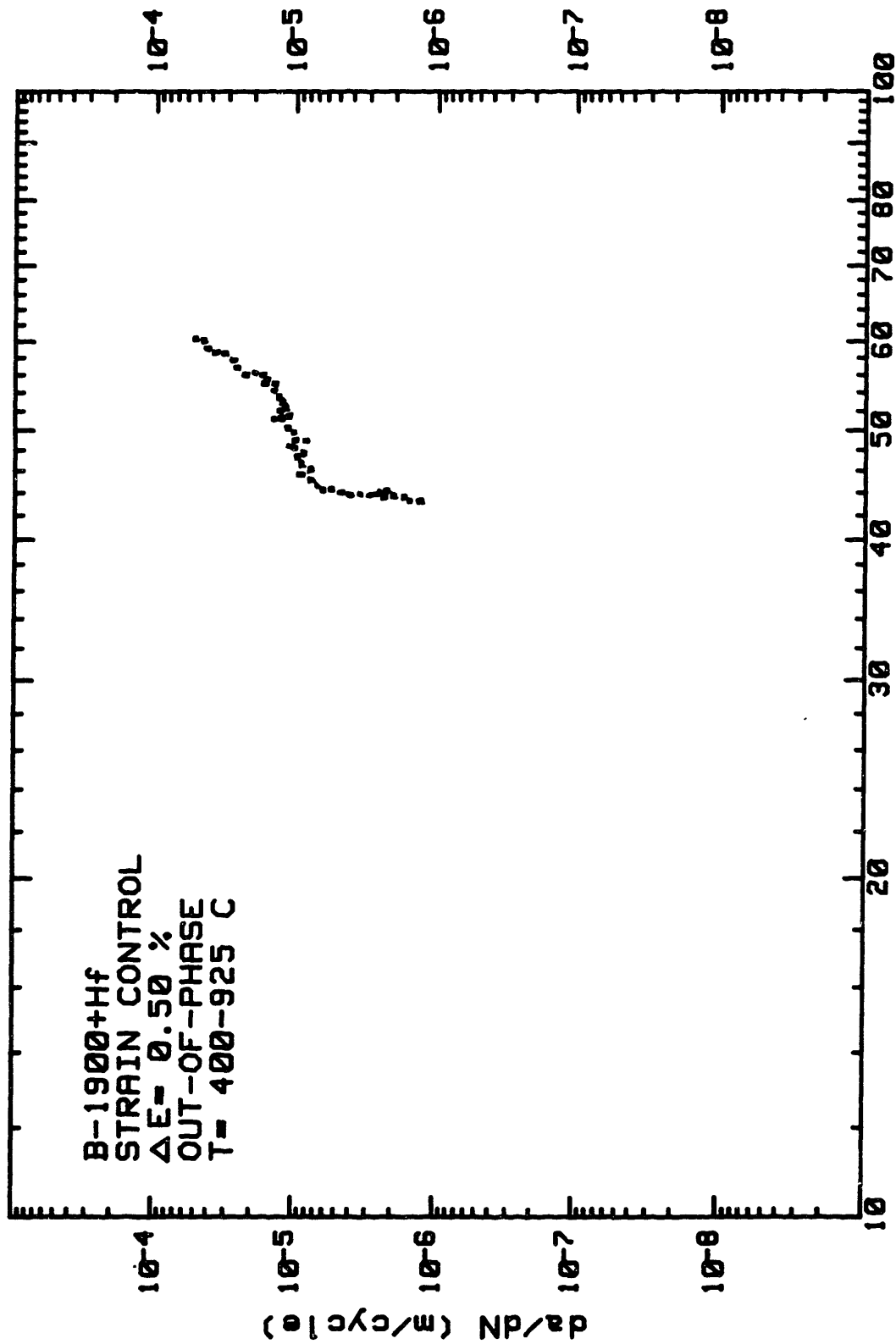
FATIGUE CRACK PROPAGATION

B-1900+Hf
STRAIN CONTROL
 $\Delta E = 0.25\%$
ISOTHERMAL
T=924-926 C
Freq. = 0.1 Hz



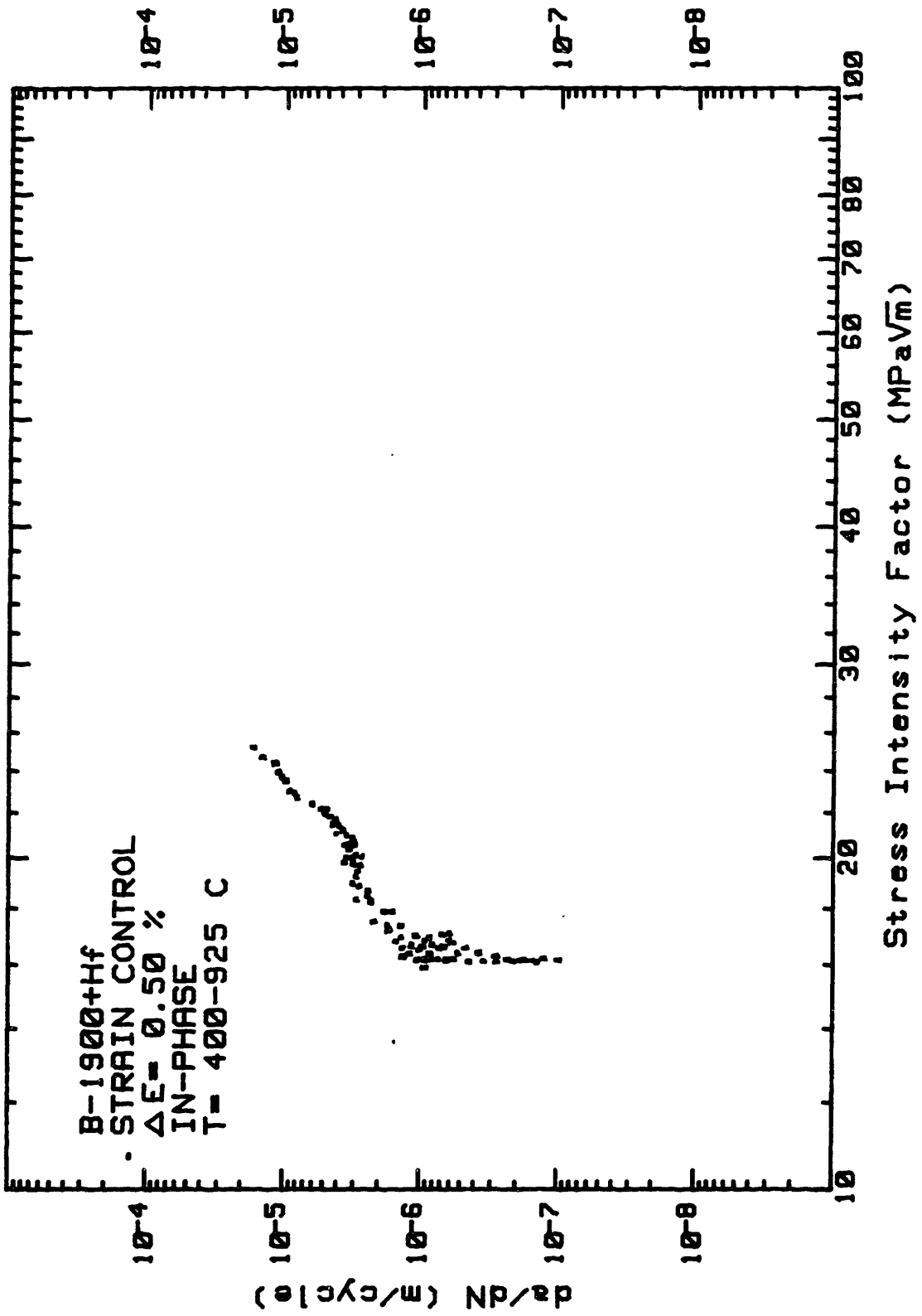
FATIGUE CRACK PROPAGATION

B-1900+Hf
STRAIN CONTROL
 $\Delta E = 0.50\%$
OUT-OF-PHASE
T = 400-925 C



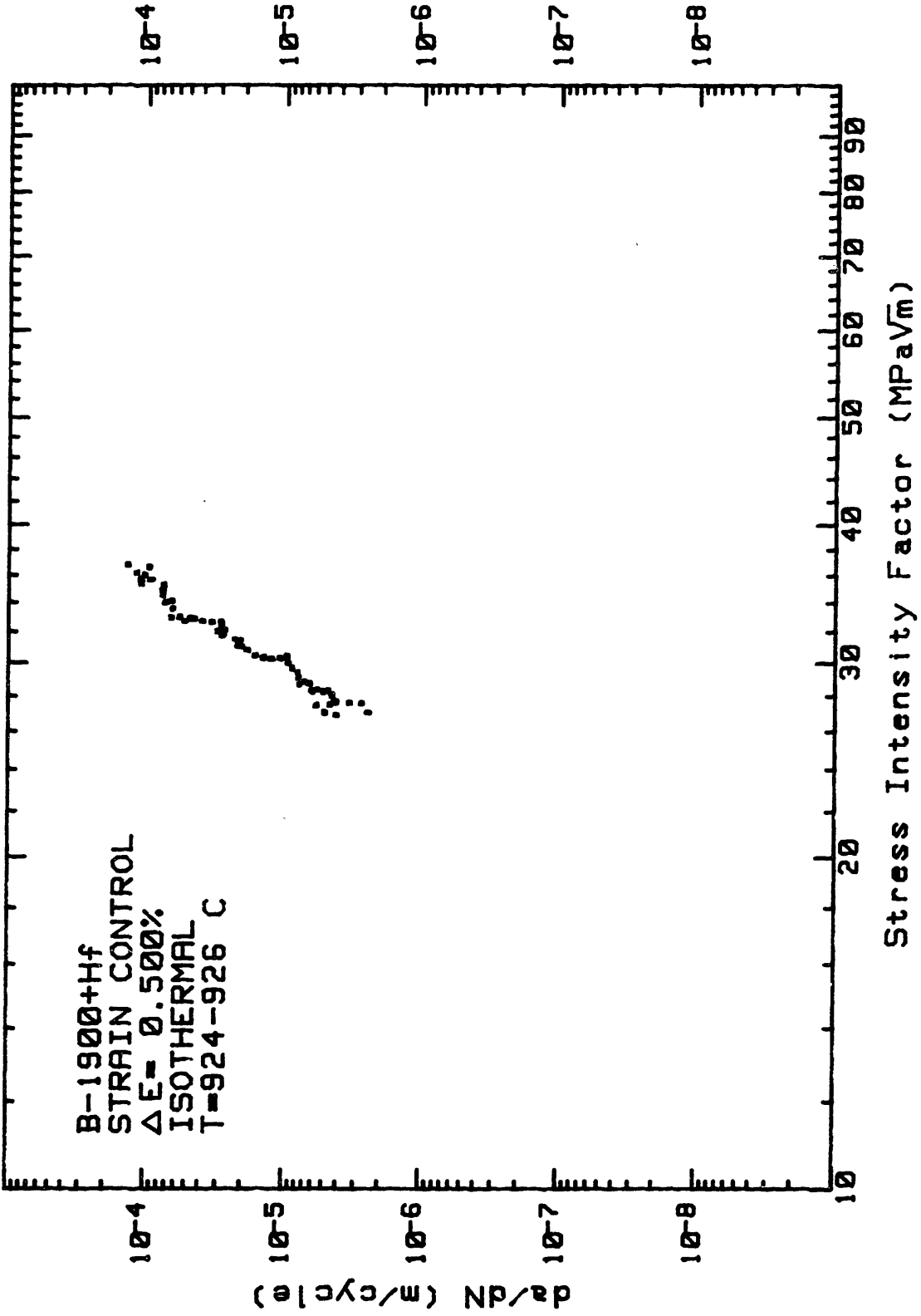
FATIGUE CRACK PROPAGATION

B-1900+Hf
- STRAIN CONTROL
 $\Delta E = 0.50\%$
IN-PHASE
T = 400-925 C



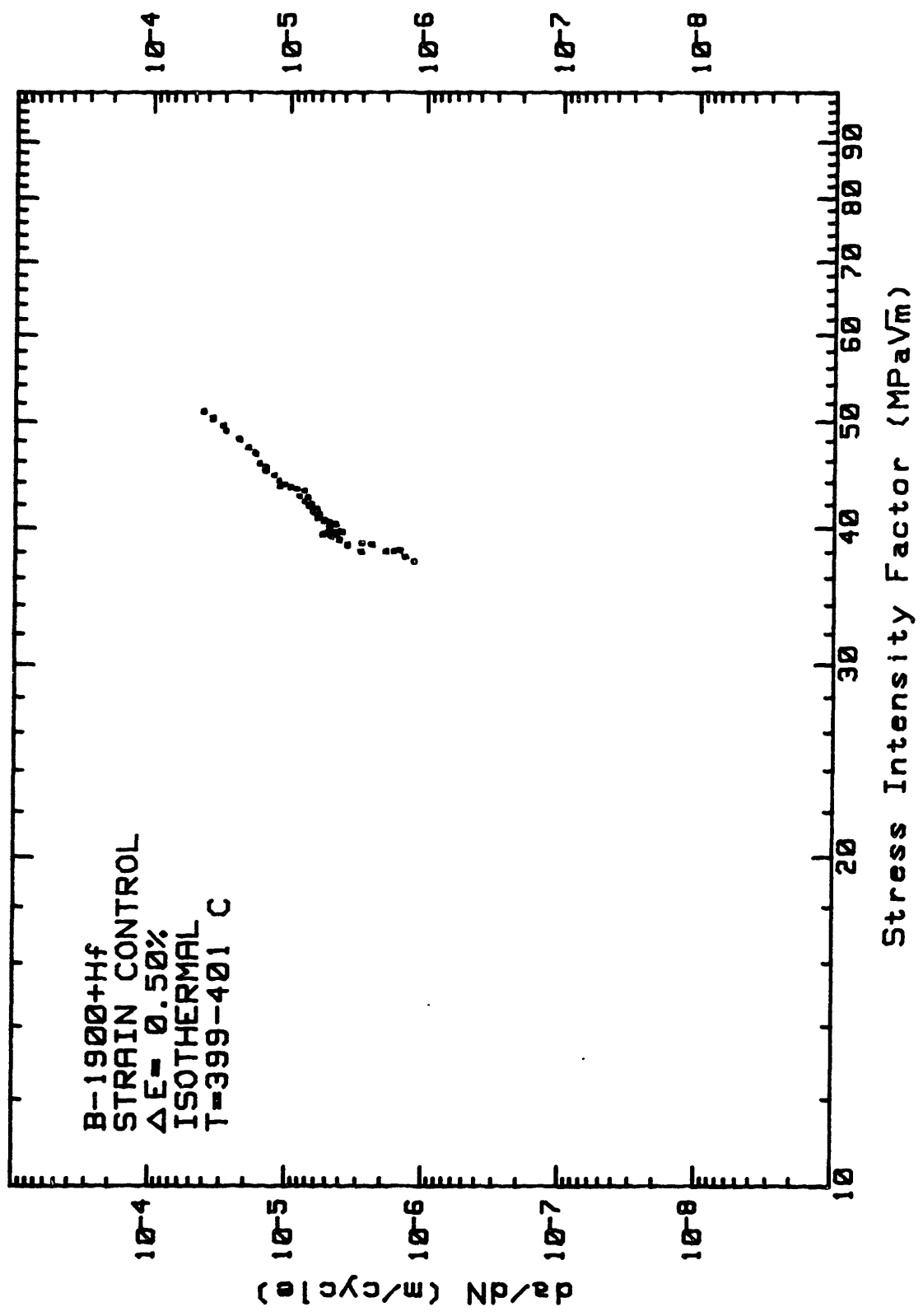
FATIGUE CRACK PROPAGATION

B-1900+Hf
STRAIN CONTROL
 $\Delta E = 0.500\%$
ISOTHERMAL
T=924-926 C



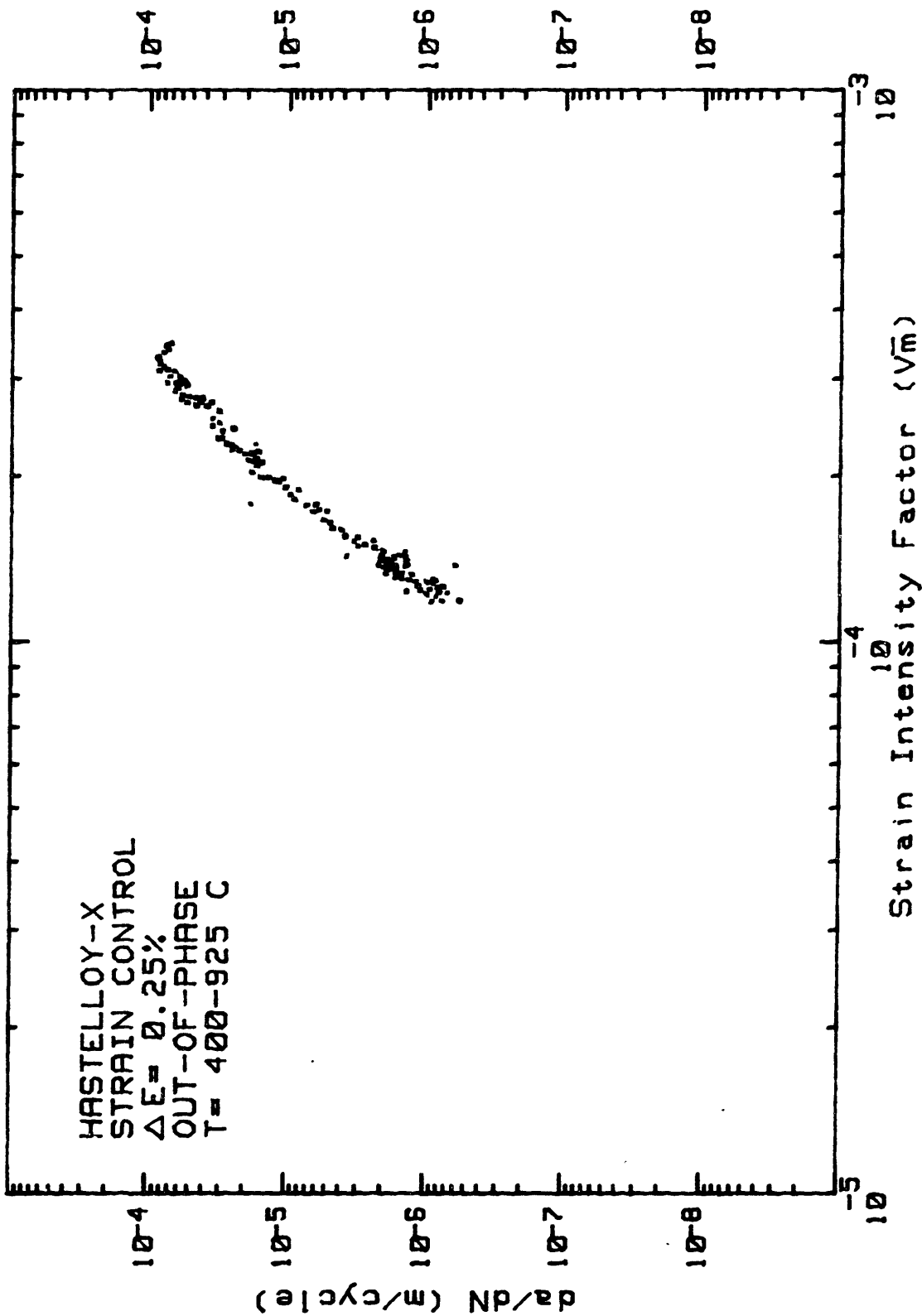
FATIGUE CRACK PROPAGATION

B-1900+Hf
STRAIN CONTROL
 $\Delta E = 0.50\%$
ISOTHERMAL
T=399-401 C



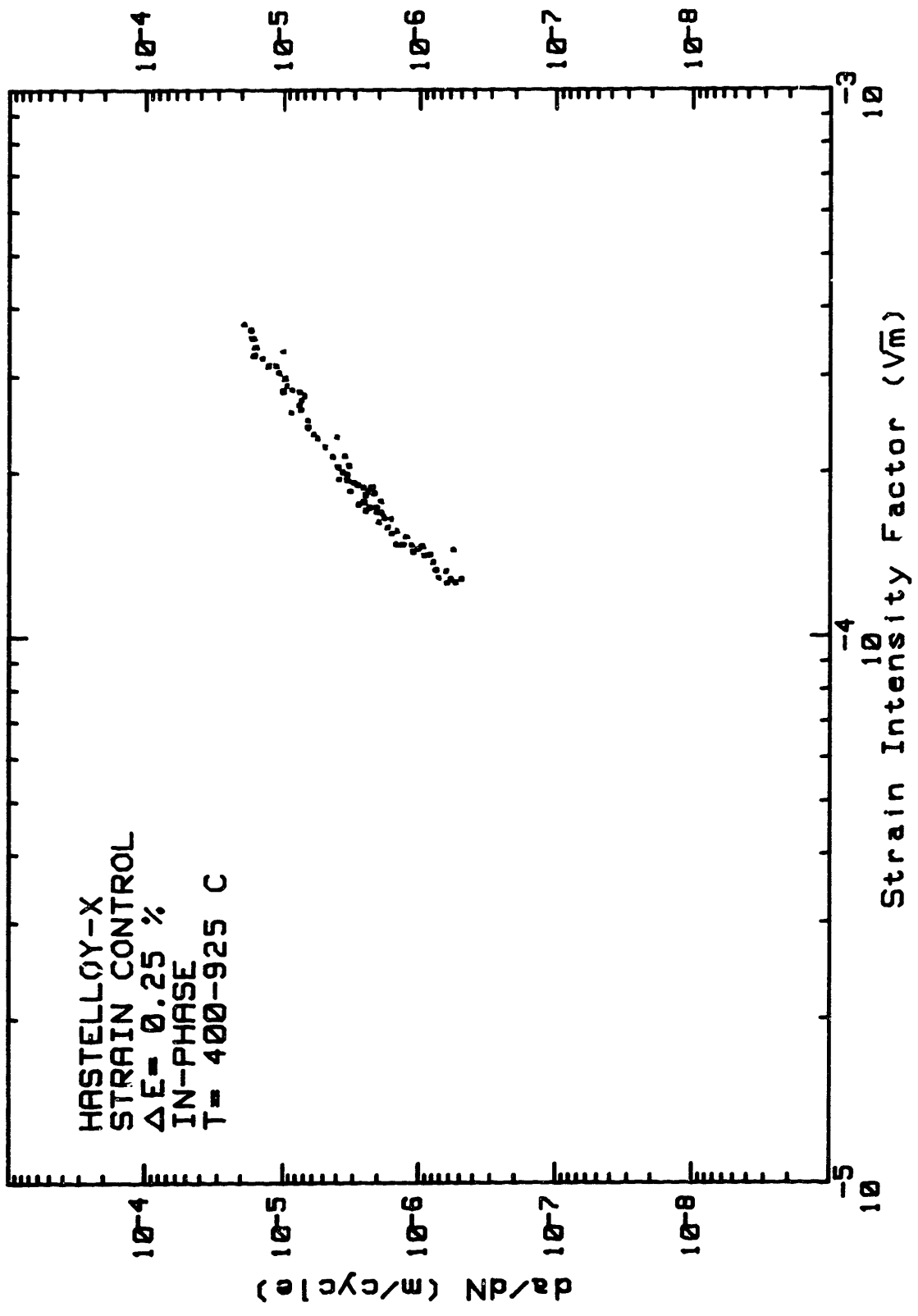
FATIGUE CRACK PROPAGATION

HASTELLOY-X
STRAIN CONTROL
 $\Delta E = 0.25\%$
OUT-OF-PHASE
T = 400-925 C



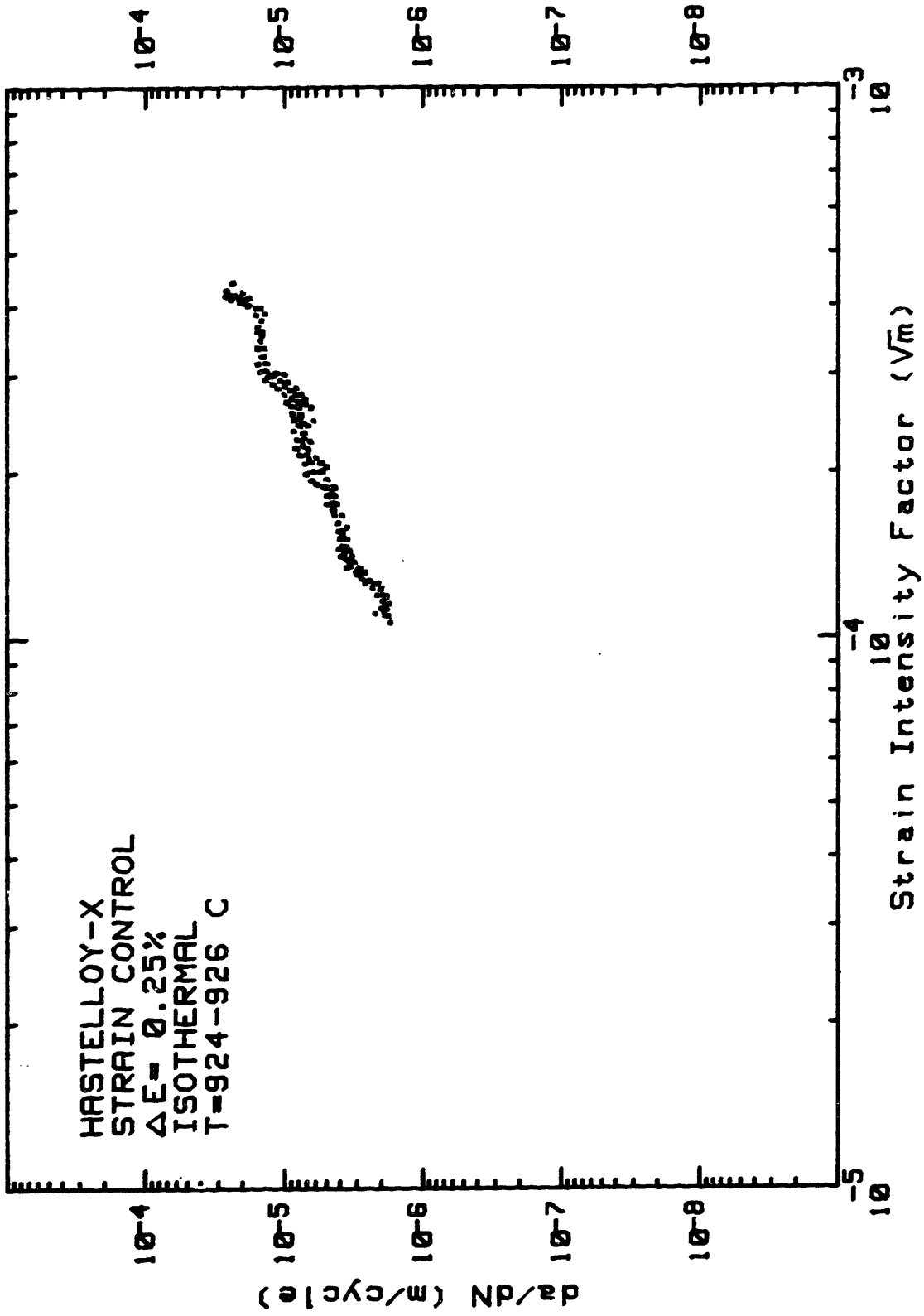
FATIGUE CRACK PROPAGATION

HASTELLOY-X
STRAIN CONTROL
 $\Delta E = 0.25\%$
IN-PHASE
T = 400-925 C



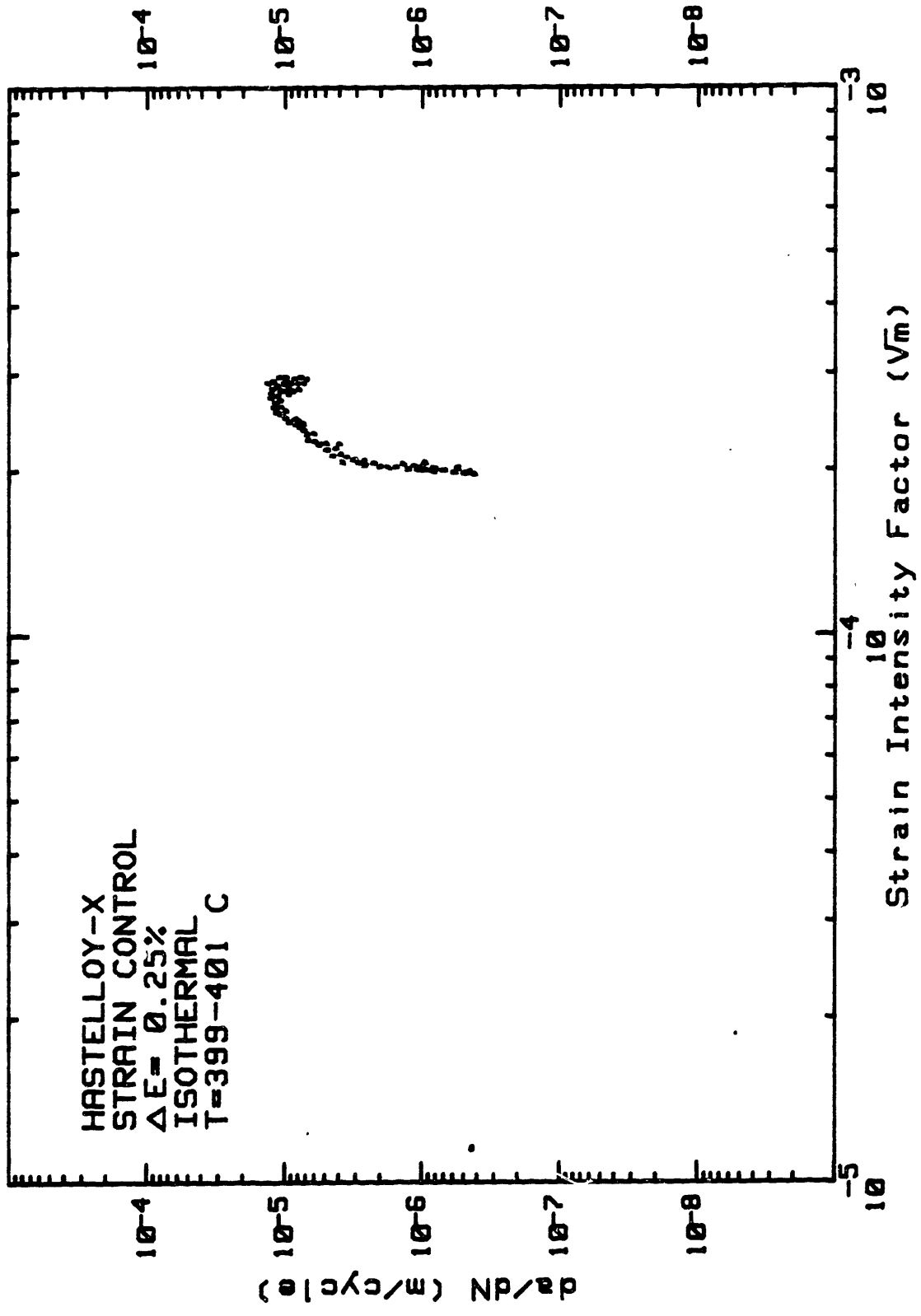
FATIGUE CRACK PROPAGATION

HASTELLOY-X
STRAIN CONTROL
 $\Delta E = 0.25\%$
ISOTHERMAL
T=924-926 C



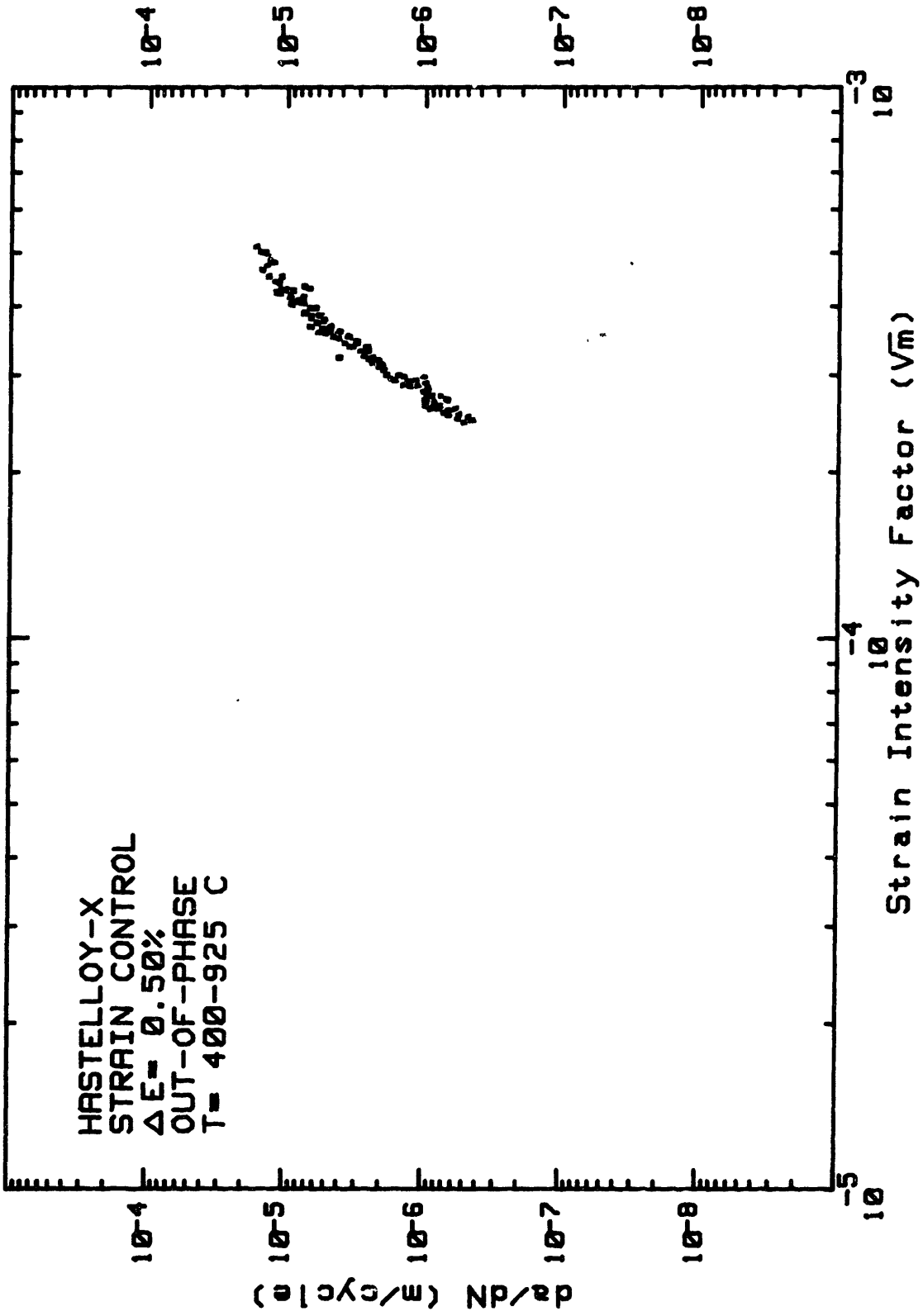
FATIGUE CRACK PROPAGATION

HASTELLOY-X
STRAIN CONTROL
 $\Delta E = 0.25\%$
ISOTHERMAL
 $T = 399 - 401 \text{ } ^\circ\text{C}$



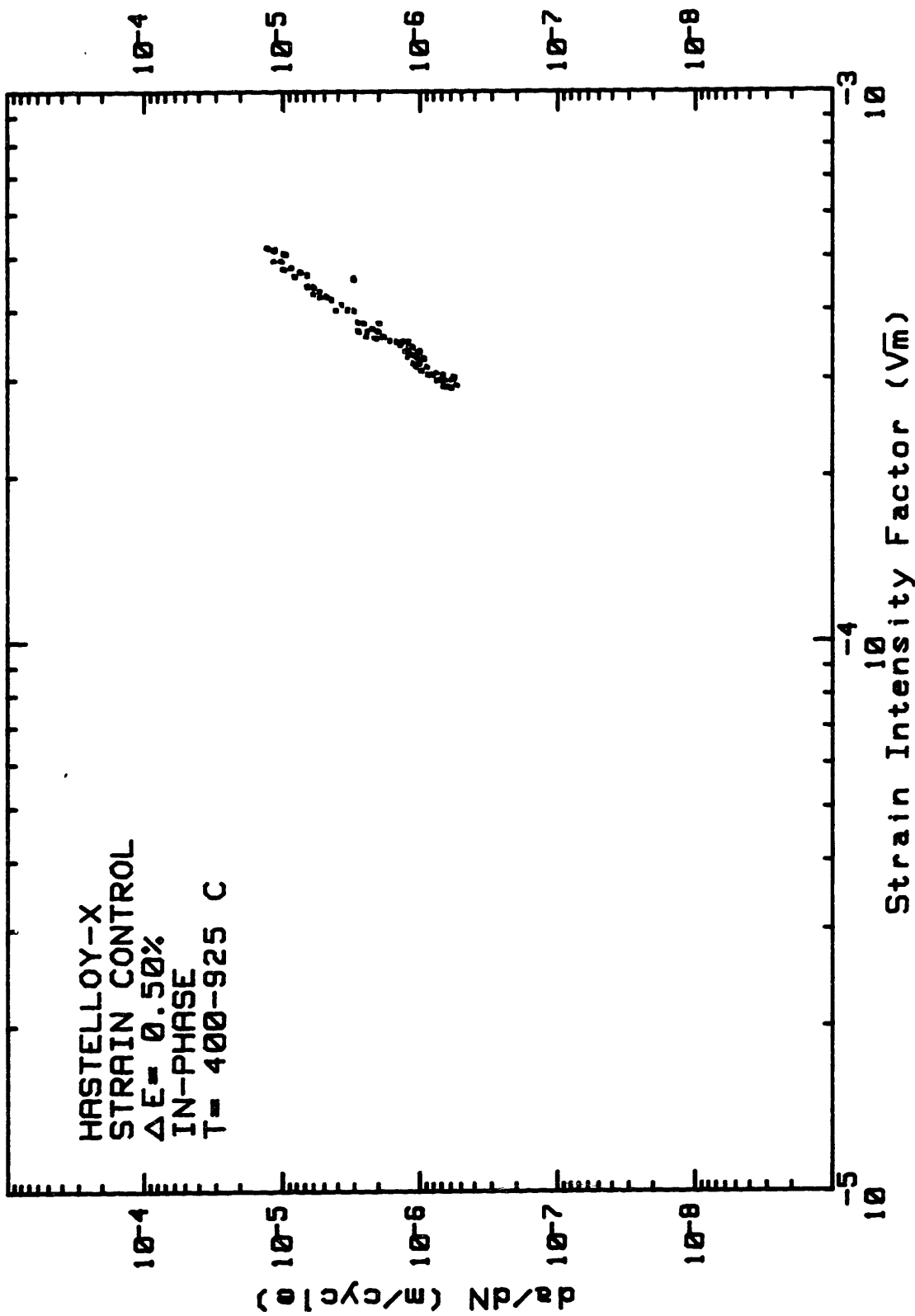
FATIGUE CRACK PROPAGATION

HASTELLOY-X
STRAIN CONTROL
 $\Delta E = 0.50\%$
OUT-OF-PHASE
 $T = 400-925\text{ C}$



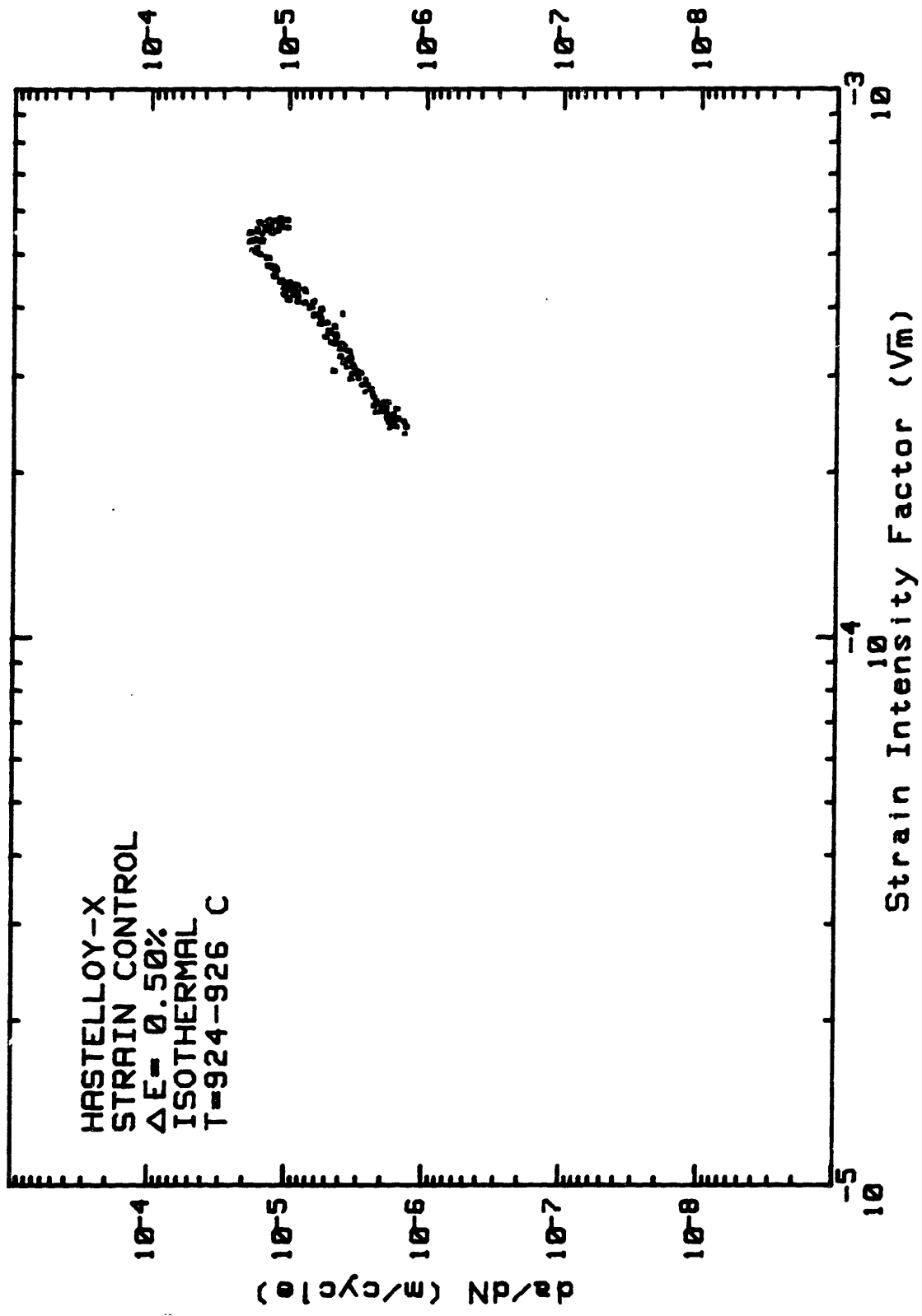
FATIGUE CRACK PROPAGATION

HASTELLOY-X
STRAIN CONTROL
 $\Delta E = 0.50\%$
IN-PHASE
T = 400-925 C



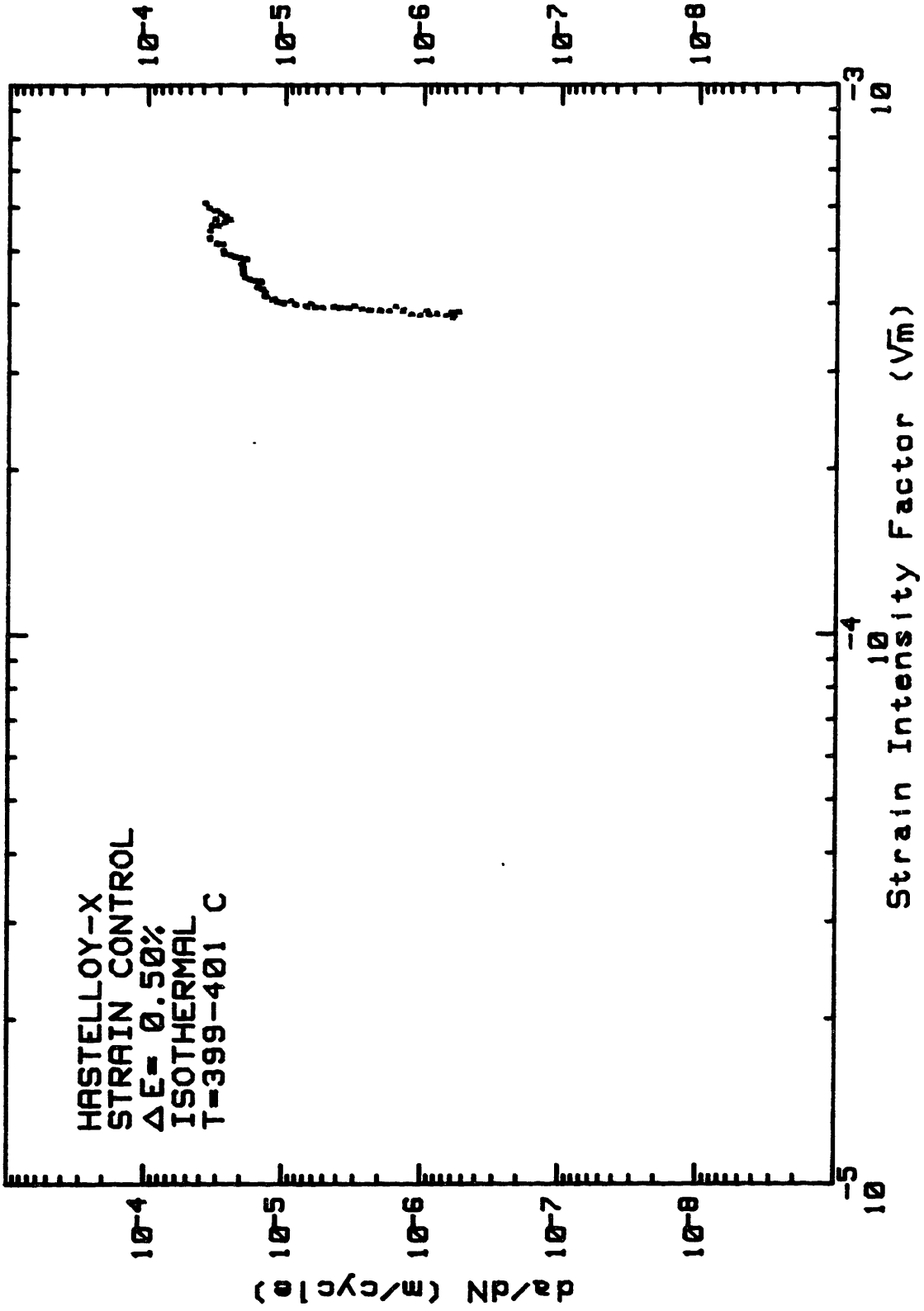
FATIGUE CRACK PROPAGATION

HASTELLOY-X
STRAIN CONTROL
 $\Delta E = 0.50\%$
ISOTHERMAL
T=924-926 C



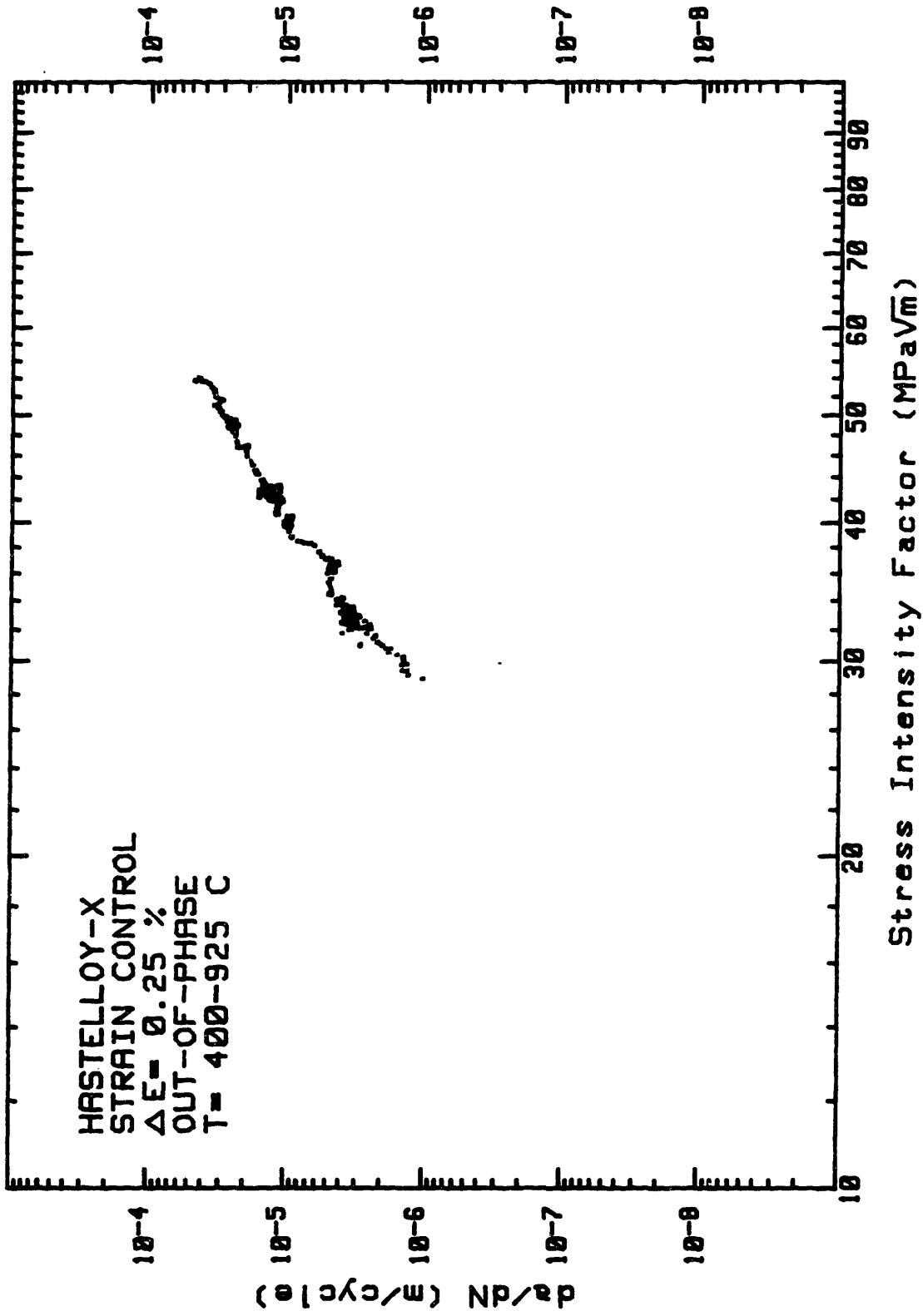
FATIGUE CRACK PROPAGATION

HASTELLOY-X
STRAIN CONTROL
 $\Delta E = 0.50\%$
ISOTHERMAL
T=399-401 C

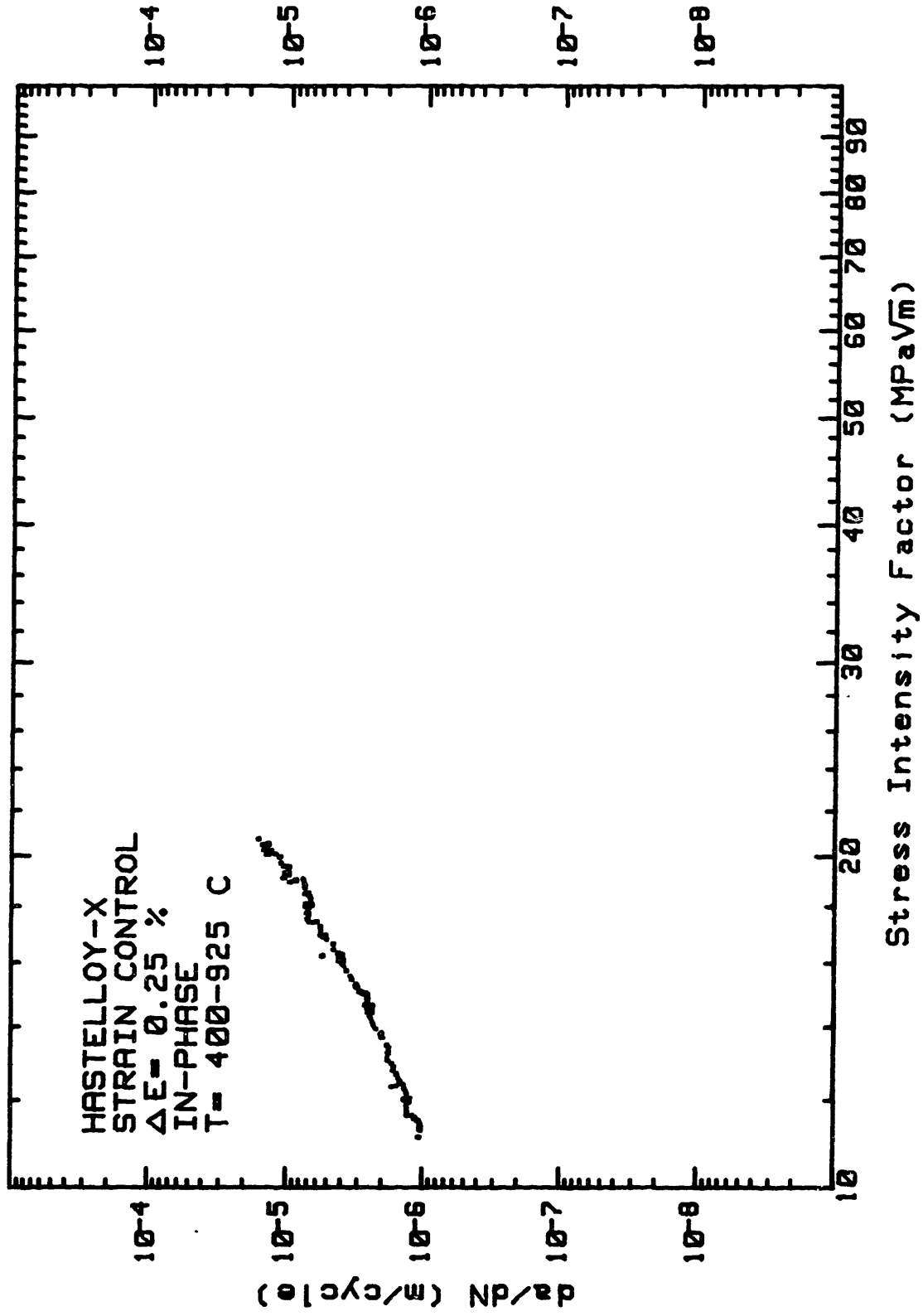


FATIGUE CRACK PROPAGATION

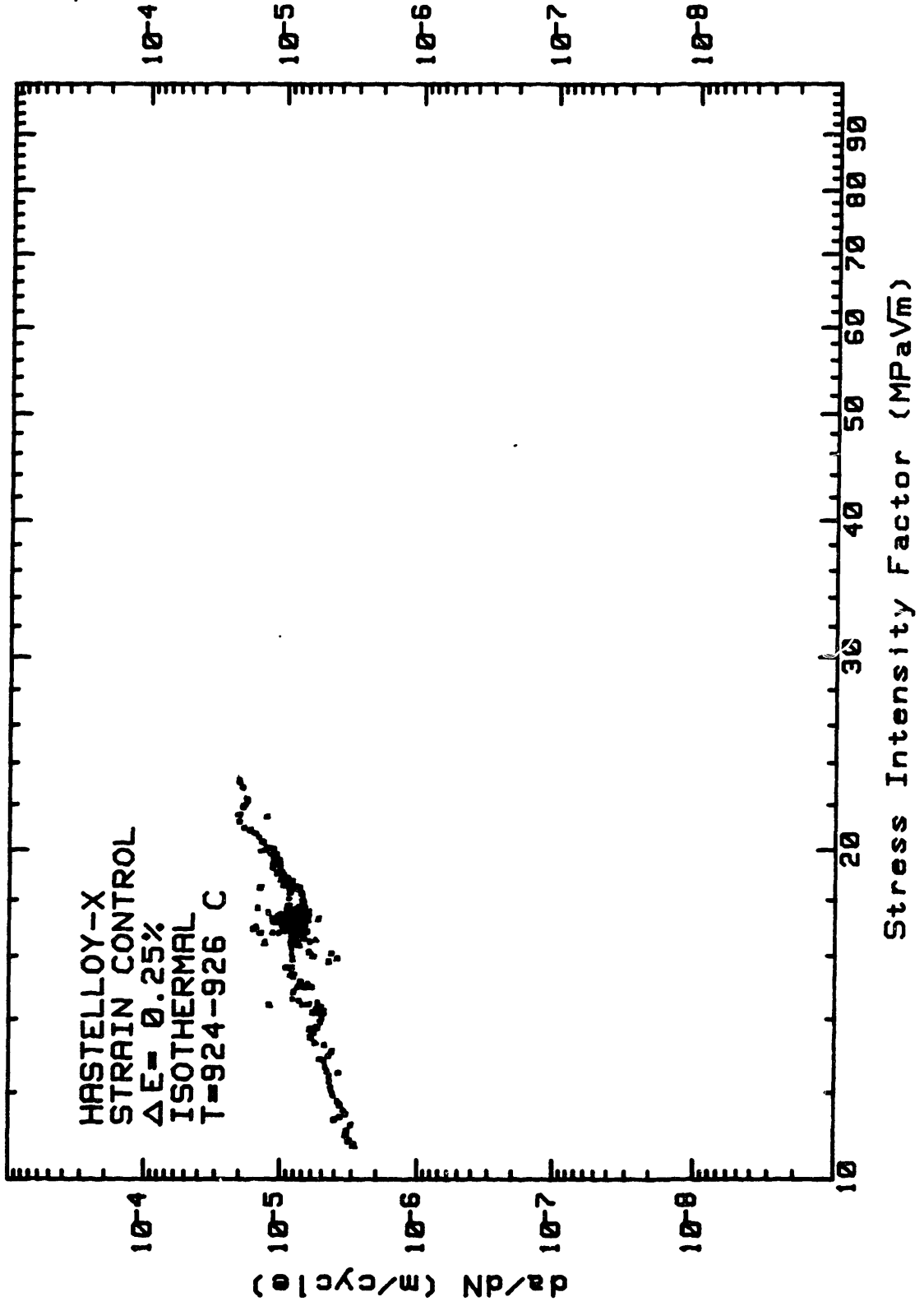
HASTELLOY-X
STRAIN CONTROL
 $\Delta E = 0.25\%$
OUT-OF-PHASE
 $T = 400-925\text{ C}$



FATIGUE CRACK PROPAGATION

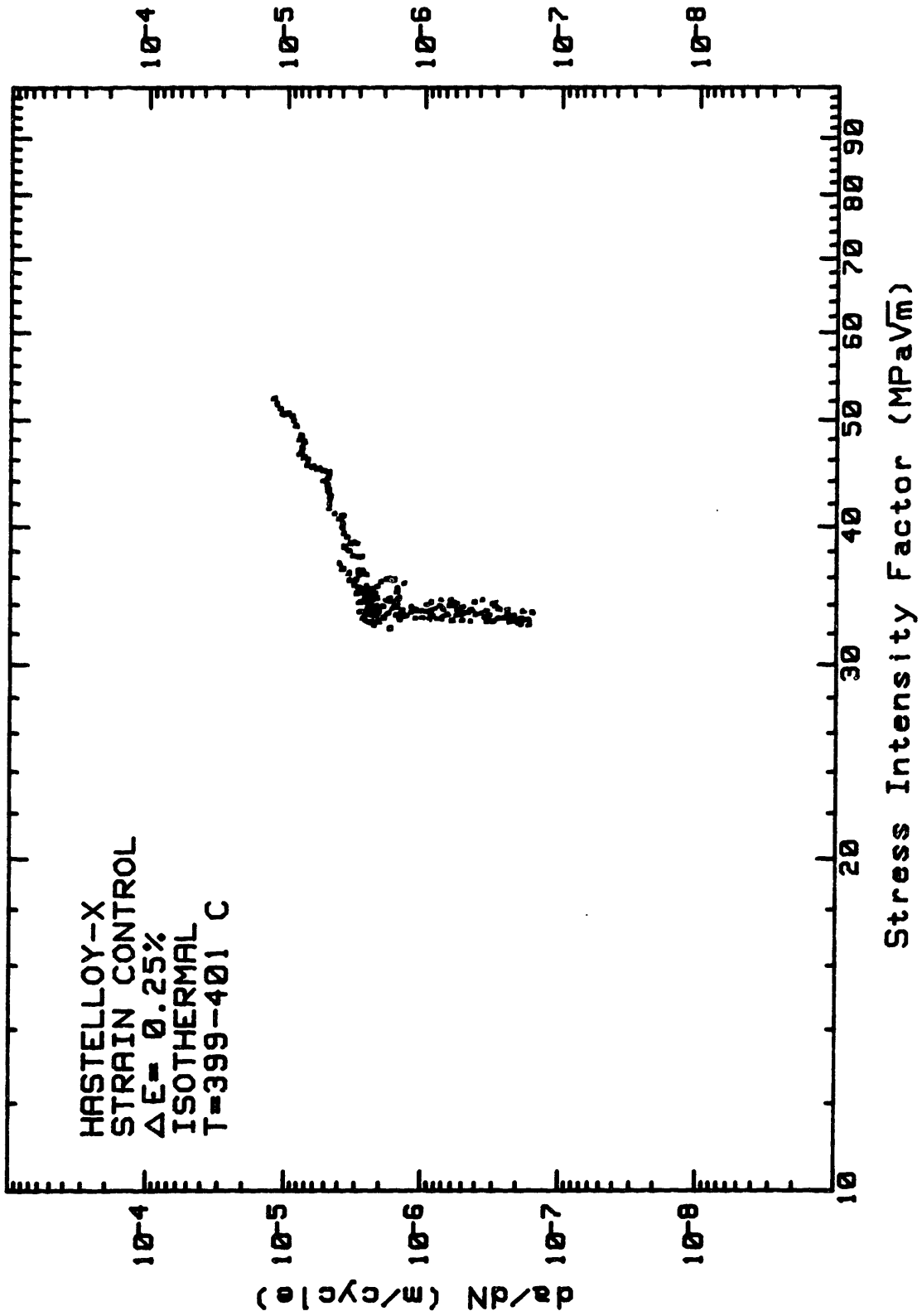


FATIGUE CRACK PROPAGATION



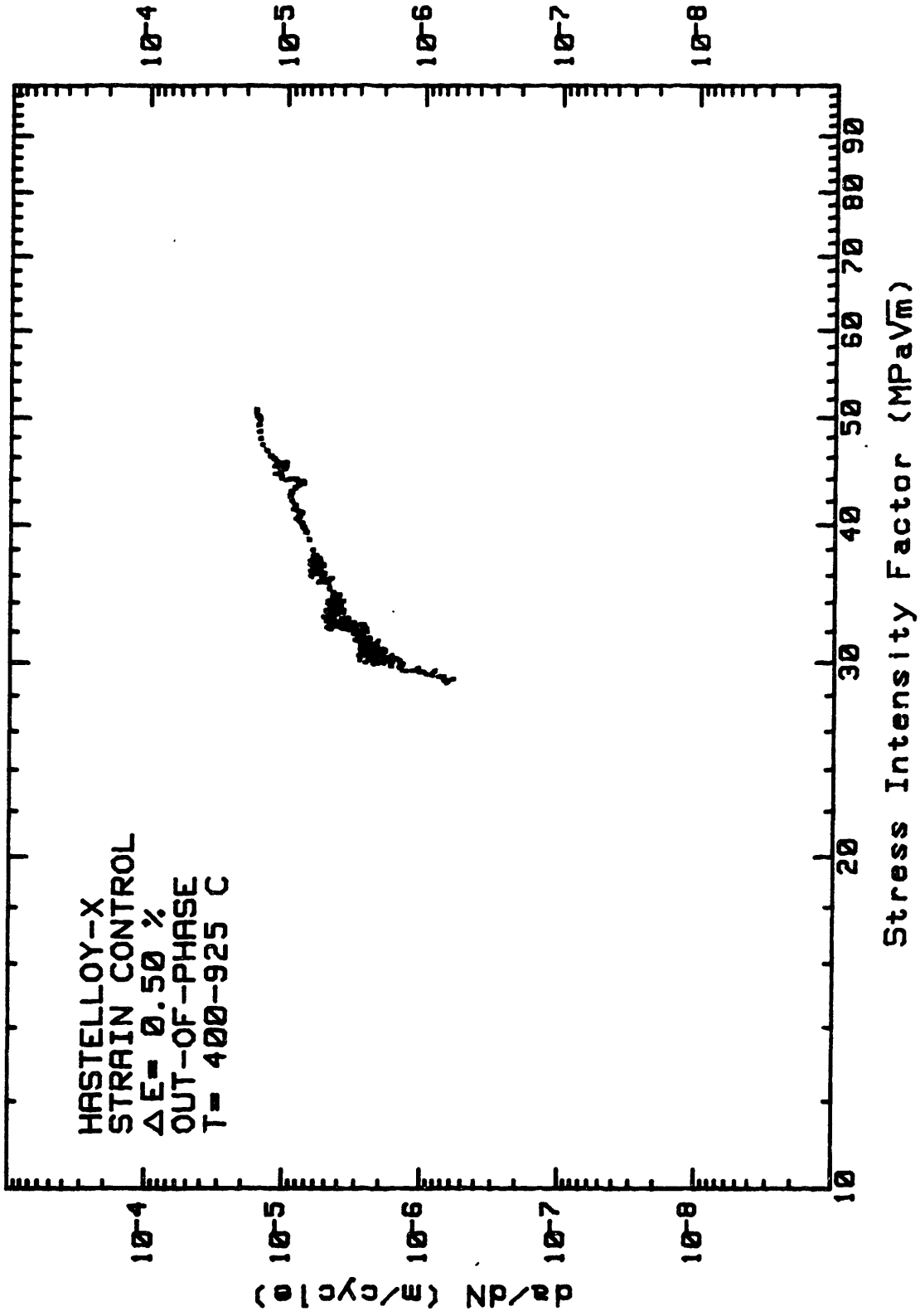
FATIGUE CRACK PROPAGATION

HASTELLOY-X
STRAIN CONTROL
 $\Delta E = 0.25\%$
ISOTHERMAL
 $T = 399 - 401 \text{ } ^\circ\text{C}$

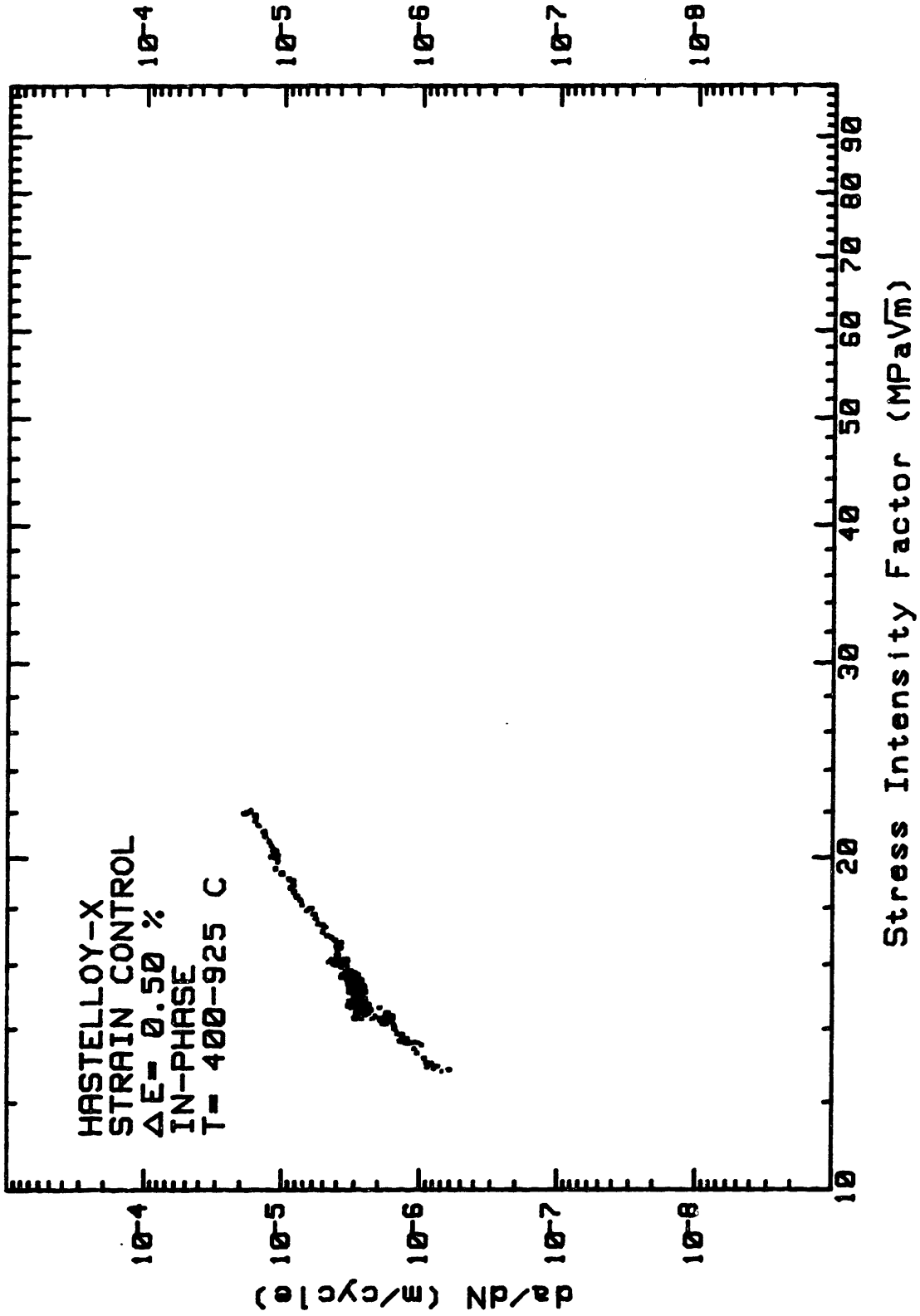


FATIGUE CRACK PROPAGATION

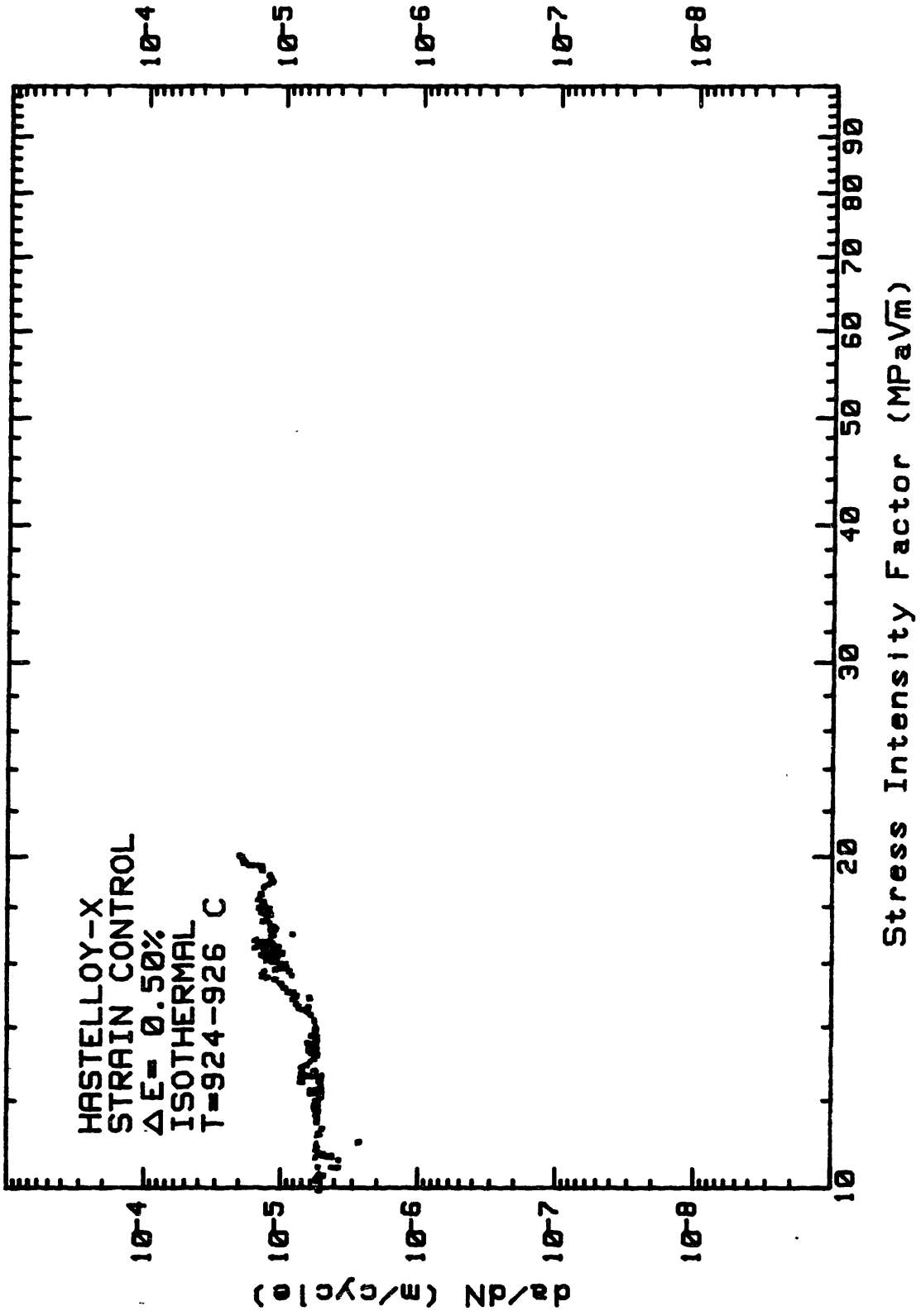
HASTELLOY-X
STRAIN CONTROL
 $\Delta E = 0.50\%$
OUT-OF-PHASE
T = 400-925 C



FATIGUE CRACK PROPAGATION

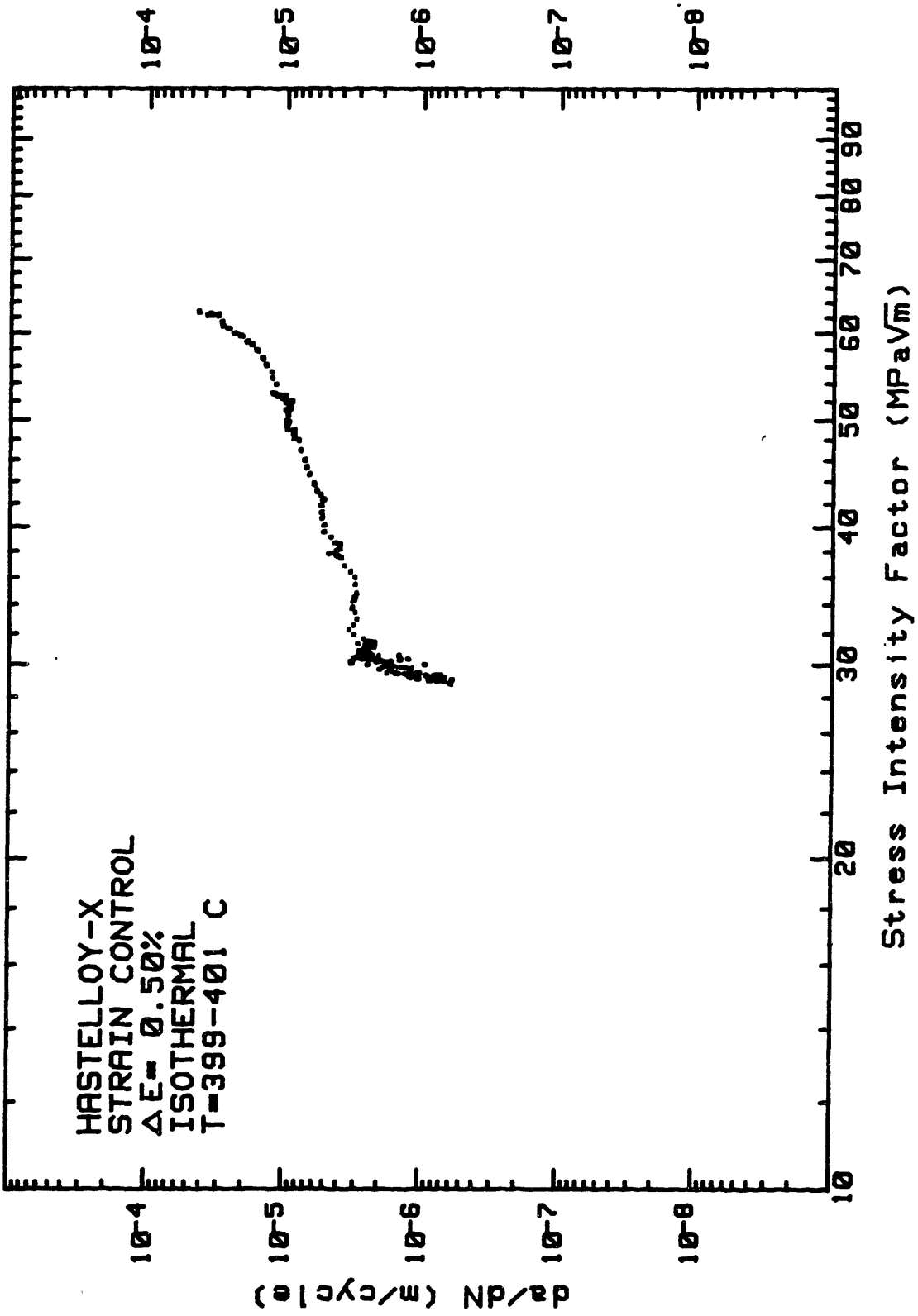


FATIGUE CRACK PROPAGATION



FATIGUE CRACK PROPAGATION

HASTELLOY-X
STRAIN CONTROL
 $\Delta E = 0.50\%$
ISOTHERMAL
 $T = 399 - 401 \text{ } ^\circ\text{C}$



Appendix V

K_I - Solutions for Single Edge Notch Specimens
Under Fixed End Displacements

INTRODUCTION

The single-edge-notch (SEN) geometry with end constraints has received considerable attention in analytical fracture mechanics because of its frequent use as a test specimen. The problem of a SEN specimen with fixed-end displacements has been studied by several authors [1-3]. In particular, the formulation of Harris [2] has received much attention because of its ease of application. However, we felt that the closing bending moments associated with zero far-field relative rotation were perhaps more significant than those implied by Harris' solution, and this premise motivated the present analysis.

ANALYSIS

The presence of a crack in a rectangular sheet of thickness B loaded by uniform imposed end displacements cause the line of action of the applied load to shift relative to the specimen centerline. This shift produces a bending moment that tends to close the crack. For the SEN geometries, the only known boundary conditions are the imposed displacements, and the applied stresses are not known a priori and must be determined.

We consider an isotropic linear elastic sub-specimen of length L that is "sufficiently long" compared to crack length (a) and specimen width (W). The specimen is of thickness B and is subject to opposing forces N and moments M as shown schematically in Fig. 1. The line of action of the force N is taken as the mid-specimen. The following considerations are restricted to mode I behavior although the argument can be

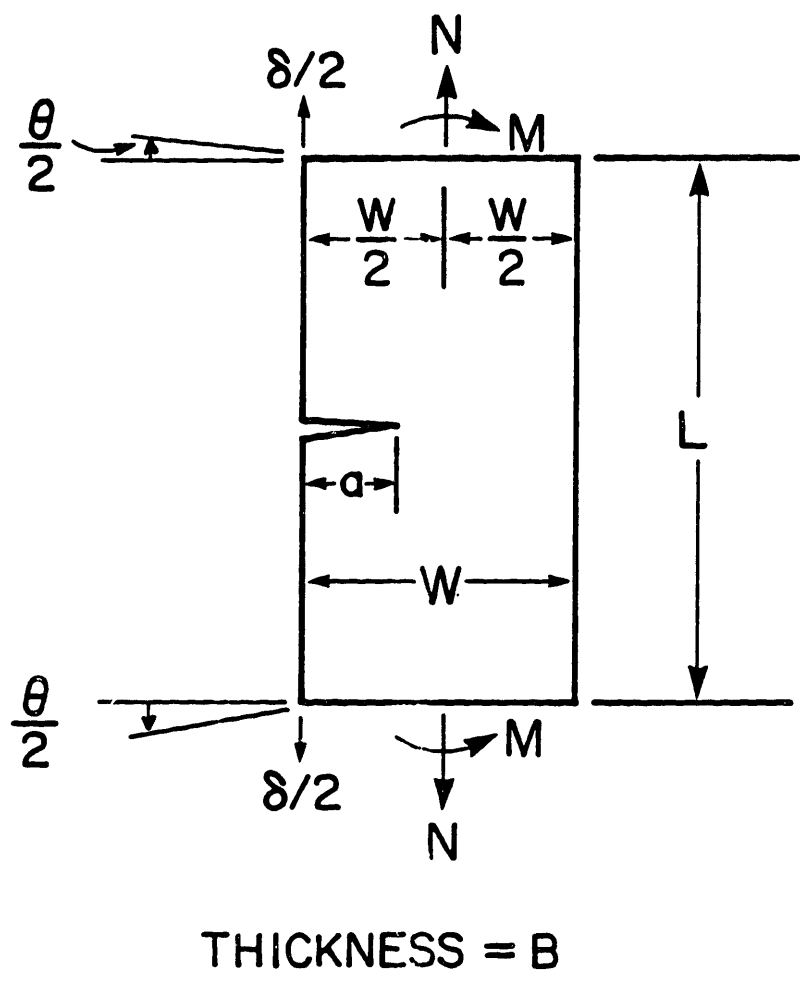


Figure 1. Resultant force N and moment M transmitted by the grips to a SEN specimen.

generalized to include other modes.

The relative displacement δ and rotation θ of the specimen ends can be taken as the sum of a "crack" and "no-crack" parts:

$$\begin{bmatrix} \delta_{\text{tot}} \\ \theta_{\text{tot}} \end{bmatrix} = \begin{bmatrix} \delta_c \\ \theta_c \end{bmatrix} + \begin{bmatrix} \delta_{\text{nc}} \\ \theta_{\text{nc}} \end{bmatrix} . \quad (1)$$

The compliance of the "no-crack" beam gives its extension δ_{nc} and rotation θ_{nc} in terms of the tensile force N acting throughout its center and the corresponding moment M [4]:

$$\begin{bmatrix} \delta_{\text{nc}} \\ \theta_{\text{nc}} \end{bmatrix} = \begin{bmatrix} L/E'A & 0 \\ 0 & L/E'I \end{bmatrix} \begin{bmatrix} N \\ M \end{bmatrix} , \quad (2)$$

where $E' = E$ (Young's modulus) for plane stress and $E/(1-\nu^2)$ for plane strain, ν being the Poisson's ratio. The section moment of inertia $I = BW^3/12$ and the cross section area $A = BW$ can be substituted into Eq. 2 to yield:

$$\begin{bmatrix} \delta_{\text{nc}} \\ \theta_{\text{nc}} \end{bmatrix} = \begin{bmatrix} L/E'BW & 0 \\ 0 & 12L/E'BW^3 \end{bmatrix} \begin{bmatrix} N \\ M \end{bmatrix} \quad (3)$$

The expression for the "cracked" terms are obtained by considering the complementary energy of the specimen U in terms of N and M ,

$$U(N,M) = \frac{1}{2} [N \ M] \left[\begin{array}{c} \delta_{nc} \\ \theta_{nc} \end{array} \right] + \left[\begin{array}{c} \delta_c \\ \theta_c \end{array} \right] , \quad (4)$$

where the matrix scalar product is indicated. Since the "no-crack" terms given in Eq. 3 are independent of crack length, the energy release rate is

$$\frac{\partial U}{\partial a} = \frac{1}{2} [N \ M] \cdot \left[\begin{array}{c} \partial \delta_c / \partial a \\ \partial \theta_c / \partial a \end{array} \right] . \quad (5)$$

With the standard relation between G (fracture mechanics energy release rate) and K_I , the change in complementary energy with respect to crack length a is equal to [5]:

$$\frac{\partial U}{\partial a} = B \frac{K_I^2}{E'} . \quad (6)$$

The stress intensity factor for combined tension and bending can be obtained by superposition of the stress intensity factors applicable to tension and bending. Therefore, in matrix form

$$K_I = \left[\begin{array}{cc} \frac{\partial K}{\partial N} & \frac{\partial K}{\partial M} \end{array} \right] \left[\begin{array}{c} N \\ M \end{array} \right] . \quad (7)$$

Highly accurate functional forms of $\partial K / \partial N$ and $\partial K / \partial M$ can be obtained from the compilations of Tada et. al. [5] where, for example

$$\frac{\partial K}{\partial N} = \frac{(\pi a)^{1/2}}{BW} \sqrt{\frac{2W}{\pi a} \tan\left(\frac{\pi a}{2W}\right)} \left[\frac{0.752 + 2.02\left(\frac{a}{W}\right) + 0.37\left(1 - \sin\left(\frac{\pi a}{2W}\right)\right)^3}{\cos\left(\frac{\pi a}{2W}\right)} \right] \quad (8.1a)$$

$$\equiv (\pi a)^{1/2} \cdot F_1\left(\frac{a}{W}\right) / BW, \quad (8.1b)$$

$$\frac{\partial K}{\partial M} = \frac{6(\pi a)^{1/2}}{BW^2} \sqrt{\frac{2W}{\pi a} \tan\left(\frac{\pi a}{2W}\right)} \left[\frac{0.923 + 0.199\left(1 - \sin\left(\frac{\pi a}{2W}\right)\right)^4}{\cos\left(\frac{\pi a}{2W}\right)} \right] \quad (8.2a)$$

$$\equiv (\pi a)^{1/2} \cdot F_2\left(\frac{a}{W}\right) \cdot \frac{6}{BW^2} \quad (8.2b)$$

Note that in Eq. (8.1b, 8.2b), alternative non-dimensional function F_1, F_2 are introduced in such a manner as to facilitate K-calibrations in terms of a nominal stress " σ " as $K_I = F \cdot \sigma \cdot (\pi a)^{1/2}$. For tension, $\sigma = N/BW$, while for bending $\sigma = 6M/BW^2$. Now equating Eq. 5 and Eq. 6 and inserting Eq. 7 into Eq. 6, one obtains

$$\frac{1}{2} \begin{bmatrix} \frac{\partial \delta_c}{\partial a} \\ \frac{\partial \theta_c}{\partial a} \end{bmatrix} = \frac{B}{E'} \begin{bmatrix} \left(\frac{\partial K}{\partial N}\right)^2 & \left(\frac{\partial K}{\partial N}\right) \left(\frac{\partial K}{\partial M}\right) \\ \left(\frac{\partial K}{\partial N}\right) \left(\frac{\partial K}{\partial M}\right) & \left(\frac{\partial K}{\partial M}\right)^2 \end{bmatrix} \begin{bmatrix} N \\ M \end{bmatrix} \quad (9)$$

Integrating Eq. 9 with respect to "a" provides the "crack" compliance matrix:

$$\begin{bmatrix} \delta_c \\ \theta_c \end{bmatrix} = \begin{bmatrix} C_{11} & C_{12} \\ C_{21} & C_{22} \end{bmatrix} \begin{bmatrix} N \\ M \end{bmatrix} \quad (10)$$

where

$$C_{11} = \frac{2B}{E'} \int_0^a \left[\left(\frac{\partial K(a')}{\partial N} \right) \right]^2 da' = \frac{\partial \delta_c}{\partial N} \quad (11.1)$$

$$C_{12} = C_{21} = \frac{2B}{E'} \int_0^a \left(\frac{\partial K(a')}{\partial N} \right) \left(\frac{\partial K(a')}{\partial M} \right) da' = \frac{\partial \delta_c}{\partial M} = \frac{\partial \theta_c}{\partial N} \quad (11.2)$$

$$C_{22} = \frac{2B}{E'} \int_0^a \left[\left(\frac{\partial K(a')}{\partial M} \right) \right]^2 da' = \frac{\partial \theta_c}{\partial M} \quad (11.3)$$

The generalized forces N, M can now be evaluated in terms of imposed displacements $\delta_{tot}, \theta_{tot}$ by using Eqs. 1, 3 and 10, providing

$$\theta_{\text{tot}} = \frac{12L}{E'BW^3} M + C_{22}M + C_{21}N \quad (12.1)$$

$$\delta_{\text{tot}} = \frac{L}{E'BW} N + C_{11}N + C_{21}M, \quad (12.2)$$

or, on multiplying by E'B;

$$E'B\theta_{\text{tot}} = \frac{12L}{W^3} M + E'BC_{22}M + E'BC_{21}N \quad (13.1)$$

$$E'B\delta_{\text{tot}} = \frac{L}{W} N + E'BC_{11}N + E'BC_{21}M. \quad (13.2)$$

For fixed-end displacement with no shear force $\theta_{\text{tot}} = 0$ and $\delta_{\text{tot}} = \delta$.

Then from Eq. 13.1 we get

$$\frac{M}{W} = - \left[\frac{E'BC_{12}}{12(L/W) + EBW^2 C_{22}} \right] N, \quad (14)$$

while Eq. 13.2 can be re-written

$$E'B\delta = \left[\frac{L}{W} + E'BC_{11} \right] N + E'BWC_{21} \left(\frac{M}{W} \right) . \quad (15)$$

On defining the dimensionless cracked compliance \hat{C}_{ij} as

$$\hat{C}_{11} = E'BC_{11} \quad (16.1)$$

$$\hat{C}_{22} = E'BW^2C_{22} \quad (16.2)$$

$$\hat{C}_{12} = \hat{C}_{21} = E'BWC_{12} = E'BWC_{21} , \quad (16.3)$$

Eq. 14 simplifies to

$$\frac{M}{W} = \frac{-\hat{C}_{12}}{12\left(\frac{L}{W}\right) + \hat{C}_{22}} \cdot N \quad (17)$$

while Eq. 15 simplifies to

$$E'B\delta = \left(\frac{L}{W} + \hat{C}_{11} \right) N + \hat{C}_{12} \frac{M}{W} . \quad (18)$$

When Eq. 17 is inserted into Eq. 18, the axial force N can be obtained as

$$N = E'BW \frac{\delta}{L} \cdot \frac{1}{\left\{ 1 + \frac{W}{L} \left[\hat{C}_{11} - \frac{(\hat{C}_{12})^2}{(12\frac{L}{W}) + \hat{C}_{22}} \right] \right\}} \quad (19)$$

The substitution of Eq. 19 into Eq. 17 provides

$$\frac{M}{W} = \frac{E'BW\delta}{L} \cdot \frac{\left\{ \frac{-\hat{C}_{12}}{(12(L/W) + \hat{C}_{22})} \right\}}{\left\{ 1 + \frac{W}{L} \left[\hat{C}_{11} - \frac{(\hat{C}_{12})^2}{(12(L/W) + \hat{C}_{22})} \right] \right\}} \quad (20)$$

Eq. 19 and 20, respectively provide the force N and bending moment M applied to the crack in terms of the imposed relative displacement δ under conditions of zero relative rotation. Note from Eq. 20 that, since the \hat{C}_{ij} are inherently non-negative, the sign of M is indeed negative, tending to close the crack.

The total stress intensity factor for this specimen is, by superposition, the sum of that due to tension and that due to bending. Due to linearity,

$$K_I = \frac{\partial K}{\partial N} \cdot N + \frac{\partial K}{\partial M} \cdot M \quad , \quad (21)$$

and on combining Eqs. (8.1b, 8.2b, 19, 20) we obtain

$$K_I = \frac{E' \delta}{L} \cdot (\pi a)^{1/2} \cdot \frac{F_1(\xi) \left\{ 1 - 6 \cdot \frac{F_2(\xi)}{F_1(\xi)} \cdot \frac{\hat{C}_{12}(\xi)}{12 \left(\frac{L}{W}\right) + \hat{C}_{22}(\xi)} \right\}}{\left\{ 1 + \frac{W}{L} \left[\hat{C}_{11}(\xi) - \frac{\hat{C}_{12}^2(\xi)}{12 \left(\frac{L}{W}\right) + \hat{C}_{22}(\xi)} \right] \right\}} \quad , \quad (22)$$

where $\xi = a/W$. As shown in [6], the terms $\hat{C}_{ij}(\xi)$ are normalized dimensionless cracked compliances which need be calculated only once. In the present application, the integrals of Eq. 11 were numerically evaluated in increments of dimensionless crack length $\Delta\xi = \Delta a/W$ of size 0.01 using Simpson's rule. If we now substitute the nominal stress value $\sigma \equiv E' \delta/L$ into Eq. 22, we recover the familiar form

$$K_I = \sigma\sqrt{\pi a} \cdot G(\xi, \eta) , \quad (23)$$

where

$$G(\xi, \eta) = \frac{F_1(\xi) \cdot \left\{ 1 - \frac{6F_2(\xi) \cdot \hat{C}_{12}(\xi)}{F_1(\xi) [12\eta + \hat{C}_{22}(\xi)]} \right\}}{\left\{ 1 + \frac{1}{\eta} \left[\hat{C}_{11}(\xi) - \frac{\hat{C}_{12}(\xi)^2}{(12\eta + \hat{C}_{22}(\xi))} \right] \right\}} , \quad (24)$$

and $\xi = a/W$, $\eta = L/W$.

In Fig. 2, plots of $G(\xi, \eta)$ versus a/W are given for different values of L/W . The dimensionless functions F_1 and F_2 of Tada et. al. [5] (see Eqs. 8.1b, 8.2b) for pure tension and pure bending, respectively, are also shown for reference purposes. Finally, Fig. 2 also shows the approximate stress intensity factor calibration of the SEN specimen due to Harris [2], who gives

$$K_I = \sigma\sqrt{\pi a} F_H(a/W) \quad (25a)$$

with

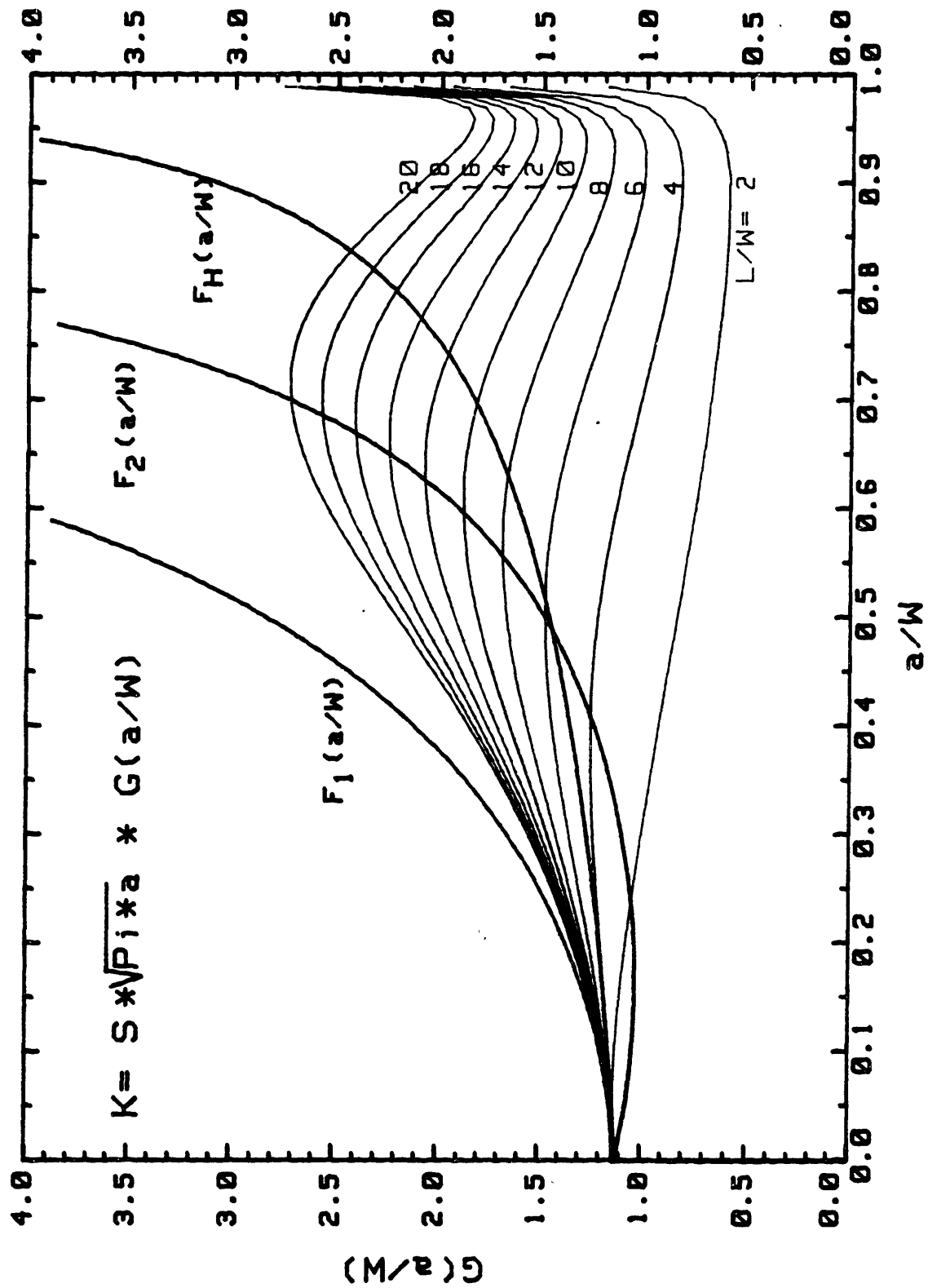


Figure 2. Geometrical factors F_1 , F_2 , F_H and Eq. 24 as a function of the dimensionless crack length.

$$F_H(a/W) = \left\{ \frac{25}{20 - 13(a/W) - 7(a/W)^2} \right\}^{1/2} \quad (25b)$$

In the interpretation of Eq. 25a, the nominal stress " σ " is understood to be N/BW , the nominal far-field stress, which in the present application must be determined (analysis) or measured (experiment) in terms of the imposed loading parameter δ .

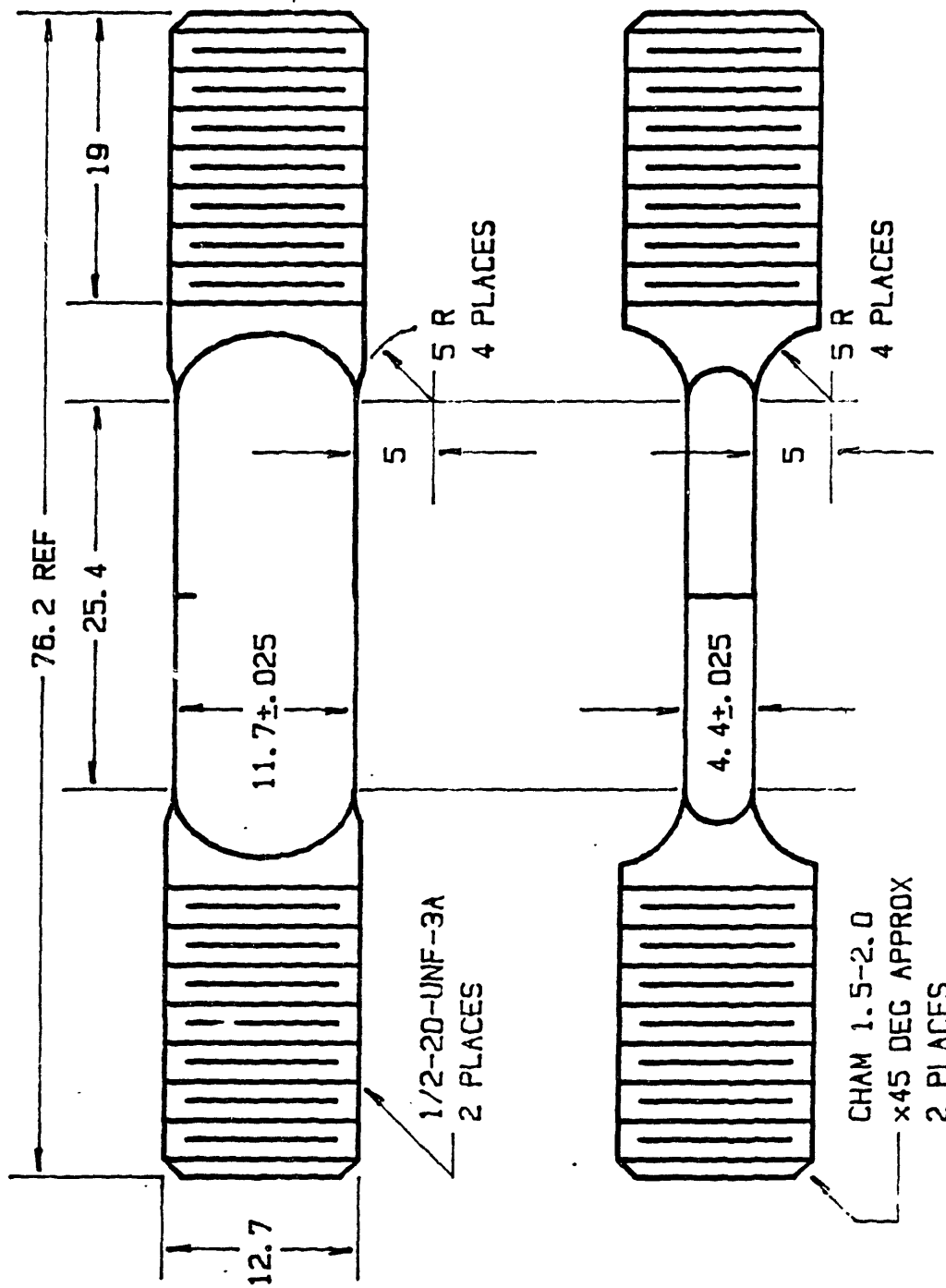
As can be seen, our solution for G is strongly dependent on both relative crack depth and specimen length-to-width ratio and shows a local maximum with respect to a/W at some intermediate value of a/W for all (L/W) ratios larger than 2. For smaller ratios, the geometric correction factor G shows a monotonic decrease with respect to a/W until very deep cracks, $a/W > .9$, are considered. Tada's and Harris' geometry correction factors which were derived for tension, F_1 and F_H , under conditions of constant remote uniform tensile stress show a monotone increase with increasing a/W . Tada's bending geometry correction factor F_2 shows a slight decrease with increasing a/W , reaching a minimum value near $a/W = 0.15$, followed by a monotonic increase.

A basic assumption of the preceding analysis is that the specimen length (L) at which displacement boundary conditions are being imposed is sufficiently long in comparison to the appropriate St. Venant decay distance for the local stress disturbance introduced by the presence of the

crack. For short cracks, $a/W \ll 1$, the characteristic decay distance is "a", so that providing $L/W > 1$, the analysis should be valid. For very deep cracks, the decay length is specimen width W , so L must in that case exceed some multiple of W . This analysis cannot precisely quantify a requisite minimum value of L/W for any particular maximum value of a/W . However, good agreement has been obtained with Bowie and Freese's solution [3] for low values of $L/W = 2$, the agreement between the two solutions was within one percent for all values of a/W covered by the analysis.

EXPERIMENTAL VERIFICATION

An experimental check of the solution was provided by performing fatigue crack growth tests on SEN specimens subject to imposed displacement loading. The dimensions of the specimen are shown in Fig. 3. The notch, about 1 mm deep, was cut by electro-discharge machining. The test material was B-1900+Hf, a high-strength/low ductility superalloy with good creep and oxidation resistance at elevated temperature. The tests were run under fully reversed strain control condition in the elastic regime ($\Delta\epsilon = 0.25\%$) in laboratory air. This nominal axial strain was controlled over a gauge length of 12.7 mm which included the crack. The temperature and frequency of the tests were 925°C and 0.1 Hz. Before starting the tests, the specimens were precracked at 10 Hz and room temperature under load-controlled conditions up to a ΔK of about 20 MPa \sqrt{m} (Harris' solution) which corresponds to an a/W ratio of 0.125. Details of the experimental set-up and crack growth measurement technique are given elsewhere [7,8].



Dimensions in mm.

Figure 3. Single edge notched (SEN) specimen used for the testing (notch: 1 mm deep x 0.025 mm wide).

Fig. 4 shows the crack growth rates as a function of the strain intensity factor ΔK_{ϵ} . The ΔK_{ϵ} is used for convenience because fatigue at high temperature is a strain-controlled process. It is defined as follows [9,10]:

$$\Delta K_{\epsilon} = \Delta \epsilon \cdot \sqrt{\pi a} \cdot G(a/W) . \quad (26)$$

In the above expression, $G(a/W)$ is the same geometric correction term derived in connection with the stress intensity factor. That is, in Fig. 4, the strain intensity is calculated as $\Delta \epsilon \cdot \sqrt{\pi a} \cdot F_H(a/W)$ with $\Delta \epsilon = .25\%$. In spite of the fact that ΔK_{ϵ} , so-defined, lacks a rigorous mechanics interpretation, it has been used for correlating crack growth data under strain-controlled conditions [9-12]. Clearly, the non-monotone correlation of fatigue crack growth rate with strain intensity factor range is not to be expected in cracks of macroscopic dimension. Thus, the non-monotonic nature of this correlation strongly suggests that there are deficiencies in this analysis of the strain intensity factor.

To provide a more rigorous understanding of the result, the ΔK_{ϵ} were re-defined as

$$\Delta K_{\epsilon} = \Delta K / E' \quad (27)$$

FATIGUE CRACK PROPAGATION

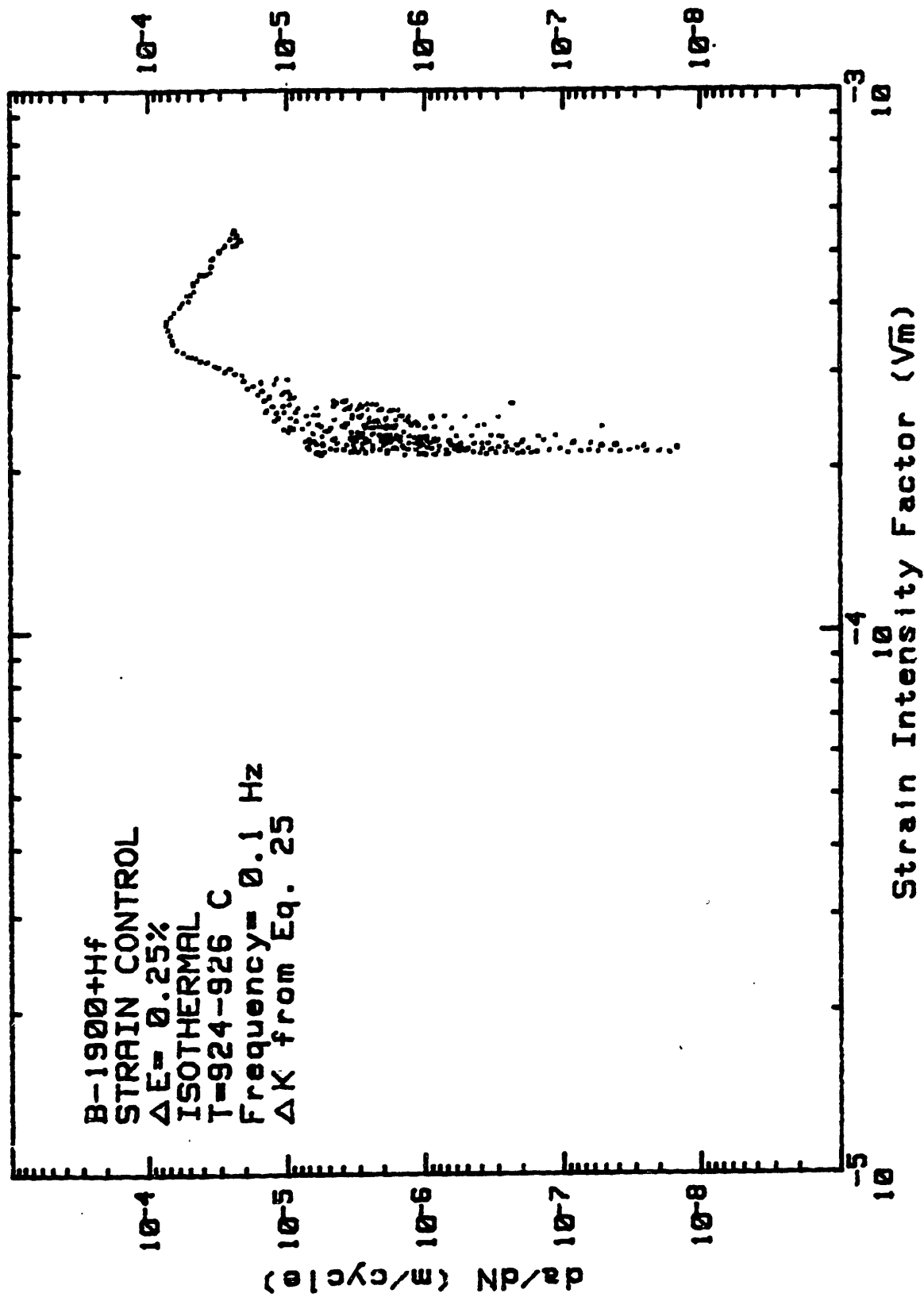


Figure 4. FCP rates as a function of the strain intensity factor calculated using Eq. 22.

where the ΔK is the stress intensity factor derived for stress-controlled (Eq. 25) or displacement-controlled (Eq. 23) conditions. In cases of predominantly elastic behavior, this definition of strain intensity factor is consistent with standard fracture mechanics. Fig.5 re-plots the fatigue crack growth rate versus the cyclic strain intensity factor deduced from Eq. 25 and from the current analysis (Eq. 23) using the value of $L/W = 2.17$ corresponding to the length of the uniform reduced gauge section of the specimen. In the application of Harris' formulation, the nominal stress σ was calculated using the tensile force N measured by the load cell. It should be noted that the load cell output is insensitive to the shift in load line which is associated with longer cracks. Again, the curve indicates that the correlation between measured fatigue crack growth rate and inferred strain intensity factor is non-monotone. Note, however, that the correlation is somewhat better than that shown in Fig. 4 because the inferred range of ΔK_{ϵ} occurring during the tests is reduced. The lower inferred range in the present case is due to the use of the measured load value, which decreases under fixed displacement conditions, due to the increasing crack compliance. This load-shedding is not reflected in the previous definition of ΔK_{ϵ} as $\Delta \epsilon \cdot \sqrt{\pi a} \cdot F_H(a/W)$. The importance of load-shedding in the determination of the actual driving force has been recognized by Leis et. al. [13-14] which also used the measured load in their K calculations.

At this point, it is useful to consider more carefully the mathematical model of an imposed displacement with no rotation over a length "L"

FATIGUE CRACK PROPAGATION

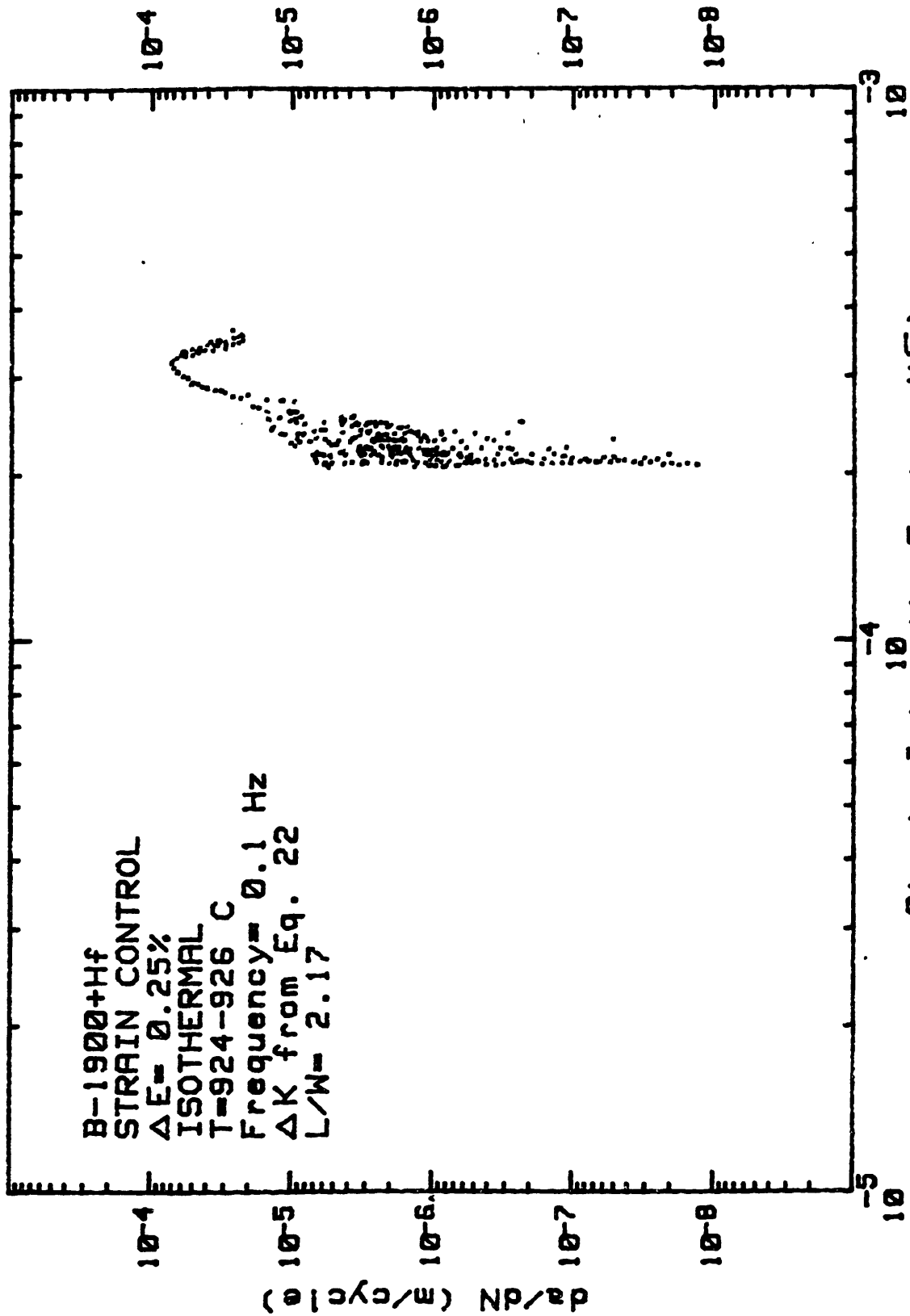


Figure 5. FCP rates as a function of the strain intensity factor calculated using Eq. 25.

as it relates to an actual specimen, such as that in Fig. 3, and its grips. Two points need to be reviewed. First, the applicability of the zero rotation conditions and secondly, the implication of measuring and controlling the imposed displacement at the back face of the specimen.

In the present case, the zero rotation condition is effectively enforced at the base of the threaded ends of the specimen. Thus, the effective value of L/W for the specimen might be expected to be somewhat greater than that based on the length of uniform reduced gage section. The additional effective length would correspond to the no-crack bending compliance of the tapered shoulders connecting gage section and threaded ends. The tensile part of the additional compliance is not required, since the mean extension δ is measured over the gauge length of $L_{\text{gauge}} = 2.17 \cdot W = 25.4$ mm. If we let L_b denote the augmented effective bending length of the specimen, and $\eta_b = L_b/W$, then the modified versions of Eq. 22 is (see Appendix V.a).

$$K_I = \frac{E' \delta}{L} \cdot (\pi a)^{1/2} \cdot G(\xi, \eta, \eta_b) \quad (28)$$

where

$$G(\xi, \eta, \eta_b) = \frac{F_1(\xi) \left\{ 1 - \frac{6F_2(\xi)}{F_1(\xi)} \cdot \frac{\hat{C}_{12}(\xi)}{(12\eta_b + C_{22}(\xi))} \right\}}{\left\{ 1 + \frac{1}{\eta} \left[\hat{C}_{11}(\xi) - \frac{\hat{C}_{12}^2(\xi)}{(12\eta_b + C_{22}(\xi))} \right] \right\}} \quad (29)$$

and, again, $\eta = L/W$.

The other point to consider is the consequence of controlling the back face displacement, δ_{BF} (see Fig. 3) instead of at the centerline of the specimen. Because the displacement δ is controlled at L instead of L_b where no-rotation is effectively enforced, the displacement at the back face is equal to the displacement at the centerline (δ_{c1}) minus the displacement induced by rotation, θ_L , at L , i.e.,

$$\delta_{BF} = \delta_{c1}(L) - \frac{W}{2} \cdot \theta_L. \quad (30)$$

Now, using Eq. 30 with $\delta_{c1}(L)$ given by Eq. 12.2, the final corrected version K_I which takes into account both the effective length (L_b) and back face displacement is given by (See Appendix V.a).

$$K_I = \frac{E'\delta}{L} \cdot (\pi a)^{1/2} \cdot G_c(\xi, \eta, \eta_b) \quad (31)$$

where

$$G_c(\xi, \eta, \eta_b) = \frac{F_1(\xi) \left\{ 1 - \frac{6F_2(\xi)}{F_1(\xi)} \cdot \frac{\hat{C}_{12}(\xi)}{(12\eta_b + \hat{C}_{22}(\xi))} \right\}}{\left\{ 1 + \frac{1}{\eta} \left[\hat{C}_{11}(\xi) - \frac{\hat{C}_{12}^2(\xi)}{12\eta_b + \hat{C}_{22}(\xi)} + \frac{6\hat{C}_{12}(\xi)(\eta - \eta_b)}{12\eta_b + \hat{C}_{22}(\xi)} \right] \right\}} \quad (32)$$

with η , η_b and ξ defined as before. The additional term appearing in the denominator of Eq. 32, as compared to Eq. 29, is of little consequence for shorter cracks, and small values of $\eta_b - \eta$. Thus, the fact that back face, as opposed to centerline displacement is monitored is generally of minor significance.

Based on the assumption that $(da/dN)_{\max}$ coincides with a maximum in the ΔK_ϵ (i.e., the correlation is monotone), plots of da/dN versus a/W were compared with plots of $G'_c(a/W)$ versus a/W where

$$G'_c(a/W) \equiv (\pi\xi)^{1/2} \cdot G_c(\xi, \eta, \eta_b) \quad (33)$$

for various values of η_b . Note from Eq. 33 that for prescribed δ , ΔK_ϵ is linearly proportional to $G'_c(\xi)$. The results are plotted in Fig. 6 versus relative crack depth, a/W . The maximum growth rate, occurring at $a/W = 0.52$, coincides with the location of maximum $G'_c(\xi, \eta, \eta_b)$ for the case of $\eta_b = 2.5$. A plot of da/dN versus ΔK_ϵ inferred from the present analysis with $L_b/W = 2.5$ is shown in Fig. 7. A very tight correlation between the crack growth rates and the ΔK_ϵ 's is observed with a monotone correlation, within reasonable limits of experimental scatter. One concludes that our K-solutions (Eq. 28, 31) correlate the data providing the proper "effective" bending length is used. It should be pointed out, that an L_b/W ratio of 2.5 (which corresponds to a length of 29 mm) is the distance between the mid-shoulders of the specimen.

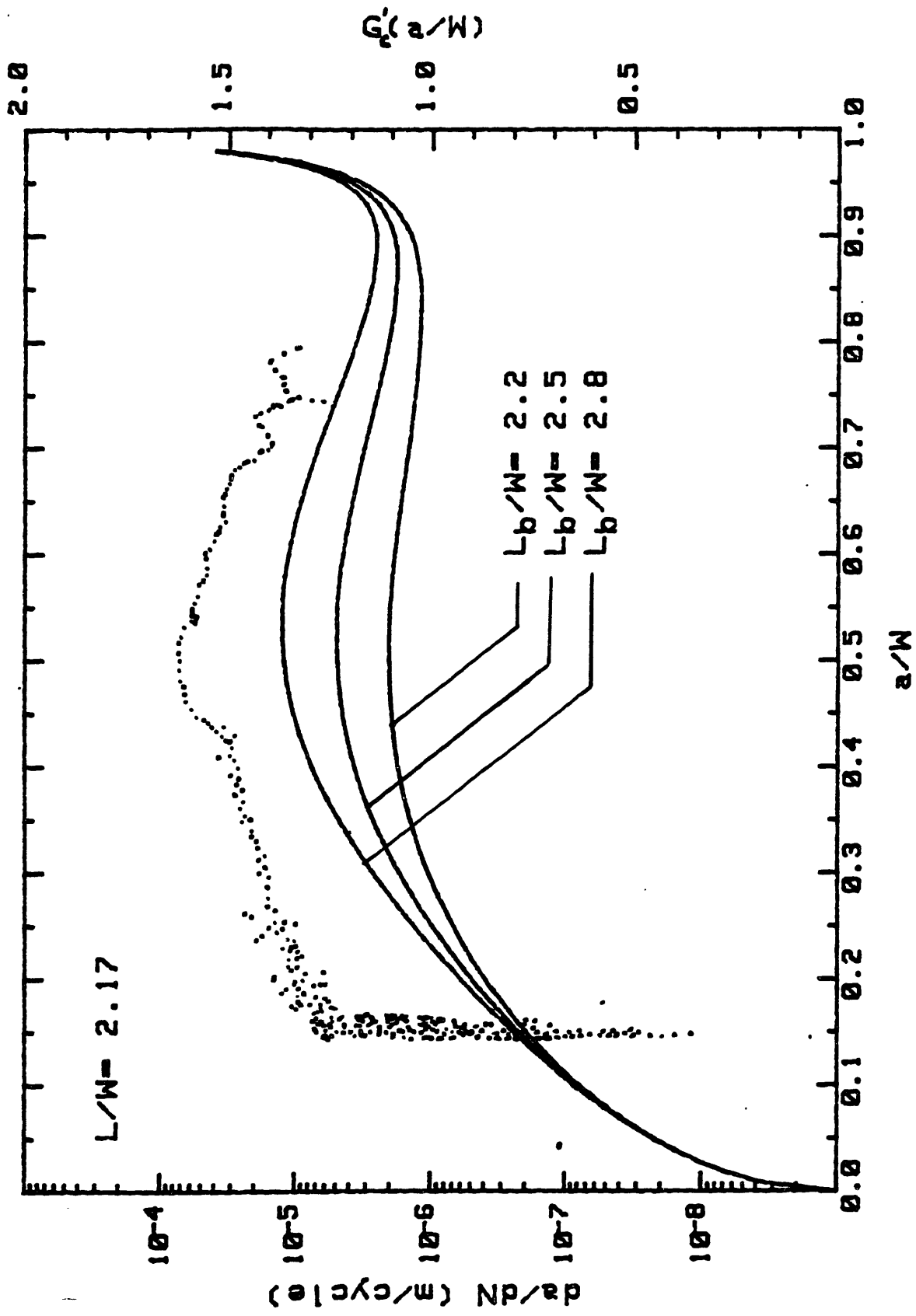


Figure 6. FCP rates as a function of a/W and Eq. 33 as a function of a/W for various η_b ratios.

FATIGUE CRACK PROPAGATION

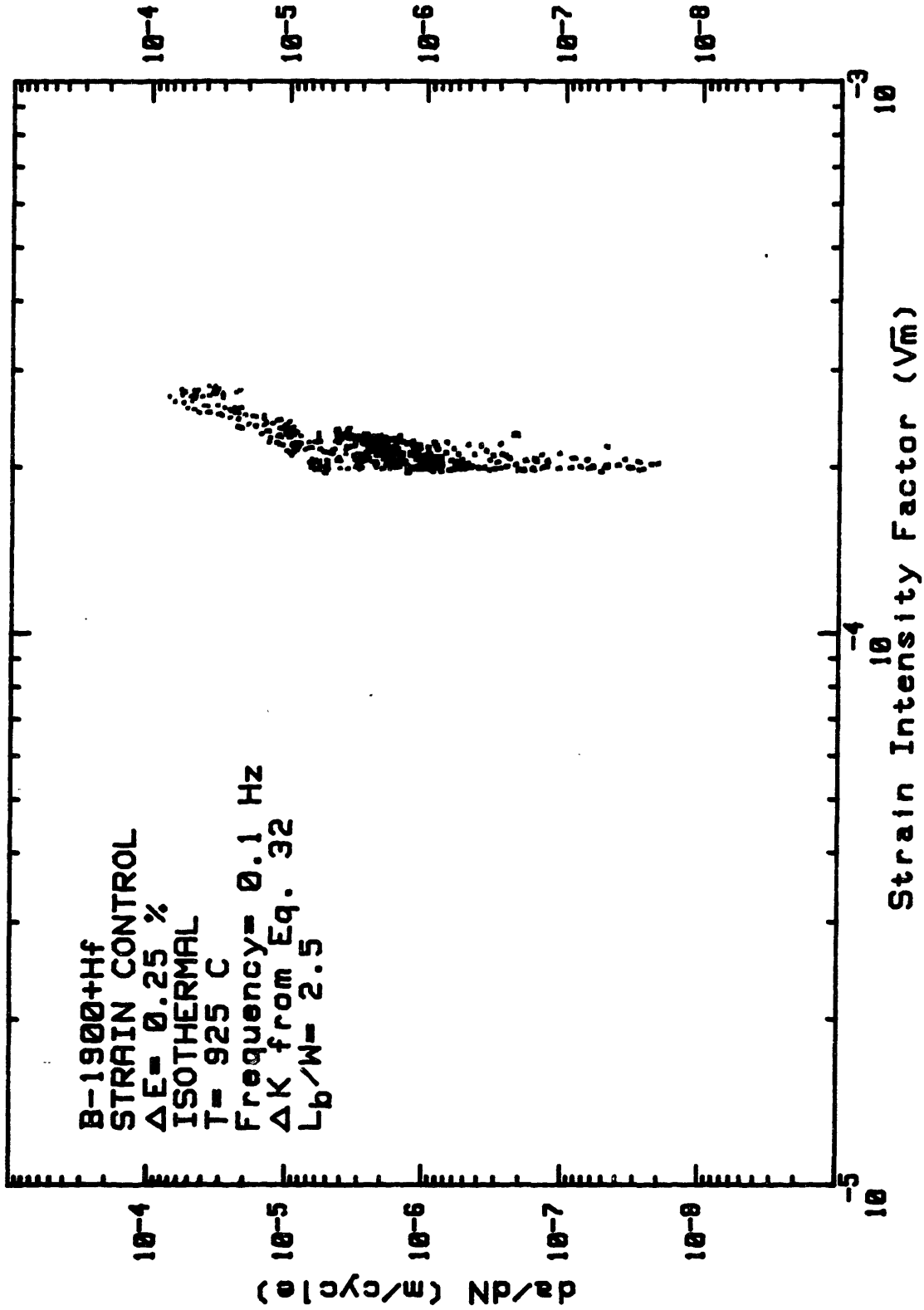


Figure 7. FCP rates as a function of the strain intensity factor calculated using Eq. 32.

CONCLUSION

For a given geometry and applied end-displacements, Figs. 4 to 6, show that the uncritical use of conventional stress-derived K_I solutions can substantially overestimate the K_I values. While such an eventuality is conservative in application, it is non-conservative when testing to obtain basic materials behavior.

In the present case, the use of the strain intensity factor as represented by Eq. 26 seems to have two important limitations, both of which grow in importance at higher a/W levels. First, this definition of strain intensity factor as crack growth driving parameter does not account for the substantial load-shedding associated with the increasing crack compliance. This limitation can, in part, be mitigated (as in Fig. 5), by monitoring the decreasing load amplitude as the crack extends, and substituting this crack-length-dependent load into a tensile loading intensity factor calibration. The second major limitation of the traditional strain intensity factor definition is that it fails to account for the development of a closing bending moment, associated with the prescribed zero-rotation boundary condition. This closing bending moment further reduces the effective crack driving force. A complete analysis of tension and bending moment in the specimen is required. When the K -solutions are derived from a line-spring analysis and combined with an effective specimen length, good correlations are found between K and the experimental fatigue crack growth data.

REFERENCES

1. J.M. Bloom, International Journal of Fracture, Vol. 3 (1967), pp. 235-242.
2. D.O. Harris, Trans. of ASME, Journal of Basic Engineering, Vol. 89 (1969), pp. 49-54.
3. O.L. Bowie and C.E. Freese, Engineering Fracture Mechanics, Vol. 14 (1981), pp. 519-526.
4. E.P. Popov, Introduction to Mechanics of Solids, Prentice Hall, Englewood Cliffs (1968).
5. H. Tada, P.C. Paris, and G.R. Irwin, The Stress Analysis of Cracks Handbook, Del Research Corporation, Hellentown (1973).
6. F.A. McClintock, D.M. Parks, J.W. Holmes, and K.W. Bain, Engineering Fracture Mechanics, Vol. 20 (1985), pp. 159-167.
7. N. Marchand and R.M. Pelloux, "A Computerized Test System for Thermal Mechanical Fatigue Crack Growth", submitted for publication.
8. N. Marchand and R.M. Pelloux, in Time-Dependent Fracture, Martinus Nijhoff (1985), pp. 167-179.
9. R.C. Boettner, C. Laird, and A.J. McEvily, Trans. of Metallurgical Society of AIME, Vol. 233 (1965), pp. 379-387.
10. A.J. McEvily, "Fatigue Crack Growth and the Strain Intensity Factor", in Fatigue and Fracture of Aircraft Structures and Materials, AFFDL-TR-70-144 (1970).
11. A.E. Gemma, F.X. Ashland, and R.M. Masci, ASTM Journal of Testing and Evaluation, Vol. 9 (1981), pp. 209-213.
12. T. Koizumi and M. Okazaki, Fatigue of Engineering Materials and Structure, Vol. 1 (1979), pp. 509-520.
13. B.N. Leis and T.F. Forte, ASTM STP 743 (1981), pp. 100-124.
14. B.N. Leis, Engineering Fracture Mechanics, Vol. 22 (1985), pp. 279-293.

APPENDIX V.a

Consider a specimen of gage length L with its associated shoulders. Let's define L_b the effective length at which the zero rotation is enforced ($\theta|_{L_b} = 0$). Obviously $L_b > L$ and, as a consequence the back face displacement δ_{BF} measured at L will be equal to the centerline displacement minus the angular displacement at L , i.e., $\frac{W}{2} \cdot \theta_L$. Therefore, the known quantities are δ_{BF} (measured at L) and θ_{tot} across L_b . Equations 12.1 and 12.2 can now be written as

$$0 = \theta_{tot}(L_b) = \theta(L_b) = \theta_{nc}(L_b) + \theta_c \quad (A.1)$$

$$\delta_{BF} = \delta_{tot}(L) = \delta_{nc}(L) + \delta_c(L) - \frac{W}{2} \theta(L) \quad (A.2)$$

Substitute Eq. 10 into A.1 and re-arranging, yielding

$$\frac{M}{W} = \frac{-C_{12} E' BW}{12 \eta_b + C_{22} E' BW} \cdot N \quad (A.3)$$

On using the dimensionless crack compliance defined by Eqns. 16.1 to 16.3,

Eq. A.3 simplifies to

$$\frac{M}{W} = \frac{-\hat{C}_{12}}{12 \eta_b + \hat{C}_{22}} \cdot N \quad (\text{A.4})$$

where $\eta_b = L_b/W$. Noting that $M(L_b) = M(L)$, the displacement δ_{BF} (Eq. A.2) is, using Eq. 10 and A.1,

$$\delta_{BF} = \left[\frac{NL}{BWE'} + C_{11}N + C_{12}M \right] - \frac{W}{2} \left[\frac{12ML}{E'BW^3} + C_{22}M + C_{12}N \right] \quad (\text{A.5})$$

which, upon re-arranging and using the dimensionless crack compliance (Eqns. 16.1-16.3) yields

$$N = E'BW \frac{\delta_{BF}}{L} \cdot \frac{1}{\left\{ 1 + \frac{1}{\eta} \left[\hat{C}_{11}(\xi) - \frac{\hat{C}_{12}^2(\xi)}{(12\eta_b + \hat{C}_{22}(\xi))} + \frac{6\hat{C}_{12}(\xi)(\eta - \eta_b)}{(12\eta_b + \hat{C}_{22}(\xi))} \right] \right\}} \quad (\text{A.6})$$

Finally, recalling that

$$K_I = \frac{N}{BW} \sqrt{\pi a} \cdot F_1(\xi) + \frac{6M}{BW^2} \cdot \sqrt{\pi a} \cdot F_2(\xi) \quad (\text{A.7})$$

and upon substitution of Eqns. A.4 and A.6 into A.7, we get

$$K_I = \frac{E' \delta_{BF}}{L} \cdot \sqrt{\pi a} \cdot \frac{F_1(\xi) \left\{ 1 - \frac{6F_2(\xi)}{F_1(\xi)} \cdot \frac{\hat{C}_{12}}{(12\eta_b + \hat{C}_{22})} \right\}}{\left\{ 1 + \frac{1}{\eta} \left[\hat{C}_{11}(\xi) - \frac{\hat{C}_{12}^2}{12\eta_b + \hat{C}_{22}(\xi)} + \frac{6\hat{C}_{12}(\xi)(\eta - \eta_b)}{12\eta_b + \hat{C}_{22}} \right] \right\}} \quad (\text{A.8})$$

Equation A.8 corrects for the fact that actual displacements are measured at back face instead of the centerline, and for the fact that the zero-rotation condition is imposed not at L , but at some distance L_b close to the actual grips.